

University of South Wales



2053156

*Bound by* **Abbey**  
Bookbinding Co.  
Cardiff, South Wales  
Tel: (01 222) 395882

The Characterization of Olive  
Oils by Various Chromatographic and  
Spectroscopic Techniques

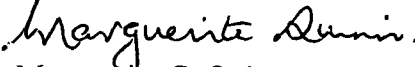
Marguerite Claire Quinn

A Thesis submitted to the  
University of Glamorgan for the  
Degree of Doctor of Philosophy  
1997

School of Applied Sciences,  
The University of Glamorgan,  
UK.

## Declaration

This thesis has not been nor is being currently submitted for the award of any other degree or similar qualification.

  
Marguerite C. Quinn

## ABSTRACT

The aim of this study is to develop an integrated set of analytical methods to characterize olive oil in terms of geographical origin, variety and extraction technology. Emphasis was also placed on the analysis of high quality extra virgin oils adulterated with lower quality sunflower oil.

This research involved the study of novel methodologies for solving olive oil authentication issues as well as the replacement of traditional wet chemistry methods with faster and more efficient means of olive oil analysis. These techniques included gas chromatography, supercritical fluid chromatography, Raman spectroscopy, Infrared spectroscopy and carbon and proton NMR.

Statistical analysis of the data obtained was used to identify the relationship between the measured parameters. The statistical analysis was carried out using both Win - Discrim and Unscrambler (Camo AS, 1996). These programs were designed to classify samples by hard modelling discriminant analysis and by soft independent modelling of class analogy (SIMCA) respectively.

# CONTENTS

ABSTRACT .....	i
CONTENTS .....	ii
LIST OF TABLES .....	xi
LIST OF FIGURES .....	xxii
ACKNOWLEDGEMENTS .....	xxvii
CHAPTER 1 .....	1
1. INTRODUCTION .....	1
1.1 Olive oil and why it is adulterated.....	1
1.2 Nutritional aspects and functions of fats and oils .....	5
1.3 Natural lipids in plants and animals.....	6
1.3.1 Simple lipids.....	7
1.3.1.1 Glycerides .....	7
1.3.1.2 Sterol esters .....	9
1.3.2 Complex lipids .....	10
1.3.2.1 Phospholipids.....	10
1.3.2.2 Glycolipids.....	11

1.3.2.3 Sphingolipids .....	12
1.3.3 Other minor components.....	12
1.3.3.1 Vitamins and antioxidants.....	12
1.3.3.2 Pigments .....	12
1.4 The composition of olive oil and its potential adulterants.....	13
1.5 Instrumentation.....	21
1.5.1 Gas chromatography.....	21
1.5.1.1 Carrier gas .....	21
1.5.1.2 Injection systems.....	22
1.5.1.3 GC analysis of the fatty acid methyl esters of oils.....	23
1.5.1.4 GC analysis of triglycerides .....	24
1.5.2. Supercritical fluid chromatography and supercritical fluid extraction.....	27
1.5.2.1 Supercritical fluid chromatography.....	29
1.5.2.2 Supercritical fluid extraction.....	32
1.5.3 Nuclear magnetic resonance.....	34
1.5.3.1 Application of proton NMR to lipid analysis.....	36
1.5.3.2 Application of carbon NMR to lipid analysis.....	37

1.5.4 Mid - infrared spectroscopy.....	42
1.5.5 Raman spectroscopy .....	47
1.5.6 Pattern recognition.....	50
1.6 Project objectives.....	57
CHAPTER 2 .....	59
2. THE CHARACTERIZATION OF OLIVE OIL BY CHROMATOGRAPHIC TECHNIQUES.....	59
2.1 The transesterification of triglycerides.....	59
2.1.1 Quantitation of the transesterification of methyl esters.....	63
2.1.2 The American Oil Society method (1973).....	65
2.1.3 Material and methods.....	65
2.1.3.1 Procedure .....	66
2.1.4 The low temperature sulphuric acid method (Mc Ginnis and Duggan, 1964).....	66
2.1.5 Materials and methods .....	66
2.1.5.1 Procedure .....	66
2.1.6 The base - catalyzed transesterification method using tetrahydrofuran (Christie, 1982) .....	67

2.1.7 Materials and methods .....	67
2.1.7.1 Procedure .....	67
2.1.8 The EC reflux method (Official Journal of EC, 1991). .....	67
2.1.9 Materials and methods .....	67
2.1.9.1 Procedure .....	68
2.2 GC results and discussion of FAME analysis by GC .....	69
2.3 GC analysis of the triglycerides of the Greek oils by total carbon number and by degree of unsaturation .....	79
2.3.1 Materials and methods .....	80
2.3.1.1 Procedure .....	81
2.3.1.2 Partial least squares regression application on the triglyceride olive oil standards	81
2.4 Discussion of GC triglyceride results .....	86
2.5 Conclusion .....	90
CHAPTER 3 .....	91
3. SUPERCRITICAL FLUID EXTRACTION AND SUPERCRITICAL FLUID ARGENTATION CHROMATOGRAPHY ANALYSIS OF VARIOUS OILS ...	91
3.1 Supercritical fluid argentation chromatography .....	91



3.1.1 Materials and methods .....	92
3.1.1.1 Procedure .....	93
3.2 Results and discussion on the supercritical fluid Chromatographic analysis of the various oils .....	94
3.2.1 SFC results and discussion on the supercritical fluid chromatographic analysis of the Greek oils using UV detection .....	103
3.2.2 SFC results and discussion on the supercritical fluid chromatographic analysis of the Greek oils using light scattering detection .....	
3.3 The supercritical fluid extraction of various oils .....	108
3.3.1 The supercritical fluid extraction of oil from sunflower and sesame seeds .....	108
3.3.1.1 Materials and methods .....	109
3.3.2 On - line supercritical fluid extraction and supercritical fluid chromatography of the triglycerides from olives and seed oils .....	110
3.3.2.1 Materials and methods .....	110
3.3.3 The derivatisation of triglycerides to FAME using lipase .....	110
3.3.3.1 Materials and method .....	111
3.3.3.3.1 Procedure .....	111
3.3.4 Results and discussion of SFE oil extractions .....	112

3.4 Conclusion .....	115
 CHAPTER 4 .....	 117
4. THE CHARACTERIZATION OF OLIVE OIL BY RAMAN AND INFRARED SPECTROSCOPY .....	117
4.1 The application of FT - Raman spectroscopy and SIMCA modelling in the data of authentic olive oil .....	117
4.1.1 Material and methods .....	117
4.1.1.1 Procedure .....	117
4.1.2 Results and discussion .....	118
4.1.2.1 SIMCA classification of whole Raman spectral data .....	119
4.1.2.2 SIMCA classification of whole Raman spectral data using full cross validation .	122
4.1.2.3 SIMCA classification of whole Raman spectral data using randomly chosen test sets .....	125
4.1.2.4 SIMCA classification of Raman fingerprint region spectral data.....	127
4.1.2.5 SIMCA classification of Raman fingerprint spectral data using randomly chosen test sets.....	136
4.1.2.6 SIMCA classification on the Peloponese and Crete varieties within the authentic oils on the Raman whole data set .....	140

4.1.2.7 SIMCA classification on the Peloponese and Crete varieties within the authentic oils on the Raman fingerprint .....	142
4.1.3 Conclusion on Raman analysis.....	145
4.2. Infrared analysis .....	146
4.2.1 Materials and methods .....	146
4.2.1.1 Procedure .....	146
4.2.2 Results and discussion.....	147
4.2.2.1 Discriminant statistical analysis of Infrared data.....	148
4.2.2.2 Discriminant analysis using the authentic samples and sunflower adulterated samples (5 % w/w and 10 % w/w sunflower respectively).....	153
4.2.2.3 Discriminant analysis using the authentic samples and 10 % w/w sunflower adulterated samples and the selective infrared absorptions.....	156
4.2.2.4 Discriminant analysis using the authentic samples and 10 % sunflower adulterated samples on the selective infrared absorptions .....	161
4.2.2.5 SIMCA classification of the Infrared data regions 3100 - 2500 and 1800 - 1000 .....	164
4.2.2.6 SIMCA classification of the Infrared data regions 3050 - 2752 .....	165
4.2.2.7 SIMCA classification of the selective Infrared data regions.....	165

Conclusion.....	166
CHAPTER 5 .....	167
5.1 The analysis of olive oils using $^{13}\text{C}$ and proton nuclear magnetic resonance.....	167
5.1.1 Materials and methods for $^{13}\text{C}$ NMR and $^1\text{H}$ NMR.....	168
5.1.1.2 Procedure .....	168
5.1.2 NMR results and discussion. ....	169
5.1.3 The statistical analysis of the $^{13}\text{C}$ NMR and $^1\text{H}$ NMR data.....	174
5.1.3.1 Hard modelling discriminant analysis of data from whole $^{13}\text{C}$ NMR Spectrum... 175	
5.1.3.2 Hard modelling discriminant analysis of data from the alkene region of $^{13}\text{C}$ NMR spectrum .....	180
5.1.3.3 Hard modeling discriminant analysis of data from proton NMR olive oil spectra .....	182
5.1.3.4 SIMCA classification of the data from the whole $^{13}\text{C}$ NMR data.....	186
5.1.3.5. SIMCA classification of the data from the alkene region of $^{13}\text{C}$ NMR data .....	189
5.1.3.6 SIMCA classification of the data from the proton NMR .....	193
5.1.3.7 SIMCA classification of the Peloponese and Crete varieties in the authentic Greek oils using carbon and proton NMR data.....	197
5.1.4 Conclusion.....	197

CHAPTER 6 .....	198
6.1 CONCLUSION .....	198
6.1.1 Chromatographic analysis of olive oils.....	199
6.1.2 Spectroscopic analysis of olive oils.....	200

## LIST OF TABLES

Table 1.1 Fatty acid profiles (% composition) for animal and vegetable lipids (Formo et al., 1979) .....	9
Table 1.2 Composition of virgin olive oil (Suarez and Mendoza, 1986) .....	15
Table 1.3 Individual triglycerides found in olive oil ( Suarez and Mendoza, 1986) .....	16
Table 1.4 Composition of the unsaponifiables of olive oil and oil cake (Suarez and Mendoza, 1986) .....	16
Table 1.5 Data from the Italian government specifications (1983), the Codex standards on olive oil (1970) and the International Olive Oil Council (1993) .....	19
Table 1.6 <sup>1</sup> H NMR spectral assignments of the triglyceride components for olive oils ( Shiao & Shiao, 1989).....	37
Table 1.7 <sup>13</sup> C NMR spectral assignments of the triglyceride components for olive oils....	38
Table 1.8 Characteristic attenuated total reflectance infrared absorption band of oil ( Safar et al., 1994).....	47
Table 1.9 Raman scatter bands for fats and oils ( Sadeghi - Jorabchi et al., 1991).....	49
Table 1.10 Characteristic infrared absorption and Raman scattering bands for sunflower oil (Sadeghi - Jorabchi et al., 1990) .....	50
Table 1.11 A detailed description of the Greek olive oil sample set provided for this research.....	56

Table 2.1 GC FAME parameters.....	69
Table 2.2 GC FAME analysis using different methods of transesterification of Kalamata extra virgin oil (% w/w).....	72
Table 2.3. Repeated results for Kalamata extra virgin olive oil using the tetrahydrofuran transesterification method (percentage area).....	73
Table 2.4 Coefficient of Variation for the tetrahydrofuran method of transesterification of Kalamata extra virgin olive oil.....	74
Table 2.5 GC FAME analysis of transesterified adulterated samples of Kalamata extra virgin oil (area percentage).....	75
Table 2.6 FAME analysis of Greek oils by GC (area percentage report).....	76
Table 2.7 Greek results of FAME analysis by GC (area percentage report).....	77
Table 2.8 Paired Student's t - test on the GC analysis of the oil samples (D1 - D22).....	78
Table 2.9 GC parameters for the triglyceride analysis of oils by total carbon number (TCN).....	80
Table 2.10 GC parameters for the triglyceride analysis of oils by TCN using BPX5 column (25 mm x 0.32 ID), precolumn BPX5 (25 mm x 0.53 ID).....	81
Table 2.11 GC parameters for the triglyceride analysis of oils by degree of unsaturation.....	81
Table 2.12 Design matrix (uncoded) for GC analysis of triglyceride mixtures (mg dm <sup>-3</sup> ).....	83
Table 2.13 Design matrix (coded) for GC analysis of triglyceride mixtures.....	84

Table 2.14 GC analysis of triglycerides mixtures by TCN (ISTD response area ) .....	86
Table 3.1 SFC parameters using UV detection/light scattering detection .....	94
Table 3.2 Comparison of resolution, selectivity and column efficiency on oils separated both with 2 columns and with 3 columns connected in series .....	100
Table 3.3 Results of SFC analysis of the Greek oils using UV Detector ( % area).....	101
Table 3.4 Reproducibility study on retention times (min) of samples analyzed by SFC using UV detection.....	102
Table 3.5 SFC analysis of the Greek oils using the light scattering detector .....	104
Table 3.6 SFC analysis of the Greek oils (adulterated with 10 % sunflower oil) using the light scattering detector .....	105
Table 3.7 Repeatability test on samples analyzed by SFC using light scattering detection	106
Table 3.8 Reproducibility test on retention times of samples analyzed by SFC using light scattering detection .....	107
Table 3.9 SFE parameters for the supercritical fluid extraction of oil from sunflower seeds and sesame seeds by the Hewlett Packard extractor .....	109
Table 3.10 The parameters for the derivatization of olive oil triglycerides to FAME using lipase as the catalyst in a Hewlett Packard SFE extraction cell .....	112
Table 4.1 Raman Parameters for olive oil analysis .....	118
Table 4.2 Raman spectral region from which data was extracted from for statistical analysis	



.....	119
Table 4.3 Complete training sets consisting of authentic Greek oils and their adulterated mixture sets.....	120
Table 4.4 Complete test set for the validation of the authentic set and its adulterated mixture sets.....	121
Table 4.5 Percentage variance accounted for in the first 2 PCs in the model formed using leverage validation.....	121
Table 4.6 Classification of the test set with the class models for the authentic oils and their adulterated mixtures on the whole data region using leverage validation .....	122
Table 4.7 Complete Training sets for the authentic oil sets and their adulterated mixture sets using FCV.....	123
Table 4.8 Complete Test set for the validation of the authentic set and its adulterated mixture sets on the whole Raman data set using FCV .....	123
Table 4.9 Percentage variance accounted for in the first 2 PCs in the model formed using FCV validation.....	124
Table 4.10 Classification of the test set with the class models for the authentic oils and their adulterated mixtures on the whole region using FCV validation .....	124
Table 4.11 Composition of the Training sets for the authentic oil sets and their adulterated mixture sets on the whole data using FCV with 3 samples in each test set.....	126
Table 4.12 Composition of the Test set for the validation of the authentic set and its	

adulterated mixture sets on the whole data region using FCV with 3 samples in each test set.....	126
Table 4.13 Percentage variance accounted for in the first 2 PCs in the model formed on the whole region using FCV with 3 samples in the test set .....	127
Table 4.14 Classification of the test set with the class models for the authentic oils and their adulterated mixtures on the whole data set using FCV with 3 samples in the test set. ....	127
Table 4.15 Composition of the Training sets of samples used for the authentic oil sets and their adulterated mixture sets on the Raman fingerprint region.....	129
Table 4.16 Composition of the Test set composition for the validation of the authentic set and its adulterated mixture sets on the Raman fingerprint region.....	129
Table 4.17 Percentage variance accounted for in the first 2 PCs in the model formed on the fingerprint region.....	130
Table 4.18 Classification of the test set with the class models for the authentic oils and their adulterated mixtures on the fingerprint region using full cross validation with 5 samples in the test set .....	133
Table 4.19 Composition of the Training sets for the authentic oil sets and their adulterated mixture sets on the Raman fingerprint region.....	137
Table 4.20 Composition of the Test set for the validation of the authentic set and its adulterated mixture sets on the Raman fingerprint region using full cross validation	

with 3 samples in the test set .....	137
Table 4.21 Percentage variance accounted for in the first 2 PCs in the model formed on the fingerprint region.....	138
Table 4.22 Classification of the test set with the class models for the authentic oils and their adulterated mixtures on the Raman fingerprint region .....	138
Table 4.23 Composition of the Training sets for the authentic oil sets and their adulterated mixture sets on the Raman fingerprint region using FCV validation and 8 samples in the test set.....	138
Table 4.24 Composition of the Test set for the validation of the authentic set and its adulterated mixture sets using FCV validation and 8 samples in the test set.....	139
Table 4.25 Percentage variance accounted for in the first 2 PCs in the model formed on the fingerprint region of the authentic oils and their adulterated mixture sets.....	139
Table 4.26 Classification of the test set with the class models for the authentic oils and their adulterated mixtures on the on the fingerprint region .....	139
Table 4.27 Composition of the Training sets for the authentic Peloponese oil sets and their adulterated mixture sets on the whole data region.....	140
Table 4.28 Composition of the Test set for the validation of the authentic Peloponese set and its adulterated mixture sets on the whole data region.....	141
Table 4.29. Percentage variance accounted for in the first 2 PCs in the model formed on the whole region of Peloponese oil and its adulterated mixture sets .....	141

Table 4.30 Classification of the test set with the class models for the authentic Peloponese oils and their adulterated mixtures on the whole region.....	141
Table 4.31 Composition of the Training sets for the authentic Peloponese oil sets and their adulterated mixture sets on the fingerprint region.....	142
Table 4.32 Composition of the Test set for the validation of the authentic Peloponese set and its adulterated mixture sets on the fingerprint region.....	142
Table 4.33 Percentage variance accounted for in the first 2 PCs in the model formed on the fingerprint region of Peloponese oil and its adulterated mixture sets.....	143
Table 4.34 Classification of the test set with the class models for the authentic Peloponese oils and their adulterated mixtures on the fingerprint region .....	143
Table 4.35 Composition of the Training sets for the authentic Crete oil sets and their adulterated mixture sets on the on the fingerprint region using FCV with 1 sample in the test set.....	144
Table 4.36 Composition of the Test set for the validation of the authentic Crete set and its adulterated mixture sets on the fingerprint region using FCV with 1 sample in the test set.....	144
Table 4.37 Percentage variance accounted for in the first 2 PCs in the model formed on the fingerprint region of Crete oil and its adulterated mixture sets using full cross validation with 1 samples in the test set.....	144
Table 4.38 Composition of the Test set for the authentic Crete oils, Peloponese oils and the	

Crete adulterated mixtures on the fingerprint region using FCV with 1 sample in the test set.....	145
Table 4.39 Infrared experimental parameters .....	147
Table 4.40 Composition of the Training set used in the development of the Greek10 % discriminant model .....	149
Table 4.41 Composition of Test set used in the validation of the Greek/10 % discriminant model.....	150
Table 4.42 Percentage variance account for in the development of the Greek/10 % discriminant model .....	151
Table 4.43 Validation of results for the test for Greek/10 % Test Discriminant model...	152
Table 4.44 Composition of the Training set used in the development of the AllGreek model .....	153
Table 4.45 Composition of the AllGreek Test set .....	154
Table 4.46 Prediction of Allgreek Test using AllGreek discriminant model .....	155
Table 4.47 The selected IR absorptions used in discriminant analysis.....	156
Table 4.48 Composition of the Training set used in the development of the Allsel model....	158

Table 4.49 Composition of the Allsel test set.....	158
Table 4.50 Percentage variance account for in the development of Allsel.....	159
Table 4.51 Prediction of Allsel test using Allsel discriminant model .....	160
Table 4.52 Comparison of Training set used in the development of sel/10 % PC model	162
Table 4.53 Comparison of Test set used in the validation of the Sel/10 % Test .....	162
Table 4.54 Classification of Sel/10 % Test.....	163
Table 4.55 Composition of training sets used in SIMCA analysis of the infrared data ..	164
Table 4.56 Test set used in statistical analysis of the infrared data .....	165
Table 5.1 <sup>13</sup> C NMR experimental parameters.....	168
Table 5.2 <sup>1</sup> H NMR experimental parameters.....	169
Table 5.3 Peak height intensities for specific carbon signals in each region of the spectrum .....	174
Table 5.4 Composition of the training sets for the authentic oil sets and their adulterated mixture sets on the whole <sup>13</sup> C NMR data region.....	176
Table 5.5 Composition of the test set for the validation of the authentic set and its adulterated mixture sets on the whole <sup>13</sup> C NMR data region.....	176
Table 5.6 PCA variance analysis in the development of discriminant analysis on the whole <sup>13</sup> C NMR data training set.....	178

Table 5.7 Composition of training sets for the authentic oil sets and their adulterated mixture sets on the $^{13}\text{C}$ NMR alkene region.....	180
Table 5.8 Composition of Test set for the validation of the authentic set and its adulterated mixture sets on the $^{13}\text{C}$ NMR alkene data region.....	181
Table 5.9 $^1\text{H}$ NMR spectral assignments of the triglyceride components for olive oils (from Shiao & Shiao, 1989). .....	183
Table 5.10 Composition of training sets for the authentic oil sets and their adulterated mixture sets from proton NMR.....	184
Table 5.11 Composition of test set for the validation of the authentic set and its adulterated mixture sets from the proton data region .....	184
Table 5.12 Composition of the training sets for the authentic oil sets and their adulterated mixture sets on the whole $^{13}\text{C}$ NMR data .....	188
Table 5.13 Composition of the test set for the validation of the authentic set and its adulterated mixture sets.....	188
Table 5.14 Percentage variance accounted for in the first 4 PCs in the model formed on the whole $^{13}\text{C}$ NMR region.....	189
Table 5.15 Classification of the test set with the class models for the authentic oils and their adulterated mixtures from the whole $^{13}\text{C}$ NMR data.....	189
Table 5.16 Composition of the training sets for the authentic oil sets and their adulterated mixture sets on the alkene region of $^{13}\text{C}$ NMR data.....	191

Table 5.17 Composition of the test set for the validation of the authentic set and its adulterated mixture sets for the alkene region of the $^{13}\text{C}$ NMR data .....	192
Table 5.18 Percentage variance accounted for in the first 4 PCs in the model formed on the alkene $^{13}\text{C}$ NMR region .....	192
Table 5.19 Classification of the test set with the class models for the authentic oils and their adulterated mixtures on the $^{13}\text{C}$ NMR alkene region.....	192
Table 5.20 Training sets for the authentic oil sets and their adulterated mixture sets on the $^1\text{H}$ NMR data .....	195
Table 5.21 Test set for the authentic oil set and its adulterated mixture sets for $^1\text{H}$ NMR data.....	195
Table 5.22 Percentage variance accounted for in the first 4 PCs in the model formed on the $^1\text{H}$ NMR region.....	196
Table 5.23 Classification of the test set with the class models for the authentic oils and their adulterated mixtures on the $^1\text{H}$ NMR region .....	196



## LIST OF FIGURES

Figure 1.1 Olive oil extraction (Fedeli, 1977) .....	4
Figure 1.2 Lipid glycerides; a: glycerol; b: monoglyceride; c: diglyceride; d: triglyceride (Christie, 1982) .....	7
Figure 1.3 Sterol esters of lipids; a: free cholesterol; b: $\beta$ -sitosterol and c: stigmasterol (Formo et al., 1979) .....	10
Figure 1.4 Typical structural arrangement of phosphatidic acid (Christie, 1982) .....	11
Figure 1.5 Phospholipids; a: phosphatidylglycerol; b: cardiolipin (Christie, 1982) .....	11
Figure 1.6 Phosphatidylethanolamine (Christie, 1982) .....	11
Figure 1.7 Sphingolipids; a: phytosphingosine; b: sphingosine (Christie, 1982) .....	12
Figure 1.8 Structure of a triglyceride (Christie, 1982).....	13
Figure 1.9 General transesterification method of a triglycerides to a fatty acid methyl ester (Ke-shun, 1994) .....	23
Figure 1.10 Pressure/temperature phase diagram of a substance ( Lee and Markides, 1990) .....	28
Figure 1.11 Schematic diagram of SFC instrumentation (Bartle and Clifford, 1994).....	29
Figure 2.1 General transesterification method (Ke-Shun, 1994) .....	60
Figure 2.2 a: acid hydrolysis; b: alkaline hydrolysis; c: saponification hydrolysis (Ke-Shun,	

1994) .....	60
Figure 2.3 The preparation of 0.5 M sodium methoxide (Ke-Shun, 1994) .....	62
Figure 2.4 FAME chromatogram of a Kalamata extra virgin olive oil .....	70
Figure 2.5 GC analysis of an olive oil by TCN using the hot evaporative injection technique.....	87
Figure 2.6 GC analysis of an olive oil by TCN using the cool on - column injection technique.....	87
Figure 2.7 GC chromatogram of olive oil by TCN separation using the Perkin Elmer auto sampler.....	88
Figure 3.1 The formation of charge - transfer complexes between silver and alkenes (from Demirbuker and Blomberg, 1990).....	91
Figure 3.2 Schematic diagram of a light scattering detector .....	93
Figure 3.3 SFC chromatogram of extra virgin olive oil .....	95
Figure 3.4 SFC chromatogram of sunflower oil using 2 columns in series.....	96
Figure 3.5 SFC chromatogram of sunflower oil using 3 columns in series.....	96
Figure 3.6 SFC chromatograph of a mixture of olive oil and sunflower oil.....	97
Figure 3.7 SFC chromatograph of sesame seed oil .....	97
Figure 3.8 SFC chromatogram of walnut oil.....	98

Figure 3.9 SFC chromatogram of soya bean oil .....	98
.....	
Figure 3.10 SFC chromatogram for Tesco vegetable oil .....	99
Figure 3.11 SFC chromatogram of extra virgin oil using light scattering detection .....	103
Figure 3.12 Off - line supercritical fluid chromatogram of sunflower extract .....	113
Figure 3.13 On - line supercritical fluid chromatogram of sunflower extract .....	113
Figure 3.14 SFC chromatogram of FAME standard .....	114
Figure 3.15 SFC chromatogram of the lipase transesterification of olive oil .....	115
Figure 4.1 Raman spectral region of the extra virgin olive oil D1 and its adulterated sunflower mixtures of 2 % w/w, 5 % w/w and 10 % w/w respectively .....	119
Figure 4.2 Fingerprint region of D1 and its sunflower adulterated mixtures .....	128
Figure 4.3 Residual variance plot of the authentic olive oils .....	130
Figure 4.4 Residual variance plot of the authentic olive oils .....	131
Figure 4.5 Score plot of PC1 versus PC2 for the authentic olive oils training set .....	132
Figure 4.6 Loadings plot of the authentic olive oils training set .....	132
Figure 4.7 Plot of the model distance between the authentic oil class model and the class model of oils adulterated with 2 % w/w sunflower .....	134
Figure 4.8. Coomans plot of the Finorg class versus Fin/2 % .....	134

Figure 4.9. Coomans plot of the Finorg class versus Fin/5 %.....	135
Figure 4.10 Coomans plot of the Finorg class versus Fin/10 %.....	135
Figure 4.11 Mid - infrared absorbance spectra of an extra virgin oil and its adulterated sunflower mixtures (2 % w/w, 5 % w/w, 10 % w/w respectively) .....	148
Figure 4.12 Canonical variate plot of the Greek10 % .....	152
Figure 4.13 Canonical variate plot of the Allgreek.....	156
Figure 4.14 Canonical variate plot of the Allsel Test set .....	161
Figure 4.15 Canonical variate of Sel/10%.....	163
Figure 5.1 Full spectrum of D12 extra virgin olive oil.....	169
Figure 5.2 Full spectrum of D12 extra virgin olive oil adulterated with 10 % sunflower oil .....	170
Figure 5.3 NMR alkene region of sample D12.....	171
Figure 5.4 NMR alkene region of sample D12 adulterated with 10 % sunflower oil .....	171
Figure 5.5 Full proton spectrum of sample D8.....	173
Figure 5.6 Full spectrum proton of sample D8 adulterated with 10 % w/w sunflower oil .... .....	173
Figure 5.7 Canonical variate analysis of NMR data set .....	179
Figure 5.8 Canonical variate analysis of Alkene data set .....	182

Figure 5.9 Loadings plot for whole <sup>13</sup>C NMR data set based on the first 2 PCs..... 186

Figure 5.10 Scores plot for whole <sup>13</sup>C NMR data set based on the first 2 PCs..... 186

Figure 5.11 Loadings plot for the alkene model developed using <sup>13</sup>C NMR data from the  
alkene region..... 190

Figure 5.12 Scores plot for the for the alkene model developed using <sup>13</sup>C NMR data from  
the alkene region..... 190

Figure 5.13 Cooman’s plot of Caralkorg and Caralk10..... 193

Figure 5.14 Loadings plot for the proton NMR data using the first 2 PCs..... 194

Figure 5.15 Scores plot for the proton NMR data using the first 2 PCs..... 194

Figure 5.16 Cooman’s plot of the authentic oils and their adulterated mixtures using the  
proton NMR data..... 197

## **ACKNOWLEDGEMENTS**

I would like to thank the following people for their help and guidance during the preparation of this thesis.

My supervisors: Dr. Peter M<sup>c</sup> Intyre; Dr. Edward Morgan and Dr. Anthony Berry, whose continued support and guidance has been of enormous help.

Dr. T. Davies for obtaining analytical Raman spectra and Dr. R. Wilson for supplying the Win - Discrim statistical package.

I would also like to thank the technical staff at the University of Glamorgan for their help and assistance in the laboratory.

On a personal note, I would like to thank my parents, family and friends for their enormous encouragement at all times and especially throughout the last year.

Fatty acids commonly found in olive oil.

Myristic acid (14:0):	$\text{CH}_3(\text{CH}_2)_{12}\text{CO}_2\text{H}$
Palmitic acid (16:0)	$\text{CH}_3(\text{CH}_2)_{14}\text{CO}_2\text{H}$
Palmitoleic acid: (16:1)	$\text{CH}_3(\text{CH}_2)_4\text{CH}=\text{CH}(\text{CH}_2)_8\text{CO}_2\text{H}$
Heptadecanoic acid (17:0):	$\text{CH}_3(\text{CH}_2)_{15}\text{CO}_2\text{H}$
Stearic acid (18:0):	$\text{CH}_3(\text{CH}_2)_{16}\text{CO}_2\text{H}$
Oleic acid (18:1):	$\text{CH}_3(\text{CH}_2)_4\text{CH}=\text{CH}(\text{CH}_2)_{10}\text{CO}_2\text{H}$
Linoleic acid (18:2):	$\text{CH}_3(\text{CH}_2)_4\text{CH}=\text{CHCH}_2\text{CH}=\text{CH}(\text{CH}_2)_7\text{CO}_2\text{H}$
Linolenic acid (18:3):	$\text{CH}_3(\text{CH}_2)_4\text{CH}=\text{CHCH}_2\text{CH}=\text{CHCH}_2\text{CH}=\text{CH}(\text{CH}_2)_4\text{CO}_2\text{H}$
Arachidic acid: (20:0)	$\text{CH}_3(\text{CH}_2)_{18}\text{CO}_2\text{H}$
Eicosenoic acid: (20:1)	$\text{CH}_3(\text{CH}_2)_4\text{CH}=\text{CH}(\text{CH}_2)_{12}\text{CO}_2\text{H}$
Eicosatridienoic acid: (20:2)	$\text{CH}_3(\text{CH}_2)_4\text{CH}=\text{CHCH}_2\text{CH}=\text{CH}(\text{CH}_2)_9\text{CO}_2\text{H}$
Behenic acid (22:0)	$\text{CH}_3(\text{CH}_2)_{20}\text{CO}_2\text{H}$

## ABBREVIATIONS

ATR: attenuated total reflectance cell

CSFC-FID: capillary SFC combined with flame ionisation detection

EU: European Union

FID detector: flame ionisation detector

G<sub>NU</sub>: triglyceride group number

LDL: low density lipoprotein

Low Density Lipoprotein, LDL

NOE: nuclear overhauser effect

Nuclesial SA: sulfonic acid stationary phase

OCL: cool on - column injection

PLS: partial least squared

PUFA: polyunsaturated fatty acids

SIMCA: soft independent modelling of class analogy

T<sub>1</sub>: NMR relaxation time

TC: total cholesterol

tp: pulse width (length or duration) used in NMR

WHO: World Health Organisation



# CHAPTER 1

## INTRODUCTION

### *1.1 Olive oil and why it is adulterated*

Throughout the last decade the nutritional aspects and physiological effects of different fats have become important issues. According to the Food and Agriculture Organization of the United Nations, the main nutritional problem of the developing countries is a deficiency in dietary energy, whereas that of developed countries is the over - consumption of fat (FAO, 1980). Essential fatty acids are not produced in the body and are required regularly for the normal growth and functions of all tissues (Lichtenwalter, 1981). However, over - consumption of certain fats leads to serious health implications and inimical effects on atherosclerosis and obesity (FAO, 1980).

Revision of current views about the safety and quality of dietary fats has led to interest in the healthy nature of the Mediterranean diet and has focused attention on the nutritional aspect of olive oil. The quality of olive oil is variable being mainly associated with the geographical area of production, year of production, climatic factors and even the cultivar and maturity of the olive. The quality of the oil is also influenced by the extraction process itself, from the highest quality “Extra virgin oil”, obtained by low temperature and pressure extraction to the lowest quality grade solvent-extracted pomace oil. The high premium attached to olive oil as a “health product” and its high quality categories has led to an increase in the marketing of olive oil as a consumer product and inevitably adulteration with lower - grade cheaper olive oils and oils from other species.

This project, a study of the chemical methods for monitoring the adulteration of olive oil is partially financed by the European Union, EU, as a direct result of its responsibility for the quality of oils.

*“Olive oil is obtained from the fruits of the evergreen olive tree *Olea europaea*. The whole fruit may contain 35 - 70 % of oil (dry weight), and the dry pulp contains more than 75 %. The oil usually has a greenish - yellow colour and a characteristic flavour and odour”* (Formo et al., 1979).

According to Mangold (1991), the Assyrians of Northern Mesopotamia were the first to grow and press olives for their oil five thousand years ago. Two thousand years later, the Phoenicians initiated the cultivation of the olive crop throughout Asia minor, the Aegean Islands of Greece and Carthage in North Africa. The growth of the olive tree extended to the Mediterranean coastal areas with the rise of the Greek and then the Roman civilization.

Today, the annual olive oil production throughout the world is 1,550,000 metric tons (Suarez and Mendoza, 1986). The leading producers are Spain 42 %, Italy 24 % and Greece 12 %. Other minor producers are in the Orient, N. Africa, South America and the USA (Fedeli, 1977).

The olive tree is raised from cuttings and thrives in the Mediterranean climate of hot summers and wet winters. The tree starts to flower after two years. However, the commercial production of olives does not start until the tree is in its eighth or ninth year. The olive fruits ripen in the summer months and begin to fall in autumn (De Bussy, 1970).

*“A low content of free fatty acid expressed as oleic acid is an indicator of a good quality olive oil”* (Pallotta, 1995). Extra virgin oil has the highest quality rating of less than 1 %

acidity, *“it possesses properties and characteristics that meet both the explicit flavour, processing, marketing, implicit nutritional and health requisites for such a product”* (Galoppini and Fiorentini, 1991; Tomassi, 1991).. Oils with a free fatty acid content of less than or equal to 3.3 % may be classified as virgin oil. Higher concentrations of free fatty acids in oils result in lampante oils which must be chemically treated before they may be used as table oils (Pallotta, 1995).

The time of gathering of the olives is critical to the characteristics of the oil produced. The fruit is collected when they contain the highest quality of oil in the best condition (Suarez and Mendoza, 1986). This stage of ripeness of the olives is determined analytically. The fruit should be hand - picked in order to contain the best quality of oil from the fruit. *“Bruising of the fruit which is caused by falling, sets free enzymes, which start hydrolysis of the oils with consequent formation of free fatty acids in the oil while the fruit is waiting to be processed”* (De Bussy, 1970).

Ideally, the oil should be obtained from the olives at the same time as the gathering takes place. However, this is not always possible and certain conservation measurements must be taken to ensure that the characteristics of the oil do not change during storage (Suarez and Mendoza, 1986). The main conservation problems are linked to the physical, chemical and biological changes that the oil suffers due to its components and extraneous material. These changes have been reviewed in detail by Suarez and Mendoza (1986).

The traditional extraction process that is followed has been outlined by Fedeli (1977) as shown in Figure 1.1.

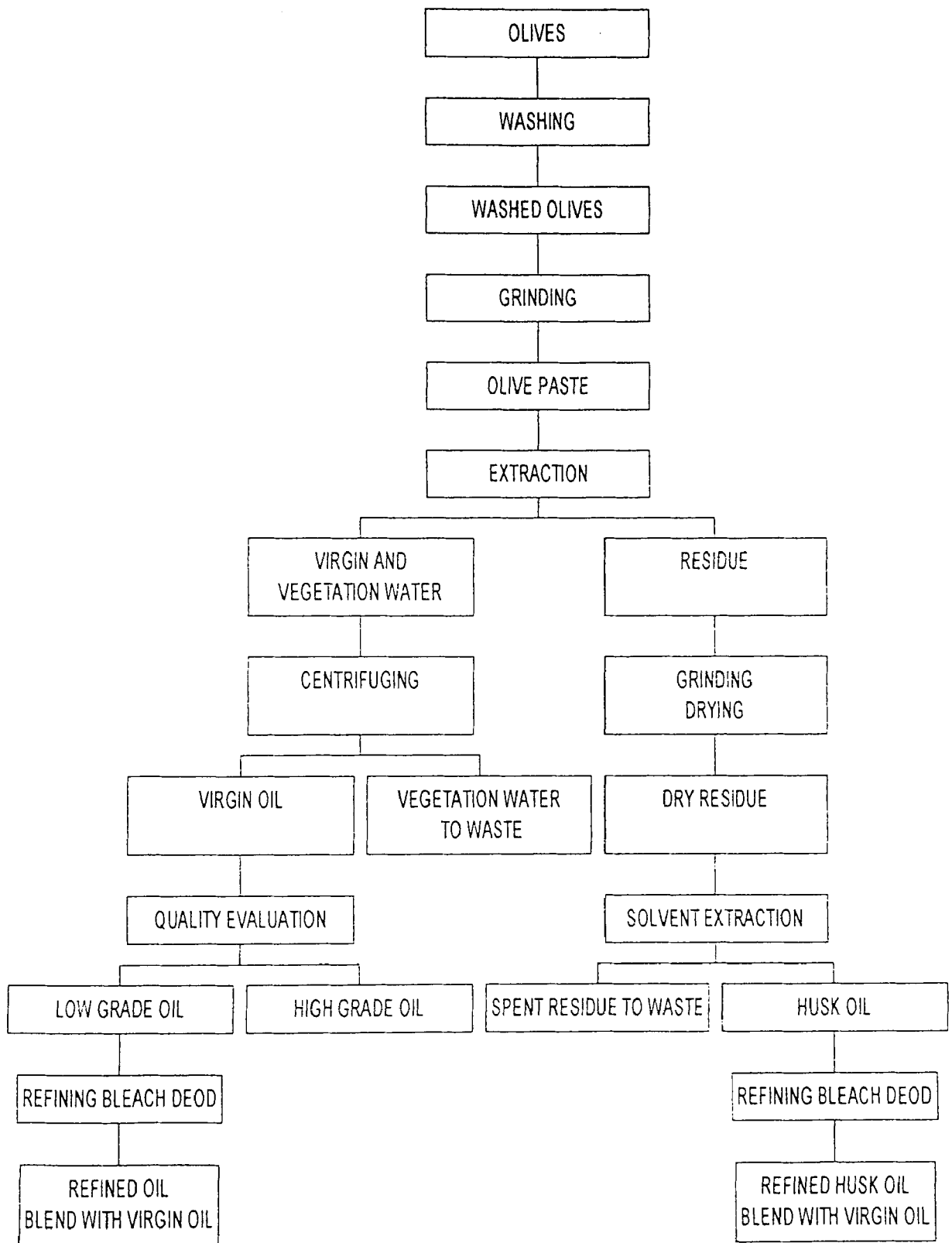


Figure 1.1 Olive oil extraction (Fedeli,1977)

The various steps during the extraction of the oil from the olive also influence the quality of oil produced. Excessive heating during the milling stage may lead to an overall increase in oil temperature by 25 °C, resulting in the loss of volatile constituents that contribute to the special odour of high quality oils (Suarez and Mendoza, 1986). Care should also be taken during the separation of the virgin oil from its vegetable water to reduce the time the oil is in contact with impurities. These impurities may influence the organoleptic qualities of the oil (Suarez and Mendoza, 1986).

The olive oil extracted from the milling process does not always contain the best quality of olive oil. Therefore, these oils must be refined in order to improve their quality and palatability. The refining process is usually a sequence of procedure; centrifuging, alkali refining, decolouration with bleaching clays, steam deodorization and winterization (Suarez and Mendoza, 1986).

The economic value of an oil is therefore associated with its quality. The profitability of olive oil depends on how much extra virgin oil can be produced from pressing as refining increases cost and lowers quality by raising the acidity and creates losses of 1.1 - 2.5 % depending on the quality of the oil and the variety of the tree (Fedeli, 1977). Thus, the economic incentive to adulterate oils is great since the high demand on extra virgin oil is matched by a scarcity of its supply.

## ***1.2 Nutritional aspects and functions of fats and oils***

Fats and oils provide essential fatty acids, a constant source of energy and serve as carriers for fat - soluble vitamins and antioxidants. They also provide a feeling of satiety and add flavour and texture to food products (Hasenhuettl, 1995). However, overconsumption of fatty foods has been associated with human disease conditions including an effect on

cardiovascular disease and atherosclerosis (De Bussy, 1970). Saturated fats have been associated with increases in Total Cholesterol, TC and Low Density Lipoprotein, LDL, (Hasenhuettl, 1993). Society's awareness of these facts has led to the replacement of saturated fats in the diet with fats that are high in unsaturates (DHSS, 1984). These unsaturates are found in oleic and linoleic oils such as olive oil (Hasenhuettl, 1993).

The nutritional benefits of olive have been reported by Pallotta (1995) as including: *“physical development in children; a delay in the onset in ageing; the prevention of cardiovascular disease, malignant neoplasia and various liver, bile - duct and gastroduodenal disorders and the functionality of some cellular membranes”*.

### ***1.3 Natural lipids in plants and animals***

Fats and oils are substances of plant and animal origin. Along with proteins and carbohydrates, they provide essential nutrients to the body. Proteins and carbohydrates may be converted to fat in the body but they fail to provide certain fatty acids such as linoleic acid which must be supplied in the diet (Lichtenwalter, 1981). Lipids may be classified into simple and complex compounds (Christie, 1982). Simple lipids are lipids which contain fatty acids and alcohol only. The alcohol is usually glycerol but may in some cases be a long chain alcohol or a sterol (Christie, 1982). Complex lipids are often polar compounds, some of which may be insoluble in fat solvents such as ether, chloroform or benzene and soluble in water. Simple lipids form part of an energy store, while complex polar lipids are important in the structure of cell membranes (Hammond, 1993). The following subsections describe the different types of chemical compounds commonly found in olive oil. These substances may enter the oil during pressing or during the solvent extraction of oil from the oil cake.

extraction of oil from the oil cake.

### 1.3.1 Simple lipids

#### 1.3.1.1 Glycerides

The main component of lipids are glycerides. These are esters of glycerol (Figure 1.2 a), a trihydric alcohol (Christie, 1982). They may be monoglycerides (Figure 1.2 b), diglycerides (Figure 1.2 c), or triglycerides (Figure 1.2 d). Note that two monoester isomers and three diester isomers exist although only one of these possibilities is given below. The acid is variable (commonly R contains between 13 and 21 carbons), and naturally occurring oils contain a mixture of chain lengths and degree of unsaturation of the acid. The fatty acid chains constitute 95 % of the triglyceride and largely determine the physical and chemical properties of the oil in question (Lichtenwalter, 1981).

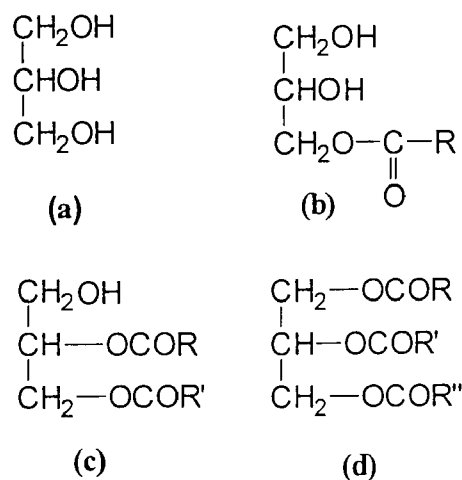


**Figure 1.2 Lipid glycerides; a: glycerol; b: monoglyceride; c: diglyceride; d: triglyceride (Christie, 1982)**

In lipids of non - ruminant origin the configuration of the double bond in the fatty acid is *cis*, even when more than one double bond is present. *Trans* isomers may be present in vegetable oils, but this is because of autoxidation, often associated with age (DHSS, 1984). *Trans* isomers also occur in hydrogenated fats, i.e. margarine and spreads where they

major controversy in the medical world over the importance of these geometrical isomers in the human diet in relation to heart disease. This may emphasize even more the importance of the “Mediterranean diet” phenomenon when one considers olive oil and the low consumption of hardened fats in this diet (DHSS, 1984).

The relative proportion of each acid, determined by gas chromatography after hydrolysis and esterification to the methyl esters has been widely used as a method of determining the source of the lipid mixture (Traitler, 1987). However, this profile is by no means constant and varies depending on sub - species, climate, soil etc. for vegetable oils, and that of the animal species (and its diet) in lipids of animal origin (Formo et al., 1979). A typical fatty acid profile is given for some animal and vegetable fats in Table 1.1.



**Table 1.1. Fatty acid profiles (% composition) for animal and vegetable lipids (Formo et al., 1979)**

Fatty acid*	Butter	Corn	Olive	Soya	Sunflower	Sesame
4:0	2.8 - 4.0	-	-	-	-	-
6:0	1.4 - 3.0	-	-	-	-	-
8:0	0.5 - 1.7	-	-	-	-	-
10:0	1.7 - 3.2	-	-	-	-	-
12:0	2.2 - 4.5	-	-	-	-	-
14:0	5.4 - 14.6	Tr* - 1.7	-	Tr* - 0.5	<0.5	<0.5
16:0	26 - 41	8 - 12	7.5 - 18	7 - 11	3 - 10	7.0 - 12
16:1	6.1 - 11.2	<0.5	0.5 - 3.0	2 - 6	<1	<0.5
18:0	1.2 - 2.4	Tr* - 0.2	0.5 - 3.0	0.3 - 3	1 - 10	3.5 - 6.0
18:1	18.7 - 33.4	19 - 49	63.0 - 83.0	15 - 33	14 - 65	35 - 50
18:2	0.9 - 3.7	34 - 62	3.5 - 20	43 - 56	20 - 75	35 - 50
18:3	1.2		0.1 - 0.6	5 - 11	<0.7	<1.0
20:0 - 22:0	0.8 - 3.0	Tr* - 0.2	0.1 - 0.8	0.3 - 3	0.5 - 1.0	0.5 - 1.0

\* Number of carbon atoms : number of double bonds; Tr: trace amounts of fatty acids present

### *1.3.1.2 Sterol esters*

Sterols are tetracyclic compounds derived from terpenes (Hasenhuettl, 1993). The main sterol esters present in plants, are from free cholesterol (Figure 1.3 a),  $\beta$ -sitosterol (Figure 1.3 b) stigmasterol (Figure 1.3 c) and campesterol (Christie, 1982). The functions of these sterols in plant metabolism has not yet been defined. However, the amounts of sterols and sterol esters present in vegetable oils have been used for authentication purposes (Eisner, 1963).

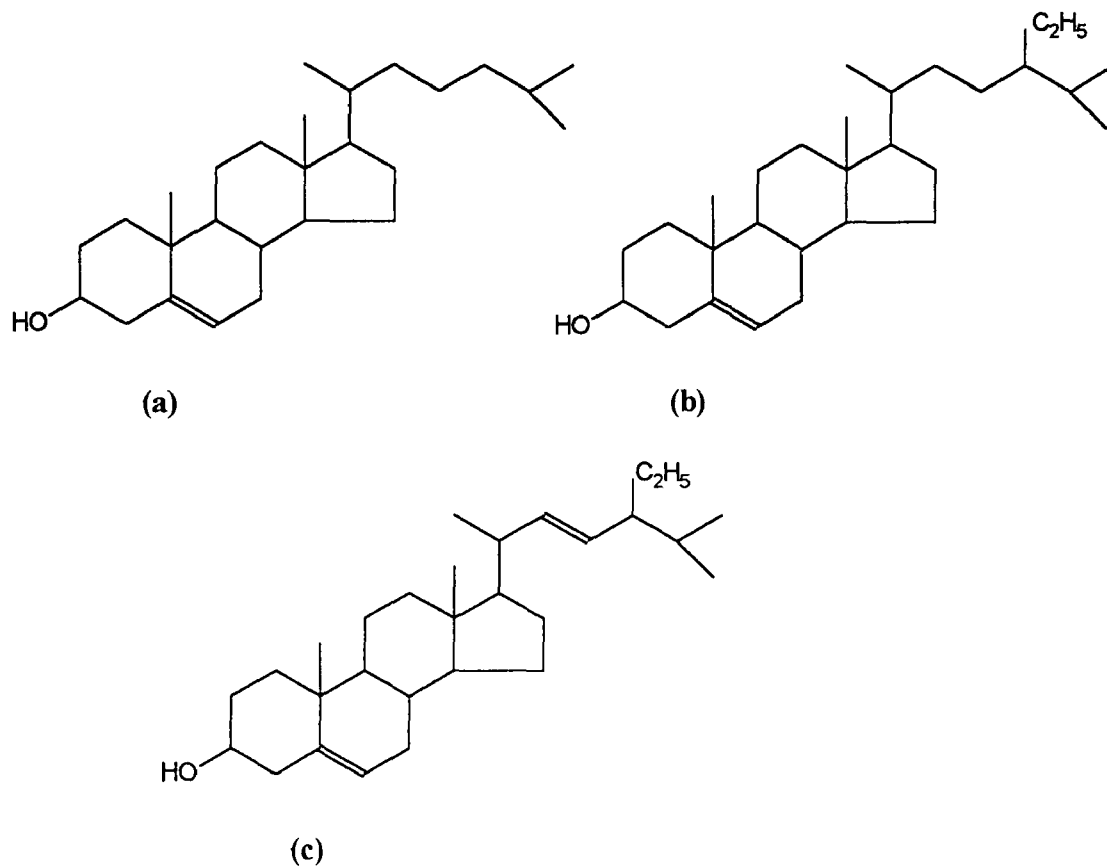


**Figure 1.3 Sterol esters of lipids; a: free cholesterol; b:  $\beta$ -sitosterol and c: stigmasterol (Formo et al., 1979)**

### 1.3.2 Complex lipids

#### 1.3.2.1 Phospholipids

As well as a phosphate group phospholipids can contain glycerol, fatty acids and nitrogenous bases (Christie 1982). The simplest members of the group are phosphatidic acids (Figure 1.4), which contain glycerol, two of the OH groups being esterified with long chain fatty acids as in triglycerides, while the third is esterified with phosphoric acid (Formo et al., 1979).

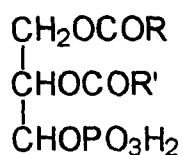


**Figure 1.4 Typical structural arrangement of phosphatidic acid (Christie, 1982)**

More complex members of the group contain two or three glycerol molecules, as in phosphatidylglycerol (Figure 1.5 a) and cardiolipin (Figure 1.5 b). These are acidic lipids and on hydrolysis yield glycerol, fatty acids and phosphoric acid in various molar proportions (Christie, 1982). The most common phospholipids found in vegetable and plant tissue is phosphatidylcholine (Lecithin). It is usually extracted from soya bean oil in commercial quantities (Lichtenwalter, 1981).

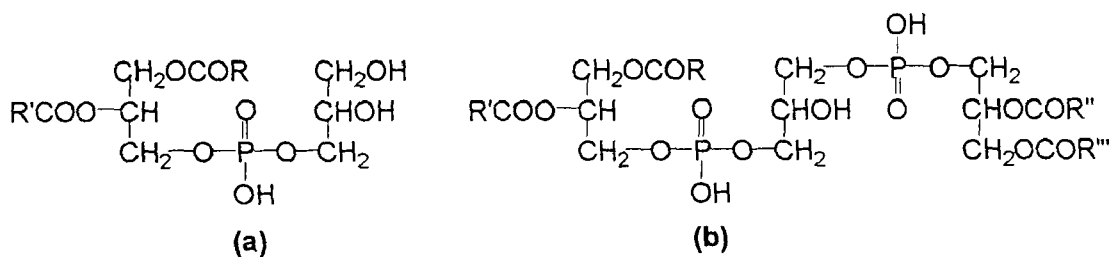


**Figure 1.5 Phospholipids; a: phosphatidylglycerol; b: cardiolipin (Christie, 1982)**

Other common phospholipids contain (choline, ethanolamine or serine) esterified to a phosphate group e.g. phosphatidylethanolamine (Figure 1.6).

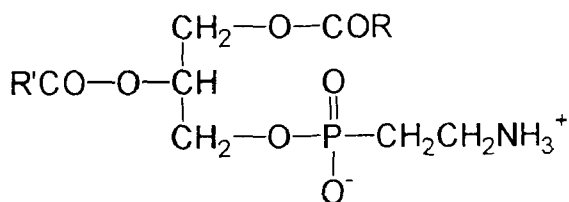


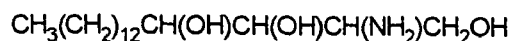
**Figure 1.6 Phosphatidylethanolamine (Christie, 1982)**

### 1.3.2.2 Glycolipids

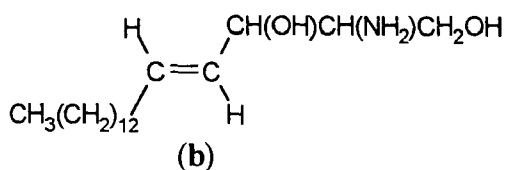
Plant glycolipids are lipids which contain carbohydrate residues (Christie, 1982). They play an important role in photosynthesis.

### 1.3.2.3 Sphingolipids

Sphingolipids are lipids that contain the amino alcohol sphingosine and its derivatives (Christie, 1982). Sphingolipids occur both in animal and plant lipids, but differ in that the commonest base in plants is phytosphingosine (Figure 1.7a), but sphingosine (Figure 1.7 b) in animal fat.



(a)



(b)

**Figure 1.7 Sphingolipids; a: phytosphingosine; b: sphingosine (Christie, 1982)**

Phytoglycolipids are other complex lipids found in a variety of plant seeds which consist of ceramides. Ceramides are amines of fatty acids with long chain di - and hydroxy - bases, they contain 12 - 22 carbon atoms in the aliphatic chain (Christie, 1982).

### 1.3.3 Other minor components

#### 1.3.3.1 Vitamins and antioxidants

Tocopherols and phenolic materials function as antioxidants in edible oils with the former being vitamin E active (Hassenhuettl, 1993). The concentration of tocopherol in edible oil differs for each variety. Its concentration ranges from 0.05 - 0.2 % and its presence accounts for the greater oxidative stability of oils as compared to animal fats which contain little or no antioxidants (Hassenhuettl, 1993).

#### 1.3.3.2 Pigments

The main pigment found in vegetable oils are carotenoids. These contain conjugated double bonds and a strong chromophore which produces red and yellow colouration in vegetable

oils (Hassenhuettl, 1993). Some chlorophylls; chlorophyll a and chlorophyll b compounds are also found in olive oil and oils extracted from immature or damaged oils. These chlorophylls can easily degrade to form pheophytins if exposed to sunlight and hence affect the storage life of oils (Fedeli, 1977).

#### ***1.4 The composition of olive oil and its potential adulterants***

Olive oil is distinctive among vegetable oils for its low content of linoleic acid (Formo et al., 1979). This chemical peculiarity and the fact that olive oil retains its natural antioxidants (tocopherol and polyphenols) makes it more stable to oxidation than most liquid oils (Hassenhuettl, 1993). *“Like most vegetable oils, olive oil tends to be more unsaturated as the climate becomes colder (i.e. grown at altitude or in a more northern location) and the unsaturation of the oil also increases with advancing maturity of the fruit”* (Formo et al., 1979).

The major component of olive oil is oleic acid, its percentage composition ranges from 65 - 85 % in the majority of oils studied in the literature. This depends on geographical location and cultivar (Formo et al., 1979). The composition of olive oil is defined in terms of the nature and distribution of the fatty acids in the triglycerides present and also the positions at which these fatty acids are attached to the glycerol backbone as shown in Figure 1.8 (Wollenberg, 1990).

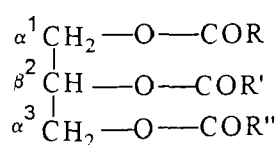


**Figure 1.8 Structure of a triglyceride (Christie, 1982)**

The position of the acyl groups COR, COR' and COR" can be defined as attached to the CH<sub>2</sub> in position 1 or 3 (alpha position) or CH group in position 2 (beta position) (Wollenberg, 1990).

Both the acyl distribution and the acyl positional distribution in the triglycerides mixture can vary greatly between different oil varieties (Wollenberg, 1990). All natural occurring oils are said to adopt the 1,3 and 2 random distribution theory in the positioning of their fatty acids on the glycerol backbone (Pallotta, 1995). In olive oils, the amount of the saturated fatty acids in the 2 - glycerol position is less than 2 % of the total fatty acids (Fedili, 1977). Thus the presence of saturated fats (exceeding the threshold limit of 2 %) in the 2 - glycerol position is indicative of the adulteration of olive oil with esterified oil.

The following tables (Table 1.2, Table 1.3 and Table 1.4) which were reported by Suarez and Mendoza (1986) show the triglycerides and fatty acid profiles of olive oil and also the unsaponifiable components present.

**Table 1.2 Composition of virgin olive oil (Suarez and Mendoza, 1986)**

Component	Typical percentage
Fatty acids:	
Oleic	63.0 - 83.0
Linoleic	3.5 - 20.0
Palmitic	7.5 - 18
Palmitoleic	0.5 - 3.0
Stearic	0.5 - 3.0
Linolenic	0.1 - 0.6
Arachidic	0.1 - 0.8
Behenic	Tr* - 0.8
Unsaponifiable (ethyl ester)	0.6 - 2.0
Unsaponifiable (petroleum ester)	0.3 - 1.4
Total hydrocarbons	0.125 - 0.750
Squalene	0.125 - 0.7
Sterols	0.125 - 0.250
Triterphenethyl alcohol	500 ppm (approx.)
Chlorophyll	0.6 - 2.2
Carotene (as $\beta$ -carotene)	0.6 - 9.5
$\alpha$ -tocopherol	175 ppm - 200 ppm
Polyphenols (as caffeic acid)	50 ppm - 500 ppm

Tr: traces

**Table 1.3 Individual triglycerides found in olive oil ( Suarez and Mendoza, 1986)**

Triglycerides of olive oil	Typical percentage
OOO	40
POO	24
LOO	9
OLO	6
POL	5
POP	4
PLO	4
Others	8

P: palmitic acid; O: oleic acid; L: linoleic acid

**Table 1.4 Composition of the unsaponifiables of olive oil and oil cake (Suarez and Mendoza, 1986)**

Constituents	Olive oil	Oil cake
Saturated hydrocarbons	7	8
Squalane and unsaturated	30	10
Waxes	-	2.4
Esters of sterols	-	1.2
Fatty alcohols	-	15.3
Triterphenethyl alcohol	9	9
Sterols	17	25
Others	36	27

Squalene is the main hydrocarbon found in olive oil, although traces of saturated, branched and aromatic hydrocarbons can also be found (Suarez and Mendoza, 1986). The main carotene present in the oil is  $\beta$  - Carotene. These compounds are dissolved in the oil inside the cells of the olives. Substances such as fatty alcohols, triterphenethyl alcohols (erythrodiol



and uvaol), sterols (free or esterified with fatty acids), waxes and triterphenethyl acids are part of the membranes and of the exterior cuticle (Suarez and Mendoza, 1986).

The standard definition for the physico - chemical, chemical and sensory parameters of olive oil are outlined by the current EC legislation (OJEC, 1991 and 1992). These standards certify the quality and authenticity of each category of olive oil. An oil failing to meet a particular standard is downgraded and reclassified (Pallotta, 1995).

The authenticity of olive oil is determined via instrumental analysis of its composition parameters such as sterol fraction, trilinolein content, fatty acids in position 2 of the triglycerides, etc.. The acid value and peroxide number of oils are the most reliable methods for measuring the quality of olive oil since *“free acidity indicates the percentage of free fatty acids that form in the oil as a result of enzymatic attack on the triglycerides”* (Pallotta, 1985). The value is indicative of the quality of oil, its ripeness, storage life and processing suitability (Pallotta, 1995).

Where an oil exceeds the maximum of 0.9 % for linolenic acid it is indicative that seed oil adulteration of an extra virgin oil has taken place (Pallotta, 1995). The sterol content reveals the botanical origin of the oil. The total sterol content determines the presence of any processed or desterolized oils in the extra virgin variety and the presence of alkenes that have been produced as a result of sterol degradation (Pallotta, 1995). The presence of aliphatic alcohols and the triterpene dialcohols, erythrodiol and uvaol, indicate that extra virgin olive oil has been blended with residue olive oil. Also certain structural changes in olive oils, induced by processing and by autoxidation in fatty acid molecules may be detected by UV spectrophotometry.

A more detailed account of the detection of the above adulterants has been produced by Pallotta (1995). A combination of complementary techniques is used to authenticate olive oils according to EC standards. This approach heightens reliability and reduces analytical error. These standards are continually being updated with advances in analytical methods (Pallotta, 1995).

The following table (Table 1.5) compiled from Italian government specifications on olive oil (1983) and the Codex standards on olive oil (1970) and the International Olive Oil Council (1993) and identifies the parameters that an oil must comply with in order to be classified as an olive oil (the Italian government specifications, 1983; Codex, 1970; IOOC, 1993).

**Table 1.5 Data from the Italian government specifications (1983), the Codex standards on olive oil (1970) and the International Olive Oil Council (1993)**

Characteristics	Extra virgin	Virgin oil	Refined olive oil	Refined olive oil residue
% of 16:0 in the 2 position of triglycerides	<1.3	<1.8	<1.8	<2.2
Specific extinction in UV; K232	<2.40	-	<3.50	<6.50
Specific extinction in UV; K268	<0.20	<0.25	<1.10	<2.00
Specific extinction in UV; ΔK	<0.01	<0.01	<0.16	<0.20
% of total sterols + Erythrodiol and uvaol	<4.5	<5.0	<5.0	-
Acidity expressed as oleic acid	<1	<4.0	<0.3	<0.3
14:0	<0.05	<0.05	<0.05	<0.05
16:0	7.5-20	7.5-20	7.5-20	7.5-20
17:0	<0.3	-	-	-
17:1	<0.3	-	-	-
18:0	0.5-5.0	0.3-3.5	0.3-3.5	0.3-3.5
18:1	55-83	56-83	56-83	56-83
18:2	3.5-21	3.5-20	3.5-20	3.5-20
18:3	<0.90	<1.5	<1.5	<1.5
20:0	<0.6	Tr	Tr	Tr
20:1	<0.4	-	-	-
22:0	<0.2	Tr	Tr	Tr
24:0	<0.2	-	-	-
Cholesterol	<0.5	<0.5	<0.5	<0.5
Campesterol	<4	<4.0	<4.0	<4.0
Stigmasterol	*	*	*	*
β-sitosterol	>93	>93	>93	>93
Δ <sup>7</sup> -stigmasterol	<0.5	<0.5	<0.5	<0.5

\* less than percentage stated for campesterol. Tr: trace amounts of components present

In spite of the efforts made to prevent the adulteration of extra virgin oil, there is still an ongoing battle between the government and industry who implement quality standard controls on olive oil, and adulterers who look for ways to produce the perfect substitute to circumvent their efforts (Firestone and Summers, 1985). The problem is further complicated by the lack of clear definition for enforcement purposes. Certain discrepancies have arisen in regard to specific thresholds for the fatty acid lignoceric acid and for  $\beta$ -sitosterol. Additionally, there are no EC standards set for undesirable substances such as pesticides, heavy metals and aromatic polycyclic hydrocarbons (Pallotta, 1994).

The adulteration of olive oil has certain impacts on society since it may lead to the production of substances which are harmful to health. The Spanish toxic syndrome of 1982 is a classical example of this. In this case a product sold as olive oil was found to contain a mixture of refined oil and 2 % aniline. The consumption of this product caused the death of 450 people (WHO, 1984 and 1992).

Further adulteration has been found in imported Italian oils in America. In 1982, the Food and Drug Administration carried out an inspection programme to control this adulteration and misbranding of olive oil (Firestone et al., 1988). Undeclared esterified oil was found in 65 % of the oils examined. However, the on going survey in 1985 - 1986 showed a significant reduction of 65 % to 13 % undeclared esterified oil (Firestone et al., 1988).

However, there is still a need for analytical guidelines to be determined in order to stimulate crop improvement, processing techniques and consumer protection. The analysis of oils needs to keep ahead of possible forms of adulteration together with strict legislation which would no longer make it attractive to adulterate oil.

There is also a need for the development of faster and more efficient methods of analysis to replace time consuming traditional methods which require many preparative steps.

In view of these facts this project was developed to investigate various techniques used in the analysis of oils to try and find an effective technique which could clearly classify authentic oils and identify the addition of possible adulterants. The following sections (sections 1.5 and 1.6) describes the instrumentation used in this study and outline the objectives of this study.

## ***1.5 Instrumentation***

### **1.5.1 Gas chromatography**

Gas chromatography involves the separation of an analyte using a gaseous mobile phase and a liquid stationary phase. The retention of the analyte is determined by its volatility and by the degree of its interaction with the liquid phase. (Smith, 1988).

The technical instrumental parameters, oven design, detector, quality of gas pressure and flow regulation should automatically be a part of any good quality instrument. These factors can also effect the analysis of lipids (Mares, 1988, Smith, 1988). The review presented is limited to the specialized techniques used in the analysis of lipids.

#### ***1.5.1.1 Carrier gas***

Grob and Grob (1979) have reported the advantages of hydrogen over nitrogen and helium, as a carrier gas. The low elution temperature of hydrogen gas compared to nitrogen and helium, leads to shorter analysis times and consequently, lower thermal degradation and decrease in the loss of sensitive unsaturated lipids during analysis. However, Davies (1984) has reported that the use of hydrogen, as a carrier gas, in a temperature program for triglyceride detection has led to a significant decrease in the flow rate with increasing

temperature. It has also been shown that the linear velocity of hydrogen affected the triglyceride recovery (Davies, 1984). Helium has been reported as being the preferred gas in lipid analysis as it is inert, non flammable and unlike hydrogen does not run the risk of explosion because of leakage in the oven during operation (Traitlet, 1987).

#### ***1.5.1.2 Injection systems***

In capillary GC, there are two types of injection types. These are evaporative injection and on - column injection of the sample in liquid phase (Traitlet, 1987).

As reviewed by Traitlet (1987) the evaporative technique is carried out using hot injectors and the sample may be split in a pre - set ratio. In cool on - column the sample enters the column via a cold injection in the liquid state. Evaporation of the sample other than the solvent begins only when the temperature program is started. To guarantee the introduction of the sample in the liquid state, the point of injection must be kept cold and this is achieved by the external cooling device or by removing the front part of the column from the oven. In this study the SGE OCI - 5 cool on - column injection system was used. The head cooling system of the OCI - 5 on - column eliminates heat build up in the injector when the oven is at high temperatures (SGE, 1993 b).

Cool on - column injection (OCI) has the advantage over hot injector techniques in that it is quantitatively linear over a wide range of molecular weights. It allows the direct analysis of triglycerides without derivatization to fatty acid methyl esters and prevents the loss of triglycerides due to catalytic or thermal degradation in injection ports (SGE 1993 b). All the sample is transferred to the column so that there can be no discrimination or needle volatilization effects (Traitlet, 1987). One difficulty encountered with on - column injection is the transfer of low volatile impurities onto the column which are not subsequently eluted.

This problem may be eliminated by cutting of a small piece of the column after prolonged use. A pre-column (retention gap) may be attached to the column to act as a deposit site for these low volatile impurities. This retention gap also has the added advantage of refocusing the injected sample in order to avoid peak splitting which can occur in cool on - column injection (Traitlet, 1987).

### 1.5.1.3 GC analysis of the fatty acid methyl esters of oils

In relation to oils, the GC analysis of derivatized samples as fatty acid methyl esters is one of the most widely used techniques (Traitlet, 1987). However, the technique has limitations in that it fails to separate positional and geometric isomers without combination with other chromatographic methods. Double bond isomers are separated on medium to high polarity stationary phases but the fact that the separation is not baseline makes quantitation difficult (Traitlet, 1987). In this research, group separation of the total isomers was carried on the fatty acid methyl esters of the Greek oils provided and the analytical data obtained from these results were used in conjunction with other techniques to give additional information on the characteristics of the oils studied.

The usual chemical equation for triglycerides to the conversion to fatty acid methyl esters (FAMES) is displayed in Figure 1.9.

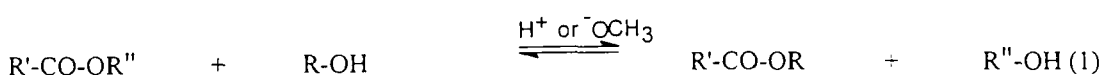


**Figure 1.9 General transesterification method of a triglycerides to a fatty acid methyl ester (Ke-shun, 1994)**

The GC analysis of FAMES olive oils was carried out using a SGE BPX70 column. This column "is a terminally modified siloxane phase containing a high concentration of

*cyanopropyl groups. The cyano groups are strongly electro attracting and interact with p groups, such as alkenes, phenyl rings, carbonyl groups, and esters” (SGE, 1993 a).*

#### **1.5.1.4 GC analysis of triglycerides**

The analysis of intact lipids by GC is one of the most difficult applications of this technique *“These difficulties are associated with the low volatility content of the lipids and the thermal instability of unsaturated compounds”* (Mares, 1988). Notwithstanding the progress made in GC, the problems of the analysis of lipids have not being fully resolved. These problems include *“losses and discrimination of substances during injection, losses during separation on the column and the stability of the column under conditions that can still be considered borderline in GC”* (Mares, 1988). Heated injectors, however, may be used for the separation of triglycerides by total carbon number, TCN, with acceptable linearity of response factors of the different carbon numbers of the triglycerides (Monseigny et al., 1979).

This type of analysis has been demonstrated on a non - polar dimethylpolysiloxane column using injection temperatures as high as 400 °C (Monseigny et al., 1979). Triglycerides were partially separated on a polar column with the aid of the cool on - column technique (Grob et al., 1980). This technique had being designed by Gailli et al. (1979) a year previously, in order to prevent losses and discrimination of less volatile parts of the sample.

Baseline separation of triglycerides based on total carbon number was eventually achieved using the cool on - column technique (Traitler and Prevot, 1981). Separation by degree of unsaturation was based on the total number of double bonds in one triglyceride molecule and no distinction was made between positional isomers. Further research in this area led to the separation of these isomers on capillary dimethylpolysiloxane columns containing



inorganic salts (Traitlet and Rossier, 1982). However, the analysis time was long and in complex mixtures gave poor resolution of the different species.

Traitlet (1987) has reported that a stationary phase of 'quarter polarity' (e.g. OV - 17) gave better separation of triglycerides by degree of unsaturation than non - polar dimethylpolysiloxane phases. The former has a higher temperature stability and its increased polarity resolves substances varying only slightly in polarity. Another property of the OV - 17 column is its elution pattern over a range of temperatures. At temperatures up to 250 °C the normal order of elution is that unsaturates elute before saturates, but at temperatures above 250 °C, the elution pattern changes to saturates before unsaturates. Therefore, a temperature program over a full temperature range would result in a remixing of the separated compounds in the column and hence a decrease in resolution. This phenomenon is discussed in more detail in advances in capillary GC by Traitlet (1987).

The analysis of triglycerides requires the use of temperatures in the range of 300 °C - 360 °C and as stated previously, the cool on - column technique is essential for this analysis in order to ensure that the sample goes to the column in the liquid state at the initial high temperatures of 300 °C. However, Frega et al. (1990) stated that the separation of triglycerides by degree of unsaturation could be achieved on a 50 % phenyl- / 50 % methyl - polysiloxane column using the evaporative injector technique. The results obtained from this analysis showed a constant quantitative composition for each oil analyzed (Frega et al., 1990). Antoniosi et al. (1993) also carried out a similar high temperature capillary GC analysis to detect the adulteration of soybean in olive oil by profile comparison.

The moveable on - column injector was first introduced by Geeraert and De Schepper (1983) for the analysis of triglycerides. Geeraert and Sandra (1985) applied this injector

technique to both high temperature and to normal temperature GC analysis of intact lipids. On non - polar columns, triglycerides were separated according to total carbon number. High resolution was also observed for the separation of unsaturates on a polar column (Geeraert and Sandra, 1985). Hinshaw (1986) has published some work on the analysis of triglycerides using the programmed temperature vaporizer as the injection technique. Similar results to the moveable on - column injector were obtained. However, to date, only two papers have been published using this injector (Hinshaw 1986 a and 1986 b).

It has been reported that the recovery of triglycerides on polar columns, (especially trilinolenin) depends on the carrier gas velocity and the mass of sample injected (Mares, 1987). However, under a set of programmed conditions the losses of triglycerides are reproducible with losses being higher for polyunsaturated triglycerides (Mares, 1987). Gilkison (1989) published a similar study on a column with a stationary phase of 65 % phenyl - methyl silicone. This study resulted in a low recovery of trilinolein which indicated that the quantitation of triglycerides was inadvisable by high temperature GC.

In this study triglycerides were determined by TCN on a BPX5 non - polar column. This SGE BPX5 column consists of 5 % diphenylpolysiloxane groups cross bonded to the column wall. Silphenylene is added into the backbone of these non - polar phenyl groups in order to improve the terminal stability of the stationary phase. This terminal improvement allows the column to be stable at temperatures up to 370 °C and the non - polar groups allow individual triglycerides to be eluted according to the relative molecular weight (SGE 1983). On non - polar columns, separation of the triglycerides is based on overall chain length and vapour pressure. Finer structure of the triglycerides can be observed in the carbon number peak by using a narrower bore column and a longer analysis time. The

triglycerides are resolved according to the number of unsaturated fatty acids in the triglyceride molecule. This separation is due to the difference in vapour pressure of saturated and unsaturated fatty acids but not between the unsaturated fatty acid themselves (Geeraert and Sandra, 1985).

The separation of triglycerides, by degree of unsaturation has also been investigated using a DB<sup>Tm</sup> - 17ht column. This column consists of 50 % phenyl - methyl silicone which had the equivalent polarity to the OV - 17 column which has already been described by Traitler (1987). The separation on this column is based on chain length, each carbon number peak being split up due to polarity differences in the triglyceride. Polarity increases with the degree of unsaturation in the fatty acid and with the total number of double bonds in the triglycerides (Geeraert and Sandra, 1985).

### **1.5.2. Supercritical fluid chromatography and supercritical fluid extraction**

*“A supercritical fluid is a substance above its critical temperature and pressure. Above its critical temperature the supercritical fluid does not condense or evaporate to form a liquid or a gas but is a fluid with properties changing from gas like to liquid like as the pressure increases”* (Bartle and Clifford, 1994). This definition is described by the pressure and temperature phase diagram (Figure 1.9) which displays the relationship of the gas, liquid and solid states of a substance as a function of temperature and pressure (Lee and Markides, 1990).

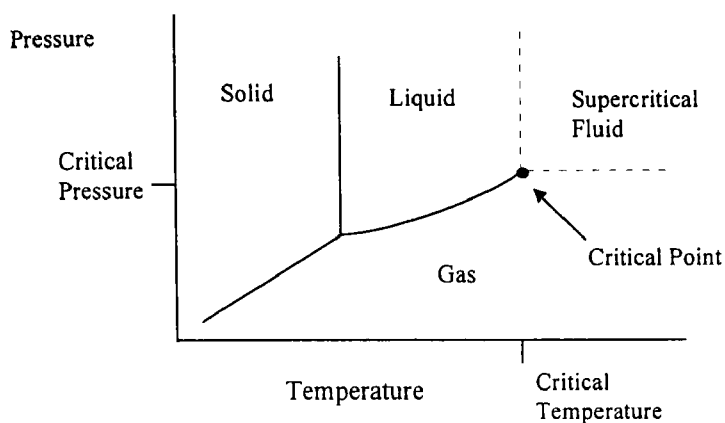


**Figure 1.10 Pressure/temperature phase diagram of a substance ( Lee and Markides, 1990)**

The most commonly used supercritical fluid is carbon dioxide, it is cheap, non - toxic and has a convenient critical temperature of 31.3 °C. Carbon dioxide is classified as a non - polar solvent. Therefore, modifier such as an alcohol must be added in order to separate polar solutes. In this case it is important to keep the mixture supercritical or close to the critical point.

The principles of operation of supercritical fluid chromatography and supercritical fluid extraction are based on the fact that the properties of a supercritical fluid can be controlled by changes in temperature or pressure; *“its density is related to its solvating power, its viscosity is related to flow rates and its diffusion coefficient is related to the mass transfer within the fluid”* (Bartle and Clifford, 1994). The limited application of high temperature GC in the analysis of lipids has led to interest in SFC as a potential technique in this area (Mares, 1987). SFC is capable of separating thermally labile and non - volatile compounds, without prior derivatization. The high diffusion coefficients of SFC produces narrower chromatographic peaks and better separation for a given analysis time (Bartle and Clifford, 1994).

The advantages of carbon dioxide as an extraction solvent over the traditional soxhlet methods are due to the fact that it is rapid, cheap and non toxic. The latter property is important in the extraction and processing of food products (Brogle, 1982).

### 1.5.2.1 Supercritical fluid chromatography

The main components of a supercritical fluid chromatograph are a high pressure pump, an injection valve, a pressure regulator, oven, a detector, amplifier and a microcomputer linked both to detector and the oven.

The basic principles and operating procedures of SFC have been described by Bartle and Clifford (1994). A schematic diagram of this instrument is shown in Figure 1.11.

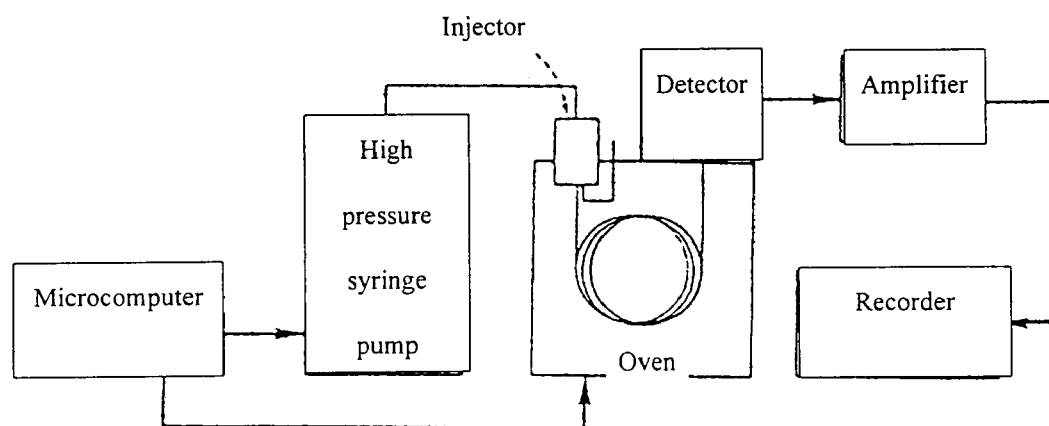


**Figure 1.11 Schematic diagram of SFC instrumentation (Bartle and Clifford, 1994)**

The choice of column is based on the selectivity, efficiency, sample capacity and speed of analysis required (Lee and Markides, 1990). According to Demirbucker and Blomberg (1994) packed column SFC is more efficient than open tubular SFC. *"In open tubular SFC, the low diffusion in supercritical media, at high densities, causes low optimal flow rates"* (Demirbucker and Blomberg, 1994). This reduces the separation efficiency and lengthens the analysis time.

The use of non - polar phases for capillary SFC, such as cross - linked methypolysiloxane, allows lipids to be separated by their carbon number. More polar phases such as phenyl siloxane, cyanopropylsiloxane and carbowax 20M have been used to achieve separation by degree of unsaturation (Lee and Markides, 1990). The advent of packed capillary columns in SFC provided a column that could combine the properties of both approaches. These columns have been reviewed by Wenbao et al. (1994) and have been shown to have low flow rates, shorter analysis times, choice of a wide variety of stationary phases and improved reproducibility in injection and detection of the samples analyzed (Wenbao et al., 1994).

In this research, columns packed with silver nitrate impregnated silica were used to separate triglycerides by degree of unsaturation. Three packed columns were connected in series to produce a similar chromatographic characteristics to the packed capillary columns described by Wenbao et al. (1994).

The type of detector used in SFC depends on the type of compounds being analyzed and on whether modifier is added to the mobile phase. The flame ionization detector, FID detector can be used with SFC. However, it responds to organic carbon molecules and the addition of modifier to the mobile phase limits its application (Lee and Markides, 1990). The fixed UV detector is a non - destructive detector that exhibits molar absorbitivities for compounds that contain chromophores. The UV detector is set at a fixed wavelength which is the characteristic absorption wavelength for the compound being analyzed. The light scattering detector may also be adopted in SFC and its basic principles involve “*nebulizing the column effluent, evaporating the solvent from droplets generated in the nebulizer, illuminating the solute particles and measuring the intensity of the scattered light*” (Lee and Markides, 1990). Carraud et al. (1987) have reported the use of packed columns

combined with a light scattering detector in the analysis of triglycerides. The results obtained from this report showed sensitivity five times greater than that obtained by LC. Rawdon and Norris (1984) succeeded in separating oleic acid and mono-, di- and triglycerides. This was achieved using a reversed phase packed HPLC column (ODS bonded) in conjunction with CO<sub>2</sub>/methanol mobile phase and a UV detector. Perrin and Peverot (1988) carried out similar research on the separation of triglycerides, using adsorption SFC in which they achieved a rapid separation of mono-, di- and triglycerides using a silica column with a methanol/modified CO<sub>2</sub> mobile phase. They also achieved separation of the triglycerides in sunflower oil, by number of double bonds on an ODS column.

Further research in the analysis of triglycerides by SFC, was carried out by Bartle and Clifford (1994). Partial separation between saturated triglycerides and unsaturated triglycerides was performed utilizing a polar cyanopropyl silica column. Chester (1984), White and Houck (1986) were some of the first researchers to introduce capillary columns to SFC. This resulted in the separation of lipids by capillary SFC at relatively low temperatures which was only attainable before by high temperature GC. Giron et al. (1992) reported on the accuracy and selective analysis of mono-, di- and triglycerides by CSFC-FID (capillary SFC combined with flame ionization detection) by comparing the analytical data obtained to the GC analytical data on their fatty acid content.

SFC has been used for studies in food adulteration. In 1991, France et al. (1991) demonstrated how packed - microbore SFC combined with a FID detector could be used in the detection of abused vegetable oils.

supercritical fluid chromatography was first introduced by Demirbaker and Blomberg (1990, 1991) for the study of lipids. Here, micropacked columns containing silica-based cation exchanger impregnated with silver nitrate were used (Demirbaker and Blomberg, 1990, 1991). These capillary columns were slurry packed with Nucleosil SA, sulfonic acid stationary phase. The mobile phase consisted of carbon dioxide - acetonitrile - isopropanol in the ratio of 92.8:6.5:0.7. The selectivity of separation of the triglycerides was based on the alkyl chain length and the position of the double bonds.

This technique was investigated as a potential technique for the separation of the triglycerides present in Greek olive oils and their adulterated mixtures. This information would possibly be used in conjunction with high temperature GC in the profiling of these oils.

#### ***1.5.2.2 Supercritical fluid extraction***

SFE provides the selective extraction of specific solutes by varying temperature and pressure of the extraction medium (Lee and Markides, 1990). A detailed review on the properties and applications of carbon dioxide as an extraction solvent has been given by Brogle (1982) and Lee and Markides (1990). SFE may be performed using both dynamic and static modes. In dynamic mode there is a constant flow of supercritical fluid through the extraction cell, while in static mode the matrix is soaked in extraction medium for a period of time which is then followed by decompression and extract collection (Lee and Markides, 1990).

SFE is influenced by four fundamental parameters. These are: the threshold pressure; the pressure at which the solute has maximum solubility in the extraction medium; the fractionation pressure range and the solute's physical properties. The theory underlying the



fractionation pressure range and the solute's physical properties. The theory underlying the effect of these parameters has been reviewed extensively by King (1989) who stated that knowledge of these parameters was vital to SFE optimization.

Stahl et al. (1980) have reported that the yields obtained for the extraction of oil seeds, using the extraction of both liquid and supercritical carbon dioxide are influenced by pressure and temperature parameters during the extraction and also on the size and shape of the seeds. They also suggest that seed oils should be extracted at pressures above 250 bar. At pressures below this value the concentration of oil is higher in liquid CO<sub>2</sub> than in supercritical CO<sub>2</sub>. The pressure has more of an effect on the solubility of the seeds when supercritical carbon dioxide is used for extraction (Stahl et al., 1980). Similarly, King (1989) has observed an increase in triglyceride solubility with increasing extraction pressure. Taylor et al. (1993) found that the amount of oil extracted in oil seeds by SFE was comparable to the amount of oil extracted from the oil seeds by the soxhlet method.

Tilly et al. (1990) described the effect of temperature (40 - 80 °C) and pressure (100 - 300 bar) on the extraction of triglycerides from oils. The solubility of the triglycerides was reported to be dependent on the solvent density and the solute volatility.

In our studies, the use of on - line SFE/SFC analysis and off - line SFE/SFC were investigated for the extraction and separation of triglyceride components of olives and various other seed oils. In this work the SFE system was coupled to the supercritical fluid chromatograph. The mobile phase was used as the extraction medium. In order to maintain chromatographic integrity, a focusing device for concentrating the extracted solutes was used prior to SFC (Lee and Markides, 1990).

Sample derivatization using SFE conditions has also been investigated. Here the transesterification of triglycerides to fatty acid methyl esters was performed in the extraction cell prior to extractions. King et al. (1992) carried out an on - line SFE - GC method of in - situ extraction, derivatization and analysis of the fatty acids in oil seeds. The fatty acid composition of the oil seeds were similar to recorded literature values for evening primrose seeds. Berg et al. (1993) used immobilized lipase to transesterify edible fat to FAMES. This reaction was carried out using on - line SFE - SFC and high yields of FAMES were observed.

In view of the transesterification methods investigated by gas chromatography the in situ derivatization of triglycerides to FAMES in a SFE extraction cell was also studied. This method of derivatization was first introduced by Berg et al (1993) who carried out the transesterification of edible fat as a on - line SFE/SFC extraction. Immobilized lipase was investigated as a potential catalyst to convert triglycerides of olive oil to fatty acid methyl esters in the supercritical fluid medium prior to extraction. The extracted FAME sample was analyzed by SFC after transesterification.

The volatiles of olive oils were also extracted using the Hewlard Packard Supercritical Fluid Extractor. The volatiles were extracted at low pressure and were collected on to a Tenax trap at the venting outlet of the instrument with subsequent analysis using thermal desorption GC/MS.

### **1.5.3 Nuclear magnetic resonance.**

Nuclear magnetic resonance is a spectroscopic technique used to obtain molecular information about pure compounds and mixtures. Several books describing in detail the theoretical aspects of NMR have been published (Martin and Martin, 1980; Becker, 1980;

Pollard, 1986). Modern NMR spectroscopy is carried out in fast Fourier transformation. The Nuclear spins are excited by a powerful field in the form of a broad band short radiofrequency pulse. This pulse excites all the absorption frequencies in the molecule at the same time (Mason, 1984). *“The transient response, the so - called free induction decay signal, the FID, of all the excited spins, is detected, amplified, digitized (by an analogue - to - digital converter) and stored in a dedicated computer as a function of time. The pulsing is repeated and the FID's are added coherently”* (Mason, 1984). The data are then converted by Fourier transformation into a plot of frequency against strength of absorption (Mason, 1984).

*“In FT NMR relaxation times determine the rate of pulsing and accumulation; fast pulsing is possible for quadrupole nuclei, which makes up for low receptivity. The pulse width (length or duration),  $t_p$ , determines the range of frequencies produced (the shorter the pulse, the wider the range)’* (Mason, 1984).

In conjunction with experimental consideration, care must be taken to avoid subjecting an analysis to additional inaccuracies in the course of processing the data. Digital resolution is determined from the number of data points used to digitize the free induction decay. This resolution should be effective in resolving the narrowest feature in the transformed spectrum (Levy, 1984). *“High spectral definition is particularly important if peak height, rather than area are used to represent intensities since it is essential that a data point resides at the apex of the peak when this method is used”* (Levy, 1984).

The maximum value of the number of data points,  $N$ , is determined by the size of the memory area reserved for data acquisition. This memory is reduced by 4K (approx.), for data handling purposes and program storage e.g. 16K data points for a memory of 20K

as 8192 or 16384. The most suitable value is determined by considering the conflicting requirements of sensitivity and resolution. A large number of data points are required for a good digital resolution and this lengthens the acquisition time and increases the number of scans. In practice, a compromise on the resolution is usually made to limit its value to the smallest compatible size that will produce an accurate reconstruction of the spectrum (Martin, 1980).

In relation to sample preparation for NMR analysis, a deuterated compound such as  $\text{CDCl}_3$  is chosen as solvent, since it satisfies particular NMR specifications regarding locking ability, spectral transparency and magnetic properties. The residual  $\text{CDCl}_3$  in the solvent gives a small peak in the NMR spectra, which is generally easily distinguishable from those arising from the sample.

#### *1.5.3.1 Application of proton NMR to lipid analysis*

In a  $^1\text{H}$  NMR spectrum the components of the samples are represented as multiplets from  $^1\text{H}$  -  $^1\text{H}$  spin - spin coupling (Pollard, 1986). The integral of the resonance is proportional to the number of protons producing that resonance (Pollard, 1986). The  $^{13}\text{C}$  NMR analysis is obtained in proton noise decoupling which removes  $^1\text{H}$  -  $^{13}\text{C}$  spin - spin coupling. This enhances the sensitivity by nuclear overhauser effect, NOE, and by collapsing multiplets to a single line (Pollard, 1986). In order to carry out a quantitative  $^{13}\text{C}$  NMR analysis the gated decoupling pulse sequence is required to suppress the NOE and long pulse delays are needed to allow  $^{13}\text{C}$  nuclei with longer spin relaxation times to relax completely (Ng and Ng, 1983).

The application of NMR to lipids was first described by Johnson and Shoolery (1977). They demonstrated the ability of  $^1\text{H}$  NMR to characterize oils and fats. Shiao and Shiao (1989)

demonstrated that  $^1\text{H}$  NMR was a rapid and informative method in the determination of contents and ratio of total saturated to unsaturated fatty acids and the molar percentage of polyunsaturated fatty acids in natural occurring triglycerides. High field  $^1\text{H}$  NMR was applied by Sacchi et al. (1996) in the analysis of virgin olive oil obtained from different olive varieties in different regions in central Italy. The analysis involved the quantitative measure of the fatty acid composition and the minor components of the oils involved. A statistical analysis was performed on the volatile component data classifying the oils according to the same olive variety (Sacchi et al., 1996).

The chemical shifts for  $^1\text{H}$  NMR signals are recorded in Table 1.6.

**Table 1.6  $^1\text{H}$  NMR spectral assignments of the triglyceride components for olive oils (Shiao & Shiao, 1989).**

Assignments	$\delta/\text{ppm}$
Total alkene protons + 1 proton of H-2 of glycerol	5.2 - 5.4
4 protons of glycerol H-1 and H-3	4.1 - 4.3
$\alpha$ -linoleic. PUFA	2.78
$-\text{O}-\text{CO}-\text{CH}_2^-$	2.30
Allylic methylene	2.05
$\alpha$ -linolenic. PUFA	0.97
Methyl signal	0.88

### *1.5.3.2 Application of carbon NMR to lipid analysis*

Reports by Ng (1983,1984,1985), Wollenberg (1990) and Gunstone (1991) have shown that high resolution  $^{13}\text{C}$  NMR can provide structural information on triglycerides regarding fatty acid composition, acyl chain length, as well as numbers, location and stereochemistry

of double bonds. Such information is useful in the characterization and classification of various types of oils.

Four groups of carbon atom are distinguished in the  $^{13}\text{C}$  NMR spectra of lipids, the glycerol atoms, the carbonyl atoms, the central ethylenic C - atoms and the methylene groups towards the terminal methyl groups. The chemical shifts of these groups are recorded in Table 1.7.

**Table 1.7  $^{13}\text{C}$  NMR spectral assignments of the triglyceride components for olive oils.**

Assignments	$\delta/\text{ppm}$
Carbonyl region	173.5 - 172.5
Ethylenic region	130.5 - 128.0
Glycerol C - atoms	69 and 63
Methylene envelope	31-14

The difference in the electronic environment of the fatty acids attached to the 1,3 and 2 positions of the glycerol backbone give rise to two different signals for the carbonyl and methylenic and ethylenic C - atoms. It is possible to calculate ratios, 1,3:2, for each fatty acid moiety and also the 1,3 or 2: saturates using the carbonyl peaks (Ng, 1983). The carbonyl carbons of the saturated, oleic and linoleic acyl groups of palm oil at the 1,3 glycerol positions and at the 2 glycerol positions also have different chemical shifts (Ng, 1983). The carbonyl carbons may also be used for the quantitative analysis of the fatty acid composition at the glycerol position (Ng, 1985). These were found to have identical NOEs and similar  $T_{1\rho}$ s thus indicating the quantitative analysis could be carried out in proton decoupling mode.

The chemical shift difference in the alkene carbons of palm oil was characteristic of the chain's glycerol position (Ng, 1984). However, the alkene carbons did not have identical NOEs or similar  $T_1$ s and thus the  $^{13}\text{C}$  NMR gated decoupling pulse sequence was required for the quantitative determination of the degree of unsaturates present in the oil.

The advantages and disadvantages of the analysis of the carbonyl as opposed to the analysis of the alkene region of the  $^{13}\text{C}$  NMR has been reviewed both by Ng (1985) and by Wollenberg (1990). These reports agree with each other stating that the main advantages of using the carbonyl region over the alkene region is the fact that the saturate's concentration and 1,3:2 saturate ratio is obtainable only from the carbonyl region. As stated previously, the carbonyl region also has identical NOE values and similar carbonyl  $T_1$  values. This means that quantitative  $^{13}\text{C}$  NMR can be carried out with relaxation times less than  $5 T_1$  which is the value necessary for quantitative conditions. The long acquisition time enhances the spectral resolution and the spin system can fully relax back to thermal equilibrium without a long relaxation delay time (Wollenberg, 1990). This results in an experimental time that is half that required for the alkene region. The alkenic carbons have different NOEs. Thus, the relaxation delay time should be greater than  $5T_1$  to allow for an effective time period to quench NOE build up regardless of the total  $T_1$  relaxation time period.

The disadvantage of the analysis of the carbonyl region was that no distinction was made between the saturated fatty acids present in the oil, linoleic and linolenic fatty acids were not resolved in the carbonyl region and also the low sensitivity of the carbonyl carbons prevented the presence of trace amounts of an acyl group from being detected. Wollenberg (1990) has suggested that both the alkene and the carbonyl region are required as a single

experiment since the saturated fatty acids cannot be resolved in the alkene region. Wollenberg (1990) also reported on the acyl distribution and acyl positional distribution of the fatty acids present in three natural oils. The positional distribution data of these oils indicated that the polyunsaturates are replaced in the glycerol 1,3 positions by saturates while the fatty acid oleyl is randomly distributed. In contrast, the distribution of linoleyl in the high oleic sunflower oil was more randomly distributed (Wollenberg, 1990).

The determination of the mole fractions of the saturated, monoene and diene acid chains was carried out by Ng (1985) from the  $^{13}\text{C}$  NMR spectra of the saturated and olefinic carbons in palm oil (Ng, 1985). These results proved more informative than the iodine values used to measure the total unsaturation in the fatty acids. For this quantitative analysis it was suggested that the gated decoupling technique should be used in which the pulse repetition time should be at least  $5T_1$  and preferably  $10T_1$  times the longest  $T_1$  of the carbons concerned.

Shiao and Shiao (1989) found the  $^{13}\text{C}$  NMR of plant seed oils to have characteristic chemical shifts in the region of  $\delta$  13 - 40 and  $\delta$  128 - 131. This analysis was carried out in broad band decoupling mode and the profile obtained served as a fingerprint for identification. Gunstone (1991) studied the mono-, di- and triglycerides and found that characteristic chemical shifts for the three glycerol carbon atoms and for C1 and C2 in each acyl chain.

Further research by Gunstone showed that the carbon atom signal for the  $\omega$ 1, terminal methyl group of the fatty acid chain of the triglyceride,  $\omega$ 2, methylene group attached to the methyl group of the fatty acid chain of the triglyceride and  $\omega$ 3, the second methylene group from the end of the fatty acid chain of the triglyceride, provided information on the cis and



trans isomers of C15, C14 and C12 of oleic esters (Gunstone, 1993). Sacchi et al. (1992) carried out an analysis of the positional distribution of fatty acids in olive oil triglycerides by high resolution  $^{13}\text{C}$  NMR of the carbonyl region and showed how the analysis of this region could be used to quantitatively detect the synthetic esterified oils in olive oil. It was reported that when esterification occurs a random distribution of the fatty acids were observed with the relative same level of saturated fats in the 1,3 and 2 glycerol positions (Sacchi et al., 1992).

The majority of the literature cited above has focussed on the analysis of oils by  $^{13}\text{C}$  NMR. As stated previously, quantitatively  $^{13}\text{C}$  NMR (with the exception of the carbonyl region) requires a gated decoupling pulse sequence to suppress the NOE and long pulse delays are needed to allow  $^{13}\text{C}$  nuclei with longer spin relaxation times to relax completely. These changes require a long experimental time and are not practical when a large number of samples need to be analyzed. In relation to oils, the application of chemometrics to NMR data has been limited to the study of the unsaponifiable matter from different oils by Zamora and Hidalgo (1994), the analysis of  $^{13}\text{C}$  NMR of petroleum distillates by Brekke et al. (1989), the characterization of crude oils by Kvalheim et al. (1985) and the  $^1\text{H}$  NMR analysis of the volatile components in olive oils (Sacchi et al., 1996). This research applied statistical analysis to  $^{13}\text{C}$  NMR and  $^1\text{H}$  NMR peak height intensity data of olive oils. The  $^{13}\text{C}$  NMR was carried out in proton decoupling mode and the influences of NOE were eliminated by using the relative peak height intensities of each oil as statistical data. The peak height intensities were referenced to specific carbon signals in each region of the spectrum.

#### 1.5.4 Mid - infrared spectroscopy

A molecule absorbs infrared electromagnetic radiation that corresponds to transitions between vibrational levels of the ground electronic state of the molecule (Twadowski and Anzenbacher, 1994). The absorption of mid - infrared radiation occurs at a frequency from  $4000\text{ cm}^{-1}$  to  $600\text{ cm}^{-1}$ .

*Stretching vibrations produce changes in the bond length of a molecule while bending vibrations cause changes in the bond angle. Such vibrations may cause a change in the dipole moment of the molecule and result in the absorption of radiation that can be monitored by a spectrophotometer. The frequency at which molecules absorb depends on the types of bonds present. The stretching frequency of the bond is related to the masses of the two atoms involved in the bond and to the strength of the bond (Ege, 1989).*

The main components of the infrared spectrophotometer are a source, an absorption cell, a dispersive element and a detector. These components and their functions have been described in detail by Twadowski and Anzenbacher (1994).

In the past, mid - infrared spectroscopy has been excluded for the analysis of food. The main reasons for this were due to instrumentation and sampling problems (Wilson, 1990). Food samples are opaque, highly scattering and they contain water which absorbs strongly in the mid - infrared region. The preparation of food samples as mull or pellets was difficult and dispersive mid - IR measurements were relatively slow. The absorption bands of the mid - infrared region are however, well resolved and are component specific (Wilson, 1990). The use of an interferometer with Fourier transformation, in place of dispersive measurements, has led to improvements in the mid - infrared spectroscopy.

These improvements include more energy at the sample, higher signal to noise ratios and faster spectra acquisition (Wilson, 1990).

The attenuated total reflectance technique has also made mid - IR applicable to food analysis. This technique shortens the time required for obtaining high quality infrared spectra for various samples and it allows for the analysis of samples which transmits infrared radiation poorly. It is also useful in the preservation of the intact character of the sample (Twadowski and Anzenbacher, 1994).

The attenuated total reflectance cell consists of a crystal of high refractive index. This crystal is usually made from Ge or ZnSe (Wilson, 1990). *“The sample is placed in direct contact with the ATR crystal. The infrared radiation enters the ATR crystal and strikes the sample of lower refractive index once or more at an angle above the critical angle at the reflecting interface. The radiation penetrates the sample to a depth of 5  $\mu\text{m}$  or less. The beam then leaves the crystal through another end (both ends have an angle of 45 °C face) and emerges in the dispersing element”* (Twadowski and Anzenbacher, 1994).

The advent of Fourier transformation, the ATR sampling technique, data manipulation and chemometric software has made mid - infrared spectroscopy favourable to the analysis of oils. The oils may be applied in their neat form to the ATR crystal and there is no problems associated with sample handling (Ismail et al., 1993). Oils contain the same fatty acids and the mid - IR spectra of their triglyceride profiles are quite similar and are dominated by the C-H and C-O vibrations of the polymethylene chains. According to Lai et al. (1984) subtle difference are observed between these polymethylene chains.

In relation to the application of infrared spectroscopy to lipid analysis the following papers have been reviewed. In 1988, the AOCS introduced a method for the determination of the trans isomer content of oils and fats. This method had however involved the use of CS<sub>2</sub> and saponification and methylation was required for trans contents less than 15 %. Lanser and Emken (1988) used the peak area of the trans absorbance band at 966 cm<sup>-1</sup> to determine the trans unsaturation of fats and oils. These results compared well with the results obtained by capillary gas chromatography. Belton et al. (1988) used FTIR and attenuated total reflectance in the estimation of isolated trans double bonds in oils and fats. Sleeter and Matlock (1989) developed an FTIR method using a KBr cell to measure the trans isomers of oils. Ulberth and Haider (1992) used an FTIR spectral subtraction technique and PLS to determine low concentrations of isolated trans double bonds in hydrogenated fats such as margarines and shortenings.

Ismail et al. (1993) developed a rapid method in the determination of free fatty acids in fats and oils by Fourier transform infrared spectroscopy. This method involved the preparation of calibration curves by adding oleic acid to the oil chosen for analysis and the measurement of the carbonyl group at 1711 cm<sup>-1</sup> after ratioing the sample spectrum against that of the same oil free of fatty acids.

Sato (1994) used principal component analysis on NIR spectroscopic data for classification of vegetable oils: soybean, corn, cottonseed, olive, rice bran, peanut, rapeseed, sesame and coconut oils.

Bewig et al. (1994) developed a four wavelength discriminant analysis equation using near - infrared reflectance (NIR) to separate the spectra of four different vegetable oil types. This equation proved successful in classifying oils not used in the equation.

Sato et al. (1991) developed a foundation for the rapid determination of fatty acid composition in fats and oils by NIR spectroscopy. NIR spectral patterns were reconstructed by combining the spectral patterns of pure triglycerides. The original and the calculated spectra were examined

Kaplan et al. (1994) carried out a study of triglycerides by CSFC - FT - IR. The on - line FT - IR spectra of the components showed that the antisymmetric  $\text{CH}_2$  stretching and carbonyl stretching modes of infrared peaks related to the carbon number of an individual triglyceride. Lai et al. (1994) used FT - IR in conjunction with principal component analysis and discriminant analysis to investigate the potential of the technique for determining the authenticity of vegetable oils. The statistical analysis was carried out on the oil data extracted from the mid - IR regions between  $3100 \text{ cm}^{-1}$  -  $2800 \text{ cm}^{-1}$  and  $1800 \text{ cm}^{-1}$  -  $1000 \text{ cm}^{-1}$ . This analysis revealed clustering of the seed oils according to the plant species. It was also noted that a high signal to noise ratio in the region of  $1600 \text{ cm}^{-1}$  indicated that the spectra was contaminated by water vapour and this contamination affected the ability to carry out discriminant analysis.

Further research in this area by Lai et al. (1995) involved the successful quantitative analysis of potential adulterants of extra virgin olive oil using mid - infrared spectroscopy. The method involved the use of ATR as a sampling technique and partial least squares multivariate analysis. Safar et al. (1994) also used a combination of mid - IR spectroscopy, attenuated total reflectance sampling with statistical multidimensional techniques to characterize edible oils, butters and margarines. In this case, the foods were differentiated as a function of their water content. The water absorption peaks were observed in the region  $3600 \text{ cm}^{-1}$ - $3000 \text{ cm}^{-1}$  and at  $1650 \text{ cm}^{-1}$ . The PCA analysis was applied

on the normalized spectra in the range of  $4000\text{ cm}^{-1}$  to  $1560\text{ cm}^{-1}$ . Principal component analysis of FTIR spectra was also performed by Dupuy et al. (1996) to classify edible fats and oils according to their origin. The two sampling methods used were attenuated total reflectance for fats and mid - IR optical fibre method for oils. The fats were classified according to their concentration of their unsaturated fats while the oil were classed according to the different concentrations of linoleic acid in the case of oils (sunflower, olive and peanut oils). Van der Voort et al. (1995) designed an industrial sample - holder accessory for fats and oils. This sampling technique was used in conjunction with partial least squares calibration to determine the cis and trans isomers of fats and oils.

Welsley et al. (1995) presented a method for the prediction of adulterated olive oils by near - infrared spectroscopy. PCA was used to predict the type of adulterant. Beaten et al. (1996) used FT - IR to predict adulteration in virgin oil samples that were adulterated with soybean, corn and olive oil residues.

The characteristic attenuated total reflectance infrared absorption bands of oil (Safar et al., 1994) are displayed in Table 1.8.

**Table 1.8 Characteristic attenuated total reflectance infrared absorption band of oil (Safar et al., 1994)**

Wavenumber	Group	Type of vibration	Remarks
3450 m	O-H	Str	Intermolecular bonded
3005 w	C-H	Sym. str	-CH=CH-(cis olefin)
2953 m	C-H	Asym str	Aliphatic (-CH <sub>3</sub> )
2922 s	C-H	Asym str	Aliphatic (-CH <sub>2</sub> )
2853 s	C-H	Sym. str	Aliphatic (-CH <sub>2</sub> )
1743 s	C=O	Str	$\nu$ (C=O)ester
1640 m	O-H	Def.	$\delta$ (O-H)water
1462 m	C-H	Scissoring	Aliphatic (-CH <sub>2</sub> )
1377 w	C-H	Sym.def.	Aliphatic (-CH <sub>3</sub> )
1238 m	C-H	Out-of-plane bend	Aliphatic (-CH <sub>2</sub> )
1162 s	C-O	Str.	$\nu$ (C-O)ester
1025 vw	C-O-C	Str.	$\nu$ (C-O-C)ester
966 vw	C-H	Out-of-plane bend	Trans (-CH=CH-)
722 m	C-H	Rocking	Aliphatic (-CH <sub>2</sub> )

s: strong; m: medium; w: weak; vw: very weak; asym: asymmetrical; def.: deformation; str; stretching, sym: symmetrical

The review of the literature cited above led to the investigation of the authentic Greek oils and their adulterated mixtures using mid - infrared analysis with ATR sampling in this study. The data obtained were statistically analyzed to try to characterize and differentiate between each sample set of authentic and adulterated samples.

### 1.5.5 Raman spectroscopy

Raman spectroscopy is based on the detection of inelastic scattered photons (Williams et al., 1990). Radiation is scattered when a sample is irradiated with monochromatic light of a wavenumber outside an absorption band. Most of the radiation is Rayleigh scattering. However, some of the incident radiation interacts inelastically with molecules and

is called Raman scattering (Hamilton, 1995). This Raman scattering relies on the change in the polarizability in a molecule as it vibrates. Infrared absorption and Raman scattering are both associated with the vibrational energy levels of the sample molecules and to the stretching or bending vibrations of the molecular bonds (Colthup et al., 1990). These techniques work in complement with each other and give rise to different relative intensities and profiles of the same molecule (Colthup et al., 1990). The Raman scattering bands for fats and oils and the characteristic Infrared absorption and Raman scattering bands for sunflower oil (Sadeghi-Jorabchi et al., 1990) are shown in Table 1.10 and Table 1.11.

Due to the low efficiency of the Raman scattering process the laser is used as the main source of monochromatic radiation and a photomultiplier is required for the detection of the scattered radiation (Twadowski and Anzenbacher, 1994). A detailed description of how the laser action is achieved and on how the photomultiplier operates is given in Twadowski and Anzenbacher (1994).

The application of Fourier transform instrumentation to vibrational spectroscopy has led to an improved signal - to - noise ratio, better light throughput and improved speed of analysis. The use of near - IR excitation increases the reproducibility frequency calibration and provides fluorescence - free Raman spectra. Such developments have made Raman spectroscopy a fast and efficient analytical technique (Marigheto and Wilson, 1996).

In relation to fats and oils, the Raman analysis has been used to measure the degree of unsaturation and the determination of cis/trans isomer ratios. Bailey and Horvat (1972) determined the cis/trans isomer content of edible vegetable oils by measuring the intensities of C=C stretching absorptions of cis and trans isomers at 1656 and 1670  $\text{cm}^{-1}$



respectively. Sadeghi - Jorabchi et al. (1990) reported how FT - Raman could be used in the determination of total unsaturation of oils and margarines. The Iodine Value of margarines was calculated from the ratio of the peak height of the C=C stretching to the peak height ratio of the CH<sub>2</sub> scissoring deformation. Further research by Sadeghi - Jorabchi et al. (1991) showed how FT - Raman could be used to determine cis and trans isomers. Ozaki et al. (1992) also published a report on how to determine the level of unsaturation of a wide range of fat - containing foods.

This study centered on the FT Raman analysis of the Greek olive oils provided and the statistical classification of the oils into groups based on the analytical data obtained.

**Table 1.9. Raman scatter bands for fats and oils (Sadeghi - Jorabchi et al., 1991)**

Absorbance	Assignment
Baseline (1700 - 1601)	area of C=C
standards, baseline (1790 - 1713)	area of C=O
standards, baseline (1543 - 1382)	CH <sub>2</sub> scissoring
1661 (baseline: 1628 - 1694)	C=C
1441 (baseline: 1382 - 1512)	CH <sub>2</sub> scissoring
Margarine (baseline: 1628 - 1694)	C=C
Margarine (baseline: 1382 - 1512)	CH <sub>2</sub> scissoring
Area of C=C : C=O/CH <sub>2</sub>	total unsaturation
1265:1303	total cis isomer
1667:1657	total trans isomer
1200 - 700	fingerprint region
720	C - N of phosphatidylcholines
1000 - 1150	C - C vibrational modes
1064, 1133	all trans formations

**Table 1.10 Characteristic infrared absorption and Raman scattering bands for sunflower oil (Sadeghi - Jorabchi et al., 1990)**

Peak	Wavenumber	Ft - Raman	FTIR	Assignments
1	3014	*	-	$\nu$ asym (=C - H)
2	3007	-	*	$\nu$ sym (=C - H)
3	2926	* (shifted)	*	$\nu$ asym (- C - H)
4	2855	*	*	$\nu$ sym (=C - H)
5	1745	* (weak)	*	$\nu$ (C=O)
6	1661	*	* (v. weak)	$\nu$ (C=C)
7	1444	*	-	$\delta$ (CH <sub>2</sub> )
8	1306	*	-	methylene twisting
9	1272	*	-	in plane =C - H deformation in cis
10	1163	-	*	C - O stretch in ester $\nu$ (C - O)
11	724	-	*	=C - H planar bending

### 1.5.6 Pattern recognition

Pattern recognition involves the use of statistical and mathematical methods in experimental design and in the analysis of data. Principal component analysis (PCA) was first introduced by Malinowski in the 1960s. Since then it has been widely used in chemical applications. The first major publications in this area are from Malinowski (1980) and Kowalski et al. (1984). One aim of PCA is to find classes of similar objects and this is associated with the detection of outliers which do not belong to known classes (Wold, 1992).

PCA reduces the original data into the minimum number of principal components so that only a few of the original variables account for the variability observed in the original data (Mardia et al., 1979). In PCA, the axis representing the original variables are rotated and transformed to form a new axis. This newly formed axes lies along the direction of maximum variance of the data and represents the first PC of the variables (Adams, 1995).

The second PC, which is orthogonal to the first PC, describes the variance in the data set which has not already been accounted for. This PC extraction process is continued until all the variance in the data set is described (Howells et. al, 1992). The eigenvector of the first principal component is represented by the slope of the major axis and its eigenvalue corresponds to the length of this major axis. Similarly the second principal component is represented by the second eigenvector and eigenvalue. PCA is visually represented by plotting pairs of the first few PCs. Each PC is associated with a set of coefficients called loadings. Loadings are defined as the projection of each variable on to the principal component. The size of the loading is related to the importance of a variable on an eigenvector. Scores are described as the projection of the samples on to a PC and are calculated from the eigenvectors:

$$(\text{Scores}) = (\text{Data})(\text{Eigenvectors}).$$

This calculation gives the scores matrix the dimensions of samples by real factors.

The application of soft independent modelling of class analogy (SIMCA) to analytical data relies on the fact of data homogeneity within a modelled class and on the absence of strong outliers or subgroups (Wold, 1983). In SIMCA, a principal component model is fitted to each category and confidence envelopes are constructed around the model to contain the data points. The closed class envelope for each category is derived by first carrying out a PCA analysis separately on each class. In SIMCA, the classification of each model is validated to ensure that only informative PCs are used in the development of the model. The types of validation method used may be leverage or cross validation, the former being an over - optimistic method and should only be used in the initial stages of the analysis to get a quick answer (Camo AS, 1996). Cross validation represents a more efficient method of

validation. It involves dividing the analytical data into several subsets, each subset being representative of the total data set. The validation process is carried out by creating a model using all the samples except one. The excluded sample is then used to validate the model. This process is repeated until each sample is excluded in turn (Martens and Naes, 1989). The PC model is described by the variances, loadings and scores. The statistical terms used in SIMCA classification are: *total residual variance* is the variance of the error part of the data and describes the overall modelling error; *total explained variance* describes how much of the original data is described by the model; *calibration variance* is a measure of how well the calibration data fit the model; *validation variance* is measured by testing the model on data that were not used to build the model (Camo AS, 1996).

Once the model has been developed, the classification rule is tested using a test set of known samples that were not used in the development of the models. The numerical results for each classified sample are displayed in a classification table. The two closest models with respect to sample to model distance ( $S_i$ ) are shown for each sample. A doubly - classified sample is indicative that the class model may not be precise and may need more samples in the calibration set and additional variables. However, the sample to model distance ( $S_i$ ) and the leverage ( $H_i$ ) should be studied to find the best fit. Samples with similar  $S_i$  values are classified to the model that has the smallest leverage (Camo AS, 1996).

The Cooman's plots show the orthogonal distances from the new objects to the different class models. It is a plot of  $S_i$  versus  $S_i$ , which is the sample to model distance of the two models plotted against each other. Samples which fall within the membership limits will belong to that class (Camo AS, 1996). The model distance plot indicates the distance between one class and the other classes. Good separation between the classes is achieved if

the distance between the classes is greater than three since *“This separation is calculated by the pooled variance of the residuals obtained when objects of class model one are fitted to class model two and visa versa, divided by the pooled residual variance obtained when the objects are fitted to their own classes. The obtained value can then be compared with F - statistics to judge the significance of the class separation”* (Wold et al., 1983). Camo (1996) has reported that this value should be compared to the value of 1 which is the distance of the model to itself. *“A model distance much greater than 1 (for instance 3 or more) shows that the two models are quite different, which in turn implies that the two classes are likely to be well distinguished from each other”* (Camo, 1996).

Discriminant analysis is a supervised pattern recognition technique in which the parent groups are predetermined and the samples being analyzed are representative of each of these groups (Adams, 1995). The data are first reduced by principal component analysis and a discriminant rule is applied to assign each of the unclassified samples to one of the parent groups (Adams, 1995). This discriminant rule is developed from the preassigned samples (the training set). Once the discriminant rule is established, the predictability of the rule is tested. This involves the classification of a new independent set of samples, of known origin, that were not used in the development of the discriminant rule. This set of samples is known as the test set. The discriminant rule may be developed using various pattern recognition techniques. The technique used in this study is squared Mahalanobis distance metric. In this case, the square of the distance between the pattern vector of the unclassified sample and every classified sample from the training set is calculated and the samples with the smallest distances to a group are assigned to that group. A plot of this straight line which defines the discriminant function is known as a canonical variate plot.

Discriminant analysis differs from SIMCA in that it is a hard modelling technique and all samples are forced to belong to one of the predetermined classes. The advantage of SIMCA over discriminant analysis is the fact that the models are developed separately and the separation of the classes is not overestimated (Vogt, 1987).

The applications of chemometrics to lipid analysis have been reviewed intensively by Kaufmann (1991). These applications involve method development, classification and modelling of properties. In relation to olive oils, regional classification has been achieved using fatty acid, sterol and triterpenic analytical data. This classification has been carried out using principal component analysis or partial least squares regression.

Kaufmann and Herslof (1991) applied multivariate statistical analysis to the fatty acid methyl ester and triglyceride data of different oils as a means of classification. A class model was developed for each of the different oils. This model provided an objective and quantitative means of identification, through nearness in a multidimensional measurement space.

A similar multivariate approach was adopted by Garcia and Aparicio (1993) which involved the analysis of the relationship between fatty acids and triglycerides in virgin oils. A chemical significance of factors between both sets was established by applying PCA. This analysis provided information about the biosynthetic route of fatty acids and its regulation. Multiple regression was also proposed for the determining the triglyceride composition of an oil according to its fatty acid composition (Garcia and Aparicio, 1993). The discrimination between authentic oils and adulterated mixtures proved successful using fatty acid, triglyceride and sterol profiles.

Tsimidou and Macrae (1987) applied PCA to the fatty acid and triglyceride compositional data of a wide range of authentic oils. This application succeeded in classifying olive oils into distinct groups using either the fatty acid methyl ester data or the triglyceride data. This statistical analysis was extended further to try and discriminate between adulterated and authentic oils. Discrimination was clearly observed among the authentic oils and the oils adulterated at levels of 20 %. However, there was no clear distinction between the original oils and its adulterated mixtures at level of 10 %. The triglyceride profiles of the oils by HPLC were found to be more discriminating than the fatty acids compositions obtained by GC (Tsimidou and Macrae, 1987).

Damiani et al. (1983) used pattern recognition techniques to define the relationship between triglyceride groups and the fatty acid composition in olive oil. They succeeded in estimating the triglyceride group number ( $G_{NU}$  groups) from the fatty acid composition data of total triglycerides and by means of suitable regression models. The  $G_{NU}$  groups, which contain all the molecular species with the same carbon number and the same degree of unsaturation, are different for each variety of oil and can be used in fingerprinting different oils.

Aparicio et al. (1992) carried out a chemometric study of the Hilditch theory applied to virgin oil. The virgin oil was characterized by its triglyceride content and their total and  $\beta$  - position fatty acids, The influence of extraction methodology on the composition of virgin olive oil was investigated using stepwise discriminant analysis. This research showed that aliphatic alcohols could be used to distinguish oils by their extraction systems.

In this research, the analytical data obtained from the various analytical techniques were classified into groups. The aim was to differentiate between the Greek oils and their adulterated mixtures and to differentiate between each level of adulteration. The statistical programs used were SIMCA and hard modelling discriminant analysis.

The analysis was carried out on the Greek oils provided by Elias SA. A detailed description of these oils is given in Table 1.11.

**Table 1.11 A detailed description of the Greek olive oil sample set provided for this research.**

Name	Place	District	Variety	Acidity	Altitude	Ripeness
D1	Crete	Chania	koroneiki	0.84	mid - mountain	semi - ripe
D2	Crete	Chania	koroneiki	0.55	plain	semi - ripe
D3	Crete	Chania	koroneiki	0.49	plain	semi - ripe
D4	Crete	Heraklion	koroneiki	0.33	mid - mountain	ripe
D5	Crete	Lassithi	koroneiki	0.35	mid - mountain	ripe
D6	Crete	Lassithi	koroneiki	0.47	mid - mountain	ripe
D7	Peloponese	Argolida	40 % tsoun + 60 %	0.80	mid - mountain	ripe
D8	Peloponese	Korinthia	patrini	0.37	mid - mountain	semi - ripe
D9	Peloponese	Lakonia	50 % koroneiki + 50 %	0.40	mid - mountain	ripe
D10	Peloponese	Lakonia	40 % koroneiki + 60 %	0.45	mid - mountain	ripe
D11	Peloponese	Lakonia	koroneiki	0.79	mid - mountain	-
D12	Peloponese	Llia	botsikoelia	0.65	mid - mountain	ripe
D13	Peloponese	Llia	koroneiki	0.51	mid - mountain	ripe
D14	Peloponese	Messinia	koroneiki	0.25	plain	ripe
D15	Peloponese	Messinia	koroneiki	0.36	mid - mountain	ripe
D16	Peloponese	Messinia	koroneiki	1.05	mid - mountain	ripe
D17	Peloponese	Messinia	koroneiki	0.98	plain	ripe
D18	Peloponese	Messinia	koroneiki	0.78	plain	ripe
D19	Evia Island	Evia	Chondrolia + Amphissa	1.62	mid - mountain	unripe
D20	Central	Fthiotida	Amphissa + Megaritikes	1.23	mid - mountain	semi - ripe
D21	Ionian	Kefalinia	koroneiki + ordinaria	0.91	mountain	ripe
D22	Ionian	Zakynthos	koroneiki	0.21	mid - mountain	ripe



## ***1.6 Project objectives***

The natural variability of olive oil due to maturity, geographical origin, climatic factors, processing and storage techniques have provided opportunities for research in both chromatographic and spectroscopic techniques. Analysis of this type of data and differentiation between authentic and adulterated samples require the use of computer - based statistical programs (Simkins and Harrison, 1995). An objective of this project was the development of a set of techniques which could be used in complement in the characterization and adulteration of extra virgin olive oils.

This research involved the study of novel methodologies for solving olive oil authentication issues as well as the replacement of traditional wet chemistry methods with faster and more efficient means of olive oil analysis. Various chromatographic techniques were investigated which included GC FAME analysis of olive oils, the direct analyses of olive oil triglycerides by high temperature GC and the separation of olive oil triglycerides by argentation SFC.

The spectroscopic techniques used in this analyses were Raman spectroscopy, mid - infrared spectroscopy and nuclear magnetic resonance. The molecular vibrations studied by Raman and mid - infrared spectroscopy are the same and in this respect these techniques provided complementary information. Proton and carbon NMR analyses of the fatty acid composition of olive oils were carried out to obtain information on the positional distribution of the fatty acids on the glycerol molecule.

The adulterant oil used in this study was sunflower oil. The adulterant oil is in itself a nutritional oil with a high linoleic content. However, its high linoleic content makes it more susceptible to oxidation and its presence in olive oil will reduce its antioxidative abilities. Its presence also changes the organoleptic qualities of olive oil and diminishes its value.

The range of sunflower adulterant concentration examined in the extra virgin olive oil were 2 - 10 % w/w. The level of adulteration of olive oil typically practised depend on the market price of the adulterants at a given time. Thus higher levels of adulteration of olive oil is found if the market price of the adulterant oil is low.

Statistical analysis of the data obtained was used to identify the relationship between the measured parameters. The statistical analysis was carried out using both Win - Discrim and Unscrambler (Camo AS, 1996). These programs were designed to classify samples by hard modelling discriminant analysis and by soft independent modelling of class analogy (SIMCA) respectively.

## CHAPTER 2

# THE CHARACTERIZATION OF OLIVE OIL BY CHROMATOGRAPHIC TECHNIQUES

### *2.1 The transesterification of triglycerides*

Fatty acids are defined in terms of saturated (those which contain no double bonds) and unsaturated (those which contain double bonds). The degree of unsaturation in an oil depends on the average number of double bonds in its fatty acids (Formo et al., 1979). In terms of triglycerides, the fatty acids contribute 94 - 96 % of the total weight of the molecule and hence are greatly influence both the physical and chemical characteristics of the triglycerides (Formo et al., 1979).

The most commonly found unsaturated fatty acids in extra virgin olive oil are palmitic, stearic, oleic and linoleic (Suarez and Mendoza, 1986). With few exceptions, naturally occurring unsaturated fatty acids are cis - isomers. Cis - isomer fatty acids, however, may be converted to trans - isomers in the course of processing which may involve heat and exposure to certain catalysts (Formo et al., 1979).

The fatty acid composition of oil is generally determined analytically by conversion of its triglycerides to mixed methyl esters (Fatty Acid Methyl Esters, FAMES) by transesterification and then followed by analysis and separation of the FAMES by GC (Formo et al., 1979). This transesterification process changes the volatility of the oil and improves the peak shape in the gas chromatogram to give a better separation (Smith, 1988).

Transesterification is the conversion of an ester to another ester by heating it with an excess of an alcohol or a carboxylic acid in the presence of an acidic or basic catalyst. In an

equilibrium reaction, either the alcohol or the acid portion of the original ester is freed (Christie, 1982). These transesterification methods are displayed in Figure 2.1.

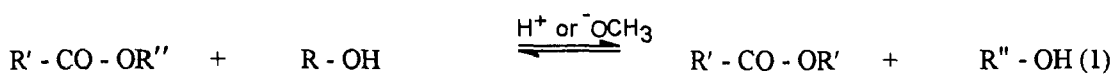


**Figure 2.1 General transesterification method (Ke-Shun, 1994)**

The equilibrium of this reaction may be shifted to the right by the addition of a large excess of alcohol or by the removal of one of the products from the reaction. The latter choice drives the reaction to near - completion (Ke-Shun, 1994). The presence of water, however, interferes with the transesterification process, since it can hydrolyze the newly formed esters to reverse the transesterification reaction. In the case of the alkali hydrolysis, this reaction is irreversible as the carboxylate anion will not react with alcohol but it will react with Na<sup>+</sup> or K<sup>+</sup> present in the reaction mixture to form a stable salt known as a soap. This alkaline process is otherwise known as saponification (Ke-Shun, 1994). These hydrolysis methods are displayed in Figure 2.2.

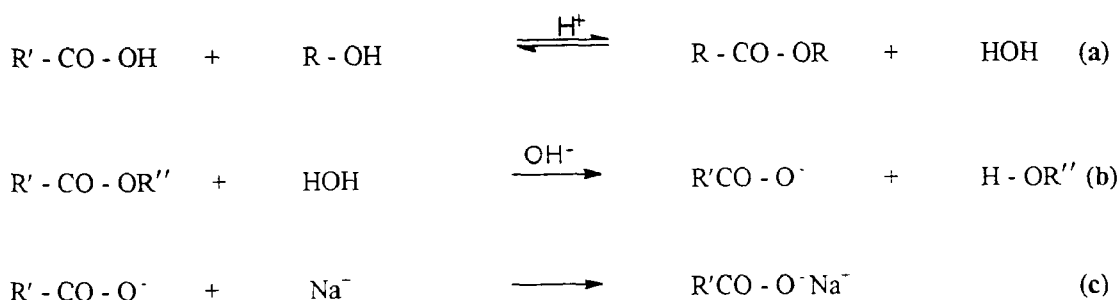


**Figure 2.2 a: acid hydrolysis; b: alkaline hydrolysis; c: saponification hydrolysis (Ke-Shun, 1994)**

There are various methods of transesterification of oils. However, the methods investigated in this study were:

- (i) The American Oil Society method (1973).
- (ii) Low temperature sulphuric acid method (M<sup>c</sup> Ginnis and Duggan, 1964).
- (iii) Base - catalyzed transesterification method using tetrahydrofuran (Christie, 1982).
- (iv) The EC reflux method (Official Journal of EC, 1991).

Acid - catalyzed transesterifications of triglycerides and esterifications of free fatty acids are carried out by heating with a large excess of anhydrous methanol in the presence of an acidic catalyst (Christie, 1982). The American Oil Society method is an example of this type of esterification. In this case, the reagent used is 10 % acetyl chloride in methanol. This reagent is produced by slowly adding acetyl chloride to methanol. However, as reviewed by Ke-Shun (1994) the reagent has limited stability and should be used immediately after its preparation. This type of acid - catalyzed transesterification was first introduced 35 years ago by Stoffel (1959), and Craske (1994) has found it to be the best general purpose reagent.

The low temperature sulphuric acid method involves the formation of a sulphuric acid complex of the lipid in ethyl ether at room temperature. Decomposition of the complex with methanol results in the direct formation of methyl esters of fatty acids (M<sup>c</sup> Ginnis and Duggan, 1964).

Base - catalyzed transesterifications proceed at a faster rate than acid - catalyzed transesterifications (Ke-Shun, 1994). Free fatty acids are not esterified, however and care

must be taken to exclude water from the reaction medium to prevent their formation as a result of hydrolysis of lipids (Mc Ginnis and Duggan, 1964). The EC reflux method and the tetrahydrofuran method are both examples of base - catalyzed transesterifications.

The preferred catalyst for base - catalyzed transesterifications is 0.5 M sodium methoxide in anhydrous methanol. This catalyst is prepared by dissolving sodium metal in dry methanol. The preparation of 0.5 M sodium methoxide is described in Figure 2.3.

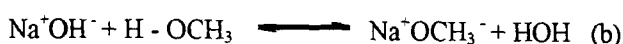
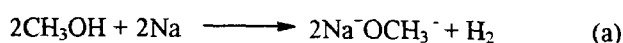


**Figure 2.3 The preparation of 0.5 M sodium methoxide (Ke-Shun, 1994)**

Bannon et al. (1982) proposed the use of sodium methoxide as an alkaline catalyst, since the use of sodium hydroxide or potassium hydroxide leads to the production of traces of water (Figure 2.3 b). As mentioned earlier, the presence of water in an alkaline transesterification reaction leads to irreversible saponification (Figures 2.2 b and 2.2 c). In order to ensure that saponification does not occur after alkaline catalyzed reactions, the reaction mixture is neutralized or washed repeatedly with water. Long storage times of the reaction mixtures should also be avoided (Ke-Shun, 1994).

Craske et al. (1988). also suggested using sodium methoxide under a refluxing temperature when samples contain long chain fatty acids, as employed in the EC reflux method. However, Christie (1982) has stated that an equally effective esterification is obtained if the reaction mixture is heated in a stoppered tube at 50 °C for a shorter time interval. This approach was adopted in the tetrahydrofuran method.

Ke-Shun (1994) has reported that the solubility of the lipids in a methanol medium also

affects the rate of the reaction. Non - polar triglycerides have poor solubility in methanol and this insolubility retards the rate at which the reaction progresses. The addition of another solvent into the reaction system, however, improves the dissolution of the triglycerides (Ke-Shun, 1994).

For all the methods used in this study the FAMES were extracted with hexane, dried with anhydrous sodium sulphate and a suitable concentration of each sample in hexane (200 - 600 ppm) was analyzed by the Perkin - Elmer autosampler gas chromatograph, using turbochrom software.

### **2.1.1 Quantitation of the transesterification of methyl esters**

As defined by Bannon et al. (1985), “*quantitative methylation is a solution of the esters obtained with a fatty acid composition representative of that of the original sample*”. According to Ke-Shun (1994) the quantitation of methylation in many methods has been associated with the completion of transesterification. However, as stated previously, the transesterification process is a reversible reaction and even in the presence of excess alcohol, the reaction does not go to completion. An equilibrium is reached at any stage between 0 % and 100 % completion of the transesterification (Ke-Shun, 1994).

Bannon et al. (1985) has stated that the main errors associated with FAMES production are; “*the failure to transesterify quantitatively; the failure to transfer esters quantitatively into an organic layer; the evaporative loss of esters during work - up or storage and the saponification of the esters after methylation when an alkaline catalyst is used.*”

These errors mainly occur in the post - reaction work - up step and have been described by Ke-Shun (1994) as a vital step in obtaining an accurate and reliable analysis. This step

*“involves neutralizing the reaction mixture, extracting the FAMEs with an organic solvent, salting out with a salt solution, washing with water, separating layers of solvents, and drying the organic layer with a drying agent”* (Ke-Shun, 1994). Many other researchers have failed to place an emphasis on this stage of analysis and have kept it to a minimum. The reason for this may be that extensive work - up may lead to losses of esters by evaporation and oxidation. This work - up stage also lengthens the operation time (Ke-Shun, 1994). Bannon et al. (1985) however, verified the importance of the work - up stage by demonstrating that significant losses in low molecular weights were reduced when the FAMEs, produced by the AOCS method using  $\text{BF}_3$  as a catalyst, were extracted under tepid conditions and shaken for more than 15 seconds.

Lepage (1988) has reported that the addition of an internal standard, prior to derivatization, can assure quantitative analysis without the requirement of the reaction going to completion. Browse (1986) also stated that losses of esters during the reaction may also be accounted for by the addition of the internal standard.

In the present study, an internal standard was added only as a correction factor for constant volume injection. The fatty acids were quantified using the internal standard calculation method. This was performed by adding a measured amount of pentadecanoic acid to each sample as an internal standard. The areas of all the peaks were then related to that of the standard. The method required calibration, with the standard also being present in the calibration sample. The calculation is shown as follows:



***The Internal Standard Calculation Method (Perkin Elmer, 1983).***

$$\text{Amount} = S \times \frac{\text{RF}_i}{\text{RFS}} \times \frac{\text{Area}_i}{\text{Area}_s} \times \frac{\text{Std amount}}{\text{Smp amount}}$$

Amount = The amount of component i

S = Scaling factor

RF<sub>i</sub> = Absolute response factor of component i

RFS = Absolute response factor of the internal standard component

Area<sub>i</sub> = Area of peak i

Area<sub>s</sub> = Peak area of the internal standard included in the analysis

Std amount = The amount of the internal standard

Smp = The quality of the analysis sample or it is set to 1

The following sections describe the procedures carried out in each of the transesterification methods studied.

**2.1.2 The American Oil Society method (1973)**

**2.1.3 Material and methods**

6 boiling tubes

50 cm<sup>3</sup> separating funnel

10 % acetyl chloride in methanol

2 % NaCl solution

Hexane (HPLC grade)

2 % NaHCO<sub>3</sub> solution

MgSO<sub>4</sub> (drying agent)

### **2.1.3.1 Procedure**

Transesterification was carried out by dissolving 130 mg of the olive oil in 2 cm<sup>3</sup> of a 10 % solution of acetyl chloride in anhydrous methanol. The mixture was then heated in an oven at 60 °C for 1 hour. Upon cooling, 4 cm<sup>3</sup> of the NaCl solution was added. The methyl esters were extracted twice with hexane (2 x 3 cm<sup>3</sup>). Both extractions were combined and washed with 2 cm<sup>3</sup> of NaHCO<sub>3</sub>.

### **2.1.4 The low temperature sulphuric acid method (M<sup>c</sup> Ginnis and Duggan, 1964)**

#### **2.1.5 Materials and methods**

125 cm<sup>3</sup> Erlenmeyer flask

Magnetic stirrer

10 cm<sup>3</sup> microburette

500 cm<sup>3</sup> separating funnel

Peroxide free diethyl ether

Sulphuric acid (conc)

Absolute methanol

NaCl solution (saturated)

35 % methanoic KOH solution

Hexane (HPLC grade)

#### **2.1.5.1 Procedure**

The olive oil sample (200 mg) was dissolved in 20 cm<sup>3</sup> of peroxide free diethyl ether in a 150 cm<sup>3</sup> flask. The mixture was stirred by means of an magnetic stirrer. Concentrated sulphuric acid (2 cm<sup>3</sup>) was then added to the stirred mixture from a 10 cm<sup>3</sup> microburette at a rate of 1 cm min<sup>-1</sup>. Absolute methanol (15 cm<sup>3</sup>) followed by methanolic KOH were added.

The mixture was then transferred to a separating funnel and water was added (150 cm<sup>3</sup>).

The methyl esters were extracted twice with hexane (2 x 15 cm<sup>3</sup>).

### **2.1.6 The base - catalyzed transesterification method using tetrahydrofuran (Christie, 1982)**

#### **2.1.7 Materials and methods**

10 cm<sup>3</sup> test tube

0.1 cm<sup>3</sup> pipette

Pasteur pipettes

1 cm<sup>3</sup> pipette

0.5 M sodium methoxide in anhydrous methanol

Glacial acetic acid

Hexane

Anhydrous sodium sulphate

#### **2.1.7.1 Procedure**

The olive oil sample (50 mg) was dissolved in tetrahydrofuran (1 cm<sup>3</sup>) in a test tube and 0.5 M sodium methoxide in anhydrous methanol (2 cm<sup>3</sup>) was added. The mixture was heated for 10 minutes at 50 °C. Glacial acetic acid (0.1 cm<sup>3</sup>) was then added, this was followed by the addition of 5 cm<sup>3</sup> of water. The required esters were extracted with hexane. The hexane layer was dried using anhydrous sodium sulphate.

### **2.1.8 The EC reflux method (Official Journal of EC, 1991).**

#### **2.1.9 Materials and methods**

100 cm<sup>3</sup> flask, with a reflux condenser with ground glass joints fitted with a soda lime tube.

50 cm<sup>3</sup> measuring cylinder

5 cm<sup>3</sup> measuring pipette

250 cm<sup>3</sup> separating funnel

200 cm<sup>3</sup> flask

Anhydrous methanol

1 % sodium methylate in methanol

Hexane (HPLC grade)

10 % NaCl solution

#### ***2.1.9.1 Procedure***

The oil sample (2 g) was placed in a 100 cm<sup>3</sup> flask with anhydrous methanol (35 cm<sup>3</sup>). A condenser was fitted and the mixture was allowed to boil under reflux for a few minutes. The heating process was stopped, the condenser was removed and 3.5 cm<sup>3</sup> sodium methylate solution was added. The reagent mixture was allowed to boil under reflux for 3 hours. The mixture was cooled and transferred to a separating funnel. Hexane (35 cm<sup>3</sup>), water (100 cm<sup>3</sup>) and the NaCl solution (6 cm<sup>3</sup>) were added. The layers were allowed to separate and the aqueous layer was transferred to a second separating funnel and extracted again with hexane (25 cm<sup>3</sup>). The combined hexane layers were extracted with water, and dried with sodium sulphate.

The derivatized samples from each of these methods were analyzed by GC using the parameters in Table 2.1

**Table 2.1 GC FAME parameters**

GC components	Parameters
Column	BPX70
Initial temp (°C)	150
Iso temp (min <sup>-1</sup> )	1.5
Ramp rate (°C min <sup>-1</sup> )	7
Temp 2 (°C)	190
Iso temp 2 (°C)	-
Temp 3 (°C)	220
Carrier	Helium
Injector	On - column
Detector	FID

## ***2.2 GC results and discussion of FAME analysis by GC***

Four methods of transesterification were investigated to find a fast and efficient method of transesterifying triglycerides to fatty acid methyl esters. The transesterifications were carried out on a sample of Kalamata extra virgin oil and the analysis was repeated four times for each method. Each analysis was carried out quantitatively and the results are shown in Table 2.2. The results were calculated as percentage weight in the oil. All the transesterified samples were analysed using a BPX70 polar column.

A typical FAME chromatogram of an extra virgin oil (Kalamata) is shown in Figure 2.4. Eight peaks were easily separated in this chromatogram. These were palmitic acid, palmitoleic acid, stearic acid, oleic acid, linoleic acid, linolenic acid, eicosenoic acid and arachidic acid. The identification of these peaks was carried out by comparison with the retention times of FAME standards.

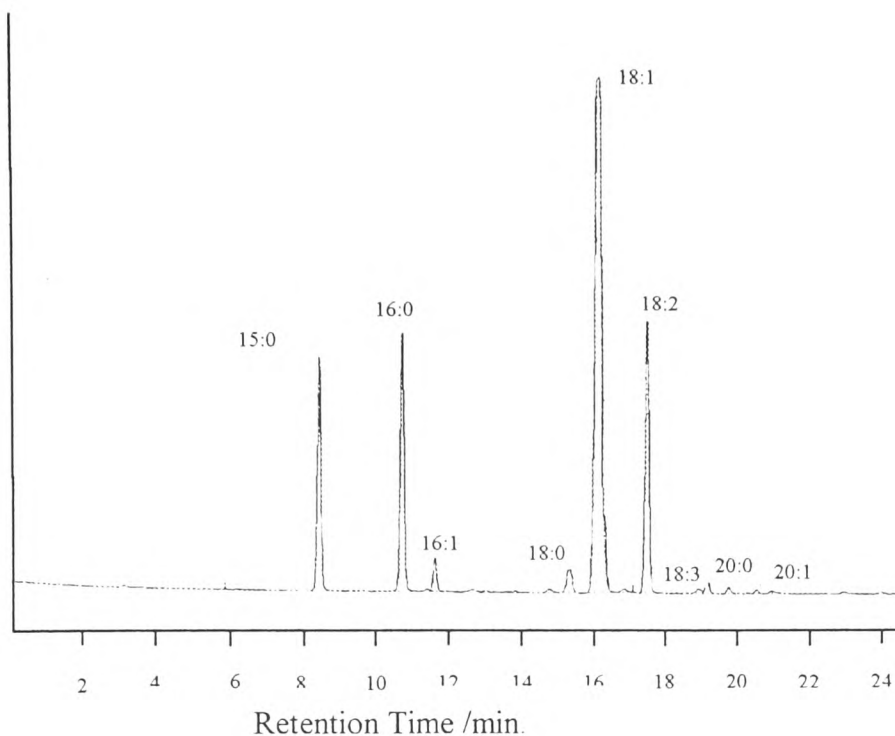


**Figure 2.4 FAME chromatogram of a Kalamata extra virgin olive oil**

15:0: pentadecanoic acid; 16:0: palmitic acid; 16:1: palmitoleic acid; 18:0: stearic acid; 18:1: oleic acid; 18:2: linoleic acid; 18:3: linolenic acid; 20:0: arachidic acid; 20:1: cis - 9 - eicosenoic acid

High yields of fatty acids were observed for the American Oil Society and the EC reflux methods. However, the repeated results lacked precision. The sulphuric acid method gave a low yield of fatty acids and showed inconsistency in the analysis of the replicate samples. The tetrahydrofuran method, on the other hand, gave a low yield for the FAMEs but was more precise than the other methods of transesterification involved in the study.

In this analysis, the exact fatty acid composition of the Kalamata extra virgin oil was not known and the true answer could not be based on the average results since each method of transesterification gave different results for each individual FAME. The mean percentages and standard deviations for each method of transesterification were estimated and are shown in Table 2.2.

All the transesterified samples were analyzed using the same chromatographic conditions,

implying that the low yields of each transesterification were possibly due to chemical error in the work - up stage of each method.

Ke-Shun (1994) has reviewed the preparation of fatty acid methyl esters extensively and has indicated that esters are frequently lost during the work - up stage in the transesterification process. It has also been stated that the standard methods of transesterification need to be improved and additional research on the factors affecting each step of FAME preparation are requisite (Ke-Shun, 1994). The results obtained in this study are in agreement with the above conclusions of Ke-Shun (1994) since rigidly following each of the procedures for the standard methods does not necessarily give the optimum yields of FAMEs.

**Table 2.2 GC FAME analysis using different methods of transesterification of Kalamata extra virgin oil (% w/w)**

Name	C16:0	C16:1	C18:0	C18:1	C18:2	C18:3	C20:0	C20:1
American oil (R1)	13.45	0.93	3.16	77.84	7.78	0.88	Tr	Tr
American oil (R2)	17.03	1.41	4.21	69.92	10.14	1.14	0.65	Tr
American oil (R3)	20.03	1.61	4.68	75.32	11.27	1.27	0.77	Tr
American oil (R4)	14.75	1.10	3.30	61.72	8.33	0.89	Tr	Tr
American oil (R5)	8.16	0.65	1.98	44.33	4.53	0.55	Tr	Tr
<b>Mean</b>	<b>14.68</b>	<b>1.14</b>	<b>3.47</b>	<b>65.83</b>	<b>8.41</b>	<b>0.95</b>	-	-
$\sigma$	4.42	0.34	0.93	13.51	2.58	0.28	-	-
EC Reflux (R1)	21.79	1.68	4.78	68.18	12.34	1.31	0.60	Tr
EC Reflux (R2)	22.28	1.70	5.00	71.64	12.64	1.36	0.78	Tr
EC Reflux (R3)	20.27	1.76	4.50	85.65	11.81	1.30	Tr	Tr
EC Reflux (R4)	16.77	1.27	4.03	72.67	9.63	0.99	Tr	Tr
EC Reflux (R5)	19.85	1.51	4.50	65.34	11.48	1.23	0.75	Tr
<b>Mean</b>	<b>20.19</b>	<b>1.58</b>	<b>4.56</b>	<b>72.70</b>	<b>11.58</b>	<b>1.24</b>	-	-
$\sigma$	2.16	0.20	0.36	7.80	1.18	0.15	-	-
Tetrahydrofuran (R1)	12.18	0.98	3.03	46.83	7.29	0.86	Tr	Tr
Tetrahydrofuran (R2)	12.73	1.02	3.04	48.63	7.64	0.85	0.62	Tr
Tetrahydrofuran (R3)	10.97	0.92	2.76	47.59	6.44	0.79	0.44	Tr
Tetrahydrofuran (R4)	11.32	0.88	2.52	44.31	6.56	0.78	0.37	Tr
Tetrahydrofuran (R5)	12.42	1.00	3.10	47.93	7.44	0.87	0.83	Tr
<b>Mean</b>	<b>11.92</b>	<b>0.96</b>	<b>2.89</b>	<b>47.06</b>	<b>7.07</b>	<b>0.83</b>	-	-
$\sigma$	0.75	0.06	0.24	1.69	0.54	0.04	-	-
H <sub>2</sub> SO <sub>4</sub> (R1)	9.93	0.78	2.14	33.86	5.19	0.56	Tr	Tr
H <sub>2</sub> SO <sub>4</sub> (R2)	5.67	0.46	1.41	24.98	3.30	0.36	Tr	Tr
H <sub>2</sub> SO <sub>4</sub> (R3)	6.76	0.41	2.29	23.27	2.73	0.30	Tr	Tr
H <sub>2</sub> SO <sub>4</sub> (R4)	6.07	0.46	1.34	25.02	3.14	0.34	Tr	Tr
H <sub>2</sub> SO <sub>4</sub> (R5)	8.10	0.65	1.85	30.50	4.49	0.49	Tr	Tr
<b>Mean</b>	<b>7.30</b>	<b>0.55</b>	<b>1.81</b>	<b>27.52</b>	<b>3.77</b>	<b>0.41</b>	-	-
$\sigma$	1.73	0.16	0.42	4.47	1.03	0.11	-	-

R1 - R5: Replicate samples in each method. Tr: trace amount of the fatty acid present.



In light of the results obtained for the FAME analysis (Table 2.2) the tetrahydrofuran method was adopted as it appeared to give the most reproducible results even though yields were low for FAME analysis. The method was also quick and easy to carry out.

A further analysis was carried out to verify the precision of the tetrahydrofuran method. Ten replicate samples of Kalamata extra virgin oil was transesterified using this method. The results of this analysis is shown in Table 2.3.

As previously observed (Table 2.2) the precision of this method was good. However, the yield was low, even lower than for the replicate tetrahydrofuran transesterification samples used previously (Table 2.2).

**Table 2.3. Repeated results for Kalamata extra virgin olive oil using the tetrahydrofuran transesterification method (percentage area)**

Name	C16:0	C16:1	C18:0	C18:1	C18:2	C18:3	C20:0	C20:1
Tethydrofuran (R1)	11.16	0.93	2.55	36.65	6.39	0.72	0.22	0.11
Tethydrofuran (R2)	10.75	0.85	2.47	34.48	6.11	0.67	0.18	0.13
Tethydrofuran (R3)	8.89	0.59	1.99	31.08	5.03	0.56	0.20	0.11
Tethydrofuran (R4)	9.87	0.78	2.22	34.90	5.60	0.61	0.18	0.11
Tethydrofuran (R5)	9.86	0.81	2.16	37.15	5.49	0.57	0.19	0.11
Tethydrofuran (R6)	10.54	0.87	2.20	36.62	5.96	0.66	0.18	0.12
Tethydrofuran (R7)	10.77	0.90	2.20	36.00	6.01	0.68	0.16	-
Tethydrofuran (R8)	10.24	0.69	2.13	33.95	5.70	0.64	0.17	0.12
Tethydrofuran (R9)	10.17	0.85	2.13	34.96	5.76	0.64	0.20	0.12
Tethydrofuran(R10)	10.16	0.70	4.10	35.53	5.58	0.60	0.17	-
Mean	10.24	0.78	2.42	35.13	5.76	0.64	0.19	-
$\sigma$	0.63	0.11	0.61	1.76	0.38	0.05	0.02	-

R1 - R10: Replicate samples in each method.

Coefficients of variation (CV) were used in the comparison of the precision of the replicate results. The coefficient of variation (also known as relative standard deviation) describes the distribution and spread of the data (Adams, 1995). It is calculated by dividing the error

estimate by the estimate of the absolute value of the measured quantity and multiplying by 100 (Miller and Miller, 1993). The measure describes the random error of the analyte without the need to consider the analytes concentration or weight (Haswell, 1992). In this analysis the CV of all the peaks were significantly high (Figure 2.3). The highest percentages were observed for palmitoleic acid, stearic acid, linolenic acid, arachidic acid and eicosenoic acid. However, these peaks were relatively small compared to peaks of palmitic acid, oleic acid and linoleic acid. Also the separation between palmitic acid and palmitoleic acid and between stearic acid and oleic was not baseline. This lack of separation obviously influenced the precision in the repeatability test. The results of this test are shown in Table 2.4.

**Table 2.4. Coefficient of Variation for the tetrahydrofuran method of transesterification of Kalamata extra virgin olive oil**

Sample	Mean	Standard deviation	Coefficient of variation of test acceptability of variation on values/ %
C16:0	10.24	0.63	6.15*
C16:1	0.80	0.11	13.75*
C18:0	2.42	0.61	25.20*
C18:1	35.13	1.76	5.01*
C18:2	5.76	0.38	6.60*
C18:3	0.64	0.05	7.81*
C20:0	0.23	0.13	56.52*
C20:1	0.13	0.02	15.38*

Fatty acids of replicate samples that were too variable to be accepted.

A GC FAME analysis was also carried out on the Kalamata extra virgin olive oil samples adulterated with 5 % w/w and 10 % w/w sunflower oil. The samples were transesterified using the tetrahydrofuran method. The results of this GC analysis are calculated as area percentage in Table 2.5. As sunflower oil is a high linoleic oil, it is unsurprising that the linoleic acid content of the extra virgin oil increased linearly with the amount of sunflower oil adulterant (Table 2.5). In contrast, the oleic acid content of the extra virgin oil

decreased with the addition of higher concentrations of sunflower oil. In this analysis separate peaks were not observed for palmitoleic acid, arachidic acid and eicosenoic acid. The lack of formation of these methyl esters was probably a reflection of how the sodium methoxide was prepared prior to the analysis. In this case the reagent was prepared in the laboratory with methanol, while in all the other analysis in this study super - seal moisture - free, sodium methoxide was used. This further emphasizes the fact that base - catalyzed transesterifications are greatly affected by the presence of moisture in the reaction.

**Table 2.5 GC FAME analysis of transesterified adulterated samples of Kalamata extra virgin oil (area percentage)**

Name	16:0 %	18:0 %	18:1 %	18:2 %	18:3 %
Extra virgin olive	9.99	3.24	78.20	7.86	0.71
Extra virgin olive (R1)	10.47	4.00	77.86	7.66	-
Extra virgin olive (R2)	10.58	2.43	77.45	8.45	-
Adult./5 %	10.19	3.71	76.24	9.86	-
Adult./5 % (R1)	9.94	3.51	76.31	10.25	-
Adult./5 % (R2)	10.09	3.27	76.38	10.27	-
Adult./10 %	9.83	3.30	74.29	12.57	-
Adult./15 %	10.01	3.71	71.95	14.33	-
Adult./15 % (R1)	10.46	3.67	71.21	14.66	-
Adult./15 % (R2)	9.60	3.34	72.52	14.54	-

Adult./5 %: extra virgin olive oil adulterated with 5 % sunflower oil; Adult./10 %: extra virgin olive oil adulterated with 10 % sunflower oil; Adult./15 %: extra virgin olive oil adulterated with 15 % sunflower oil; R1, R2: replicate samples.

A FAME analysis of the Greek extra virgin olive oil samples was also conducted. Again the oils were transesterified using the Tetrahydrofuran method of transesterification (using super - seal sodium methoxide) and the GC analysis was carried out on a BPX70 column. The fatty acid composition of these oils were recorded as area percentage in Table 2.6.

These results were compared with the GC FAME results of the same oils, obtained from a Greek laboratory. The transesterification method used in this case was BF<sub>3</sub> which is the transesterification method adopted by the British Standards Institution (BSI, 1980). The Greek analysis of these oils was also carried out on CP - Sil 88 column.

The GC FAME results obtained from Greece were calculated as area percentages without an internal standard correction factor. Thus, the results from this research were estimated accordingly so that a comparison could be drawn between the two methods. The results of these inter - laboratory results are shown in Table 2.6 and Table 2.7.

**Table 2.6 FAME analysis of Greek oils by GC (area percentage report)**

Sample	D1	D2	D3	D4	D5	D6	D7	D8	D9	D10	D11
C14:0		-	-		-	-					
C16:1	0.80	1.13	0.93	0.69	0.94	0.95	2.02	0.75	1.01	0.79	1.02
C16:0	13.45	14.73	14.85	12.96	13.64	14.24	17.78	12.05	14.67	12.73	14.78
C18:0	3.22	2.92	3.12	3.18	3.14	2.86	2.59	3.29	2.94	3.33	3.04
C18:1	72.13	71.07	71.67	72.97	72.89	72.88	55.93	73.04	72.10	74.49	69.67
C18:2	8.58	8.37	7.62	8.57	8.50	7.26	19.74	8.24	7.45	7.01	9.80
C20:0	0.92	0.83	0.85	0.82	0.95	0.91	1.10	0.71	0.92	0.76	0.25
C20:1	0.59	0.56	0.59	0.53	0.55	0.53	0.48	0.56	0.56	0.55	0.91
C18:3	0.30	0.37	0.36	0.35	0.34	0.37	0.36	0.36	0.36	0.35	0.55
Sample	D12	D13	D14	D15	D16	D17	D18	D19	D20	D21	D22
C14:0	-	-	-	-	-	-	-	-	-	-	-
C16:1	0.93	0.96	0.89	0.92	0.97	0.85	0.74	0.99	1.32	1.61	1.45
C16:0	13.20	14.93	13.55	14.26	14.34	14.83	12.81	14.37	18.96	20.42	18.42
C18:0	2.69	3.40	3.40	3.06	3.57	2.99	2.28	2.53	3.62	4.26	4.29
C18:1	73.45	68.97	69.69	71.54	69.66	73.80	76.33	66.86	54.53	59.72	62.65
C18:2	7.73	9.78	10.33	8.18	9.16	6.18	6.19	13.12	19.08	11.28	10.11
C20:0	0.99	1.02	1.27	1.16	1.35	0.48	0.93	1.28	1.40	1.32	1.72
C20:1	0.55	0.61	0.60	0.55	0.63	0.53	0.41	0.50	0.62	0.81	0.80
C18:3	0.37	0.33	0.29	0.32	0.30	0.33	0.29	0.33	0.47	0.58	0.51

**Table 2.7 Greek results of FAME analysis by GC (area percentage report)**

Sample	D1	D2	D3	D4	D5	D6	D7	D8	D9	D10	D11
C14:0	0.02	-	-	0.02	-	-					0.02
C16:1	0.02	-	-	-	-	-					
C16:0	12.84	14.26	13.33	11.61	12.81	13.26	17.76	11.65	13.28	11.72	13.87
C17:0	0.15	0.17	0.14	0.18	0.18	0.15	0.09 -	0.16	0.14	0.48	0.16
C18:0	2.79	2.53	2.81	2.73	2.69	2.26	2.11	2.79	2.44	2.70	2.83
C18:1	75.40	74.00	75.40	76.69	75.13	76.23	61.43	76.26	76.13	77.44	73.10
C18:2	7.09	7.46	6.59	7.16	7.47	6.37	17.19	7.77	6.40	6.33	8.36
C20:0	0.52	0.44	0.53	0.48	0.46	0.42	0.40	0.42	0.45	0.43	0.49
C20:1	0.32	0.28	0.32	0.31	0.29	0.40	0.24	0.27	0.30	0.28	0.28
C18:3	0.68	0.73	0.69	0.65	0.81	0.77	0.79	0.68	0.69	0.64	0.71
C22.0	0.18	0.13	0.18	0.17	0.15	0.14	-	-	0.16	-	0.17
Sample	D12	D13	D14	D15	D16	D17	D18	D19	D20	D21	D22
C14:0	0.02	0.02	0.03	0.02	-	-	-	-	-	-	0.02
C16:0	12.82	12.70	12.83	13.00	13.50	13.36	13.03	12.24	12.98	13.95	12.00
C17:0	0.06	0.06	0.06	0.07	0.11	0.10	0.06	0.11	0.06	0.06	0.06
C16:1	0.10	0.07	0.09	0.08	0.07	0.10	0.16	0.20	0.10	0.09	0.08
C18:0	2.49	2.85	3.21	2.77	3.02	2.44	2.53	2.31	2.37	2.70	2.81
C18:1	75.68	74.48	72.49	75.21	73.52	76.90	76.48	72.57	70.36	74.70	76.67
C18:2	6.98	8.05	9.20	6.95	7.76	5.39	6.07	10.83	12.44	6.79	6.20
C20:0	0.49	0.52	0.58	0.53	0.53	0.46	0.50	0.44	0.44	0.50	0.54
C20:1	0.33	0.31	0.30	0.31	0.31	0.31	0.36	0.38	0.35	0.35	0.38
C18:3	0.84	0.75	0.99	0.85	0.99	0.76	0.66	0.77	0.76	0.68	1.02
C20:2	-	-	-	-	-	-	-	-	-	-	0.04
C22.0	0.18	0.18	0.21	0.19	0.18	0.16	0.18	0.14	0.14	0.16	0.20

Certain discrepancies were observed between both analysis. The fatty acids myristic acid heptadecanoic acid and behenic acid were clearly present in the results obtained from Greece whereas they were absent in the results obtained in this study. These differences were possibly influenced by the type of transesterification method used in each analysis.

A paired Student's t - Test was also carried out on the results of each of these analysis to test how significant the difference between each of these analysis were. In this test the null hypothesis of no significant difference between the two methods of analysis was adopted.

The mean of the differences of the two methods was tested to see if they differed significantly from zero. The five main peaks found in olive oil were used in this test. These were palmitic acid, stearic acid, oleic acid, linoleic acid and linolenic acid. In each case significant differences between both laboratory results were observed. The result of this test are shown in Table 2.8.

**Table 2.8 Paired Student's t - test on the GC analysis of the oil samples (D1 - D22)**

FAME	Mean of differences	SD of differences	PAIRED t - TEST value
16:0	26.34	1.96	62.91**
18:0	8.57	0.42	96.02**
18:1	- 81.91	4.22	91.09**
18:2	29.23	1.52	90.36**
18:3	- 8.11	0.14	270.00**

\*\* results significantly different at 99 % probability level.

For (n-1) degrees of freedom the critical value of t was 2.85 at a 99 % probability level. Since this calculated value of t for each methyl ester is far greater than its critical value the null hypothesis was rejected and the methods were shown to be significantly different.

The true fatty acid composition of each of these samples were unknown thus neither analysis can be considered to be the more accurate. The comparison of these results were indicative of how inconsistent GC FAME analysis was in the analysis of the same olive oil samples. Craske's (1993) study on the separation of instrumental and chemical errors of oils by oil has further shown inconsistencies in GC FAME analysis of oils. Here, thirty five analysts participated in the transesterification and subsequent GC FAME analysis of a standard triglyceride mixture. The methods of transesterification and experimental conditions were left to the analysts discretion. Craske (1993) reported from this study that only four analysts achieved acceptable grades of analysis. Thus, this study further

highlighted the irregularity of GC FAME method and further stressed the need for a more direct method of analyses of triglycerides present in olive oils.

### ***2.3 GC analysis of the triglycerides of the Greek oils by total carbon number and by degree of unsaturation***

As stated previously group separation of triglycerides has been achieved using non - polar silicone phases while the separation according to degree of unsaturation requires a column of quarter polarity (Hinshaw, 1986).

The type of injection system used in the analysis of triglycerides is critical. Cool on - column has being reported as the preferred technique since it reduces thermal decomposition and mass discrimination (Hinshaw, 1986).

In this study the GC analysis of the oil triglycerides by total carbon number (TCN) were carried out on a BPX5 column (12 m x 0.53 mm I.D.). This analysis was carried out on a manual GC in two different injection modes to compare the efficiency of each technique. These techniques were the hot evaporative injection technique and the cool on - column technique. The cool on - column injector used in this case was a SGE OC1 - 5 on - column injector.

Further analysis on the olive oil triglycerides was carried out on the Perkin Elmer autosampler gas chromatograph. In this case the injection mode was set - up for on - column and the injector was set to oven temperature programming, which meant that the temperature of the injector lapsed behind the temperature of the oven program by 5 °C throughout the analysis. This gave a similar effect to the cool on - column injector.

Finer structure in the separation of the triglyceride carbon number peaks (according to the

number of unsaturated fatty acid in the triglyceride molecule) was attempted on a narrower bore and longer BPX5 column (25 m x 0.32 mm I.D.).

The separation of the triglycerides by degree of unsaturation was also investigated using a DB<sup>m</sup> - 17ht column. The injector was cooled by an external device to keep the injector cool at the point of sample injection.

Triglyceride standards representing the natural variation of triglycerides in olive oil were also prepared and analyzed by the Perkin Elmer autosampler gas chromatograph. The peak area data from this analysis were statistically manipulated to try to predict the natural variation of triglycerides in unknown olive oils.

The following section describes the methods and GC parameters used in each of the GC analyses of olive oil triglycerides.

### 2.3.1 Materials and methods

**Table 2.9 GC parameters for the triglyceride analysis of oils by total carbon number (TCN)**

GC components	Parameters
Column	BPX5
Initial temp (°C)	100
Iso temp (°C)	0.5
Ramp rate (°C min <sup>-1</sup> )	45
Temp 2 (°C)	280
Ramp rate (°C min <sup>-1</sup> )	5
Temp 3 (°C)	360
Carrier (psi)	Helium
Injector	Oven programmed/on - column
Detector	FID



**Table 2.10 GC parameters for the triglyceride analysis of oils by TCN using BPX5 column (25 mm x 0.32 ID), precolumn BPX5 (25 mm x 0.53 ID)**

GC components	Parameters
Column	BPX5 (25 mm x 0.32 ID)
Initial temp (°C)	100
Ramp rate (°C min <sup>-1</sup> )	35
Temp 2 (°C)	360
Time	20
Carrier (psi)	Helium (25)
Injector	Oven programmed on - column
Detector	FID

**Table 2.11 GC parameters for the triglyceride analysis of oils by degree of unsaturation**

GC Components	Parameters
Column	DB17HT
Initial temp (°C)	250
Iso temp (°C)	—
Ramp rate (°C min <sup>-1</sup> )	5
Temp 2 (°C)	365
Iso temp 2 (°C)	1
Helium (psi)	40
Injector	Cool on - column
Detector	FID

### *2.3.1.1 Procedure*

In all the GC triglyceride analysis the oil samples were prepared in hexane (3000 ppm) and tripentadecoin was used as an internal standard.

### *2.3.1.2 Partial least squares regression application on the triglyceride olive oil standards*

In partial least squares regression, models are developed for **X** and **Y** matrices simultaneously to find the latent variables in **X** that will best predict the latent variables in **Y** (Camo AS, 1996). This model is then used to predict **Y** variable in unknown samples.

In this analysis, standard triglyceride standards were prepared according to natural variation of triglycerides found in olive oils. This natural variation is described in Table 2.12 and the coded matrix of this variation is shown in Table 2.13.

**Table 2.12 Design matrix (uncoded) for GC analysis of triglyceride mixtures (mg dm<sup>-3</sup>)**

Run	OOP	POL	OOO	OOL	OOS
1	1050	275	2100	400	150
2	750	275	2100	250	150
3	1350	275	2100	550	150
4	1050	200	2100	400	50
5	750	200	2100	250	50
6	1350	200	2100	550	50
7	1050	350	2100	400	250
8	750	350	2100	250	250
9	1350	350	2100	550	250
10	1050	275	1800	400	150
11	750	275	1800	250	150
12	1350	275	1800	550	150
13	1050	200	1800	400	50
14	750	200	1800	250	50
15	1350	200	1800	550	50
16	1050	350	1800	400	250
17	750	350	1800	250	250
18	1350	350	1800	550	250
19	1050	275	2400	400	150
20	750	275	2400	250	150
21	1350	275	2400	550	150
22	1050	200	2400	400	50
23	750	200	2400	250	50
24	1350	200	2400	550	50
25	1050	350	2400	250	250
26	750	350	2400	250	250
27	1350	350	2400	550	250

**Table 2.13 Design matrix (coded) for GC analysis of triglyceride mixtures**

Run	OOP	POL	OOO	OOL	OOS
1	0	0	0	0	0
2	-1	0	0	-1	0
3	+1	0	0	0	0
4	0	-1	0	0	-1
5	-1	-1	0	-1	-1
6	+1	-1	0	+1	-1
7	0	+1	0	0	+1
8	-1	+1	0	-1	+1
9	+1	+1	0	+1	+1
10	0	0	-1	0	0
11	-1	0	-1	-1	0
12	+1	0	-1	+1	0
13	0	-1	-1	0	-1
14	-1	-1	-1	-1	-1
15	+1	-1	-1	+1	-1
16	0	+1	-1	0	+1
17	-1	+1	-1	-1	+1
18	+1	+1	-1	+1	+1
19	0	0	+1	0	0
20	-1	0	+1	-1	0
21	+1	0	+1	+1	0
22	0	-1	+1	0	-1
23	-1	-1	+1	-1	-1
24	+1	-1	+1	+1	-1
25	0	+1	+1	0	+1
26	-1	+1	+1	-1	+1
27	+1	+1	+1	+1	+1

The aim of this analysis was to carry out a PLS regression on samples 1 - 16 (Table 2.12).

The X variable described the individual concentrations of standards present in the

mixture. These were OOP, POL, OOO, OOL and OOS. The Y variable represented by the peaks area obtained from the GC analysis of these standard mixtures. This PLS model was used to try and predict the peak areas of the samples 17 - 23. A comparison of the true peak areas of samples 17 - 23 with the prediction set was indicative of the performance of the prediction.

In practice, this analysis did not prove effective. The GC analysis of the standard triglycerides did not result in sufficient separation of the individual triglycerides present in the mixture. The TCN GC analysis of the triglyceride standard mixtures resulted in the separation of two peaks in the chromatogram. The former peaks represented the triglycerides OOP and POL (peak 3) while the latter represented the triglycerides OOO, OOL and OOS (peak 4). The peak area of each triglyceride was divided by the peak area of the internal standard and these results are shown in Table 2.14.

**Table 2.14 GC analysis of triglycerides mixtures by TCN (ISTD response area )**

Run	Peak 1	Peak 2	Peak 3	Peak 4
1	-	0.05	3.06	5.67
2	0.04	0.04	2.54	5.23
3	0.05	0.05	2.98	4.94
4	0.03	0.06	4.07	5.87
5	0.00	0.04	2.52	4.72
6	0.03	0.05	3.85	5.48
7	0.05	0.05	3.53	4.65
8	0.05	0.04	2.70	4.69
9	-	0.05	4.04	6.30
10	0.04	0.20	3.27	5.14
11	0.04	0.11	3.04	5.44
12	-	0.06	4.00	5.40
13	0.03	0.04	2.82	4.68
14	-	0.11	2.43	4.55
15	0.02	0.07	2.24	2.92
16	0.06	0.05	4.13	5.92
17	0.05	0.04	2.46	4.34
18	0.04	0.05	3.94	5.24
19	0.07	0.12	6.65	10.77
20	-	0.03	2.48	5.56
21	0.04	0.06	4.42	6.03
22	0.04	0.04	3.26	5.71
23	-	0.03	1.97	5.41
26	0.04	0.03	2.40	5.55

### ***2.4 Discussion of GC triglyceride results***

The analysis of olive oil triglycerides was investigated on a gas chromatograph by cool on - column injection and by the hot injector evaporative technique. Degradation and decomposition of the oil triglycerides was clearly observed in the chromatogram depicting the hot evaporative techniques (Figure 2.5) while no such observation was made in the chromatogram using the cool on - column technique (Figure 2.6).

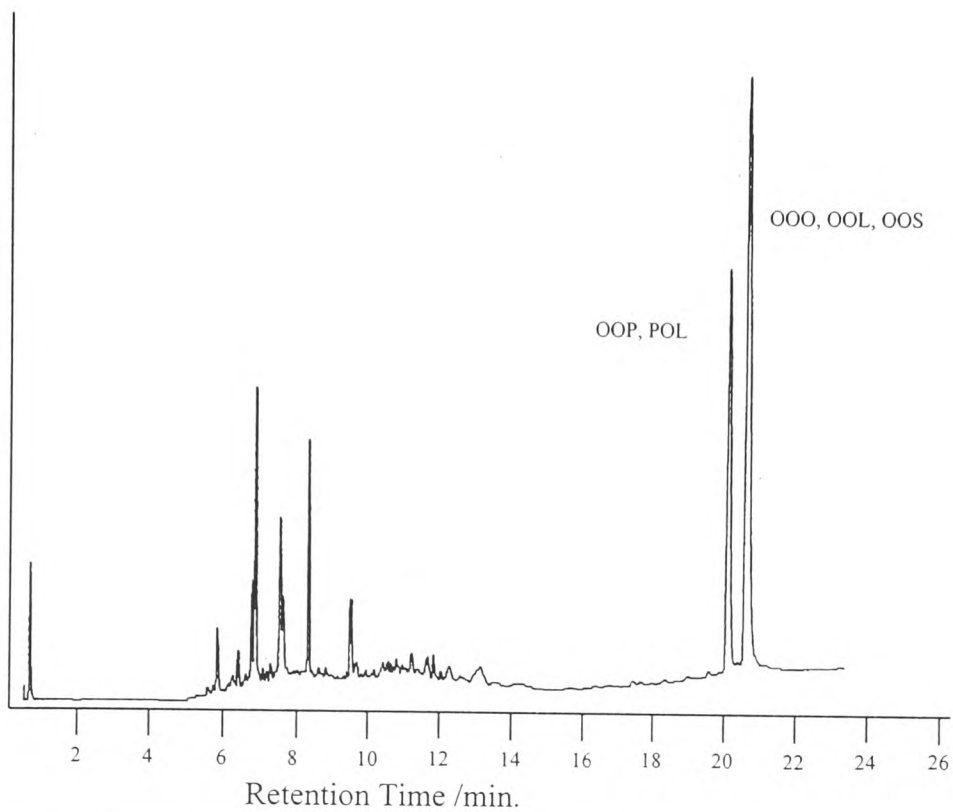


**Figure 2.5 GC analysis of an olive oil by TCN using the hot evaporative injection technique**

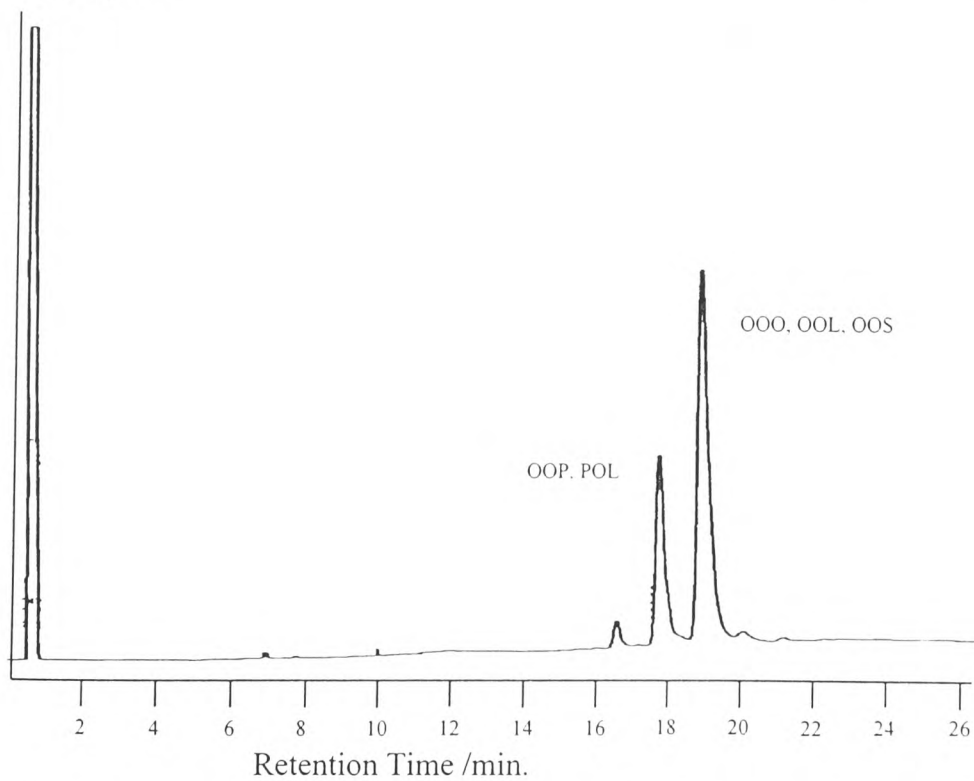


**Figure 2.6 GC analysis of an olive oil by TCN using the cool on - column injection technique**

The Perkin Elmer autosampler gas chromatograph using on - column injection with an oven programmed injector ensured consistency in injection volume and was used for further analysis of the triglycerides by TCN. The TCN separation of an olive oil on the non - polar column on the Perkin Elmer autosampler gas chromatograph is shown in Figure 2.7. The GC analysis of the oil triglycerides by total carbon number (TCN) were carried out on a BPX5 column (12 m x 0.53 mm I.D.).

In this figure the chromatogram is dominated with two peaks (peak 3 and 4). Two other minor peaks are observed but it was difficult to differentiate these peaks from the base - line (peak 1 and peak 2).

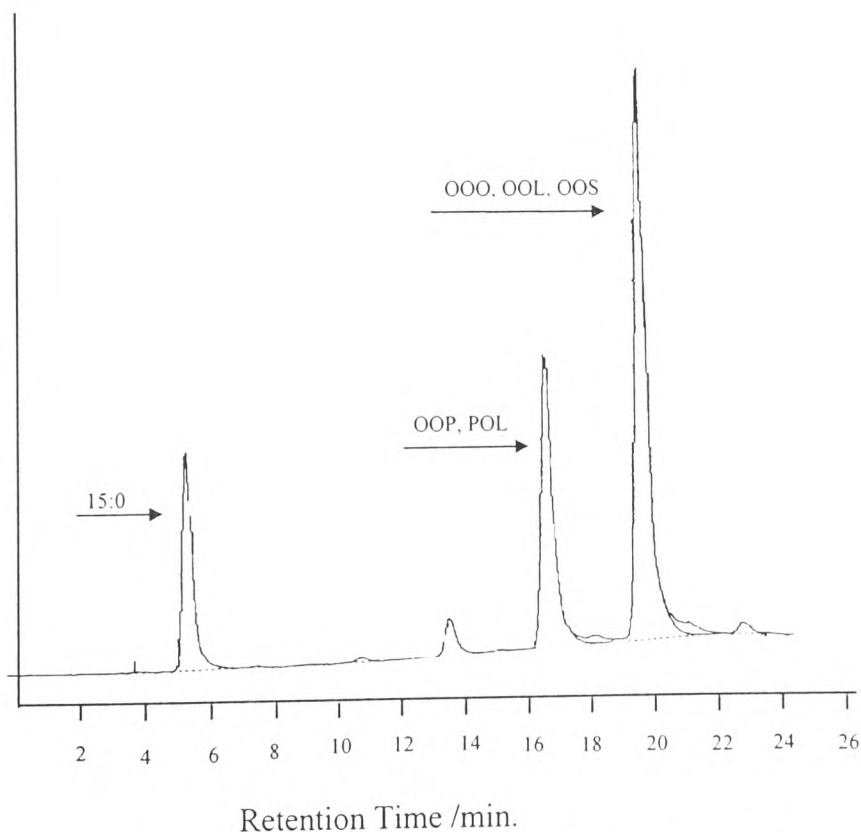


**Figure 2.7 GC chromatogram of olive oil by TCN separation using the Perkin Elmer auto sampler**

A capillary BPX5 column (0.32 ID x 25 mm) was used to try and further separate the



carbon number peaks by the number of unsaturated fatty acids in the triglyceride molecule. However the Perkin Elmer autosampler was not configured for a capillary column and a retention gap of 0.53 mm internal diameter was required for its installation. The problem with this analysis was the fact that an activated pre - column (BPX5, 0.53 ID) was used instead of a deactivated column. This meant that the sample remained on the column for longer which resulted in less resolution and peak splitting.

The separation of triglycerides by degree of unsaturation were investigated in place of carbon number separation. The information provided by TCN separation was limited and the successful separation of the triglycerides by degree of unsaturation would provide more enlightening data which could be manipulated statistically using partial least squares regression. The separation of the triglycerides by degree of unsaturation was carried out on a capillary DB<sup>m</sup> - 17ht column. This was installed in the Perkin Elmer autosampler using a deactivated precolumn. As stated previously, the majority of the literature has reported that the separation of triglycerides by degree of unsaturation requires a column of quarter polarity, at temperatures above 250 °C, combined with a moveable on - column injector (Trautler, 1987).

In order to try and achieve similar conditions in this research, carbon dioxide was used as an potential coolant to cool the injector prior to injection. This approach however, proved unsuccessful. No peaks were observed in the chromatograph which indicated that the olive oil sample was not going on the column in a liquid state. To further investigate this phenomenon the column was retested with the conditioning standard mixture that was supplied with the column. This standard consisted of mixture polar and non polar compounds. The mixture, run under conditions with the injector at 100 °C, was

successfully resolved. This indicated that the column was working efficiently and that the sample was not lost due to possible leaks in the precolumn connection. This suggested that the carbon dioxide failed to cool the injector at the point of injection at temperature as high as 250 °C which was requisite in the analysis of triglycerides. This analysis further emphasized the importance of a moveable cool on - column injector in the analysis of high molecular weight triglycerides. Analysis of the triglycerides was also carried out using a hot detector system but this failed to give any peaks on the chromatogram.

## ***2.5 Conclusion***

The factors affecting the quantitative analysis of FAMES included the type of lipids being derivatized, the concentration of the reagents, the presence of an organic solvent, reaction time and temperature and the presence of water in the reaction. Post reaction work - up also effected the quantitative recovery of FAMES. The quantitative transfer of FAMES into an organic layer without evaporative losses and side effects was difficult (Ke-Shun, 1994). The transesterification method investigated in this method produced erratic results for the analysis of the same olive oil samples.

The direct analysis of triglycerides by total carbon was successful by GC. However, this information was not sufficient in itself to classify the individual triglycerides of the olive oils. The necessary apparatus for the analysis of triglycerides by degree of unsaturation, by high temperature GC was not available for this research and therefore the application of this analysis was limited. This limited application of high temperature GC, without the necessary moveable on - column injector, led to the investigation of argentation SFC as a potential technique for the separation of triglycerides by degree of unsaturation.

## CHAPTER 3

# SUPERCritical FLUID EXTRACTION AND SUPERCritical FLUID ARGENTATION CHROMATOGRAPHY ANALYSIS OF VARIOUS OILS

### 3.1 *Supercritical fluid argentation chromatography*

Argentation SFC was investigated as a potential technique in the separation of a variety of oils and also as a technique to detect sunflower oil adulteration in olive oils.

Chromatographic separation in argentation SFC is based on the formation of charge - transfer complexes between silver ions and alkenes thus providing selectivity in the separation of triglycerides based on the degree and position of unsaturation within the molecule (Demirbuker and Blomberg, 1990).

The formation of a charge - transfer complex requires the overlap of the filled  $\pi$  orbital of the alkene with the free s orbital of silver ( $\sigma$  bond, Figure 3.1 a) and the overlap of the vacant antibonding  $\pi$  orbital of the alkene with filled d orbitals of silver ( $\pi$  bond, Figure 3.1 b) (Dewar, 1952). A silver charged transfer complex is shown in Figure 3.1.

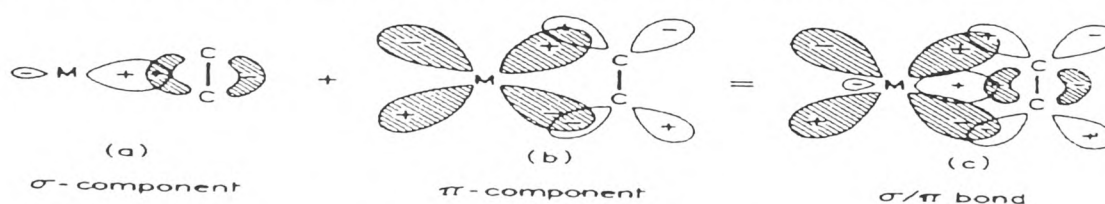


**Figure 3.1** The formation of charge - transfer complexes between silver ( $M^+$ ) and alkenes

*"The strength of the complex is determined by the accessibility of electrons in the filled orbitals and by the steric inhibition of these orbitals"* (Demirbuker and Blomberg, 1990).

The mobile phase used in this analysis was carbon dioxide - acetonitrile - isopropanol in the ratio of 92.8:6.5:0.7. Acetonitrile is added as a dynamic modifier since the cyano group present in acetonitrile is thought to form complexes with silver ions and thereby prevent the complexation of the solute with the silver ions (Demirbaker and Blomberg, 1990). Isopropanol was added to the mobile phase to improve the solubility of carbon dioxide in acetonitrile.

As stated in Chapter 1 this type of supercritical fluid chromatography was first introduced by Demirbaker and Blomberg (1990, 1991) in the study of lipids. This study differed from that performed by Demirbaker and Blomberg (1990, 1991) in that packed standard sized columns (250 mm x 4.6 mm ID) connected in series were used instead of micropacked columns (290 mm x 0.25 mm ID). The column material consisted of a silica - based cation exchanger impregnated with silver nitrate.

Various oils were analyzed by this method. These included extra virgin olive oil, sunflower oil, soya oil, sesame oil, walnut oil, a mixture of sunflower and olive oil and Tesco vegetable oil. The authentic Greek oils and their 10 % adulterated mixtures were also analyzed by this method. Two methods of detection were investigated. These were UV and evaporative light scattering.

### **3.1.1 Materials and methods**

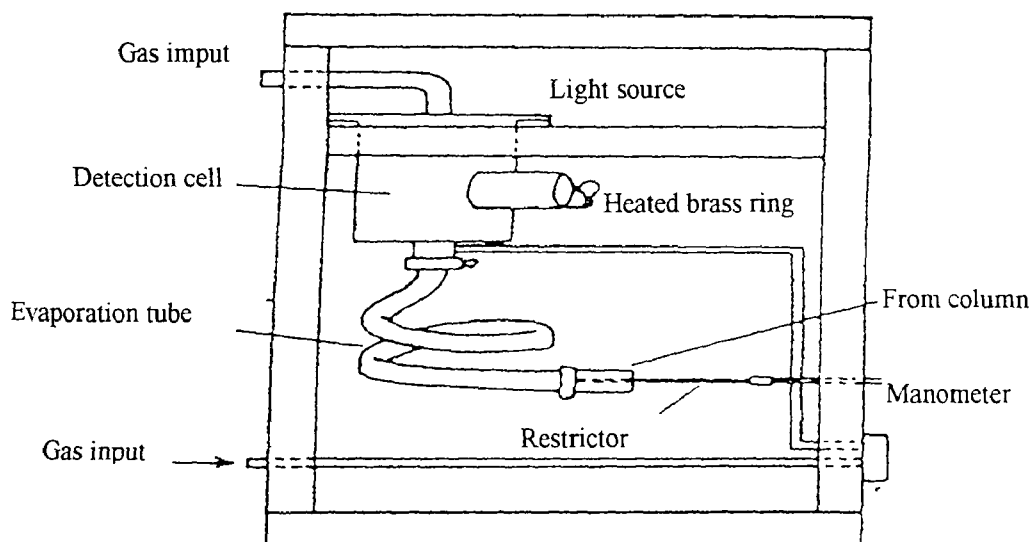
The original olive oils were supplied from Greece, other seed oils were purchased in a local supermarket. The high purity solvent, hexane, was supplied from Aldrich.

### 3.1.1.1 Procedure

The samples (authentic oils and 10 % w/w adulterated mixtures of olive oil) were prepared in hexane. These were subsequently analyzed according to the parameters outlined in Table 3.1.

The pump head of the SFC instrument was cooled to improve pump efficiency. Sample injections were made via a Rheodyne 5125 valve injector (25 -  $\mu$ l loop). In the operation of the light scattering detector modifier was added to the carbon dioxide using a second Gilson pump and the temperature of the column was controlled by a thermostated oven. The chromatograph was coupled to the detector via a low dead volume T connector and the regulator valve. The regulator valve was then attached to the back pressure regulator which in turn was linked to the nebulizer.

The diagram illustrated in Figure 3.2 gives a detailed description of the type of light scatter



used.

Figure 3.2 Schematic diagram of a light scattering detector

**Table 3.1 SFC parameters using UV detection/light scattering detection**

SFC components	Parameters
Column	2 x (10 $\mu$ m Nucleosil SA 250 mm x 4.6 mm I.D.)
Injection temperature/ $^{\circ}$ C	100
Pressure/ Kpsi	4
Mobile phase	Carbon dioxide - acetonitrile - isopropanol (93.0:6.3:0.7)
Flow rate/ $\text{cm}^3/\text{min}$	4
Detector	UV detection at 210 nm./ light scattering detector

### ***3.2 Results and discussion on the supercritical fluid Chromatographic analysis of the various oils***

Argentation SFC of olive oil triglycerides, using an UV detector, proved successful yielding similar oil fingerprints to that obtained by Demirbaker and Blomberg (1991). The experiment was performed using isocratic elution (according to the parameters described in Table 3.1) rather than the pressure and temperature programs that were used by Demirbaker and Blomberg (1991).

Triglycerides were identified by comparing their retention times with triglyceride standards. Analysis was first carried out using two columns in series. An additional column was connected in series to try and further improve the resolution of the triglyceride peaks. There was no obvious improvement in the chromatographic separation with the addition of an extra column. The chromatographic separation of sunflower oil using two column and three columns in series are shown in Figure 3.4 and Figure 3.5 respectively.

Here separation was based on degree of saturation. Each chromatogram gave distinct profiles of the individual oils analyzed which served as fingerprints for their identification (Figures 3.3 - 3.10). Some chromatographic profiles were shown to differ based according to geographical source of the oil. Distinct differences were also observed between the olive

oil chromatogram and the chromatogram for the olive and sunflower mixture. The triglyceride peak trilinolein which was clearly present in the sunflower and the olive/sunflower chromatograms (Figures 3.4 and 3.5 respectively) was absent in the olive oil chromatogram (Figure 3.3). The presence of this peak in an olive oil chromatogram is a clear indicator of sunflower adulteration in olive oil.

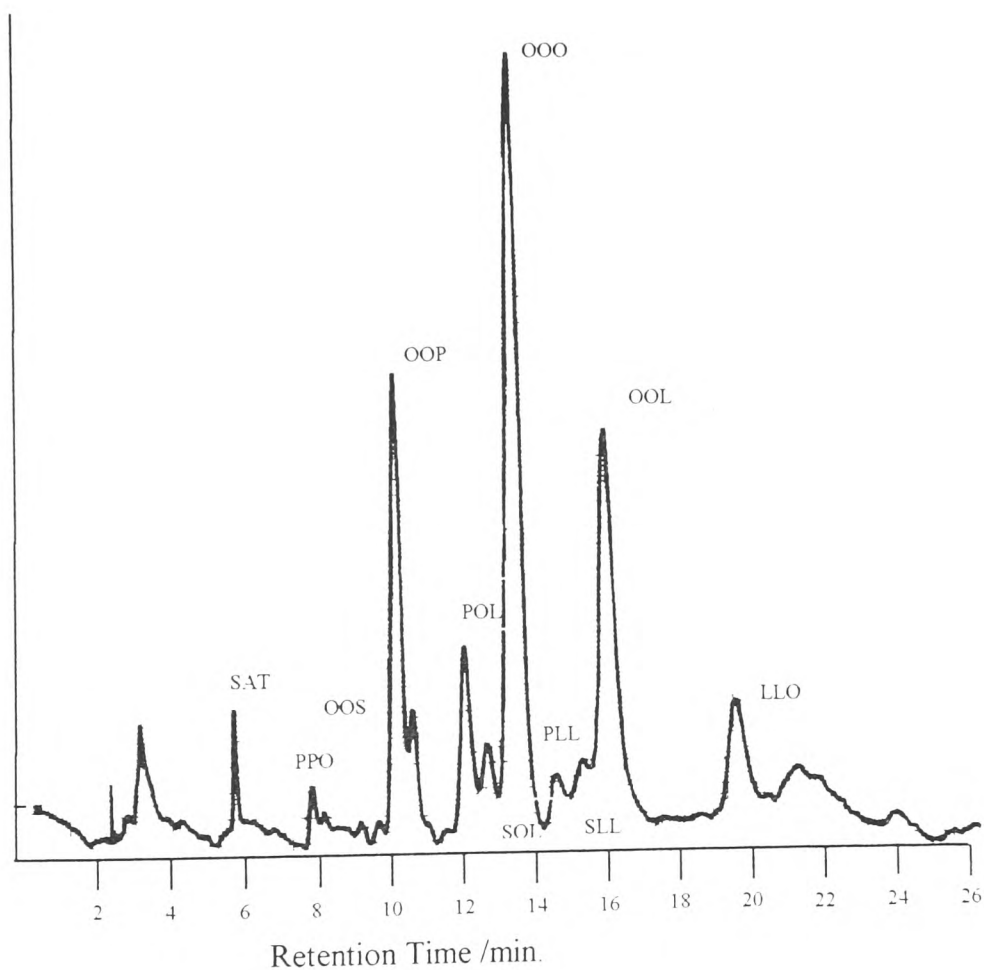


**Figure 3.3 SFC chromatogram of extra virgin olive oil**

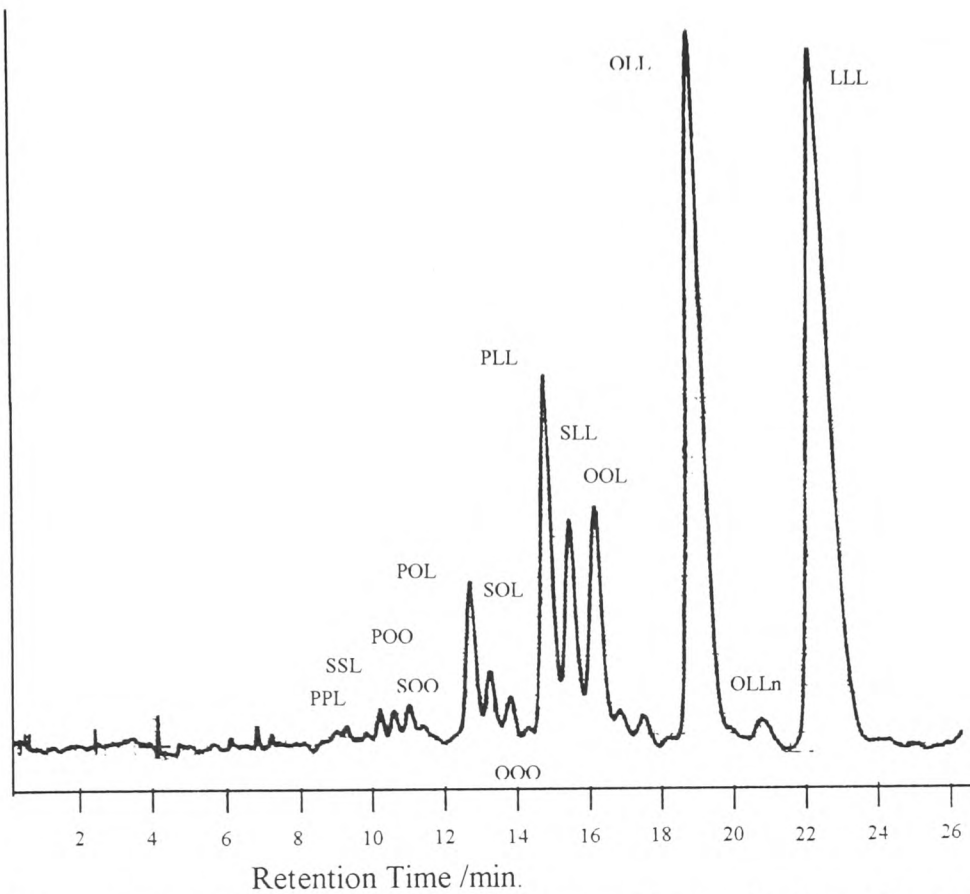


Figure 3.4 SFC chromatogram of sunflower oil using 2 columns in series

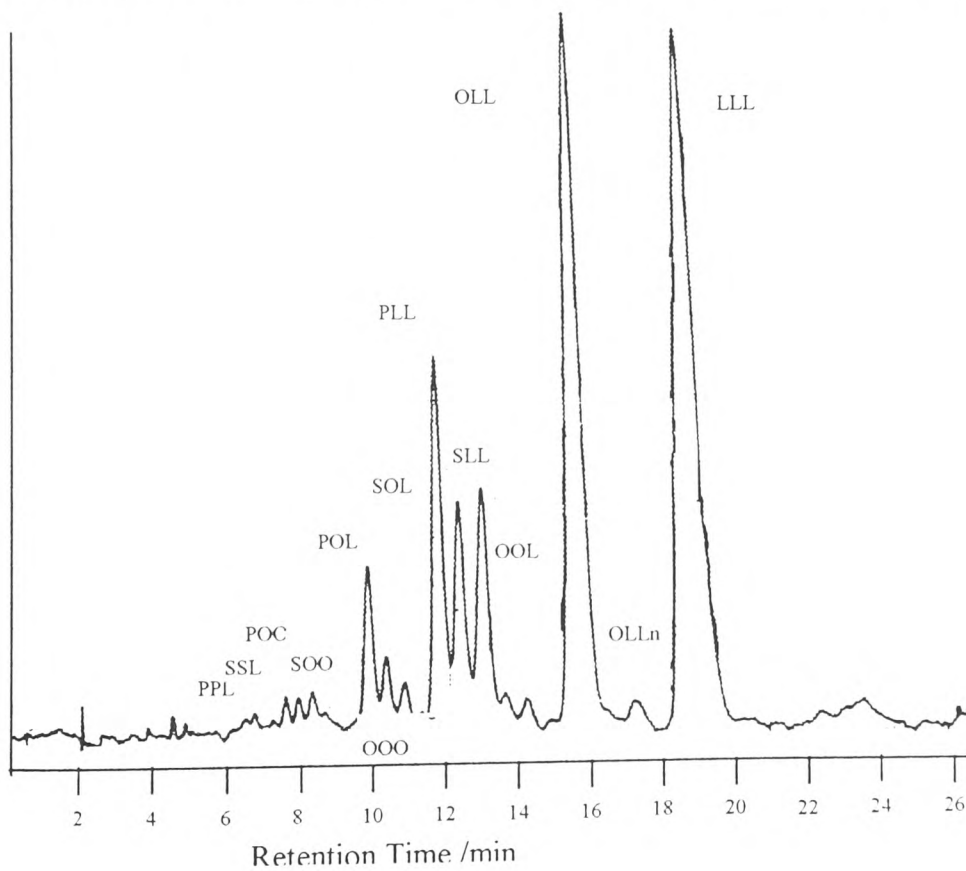
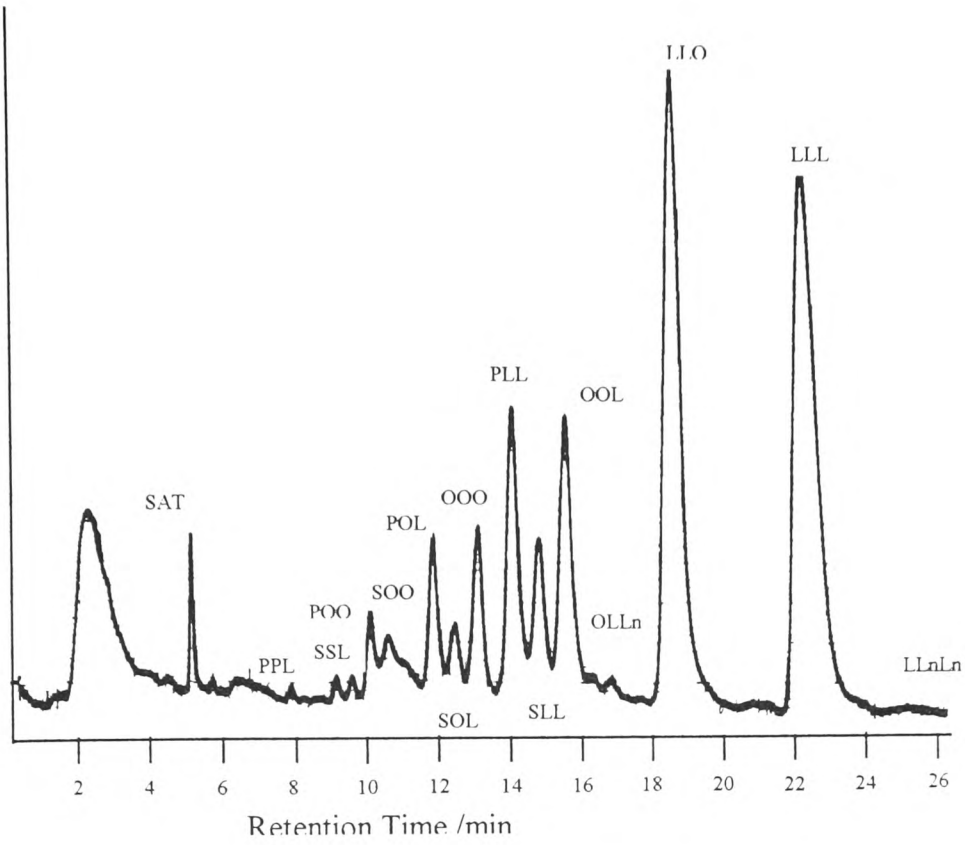
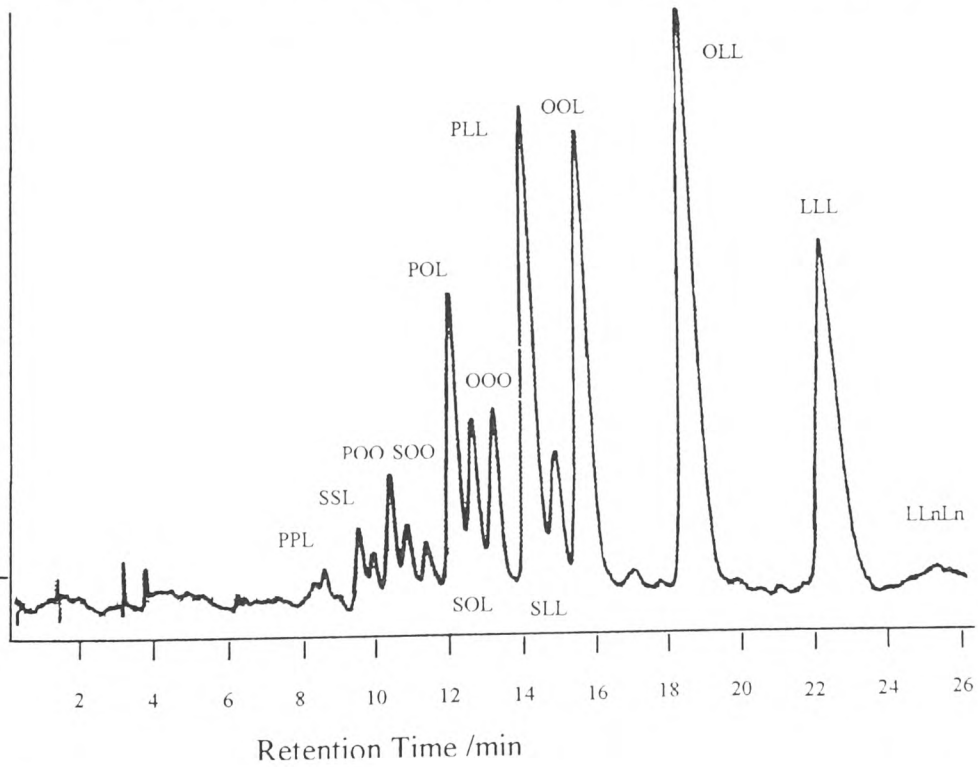


Figure 3.5 SFC chromatogram of sunflower oil using 3 columns in series





**Figure 3.6 SFC chromatograph of a mixture of olive oil and sunflower oil**



**Figure 3.7 SFC chromatograph of sesame seed oil**



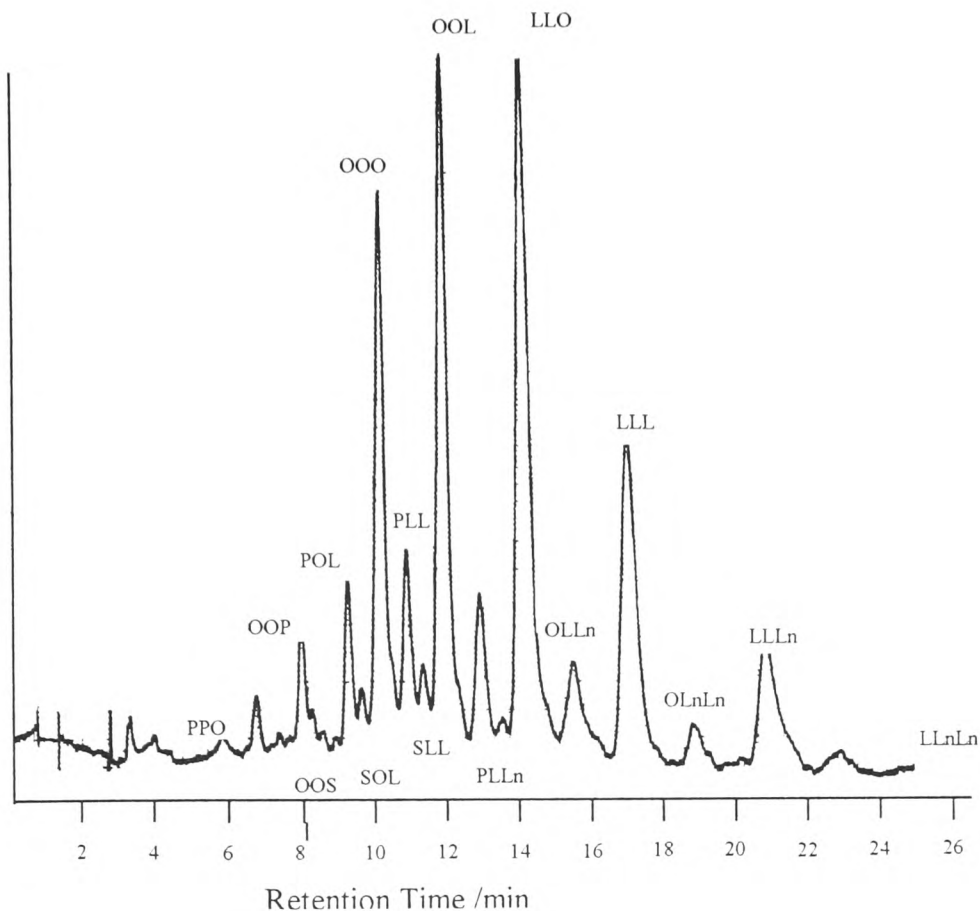


**Figure 3.10 SFC chromatogram for Tesco vegetable oil**

The resolution of the peaks PLL and SLL was calculated for the various oils analyzed. The resolution and the column efficiency of several oils separated both with two columns and with three columns in series are recorded in Table 3.2. In the case of each oil analyzed the resolution was improved giving values greater than one.

The number of theoretical plates was calculated for two columns and three columns in series. This calculation was carried out on the peak PLL. The data is shown in Table 3.2. It is evident that the number of theoretical plates increased almost two fold with the addition of an extra column in series. The selectivity of the peaks were however, not greatly effected by the addition of an extra column in series (Table 3.2).

**Table 3.2 Comparison of resolution, selectivity and column efficiency on oils separated both with 2 columns and with 3 columns connected in series**

Name of oil	No. of columns in series	Resolution	Selectivity	N° of theoretical of plates
Sunflower	2	1.50	1.06	4421
Sunflower	3	1.75	1.05	8105
Sun/olive	2	1.75	1.06	3890
Sun/olive	3	1.75	1.05	6884
Walnut	2	1.75	1.07	3890
Walnut	3	2.00	1.06	6033
Soya	2	1.75	1.06	4421
Soya	3	2.75	1.07	8754
Sesame	2	1.75	1.07	3890
Sesame	3	2.25	1.06	7791
Tesco oil	2	1.75	1.06	4579
Tesco oil	3	2.33	1.05	7584

### 3.2.1 SFC results and discussion on the supercritical fluid chromatographic analysis of the Greek oils using UV detection

Greek oils were also analyzed by SFC using UV detection. The results of this analysis are shown in Table 3.3. As shown in Figure 3.4, 10 triglyceride peaks are clearly observed in the extra virgin oil chromatogram. The triglyceride peaks OOP and OOS are not well resolved from each other and thus, their total peak areas have been recorded.

**Table 3.3 Results of SFC analysis of the Greek oils using UV Detector ( % area)**

Sample	SAT	PPO	OOP/OOS	POL	SOL	OOO	PLL	OOL	LLO
D1	11.34	2.37	19.74	7.04	2.34	38.34	1.65	15.44	1.74
D2	9.31	3.26	15.70	6.17	2.39	31.25	1.57	17.00	13.35
D3	13.16	1.27	18.45	6.09	2.43	31.98	2.55	14.13	9.93
D4	9.68	2.81	17.24	6.09	2.20	33.54	2.44	17.19	8.81
D5	12.93	1.45	17.90	5.90	2.58	35.52	2.94	20.77	13.20
D6	13.68	1.03	18.48	5.89	2.66	36.54	1.68	15.27	4.79
D7	9.75	1.66	11.41	3.75	12.36	21.14	6.21	19.69	14.02
D8	9.63	2.41	14.80	8.33	2.47	35.75	2.96	20.07	3.59
D9	11.41	1.37	17.47	5.37	2.83	35.62	2.76	16.07	7.11
D10	6.66	1.10	18.78	5.34	2.04	41.02	2.31	16.50	6.26
D11	9.84	1.62	17.84	7.85	2.33	29.94	4.11	17.66	8.80
D12	8.61	1.03	19.04	6.56	2.46	33.68	3.89	16.97	7.78
D13	8.51	0.96	15.00	5.77	2.07	30.22	2.05	20.45	14.99
D14	8.16	1.59	17.96	6.19	2.03	29.75	2.62	24.38	7.32
D15	8.33	1.17	19.10	6.63	3.20	35.80	3.42	16.17	6.17
D16	12.11	0.08	18.27	5.78	2.35	33.58	1.18	14.56	12.10
D17	11.91	1.20	20.63	3.74	0.78	37.48	3.326	17.00	7.27
D18	12.74	2.92	22.44	6.29	2.61	42.27	2.64	20.94	6.81
D19	12.54	2.49	17.35	8.47	3.09	29.06	3.68	18.96	8.06
D20	9.33	1.85	12.29	7.64	2.65	25.45	4.94	22.57	13.28
D21	6.85	1.61	19.20	6.19	1.97	33.05	3.60	19.26	8.27
D22	9.57	1.97	14.73	4.63	2.46	32.24	4.57	20.28	9.54

A reproducibility study was carried out on the triglyceride retention times of each of the Greek samples (Table 3.4). In each case the standard deviation of the triglyceride retention time is low giving good repeatability.

**Table 3.4 Reproducibility study on retention times (min) of samples analyzed by SFC using UV detection**

Name	SAT	PPO	OOP	OOS	POL	SOL	OOO	PLL	OOL	LLO
D1	5.40	7.83	9.25	10.28	12.05	12.63	13.60	14.49	16.00	19.36
D2	5.41	7.85	9.64	10.32	12.09	12.65	13.59	14.56	16.01	19.35
D3	5.48	8.05	9.46	10.57	12.40	13.00	13.97	14.85	16.45	19.90
D4	5.42	7.90	-	10.33	12.13	12.69	13.68	14.51	16.05	19.39
D5	5.49	7.56	9.45	10.59	12.40	12.99	14.00	14.86	16.39	19.81
D6	5.48	8.05	9.43	10.61	12.44	13.05	14.05	15.58	16.47	19.94
D7	5.52	8.08	9.46	10.58	11.77	12.52	13.96	14.91	16.54	19.92
D8	5.49	8.04	9.50	10.58	12.42	13.03	14.03	14.82	16.47	19.93
D9	5.48	8.03	9.44	10.54	12.36	12.98	13.94	14.85	16.38	19.83
D10	5.40	7.84	10.30	10.70	12.10	12.70	13.67	14.43	16.00	19.32
D11	5.42	7.89	9.26	10.32	12.12	12.65	13.63	14.52	16.04	19.35
D12	5.39	7.78	9.26	10.23	12.01	12.57	13.53	14.39	15.87	19.25
D13	5.41	7.89	9.20	10.34	12.14	12.70	13.67	14.56	16.06	19.38
D14	5.45	7.32	9.36	10.53	12.37	12.97	13.93	14.88	16.41	19.77
D15	5.57	8.06	9.93	10.65	12.48	13.08	14.09	14.94	16.52	19.91
D16	5.42	7.86	9.30	10.3	12.08	12.67	13.57	14.5	16.01	19.32
D17	5.50	8.04	9.46	10.61	11.48	12.45	14.07	14.91	16.50	20.00
D18	5.41	7.88	9.30	10.35	12.13	12.72	13.68	14.56	16.05	19.39
D19	5.47	8.02	9.38	10.54	11.64	12.40	13.95	14.87	16.48	19.91
D20	5.44	7.98	9.35	10.46	12.32	12.91	13.83	14.78	16.34	19.73
D21	5.46	8.05	9.41	10.57	12.39	12.94	13.96	14.84	16.41	19.74
D22	5.46	8.00	9.35	10.52	12.36	12.94	13.93	14.84	16.36	19.82
Mean	5.45	7.91	9.45	10.49	12.17	12.79	13.84	14.76	16.27	19.66
$\sigma$	0.05	0.19	0.25	0.14	0.27	0.21	0.19	0.26	0.22	0.27
CV	0.92	2.40	2.65	1.33	2.22	1.64	1.37	1.76	1.35	1.37

Chromatographic performance of the system was shown to decrease over a period of time manifested by a progressive drop in separation efficiency. In order to compensate for this the column was occasionally reconditioned with silver nitrate.

### 3.2.2 SFC results and discussion on the supercritical fluid chromatographic analysis of the Greek oils using light scattering detection

Light scattering detection is based on mass detection rather than on the presence of chromophores present in the sample, as is the case with UV detection. A typical analysis of an extra virgin oil, using SFC - light scattering detection (SFC - LS) is illustrated in Figure

3.11

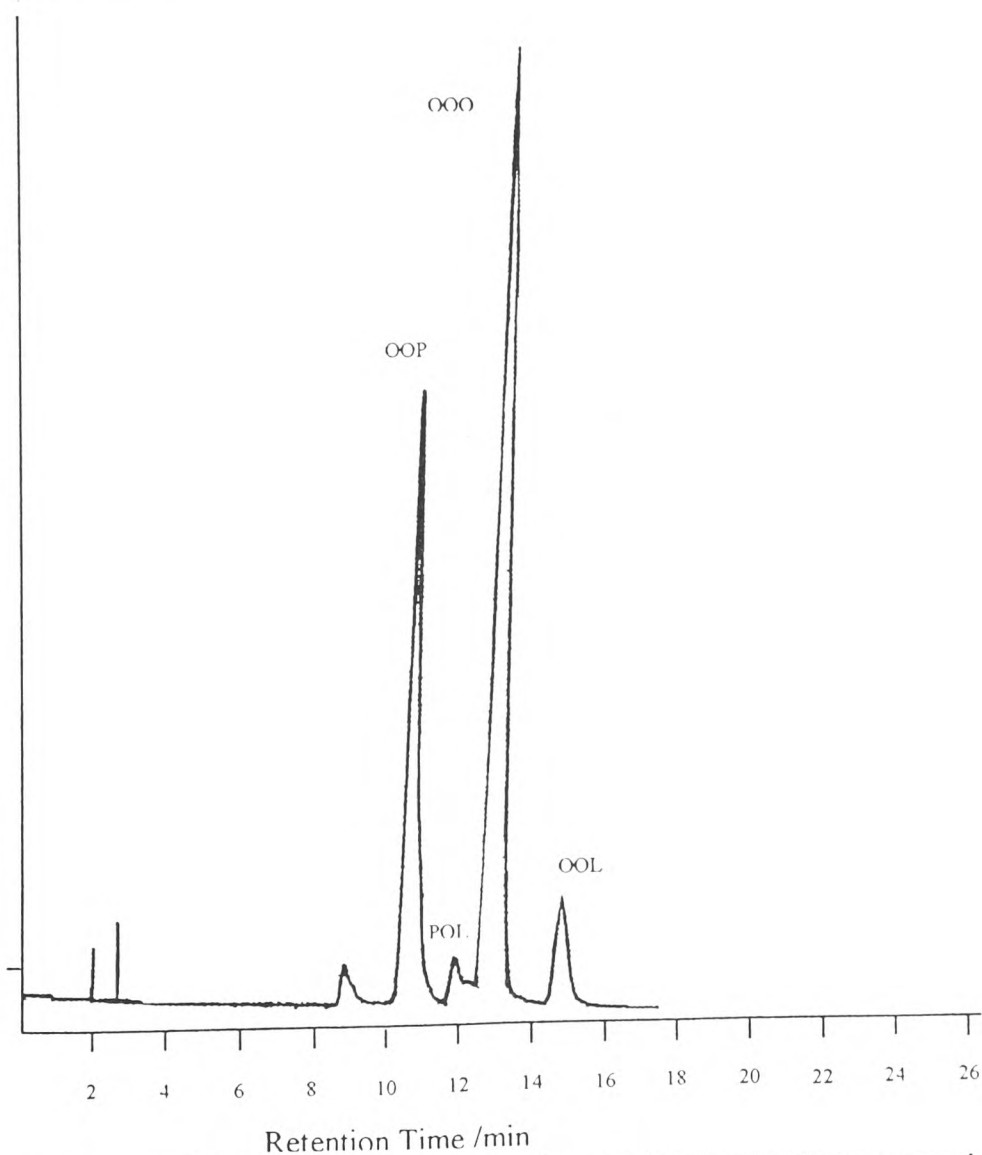


Figure 3.11 SFC chromatogram of extra virgin oil using light scattering detection

Results for the Greek oils and their adulterated mixtures of 10 % sunflower were analyzed by argentation SFC - LS are shown in Tables 3.5 and 3.6.

**Table 3.5 SFC analysis of the Greek oils using the light scattering detector**

Sample	OOP	OO	PLL	OOL	LLO	LLL
D1	2.44	32.16	2.45	55.40	6.81	0.72
D2	4.02	35.05	2.91	50.64	6.71	0.67
D3	2.72	33.69	2.47	54.43	6.02	0.67
D4	1.39	30.32	2.17	58.53	7.16	0.42
D5	2.38	30.97	2.52	56.00	7.33	0.80
D6	2.32	31.85	1.95	56.72	7.09	0.07
D7	3.93	30.40	12.16	36.30	13.96	3.25
D8	1.63	28.26	2.04	59.76	7.68	0.62
D9	3.03	31.85	2.01	55.75	6.74	0.62
D10	2.12	29.80	1.85	60.12	6.08	0.60
D11	2.96	32.28	3.93	49.74	9.19	1.90
D12	2.61	31.75	2.87	54.96	6.41	1.40
D13	2.50	32.21	3.47	52.57	8.17	0.37
D14	2.39	33.51	4.72	51.69	8.02	0.97
D15	2.56	32.61	2.58	58.71	2.82	0.72
D16	2.42	32.11	2.70	55.31	6.53	0.93
D17	2.75	33.25	0.37	55.46	7.18	0.99
D18	2.47	31.80	3.31	54.52	6.38	1.53
D19	1.15	28.14	4.27	53.74	11.97	0.72
D20	2.13	27.09	6.31	49.62	13.13	1.72
D21	3.11	32.24	3.84	53.44	6.11	1.25
D22	2.61	28.93	2.01	59.15	6.04	1.26



**Table 3.6 SFC analysis of the Greek oils (adulterated with 10 % sunflower oil) using the light scattering detector**

Sample	OOP	OOO	PLL	OOL	LLO	LLL
D1/10	2.50	30.95	3.05	55.17	6.12	2.23
D2/10	2.96	31.86	4.61	51.30	7.02	2.26
D3/10	2.47	32.79	3.66	52.25	6.48	2.35
D4/10	2.12	28.02	2.58	58.29	6.30	2.69
D5/10	0.77	29.49	3.03	54.72	7.98	4.01
D6/10	1.73	26.66	2.93	58.07	8.11	2.50
D7/10	3.65	26.72	12.40	32.72	16.74	5.25
D8/10	2.56	26.62	3.75	53.49	10.52	3.06
D9/10	2.13	30.90	1.28	56.06	6.71	2.93
D10/10	2.40	27.10	2.26	58.36	6.74	3.14
D11/10	2.63	29.12	5.31	49.76	9.94	3.24
D12/10	2.63	29.09	3.10	52.29	8.90	4.01
D13/10	2.04	29.62	4.49	52.37	8.57	2.90
D14/10	2.66	28.92	5.56	50.51	9.42	2.92
D15/10	2.39	30.02	4.11	53.33	6.54	2.19
D16/10	2.53	31.21	3.32	52.86	7.27	2.80
D17/10	1.77	34.99	1.05	56.15	4.46	1.59
D18/10	2.44	31.92	0.83	56.20	6.44	2.17
D19/10	2.09	27.77	4.57	48.82	13.06	3.70
D20/10	1.96	25.29	4.88	46.04	17.46	4.38
D21/10	2.31	20.50	2.09	33.81	4.05	3.43
D22/10	1.21	30.10	1.77	59.97	5.48	1.48

A reproducibility study was carried out on the Greek sample D12 which was adulterated with 10 % sunflower. The results of this study are shown in Table 3.7. Large standard deviations were observed for the peaks OOO, OOL, LLO and LLL.

During these studies it became apparent that the light scattering detector produced a “grass effect” on some of the chromatograms which caused peak distortion and consequently error in peak integration (Figure 3.13). This peak distortion was possibly due to the use of an

open - linear restrictor in which low solubility analytes became deposited.

Quantitation was difficult as high sample loadings were necessary and consequently high concentrations of standards would be required to produce calibration curves. Large injection volumes (6  $\mu$ l) of samples were used for the analysis in order to compensate for injection error. However, the reproducibility test (Table 3.8) showed large standard deviation in replicate samples.

**Table 3.7 Repeatability test on samples analyzed by SFC using light scattering detection**

Sample	OOP	OOO	PLL	OOL	LLO	LLL
D20/10 (R1)	1.96	25.29	4.88	46.04	17.46	4.38
D20/10 (R2)	1.01	27.39	5.65	50.01	13.00	2.94
D20/10 (R3)	1.09	27.67	4.70	50.47	13.26	2.81
D20/10 (R4)	1.87	25.74	6.76	46.32	14.19	5.12
Mean	1.48	26.52	5.50	48.21	14.48	3.81
$\sigma$	0.43	1.18	0.94	2.35	2.05	1.13

A reproducibility study was also carried out on the oil triglyceride retention times using this method of detection. The results are shown in Table 3.8 indicating that this method of detection was effective in qualitative analysis of olive oils.

**Table 3.8 Reproducibility test on retention times of samples analyzed by SFC using light scattering detection**

Name	OOP	OOO	PLL	OOL	LLO	LLL
D1/10	7.85	9.83	11.51	12.63	14.94	17.89
D2/10	7.86	9.82	11.39	12.47	14.60	17.33
D3/10	7.82	9.85	11.88	12.86	15.41	18.22
D4/10	7.93	10.01	11.69	12.89	15.21	18.19
D5/10	7.32	9.96	11.62	12.84	15.11	18.49
D6/10	7.89	9.88	11.45	12.52	14.62	16.63
D7/10	7.96	10.07	11.79	12.94	15.32	18.28
D8/10	6.95	10.01	11.84	12.97	15.58	17.70
D9/10	7.80	9.66	11.70	12.38	14.65	17.54
D10/10	7.83	9.92	11.61	12.75	14.89	17.86
D11/10	7.77	9.82	11.48	12.60	14.92	17.80
D12/10	7.80	9.85	11.45	12.65	14.86	17.75
D13/10	7.83	9.74	11.34	12.49	14.65	17.32
D14/10	7.80	9.80	11.48	12.65	14.92	17.75
D15/10	8.17	10.28	12.04	13.24	15.48	18.51
D16/10	8.23	10.33	12.47	13.29	15.75	17.57
D17/10	7.98	10.15	12.40	13.08	15.50	18.59
D18/10	8.12	10.31	12.71	13.42	16.11	19.09
D19/10	8.28	10.38	12.24	13.56	15.93	19.20
D21/10	8.11	10.22	12.52	13.27	15.72	18.51
Mean	7.87	9.99	11.83	12.88	15.21	18.01
$\sigma$	0.30	0.22	0.42	0.34	0.46	0.62

Both the UV detector and the light scattering detector proved effective in qualitatively profiling between different varieties of oil. The former approach however, provided more informative on the number of triglycerides present in the oils.

### ***3.3 The supercritical fluid extraction of various oils***

During the processing of oils the pressing stage is usually followed by an organic solvent extraction stage to achieve higher yields of oil. This technique is time consuming and the removal of organic solvents from the oil, after extraction, are prerequisite to the human consumption of the oil.

Supercritical fluid extraction, SFE, provides an alternative technique to solvent extraction. This method utilizes the supercritical fluid carbon dioxide instead of organic solvents. Carbon dioxide has an advantage over organic solvents in that it is cheap, non toxic and is easily removed from the extracted oil.

As reported by Stahl (1980) the yield of oil is dependent on the time of contact between carbon dioxide and the oil seeds, the size and physical structure of the seed particles and the temperature and pressure parameters used in the extraction. It was also stated that the sufficient extraction of non polar compounds can be carried out in the pressure range of 80 - 200 bar.

For this study sunflower and sesame seeds were extracted off - line using a pressure of 187 bar and at a temperature of 60 °C. The chromatographic profiles of these extracts were then compared with on - line SFE/SFC analysis of the same seeds.

In addition to this, the potential for lipase transesterification of triglycerides to FAMES was investigated using supercritical fluid carbon dioxide as the reaction solvent.

#### **3.3.1 The supercritical fluid extraction of oil from sunflower and sesame seeds**

Crushed sunflower and sesame seeds were extracted using supercritical fluid carbon dioxide. The extracted triglycerides were then analyzed by supercritical fluid

chromatography and their profiles were compared.

### 3.2.2 Materials and methods

The seeds were weighed into the extraction cell and the analysis was carried out according to the parameters outlined in Table 3.9

**Table 3.9 SFE parameters for the supercritical fluid extraction of oil from sunflower seeds and sesame seeds by the Hewlett Packard extractor**

SFC components	Parameters
Chamber temperature (°C)	60
Equilibration time (min)	10
Extraction time (min)	10
Thimble	7
Thimble volume	5.1
Nozzle temperature (°C)	5
Trap temperature (°C)	20
Trap packing	ODS
Void volume compensation	1.0
Fraction output	1
Solvent	Hexane
Volume (cm <sup>3</sup> )	1
Rate (cm <sup>3</sup> min <sup>-1</sup> )	2
Nozzle temperature (°C)	45
Trap temperature (°C)	40
Fluid delivery:	CO <sub>2</sub>
Density (g cm <sup>-3</sup> )	0.7
Pressure (Bar, psi)	187/2709
Flow	2.7
Extraction fluid	CO <sub>2</sub>

### **3.2.3 On - line supercritical fluid extraction and supercritical fluid chromatography of the triglycerides from olives and seed oils.**

On line SFE/SFC allowed for the quantitative transfer of all the triglycerides to the chromatographic column. This ensured maximum sensitivity and eliminated sample handling between the extraction stage and the chromatographic separation stage.

This SFE system was coupled to a SFC column using a small extraction cell. This on - line SFE/SFC technique allowed extracted and separated triglycerides from olives, sunflower seeds and sesame seeds. These profiles were then compared with those profiles obtained from the off - line SFE/SFC analyses of these oil seeds and from direct analyses of the respective oils.

### **3.2.4 Materials and methods**

The extraction cell was fitted in place of the loop of the Rheodyne valve. The injection valve was positioned in the load status and CO<sub>2</sub> was allowed to flow through the thermostatted extraction cell for 30 seconds. The resultant extract was deposited at the beginning of the column. The extraction was then stopped by switching the valve to the injection mode. At this point a mobile phase consisting of CO<sub>2</sub> and modifier (93:7) as the mobile phase was introduced into the column and the extracted oil in the extraction cell was separated chromatographically.

### **3.2.5 The derivatization of triglycerides to FAME using lipase**

The approach adopted in this analysis involved the off – line derivatization of olive oil to FAMES using SFE and the subsequent analysis of the derivatized samples using argentation SFC. Triglycerides were extracted using supercritical fluid carbon dioxide and were transesterified to fatty acid methyl esters using immobilized lipase as the catalyst.

### **3.3.3.1 Materials and method**

The method followed in this experiment was taken from Berg et al. (1993).

Extraction cell

Hexane

Methanol

Silica gel

Cotton wool

Phosphate buffer (pH 7)

Immobilized Lipase

#### ***3.3.3.1.1 Procedure***

The extraction cell was washed with methanol and dried. The bottom of the extraction cell was filled with dried  $\text{Na}_2\text{SO}_4$  and cotton wool. Oil (5-10 mg), lipase and water (absorbed onto silica) were added to the extraction cell. The silica was separated from the oil by a layer of cotton wool which had been washed with hexane. Phosphate buffer ( $2 \text{ cm}^3$ ) was added to the cell to ensure a constant pH during the reaction. A change in pH, in the reaction mixture, may arise due to the formation of carbonic acid in the cell on the contact of the water with carbon dioxide under pressure. The reaction - extraction was carried out using the Hewlett Packard SFE. The details of the parameters followed in these analyses are outlined in Tables 3.10.

**Table 3.10 The parameters for the derivatization of olive oil triglycerides to FAME using lipase as the catalyst in a Hewlett Packard SFE extraction cell**

SFE components	Parameters
Chamber temperature (°C)	50
Equilibration time (min)	4
Extraction time (min)	8.40
Thimble	7
Thimble volume (cm <sup>3</sup> )	3.2
Nozzle temperature (°C)	45
Trap temperature (°C)	40
Trap packing	ODS
Void volume compensation (cm <sup>3</sup> )	1.0
Solvent	Hexane
Volume (cm <sup>3</sup> )	1
Rate (cm min <sup>-1</sup> )	2
Nozzle temperature (°C)	45
Trap temperature (°C)	40
Fluid delivery	CO <sub>2</sub>
Density (g cm <sup>-3</sup> )	0.7
Pressure (Bar, psi)	187/2709
Flow (cm <sup>3</sup> min <sup>-1</sup> )	2.7
Extraction fluid	CO <sub>2</sub>

### 3.2.7 Results and discussion of SFE oil extractions

The off - line extraction of the sunflower gave similar profiles (Figures 3.12) to those obtained by the processed oils (Figure 3.5). On - line extractions overloaded the column producing indistinct chromatographic profiles. An on - line chromatogram obtained for sunflower seeds is shown in Figure 3.13.



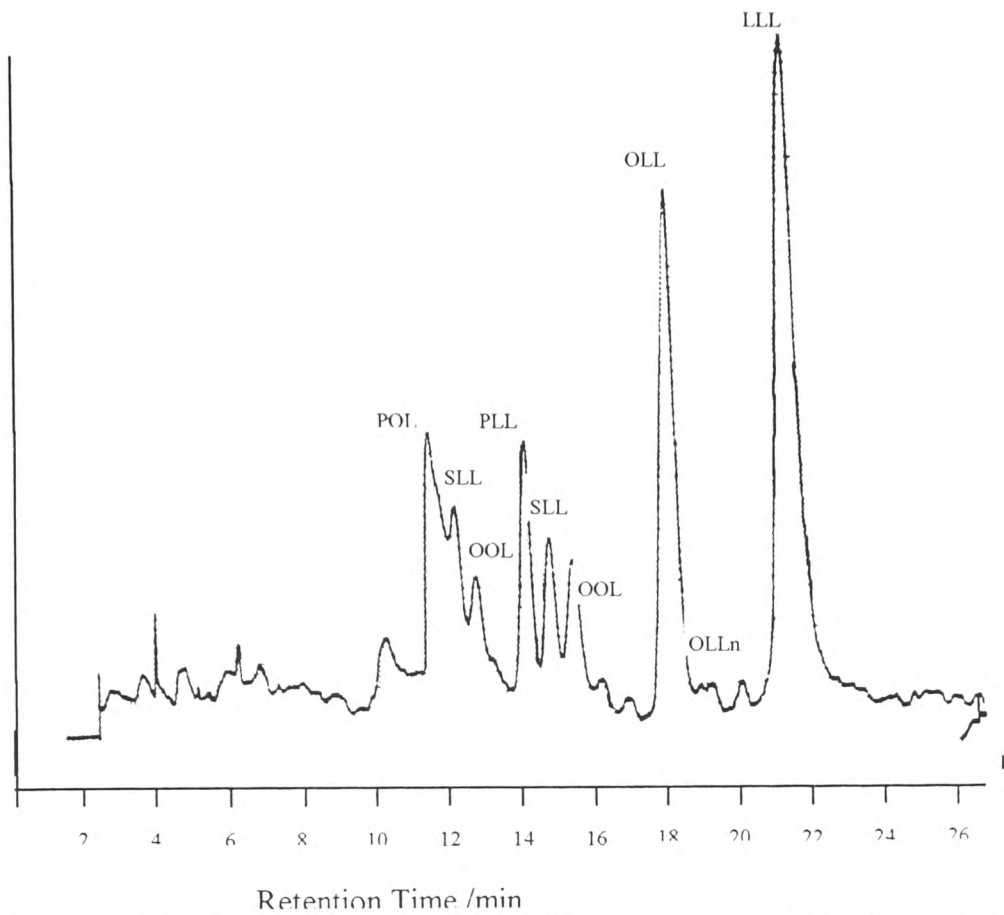


Figure 3.12 Off - line supercritical fluid chromatogram of sunflower extract

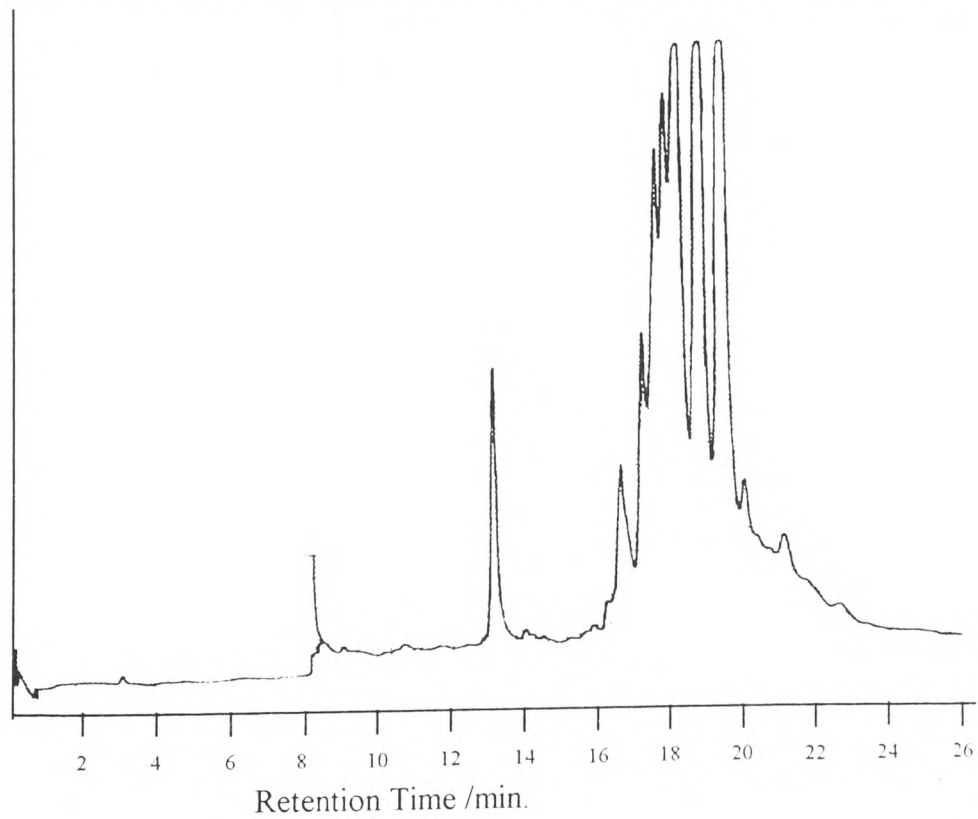
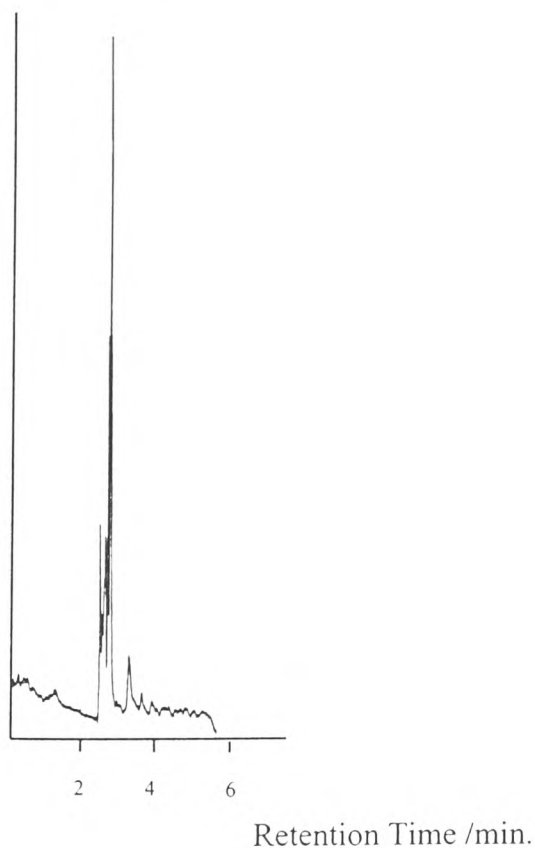
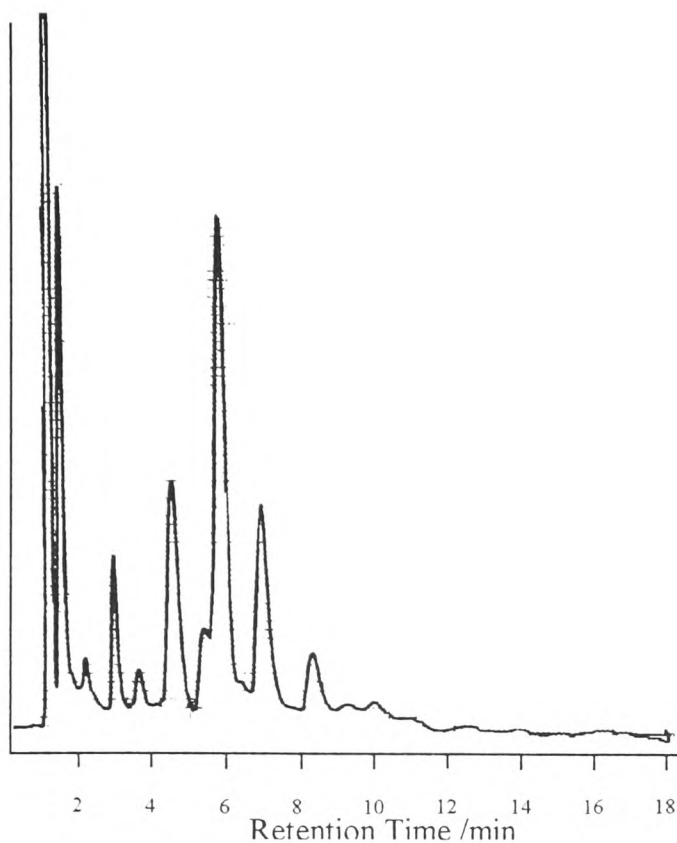


Figure 3.13 On - line supercritical fluid chromatogram of sunflower extract

Studies in to the on - line transesterification of the olive oil triglycerides, using lipase in the extraction cell were partially successful resulting in the formation of some FAMES. The SFC chromatograms of a FAME standard and of the lipase derivatized olive oil are shown in Figures 3.14 and 3.15 respectively. The comparison of these chromatograms show clearly the presence of FAMES in the transesterified olive oil chromatogram. However, the conversion was not effective enough to consider this method as viable method of transesterification. Large amounts of triglycerides were still observed in the SFC chromatograph after transesterification with the lipase catalyst (Figure 3.15). This further verifies the presence of FAMES in the transesterified sample.



**Figure 3.16 SFC chromatogram of FAME standard**



**Figure 3.15 SFC chromatogram of the lipase transesterification of olive oil**

### **3.4 Conclusion**

Argentation SFC offers an alternative to gas chromatography in providing a superior approach to the separation of triglycerides based on degree of unsaturation and overall characteristic chromatographic fingerprints for a variety of vegetable oils as well as for the authentic Greek olive oils and their adulterated mixtures.

The on - line SFE/SFC analysis of oil seeds eliminated sample preparation and minimized analysis time. However, the amount of oil extracted in this on - line process was too concentrated and the column was overloaded. This resulted in bad chromatographic separation of the triglyceride peaks. This could be improved by further looking at shorter extraction times - different extraction densities.

The studies in to on - line lipase transesterification were inconclusive. Whilst some

dervitazation of the sample were evident conversion yields were low. Further studies should centre on improving yield, reproducibility and the selectivity of dervitazation.

Finding suitable internal standards, improved detection limits of LS linked to a diode ray detector should also lead to improvement in quantitative LS - SFC.

## CHAPTER 4

### THE CHARACTERIZATION OF OLIVE OIL BY RAMAN AND INFRARED SPECTROSCOPY

#### *4.1 The application of FT - Raman spectroscopy and SIMCA modelling in the data of authentic olive oil*

As stated in Chapter 1 the use of FT - Raman spectroscopy coupled with the use of Nd/YAG lasers, Michelin interferometers and near - infrared detectors have vastly improved the applicability of this technique to the analysis of oils and fats (Hirshfeld and Schildkraut, 1974). The use of infrared lasers provides fluorescence - free Raman spectra as they operate at frequencies well below the threshold for most fluorescence processes (Williams et al, 1990). The high polarity of water and its low density makes it a poor scatterer of light. This gives Raman spectroscopy an added advantage over Infrared spectroscopy as water gives rise to intense absorption over much of the infrared spectral range. However, the molecular vibrations studied by both techniques are the same and in this respect the two are complementary to each other. In this study the application of FT - Raman spectroscopy and SIMCA modelling in the determination of authentic olive oil is described.

#### **4.1.1 Material and methods**

The olive oils were supplied from Greece and the sunflower oil was purchased at a local retailer.

#### **4.1.1.2 Procedure**

The FT - Raman spectra of the oil was carried out on a Perkin Elmer 2000 FT – Raman spectrometer. The Raman parameters used are shown in Table 4.1.

**Table 4.1 Raman Parameters for olive oil analysis**

Raman components	Parameters
Laser	Nd:YAG
Detector	InGaAS
Apodization	Filler
Resolution	4.00
OPD velocity (cm s <sup>-1</sup> )	1
Data interval (cm <sup>-1</sup> )	1/CM
Wavenumber shift	3600 - -1500
N Points	5101

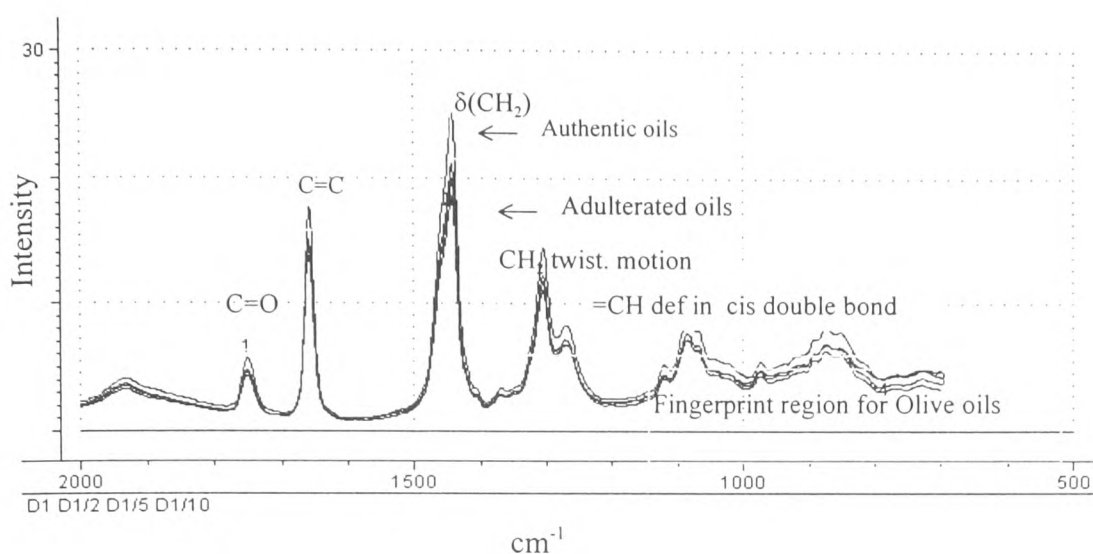
The results from this analysis were supplied by Bruker, Germany. The analytical data obtained was analyzed statistically using a SIMCA classification. Both leverage and full cross validation were used as validation methods. A full explanation of these validation methods is given in Chapter 1.

#### 4.1.2 Results and discussion

The aim of this analysis was to investigate if the statistical analysis of olive oil Raman spectral data could be used to discriminate between the authentic Greek oils and their adulterated mixtures. In this study, the FT - Raman spectra were produced over the Raman shift range of - 1500 cm<sup>-1</sup> to 3600 cm<sup>-1</sup> and all spectra were normalized at 2855 cm<sup>-1</sup>. For statistical examination the collected spectra were transferred to JCAMP DX (ASCII) format.

Figure 4.1 shows the Raman spectral region of the extra virgin olive oil (sample D1) and its adulterated mixtures of 2 % w/w, 5 % w/w and 10 % w/w. Looking at the C=O at 1730 cm<sup>-1</sup> it is possible to see clear differences in the peak heights between

adulterated mixtures.



C=O: C=O stretching in an ester; C=C: C=C stretching;  $\delta$  CH<sub>2</sub>: scissoring deformation; CH<sub>2</sub> twist. motion: in phase methylene twisting motion; =CH def. cis double bond: in plane =CH deformation in an unconjugated cis double bond.

**Figure 4.1 Raman spectral region of the extra virgin olive oil D1 and its adulterated sunflower mixtures of 2 % w/w, 5 % w/w and 10 % w/w respectively**

#### 4.1.2.1 SIMCA classification of whole Raman spectral data

A SIMCA classification was first carried out on the Raman spectra absorption regions shown in Table 4.2. This data set is referred to as the whole data set in this chapter.

**Table 4.2 Raman spectral region from which data was extracted from for statistical analysis**

Region/ cm <sup>-1</sup>	Assignment
1664 - 1628	$\nu$ (C=C)
1512 - 1382	$\delta$ (CH <sub>2</sub> )
1320 - 1240	methylene twisting
1200 - 700	fingerprint region

The data table contained 48 training set samples and 40 test samples. The training samples were divided into 4 sample sets each containing 12 samples. These sets were called

*authentic* representing the authentic olive oil samples, and *Adult/2 %*, *Adult/5 %* and *Adult/10 %* representing the sunflower/olive adulterated mixtures of 2 % w/w, 5 % w/w, and 10 % w/w respectively. The test sets were called *Authentic test* representing the authentic olive oil samples, *Test set/2 %*, *Test set/5 %* and *Test set/10 %* representing the sunflower/olive adulterated mixtures of 2 % w/w, 5 % w/w, and 10 % w/w respectively. The samples used in each of these sets are shown in Table 4.3 and Table 4.4.

**Table 4.3 Complete training sets consisting of authentic Greek oils and their adulterated mixture sets**

<b>Authentic samples</b>	<b>Adult/2 %</b>	<b>Adult/5 %</b>	<b>Adult/10 %</b>
D1	D1/2	D1/5	D1/10
D3	D4/2	D3/5	D3/10
D5*	D5/2	D4/5	D4/10
D8	D8/2	D5/5	D5/10
D10*	D10/2	D8/5	D8/10
D12	D12/2	D10/5	D10/10
D13	D13/2	D12/5	D12/10
D15	D15/2	D13/5	D13/10
D17	D17/2	D15/5	D15/10
D19	D19/2	D17/5	D17/10
D20	D20/2*	D19/5	D19/10
D21	D21/2	D21/5	D21/10

\* indicates outliers removed during the development of the class model.



**Table 4.4 Complete test set for the validation of the authentic set and its adulterated mixture sets**

Authentic test	Test set/2 %	Test set/5 %	Test set/10 %
D2	D2/2	D2/5	D2/10
D4	D6/2	D6/5	D6/10
D6	D7/2	D7/5	D7/10
D7	D9/2	D9/5	D9/10
D9	D11/2	D11/5	D11/10
D11	D14/2	D14/5	D14/10
D14	D16/2	D16/5	D16/10
D16	D18/2	D18/5	D18/10
D18	D20/2	D20/5	D20/10
D22	D22/2	D22/5	D22/10

Each of the four training sets were described by a PCA model; the model was validated by leverage, the number of components were determined for each model and outliers were found and removed separately. The first 2 PCs accounted for 99 % (approx.) of the variance in each case for each set. This is shown in Table 4.5. As stated in Chapter 1 total residual and explained variances show how well the model fits the data. Models with small total residual variance (close to zero) or large total explained variance (close to 100 %) explain most of the variation in the data (Camo AS, 1996). Thus the number of PCs that give minimal total residual variance or maximum explained variance are indicative of how many PCs to use in the model.

**Table 4.5 Percentage variance accounted for in the first 2PCs in the model formed using leverage validation**

Name of components	Authentic	Adult/2 %	Adult/5 %	Adult/10 %
PC1	77.91	92.56	92.24	87.61
PC2	99.43	98.77	99.48	99.58

The results for validating the models are shown in Table 4.6. In validation the test sets of known samples are classed using the developed model. The number of correctly classed test set samples measures the predictability of the model.

**Table 4.6 Classification of the test set with the class models for the authentic oils and their adulterated mixtures on the whole data region using leverage validation**

Class models		Test sets		Classified successfully	
Authentic	Adult/2 %	Authentic Test	Test set/2 %	7/10	6/10
Authentic	Adult/5 %	Authentic Test	Test set/5 %	7/10	5/10
Authentic	Adult/10 %	Authentic Test	Test set/10 %	7/10	7/10

This analysis using leverage validation was a preliminary test in the classification of these oils. Leverage validation results in optimistic predictions and further validation (full cross validation) is required to confirm these models (Camo AS, 1996).

#### **4.1.2.2 SIMCA classification of whole Raman spectral data using full cross validation**

The use of full cross validation (FCV) guarantees that only the relevant parts of the data are used in the model. As described in Chapter 1, in full cross validation there are as many sequences as samples. The validation process involves creating a model with all the samples except one. This excluded sample is then used to validate the model. This procedure is repeated until all the samples have been excluded in turn (Camo AS, 1996).

In FCV the training sets and test sets were given the following names: *Authfcv* represented the authentic oil training set, *Adfcv/2 %*, *Adfcv/5 %* and *Adfcv/10 %* represented the adulterated sunflower mixtures training sets of 2 % w/w, 5 % w/w and 10 % w/w respectively; *Authfcv test*, *Authfcv/2 % Test*, *Authfcv/5 %* and *Authfcv/10 % Test* represented the authentic oil test set and the 2 % w/w, 5 % w/w and 10 % w/w adulterated

mixture test sets respectively. The training and test sets used for this analysis are shown in Tables 4.7 and Table 4.8.

**Table 4.7 Complete Training sets for the authentic oil sets and their adulterated mixture sets using FCV**

Authfcv	Adfcv/2 %	Adfcv/5 %	Adfcv/10 %
D1	D1/2	D1/5	D1/10
D3	D3/2	D3/5	D3/10
D8	D8/2	D8/5	D8/10
D10*	D10/2	D10/5	D10/10
D12	D12/2	D12/5	D12/10
D13	D13/2	D13/5	D13/10
D15	D15/2	D15/5	D15/10
D17	D17/2	D17/5	D17/10
D19	D19/2	D19/5	D19/10
D20	D20/2	D20/5	D20/10
D21	D21/2	D21/5	D21/10

\* indicates outliers removed during the development of the class model.

**Table 4.8 Complete Test set for the validation of the authentic set and its adulterated mixture sets on the whole Raman data set using FCV**

Authfcv Test	Authfcv/2 % Test	Authfcv/5 % Test	Authfcv/10 % Test
D2	D2/2	D2/5	D2/10
D4	D4/2	D4/5	D2/10
D5	D5/2	D5/5	D5/10
D6	D6/2	D6/5	D6/10
D7	D7/2	D7/5	D7/10
D9	D9/2	D9/5	D9/10
D11	D11/2	D11/5	D11/10
D14	D14/2	D14/5	D14/10
D16	D16/2	D16/5	D16/10
D18	D18/2	D18/5	D18/10
D22	D22/2	D22/5	D22/10

In this application full cross validation of the data set resulted in a large number of variables in the region of  $1600\text{ cm}^{-1}$  being badly described by the model. In the authentic oil class model the total residual calibration for PC1 was low which indicated that the calibration data did not fit the model. The second PC in each model badly described a significant proportion of variables present in the data set. However these warning limits are used as only filters to highlight the extreme data in the model. They are user definable and usually have a higher limit for the analysis of spectroscopic data (Camo AS, 1996). The amount of variance accounted for in each model after two PCs extracted are shown in Table 4.9.

**Table 4.9 Percentage variance accounted for in the first 2PCs in the model formed using FCV validation**

Name of components	Authfcv	Adfcv/2 %	Adfcv/5 %	Adfcv/10 %
PC1	83.55	88.15	93.46	81.41
PC2*	96.09	99.34	99.59	99.64

\* variables poorly described by PC 2.

The classification of the test sets using these models was carried out using one PC and 6 out of 8 of the original oil test set were classified correctly. The classification are shown in Table 4.10.

**Table 4.10 Classification of the test set with the class models for the authentic oils and their adulterated mixtures on the whole region using F.C.V. validation**

Class models		Test sets		Classified successfully	
Authfcv	Adfcv/2 %	Authfcv Test	Authfcv/2 % Test	6/11	6/11
Authfcv	Afcv/5 %	Authfcv Test	Authfcv/5 % Test	6/11	6/11
Authfcv	Adfcv/10 %	Authfcv Test	Authfcv/10 % Test	6/11	6/11

As a further test on the PCA limits, the analysis was repeated using higher limits in the development of the model. This analysis resulted in all the samples in the training set fitting the model developed. However, the classification of the test sets using these model did not give as good a classification as models developed with the lower limits.

#### ***4.1.2.3 SIMCA classification of whole Raman spectral data using randomly chosen test sets***

The statistical data sets of the authentic oils and their adulterated mixtures were further manipulated to contain a randomly chosen training set with 19 samples and test set of 3 samples. Previously specific samples were assigned to the designated authentic and adulterated classes. This manipulation used a larger training set and a smaller test set. The training set for the authentic oil samples and their adulterated mixtures were called *Original, Sun/2 %, Sun/5 % and Sun/10 %* respectively. The test sets for the authentic oils and their adulterated mixtures were called *Orig, Sun Test 2 %, Sun Test 5 % and Sun Test 10 %*. These samples used for these sets are shown in Tables 4.11 and 4.12.

**Table 4.11 Composition of the Training sets for the authentic oil sets and their adulterated mixture sets on the whole data using FCV with 3 samples in each test set**

Original	Sun/2 %	Sun/5 %	Sun/10 %
D1	D1/2	D1/5	D2/10
D2	D2/2*	D2/5	D3/10
D3	D3/2*	D4/5	D4/10
D4*	D4/2	D5/5	D5/10
D5	D5/2*	D6/5	D6/10*
D6	D7/2*	D7/5	D7/10
D7	D8/2	D8/5	D9/10
D8	D9/2	D10/5	D10/10
D11	D11/2	D11/5	D11/10
D12	D13/2	D12/5	D12/10
D13	D14/2	D13/5	D13/10
D14*	D15/2	D15/5	D14/10
D15*	D16/2	D16/5	D15/10
D16*	D17/2	D16/5	D16/10
D17	D18/2	D18/5	D17/10
D19	D19/2	D19/5	D18/10
D20	D20/2*	D20/5	D20/10
D21	D21/2	D21/5	D21/10
D22*	D22/2	D22/5	D22/10

\* indicates outliers removed during the development of the class model.

**Table 4.12 Composition of the Test set for the validation of the authentic set and its adulterated mixture sets on the whole data region using FCV with 3 samples in each test set**

Orig	Sun Test/2 %	Sun Test/5 %	Sun Test/10 %
D9	D1/2	D3/5	D1/10
D10	D6/2	D9/5	D8/10
D18	D10/2	D14/5	D19/10

Variable outliers were again found to badly describe the model using both the first and

second PCs and thus, their presence in the class models did not lend itself to a good classification. A lot of sample outliers were eliminated during the development of these models, indicating that these models failed to describe all the samples in the data set. These samples outliers are identified by asterisk in Table 4.11. The percentage variance accounted for in the development of this model are shown in Table 4.13. On the basis of two PCs two out of three authentic oils test samples were classified correctly. This classification is shown in Table 4.14.

**Table 4.13 Percentage variance accounted for in the first 2 PCs in the model formed on the whole region using FCV with 3 samples in the test set**

Name of components	Original	Sun/2 %	Sun/5 %	Sun/10 %
PC1*	73.51	90.81	92.00	87.91
PC2*	91.57	99.27	99.46	99.76

\* variables poorly described.

**Table 4.14 Classification of the test set with the class models for the authentic oils and their adulterated mixtures on the whole data set using FCV with 3 samples in the test set.**

Class models		Test sets		Classified successfully	
Original	Sun/2 %	Orig	Sun Test/2 %	2/3	2/3
Original	Sun/2 %	Orig	Sun Test/5 %	2/3	2/3
Original	Sun/2 %	Orig	Sun Test/10 %	2/3	1/3

#### **4.1.2.4 SIMCA classification of Raman fingerprint region spectral data**

The Raman data was reduced further to include the fingerprint region ( $1200 - 700 \text{ cm}^{-1}$ ) only. The FT Raman fingerprint spectra of an extra virgin olive oil (sample D1) and its adulterated mixtures, over the Raman shift of  $700 - 1200 \text{ cm}^{-1}$ , are shown in Figure 4.2. Although sunflower oil is not thought to have any strong scatter bands in this region, its

addition to extra virgin oil has altered its composition and has led to distinct difference between the extra virgin oil and its adulterated mixtures. These differences in the fingerprint region are clearly observed in Figure 4.1. There are clear differences in the peak height intensity of the authentic oils and their adulterated mixtures in the absorption region of  $1100\text{ cm}^{-1}$  and in the region of  $900\text{ cm}^{-1}$ .

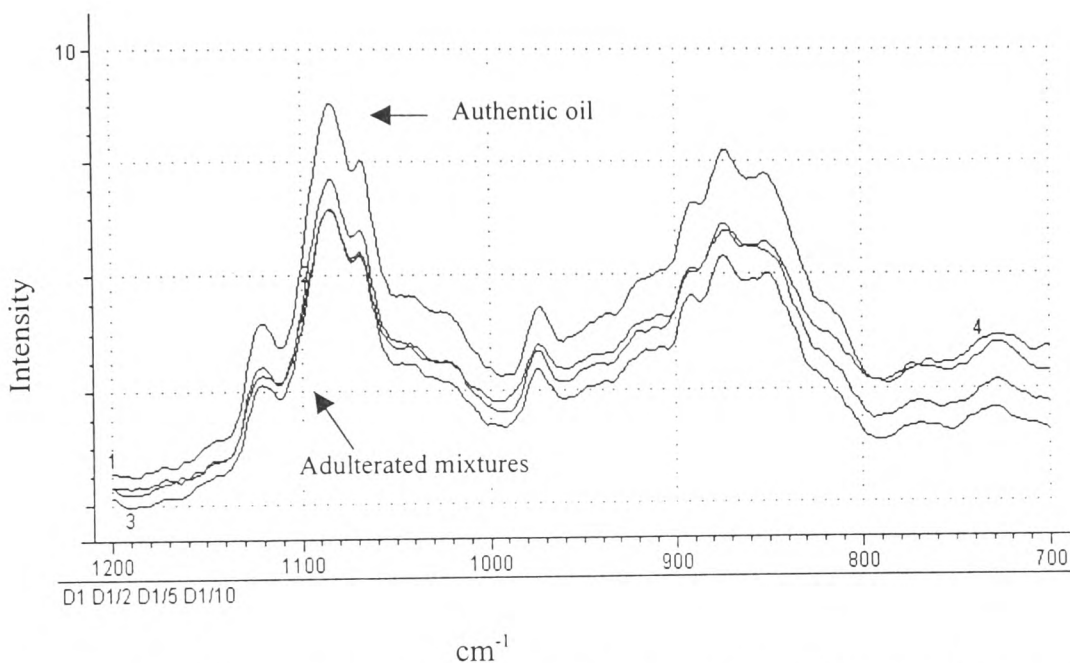


**Figure 4.2 Fingerprint region of D1 and its sunflower adulterated mixtures**

In the statistical analysis of the fingerprint region the data table consisted 17 samples in each of the training set and 20 samples in the test set samples. The training sample sets were divided into 4 sample sets each containing 19 samples. Similar, to the previous analysis these sets were divided into authentic samples and their adulterated mixtures of 2 %, 5 %, and 10 % of sunflower oil respectively. The training sets were called *Finorg*, *Fin/2 %*, *Fin/5 %* and *Fin/10 %* respectively. The test sets were called *Fin/test*, *Fin/2 % Test*, *Fin/5 % Test* and *Fin/10 % Test*. The samples comprising these sets are shown in Table 4.15 and 4.16.



**Table 4.15 Composition of the Training sets of samples used for the authentic oil sets and their adulterated mixture sets on the Raman fingerprint region**

<b>Finorg</b>	<b>Fin/2 %</b>	<b>Fin/5 %</b>	<b>Fin/10 %</b>
D1	D1/2	D1/5	D1/10
D3	D3/2	D2/5	D2/10
D4	D4/2	D3/5	D3/10
D7*	D5/2*	D5/5	D4/10
D8	D6/2	D7/5	D7/10
D10*	D7/2*	D8/5	D8/10
D12	D9/2	D9/5	D9/10
D13	D10/2	D10/5	D10/10
D14	D13/2	D11/5	D11/10
D15	D14/2	D13/5	D12/10
D16*	D15/2	D14/5	D13/10
D17	D17/2	D15/5	D14/10
D18	D18/2	D16/5	D16/10
D19	D19/2	D18/5	D17/10
D20	D20/2*	D19/5	D18/10
D21	D21/2	D20/5	D20/10
D22	D22/2	D21/5	D22/10

\* indicates outliers removed during the development of the class model.

**Table 4.16 Composition of the Test set composition for the validation of the authentic set and its adulterated mixture sets on the Raman fingerprint region**

<b>Fin/test</b>	<b>Fin/2 % Test</b>	<b>Fin/5 % Test</b>	<b>Fin/10 % Test</b>
D2	D2/2	D4/5	D5/10
D5	D8/2	D6/5	D6/10
D6	D11/2	D12/5	D15/10
D9	D12/2	D17/5	D16/10
D11	D16/2	D22/5	D21/10

This analysis was carried out using full cross validation on 4 PCs. Sample outliers were removed from the models and no variables were found to be badly described by the models. A PCA overview of the authentic class model is shown in the Figures 4.3 - 4.6. The amount of variance accounted for in each model after two PCs is shown in Table 4.17.

**Table 4.17 Percentage variance accounted for in the first 2PCs in the model formed on the fingerprint region.**

Name of components	Finorg	Fin/2 %	Fin/5 %	Fin/10 %
PC1	97.58	95.28	88.97	94.09
PC2	99.66	99.74	99.69	99.86

The first 2 PCs in all the models described greater than 99 % of the variance in the spectra respectively. The residual variance displayed in the variance plot (Figure 4.3) indicated the optimal number of PCs to use in the model while the explained variance indicated how much of the variation in the data was described by the model.

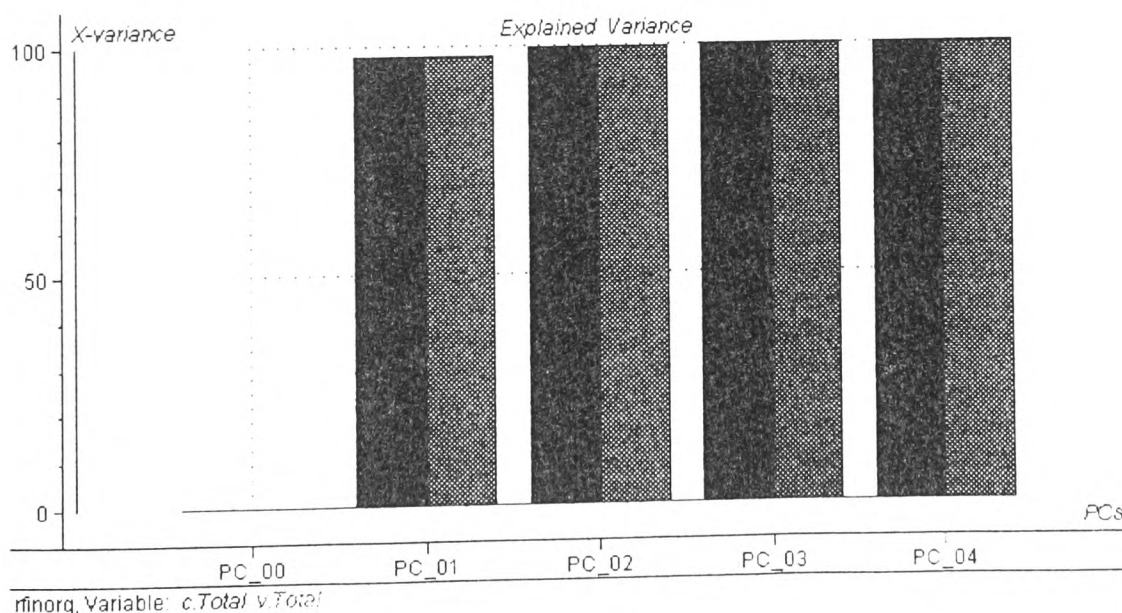


**Figure 4.3 Residual variance plot of the authentic olive oils**

The influence plot (Figure 4.4) was an indication of any outlier present in the model. This plot is a plot of squared residuals versus leverages (Camo AS, 1996). Outliers have a high leverage and a high squared residual and appear, if present, in the upper right - hand corner of this plot. In this application, samples D7, D10 and D16 were removed as outliers in the authentic model and the outliers in the adulterant models were D5/2 %, D7/2 % and D20/2 %.

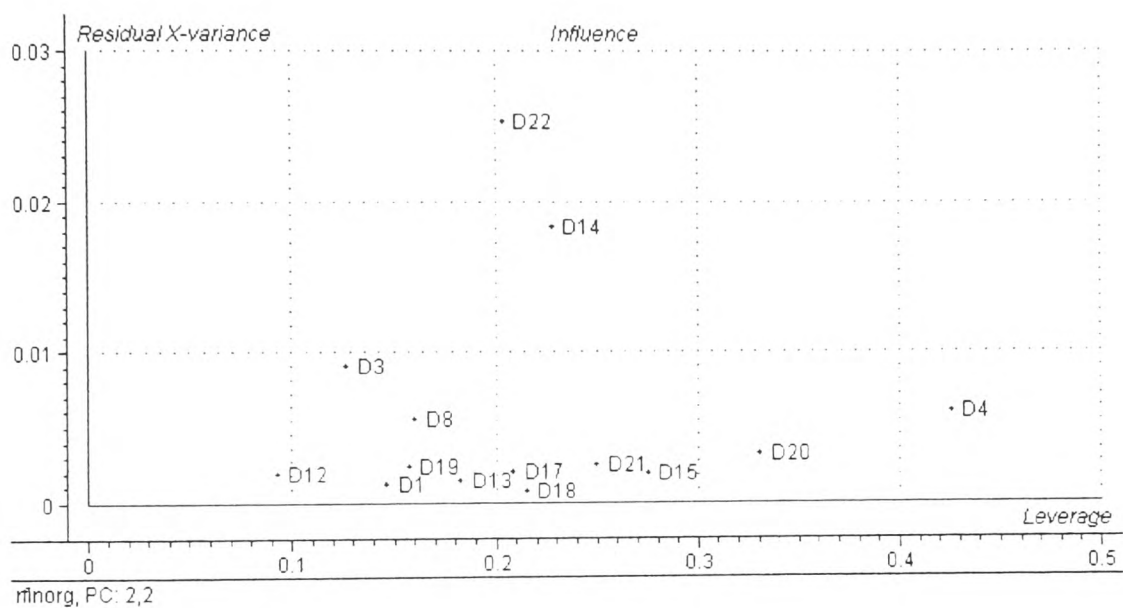


**Figure 4.4 Residual variance plot of the authentic olive oils.**

The score plots (Figure 4.5) showed the projections of the samples onto the PCs. The loadings plot (Figures 4.6) showed how much each variable contributed to the first PC and how well the PC took into account the variable's variation over the data points (Camo AS, 1996).

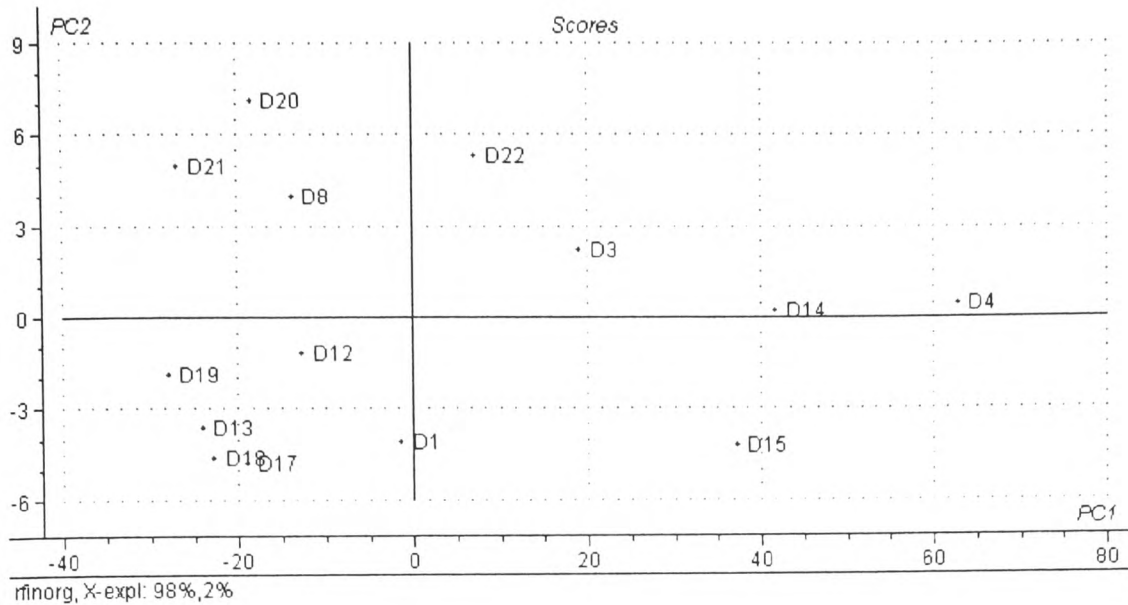


**Figure 4.5** Score plot of PC1 versus PC2 for the authentic olive oils training set

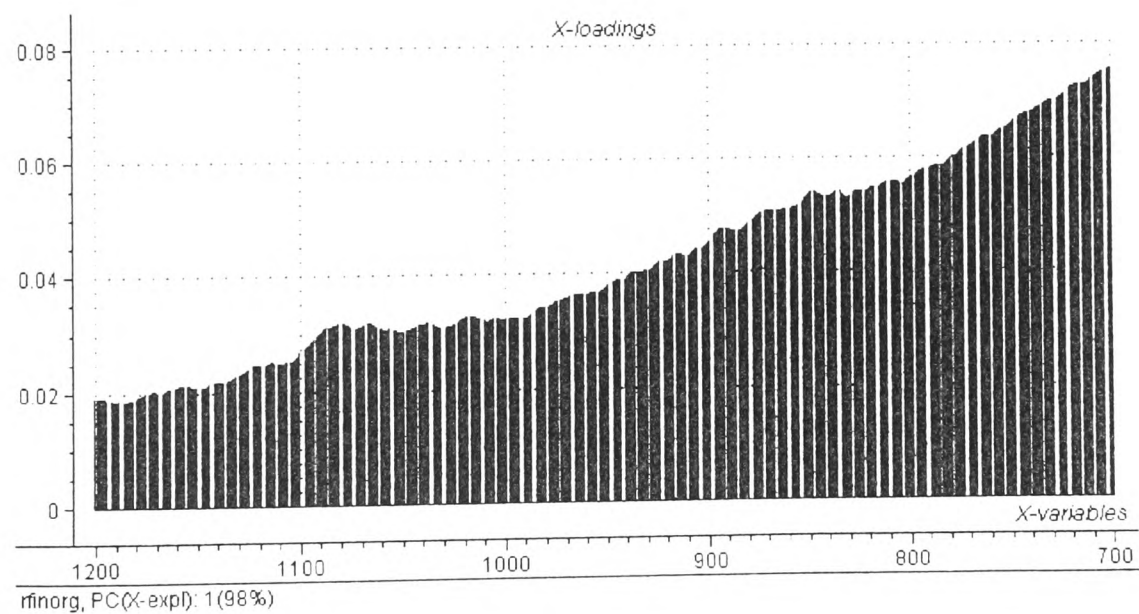


**Figure 4.6** Loadings plot of the authentic olive oils training set

Once the models were developed they were validated by the test sets. The classification of the test sets are shown in Table 4.18.

**Table 4.18 Classification of the test set with the class models for the authentic oils and their adulterated mixtures on the fingerprint region using full cross validation with 5 samples in the test set**

Class models		Test sets		Classified successfully	
Finorg	Fin/2 %	Fin test	Fin/2 % Test	5/5	5/5
Finorg	Fin/5 %	Fin test	Fin/5 % Test	5/5	5/5
Finorg	Fin/10 %	Fin test	Fin/10 % Test	5/5	4/5
All models		All test sets		5/5 Fin test	

The classification of the test set resulted in 19 out of the 20 samples used being correctly assigned. The classification table showed numerical results for each classified sample. Cooman's plots for the classification of the authentic oils and their adulterated mixtures are shown in Figures 4.8 - 4.10. As stated in Chapter 1, section 1.5.8, the development of well defined class models relies on a separation distance in the ratio of 1:3 between each class model. The discriminating plot is also indicative of good separation between the class models, and variables with a discriminating power of 1 should be eliminated from the model. A good class separation was observed between the authentic class and each of the adulterated sets in all the class models developed in this analysis. However, this separation was not observed between the adulterated sets themselves indicating that these models were useful in the detection of adulteration in olive oils, but were not efficient enough to detect the different levels of adulteration. However, this application showed that low levels of sunflower adulteration of olive oil, in the region of 2 % w/w, could be detected (Figure 4.8). Thus, the PCA analysis on the Raman authentic and adulterated oils spectra was a reliable method for distinguishing authentic olive oil from its adulterants.

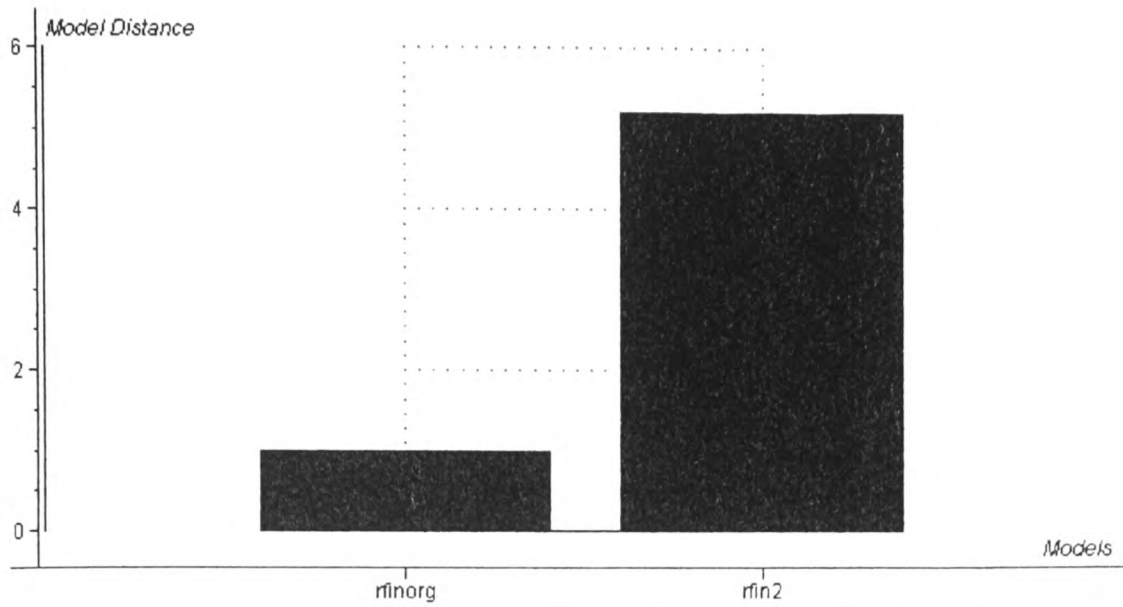
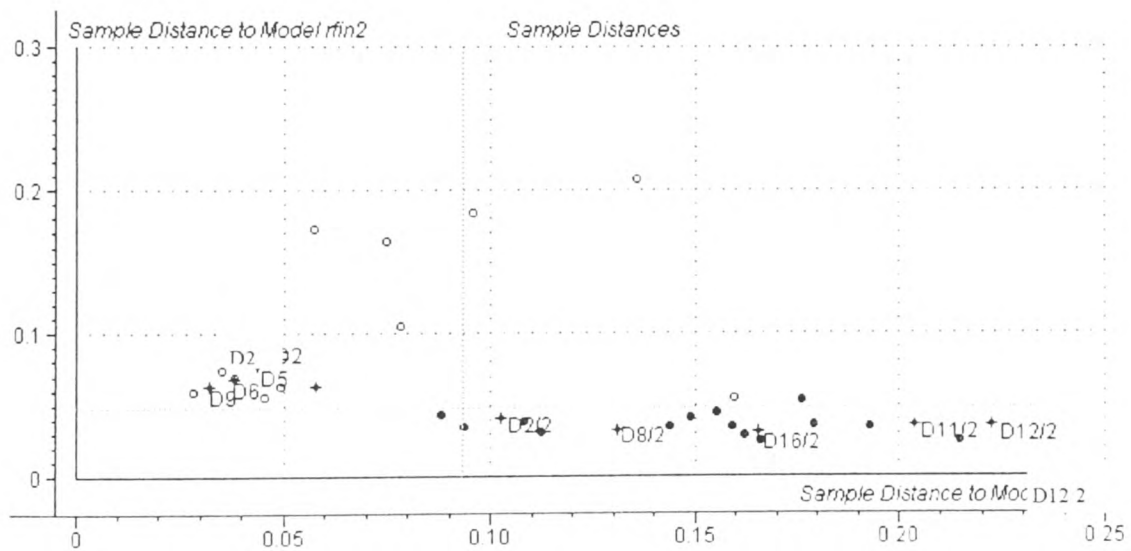
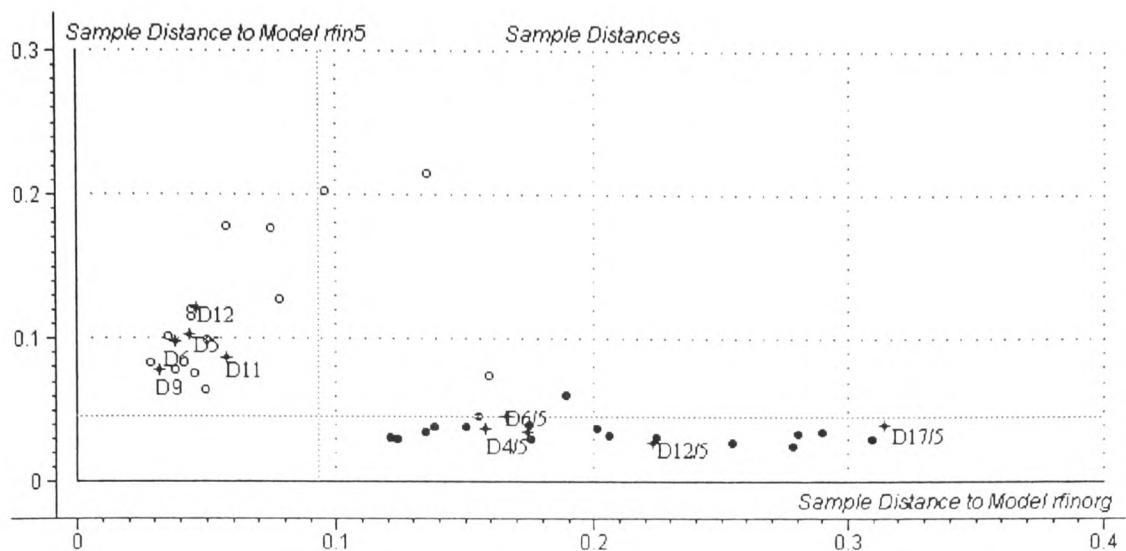


**Figure 4.7** Plot of the model distance between the authentic oil class model and the class model of oils adulterated with 2 % w/w sunflower



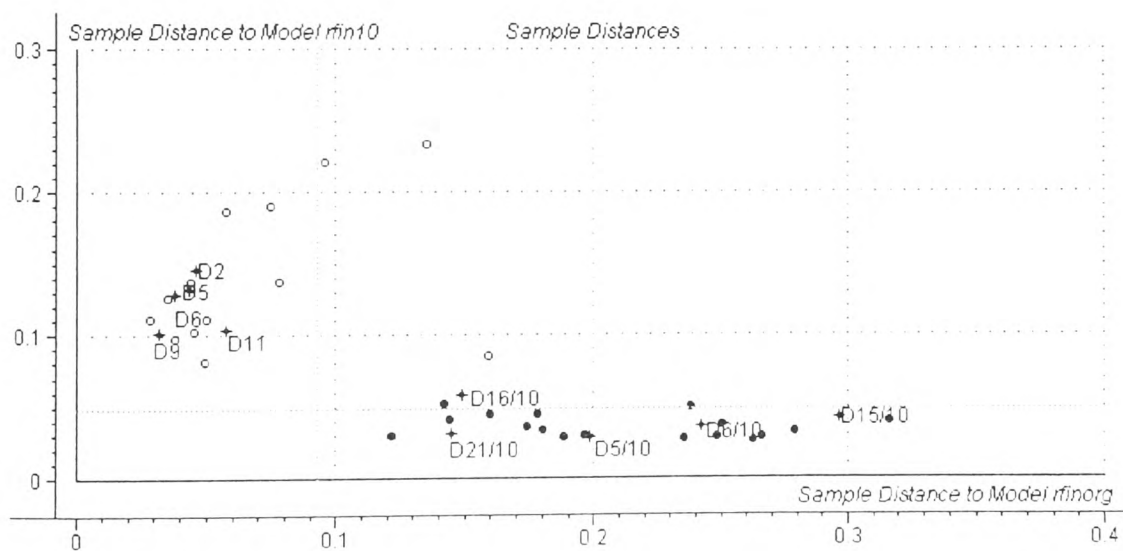
rfin2: class model of the oils adulterated with 2 % sunflower on the fingerprint region using 5 test samples.  
 Rfinorg: class model of the authentic oils on the fingerprint region using 5 test samples.

**Figure 4.8.** Coomans plot of the Finorg class versus Fin/2 %



Rfinorg: class model of the authentic oils on the fingerprint region using 5 test set samples; Rfin5: class model of the oils adulterated with 5 % sunflower on the fingerprint region using 5 test set samples.

**Figure 4.9. Coomans plot of the Finorg class versus Fin/5 %**



Rfinorg: class model of the authentic oils on the fingerprint region using 5 test set samples; Rfin10: class model of the oils adulterated with 10 % sunflower on the fingerprint region using 5 test set samples.

**Figure 4.10 Coomans plot of the Finorg class versus Fin/10 %**

#### **4.1.2.5 SIMCA classification of Raman fingerprint spectral data using randomly chosen test sets**

This analysis was further supported by the development of other models from the same data set. The number of samples used in these test sets were 3 and 8. This ensured that a bigger training set and a smaller training set (than the already developed model) were used to calibrate the models. The training set containing 19 samples each were called *Finorg3*, *Fin3/2 %*, *Fin3/5 %* and *Fin3/10 %* respectively. The Test sets of the authentic oils and its adulterated mixtures, each containing 3 samples, were called *Fin3 Test*, *Fin3/2 % Test*, *Fin3/5 % Test* and *Fin3/10 % Test*. The training set containing 14 samples were called *Finorg8*, *Fin8/2 %*, *Fin8/5 %* and *Fin8/10 %*. The test sets containing 8 samples were called *Fin8 Test*, *Fin8/2 % Test*, *Fin8/5 % Test* and *Fin8/10 % Test*. The test sets for each of these studies were randomly chosen by the computer and the data sets were set up according to Tables 4.19, 4.20, 4.21 and 4.22.



**Table 4.19 Composition of the Training sets for the authentic oil sets and their adulterated mixture sets on the Raman fingerprint region**

<b>Finorg3</b>	<b>Fin3/2 %</b>	<b>Fin3/5 %</b>	<b>Fin3/10 %</b>
D1	D1/2	D1/5	D1/10
D2	D3/2*	D2/5	D2/10
D3	D4/2	D4/5	D3/10
D4*	D5/2*	D5/5	D4/10
D5	D6/2	D6/5	D5/10
D6	D7/2*	D7/5	D6/10
D7	D8/2	D8/5	D7/10
D8	D9/2	D9/5	D8/10
D9	D10/2	D10/5	D9/10
D10*	D11/2	D11/5	D10/10
D11	D12/2	D12/5	D11/10
D12	D13/2	D13/5	D12/10
D14*	D14/2	D14/5	D13/10
D15	D15/2	D15/5	D14/10
D16*	D16/2	D18/5	D16/10*
D18	D17/2	D19/5	D17/10
D20	D18/2	D20/5	D18/10
D21	D19/2	D21/5	D20/10
D22*	D20/2	D22/5	D22/10

\* indicates outliers removed during the development of the class model.

**Table 4.20 Composition of the Test set for the validation of the authentic set and its adulterated mixture sets on the Raman fingerprint region using full cross validation with 3 samples in the test set**

<b>Fin3 Test</b>	<b>Fin3/2 % Test</b>	<b>Fin3/5 % Test</b>	<b>Fin3/10 % Test</b>
D13	D2/2	D3/5	D15/10
D17	D21/2	D16/5	D19/10
D19	D22/2	D17/5	D21/10

**Table 4.21 Percentage variance accounted for in the first 2 PCs in the model formed on the fingerprint region**

Name of components	Finorg3	Fin3/2 %	Fin3/5 %	Fin3/10 %
PC1	95.00	97.00	91.00	94.00
PC2	99.56	99.83	99.67	99.86

**Table 4.22 Classification of the test set with the class models for the authentic oils and their adulterated mixtures on the Raman fingerprint region**

Class models		Test sets		Classified successfully	
Finorg3	Fin3/2 %	Fin3 Test	Fin3/2 % Test	3/3	0/3
Finorg3	Fin3/5 %	Fin3 Test	Fin3/5 % Test	3/3	2/3
Finorg3	Fin3/10 %	Fin3 Test	Fin3/10 % Test	3/3	2/3

**Table 4.23 Composition of the Training sets for the authentic oil sets and their adulterated mixture sets on the Raman fingerprint region using FCV validation and 8 samples in the test set**

Finorg8	Fin8/2 %	Fin8/5 %	Fin8/10 %
D1	D1/2	D1/5	D1/10
D3	D3/2	D3/5	D3/10
D4	D4/2	D4/5	D4/10
D8	D8/2	D8/5	D8/10
D9	D9/2	D9/5	D9/10
D10*	D10/2	D10/5	D10/10
D12	D12/2	D12/5	D12/10
D13	D13/2	D13/5	D13/10
D14	D14/2	D14/5	D14/10
D15	D15/2	D15/5	D15/10
D17	D17/2	D17/5	D17/10
D19	D19/2	D19/5	D19/10
D20	D20/2	D20/5	D20/10
D21	D21/2	D21/5	D21/10

\* indicates outliers removed during the development of the class model.

**Table 4.24 Composition of the Test set for the validation of the authentic set and its adulterated mixture sets using FCV validation and 8 samples in the test set**

Fin8 Test	Fin8/2 % Test	Fin8/5 % Test	Fin8/10 % Test
D2	D2/2	D2/5	D2/10
D5	D5/2	D5/5	D5/10
D6	D6/2	D6/5	D6/10
D7	D7/2	D7/5	D7/10
D11	D11/2	D11/5	D11/10
D16	D16/2	D16/5	D16/10
D18	D18/2	D18/5	D18/10
D22	D22/2	D22/5	D22/10

**Table 4.25 Percentage variance accounted for in the first 2 PCs in the model formed on the fingerprint region of the authentic oils and their adulterated mixture sets**

Name of components	Finorg8	Fin8/2 %	Fin8/5 %	Fin8/10 %
PC1	97.97	94.60	92.46	92.31
PC2	99.80	99.79	99.75	99.81

**Table 4.26 Classification of the test set with the class models for the authentic oils and their adulterated mixtures on the on the fingerprint region**

Class models		Test sets		Classified successfully	
Finorg8	Fin8/2 %	Fin8 Test	Fin8/2 % Test	5/8	6/8
Finorg8	Fin8/5 %	Fin8 Test	Fin8/5 % Test	5/8	4/8
Finorg8	Fin8/10 %	Fin8 Test	Fin8/10 % Test	5/8	5/8

These models also proved successful in distinguishing the authentic oils from their adulterated mixtures. All the authentic oils in the Fin3 Test were classified correctly. Three of the samples in the Fin8 test were incorrectly assigned. However, this test set was large

and left a smaller number of samples in the training set to represent the whole fingerprint data set. The results of these model are shown in Table 4.22 and Table 4.26. Thus, the Raman fingerprint region of olive oils proved effective in the classification of the authentic oils and the detection of sunflower adulteration.

**4.1.2.6 SIMCA classification on the Peloponese and Crete varieties within the authentic oils on the Raman whole data set**

Individual models were also developed for the Peloponese oils, Crete oils and their adulterated mixtures. The Peloponese model were developed from the whole data region in Table 4.6 and from the fingerprint region alone. The training sets developed from the whole data region were called Pelop, Pelop/2 %, Pelop/5 % and Pelop/10 % represent the authentic Peloponese oils and its adulterated mixtures of 2 % w/w, 5 % w/w and 10 % w/w sunflower respectively. The test set for these olive oils were called Pelop Test, Pelop/2 % Test, Pelop/5 % Test, Pelop/10 % Test. The composition of the training sets and the test sets are shown in the following Tables 4.27 and 4.28.

**Table 4.27 Composition of the Training sets for the authentic Peloponese oil sets and their adulterated mixture sets on the whole data region**

Pelop	Pelop/2 % set	Pelop/5 %	Pelop/10 %
D8	D7/2	D7/5	D7/10
D10	D9/2	D8/5	D8/10
D11	D10/2	D9/5	D9/10
D12	D13/2	D10/5	D10/10
D13	D14/2	D13/5	D11/10
D14	D15/2	D14/5	D12/10
D15	D16/2	D16/5	D13/10
D16	D17/2	D17/5	D17/10
D17	D18/2	D18/5	D18/10

**Table 4.28 Composition of the Test set for the validation of the authentic Peloponese set and its adulterated mixture sets on the whole data region**

Pelop Test	Pelop/2 % Test	Pelop/5 % Test	Pelop/10 % Test
D7	D8/2	D11/5	D8/10
D9	D11/2	D12/5	D15/10
D18	D12/2	D15/5	D16/10

Similar to the authentic data set, using the whole data region the Peloponese samples were badly described by the model using all the absorption band regions in Table 4.2, page 119. The classification was performed on 2 PCs which again resulted in the discrimination between the authentic oil samples and their adulterated mixtures. The percentage variance accounted for in the first two PCs is recorded in Table 4.29. The results of the classification are shown in Table 4.30.

**Table 4.29. Percentage variance accounted for in the first 2PCs in the model formed on the whole region of Peloponese oil and its adulterated mixture sets**

Name of components	Pelop	Pelop/2 % set	Pelop/5 % set	Pelop/10 % set
PC1*	94.00	95.00	90.90	85.58
PC2*	99.00	99.00	99.75	99.82

\* Variables are badly described by the model.

**Table 4.30 Classification of the test set with the class models for the authentic Peloponese oils and their adulterated mixtures on the whole region**

Class models		Test sets		Classified successfully	
Pelop	Pelop/2 %	Pelop Test	Pelop/2 % Test	3/3	2/3
Pelop	Pelop/5 %	Pelop Test	Pelop/5 % Test	3/3	2/3
Pelop	Pelop/10 %	Pelop Test	Pelop/10 % Test	3/3	1/3

**4.1.2.7 SIMCA classification on the Peloponese and Crete varieties within the authentic oils on the Raman fingerprint**

The training sets developed from the fingerprint region were called Pelfin, Pel/2 %, Pel/5 % and Pel/10 %. The test sets were called Pelfin Test, Pel/2 % Test, Pel/5 % Test and Pel/10 % Test. These sets are recorded in Tables 4.31 - 4.32.

**Table 4.31 Composition of the Training sets for the authentic Peloponese oil sets and their adulterated mixture sets on the fingerprint region**

Pelfin	Pel/2 %	Pel/5 %	Pel/10 %
D7	D7/2	D7/5	D7/10
D8	D8/2	D8/5	D8/10
D10	D9/2	D10/5	D11/10
D11	D10/2	D12/5	D12/10
D12	D13/2	D13/5	D13/10
D15	D14/2	D14/5	D14/10
D16	D15/2	D15/5	D15/10
D17	D17/2	D17/5	D17/10
D18	D18/2	D18/5	D18/10

**Table 4.32 Composition of the Test set for the validation of the authentic Peloponese set and its adulterated mixture sets on the fingerprint region**

Pelfin Test	Pel/2 % Test	Pel/5 % Test	Pel/10 % Test
D9	D11/2	D9/5	D9/10
D13	D12/2	D11/5	D10/10
D14	D16/2	D16/5	D16/10

The statistical application of SIMCA to the fingerprint region of the Peloponese provided similar results to those already described for the whole Raman data region. Each variable was described by the model and the first two PCs accounted for 99 % (approx.) of the variance. This is shown in Table 4.32. Each authentic oil sample in the set was again

distinguished from the adulterant test sets. The similarities between the statistical analysis of the whole data region and the fingerprint region implied that total variation of the data could be extracted from the fingerprint region alone. The classification of the test set is shown in Table 4.34.

**Table 4.33 Percentage variance accounted for in the first 2PCs in the model formed on the fingerprint region of Peloponese oil and its adulterated mixture sets**

Name of components	Pelfin	Pel/2 %	Pel/5 %	Pel/10 %
PC1	99.52	97.96	90.90	85.58
PC2	99.85	99.79*	99.75	99.82

\* Total residual calibration variance is 0.47 (limit 0.50)

**Table 4.34 Classification of the test set with the class models for the authentic Peloponese oils and their adulterated mixtures on the fingerprint region**

Class models		Test sets		Classified successfully	
Pelfin	Pel/2 %	Pelfin Test	Pel/2 % Test	3/3	2/3
Pelfin	Pel/5 %	Pelfin Test	Pel/5 % Test	3/3	2/3
Pelfin	Pel/10 %	Pelfin Test	Pel/10 % Test	3/3	2/3

The models for the Crete oil samples and their adulterated mixtures were developed from the data obtained from the fingerprint region. The training sets and test sets for these models are shown in Tables 4.35 and 4.36. The training sets were called *Crete*, *Crete 2 %*, *Crete 5 %* and *Crete 10 %*. The test sets were called *Crete Test*, *Crete 2 % Test*, *Crete 5 % Test* and *Crete 10 % Test*.

**Table 4.35 Composition of the Training sets for the authentic Crete oil sets and their adulterated mixture sets on the on the fingerprint region using F.C.V. with 1 sample in the test set**

Crete	Crete/2 %	Crete/5 %	Crete/10 %
D1	D1/2	D1/5	D1/10
D2	D3/2	D2/5	D3/10
D3	D4/2	D4/5	D4/10
D4	D5/2	D5/5	D5/10
D6	D6/2	D6/5	D6/10

**Table 4.36 Composition of the Test set for the validation of the authentic Crete set and its adulterated mixture sets on the fingerprint region using F.C.V. with 1 sample in the test set**

Crete Test	Crete/2 % Test	Crete/5 % Test	Crete/10 % Test
D5	D2/2	D3/5	D2/10

In the development of these models, a low total residual calibration variance was observed after 1 PC. The classification was performed on 2 PCs and each test set was assigned to its class model correctly (Tables 4.37 and 4.38).

**Table 4.37 Percentage variance accounted for in the first 2 PCs in the model formed on the fingerprint region of Crete oil and its adulterated mixture sets using full cross validation with 1 samples in the test set**

Name of components	Crete	Crete/2 %	Crete/5 %	Crete/10 %
PC1	99.00	97.5*	92.35*	97.00*
PC2	99.85	99.79*	99.30	99.82

\* Total residual calibration variance is low.



**Table 4.38 Composition of the Test sets for the authentic Crete oils, Peloponese oils and the Crete adulterated mixtures on the fingerprint region using FCV with 1 sample in the test set**

Class models		Test sets		Classified successfully	
Pelop	Crete	Pelop Test	Crete Test	No differences between classes	
Crete	Crete/2 %	Crete Test	Crete/2 % Test	1/1	1/1
Crete	Crete/5 %	Crete Test	Crete/5 % Test	1/1	1/1
Crete	Crete/10 %	Crete Test	Crete/10 % Test	1/1	1/1

Using the developed models of *Pelop*, *Crete*, *Crete/2 %*, *Crete 5 %* and *Crete 10 %*, a further classification was carried out to try and differentiate between the Crete and Peloponese varieties of oils and their Crete adulterated mixtures. In this classification no differences were observed between the subgroup varieties of Peloponese and Crete. However, the subsets of these oils were small and may require a larger number in each class model to determine subtle differences between these oils. Distinctions were made between the authentic Crete oils and its adulterated mixtures. However, again, sample size was small and more samples may be required to give more conclusive results.

#### **4.1.3 Conclusion on Raman analysis**

In conclusion, this FT - Raman analysis used in complement with SIMCA classification proved a valuable tool in discriminating between olive oil and its adulterated mixtures. The Raman technique itself was rapid, reproducible and quite applicable to the analysis of oils in favour of traditional time consuming wet chemistry methods.

## **4.2. Infrared analysis**

Fourier transform infrared spectroscopy was used in conjunction with principal component analysis and discriminant analysis to investigate whether the adulteration of extra virgin olive oil could be detected. Mid - infrared spectroscopy using the attenuated total reflectance sampling technique provided a fast and efficient method for analyzing olive oils. The minor differences between the spectra of the olive oils and their adulterated mixtures can be highlighted by means of principal component analysis (Safar ,1994).

The aim of this analysis carried out in the present study was to apply a discriminant function to a data set consisting of extra virgin oil and its adulterated mixtures (2 % w/w, 5 % w/w and 10 % w/w sunflower) and to assign spectra to either the authentic or to one of the adulterated classes. SIMCA (Chapter 1) was also applied to this data set. Here again classification was the aim but involved the development of softer models which were shaped from the properties of the data and were less restrictive than hard models (Christie, 1986).

### **4.2.1 Materials and methods**

Carbon tetrachloride.

Attenuated total reflectance (ATR) cell

#### **4.2.1.1 Procedure**

The Mid - Infrared (MIR) spectra were obtained on a Perkin Elmer 1720 Fourier Transform spectrometer using attenuated total reflectance as the sampling technique. The detector used was a TGS detector. The sample was placed in contact with the ATR crystal (ZnSe crystal). Each spectrum was collected at  $2\text{ cm}^{-1}$  resolution from  $4000 - 600\text{ cm}^{-1}$  after 16 scans. Between measurements the crystal was cleaned with carbon tetrachloride and air dried. Each sample single - beam spectrum was ratioed to a single beam spectrum of a clean

ATR plate. The parameters for this experiment are recorded in Table 4.39.

**Table 4.39 Infrared experimental parameters**

Mid - Infrared components	Parameters
Detector	TGS
Apodization	Normal
Resolution	2.00
X Units	1/CM
Y Units	absorbance
Absorbance scan	4000 - 600
N points	3401

#### 4.2.2 Results and discussion

Mid - infrared spectra of a Greek oil and its adulterated mixtures (sample D1) are shown in Figure 4.11. Since vegetable oils contain similar fatty acids and triglycerides, their spectra are dominated by the C-H and C-O vibrations of the polymethylene chains (Lai, 1994). On inspection of Figure 4.11 no obvious differences were observed between each spectra. However, as reported by Lai (1994) subtle difference do exist between vegetable oil spectra in the structure of their polymethylene chains.

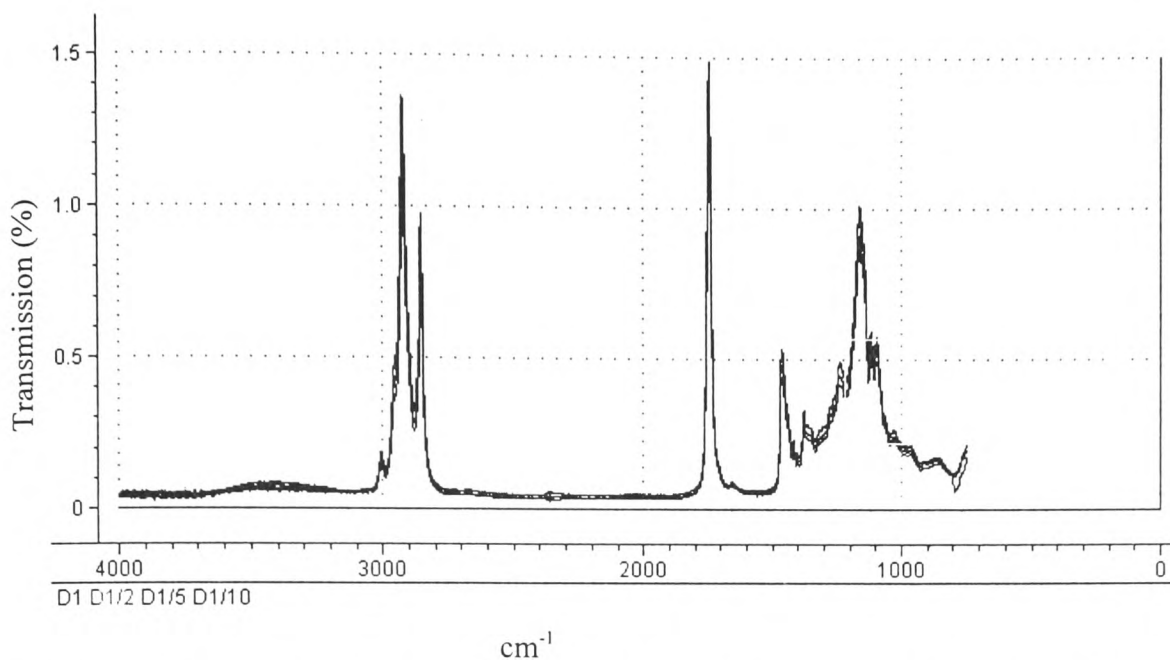


**Figure 4.6 Mid - infrared absorbance spectra of an extra virgin oil and its adulterated sunflower mixtures (2% w/w, 5% w/w, 10% w/w respectively)**

#### *4.2.2.1 Discriminant statistical analysis of Infrared data*

As a pretreatment to the data, the baseline of the spectrum was first corrected using the instrument software. Hard modelling discriminant analysis was carried out on the infrared data of 66 oils consisting of 22 authentic Greek oils and 44 of their adulterated mixtures with sunflower oil. The levels of sunflower adulteration in the olive oil were 2% 5% and 10% respectively. Lai (1994) has reported that infrared data extracted from the regions 3100 - 2800  $\text{cm}^{-1}$  and from 1800 - 800  $\text{cm}^{-1}$  provided most of the spectral information on oils (Lai, 1994). Thus, the statistical analysis on the IR data was carried out on these extracted regions. PCA was used to reduce the IR data so that the observations exceeded the variables. This data reduction is important if multivariate methods such linear discriminant analysis using as squared Mahalanobis distance are to proceed. This data reduction also simplifies the data set and gives a clearer indication of the relationships between the samples (Lai, 1994). All the data analysis was carried out using Win - Discrim

(see Chapter 1, section 1.5.6).

PCA models were first developed using the authentic oils and their sunflower mixtures (10 % w/w). This discriminant model refers to adulterated oil sample used was called *Greek10 %* and the test set was called *Greek10 % Test*. The training and test sets for this analysis are shown in Table 4.40 and 4.41 respectively.

**Table 4.40 Composition of the Training set used in the development of the Greek10 % discriminant model**

Greek/10 %	
D1	D1/10
D3*	D2/10
D4	D3/10*
D5	D4/10
D6*	D6/10
D8	D8/10
D10	D9/10*
D11	D10/10
D13	D11/10
D14	D12/10
D16	D13/10
D17	D14/10
D18	D16/10
D19	D17/10*
D20	D18/10
D21*	D20/10
D22	D22/10

\* Misclassified samples in the development of the Allsel PC model.

**Table 4.41 Composition of Test set used in the validation of the Greek/10 % discriminant model**

Greek/10 % Test	
D2	D5/10
D7	D7/10
D9	D15/10
D12	D19/10
D15	D21/10

In the application of discriminant analysis to this study, each sample in the training data set was assigned to its class, whether it was authentic extra virgin oil or extra virgin oil adulterated with 10 % w/w sunflower oil. The authentic oils were classed as group 1 and the oil adulterated with 10 % w/w sunflower were classed as group 2. The data matrix was first reduced by PCA and 15 PCs were extracted. The percentage variance accounted for by 15 PC scores are shown in Table 4.42. The variance reached a stable minimum after 14 PCs and was thus indicative of the number of PCs to use in this analysis. The percentage variance accounted for in the development of this model was however, low and only reached a maximum of 20.61 %.

**Table 4.42 Percentage variance account for in the development of the Greek/10 % discriminant model**

Score	Cumulative percentage variance
1	13.35
2	17.07
3	18.29
4	19.04
5	19.58
6	19.86
7	20.11
8	20.26
9	20.35
10	20.41
11	20.47
12	20.52
13	20.56
14	20.61
15	20.65

Using 14 PCs, the squared Malahanobis distances of each sample in the training data set from the 2 group mean sample were calculated. Each sample was reassigned to the nearest group on the basis of the calculated squared Malahanobis distance. This analysis resulted in correctly assigning 34 out of a total 51 samples to their defined classes. The misclassified samples are indicated with asterisk in Table 4.40. This class model was evaluated using the *Greek 10 % Test set*.

As previously described for the training set, the squared Mahalanobis distance of each sample in the test set from the 2 group mean samples were calculated and the samples were reassigned to their nearest parent group. The efficiency of the discrimination was reflected in how well the assignments to the correct class were performed. The test set of this model

resulted in the correct classification of 9 out of 10 samples. The misclassified sample was D7 (Table 4.43). The sample D12 also appeared as highly suspect in this analysis as the sample was far removed from authentic and adulterated models. A canonical variate analysis of Greek/10 % is shown in Figure 4.12.

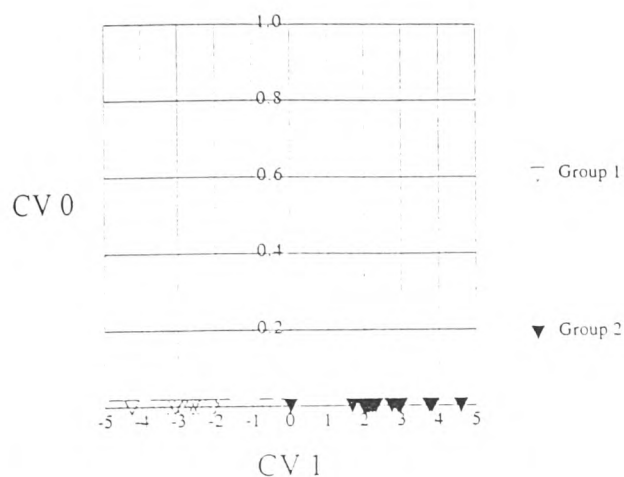


Figure 4.12 Canonical variate plot of the Greek10 %

Table 4.43 Validation of results for the test for Greek/10 % Test Discriminant model

Name	Distance	Distance from	Predicted	Assignment
D2	17.05	18.91	1.00	Correct
D7	19.63	17.31	2.00	Incorrect
D9	14.98	15.31	1.00	Correct
D12	343.27	368.90	1.00	Correct
D15	36.78	37.52	1.00	Correct
D5/10	7.68	4.68	2.00	Correct
D7/10	15.78	14.21	2.00	Correct
D15/10	21.18	17.77	2.00	Correct
D19/10	17.10	16.39	2.00	Correct
D21/10	46.38	38.19	2.00	Correct

Group 1: authentic oils. Group 2: olive oils adulterated with 10 % w/w sunflower.



**4.2.2.2 Discriminant analysis using the authentic samples and sunflower adulterated samples (5 % w/w and 10 % w/w sunflower respectively)**

A further analysis was carried out to include the oils adulterated with 5 % w/w sunflower oil. These PC models were called *AllGreek* and the test set used in the validation of the model was called *AllGreek Test*. The composition of the training set and test set for this analysis is shown in Table 4.44 and Table 4.45 respectively.

**Table 4.44 Composition of the Training set used in the development of the AllGreek model**

AllGreek Training set		
D1*	D1/5*	D1/10
D3*	D2/5*	D2/10
D4	D3/5	D3/10*
D5	D4/5	D4/10
D6*	D5/5	D6/10
D8*	D6/5*	D8/10*
D10*	D7/5*	D9/10*
D11	D8/5*	D10/10*
D13	D9/5	D11/10
D14	D10/5*	D12/10
D16	D12/5*	D13/10
D17	D14/5	D14/10
D18*	D16/58	D16/10
D19	D18/5	D17/10*
D20*	D20/5*	D18/10*
D21*	D21/5*	D20/10
D22	D22/5	D22/10

\* Misclassified samples in the development of the AllGreek PC model.

**Table 4.45 Composition of the AllGreek Test set**

Allgreek Test		
D2	D11/5	D5/10
D7	D13/5	D7/10
D9	D15/5	D15/10
D12	D17/5	D19/10
D15	D19/5	D21/10

The development of this classification resulted in the classification of 34 out of 51 samples.

In this case group 1 represented the authentic oils, group 2 represented the

oils adulterated with 5 % w/w sunflower and group 3 represented the olive oil adulterated with 10 % w/w sunflower. The misclassifications in this linear discriminant (LD) model are indicated by an asterisk in Table 4.44.

In this analysis 13 out of 20 samples were classified correctly. However, this PC linear discriminant model failed to make any distinction between the authentic oils and their 5 % w/w sunflower adulterated mixtures. The prediction of the AllGreek Test is shown in Table 4.46.

A further model was developed by removing the outlier sample 7 and its adulterated mixtures from the data set. However, this elimination did not make any improvement in the classification of the test set samples.

**Table 4.46 Prediction of Allgreek Test using AllGreek discriminant model**

Name	Distance from group 1	Distance from group 2	Distance from group 3	Predicted group	Assignment
D11/5	30.22	35.40	31.79	1.00	Incorrect
D13/5	15.78	15.60	15.46	3.00	Correct
D15/10	22.33	19.05	19.84	2.00	Incorrect
D15/5	13.74	15.18	19.90	1.00	Incorrect
D17/5	20.66	15.55	16.88	2.00	Correct
D19/10	18.90	17.82	20.56	2.00	Incorrect
D19/5	28.70	21.05	27.26	2.00	Correct
D21/10	49.82	47.22	43.87	3.00	Correct
D5/10	8.72	7.66	5.23	3.00	Correct
D7/10	14.10	13.91	14.59	2.00	Incorrect
D12	418.68	403.12	425.32	2.00	Incorrect
D15	47.20	50.27	52.10	1.00	Correct
D2	23.23	23.26	24.67	1.00	Correct
D7	21.90	21.30	22.68	2.00	Correct
D9	13.76	17.83	14.89	1.00	Incorrect

Group 1: Authentic oils. Group 2: olive oils adulterated with 5 % sunflower oil Group 3: olive oils adulterated with 10 % sunflower oil.

The prediction of the *Allgreek Test* resulted in 8 out of 15 samples being correctly classified (Table 4.46). A canonical variate plot of the allGreek Test samples are shown in Figure 4.13. In this canonical plot the authentic oils and their adulterated mixtures were not clearly distinguished from each other (Figure 4.13).

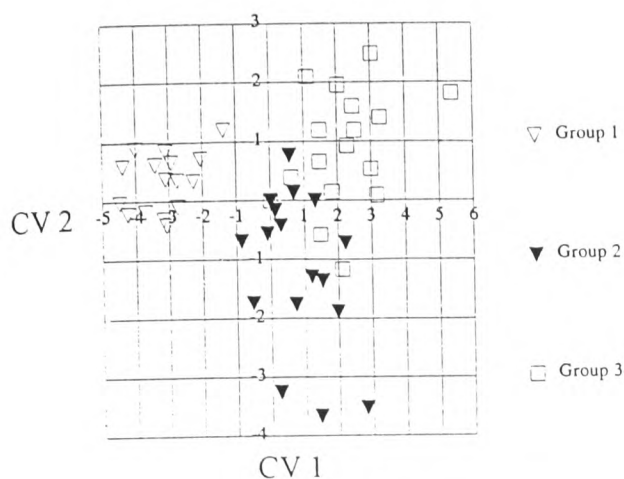


**Figure 4.13** Canonical variate plot of the Allgreek

#### 4.2.2.3 Discriminant analysis using the authentic samples and 10 % w/w sunflower adulterated samples and the selective infrared absorptions

The infrared data region was reduced further to remove possible interferences arising from varying water contents in the oils and instrumental noise. The selectivity of these wavenumber were based on the characteristic absorptions recorded in Table 1.8, page 47. The selected wavenumber are recorded in Table 4.47.

**Table 4.47** The selected IR absorptions used in discriminant analysis

Peak	Wavenumber	Assignments
1	3020 - 3000	$\nu$ asym (=C-H), $\nu$ Sam (=C-H)
2	2950 - 2900	$\nu$ asym (-C-H)
3	2880 - 2840	$\nu$ sym (=C-H)
4	1760 - 1730	$\nu$ (C=O)
5	1665 - 1650	$\nu$ (C=C)
6	1480 - 1450	$\delta$ (CH <sub>2</sub> )
7	1380 - 1260	methylene twisting,
8	1380 - 1260	in plane =C-H deformation in cis bond
9	1180 - 1150	C-O stretch in ester $\nu$ (C-O)
10	1050 - 950	trans (-CH=CH-)
11	750 - 700	=C-H planar bending

Using the *Allsel* training set and *Allsel Test* set (Table 4.48 and Table 4.49 respectively) a discriminant was developed from the selective IR data region. This discriminant was called *Allsel*. In the development of this model there was a significant increase in the percentage variance accounted for in the data over as compared to the whole data region (Table 4.42). The cumulative percentage variance, shown in Table 4.50 reached a maximum of 94.58 % after 15 PCs were estimated.

**Table 4.48 Composition of the Training set used in the development of the Allsel model**

Allsel Training set		
D1	D1/5*	D1/10
D3	D2/5	D2/10
D4	D3/5	D3/10
D5	D4/5	D4/10
D6*	D5/5	D6/10
D8	D6/5	D8/10
D10	D7/5*	D9/10
D11	D8/5	D10/10
D13	D9/5	D11/10
D14	D10/5*	D12/10
D16	D12/5	D13/10
D17	D14/5	D14/10
D18	D16/5	D16/10
D19	D18/5	D17/10*
D20*	D20/5	D18/10
D21	D21/5*	D20/10
D22	D22/5	D22/10

\* Misclassified samples in the development of the Allsel PC model.

**Table 4.49 Composition of the Allsel test set**

Allsel Test		
D2	D11/5	D5/10
D7	D13/5	D7/10
D9	D15/5	D15/10
D12	D17/5	D19/10
D15	D19/5	D21/10

**Table 4.50 Percentage variance account for in the development of Allsel**

PCs	Cumulative percentage variance
1	55.21
2	74.91
3	81.12
4	84.25
5	86.04
6	87.43
7	88.52
8	89.54
9	90.49
10	91.29
11	92.03
12	92.72
13	93.38
14	94.00
15	94.58

The development of the *Allsel* PC model resulted in the correct classification of 43 out of 51 samples. The misclassified samples in the discriminant models are indicated in Table 4.48 by an asterisk. The validations of the *Allsel* discriminant models are shown in Table 4.51.

**Table 4.51 Prediction of Allsel test using Allsel discriminant model**

Name	Distance from group 1	Distance from group 2	Distance from group 3	Predicted group	Assignment
D2	7.16	12.13	17.36	1.00	Correct
D4	10.29	12.89	17.63	1.00	Correct
D9	1.74	9.82	18.97	1.00	Correct
D12	4.07	8.32	17.76	1.00	Correct
D15	22.91	23.79	26.25	1.00	Incorrect
D11/5	15.57	10.05	9.89	3.00	Incorrect
D13/5	15.87	5.97	4.66	3.00	Incorrect
D15/5	17.69	12.57	12.70	2.00	Correct
D17/5	7.50	4.82	11.47	2.00	Correct
D19/5	15.79	8.94	7.06	3.00	Incorrect
D5/10	12.84	1.89	4.64	2.00	Incorrect
D15/10	42.98	25.92	19.68	3.00	Correct
D19/10	26.92	16.09	12.36	3.00	Correct
D21/10	13.34	10.70	10.81	2.00	Incorrect

The validation of the *Allsel* discriminant model resulted in the correct classification of the 4 out of 5 authentic oils. Thus, this analysis successfully distinguished the authentic olive oils from their adulterated mixtures.

The canonical plot of the *Allsel* test samples is shown in Figure 4.14. In contrast to the canonical plot of the *Allgreek* test samples (Figure 4.13), the *Allsel* canonical plot shows a clear separation between the authentic oils and their adulterated samples.



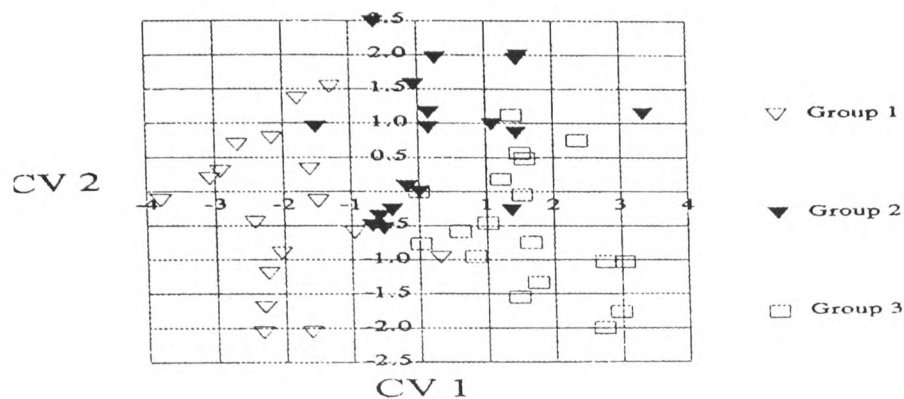


**Figure 4.14 Canonical variate plot of the Allsel model**

**4.2.2.4 Discriminant analysis using the authentic samples and 10 % sunflower adulterated samples on the selective infrared absorptions**

Discriminant analysis using the selected IR data was also used to try and distinguish between the authentic oils and their 10 % adulterated mixtures only. The training and test sets are shown in Table 4.52 and Table 4.53. The training and test sets for this application were called *Sel/10 %* and *Sel/10 % Test*.

**Table 4.52 Comparison of Training set used in the development of sel/10 % PC model**

Sel/10 %	
D1	D1/10
D3	D2/10
D4	D3/10
D8	D4/10
D10	D6/10
D11	D8/10
D13	D9/10
D14	D10/10
D16	D11/10
D17	D12/10
D18	D13/10
D19	D14/10
D21	D16/10
D22	D17/10
	D18/10
	D20/10
	D22/10

\* Misclassified samples in the development of the PC model.

**Table 4.53 Comparison of Test set used in the validation of the Sel/10 % Test**

Sel/10 % Test	
D2	D5/10
D4	D7/10
D9	D15/10
D12	D19/10
D15	D21/10

Samples 7 and 20 were removed from Sel/10 % training set as outliers and the Sel/10 % PC model resulted in correctly classifying all the samples. The Sel/10 % Test set consisting of authentic oils and adulterated mixtures were also correctly classified. The classification of

the *Sel/10 % Test* are shown in Table 4.54.

**Table 4.54 Classification of Sel/10 % Test**

Name	Distance from 1	Distance from 2	Predicted group	Assignment
D2	6.95	33.45	1.00	Correct
D4	11.83	16.08	1.00	Correct
D9	1.99	37.22	1.00	Correct
D12	6.72	26.74	1.00	Correct
D15	30.85	40.41	1.00	Correct
D5/10	24.44	3.87	2.00	Correct
D13/10	40.36	10.50	2.00	Correct
D15/10	50.45	16.46	2.00	Correct
D19/10	53.48	11.76	2.00	Correct
D21/10	24.44	8.42	2.00	Correct

This classification showed that the authentic oils and their 10 % w/w adulterated mixtures could be easily distinguished from each other. However, the distinction between the oils adulterated with the 5 % w/w adulterated sunflower oils and the oils adulterated with 10 % w/w sunflower was not clear. A canonical variate of Sel/10 % is shown in Figure 4.15.

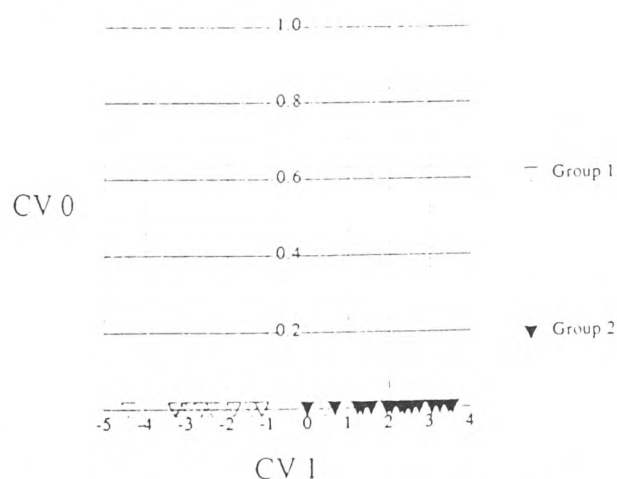


**Figure 4.15 Canonical variate of Sel/10 %**

#### 4.2.2.5 SIMCA classification of the Infrared data regions 3100 - 2500 and 1800 - 1000

The SIMCA classification on the infrared data was carried out using Unscrambler (CAMO AS, 1996). The IR data was first reduced to include the regions 3100 - 2500  $\text{cm}^{-1}$  and 1800 - 1000  $\text{cm}^{-1}$ . The data was normalized using mean normalization and the principal component analysis was carried out using no weightings on the variables. As described previously, SIMCA classification involves the development of independent models which are shaped according to the properties of the data. The training sets for the authentic oils and their adulterated mixtures were called *Authentic*, *Adult./5 %* and *Adult./10 %* and test sets were called *Authentic Test*, *Adult./5 % Test* and *Adult. 10 % Test*. These sets are shown in Table 4.55 and Table 4.56.

**Table 4.55 Composition of training sets used in SIMCA analysis of the infrared data**

<b>Authentic</b>	<b>Adult./ 5 %</b>	<b>Adult./10 %</b>
D1*	D1/5	D1/10
D3	D2/5	D2/10
D4*	D3/5	D3/10
D5	D4/5	D4/10
D6	D5/5	D6/10
D8	D6/5	D8/10
D10*	D7/5	D9/10
D11*	D8/5	D10/10
D13	D9/5	D11/10
D14	D10/5	D12/10
D16*	D12/5	D13/10
D17*	D14/5	D14/10
D18	D16/5	D16/10
D19	D18/5	D17/10
D20	D20/5	D18/10
D21	D21/5	D20/10
D22	D22/5	D22/10

**Table 4.56 Test set used in statistical analysis of the infrared data**

Authentic	Adult./5 % Test	Adult./10 % Test
D2	D11/5	D5/10
D7	D13/5	D7/10
D9	D15/5	D15/10
D12	D17/5	D19/10
D15	D19/5	D21/10

In the development of the infrared SIMCA PC model of the authentic oils 6 samples were rejected. These samples are indicated with an asterisk in Table 4.55. The variables extracted from the region  $2932 - 2909 \text{ cm}^{-1}$  and  $1749 - 1746 \text{ cm}^{-1}$  were also rejected. The rejection of these variables did not lend itself to the development of a good model as these absorptions are indicative of C-H antisymmetric stretch and the C=O stretch of an ester in the polymethylene chains respectively. The percentage variance accounted for in this model was also low.

#### ***4.2.2.6 SIMCA classification of the Infrared data regions 3050 - 2752***

IR data was further reduced to include the absorptions  $3050 - 2752 \text{ cm}^{-1}$  only. This region represented the C-H stretch of the polymethylene chain of the triglycerides. This principal component analysis did not prove successful as it resulted in many of the variables being badly described by the model. Samples D1 and D10 were removed from the model as outliers. However, a classification was carried out using developed models from the authentic oils and from the oils adulterated with 10 % sunflower oil. The model distance between these models were in the ratio 1:1.82 which indicated that there was insufficient distance between each class to give an effective separation between the oils and their adulterated mixtures (Chapter1, section 1.5.8).

#### ***4.2.2.7 SIMCA classification of the selective Infrared data regions***

Another selective data class was developed to include all the region in which olive oils absorb in the infrared region. The selective absorptions are recorded in Table 4.47.

Models were developed for the authentic oils and the oils adulterated with 10 % sunflower. Principal component analysis was carried out using full cross validation with 8 PCs. The variables were not weighted in this analysis. In the development of these models the percentage variance accounted for was also low indicating that there was little variation among the samples. The model distance between the models was 1:1.98. Again this distance was not sufficient to make a distinction between the authentic oil models and the models of their adulterated mixtures.

#### **Conclusion**

The water absorption in the Mid - infrared absorption bands of olive oils was clearly present. The varying unknown water contents greatly influenced the olive oil IR spectra and resulted in the bad classification of the authentic oils and the adulterated samples. However, the discriminant analysis of reduced selective IR data (which eliminated the absorption regions of water) was successful in partly distinguishing the Greek olive oils and their sunflower adulterants.

The soft modelling of this selective data did not prove as effective. The subtle difference between the authentic and adulterated samples were not as apparent with this statistical application. In the development of the class models several informative variables were rejected. The developed models (excluding these variables) did not have sufficient distance between each other to consider them different.

## CHAPTER 5

### *5.1 The analysis of olive oils using $^{13}\text{C}$ and proton nuclear magnetic resonance*

Nuclear magnetic resonance provides an insight into the nature of mixtures present in natural oils by acquiring useful information about its carbon and hydrogen atoms in different molecular environments. As stated in Chapter 1 the NMR analysis of olive oils provides structural information on fatty acid composition, acyl chain length, and location and stereochemistry of double bonds (Shiao, 1989). The full NMR spectrum of an oil provides characteristic chemical shifts in the carbonyl, alkene, methylene and methyl regions. These profiles serve as fingerprints for identification. In the expanded alkene region of  $^{13}\text{C}$  NMR the individual unsaturated fatty acid are completely resolved. Thus, the detection of adulteration in olive oil with sunflower oil is applicable through NMR as these oils are distinctly different in their oleic and linoleic fatty acid content.

Integration and quantitation of NMR data is time-consuming and laborious when large data sets are used. The statistical manipulation of NMR analytical data offers a fast and efficient means of comparing all the spectra simultaneously to uncover pattern similarities or differences among the spectra.

In this study the oil samples and its adulterated mixtures were analysed by both  $^1\text{H}$  NMR and  $^{13}\text{C}$  NMR. Computer-based pattern recognition methods was then used to classify the spectra into groups. The object was to try and differentiate between the authentic oils and their adulterated sunflower oil mixtures and also between the different regions that the authentic oils came from.

### 5.1.1 Materials and methods for $^{13}\text{C}$ NMR and $^1\text{H}$ NMR

$^{13}\text{C}$  NMR and  $^1\text{H}$  NMR spectra were obtained using a JEOL EX270 instrument.

Deuterated chloroform

NMR tubes (No. 528, high quality standard)

Standard triglycerides were supplied by Sigma.

#### 5.1.1.2 Procedure

The concentrations of the samples analysed by NMR varied according to the different degrees of resolution required for each experiment. High resolution full spectra  $^{13}\text{C}$  NMR of the oils were obtained using a 25 % (w/v) concentration of the oils in  $\text{CDCl}_3$  and  $^1\text{H}$  NMR of the oils were obtained using a 1 % (w/v) concentration of the oils in  $\text{CDCl}_3$ . The experimental conditions for  $^{13}\text{C}$  NMR and  $^1\text{H}$  NMR are recorded in Tables 5.1 and 5.2 respectively.

Table 5.1  $^{13}\text{C}$  NMR experimental parameters

Spectrum	Full spectra
Frequency (Hz)	12019.2
Data points	2621446
Acquisition (time $\text{s}^{-1}$ )	10.905
Pulse delay	49.095
Pulse width ( $\mu\text{s}$ )	7.5
Scans	136
Temperature ( $^{\circ}\text{C}$ )	24.5
Solvent	$\text{CDCl}_3$

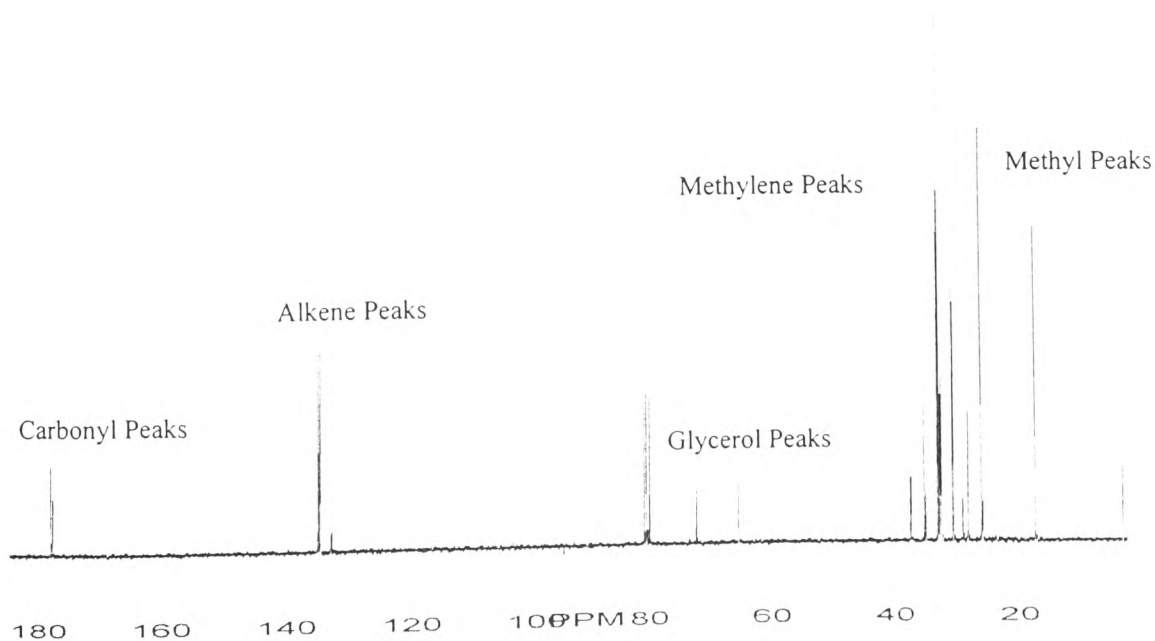


**Table 5.2  $^1\text{H}$  NMR experimental parameters**

Spectrum	Full spectra
Frequency (Hz)	5405.4
Data points	65536
Acquisition (time $\text{s}^{-1}$ )	6.062
Pulse Delay	3.969
Pulse Width ( $\mu\text{s}$ )	9.5
Scans	4
Temperature ( $^{\circ}\text{C}$ )	24.5
Solvent	$\text{CDCl}_3$

### 5.1.2 NMR results and discussion.

A typical  $^{13}\text{C}$  NMR spectrum of one of the authentic Greek oils (sample D12) is shown in Figure 5.1. Four groups of carbons are clearly observed in this spectrum. These are called the carbonyl C-atoms, the alkene C-atoms, the glycerol atoms, the methylene carbons and the terminal methyl groups. The  $^{13}\text{C}$  NMR spectrum of the same oil adulterated with 10% sunflower oil is shown in Figure 5.2. Distinct differences between these spectra are observed in their methylene and alkene regions. The NMR spectra of all the oils studied are shown in the Appendix C.

**Figure 5.1 Full spectrum of D12 extra virgin olive oil**

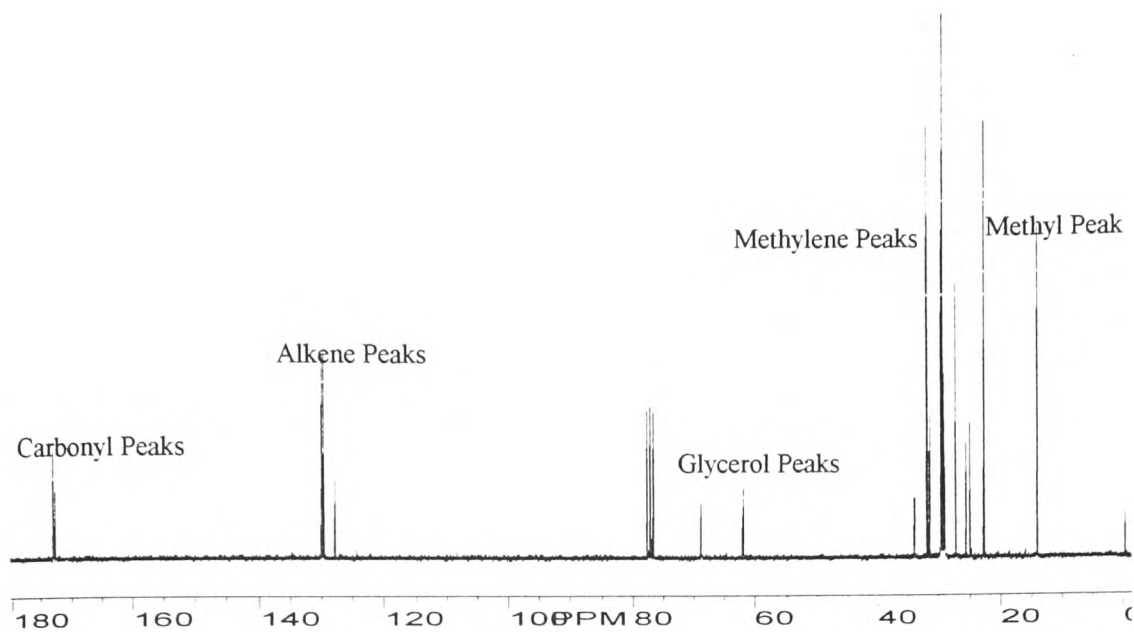


**Figure 5.2 Full spectrum of D12 extra virgin olive oil adulterated with 10 % sunflower oil**

Ng (1984) has reported that in the alkene region the small environmental differences experienced by carbon atoms in the carbon chains attached to the 1,3 and 2 carbon atoms of the glycerol backbone give rise to two small differences in chemical shift for these atoms. The distinctions between the positional distribution of unsaturated fatty acids in triglyceride mixtures depend on the structural resolution by NMR to give distinct chemical shifts of C-9 and C-10 carbons in oleic acid and C-9, C-10, C-12 and C-13 carbons in linoleic acid which are attached in the C1/C3 or C2 positions of the glycerol (Ng, 1984).

These chemical differences between oleic and linoleic acid are clearly visible in the alkene region of the  $^{13}\text{C}$  NMR spectrum of sample D12 (Figure 5.3). Significant peak height differences are observed between the authentic oil and its 10 % w/w adulterated sunflower oil mixture (Figure 5.4). In the sunflower oil adulterated mixture there is a increase in the size of the linoleic acid peaks while the oleic peaks have decreased. Thus, the investigation of the  $^{13}\text{C}$  NMR alkene region of an olive oil provide vital information on suspect adulterated oils.

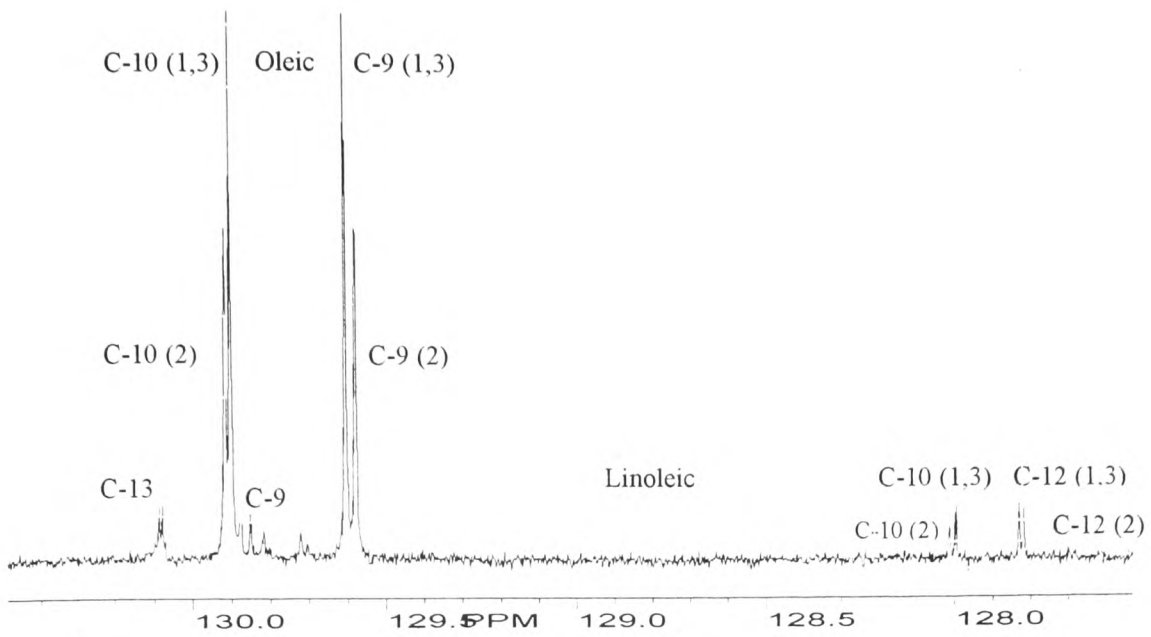


**Figure 5.3 NMR alkene region of sample D12**

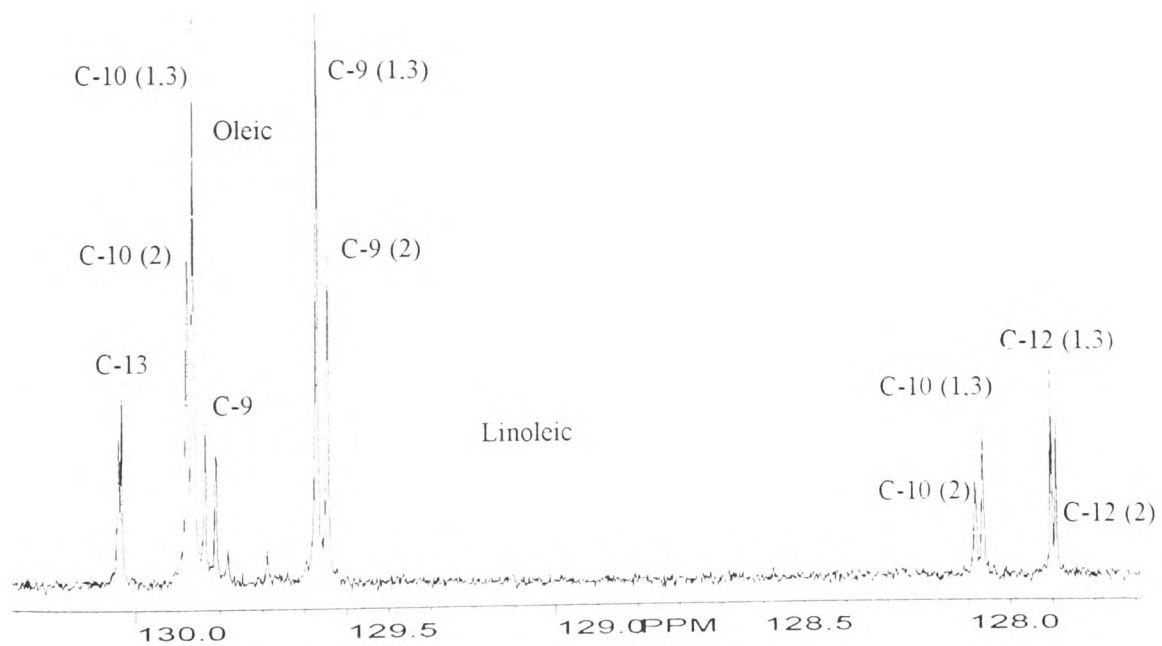


**Figure 5.4 NMR alkene region of sample D12 adulterated with 10 % sunflower oil**

As described in Chapter 1 the carbonyl region may be used in the characterization of olive oils and in the investigation of its adulteration. The similar  $T_1$ s and NOEs of the carbonyl oil

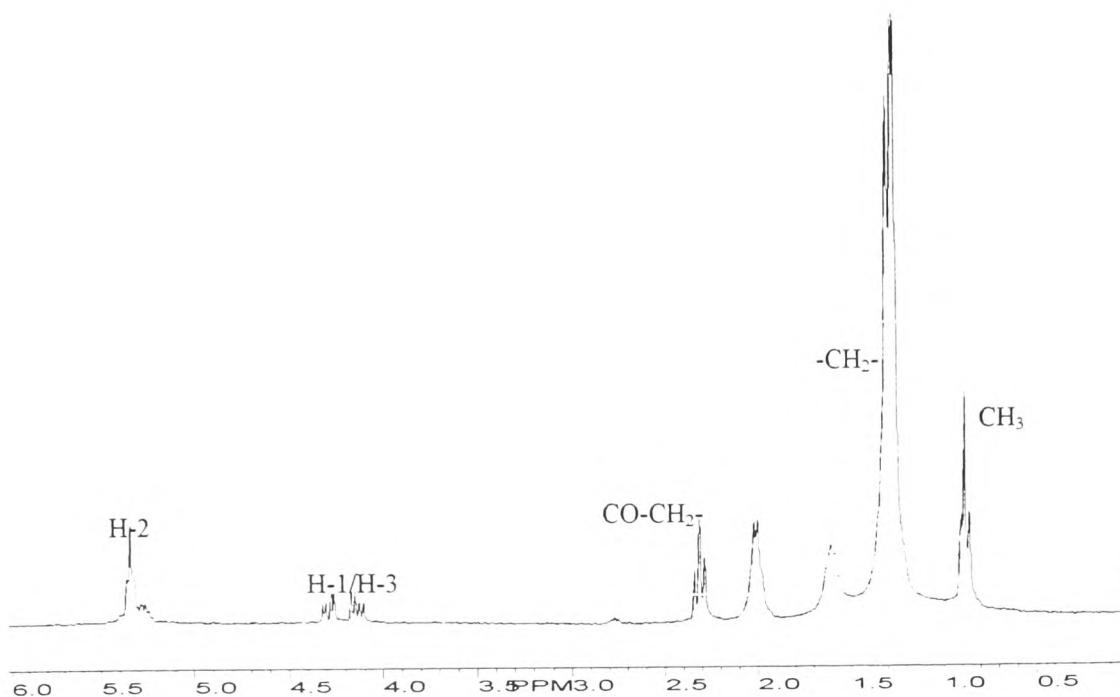
signals make this region more favourable to quantitation conditions than the alkene region as the analysis time is shorter. However in this study, the carbonyl region gave poor resolution using the conditions described in Table 5.1. This lack of resolution has also been experienced by (Mauromoustakos, 1994). The failure to resolve this region may have been due to the viscosity of the solution (25 % w/v) or due the low temperature during analysis. Ng (1985) has indicated that a higher sample temperature is required to obtain narrow lines in the spectrum of carbonyl carbons at high field, thus implying that the long correlation time associated with the slow motion of the triglyceride molecule may not hold at high magnetic fields. Hence, the  $^{13}\text{C}$  NMR statistical analysis was carried out on the alkene, glycerol, methylene and methyl regions only.

The  $^1\text{H}$  NMR spectrum of sample D8 is shown in Figure 5.5. The remaining  $^1\text{H}$  NMR oil spectra in this study are shown in Appendix E. Shiao and Shiao (1989) have reported that the total unsaturated fatty acids in an oil is represented by alkene protons in the region 5.2 - 5.4 ppm. This region is obscured by one proton from the H-2 of the chemical shift of the oil glycerol signal. However, the remaining 4 protons of glycerol produced signals in the region 4.1 - 4.3 ppm. Thus, the total degree of unsaturation of the oil can be estimated by subtracting the integrals of each of these integrated areas.

Shiao and Shiao (1989) also pointed out that the molar percentages of unsaturated fatty acids in oils can be obtained by a comparison of the peak areas of the allylic methylene (2.05 ppm) and the terminal methyl protons (0.8 - 1.03 ppm).

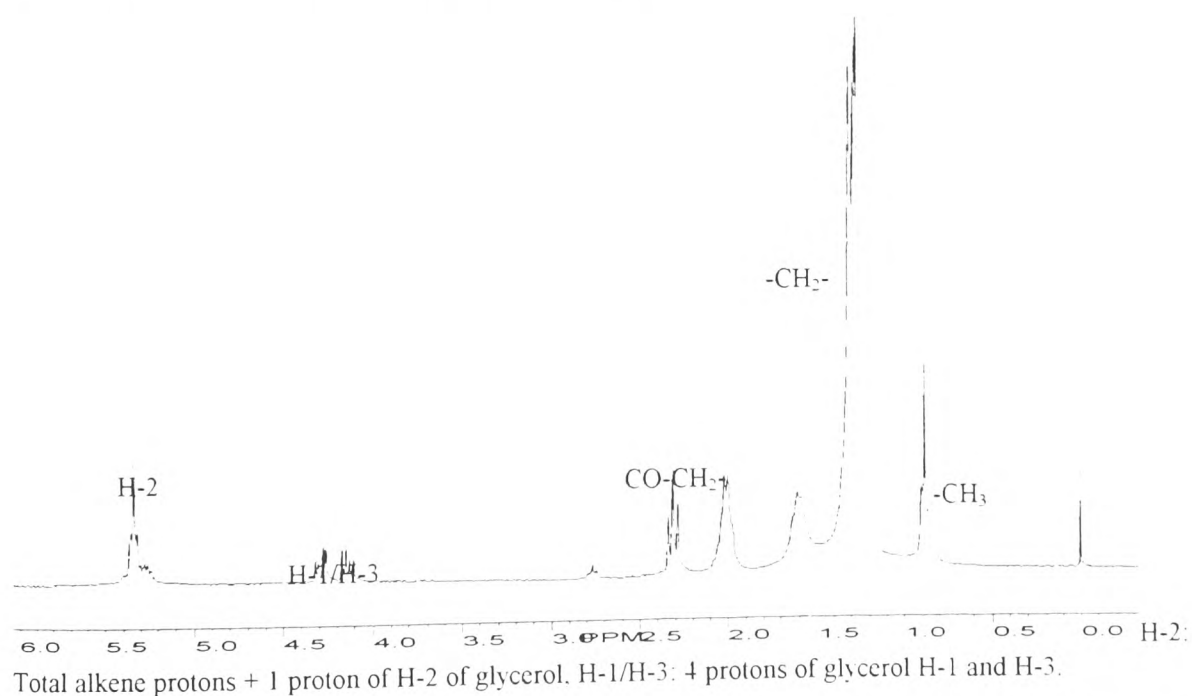
On inspection, no obvious differences between proton NMR spectra of the authentic oil (Figure 5.5) and its adulterated sunflower oil mixtures (Figure 5.6) were observed. Linear discriminant analysis and SIMCA were applied to the data extracted from the proton NMR

to try and detect adulteration in these olive oils.



H-2: Total alkene protons + 1 proton of H-2 of glycerol, H-1/H-3: 4 protons of glycerol H-1 and H-3.

Figure 5.5 Full proton spectrum of sample D8



H-2: Total alkene protons + 1 proton of H-2 of glycerol, H-1/H-3: 4 protons of glycerol H-1 and H-3.

Figure 5.6 Full spectrum proton of sample D8 adulterated with 10 % w/w sunflower oil

### 5.1.3 The statistical analysis of the $^{13}\text{C}$ NMR and $^1\text{H}$ NMR data

The large number of data points in the  $^{13}\text{C}$  NMR spectra provided high digital resolution in the NMR spectra while the large pulse delay between pulses ensured complete relaxation of all carbons with differential  $T_{1s}$  and quantitative conditions over the whole spectrum. Any influences of NOE were eliminated by using the relative peak height intensities of each oil as statistical data.

Prior to statistical analysis, the  $^{13}\text{C}$  NMR and  $^1\text{H}$  NMR spectra were Fourier Transformed using SpecNMR. After Fourier Transformation the spectra were manually phased and a base - line correction applied. The variables (39 from each  $^{13}\text{C}$  NMR spectrum and 23 from each  $^1\text{H}$  NMR spectrum) were extracted from the alkene, glycerol, methylene and methyl regions. In order to compare one spectrum with another the data was normalized. This was achieved by referencing the peak height intensities to specific carbon signals in each region of the  $^{13}\text{C}$  NMR spectra and to the  $\text{CH}_2$ - proton signal at 1.27 ppm in the  $^1\text{H}$  NMR spectra. The references for the  $^{13}\text{C}$  NMR spectra are shown in Table 5.3. Since all spectra were normalized to specific peaks, all spectra were directly comparable.

**Table 5.3 Peak height intensities for specific carbon signals in each region of the spectrum**

Reference Peaks	Assignment/ ppm
Alkene Region: (C-9 (1.3) in Oleic acid)	129.90
Glycerol Region: (G2)	62.00
Methylene Region ( $\text{CH}_2$ )	31.90
Methyl Region: ( $\text{CH}_3$ )	13.08

After pretreatment, the analytical NMR data was imported to Win - Discrim as comma

separated values and was first analysed by discriminant analysis.

#### **5.1.3.1 Hard modelling discriminant analysis of data from whole $^{13}\text{C}$ NMR Spectrum**

Discriminant analysis was used with principal components and canonical variables to distinguish between NMR spectra of extra virgin oil and its adulterated mixtures with sunflower oil.

In the  $^{13}\text{C}$  NMR statistical analysis the data set consisted of 22 authentic oils, 44 oils adulterated with levels of 5 % w/w and 10 % w/w sunflower oil respectively. From the constructed data set, three data matrices of oils were developed. The *NMR* set consisted of 17 authentic Greek oil samples and 34 adulterated mixtures of 5 % and 10 % sunflower oil. The test set *NMR Test* contained 15 oil samples which were representative of all classes. The training sets and test set are shown in Table 5.4 and Table 5.5.

**Table 5.4 Composition of the training sets for the authentic oil sets and their adulterated mixture sets on the whole <sup>13</sup>C NMR data region**

NMR		
D1	D1/5	D2/10
D2	D2/5	D3/10
D4	D3/5	D4/10
D5*	D4/5	D5/10
D6	D5/5	D6/10
D7	D7/5*	D8/10
D9	D8/5	D9/10
D11	D9/5	D10/10
D12	D10/5*	D11/10
D14*	D11/5	D13/10
D15	D12/5*	D14/10
D16	D14/5	D16/10
D17	D15/5	D17/10
D18	D16/5*	D18/10
D20	D19/5	D19/10
D21	D21/5*	D20/10
D22	D22/5	D21/10

\* indicates outliers in the class model.

**Table 5.5 Composition of the test set for the validation of the authentic set and its adulterated mixture sets on the whole <sup>13</sup>C NMR data region**

NMR Test		
D3	D6/5	D1/10
D8	D13/5*	D7/10
D10	D17/5	D12/10
D13	D18/5	D15/10
D19*	D20/5*	D22/10*

\* indicates outliers in the class model.

As described in the application of discriminant analysis to the infrared data, each NMR



sample in the training data set was assigned to its class, whether it was authentic extra virgin oil, extra virgin oil adulterated with 5 % sunflower oil or extra virgin oil adulterated with 10 % sunflower oil. The data matrix was first reduced by PCA and 15 principal components were extracted. The percentage variance accounted for by 15 PCs are shown in Table 5.6. The variance reached a stable minimum after 13 PCs and was thus indicative of the number of PCs to use in this analysis.

**Table 5.6 PCA variance analysis in the development of discriminant analysis on the whole <sup>13</sup>C NMR data training set**

Score	Cumulative percentage variance
1	27.79
2	49.29
3	62.55
4	71.27
5	76.66
6	81.45
7	84.86
8	87.57
9	90.08
10	91.98
11	93.55
12	94.96
13	96.20
14	97.05
15	97.63

Using 13 PC scores, the squared Malahanobis distances of each sample in the training data set from the 3 group mean samples were calculated. Each sample was reassigned to the nearest group on the basis of the calculated squared Malahanobis distance. This analysis resulted in correctly assigning 44 out of a total 51 samples to their defined classes. This class model was evaluated using the NMR Test set.

As previously described for the training set, the squared Malahanobis distance of each sample in the test set from the 3 group mean samples were calculated and the samples were reassigned to their nearest parent group. The efficiency of the discrimination was indicated in the number of correctly assigned samples to their own classes. This classification resulted in correctly assigning 11 out of 15 samples, with samples D19, D13/5, D20/5, and D22/10 being incorrectly assigned. In this analysis sample D7 was an outlier in the training

set model and it was far removed from the other samples in the plot and had thus a dominant influence on the fit of the class model. This sample and its adulterated mixtures were removed from the training set and a further discriminant analysis was applied to the training set. In this case 4 samples were misclassified, these were the authentic oil samples D14 and D20 which were classified as belonging to the class of oils adulterated with 10 % sunflower oil. The other samples were D16/5 and D21/5 which were classified as authentic oils instead of oils that were adulterated with 5 % sunflower oil.

The application of this model to the classification of the test set resulted in correctly assigning 12 out of 15 samples of the test set. In the test set samples D19, D13/5 and D20/5 were classified as samples belonging to the class of oils adulterated with 10 % sunflower oil. Thus, this application of NMR and linear discriminant analysis did not make a clear distinction between the authentic olive oils and their adulterated mixtures. A Cooman's plot of the NMR data set is shown in Figure 5.7

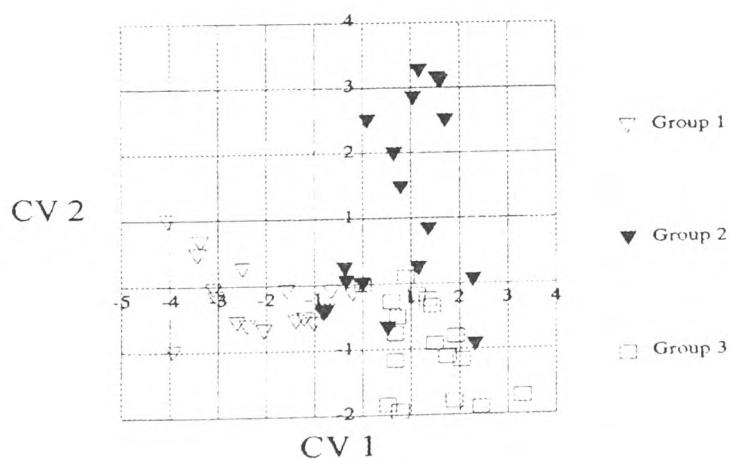


Figure 5.7 Canonical variate analysis of NMR data set

### 5.1.3.2 Hard modeling discriminant analysis of data from the alkene region of $^{13}\text{C}$ NMR spectrum

Discriminant analysis was also carried out on reduced NMR data sets which included the alkene region only. The training set was called *Alkene* which represented the authentic extra virgin and its adulterated mixtures of 2 % w/w, 5 % w/w and 10 % w/w. The test sets were called *Alkene Test*. The training sets and test set for this analysis is shown in Tables 5.7 and 5.8.

**Table 5.7 Composition of training sets for the authentic oil sets and their adulterated mixture sets on the  $^{13}\text{C}$  NMR alkene region**

Alkene		
D2	D1/5	D1/10
D3	D3/5	D2/10*
D4	D4/5	D4/10
D5	D5/5	D6/10*
D7	D6/5	D7/10
D8	D7/5	D9/10
D9	D9/5	D10/10
D10	D10/5	D11/10
D11	D11/5*	D12/10
D12	D12/5	D13/10
D13	D13/5*	D14/10
D15	D14/5	D16/10
D16	D16/5	D17/10
D18	D17/5*	D18/10
D20	D19/5	D19/10
D21	D20/5	D21/10
D22	D22/5	D22/10

\* indicates outliers in class model.

**Table 5.8 Composition of Test set for the validation of the authentic set and its adulterated mixture sets on the  $^{13}\text{C}$  NMR alkene data region**

Alkene Test		
D1	D2/5*	D3/10
D6	D8/5*	D5/10*
D14	D15/5*	D8/10
D17	D18/5*	D15/10
D19*	D21/5*	D20/10*

\* indicates outliers in class model.

In the development of this classification rule (from the reduced  $^{13}\text{C}$  NMR alkene region) 5 samples were assigned to the wrong class. These were samples D2/10, D6/10, D11/5, D13/5, D17/5. The evaluation of the discriminant model using the test set resulted in 8 out of 15 samples being misclassified. These outliers are indicated by an asterisk in Table 5.7. This analysis showed that the discriminant function developed from the reduced  $^{13}\text{C}$  NMR data did not prove as effective as the discriminant rule developed using the whole  $^{13}\text{C}$  NMR data.

However, another discriminant analysis was carried out on the  $^{13}\text{C}$  alkene Training data set after the outlier sample 7 was removed from the set. In this application 4 samples were assigned to the wrong class. These samples were D13/5, D10/10, D2/10 and D6/10. These samples were however all classified as adulterated samples, thus showing that the classification rule distinguished between the authentic oils and their adulterated mixtures but did not distinguish between the different levels of adulteration. The classification of the test set using this discriminant model, resulted in 13 out of 15 samples being assigned to the correct class. The samples that were incorrectly assigned were sample D14, which was

assigned to the class of oils adulterated with 5 % sunflower oil, and sample D8/5 which was assigned to the authentic oil class. Thus the removal of sample 7 from the Training set improved the efficiency of the class model in discriminating between the samples in the test set. A Cooman's plot of this analysis is shown in Figure 5.8

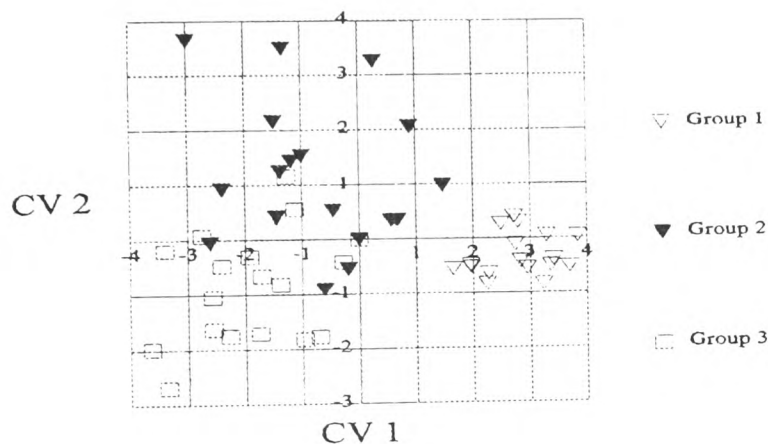


**Figure 5.8 Canonical variate analysis of Alkene data set**

### 5.1.3.3 Hard modeling discriminant analysis of data from proton NMR olive oil spectra

Discriminant analysis was also carried out using the Proton NMR data of the oils. In this analysis data were extracted from the whole  $^1\text{H}$  NMR spectrum. The regions from which data were extracted are recorded in Table 5.9.

**Table 5.9  $^1\text{H}$  NMR spectral assignments of the triglyceride components for olive oils (from Shiao & Shiao, 1989).**

Assignments	$\delta/\text{ppm}$
Total alkene protons + 1 proton of H-2 of glycerol	5.2-5.4
4 protons of glycerol H-1 and H-3	4.1-4.3
$\alpha$ -linoleic, PUFA	2.78
$-\text{O}-\text{CO}-\text{CH}_2^-$	2.30
Allylic methylene	2.05
$\alpha$ -linolenic, PUFA	0.97
Methyl signal	0.88

The proton training sets were called *Proton* which represented the authentic oils and their sunflower oil adulterated mixtures respectively. The test set was called *Proton Test*. The composition of the training sets and test set for this analysis are shown in Tables 5.10 and 5.11.

**Table 5.10 Composition of training sets for the authentic oil sets and their adulterated mixture sets from proton NMR.**

Proton		
D1	D1/5	D2/10
D2	D3/5	D4/10
D3	D4/5*	D6/10
D4	D5/5	D7/10
D5	D7/5	D8/10
D7*	D8/5	D9/10
D8*	D10/5	D10/10
D9*	D11/5	D11/10
D11	D13/5	D12/10
D12	D14/5	D13/10*
D13	D15/5	D15/10
D15	D16/5*	D16/10
D16	D18/5*	D17/10
D17	D19/5	D18/10
D18	D20/5	D19/10
D20	D21/5	D20/10
D22*	D22/5	D22/10

\* indicates outliers in class model

**Table 5.11 Composition of test set for the validation of the authentic set and its adulterated mixture sets from the proton data region**

Proton Test		
D6	D2/5	D3/10
D10	D6/5*	D5/10
D14	D9/5	D8/10
D19*	D12/5	D14/10
D21	D17/5	D21/10*

\* indicates outliers in class model

In this application, the classification model resulted in incorrectly classifying samples; D4/5, D7, D8, D9 and D22. This model was used to classify the test sets. This resulted in the correct assignment of 12 out of 15 samples. Samples D6/5, D19 and D21/10 were classified



wrongly. Similar to the steps adopted in the discriminant analysis of  $^{13}\text{C}$  NMR, sample 7 and its adulterated mixtures were removed from the training set and the discriminant analysis was repeated. In this instance the discriminant model was not improved and resulted in sample 8 being far removed from the model.

Discriminant analysis was not practical in the investigation of the subgroup region of the authentic oils as the number of samples in each of the varieties were too small. In discriminant analysis of this kind the number of observations must exceed the variables otherwise 'overfitting' will occur in which the model will calibrate well but will have no predictability (Lai, 1994). Thus, discriminant analysis can not be used in the investigation of regions classification as the Crete oil class consisted of only 5 oils.

However PCA models were developed from the Peloponese and Crete oils to prove the occurrence of 'overfitting'. The model were developed using 5 PCs and the squared Malahanobis distances of each observation in the training set from the 3 group mean observations were calculated. Ten out of the thirteen samples were classified correctly. The classification rule was applied to the test set and only one out of the five samples were classified correctly. This indicated that development of the models resulted in overfitting and an insufficient classification.

#### 5.1.3.4 SIMCA classification of the data from the whole $^{13}\text{C}$ NMR data

A PC model was first developed for the whole  $^{13}\text{C}$  NMR data set to observe the natural subgrouping of samples within the data. The loadings and scores plots for this analysis are shown in Figures 5.9 and 5.10 respectively.

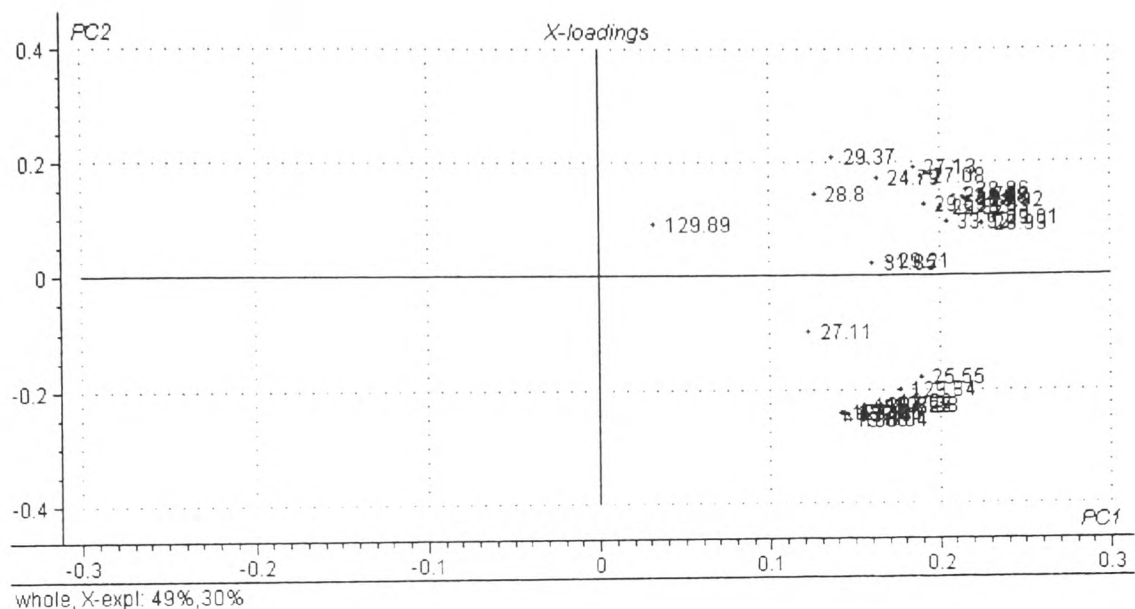


Figure 5.9 Loadings plot for whole  $^{13}\text{C}$  NMR data set based on the first 2 PCs

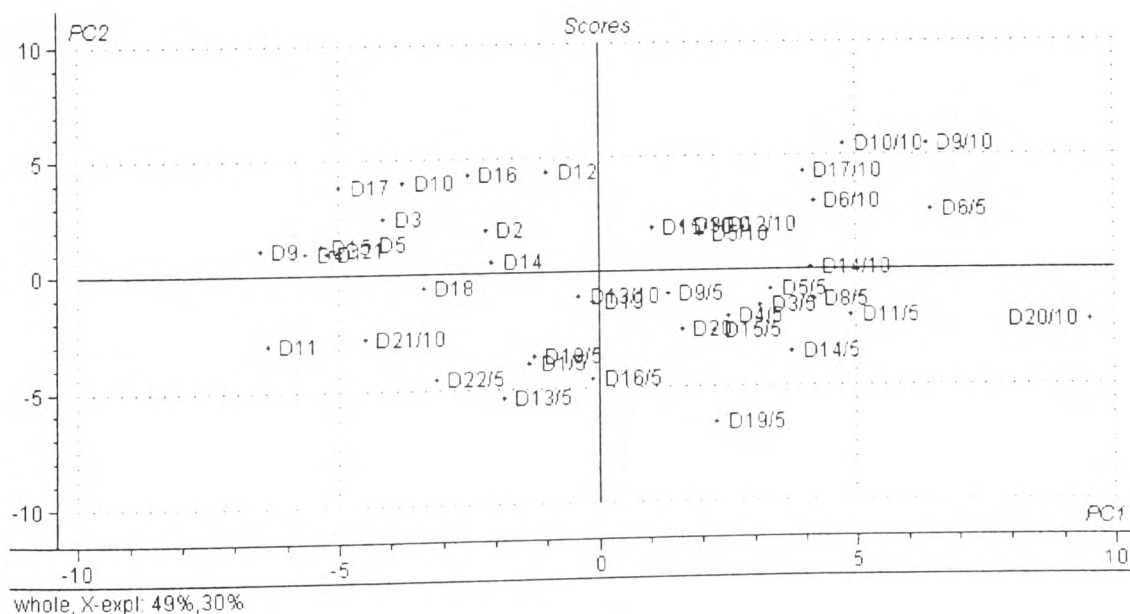


Figure 5.10 Scores plot for whole  $^{13}\text{C}$  NMR data set based on the first 2 PCs

The loadings and scores plot (Figures 5.9 and 5.10) show a positive correlation of the sunflower oil adulterated samples with the variables. In contrast, the authentic olive oil samples are in negative correlation with the variables. Separation between the oils and their adulterated samples are observed in the scores plot while the adulterated classes are overlapping (Figure 5.9).

The SIMCA classification of this  $^{13}\text{C}$  NMR data region of the oils involved the development of 3 class models for the authentic oils, the oils adulterated with 5 % sunflower oil and the oils adulterated with 10 % sunflower oil. The training sets used in the development of these sets were called Carborg, Carb5 and Carb10 respectively. Each set was fully cross validated using 8 PCs and outliers were identified and removed. These models were validated using the test sets. The composition of the test sets were called Carborg Test, Carb5 Test and Carb10 Test. The training and test sets are shown in the Table 5.12 and Table 5.13.

**Table 5.12 Composition of the training sets for the authentic oil sets and their adulterated mixture sets on the whole <sup>13</sup>C NMR data**

Carborg	Carb5	Carb10
D1	D1/5	D2/10*
D2	D2/5	D3/10
D4	D3/5	D4/10*
D5	D4/5	D5/10
D6*	D5/5	D6/10
D7*	D7/5	D8/10*
D9	D8/5	D9/10
D11	D9/5	D10/10
D12	D10/5	D11/10*
D14	D11/5	D13/10
D15*	D12/5	D14/10
D16	D14/5	D16/10*
D17	D15/5	D17/10
D18	D16/5	D18/10*
D20	D19/5	D19/10*
D21	D21/5	D20/10
D22*	D22/5	D21/10

\* indicates outliers removed during the development of the class model

**Table 5.13 Composition of the test set for the validation of the authentic set and its adulterated mixture sets**

Carborg Test	Carb5 Test	Carb10 Test
D3	D6/5	D1/10
D8	D13/5	D7/10
D10	D17/5	D12/10
D13	D18/5	D15/10
D19	D20/5	D22/10

The first 4 PCs described 80 % (approx.) of the variance in the spectra and were used in the classification of these oils. The percentage variance accounted for by the first 4 PCs are recorded in Table 5.14.

**Table 5.14 Percentage variance accounted for in the first 4 PCs in the model formed on the whole  $^{13}\text{C}$  NMR region**

Name of components	Carborg	Carb5	Carb10
PC1	35.96	50.22	29.95
PC2	72.91*	64.09*	61.75*
PC3	83.45	74.29	70.45
PC4	89.04	83.33	79.81

Total residual variance is lower than 0.5.

In the development of these models the total residual variance for PC2 of each of these classes was lower than the limit of 0.50, thus, implying that the calibration data did not fit the model perfectly. This analysis did not lend itself to a good classification, as only 2 out of 5 authentic samples were successfully classified from the adulterated oils. The results of this classification are recorded in Table 5.15.

**Table 5.15 Classification of the test set with the class models for the authentic oils and their adulterated mixtures from the whole  $^{13}\text{C}$  NMR data.**

Class models		Test sets		Classified successfully	
Carborg	Carb5	Carborg Test	Carb5 Test	2/5	2/5
Carborg	Carb10	Carborg Test	Carb10 Test	3/5*	2/5

\* Samples were doubly classed.

#### **5.1.3.5. SIMCA classification of the data from the alkene region of $^{13}\text{C}$ NMR data**

A similar classification using SIMCA was carried out on the reduced alkene  $^{13}\text{C}$  NMR data.

As a pretreatment to the data a PCA was also carried out on the whole data sets extracted

from the alkene region. The loadings and scores plot for this analysis are shown in Figures 5.11 and 5.12 respectively.

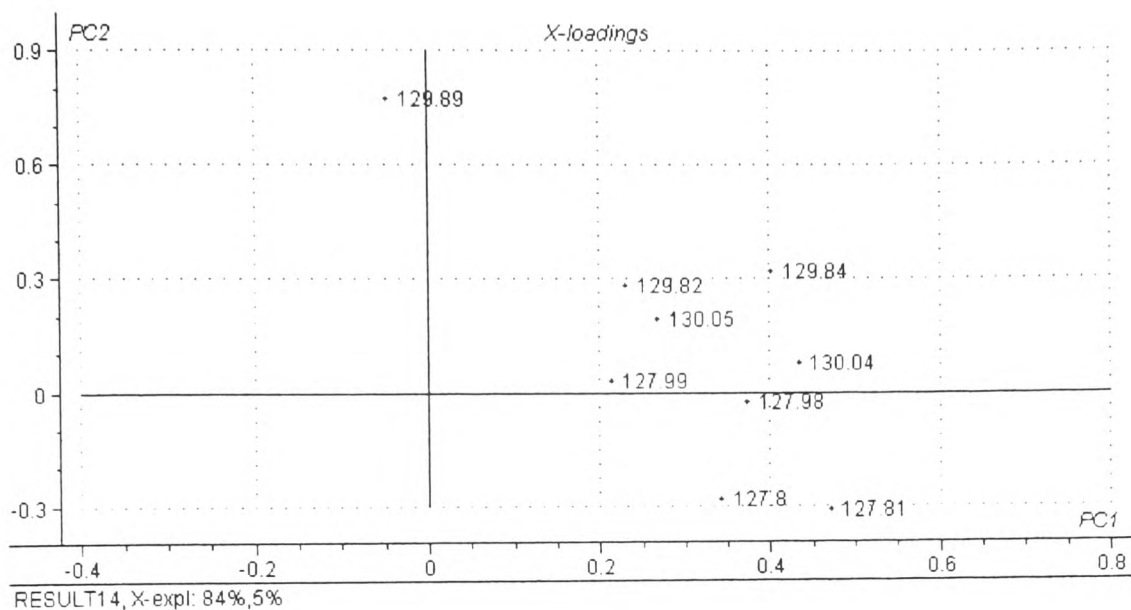


**Figure 5.11** Loadings plot for the alkene model developed using  $^{13}\text{C}$  NMR data from the alkene region.

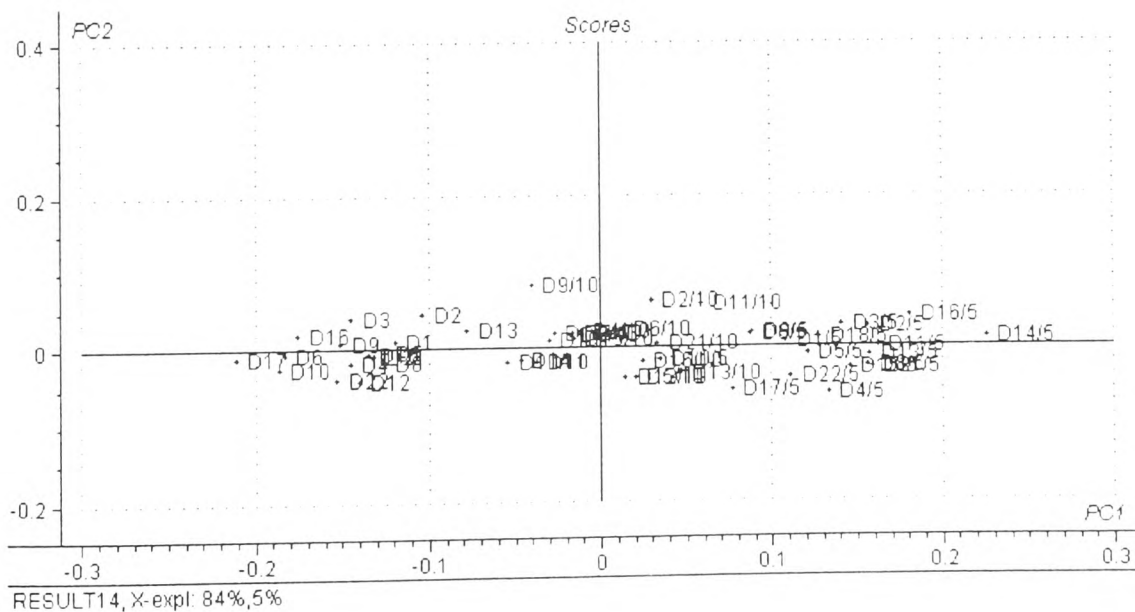


**Figure 5.12** Scores plot for the for the alkene model developed using  $^{13}\text{C}$  NMR data from the alkene region.

Similar to the PCA analysis on the full NMR data the variables were positively correlated with the adulterated samples and were negatively correlated with the authentic samples. There is a distinct separation between the authentic samples and the adulterated mixtures were observed in the scores plot. However, the separation between the samples adulterated with 5 % sunflower oil and with 10 % sunflower oil are not as apparent as that observed in the scores plot (Figure 5.7) of whole NMR data set. In the SIMCA classification using the  $^{13}\text{C}$  NMR data, the training sets were called Caralkorg, Caralk5 and Caralk10 and the test sets were called Caralkorg Test, Caralk5 Test and Caralk10 Test. These composition of these sets are shown in Tables 5.16 and 5.17.

**Table 5.16 Composition of the training sets for the authentic oil sets and their adulterated mixture sets on the alkene region of  $^{13}\text{C}$  NMR data**

Caralkorg	Caralk5	Caralk10
D1	D1/5	D2/10*
D2	D2/5	D3/10
D4	D3/5	D4/10*
D5	D4/5	D5/10
D6	D5/5	D6/10
D7*	D7/5*	D8/10*
D9	D8/5	D9/10
D11	D9/5	D10/10
D12	D10/5	D11/10*
D14	D11/5	D13/10
D15	D12/5*	D14/10*
D16	D14/5	D16/10*
D17	D15/5	D17/10
D18	D16/5	D18/10*
D20*	D19/5*	D19/10*
D21	D21/5	D20/10*
D22*	D22/5	D21/10

\* indicates outliers removed during the development of the class model.

**Table 5.17 Composition of the test set for the validation of the authentic set and its adulterated mixture sets for the alkene region of the  $^{13}\text{C}$  NMR data**

Caralkorg Test	Caralk5 Test	Caralk10 Test
D3	D6/5	D1/10
D8	D13/5	D7/10
D10	D17/5	D12/10
D13	D18/5	D15/10
D19	D20/5	D22/10

In this application, the first 4 PCs accounted for 80 % (approx.) of the variation in the data (Table 5.18) and were used in the classification of the oils.

**Table 5.18 Percentage variance accounted for in the first 4 PCs in the model formed on the alkene  $^{13}\text{C}$  NMR region**

Name of components	Caralkorg	Caralk5	Caralk10
PC1	66.49	50.22	29.95
PC2	79.30	64.09	61.75
PC3	87.60*	74.29*	70.45*
PC4	93.52	83.33	79.81

Total residual variance is lower than 0.5.

The validation of the developed alkene  $^{13}\text{C}$  NMR models resulted in the successful classification of four out of five of the authentic oils from its adulterated sunflower oil mixtures. These results are recorded in Table 5.19.

**Table 5.19 Classification of the test set with the class models for the authentic oils and their adulterated mixtures on the  $^{13}\text{C}$  NMR alkene region**

Class models		Test sets		Classified successfully	
Caralkorg	Caralk5	Caralkorg Test	Caralk5 Test	4/5	4/5
Caralkorg	Caralk10	Caralkorg Test	Caralk10 Test	4/5	3/5



Although the SIMCA classification of the alkene region did not completely distinguish between the olive oils and their adulterated mixtures, the analysis showed potential for future investigation of the adulteration. The use of a larger number of samples in the data set and the development of tighter fitting models might also furnish a better classification.

A Cooman's plot of the classification of the authentic oils and their 10 % adulterated mixtures are shown in Figure 5.11.

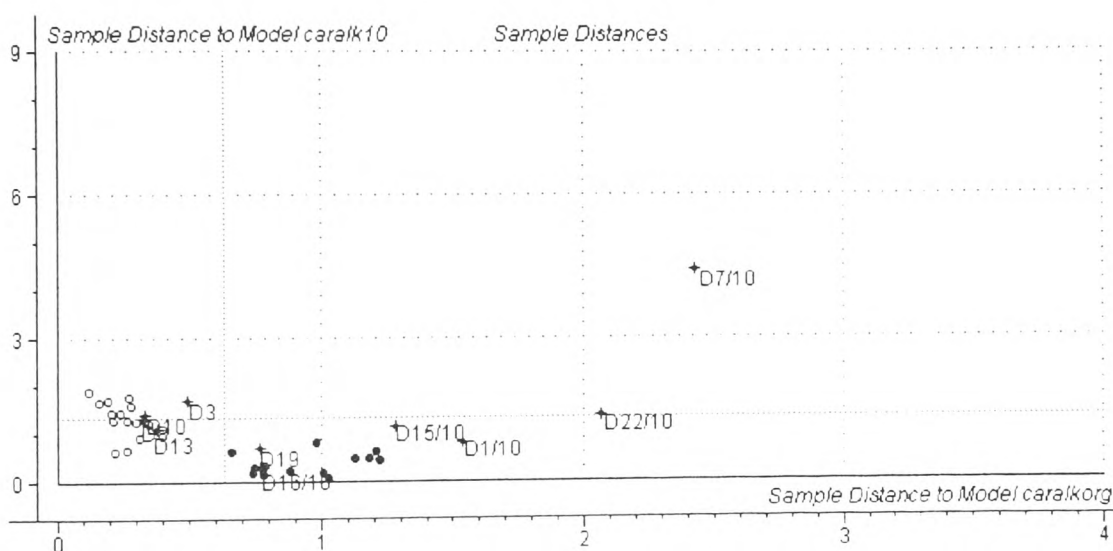


**Figure 5.13** Cooman's plot of Caralkorg and Caralk10

#### 5.1.3.6 SIMCA classification of the data from the proton NMR

A SIMCA classification was also carried out on the Proton NMR data. Similar to the  $^{13}\text{C}$  NMR analysis, the whole proton data set was reduced by PCA to try and establish sample grouping. The loadings and scores plot for this analysis are shown in Figures 5.14 and 5.15 respectively.



shown in Table 5.20 and Table 5.21.

**Table 5.20 Training sets for the authentic oil sets and their adulterated mixture sets on the  $^1\text{H}$  NMR data**

Protsorg	Prot5	Prot10
D1	D1/5	D2/10
D2	D3/5	D4/10
D3	D4/5	D6/10
D4	D5/5*	D7/10*
D58	D7/5*	D9/10
D7*	D8/5	D10/10
D8	D10/5	D11/10*
D9	D11/5*	D12/10
D11	D13/5	D13/10
D12	D14/5	D15/10
D13	D15/5	D16/10
D15*	D16/5	D17/10
D16	D18/5	D18/10
D17	D19/5	D19/10
D18	D20/5	D20/10
D21	D21/5	D21/10
D22	D22/5	

\* indicates outliers removed during the development of the class model.

**Table 5.21 Test set for the authentic oil set and its adulterated mixture sets for  $^1\text{H}$  NMR data**

Protorg Test	Prot5 Test	Prot10 Test
D6	D2/5	D3/10
D10	D6/5	D5/10
D14	D9/5	D8/10
D19	D12/5	D14/10
D21	D17/5	D21/10

In this analysis, the first 3 PCs accounted for 90 % (approx.) of the variation in the

data and were used in the classification of the oils.

**Table 5.22 Percentage variance accounted for in the first 4 PCs in the model formed on the <sup>1</sup>H NMR region**

Name of components	Protsorg	Prot5	Prot10
PC1	64.41	76.00	65.67
PC2	81.37	85.29	81.50
PC3	90.89	93.47	88.65
PC4	93.39	96.54	94.40

This classification did not prove to be successful as it failed to distinguish between the authentic oils and its adulterated mixtures. The results of this classification are recorded in Table 5.23.

**Table 5.23 Classification of the test set with the class models for the authentic oils and their adulterated mixtures on the <sup>1</sup>H NMR region**

Class models		Test sets		Classified successfully	
Protsorg	Prots5	Protsorg Test	Prots5 Test	1/5	4/5*
Protsorg	Prots10	Protsorg Test	Prots10 Test	0/5	4/5*

\*Samples were doubly classed

A Cooman's plot of the classification of the authentic oils and their 10 % w/w adulterated mixtures is shown in Figure 5.16. This plot clearly shows overlap of both the original and the adulterated model.

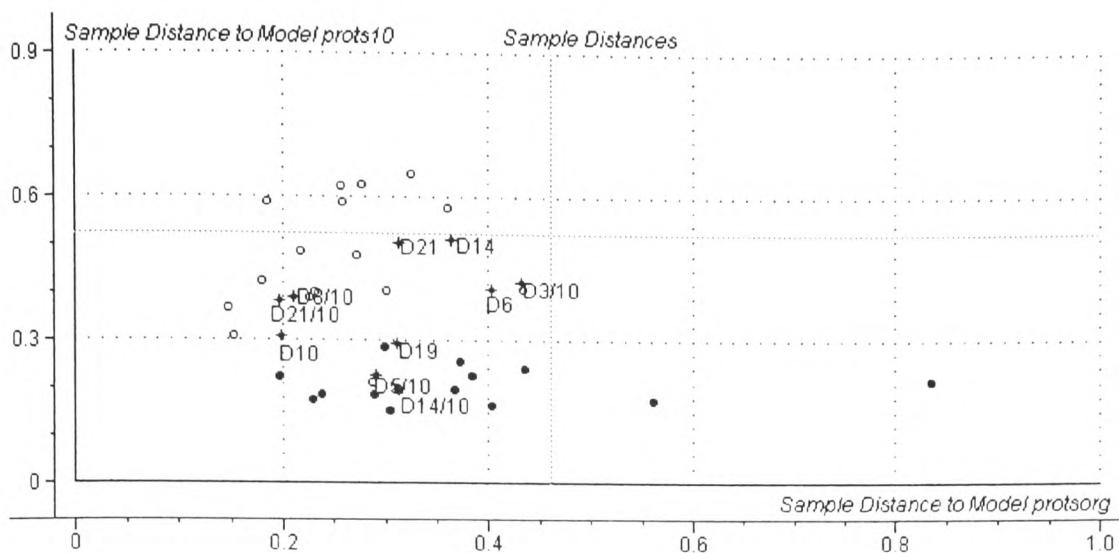


**Figure 5.16 Cooman's plot of the authentic oils and their adulterated mixtures using the proton NMR data**

### *5.1.3.7 SIMCA classification of the Peloponese and Crete varieties in the authentic Greek oils using carbon and proton NMR data*

Models were also developed for the Peloponese oils and Crete oil varieties of oils using both the  $^{13}\text{C}$  NMR data and the  $^1\text{H}$  NMR data. The aim was to try and distinguish between both varieties of oils. This classification failed to separate these oils into their subgroups of oils. However, the subgroups were small and a larger number of samples are required to represent the natural variation among the authentic oils.

### **5.1.4 Conclusion**

In summary, hard modelling discriminant analysis on NMR data showed potential in the detection of adulteration on olive oil. This type of modelling is however restrictive and samples must be assigned to one the developed classes. SIMCA modelling allowed each the oil class models to be developed independently and the samples were either classed or unclassed. The SIMCA application on the alkene analytical data succeeded in distinguishing 4/5 authentic oils from the adulterated oil thus, proving more successful than the SIMCA analysis of the full carbon and proton NMR data.

## CHAPTER 6

### 6.1 CONCLUSION

The authenticity of olive oil on the international market has become an important issue. Authenticity issues in relation to olive oil arise from variations in quality and occur from the cultivation stages of the olives to the production of the olive oil. The economic incentive of dishonest traders to adulterate high quality extra virgin oil with inferior products is great. This type of adulteration is not only illegal but has also led to serious health implications. The development of technology to classify authentic olive oils are hindered by the development of fraudulent practices which are designed to disguise olive oil adulteration.

The preparation of fraudulent mixture, that lie within the established limits for olive oils are easily prepared (Aparicio, 1995). Adulteration levels as low as 2 - 5 % are economically viable when there is a significant price difference between the extra virgin olive oil and its adulterated product thus making the detection of adulteration virtually impossible. There is a need for the development of improved methods and techniques in the analyses of olive oil to clearly define its authenticity so that tighter controls can be placed on the labelling of the olive oil product.

The traditional wet chemistry techniques have been applied to measure various constituents of olive oils. The detection of non olive oil components in the oil is indicative of adulteration and leads to a simple classification of an adulterated product. However, the authentication of an olive oil sample becomes more complicated when the oil contains only

the constituents that should naturally occur (Lees, 1995).

The diversity of olive oil authenticity criteria requires the employment of a number of integrated techniques for its analysis. These techniques used in complement provide a variety of parameters which can be manipulated statistically to distinctly differentiate between authentic oils and their adulterated mixtures.

This project investigated both the chromatographic and spectroscopic techniques used in the analysis of olive oil. The traditional wet chemistry methods were compared and contrasted with the direct and less time consuming spectroscopic techniques. The advantages and disadvantages of each technique studied were highlighted.

#### **6.1.1 Chromatographic analysis of olive oils**

The GC analysis of the olive oils in this analysis had limited application. The transesterification step in the FAME analysis process was susceptible to chemical and experimental error. The current standard transesterification methods were outdated and needed a firm revision of each step in FAME preparation. These errors were highlighted in the significant differences in FAME analysis obtained for the same oil sample using four different transesterification methods. The analysis of the Greek oil samples in this study and in a Greek laboratory resulted in significant differences in the fatty acid compositions of these oils (Chapter 2, Tables 2.6 and 2.7 respectively). This lack of consistency among the GC FAME results of the same oils led to the investigation of the more direct analysis of the olive oil triglycerides by high temperature GC. This approach did not require any prior derivatization of the oil samples. This minimized the analyses time and also reduced additional errors that occurred during the work - up stages of FAME derivatization.

The direct high temperature GC separation of the triglycerides by total carbon number resulted in the elution of two main peaks in the olive oil gas chromatogram. Finer structure in the separation according to the number of unsaturated fatty acids in the triglycerides was not however achieved. This lack of separation of the individual triglycerides meant that the PLS statistical analysis was not feasible on the basis of total carbon number data.

The gas chromatographic technique was further investigated to try and separate the triglycerides by degree of unsaturation. The separation was subject to the availability of a moveable on - column injector as the external coolant carbon dioxide failed to keep the point of sample injection sufficiently cool to allow the sample to be transferred on to the column in a liquid state.

Argentation SFC offered a novel approach to the elution of a wide range of triglycerides by degree of unsaturation. This technique used packed columns in series to give similar resolution to a capillary packed column. The SFC chromatograms gave characteristic profiles of a variety of oils. These profiles served as fingerprints for identification. On a quantitative note, this method lacked repeatability. High concentrations were required for the analysis and this limited this technique in the analysis of the triglyceride standards that represented the natural variability of olive oils.

### **6.1.2 Spectroscopic analysis of olive oils**

The advances in spectroscopic instrumentation in particular in Fourier Transformation has led to invaluable tools in the study of the physical and chemical properties of olive oil. The spectroscopic techniques of FT - Raman, IR and NMR proved to be faster and more direct in the detection of olive oil adulteration than chromatography. The spectra obtained



provided information from all the chemical compounds present in olive oil. The statistical manipulation of spectroscopic data produced distinct classifications of the authentic olive oils and its adulterated sunflower mixtures (SIMCA). However, SIMCA did not differentiate between the levels of adulteration (2 % w/w, 5 % w/w and 10 % w/w).

The SIMCA classification of the Raman fingerprint region resulted in the distinction of the authentic Greek oils from its adulterated mixtures. Sunflower adulterated olive oils were detected at limits as low as 2% w/w. FT Raman proved to be the most effective spectroscopic technique in this research. The fact that Raman was a poor scatterer of water meant that the spectra of extra virgin oils containing varying contents of water did not have water scatter interference.

Discriminant analysis on the selected infrared data showed a clear difference between the authentic oils and their adulterated mixtures. This distinction was not observed between the adulterated mixtures themselves. The SIMCA classification of the infrared data did not prove as successful as the discriminant analysis. The class models developed did not have sufficient class distance to distinguish between the authentic oils and their adulterated classes.

Lai (1994) has also found that sampling of replicates introduced variation into the data set samples thus indicating how subtle the differences among the oils and its adulterated mixtures were. This replicate variation together with the varying content of water present in the olive oil samples may explain why the classification of the authentic extra virgin oil and its adulterated mixtures was so difficult with infrared. Lai (1995) has also stated that the chemical variation between extra virgin and other olive oils is so small that high

spectral quality using a desiccated interferometer is required. This further stresses the fact that the oils with varying water content will influence the classification dramatically. This shows why the Raman technique which does not produce scatter bands from water was successful.

Similar to the IR results obtained the discriminant analysis of the NMR showed potential in the classification of olive oils. The alkene region of the  $^{13}\text{C}$  NMR data was more indicative of differences among the oils than the whole data region. Again these differences were not as apparent in the SIMCA modelling of this data. As for IR the distance between the authentic class model and the adulterated models was not great enough to ensure a good classification of the samples.

In conclusion FT Raman proved to be the most effective technique in detection of adulteration of olive oils. The technique was rapid and accurate and the statistical manipulation of its fingerprint region indicated clear differences among the authentic oils and its 2% w/w sunflower oil adulterated mixtures.

Other research in the authentication of olive oil has focused on techniques such as SNIF - NMR, pyrolysis - Mass spectrometry (PyMS) and GC - electron ionization mass spectrometry (GC - EIMS) and also on other possible adulterants with soybean, corn, peanut and rapeseed oil.

For example, Deuterium SNIF - NMR determines the deuterium content on a specific site of a molecule. These site - specific ratios vary according to location and provided information on the geographical origin of the oil (Lees, 1994). Also Meuzelaar et al. (1982) have used PyMS to distinguish between homologous series of some aliphatic components.

The usefulness of the technique in relation to extra virgin olive oil was reported by Goodacre et al. (1992) who used PyMS in complement with artificial neural networks in the detection of extra virgin olive oil adulteration (5 - 50 % w/w) with soybean, peanut, corn and refined olive oil.

As reviewed by Aparicio (1995) GC - EIMS can be used to identify the presence of small amounts of sterols found in virgin olive oil. This technique was useful in the detection of rapeseed oil in extra virgin olive oil. However this technique was not applicable to the detection of sunflower oil and corn oil adulterants.

Olive oil adulteration is a growing problem governed by market trends. Analytical techniques must be constantly developed and improved to combat the on - going development of techniques used to falsify extra virgin olive oil. The culmination of a wide variety of analytical techniques and multivariate statistical methods is required to establish a reference data base to include all natural variations of the oil in question. The development of such a database is an effective way of characterizing of olive oil and detecting various levels of adulteration.

## REFERENCES

- Ackman, R. G. 1986. Wcot (capillary) gas - liquid chromatography. Analysis of fats and oils. Ed. Hamilton, R. J., Rossell, J. Elsevier Applied Science Pub.
- Adams, M. J. 1991. Cluster analysis with infrared spectra. Analytical Proceedings, vol. 28, p. 147 - 149.
- Adams, M. J., 1995. Pattern Recognition II: supervised learning. Chemometrics in analytical chemistry, Royal Society of Chemistry.
- American Oil Chemists' society. 1973. Official and tentative methods of the American Oil Chemists' society, 3 rd Edition, Champaign, ILL.
- Antoniosi, F. N. R., Carrilho, E. and Lancas F. M. 1993. Fast quantitative analysis of soybean in olive oil by high - temperature capillary gas chromatography, JAOCS, Oct. 1993, vol. 70, no. 10, p. 1051 - 1053.
- AOCS. 1988. Official methods and recommended practices of the American Oil Chemists Society, method Cd 14-61 (3<sup>rd</sup> edition). Ed. D. Firestone. Champaign.
- Aparicio, R., Graciani, E and Ferreiro L. 1992. Chemometric study of the Hilditch theory applied to virgin olive oil. Analytica Chimica Acta, vol. 259, p. 115 - 122.
- Bailey, G. F. and Horvat, R. J. 1972. Raman spectroscopic analysis of the cis/trans isomer composition of edible vegetable oils. JAOCS, vol. 49, p. 494 - 498.
- Bamberger, T., Erickson, J. C. and Cooney, C. L., 1988. Measurement and model prediction of solubility's of pure fatty acids, pure triglycerides and mixtures of

triglycerides in supercritical carbon dioxide, American Chemical Society, J. Chem. Eng. Data, vol. 33, p. 327 - 333.

Bannon, C. D., Craske, J. D. and Hilliker, A. E. 1985. Quantitative methylation, J. Chromatogr., vol. 62, p. 1501.

Bannon, C. D., Craske, J. D., Hai, N. T., Harper, N. L., and O'Rourke, K. L. 1982. Analysis of fatty acid methyl esters with high accuracy and reliability, J. Chromatograph, vol. 247 p. 63 - 69.

Baro, T. J., Pattagini, S. C. 1993. Sample handling for mid - infrared spectroscopy. Spectroscopy, vol. 8, p. 40 - 47.

Bartle, K. D., Clifford, A. A. 1994. Supercritical fluid extraction and chromatography of lipid materials. Developments in the analysis of lipids. Ed. J.H.P. Tyman and M. H. Gordon. The Royal Society of Chemistry.

Becker. 1980. High resolution NMR. Theory and chemical applications, 2<sup>nd</sup> edition, Academic Press, New York.

Belton, P. S., Wilson, R. H., Sadeghi-Jorabchi, H. and Peers, K. E. 1988. A rapid method for the determination of isolated trans double bonds in oils and fats using Fourier transform infrared spectroscopy combined with attenuated total reflectance. Lebensm.-Wiss.u-Technol., vol. 21, p. 153 - 157.

Berg, B. E., Hansen, E. M., Greibrokk, T. 1993. Supercritical CO<sub>2</sub> as a solvent for combined precolumn chemical reaction and introduction medium in capillary supercritical fluid chromatography. The second European symposium on analytical

supercritical fluid chromatography and extraction, Palazzo Dei Congressi, Riva Del Garda, Italy; p. 195 - 203.

Bewig, K. M., Clarke, A. D., Roberts, C. and Unklesbay, N. 1994. Discriminant analysis of vegetable oils by near - infrared reflectance spectroscopy. *JAOCS*, vol. 71, p. 195 - 200

Brekke, T., Barth, T., kvalheim, O., Sletten, E. 1990. Multivariate analysis of <sup>13</sup>C nuclear magnetic resonance spectra. Identification and quantitation of average structures in petroleum distillates. *Analytical Chemistry*, vol. 62, p. 49 - 56.

Brogie, H. 1982. CO<sub>2</sub> as a solvent: Its properties and applications, CO<sub>2</sub> in solvent extraction, June 1982, *Chemistry and Industry*, no. 12, p. 385 - 396.

Browse, J., M<sup>c</sup> Court, P. J. and Somerville C. R. 1986. *Anal. Biochem*, vol. 152, p. 141.

Brumley, W., Sheppard. A. J., Rudolf, T. S., Shen, C-S. J., Yasaei. P. and Spon, J. A. 1985. Mass spectrometry and identification of sterol in vegetable oils as butyryl esters and relative quantification by gas chromatography with flame ionization detection. *J. Assoc. Off. Anal. Chem*, vol. 68, p. 701 - 709.

BSI. 1978. Preparation of methyl esters of fatty acids, British standard method of analysis of fats and fatty acids. BS 684: Section 2.34: 1980, ISO 5509 - 1978.

Camo AS., 1996. The unscrambler 6, User`s Guide.

Carraud, P., Theibaut. D., Caude, M., Rosset, R. 1987. SFC/ light scattering detector: a promising coupling for polar compounds analysis with packed columns. *Journal of Chromatographic Science*, vol. 25, p. 395 - 398.

Chester, T. L. 1984. The introduction of capillary columns to supercritical fluid chromatography. *Journal of Chromatography*, vol. 299, p. 424.

Christie, W., W. 1982. *Lipid analysis. The structure, chemistry and occurrence of lipids.* Pergamon Press.

Christie, W., W. 1986. The positional distribution of fatty acids in triglycerides. *Analysis of fats and oils*, Ed. Hamilton, R. J., Rossell J., Elsevier Applied Science Pub.

Codex Alimentarius Commission CAC/RS 33 - 1970, 1970. Recommended international standard for olive oil, virgin and refined, and for refined olive residue oil. Food and Agriculture Organization.

Colthup, N. B., Daly, L. H. and Wiberley, S. E. 1990. *Introduction to infrared and Raman spectroscopy* (3rd edition), Academic Press.

Craske, J. D. 1993. Separation of instrumental and chemical errors in the analysis of oils by gas chromatography - a collaborative evaluation, *JAOCS*, April 1993, vol. 70, no. 4, p. 325 - 334.

Craske, J. D., Bannon. C. D., Norman, L. M., 1988. The use of sodium methoxide as a catalyst in the transesterification of fatty acid methyl esters. *J. Am. Oil Chem. Soc.*, vol. 65, p.262.

Damiani, P. And Burini, G. 1983. Chemometrics in food research: relationship between triglyceride groups and fatty acid composition in olive oil. Mar. 1993, *JAOCS*, vol. 60, no. 3, p. 539 - 543.

Davies, N. W. 1984. *Anal. Chemistry*, The use of hydrogen, as a carrier gas, in a

temperature program for triglyceride detection, vol. 56, p.2600 - 2602.

De Bussy, J. H. 1970. Oleic and linoleic oils, vegetable oils and fats, edible oils and fats. Materials and technology, Longmanns, p. 45.

De Bussy, J. H. 1970. The role in nutrition, vegetable oils and fats, edible oils and fats. Materials and technology, Longmanns, p. 12.

Demirbaker, M., Blomberg, L. G. 1990. Group separation of triacylglycerides on micropacked argentation columns using supercritical media as mobile phases, Journal of Chromatographic Science, February 1990, vol. 28, p. 67 - 72.

Demirbaker, M., Blomberg, L. G. 1991. Separation of triacylglycerides by supercritical - fluid argentation chromatography, Journal of Chromatography, Elsevier Science publishers B.V., Amsterdam, vol. 550, p. 765 - 774.

Demirbaker, M., Blomberg, L. G. 1994. Analysis of triacylglycerides by argentation supercritical - fluid Developments in the analysis of lipids. Ed. J.H.P. Tyman and M. H. Gordon. The Royal Society of Chemistry.

Dewar, M. J. S. 1951. A review of the  $\pi$  complex theory. Bull. Soc. Chim., vol. 18, p. C71 - C79.

DHSS, Department of Health and Social Security. 1984. Diet and cardio - vascular diseases, report on health and social subjects, no. 28, HMSO, London. 1984.

Dupuy, N., Duponchel, L., Huvenne, J. P., Sombret, B. and Legrand, P. (1996). Classification of edible fats and oils by principal component analysis of Fourier transform



infrared spectra. *Food Chem.*, vol. 57 p. 245 - 251.

Ege, S. 1989. *Organic chemistry, Infrared spectroscopy*, second edition, D. C. Heath and Company.

Eiceman, G. A., Hill, H. H. Jr., Davani, B., Torresday, J. G. 1996. *Gas chromatography. Analytical chemistry*, June 1996, vol. 68, no. 12, p.291-308.

Eisner, J., Firestone, D. J. 1963. The determination of sterols and sterol esters in the authentication of vegetable oils. *Assoc. Off. Agric. Chem.*, vol. 46, p. 542.

El - Hamdy, A. H., El - Fizga, N. K. 1995. Detection of olive oil adulteration by measuring its authenticity factor using High Performance Liquid Chromatography, *Journal of Chromatography A*, vol. 708, p. 351 - 355.

El - Hamdy, A. H., Perkins, E. G. 1981. High performance reversed phase chromatography of natural triglyceride mixtures: critical pair separation, *JAOCS*, Sept., 1981, p.867 - 872.

FAO, Food and Agriculture Organization of the United Nations and the World Health Organization. 1980. *Dietary fats and oils in human nutrition, definitions, effects of processing on the nutritive value of fats and oils used in human nutrition*, FAO, Rome, Italy.

Fedeli, E. 1977. Fats other Lipids. *Lipids of olives*, *Prog. Chem.* vol. 15, p. 54 - 74.

Filho, N. R. A., Carrilho, E., Lancas, F. M. 1993. Fast quantitative analysis of soybean oil in olive oil by high temperature gas chromatography, *JAOCS*, Oct. 1993, vol. 70, no. 10.

Firestone, D. and Summers J. L. 1985. Detection of adulteration and misbranded olive oil

products, JAOCS, Nov. 1985, vol. 62, no. 11, p.1558 - 1562.

Firestone, D., Carson, K. L., Reina, R. J. 1988. Update on control of olive oil adulteration and misbranding in the United States, JAOCS, vol. 65, no. 5.

Food and Agriculture Organization of the United Nations and the World Health Organization 1980. FAO, Rome.

Food and Agriculture Organization of the United Nations and the World Health Organization 1980. Special Considerations, FAO, Rome.

Formo, M. W., Jungermann, E., Norris, F. A., Sonntag, N. O. V. 1979. Baileys industrial oils and fat products. Composition and characteristics of individual fats and oils. Ed. Swern, D. J Wiley and sons, Inc.. p. 289.

France, J. E., Snyder, J. M., King, J. W. 1991. Packed - microbore SFC with Flame ionization detection of abused vegetable oils, Journal of Chromatography, vol. 540, p. 271 - 278.

Frega, N., Bocci, F., Lercker, G. 1990. The HRGC determination of triglycerides, Italian Journal of Food Science, no 4, p. 257 - 264.

Frega, N., Bocci, F., Lercker, G. 1993. The high resolution gas chromatographic determination of diacylglycerols in common vegetable oils. JAOCS, Feb. 1993, vol. 70, no. 2, p. 175 - 177.

Galanos, D. S. 1965. Detection of adulteration of plant oils with special reference to olive oil, Journal of American Oil Chemist Society, Sept. 1965. vol. 42.

Galli, M., Trestianu, S., Grob, K. Jr. 1979. Special cooling system for the on - column injector in capillary gas chromatography eliminating discrimination of sample compounds, *Journal of High Resolution Chromatography and Chromatography Communications*, June 1979, vol. 2, p. 366 - 371.

Gallopini, C. and Fiorentini, R. 1991. Cited in Pallotta, U. 1995. A review of Italian research on the genuineness and quality of extra virgin olive oil, *Italian Journal of Food Science*, Chiriotti Editori, Italy.

Garcia, J. P. and Aparicio, R. L. 1993. Triacylglycerol determination based on fatty acid composition using chemometrics. *Analytica Chimica Acta*, vol. 271, p. 293 - 298.

Geeraert, E. and De Scheper, D. 1983. Design and operation of a simple movable on - column injector, *Journal of High Resolution Chromatography and Chromatography Communications*, July 1983, vol. 6, p. 386 - 387.

Geeraert, E. and Sandra, P. 1985. Capillary GC of triglycerides in fats and oils using a high temperature phenylmethylsilicone stationary phase, part. *Journal of High Resolution Chromatography and Chromatography Communications*, Aug. 1985, vol. 8, p. 415 - 422.

Gilkison, I. S. 1989. Quantitative capillary GC of triglycerides using a polarizable stationary phase, *Journal of High Resolution Chromatography and Chromatography Communications*, vol. 12, no. 7, p. 481 - 483.

Giron, D., Link, R., Bouissel, S. 1992. Analysis of mono - , di - and triglycerides in pharmaceutical excipients by capillary SFC, *Journal of Pharmaceutical and Biomedical Analysis*, vol. 10, no. 10 - 12, p. 821 - 830.

Grob, K., Grob, G. 1978. J. High resolut. Chromatogr., Chromatogr. Commun., vol. 151, p. 311 - 320.

Grob, K., Grob, G. 1979. The advantages of hydrogen over nitrogen as a carrier gas for capillary GC. J. High resolut. Chromatogr., Chromatogr. Commun., vol. 2, p. 109 - 117.

Grob, K., Jr. Nuekom, H. P. and Battaglia, R. 1980. The separation of triglycerides on a polar column with the aid of the cool on - column technique. J. Am. Oil Chem. Soc, vol. 57, p. 282.

Gunstone, F. 1991. <sup>13</sup>C NMR of mono -, di - and triacylglycerols leading to qualitative and semiquantitative information about mixtures of these glycerol esters. Chemistry and Physics of Lipids, vol. 58, p. 219 - 224.

Gunstone, F. 1993. The composition of hydrogenated fats by high resolution <sup>13</sup>C nuclear magnetic resonance spectroscopy, JAOCS, vol. 70, no. 10, p. 965 - 970.

Hamilton, R. J. 1995. Developments in fats and oils. Raman spectroscopy, p. 241, Blackie academic and professional.

Hammond, E. W. 1993. Oils and fats. Food and Nutritional Analyses - Matrices, Analytical science Encyclopaedia, p.1540 - 1546.

Hanswell, S. J. 1992. Practical guide to chemometrics. Marcel Dekker, New York.

Hasenhuettl, G. L. 1993. Fats and fatty oils. Encyclopaedia of chemical technology. Ed. Kroschivitz, J., J Wiley and Sons, p.252 - 287.

Hinshaw, J. V., Seferovic, W. 1986. Analysis of triglycerides by capillary gas

chromatography with programmed - temperature injection, Dec. 1986, Journal of high resolution chromatography and chromatography communications, p.69 - 72.

Hinshaw, J. V., Seferovic, W. 1986. Analysis of triglycerides by capillary gas chromatography with programmed - temperature injection, Journal of high resolution chromatography and chromatography communications, vol. 9, p. 731 - 736.

Hirshfeld, T. and Schildkraut, E.R.. (1974). Laser Raman Gas diagnostics. Ed. M. Lapp. p. 379-388. Plenum press, New York, NY.

Howells, S., Maxwell, R., Griffiths, J., 1992. Classification of tumour <sup>1</sup>H NMR spectra by pattern recognition, NMR in Biomedicine, vol. 5, p. 59 - 64.

International Olive Oil Council. 1993. T15/NC n. 1/Riv. 6, 10 June.

International Standard 1978. ISO 5509. Animal and vegetable fats and oils. Preparation of methyl esters of fatty acids. p. 1 - 6.

Ismail, A. A., Van de Voort, F. R., Emo, G., Sedman, J. 1993. Rapid quantitative determination of free fatty acids in fats and oils by Fourier Transform infrared Spectroscopy, JAOCS, vol. 70, no. 4, p. 335 - 341.

Italian government specifications on olive oil. 1983. Riv. Ital. Sostanze Grasse, vol. 60, p. 229.

Kaplan, M., Davidson, G., Poliakoff, M. 1994. Capillary supercritical fluid chromatography - Fourier transform infrared spectroscopy study of triglycerides and the qualitative analysis of normal and "unsaturated" cheeses. Journal of Chromatography, vol.

673, p. 231 - 237.

Kapoulas, V. M. 1981. Detection of the adulteration of olive oil with seed oils by a combination of column and gas liquid chromatography, *JAOCS*, June 1981, vol. 58, Part 6, p. 694 - 697.

Kaufmann, P. 1991. Lipid analysis and chemometrics; method development, identification and modelling of properties, *Proc. Scan. Symp. Lipids*, vol. 16, p. 70 - 83.

Kaufmann, P. and Herslof, B. G. 1991. A multivariate identification of natural triglycerides, *Fat Sci. Technol.*, Jan. 1991, no. 5, p. 179 - 183.

Ke-Shun, L. 1994. Preparation of fatty methyl esters for gas chromatographic analysis of lipids in biological materials, *JAOCS*, Nov. 1994, vol. 71, no. 11, p. 1179 - 1186.

King J W. 1989. Fundamental and applications of supercritical fluid extraction in chromatographic science. *Journal of chromatographic science*, July 1989, vol. 27 p. 355 - 363.

King, J. W. Eissler, R. L., Friedrich. J. P. 1988. Charaterization and utilization in vegetable oil extraction studies. *Supercritical fluid - adsorbate - adsorbent systems*.

King, J. W., France, J. E., Snyder J. M. 1992. On - line supercritical fluid extraction - supercritical fluid reaction - capillary gas chromatography analysis of the fatty acid composition of oilseeds. 1992. *Fresenius J. Anal. Chem.*, vol. 344, p. 474 - 478.

Kishimoto, Y., Redin, N. S. J. 1959. *Lipid Res.* vol. 1, p. 72.

Knauss, K., Fullemann, J. and Turner, H. P. 1981. *High Resolut. Chromatogr.*,

Chromatogr. Commun, vol., p. 641.

Kowalski, B. R. 1984. Chemometrics: mathematics and statistics in chemistry, D. Reidel publishing company.

Kvalheim, O., Aksnes, D., Brekke, T., Eide, M., Sletten, E. 1985. Crude oil characterization and correlation by principal component analysis of  $^{13}\text{C}$  nuclear magnetic resonance spectra. Analytical Chemistry, Dec. 1985, vol. 57, no. 14, p. 2858 - 2865.

Lai, Y. W., Kemsley, K., Wilson, R. H. 1994. Potential of Fourier Transform infrared spectroscopy for the authentication of vegetable oils, J. Agric. Food Chem., vol. 42, p. 1154 - 1159.

Lai, Y. W., Kemsley, K., Wilson, R. H. 1995. Quantitative analysis of potential adulterants of extra virgin olive oil using infrared spectroscopy, Food Chemistry, vol. 53, p. 95 - 98.

Lanser, A. C. and Emken, E. A. 1988. Comparison of FTIR and capillary GC chromatographic methods for quantitation for trans unsaturation in fatty acid methyl esters. JAOCS, vol. 65, p. 1483 - 1487.

Lee, M. L., Markides, K. E. 1990. Analytical supercritical fluid chromatography and extraction. Chromatography Conferences, Inc.

Lees, M. 1994. Compositional and distribution analysis of TAG's using  $^{13}\text{C}$  NMR. Personal communications, Nantes.

Lees, M. 1995 Food authentication: issues and methodologies, Personal communications, Nantes.

Lepage, G., Roy, C. C. 1986. The quantitative analysis of fatty acid methyl esters using an internal standard prior to derivatization. *J. Lipid Res.*, vol. 27, p. 114.

Levy, G. 1984. High accuracy quantitative analysis. *Topics in <sup>13</sup>C NMR spectroscopy*. Wiley - interscience.

Lichtenwalter, G. 1981. Fats and fatty acids. *Encyclopaedia of Chemical Processing and Design*, Ed. M<sup>c</sup> Ketta J.

Magnus, H. J., Bergqvist and Kaufmann, P. 1993. A multivariate optimization of triacylglycerol analysis by high performance liquid chromatography. *Lipids*, vol. 28, no. 7, p. 667 - 675.

Malinowski, E., R. 1960. *Factor analysis in chemistry*, a Wiley - Interscience publication.

Mangold, H. K. 1991. Olives oils and the Mediterranean. proceedings of the conference "Qualita dell'Olio d'Oliva: Naturalita, Ricerca e Technologie, Venice, 6 - 7 June 1991, p. 71.

Mardia, K. V., Kent, J. T., Bibby, J. M., 1979. *Multivariate analysis*. Academia Press, new York,

Mares, P. 1988. High temperature capillary gas liquid chromatography of triacylglycerols and other lipids. *Prog. Lipid Res.*, vol. 27, p. 107 - 133.

Mares, P., Skorepa, J., Sindelkova, E., Tvrzicka, E. 1993. Gas - liquid chromatographic analysis of intact long chain triglycerides, *Journal of High Chromatography*, vol. 273, p. 172 - 179.



Marigheto, N. A., Wilson, R. H. 1996. Spectroscopy in oils and fats authentication. Institute of food research. Norwich, Personal communications.

Martens, H. and Naes, T. M. 1989. Multivariate calibration. J. Wiley, New York, USA.

Martin, M. L. and Martin, G. 1980. Ed. Delpuech, J.J. Practical NMR spectroscopy, Heyden and son Ltd.

Mason, J. 1987. The Fourier Transform technique. Multinuclear NMR, Plenum press, New York, London.

Mauromoustakos, T. 1994. Personal communications. National Hellenic Research Foundation- Institute of Organic and Pharmaceutical Chemistry, Athens. Greece.

M<sup>c</sup> Ginnis G. W. and Duggan, L. R. 1964. A rapid low temperature method for preparation of methyl esters of fatty acids, JAOCS, April 1965, vol. 4, p. 305 - 312.

Monseigny, A., Vigneron, P. Y., Levacq, M., Zwobada, F. 1979. The separation of triglycerides by total carbon number, TCN using a heated injector, Rev. Fr. Corps Gras, vol. 26, p. 107.

Myher, J. J., Kuksis, A. 1982. Resolution of diacylglycerol moieties of natural glycerophospholipids by gas - liquid chromatography on polar capillary columns. National Research Council of Canada, vol. 60, p. 638 - 650.

Ng, S. 1984. High field <sup>13</sup>C nuclear magnetic resonance spectrum of the olefinic carbons of the triglycerides of palm oil. Lipids, vol. 19, no. 1, p. 56 - 59.

Ng, S. 1985. Analysis of positional distribution of fatty acids in palm oil by <sup>13</sup>C NMR

spectroscopy. *Lipids*, vol. 20, no. 11, p. 778 - 781.

Ng, S. and Ng, W. 1983.  $^{13}\text{C}$  NMR spectroscopic analysis of the fatty acid composition of palm oil, *JAOCS*, July 1983, vol. 60, no. 7, p. 1266 - 1269.

Ng, S. and NG, W. L. 1983. Quantitative compositional analysis of palm oil, *J. Am. Oil Chem. Soc.*, 60, p. 1266.

O.J.E.C. (Official Journal of the European Communities) 1991. Italian Edition, L.248, 5 Sept., 1991.

O.J.E.C. 1992. (Official Journal of the European Communities), Italian Edition, L.248, 5 Sept. 1992.

Ozaki, Y., Cho, R., Ikegaya, K., Muraishi, S. and Kawauchi, K. (1992). Potential of near - infrared Fourier transform Raman spectroscopy in food analysis. *App. Spectrosc.*, vol. 46, p. 1503 - 1507.

Pallotta, U. 1995. A review of Italian research on the genuineness and quality of extra virgin olive oil. *Italian Journal of food science*, Chiriotti Editori, Italy.

Perkin Elmer, 1983. Perkin Elmer Instruction Manual.

Perrin, J. L., Prevot. A., 1988. The separation of mono, di and triglycerides using adsorption SFC, *Rev. Fr. Corps. Gras*, vol. 35, p. 485.

Pollard, M. 1986. Nuclear magnetic resonance spectroscopy (high resolution). Analysis of fats and oils, Ed. Hamilton, R. J., Rossell, J., Elsevier Applied Science Publication, Chapter 9, p. 401 - 429.

Proot, M., Sandra, P. 1986. Resolution of triglycerides in capillary SFC as a function of column temperature, *Journal of High Resolution Chromatography and Chromatography Communications*, vol. 9, p. 189 - 192.

Rawdon, M. G., Norris, T. A. 1984. Supercritical fluid chromatography as a routine analytical technique. *International Laboratory*, June 1984, p. 12 - 23.

Rousseva, N. 1989. Gas chromatographic analysis of the methyl esters of higher fatty acids on porapak, vol. 42, p. 81 - 84.

Sacchi, R., Addeo, F., Giudicianni, I., Paolillo, L. 1992. Analysis of the positional distribution of fatty acids in olive oil triacylglycerols by high resolution  $^{13}\text{C}$  NMR of the carbonyl region, *Short communications, Ital. J. Food Sci.*, no. 2, p. 117 - 123.

Sacchi, R., Paolillo, L., Giudicianni I and Addeo F. 1991. Rapid  $^1\text{H}$  - NMR determination of 1, 2 and 1,3 diglycerides in virgin olive oils, *JAOCS*, vol., no. 6, p. 747 - 758.

Sacchi, R., Patumi, M., Fontanazza, G., Barone, P., Fiordiponti, L., Mannina, L., Rossi, E., Segre, A. L. 1996. A high field  $^1\text{H}$  nuclear magnetic study of the minor components in virgin olive oil, *JAOCS*, no. 2, p. 117 - 123.

Sadeghi-Jorabchi H., Wilson, R. H. and Belton, P. S., Edwards-Webb, J. D. and Coxon, D. T. 1991. Quantitative analysis of oils and fats by Fourier transform Raman spectroscopy. *Spectrochim. Acta*, vol. 47A, p. 1449 - 1458.

Sadeghi-Jorabchi, H., Hendra, P. J., Wilson, R. H. and Belton, P. S. 1990. Determination of the total unsaturation in oils and margarines by Fourier transform Raman spectroscopy.

JAOCS, vol. 67, p. 483 - 486.

Sadeghi-Jorabchi, H., Hendra, P. J., Wilson, R. H. and Belton, P. S. 1990. Determination of the total unsaturation in oils and margarines by Fourier transform Raman spectroscopy. JAOCS, vol. 67, p. 483 - 486.

Safar, M., Bertrand, D., Robert, P., Devaux, M. F., Genot, C. 1994. Characterization of edible oils, butters and margarines by Fourier Transform infrared spectroscopy with attenuated total reflectance, JAOCS, vol. 71, no. 4, p. 371 - 377.

Sandra, P., David, F., Munari, F., Mapelli, G., Trestianu, S. 1988. HT - CGC and CSFC for the analysis of relative high molecular weight compounds, Supercritical Fluid Chromatography Royal Society of Chemistry, Chapter 5, p. 137 - 158.

Sato, T. 1994. Application of principal component analysis on near-infrared spectroscopic data of vegetable oils for their classification. JAOCS, vol. 71, p. 293 - 298.

Sato, T., Kawano, S., Iwamoto, M. 1991. Near infrared spectral patterns of fatty acid analysis from fats and oils, JAOCS, vol. 68, no. 11, p. 827 - 833.

SGE applications, 1993a. BPX5, triglycerides, fatty food guide, Publication no. AP.- 0036 - C Rev:01. Nov. 1993.

SGE. 1993b. SGE applications, BPX70. Fatty acid distribution in edible oils, Publication no. 5000273, July 1993.

SGE. 1993c. SGE production data. OCI - 5, on - column injection system, Oct. 1993. Publication no. PD - 0005 - A Rev:00.

- Shiao, T., Shiao, M., 1989. Determination of fatty acid compositions of triacylglycerols by high resolution NMR spectroscopy. Botanical bulletin of academia Sinica, vol. 30, p. 191 - 199.
- Shoolery, J. N. 1977. Quantitative  $^{13}\text{C}$  NMR analytical method for determining the composition of fats and oils. Prog. Nucl. Magn. Reson. Spectrosc., vol. 11, p. 79 -83
- Simpkins, W., Harrison, M. 1995. The state of the art of in authenticity testing. Trend in Food Science and Technology, Oct. 1995, vol. 61, p. 321 - 328.
- Sleeter, R. T. and Matlock, M. G. 1989. Automated quantitative analysis of isolated (non - conjugated) *trans* isomers using Fourier Transform infrared spectroscopy incorporating improvements in the procedure. JAOCS, vol. 66., p. 121 - 127.
- Smith, R. M. 1988. Gas and liquid chromatography in analytical chemistry. Gas liquid chromatography: Instrumentation. J Wiley and Sons Ltd.
- Stahl, E., Schutz, E. and Mangold, H. K. 1980. Extraction of seed oils with liquid and supercritical carbon dioxide, J. Agric. Food Chem., vol. 28, p. 1153 - 1157.
- Stoffel, W. F., Chu, F and Ahrens, E. H. 1959. JR., Anal. Chem., vol. 31, p. 307.
- Suarez, J. M. M., Mendoza, J. A. 1986. Olive oil processing and related aspects. Extraction and refining: general aspects, Proc. - World Conf. Emerging Technol, p. 299 - 305.
- Sumar, S., Ismail, H. 1995. Adulteration of foods - past and present. Nutrition and Food Science, July/August. no. 4, p. 11 - 15.

Sutcliffe, L. 1995. Basic principles and application of magnetic resonance. Magnetic resonance in food science. Ed. Belton, P., Delgadillo, I., Gil, A., Webb, G.. The Royal Society of Chemistry.

Taylor, S., King, J. W., List, G. R. 1993. Determination of oil content in oilseeds by analytical supercritical fluid extraction, April 1993, JAOCS, vol. 70, no. 4, p. 437 - 439.

Tilly, K., Chaplin, R. P., Foster, N. R. 1990. Supercritical fluid extraction of the triglycerides in vegetable oils. Separation science and technology, vol. 25, no. 4, p. 357 - 367.

Tomassi, G. 1991. Cited in Pallotta, U. 1995. A review of Italian research on the genuineness and quality of extra virgin olive oil, Italian Journal of Food Science, Chiriotti Editori, Italy.

Traitler, H. 1987. Recent advances in capillary gas chromatography applied to lipid analysis. Prog. Lipid Res., vol. 26, p. 257 - 280.

Tsimidou, M., 1995. The use of HPLC in the quality control of virgin olive oil, Aug./Sept. 1995. Chromatography and Analysis, p.5 - 7.

Tsimidou, M., Macrae, R. and Wilson, I. 1987. Authentication of virgin olive oils using principal component analysis of triglycerides and fatty acid profiles: Part I - Classification of Greek olive oils. Food Chemistry, vol. 25, p. 227 - 239.

Twadowski, J., Anzenbacher, P. 1994. Raman and IR spectroscopy in biology and biochemistry. Polish scientific Publisher, PWN Ltd, Warsaw.

Ulberth, F. and Haider, H. 1992. Determination of low level trans unsaturation in fats by Fourier Transform infrared spectroscopy. *J. Food Sci.*, vol. 57, p. 1444 - 1447.

Van der Voort, F. R., Ismail, A. A. and Sedman, J. (1995). A rapid, automated method for the determination of *cis* and *trans* content of fats and oils by Fourier transform infrared spectroscopy. *JAOCS*, vol. 72, p. 873 - 880.

Vander Wal, R. J. 1960. Calculation of the distribution of the saturated and unsaturated acyl groups in fats, from pancreatic lipase hydrolysis data, *Journal of the American Oil Chemical Society*, p. 18 - 20.

Vogt, N. B. 1987. Chemometrics tutorials, soft modelling and chemosystematics, *Chemometrics and Intelligent Laboratory Systems*, vol. 1, p. 213 - 231.

Wenbao, L., Malik, A., Milton, L. L. 1994. Fused silica packed capillary Columns in SFC. *J. Microcol. Sep.*, vol. 6, p. 557 - 563.

Wesley, I. J., Barnes, R. J. and M<sup>c</sup> Gill. A. E. J. 1995. Measurement of adulteration of olive oils by near-infrared spectroscopy. *JAOCS*, vol. 72, p. 289 - 292.

White, C. M. and Houck, R. K. 1986. *Journal of high resolution chromatography*, vol. 9, p. 424.

WHO, World Health Organization, 1984. Toxic oil syndrome: mass food poisoning in Spain; WHO: Copenhagen.

WHO, World Health Organization, 1992. Toxic oil syndrome: current knowledge and current perspective; WHO: Copenhagen.

Williams, K. P. L., Mason, S. M. 1990. Future direction for Fourier Transform Raman spectroscopy in industrial analysis, *Spectrochim Acta*, vol. 46A, p. 187 - 196.

Wilson, R. H. 1990. Fourier Transform mid - infrared spectroscopy for food analysis. *Trends in analytical chemistry*, vol. 9, no. 4, p. 127 - 131.

Wold S., Albano C., Dunn, W. J., Esbensen K., Hellberg, S., Johansson, E and Sjostrom M. 1983. Pattern recognition : Finding and using regularities in multivariate data, Eds. H. Martens and H. Russwurm Jr. Food research and data analysis, Applied Science Publishers, London.

Wollenberg, K. F. 1990. Quantitative high resolution  $^{13}\text{C}$  nuclear magnetic resonance of the olefinic and carbonyl carbons of edible vegetable oils, *JAOCS*. vol. 67, no 8, p. 487 - 495.

Wood, G. M., Slack, P. T., Rossell, J. B., Mann, P. J., Farnell, P. J. 1994. Spanish toxic oil syndrome (1981): Progress in the identification of suspected toxic components in simulated oils, *J. Agric Food Chem.*, vol. 42. no. 11, p. 2525 - 2530.

Zamora, R., Navarro, J. L., Hidalgo, F. J. 1994. Identification and classification of olive oils by high resolution  $^{13}\text{C}$  nuclear magnetic resonance, *JAOCS*, vol. 71, no. 4, p. 361 - 364.



## APPENDIX A

Figure A1 Raman spectra of sample D1 and its adulterated mixtures of sunflower oil ....	A1
Figure A2 Raman fingerprint spectra of sample D1 and its adulterated mixtures of sunflower oil .....	A1
Figure A3 Raman spectra of sample D2 and its adulterated mixtures of sunflower oil ....	A1
Figure A4 Raman fingerprint spectra of sample D2 and its adulterated mixtures of sunflower oil .....	A2
Figure A5 Raman spectra of sample D3 and its adulterated mixtures of sunflower oil ....	A2
Figure A6 Raman fingerprint spectra of sample D3 and its adulterated mixtures of sunflower oil .....	A2
Figure A7 Raman spectra of sample D4 and its adulterated mixtures of sunflower oil ....	A3
Figure A8 Raman fingerprint spectra of sample D4 and its adulterated mixtures of sunflower oil .....	A3
Figure A9 Raman spectra of sample D5 and its adulterated mixtures of sunflower oil ....	A3
Figure A10 Raman fingerprint spectra of sample D5 and its adulterated mixtures of sunflower oil .....	A4
Figure A11 Raman spectra of sample D6 and its adulterated mixtures of sunflower oil ..	A4
Figure A12 Raman fingerprint spectra of sample D6 and its adulterated mixtures of sunflower oil .....	A4

Figure A13 Raman spectra of sample D7 and its adulterated mixtures of sunflower oil .. A5

Figure A14 Raman fingerprint spectra of sample D7 and its adulterated mixtures of sunflower oil ..... A5

Figure A15 Raman spectra of sample D8 and its adulterated mixtures of sunflower oil .. A5

Figure A16 Raman fingerprint spectra of sample D8 and its adulterated mixtures of sunflower oil ..... A6

Figure A17 Raman spectra of sample D9 and its adulterated mixtures of sunflower oil .. A6

Figure A18 Fingerprint Raman spectra of sample D9 and its adulterated mixtures of sunflower oil ..... A6

Figure A19 Raman spectra of sample D10 and its adulterated mixtures of sunflower oil A7

Figure A20 Fingerprint Raman spectra of sample D10 and its adulterated mixtures of sunflower oil ..... A7

Figure A21 Raman spectra of sample D11 and its adulterated mixtures of sunflower oil A7

Figure A22 Raman fingerprint spectra of sample D11 and its adulterated mixtures of sunflower oil ..... A8

Figure A23 Raman spectra of the sample D12 and its adulterated mixtures of sunflower oil ..... A8

Figure A24 Raman fingerprint spectra of sample D12 and its adulterated mixtures of sunflower oil ..... A8

Figure A25 Raman Fingerprint spectra of sample D13 and its adulterated mixtures of sunflower oil .....	A9
Figure A26 Raman fingerprint spectra of sample D13 and its adulterated mixtures of sunflower oil .....	A9
Figure A27 Raman fingerprint spectra of sample D14 and its adulterated mixtures of sunflower oil .....	A9
Figure A28 Raman fingerprint spectra of sample D14 and its adulterated mixtures of sunflower oil .....	A10
Figure A29 Raman fingerprint spectra of sample D15 and its adulterated mixtures of sunflower oil .....	A10
Figure A30 Raman fingerprint spectra of sample D15 and its adulterated mixtures of sunflower oil .....	A10
Figure A31 Raman spectra of sample D16 and its adulterated mixtures of sunflower oil .....	A11
Figure A32 Raman fingerprint spectra of sample D16 and its adulterated mixtures of .....	
sunflower oil .....	A11
Figure A33 Raman spectra of sample D17 and its adulterated mixtures of sunflower oil .....	
.....	A11
Figure A34 Raman fingerprint spectra of sample D18 and its adulterated mixtures of sunflower oil .....	A12

Figure A35 Raman fingerprint spectra of sample D18 and its adulterated mixtures of sunflower oil ..... A12

Figure A36 Raman fingerprint spectra of sample D18 and its adulterated mixtures of sunflower oil ..... A12

Figure A37 Raman spectra of sample D19 and its adulterated mixtures of sunflower oil ..... A13

Figure A38 Raman spectra of sample D19 and its adulterated mixtures of sunflower oil ..... A13

Figure A39 Raman spectra of sample D20 and its adulterated mixtures of sunflower oil ..... A13

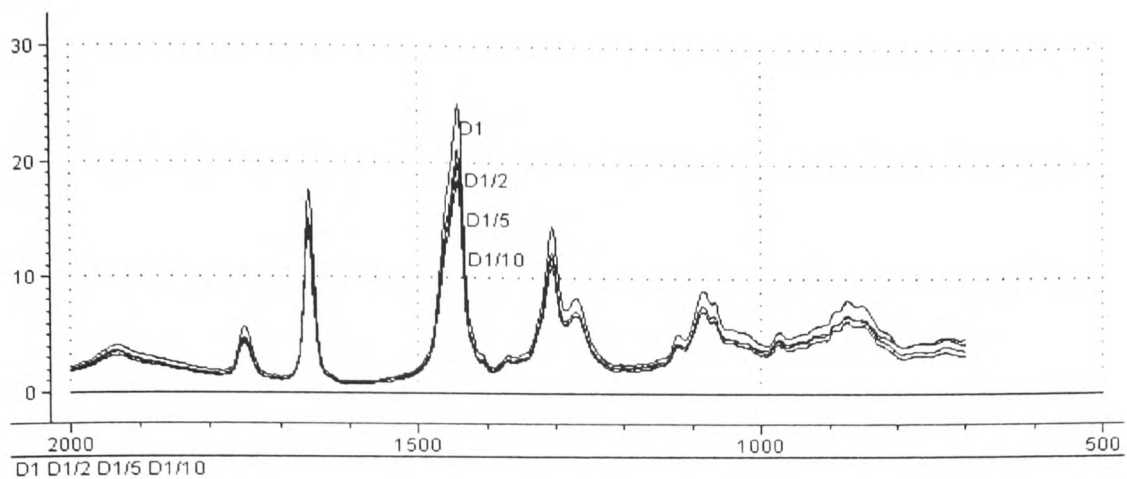
Figure A40 Raman fingerprint spectra of sample D20 and its adulterated mixtures of sunflower oil ..... A14

Figure A41 Raman spectra of sample D21 and its adulterated mixtures of sunflower oil ..... A14

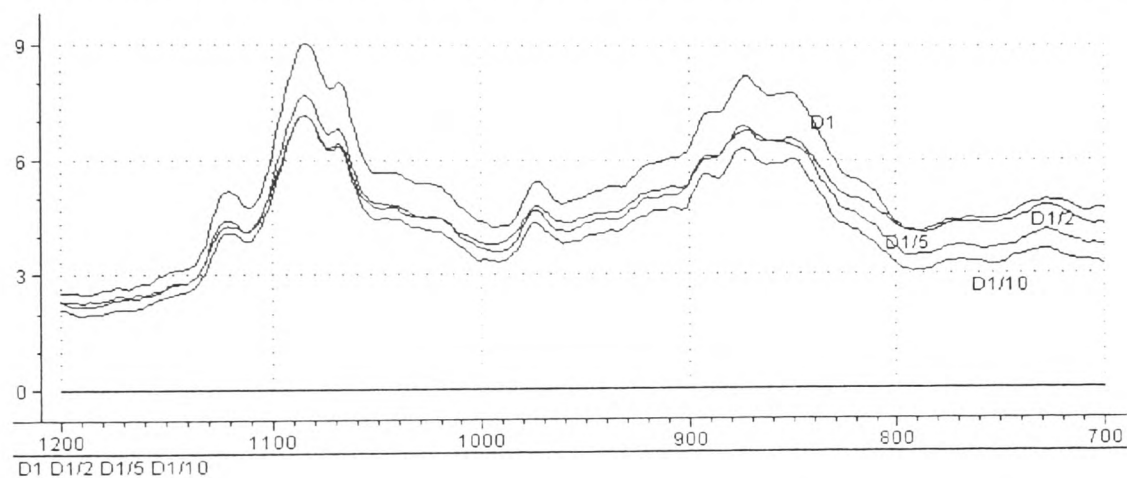
Figure A42 Raman fingerprint spectra of sample D21 and its adulterated mixtures of sunflower oil ..... A14

Figure A43 Raman spectra of sample D22 and its adulterated mixtures of sunflower oil ..... A15

Figure A44 Raman fingerprint spectra sample D22 and its adulterated mixtures of sunflower oil ..... A15



**Figure A1 Raman spectra of sample D1 and its adulterated mixtures of sunflower oil**



**Figure A2 Raman fingerprint spectra of sample D1 and its adulterated mixtures of sunflower oil**

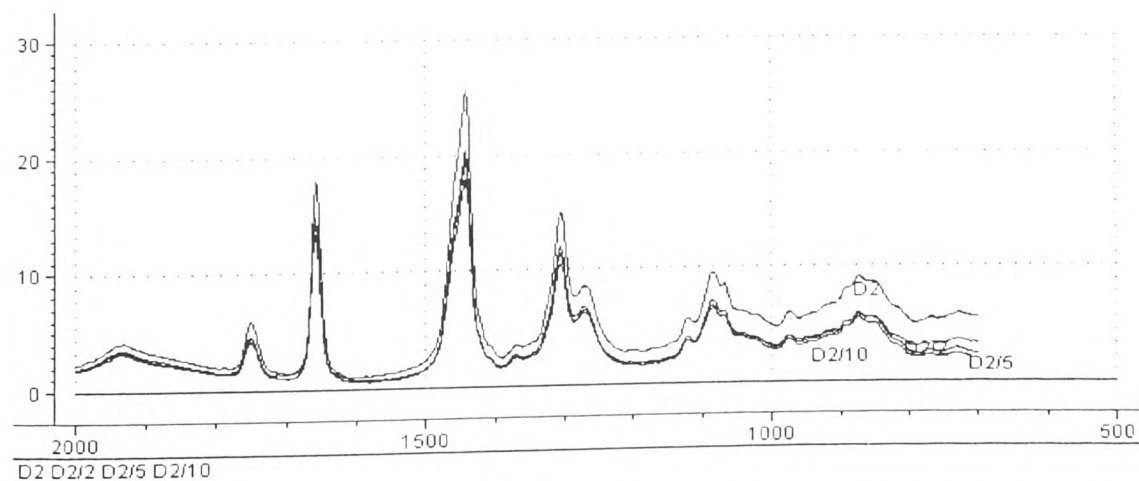


**Figure A3 Raman spectra of sample D2 and its adulterated mixtures of sunflower oil**

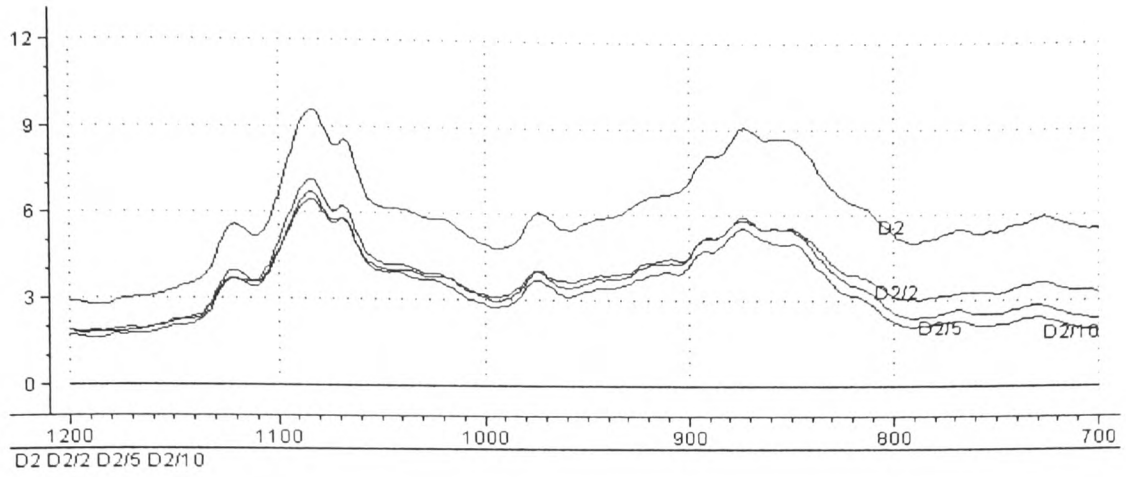


**Figure A4 Raman fingerprint spectra of sample D2 and its adulterated mixtures of sunflower oil**

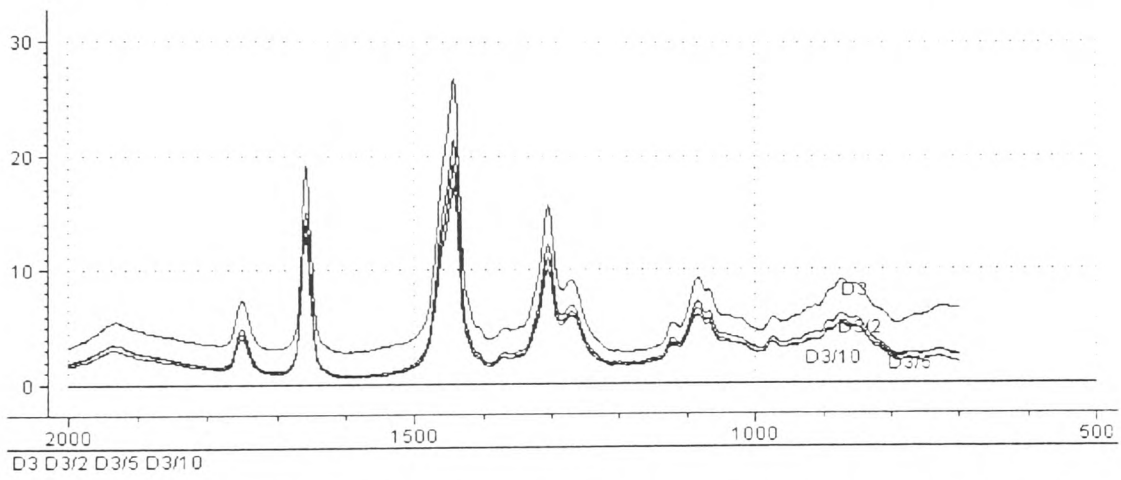


**Figure A5 Raman spectra of sample D3 and its adulterated mixtures of sunflower oil**

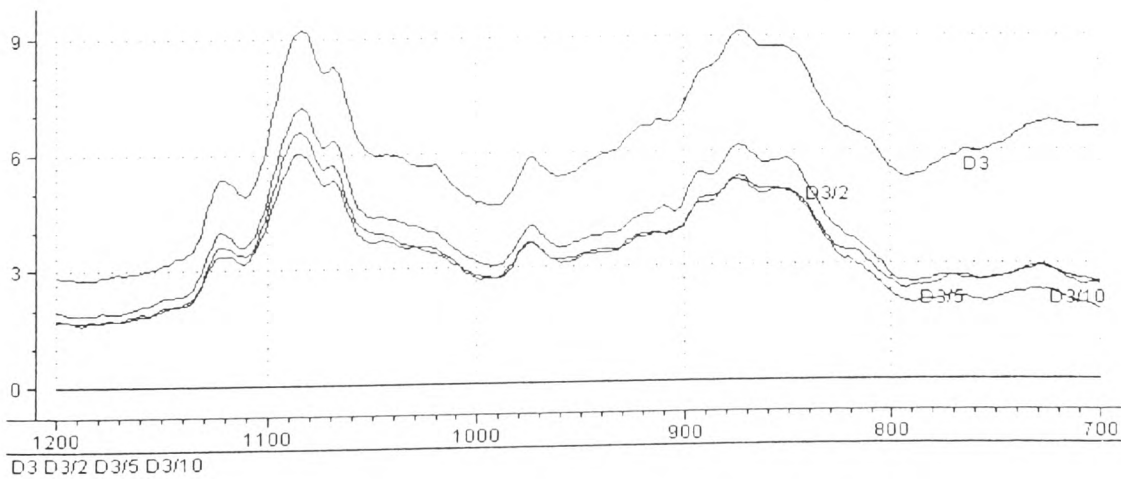


**Figure A6 Raman fingerprint spectra of sample D3 and its adulterated mixtures of sunflower oil**

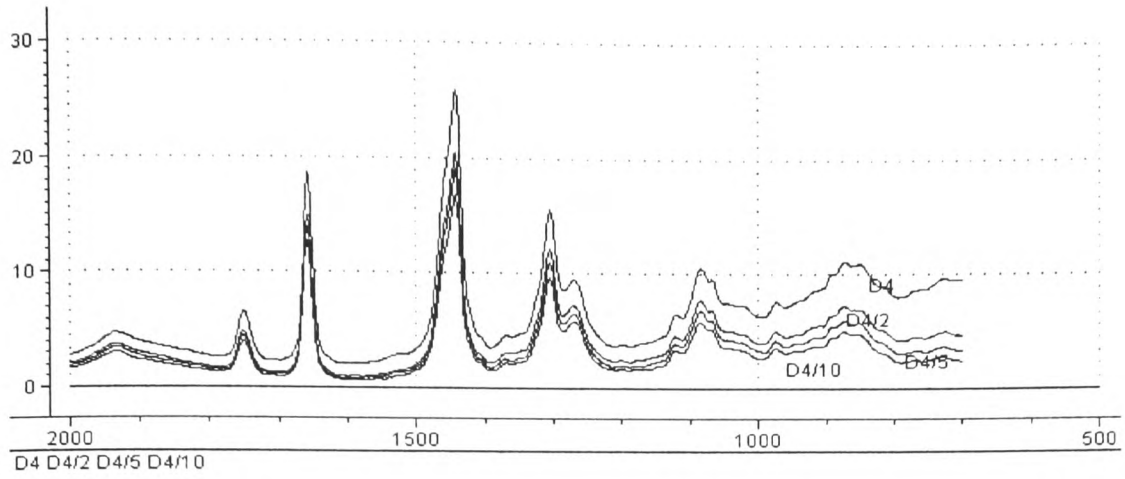


**Figure A7 Raman spectra of sample D4 and its adulterated mixtures of sunflower oil**

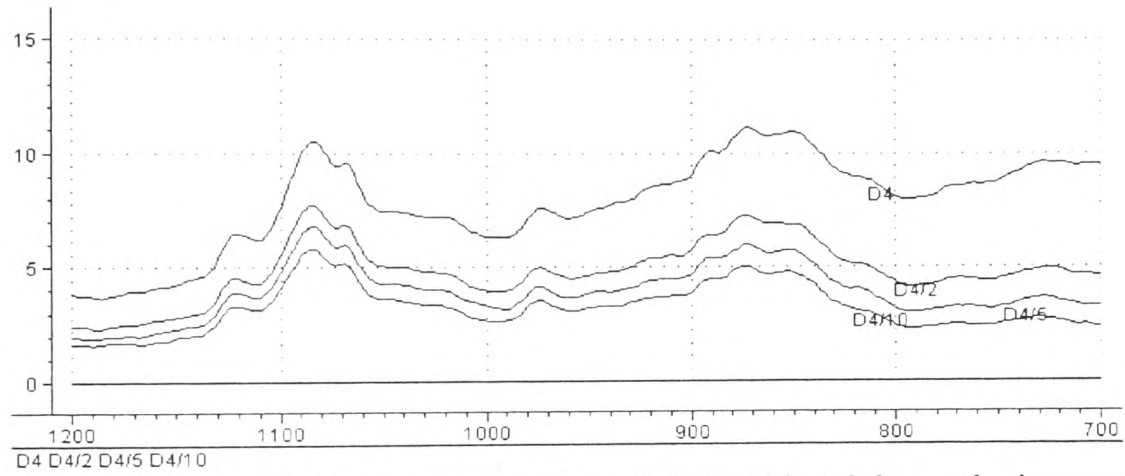


**Figure A8 Raman fingerprint spectra of sample D4 and its adulterated mixtures of sunflower oil**

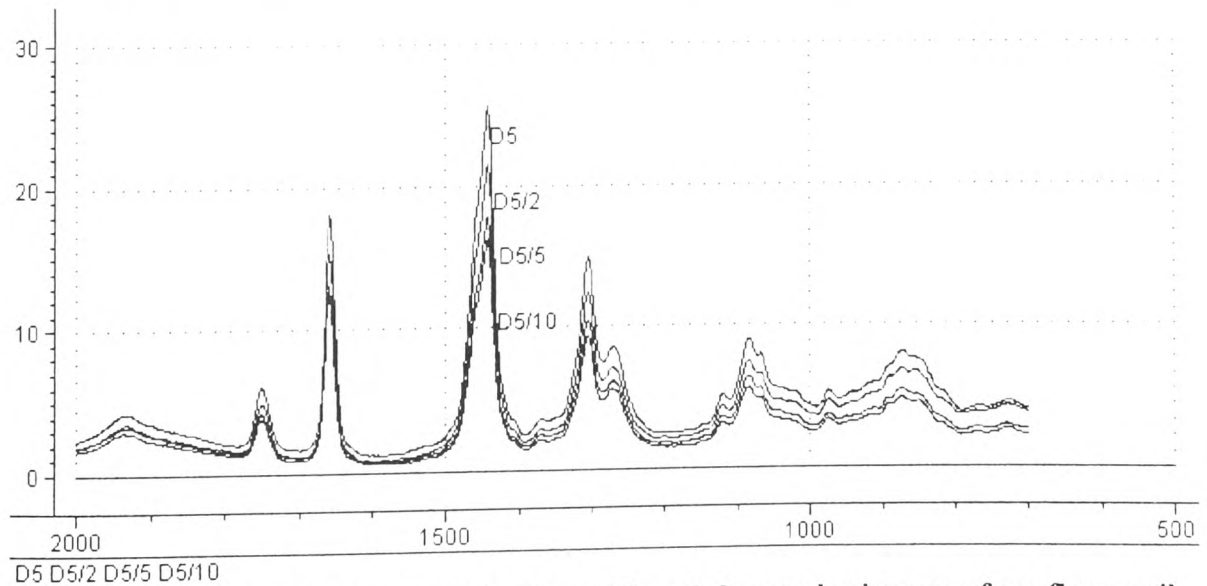


**Figure A9 Raman spectra of sample D5 and its adulterated mixtures of sunflower oil**

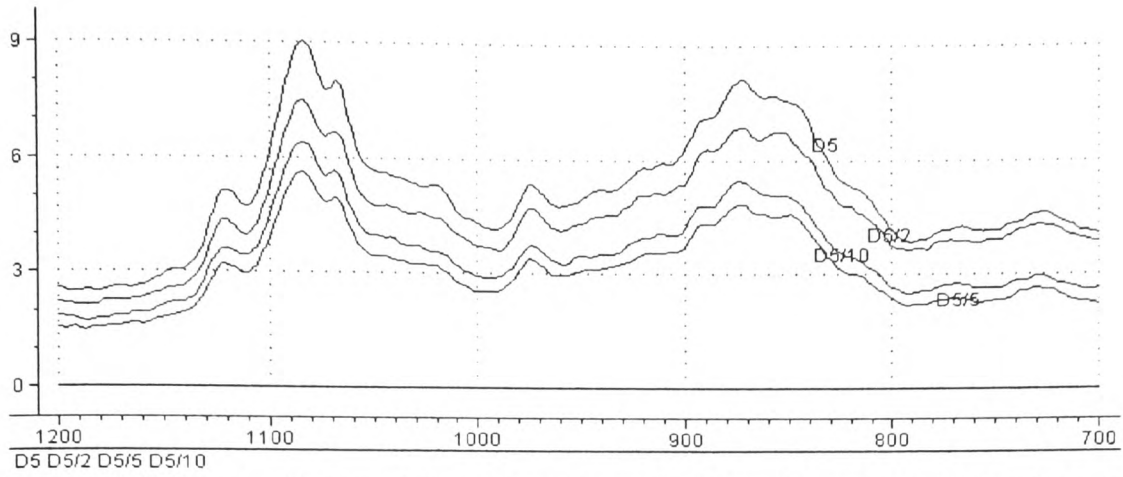


**Figure A10 Raman fingerprint spectra of sample D5 and its adulterated mixtures of sunflower oil**

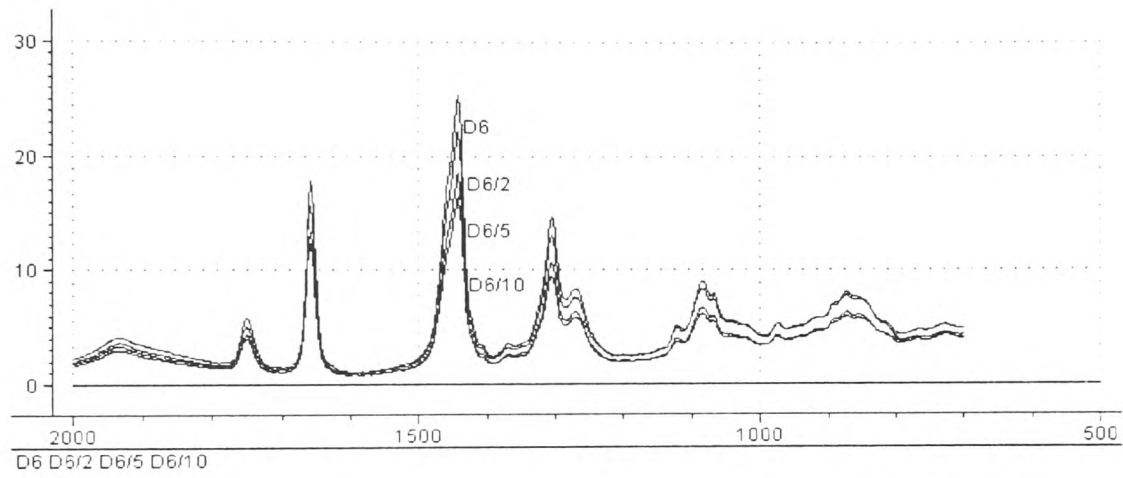


**Figure A11 Raman spectra of sample D6 and its adulterated mixtures of sunflower oil**

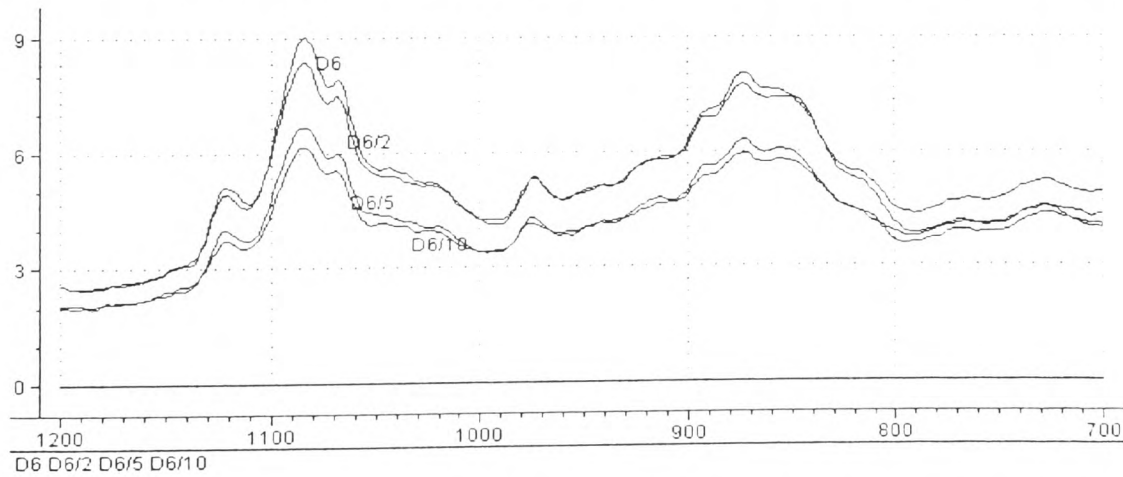


**Figure A12 Raman fingerprint region spectra of sample D6 and its adulterated mixtures of sunflower oil**



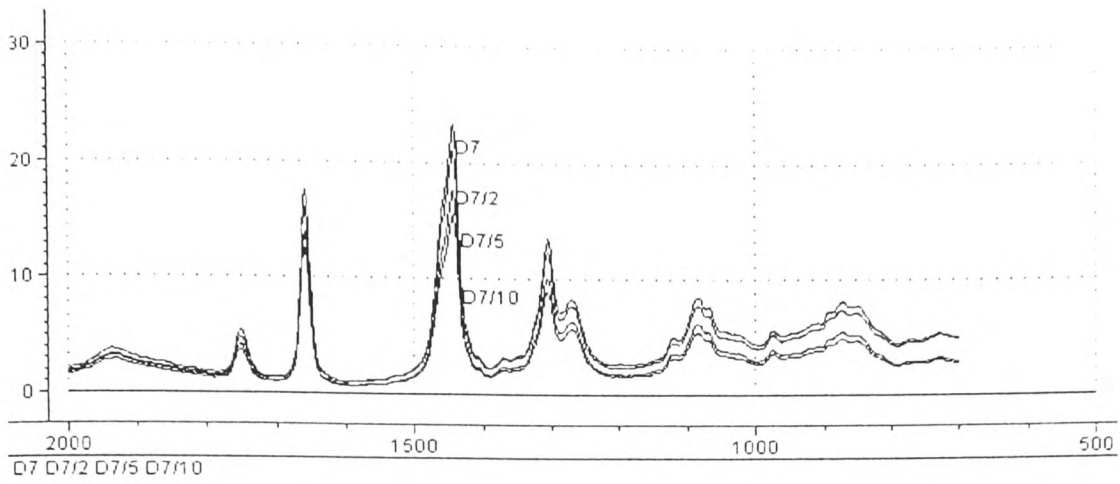


Figure A13 Raman spectra of sample D7 and its adulterated mixtures of sunflower oil

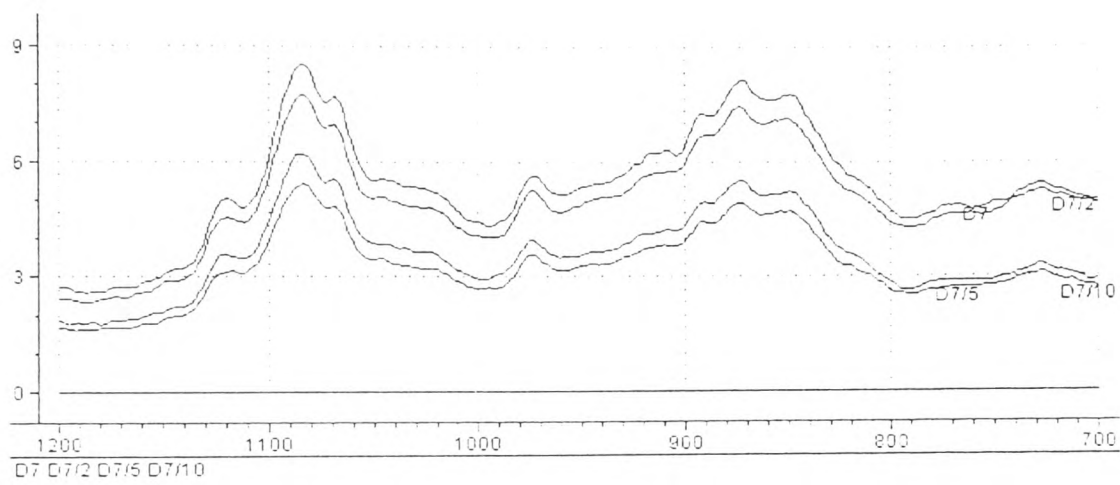


Figure A14 Raman fingerprint region spectra of sample D7 and its adulterated mixtures of sunflower oil

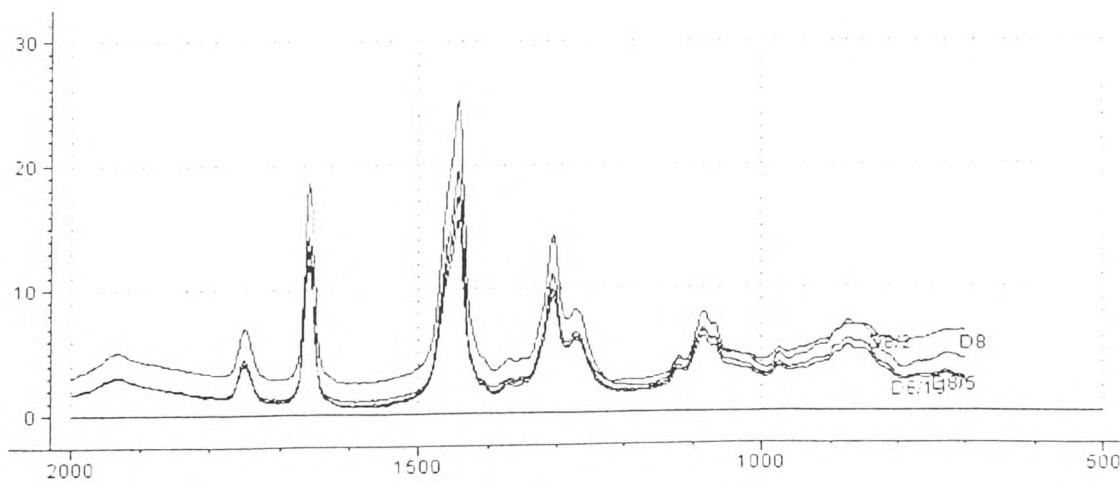
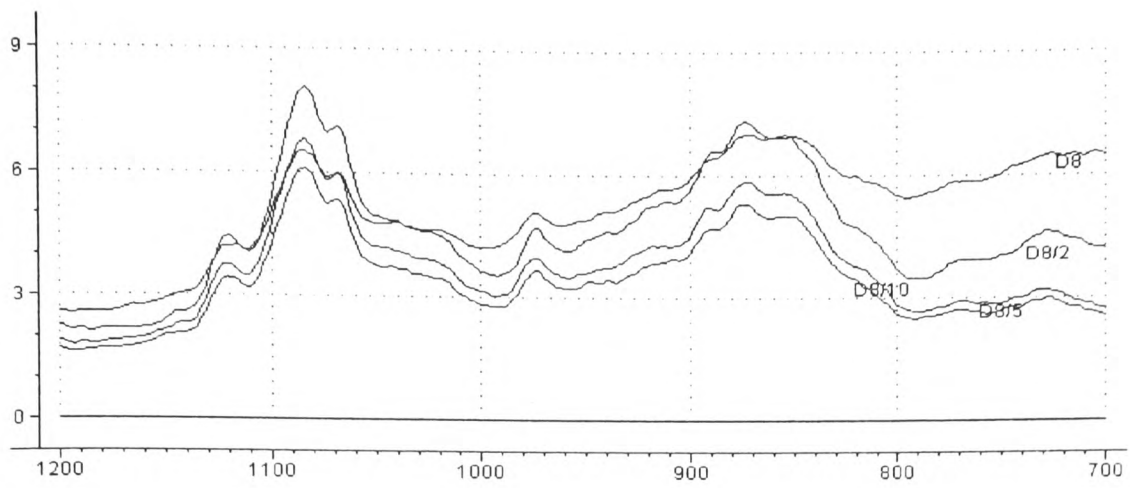
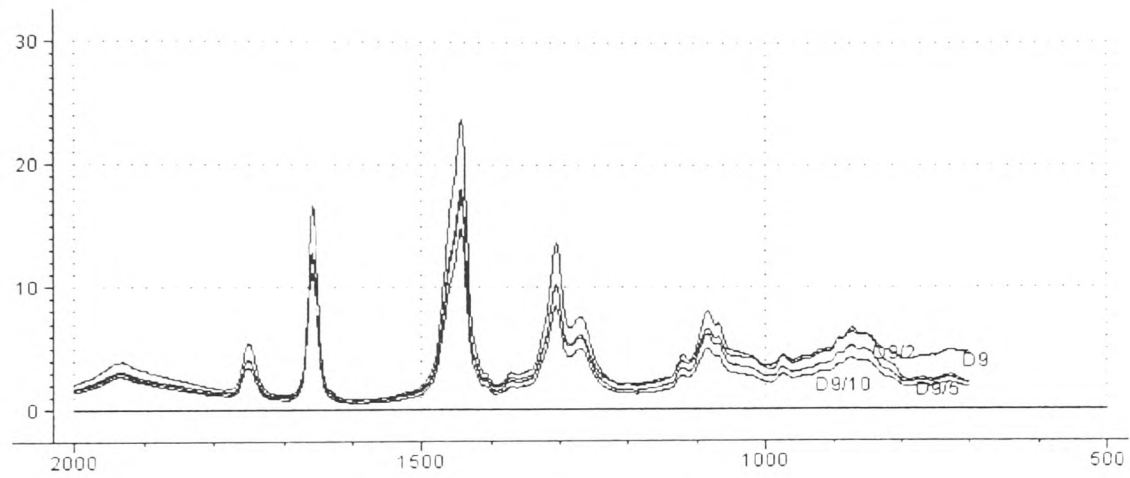


Figure A15 Raman spectra of sample D8 and its adulterated mixtures of sunflower oil (2 % w/w, 5 % w/w, 10 % w/w respectively)



**Figure A16 Raman fingerprint spectra of sample D8 and its adulterated mixtures of sunflower oil**



**Figure A17 Raman spectra of sample D9 and its adulterated mixtures of sunflower oil**

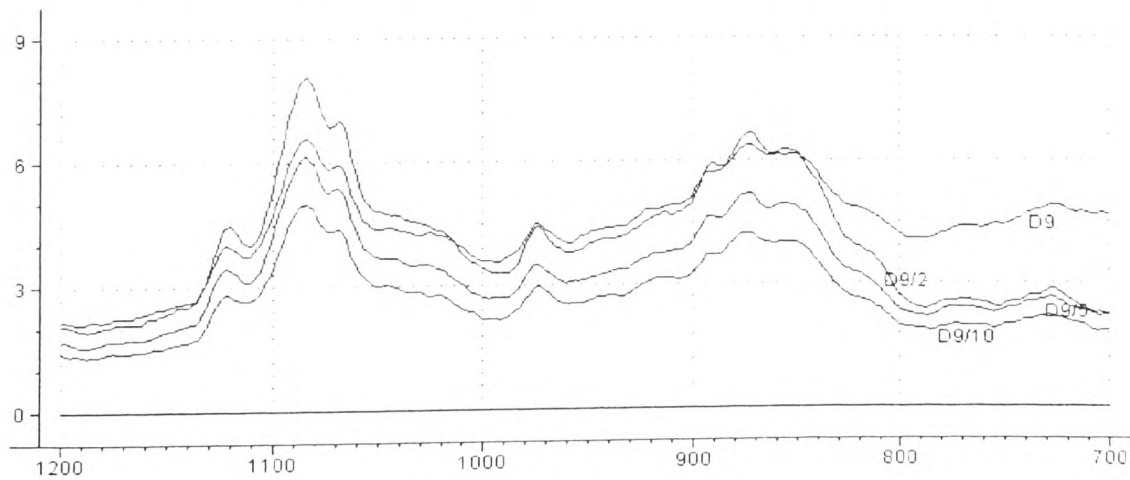


**Figure A18 Raman fingerprint spectra of sample D9 and its adulterated mixtures of sunflower oil**

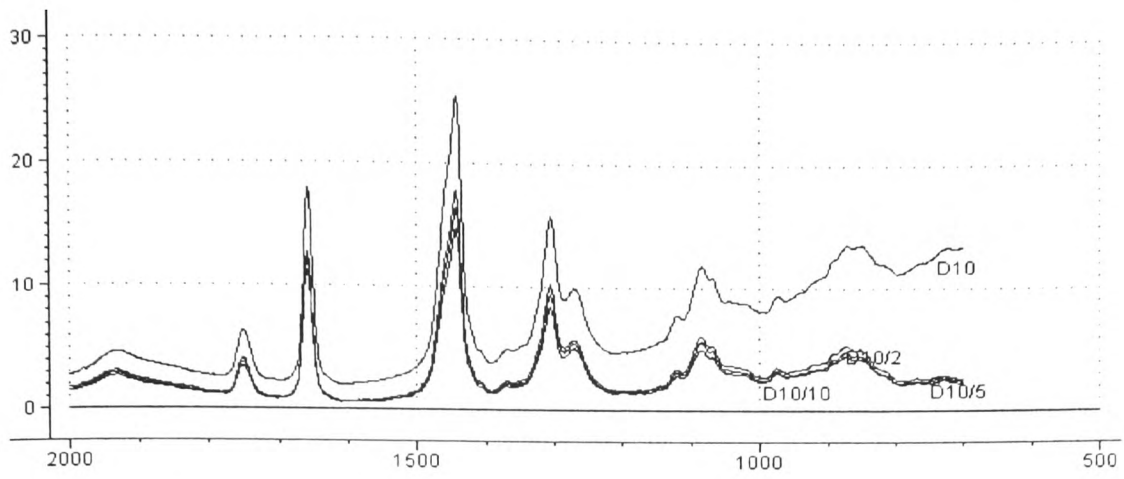


Figure A19 Raman spectra of sample D10 and its adulterated mixtures of sunflower oil

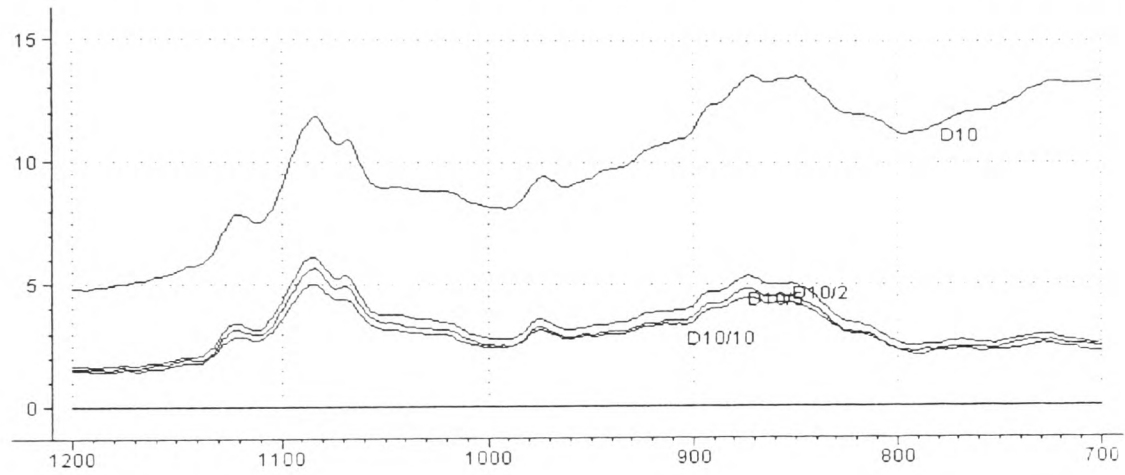


Figure A20 Fingerprint Raman spectra of sample D10 and its adulterated mixtures of sunflower oil

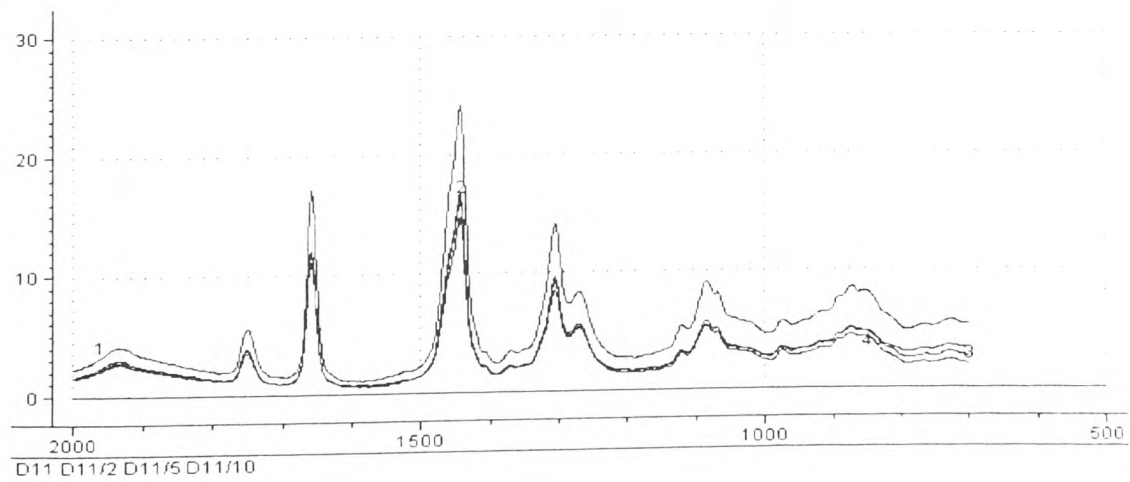
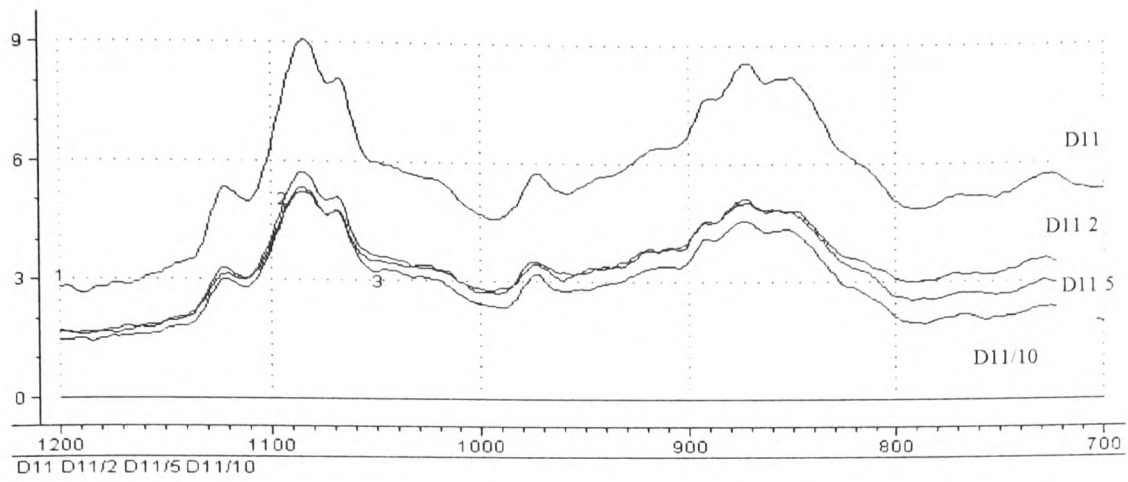
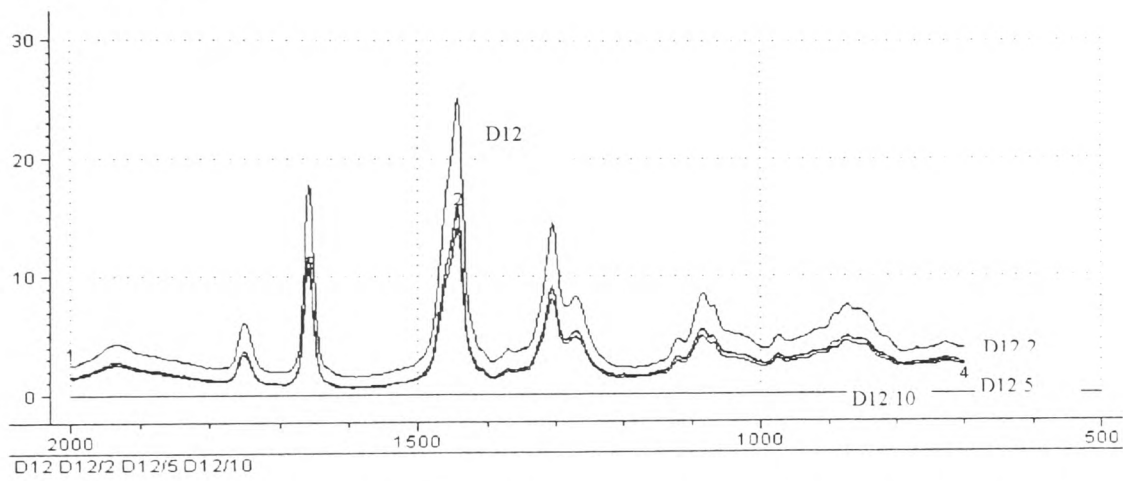


Figure A21 Raman spectra of sample D11 and its adulterated mixtures of sunflower oil



**Figure A22 Raman fingerprint spectra of sample D11 and its adulterated mixtures of sunflower oil**



**Figure A23 Raman spectra of the sample D12 and its adulterated mixtures of sunflower oil**

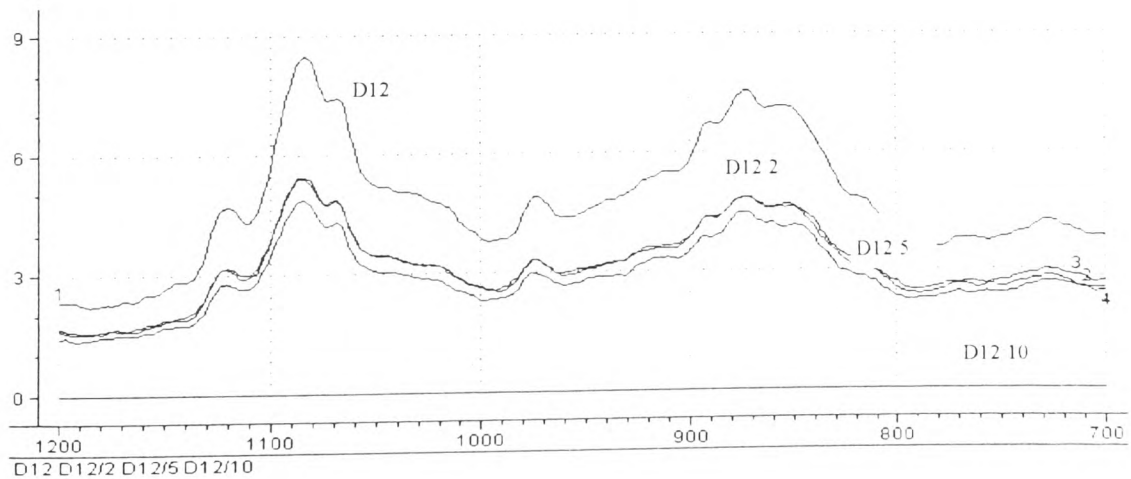


**Figure A24 Raman fingerprint spectra of sample D12 and its adulterated mixtures of sunflower oil**

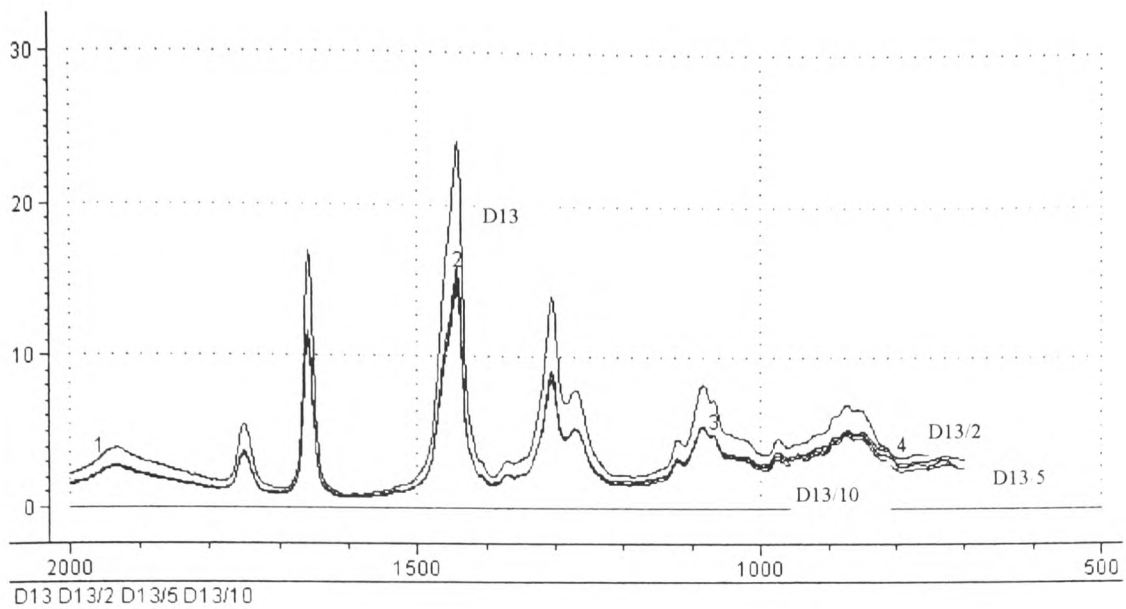


Figure A25 Raman spectra of sample D13 and its adulterated mixtures of sunflower oil

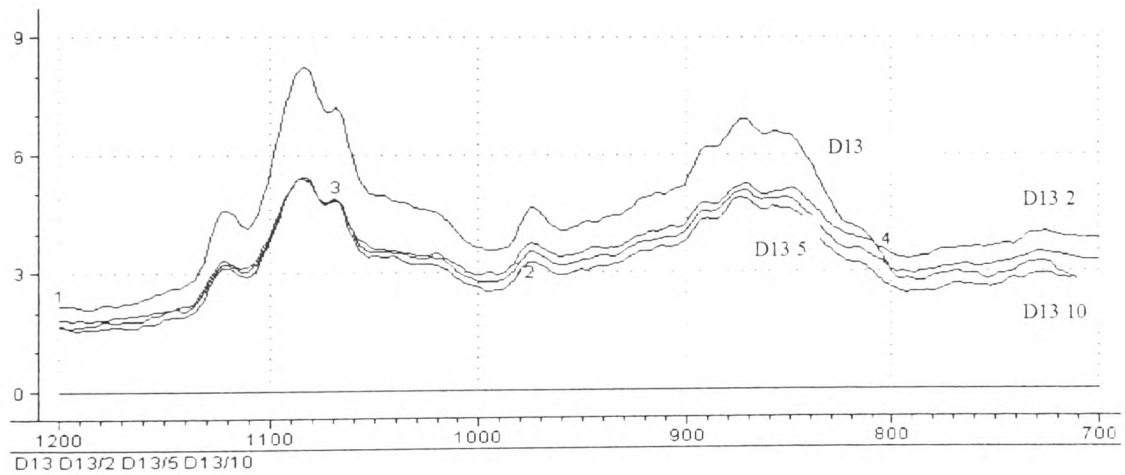


Figure A26 Raman fingerprint spectra of sample D13 and its adulterated mixtures of sunflower oil

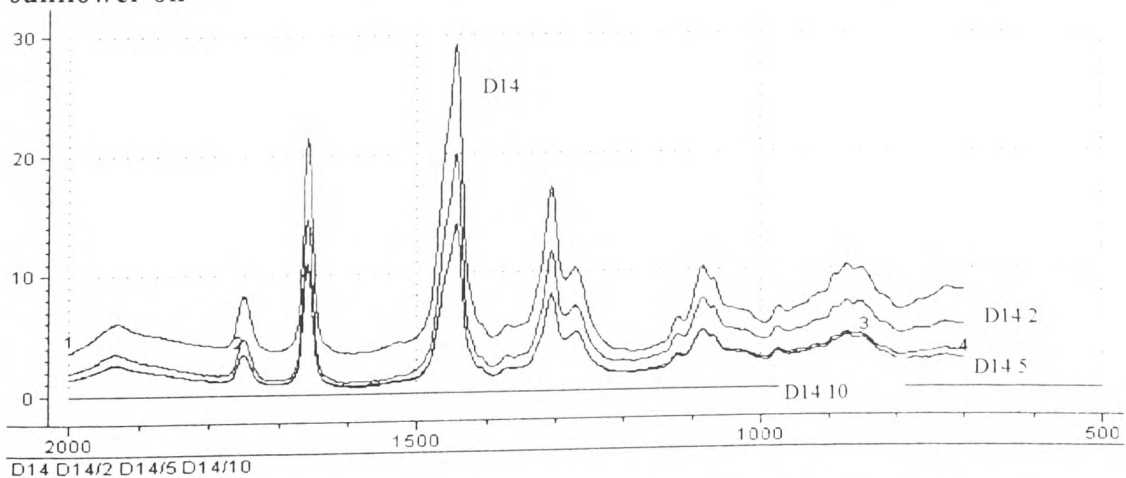
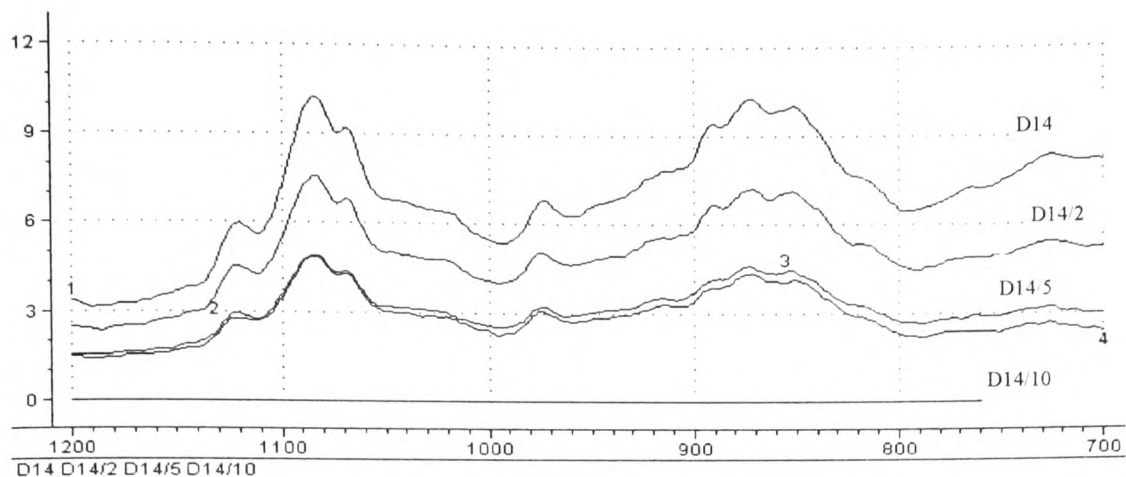
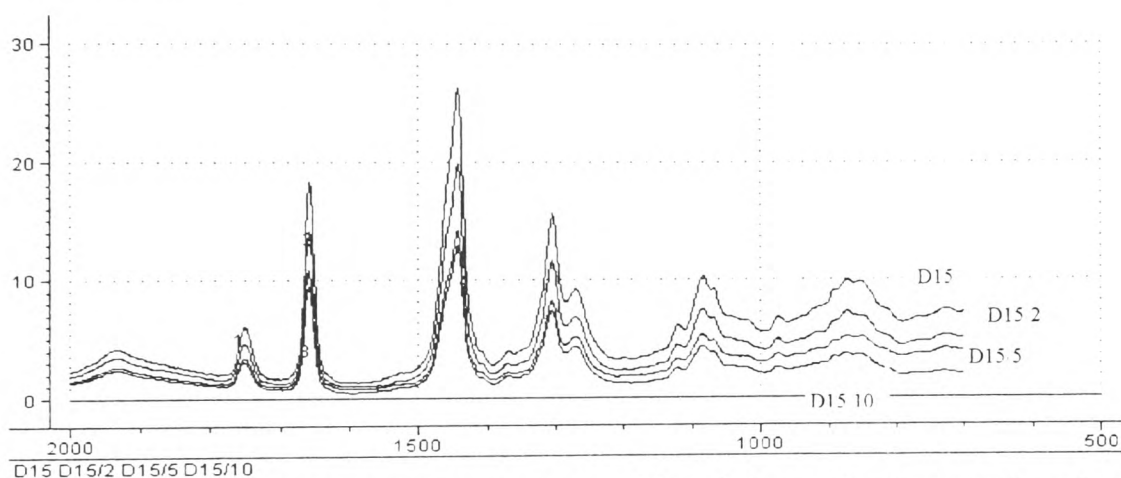


Figure A27 Raman spectra of sample D14 and its adulterated mixtures of sunflower oil



**Figure A28 Raman fingerprint spectra of sample D14 and its adulterated mixtures of sunflower oil**



**Figure A29 Raman spectra of sample D15 and its adulterated mixtures of sunflower oil**

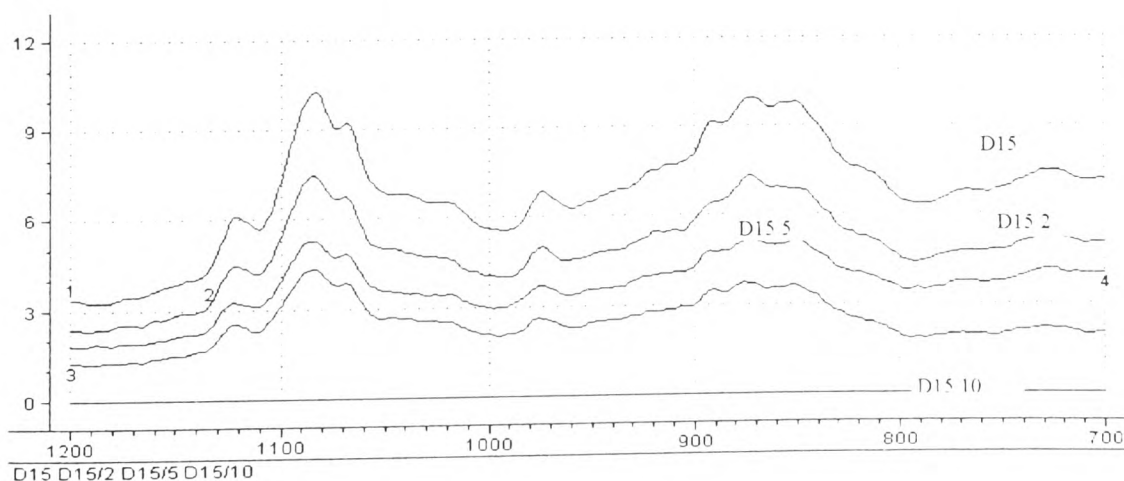


**Figure A30 Raman fingerprint spectra of sample D15 and its adulterated mixtures of sunflower oil**

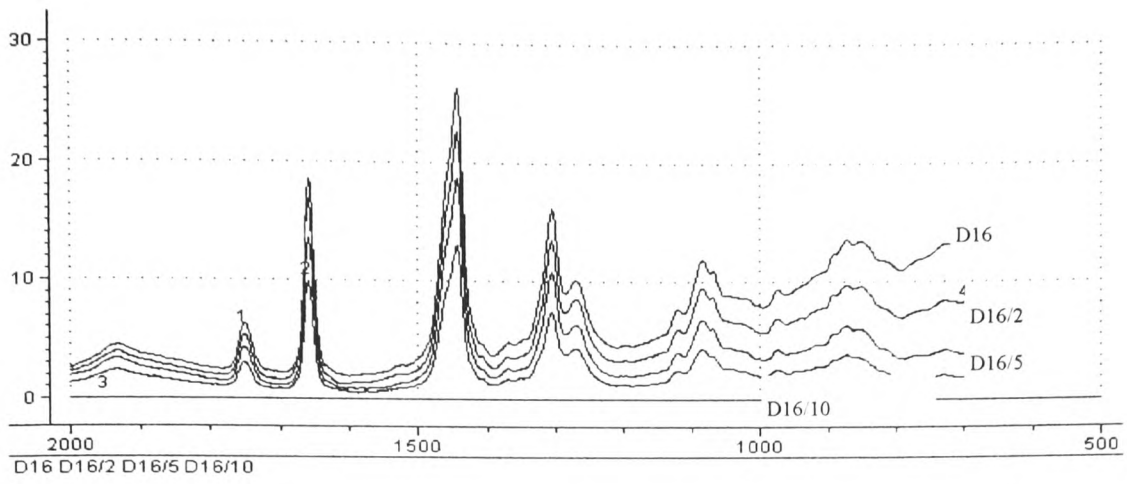


**Figure A31 Raman spectra of sample D16 and its adulterated mixtures of sunflower oil**

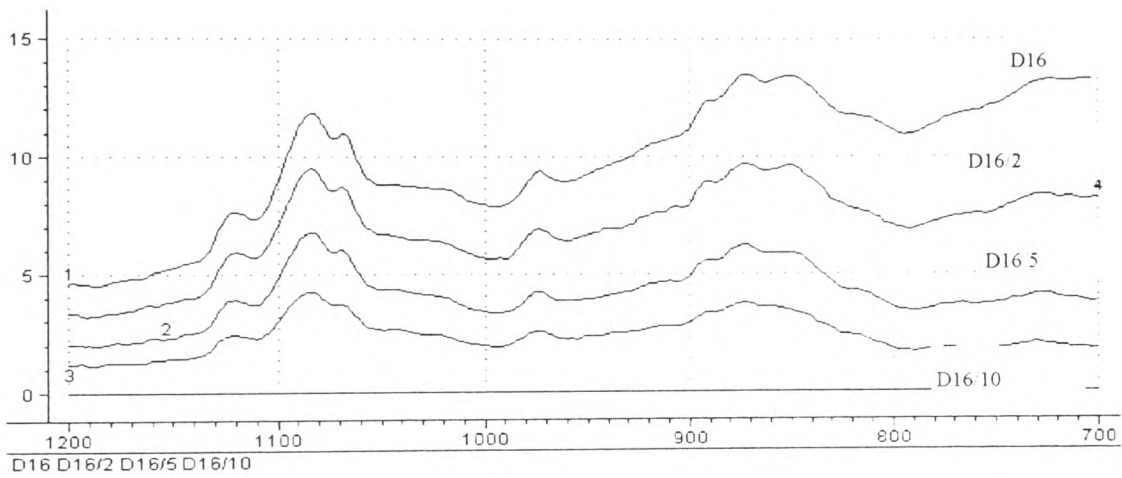


**Figure A32 Raman fingerprint spectra of sample D16 and its adulterated mixtures of sunflower oil**

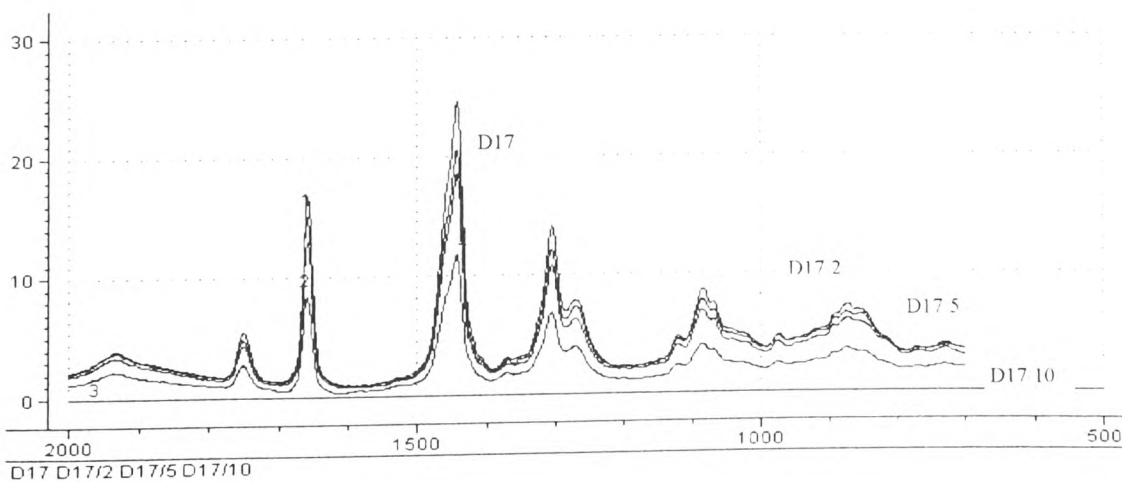


**Figure A33 Raman spectra of sample D17 and its adulterated mixtures of sunflower oil**

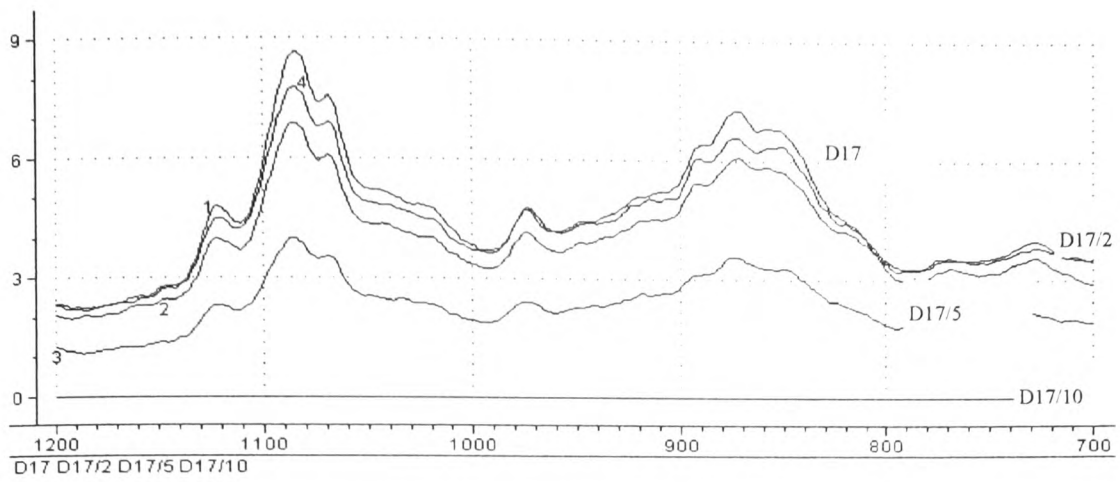


**Figure A34 Raman fingerprint spectra of sample D17 and its adulterated mixtures of sunflower oil**

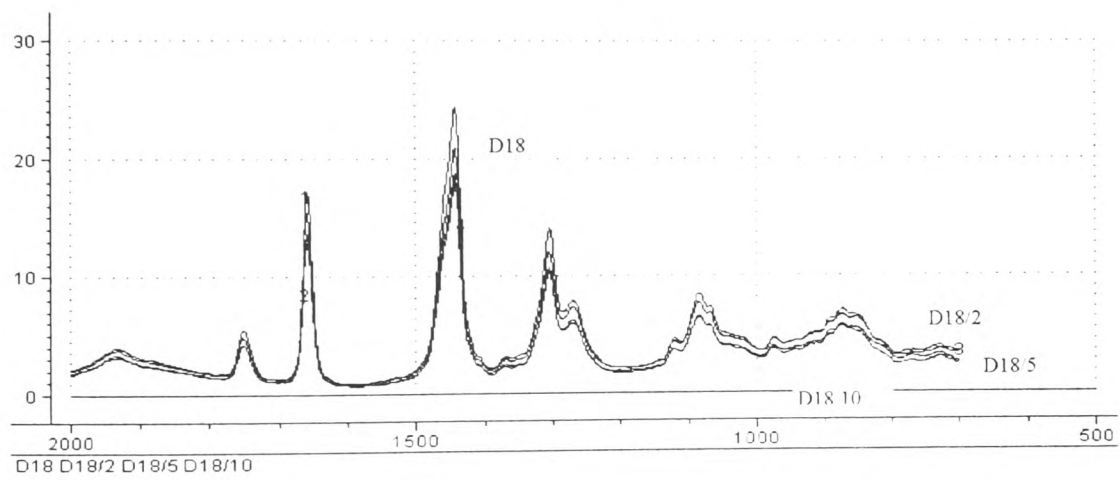


**Figure A35 Raman spectra of sample D18 and its adulterated mixtures of sunflower oil**

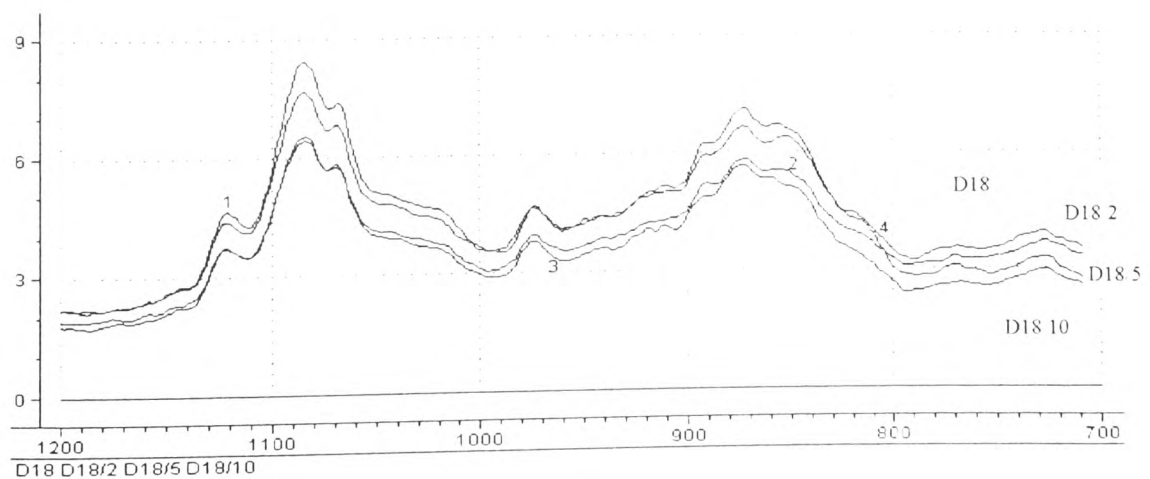


**Figure A36 Raman fingerprint spectra of sample D18 and its adulterated mixtures of sunflower oil**



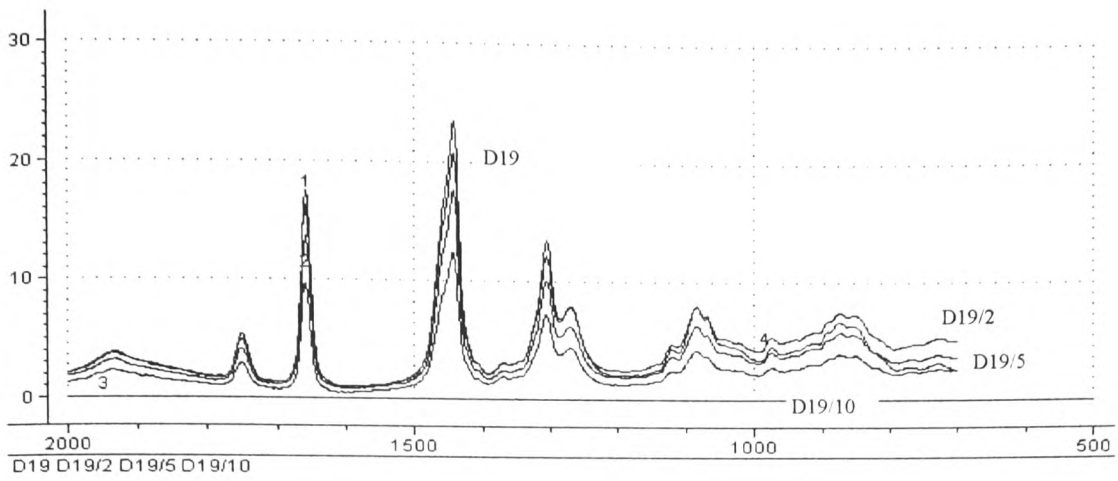


**Figure A37 Raman spectra of sample D19 and its adulterated mixtures of sunflower oil**

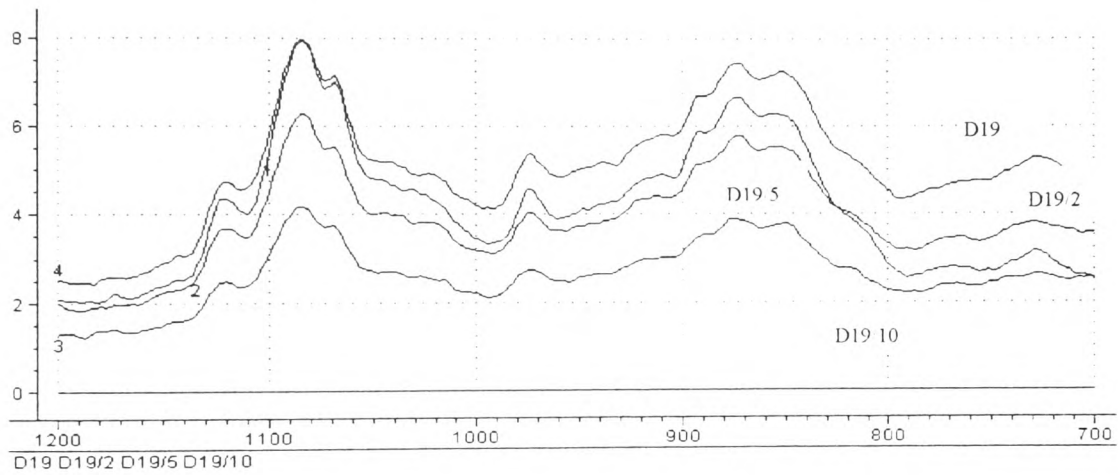


**Figure A38 Raman fingerprint spectra of sample D19 and its adulterated mixtures of sunflower oil**

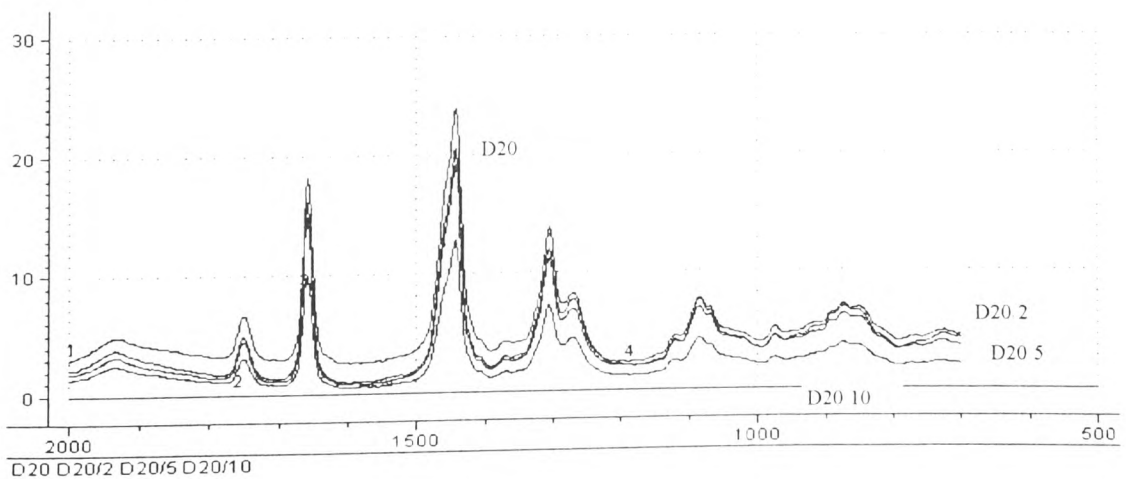


**Figure A39 Raman spectra of sample D20 and its adulterated mixtures of sunflower oil**

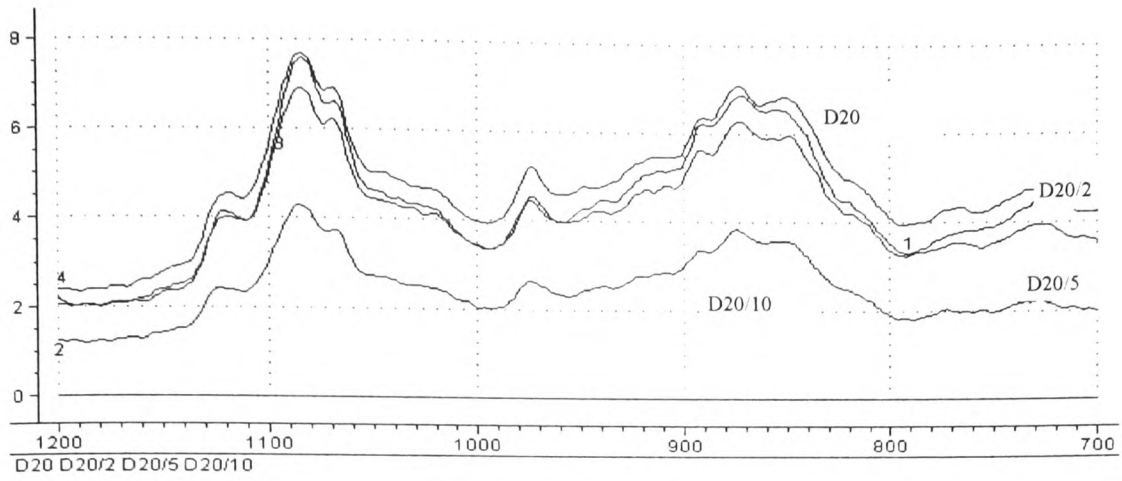


**Figure A40 Raman fingerprint spectra of sample D20 and its adulterated mixtures of sunflower oil**

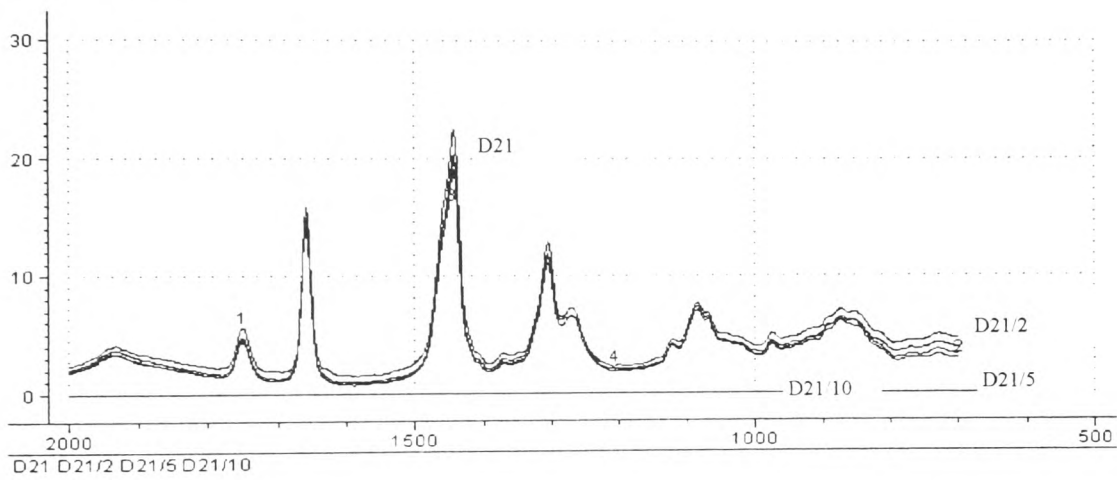


**Figure A41 Raman spectra of sample D21 and its adulterated mixtures of sunflower oil**

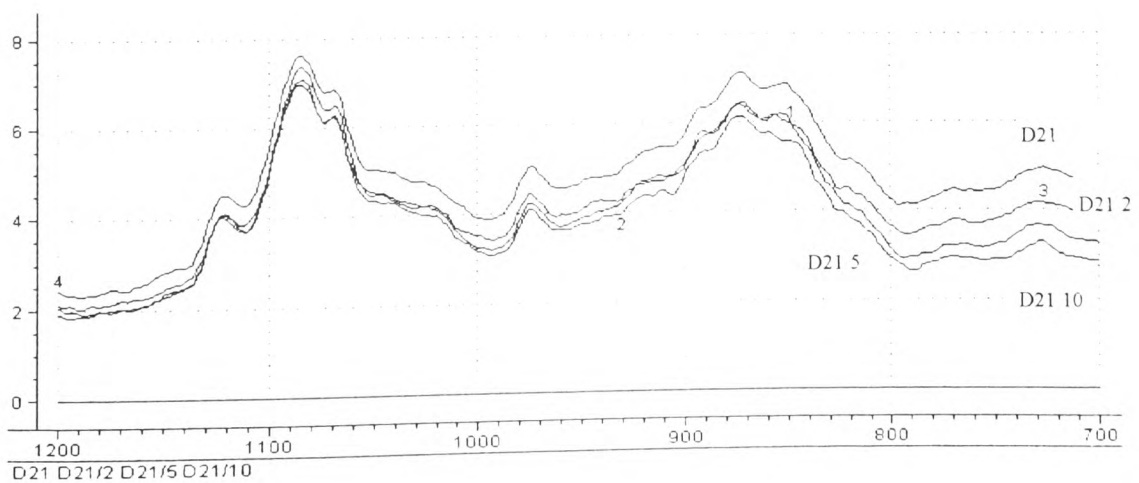


**Figure A42 Raman fingerprint spectra of sample D21 and its adulterated mixtures of sunflower oil**

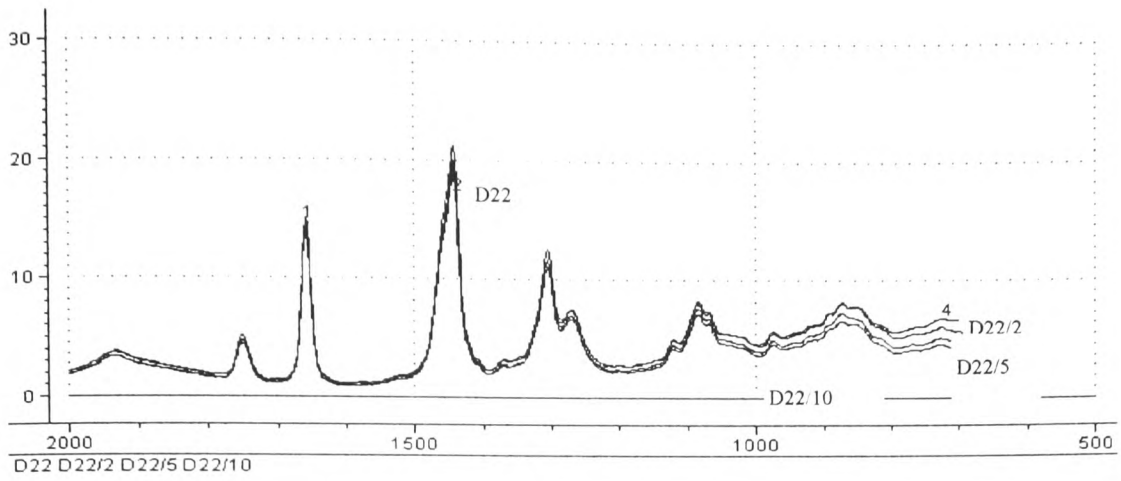


**Figure A43 Raman spectra of sample D22 and its adulterated mixtures of sunflower oil**

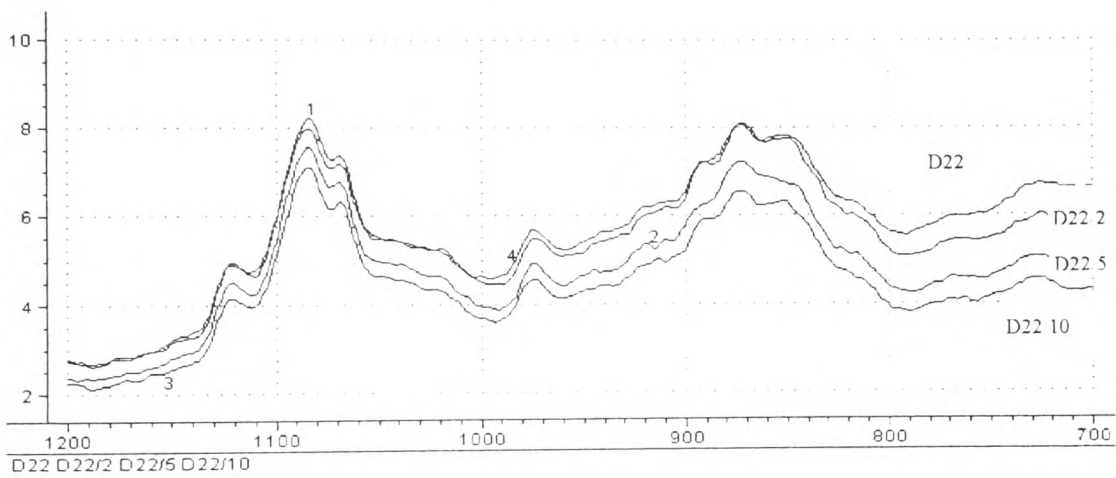
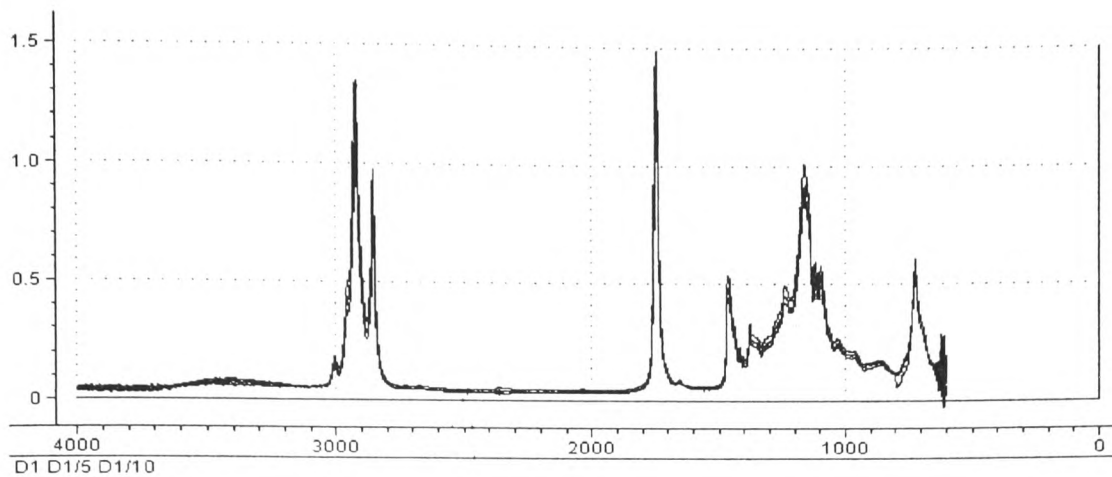


**Figure A44 Raman fingerprint spectra of sample D22 and its adulterated mixtures of sunflower oil**

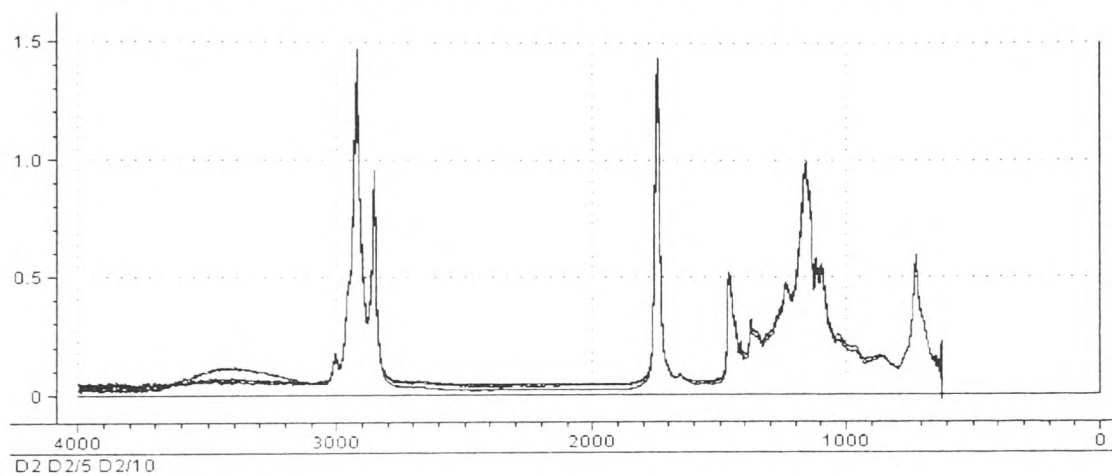
## APPENDIX B

Figure B1 Mid - infrared spectra of sample D1 and its adulterated mixtures.....	B1
Figure B2 Mid - infrared spectra of sample D2 and its adulterated mixtures.....	B1
Figure B3 Mid - infrared spectra of sample D3 and its adulterated mixtures.....	B1
Figure B4 Mid - infrared spectra of sample D4 and its adulterated mixtures.....	B2
Figure B5 Mid - infrared spectra of sample D5 and its adulterated mixtures.....	B2
Figure B6 Mid - infrared spectra of sample D6 and its adulterated mixtures.....	B2
Figure B7 Mid - infrared spectra of sample D7 and its adulterated mixtures.....	B3
Figure B8 Mid - infrared spectra of sample D8 and its adulterated mixtures.....	B3
Figure B9 Mid - infrared spectra of sample D9 and its adulterated mixtures.....	B3
Figure B10 Mid - infrared spectra of sample D10 and its adulterated mixtures.....	B4
Figure B11 Mid - infrared spectra of sample D11 and its adulterated mixtures.....	B4
Figure B12 Mid - infrared spectra of sample D12 and its adulterated mixtures.....	B4
Figure B13 Mid - infrared spectra of sample D13 and its adulterated mixtures.....	B5
Figure B14 Mid - infrared spectra of sample D14 and its adulterated mixtures.....	B5
Figure B15 Mid - infrared spectra of sample D15 and its adulterated mixtures.....	B5
Figure B16 Mid - infrared spectra of sample D16 and its adulterated mixtures.....	B6

Figure B17 Mid - infrared spectra of sample D17 and its adulterated mixtures.....	B6
Figure B18 Mid - infrared spectra of sample D18 and its adulterated mixtures.....	B6
Figure B19 Mid - infrared spectra of sample D19 and its adulterated mixtures.....	B7
Figure B20 Mid - infrared spectra of sample D20 and its adulterated mixtures.....	B7
Figure B21 Mid - infrared spectra of sample D21 and its adulterated mixtures.....	B7
Figure B22 Mid - infrared spectra of sample D22 and its adulterated mixtures.....	B8



**Figure B1** Mid - infrared spectra of sample D1 and its adulterated mixtures



**Figure B2** Mid - infrared spectra of sample D2 and its adulterated mixtures

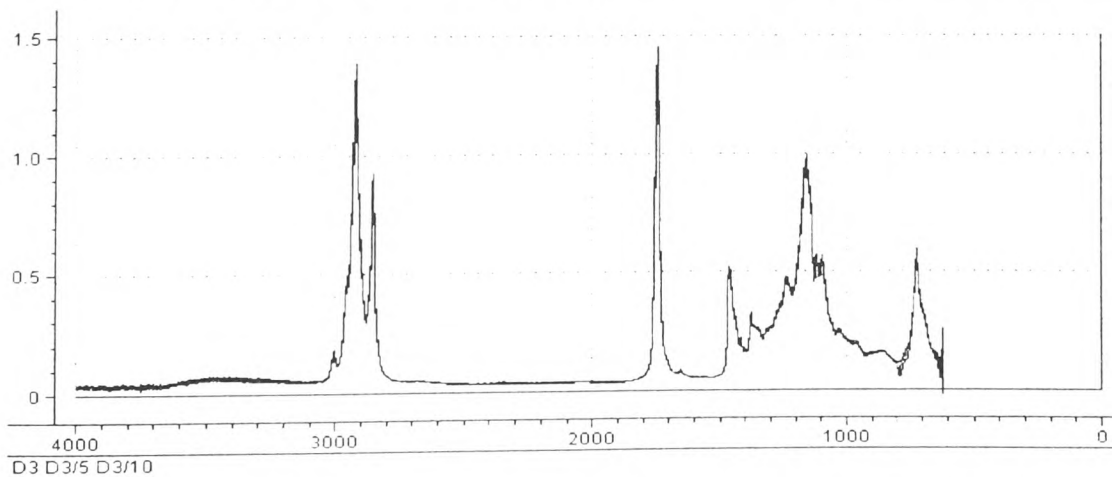


**Figure B3** Mid - infrared spectra of sample D3 and its adulterated mixtures

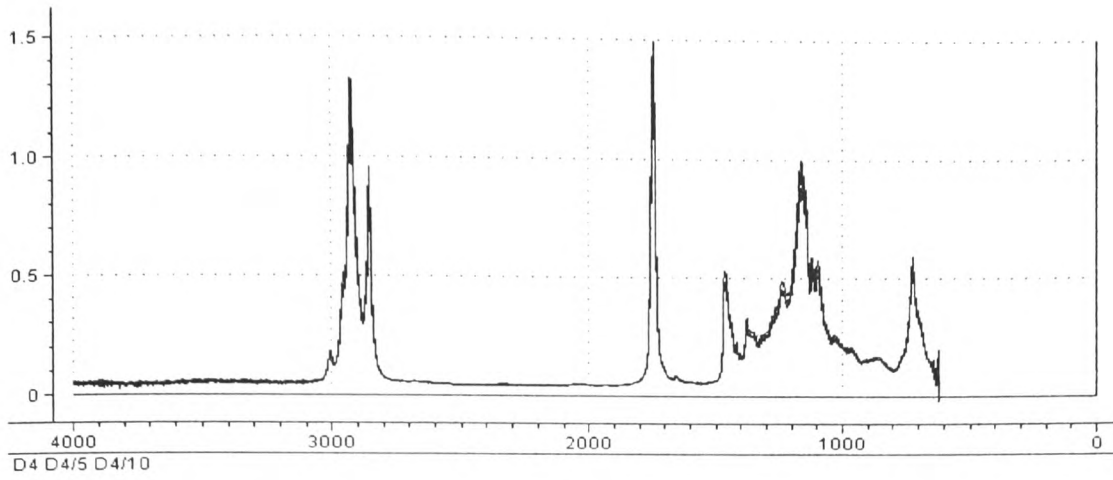


**Figure B4 Mid - infrared spectra of sample D4 and its adulterated mixtures**

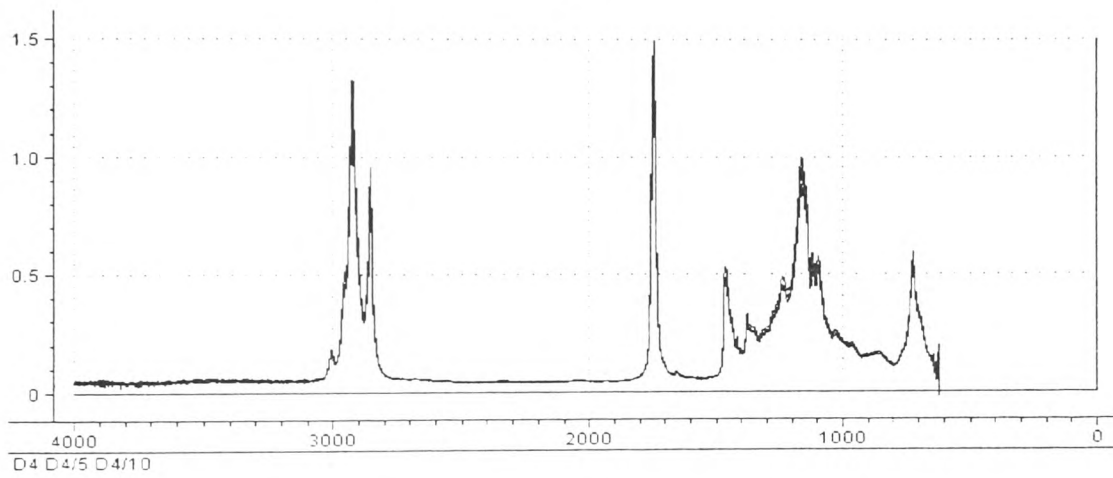


**Figure B5 Mid - infrared spectra of sample D5 and its adulterated mixtures**

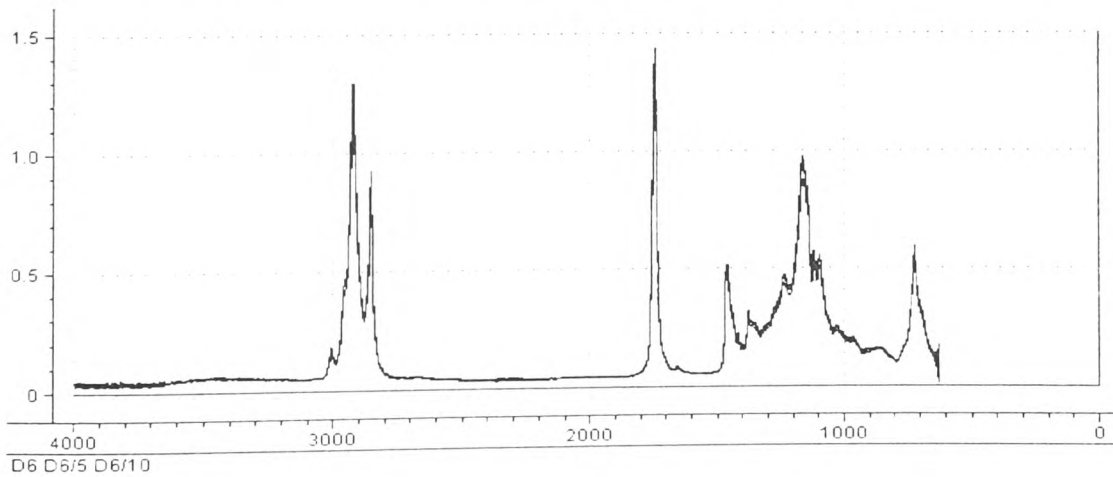


**Figure B6 Mid - infrared spectra of sample D6 and its adulterated mixtures**

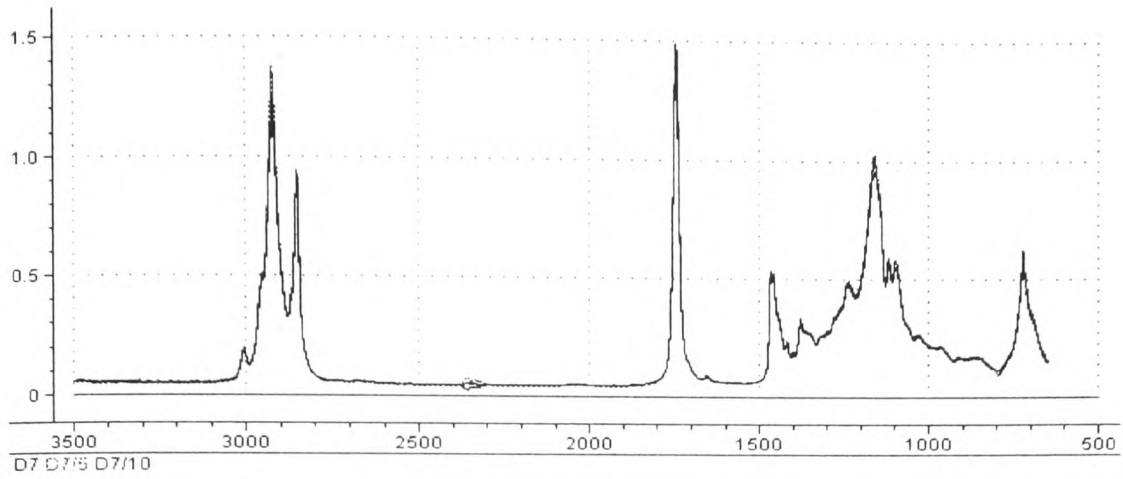


**Figure B7** Mid - infrared spectra of sample D7 and its adulterated mixtures

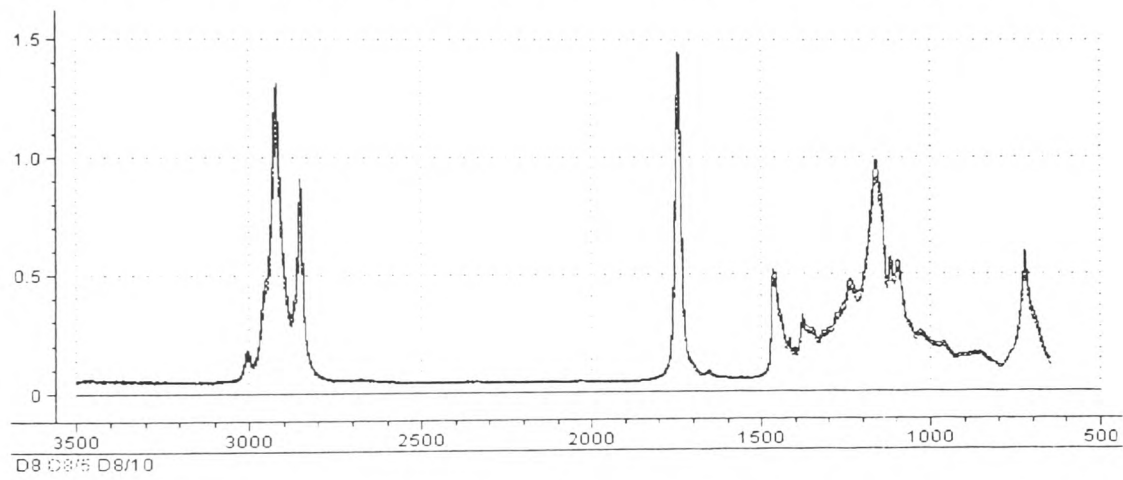


**Figure B8** Mid - infrared spectra of sample D8 and its adulterated mixtures

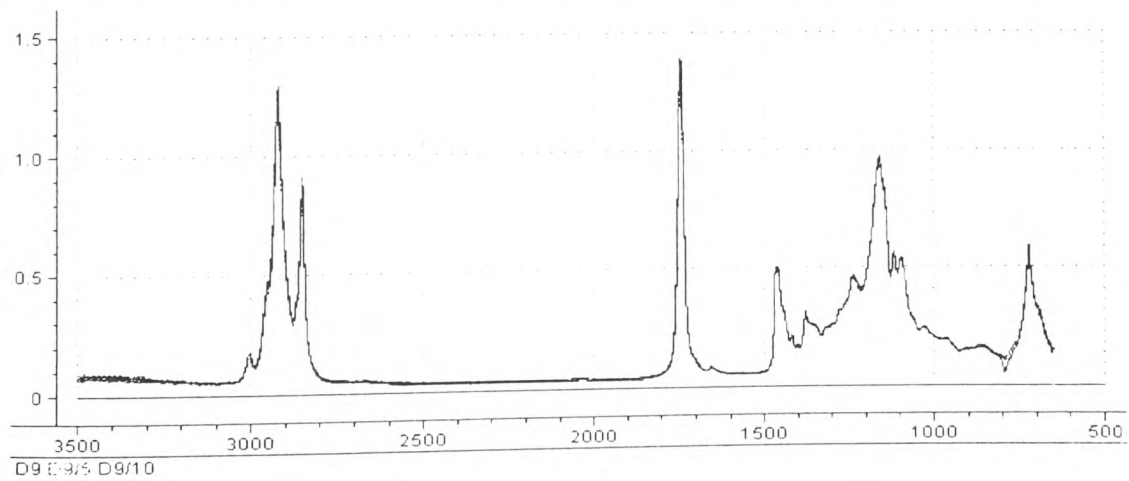


**Figure B9** Mid - infrared spectra of sample D9 and its adulterated mixtures



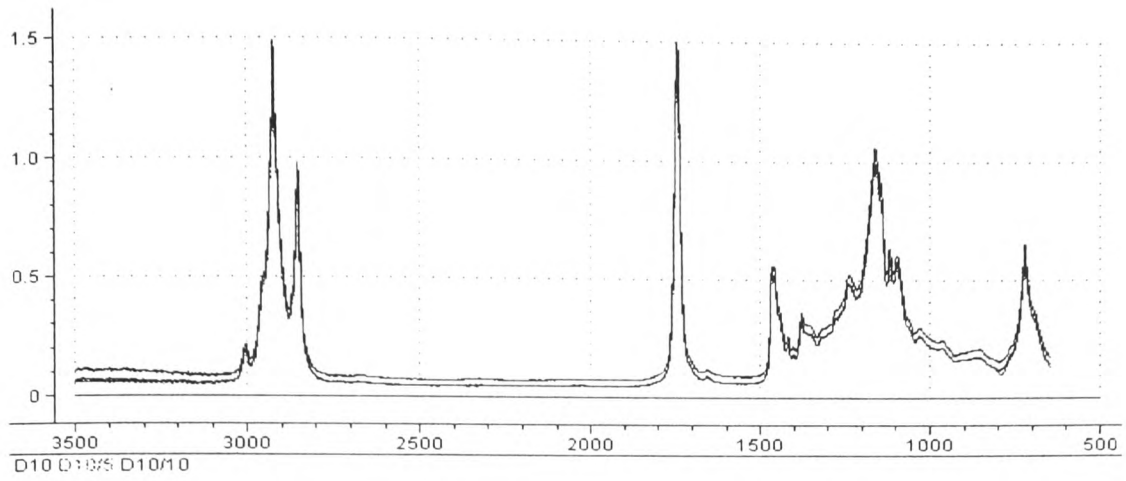


**Figure B10 Mid - infrared spectra of sample D10 and its adulterated mixtures**

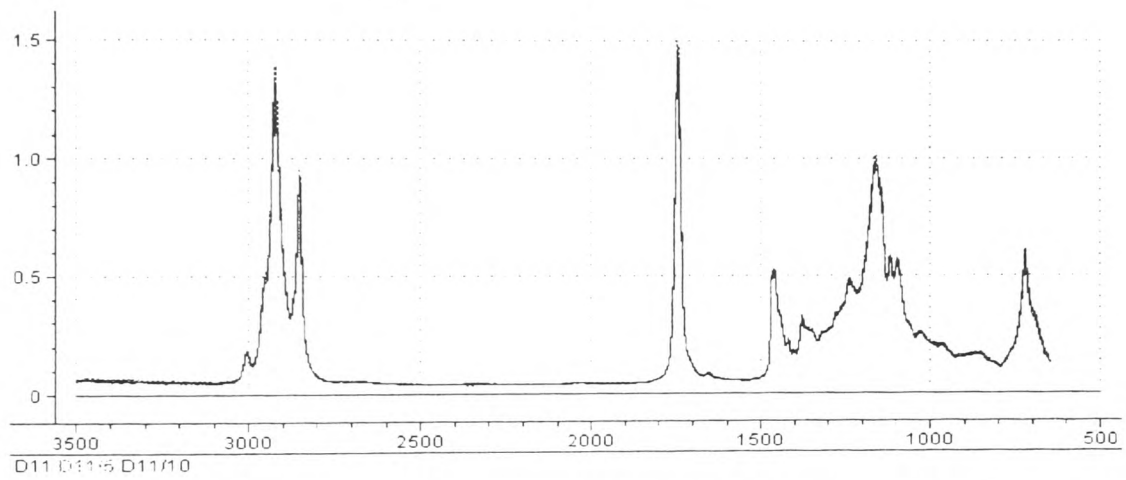


**Figure B11 Mid - infrared spectra of sample D11 and its adulterated mixtures**

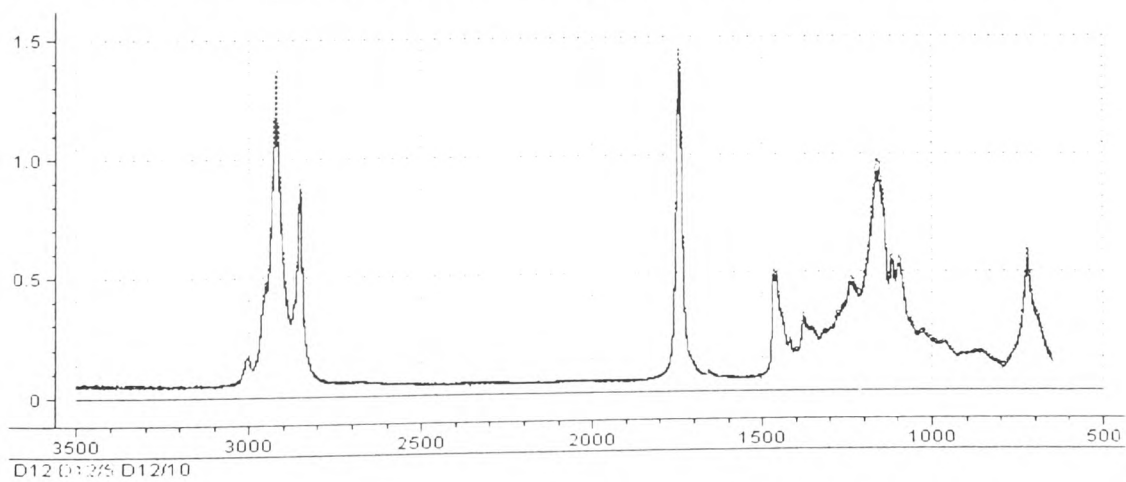


**Figure B12 Mid - infrared spectra of sample D12 and its adulterated mixtures**

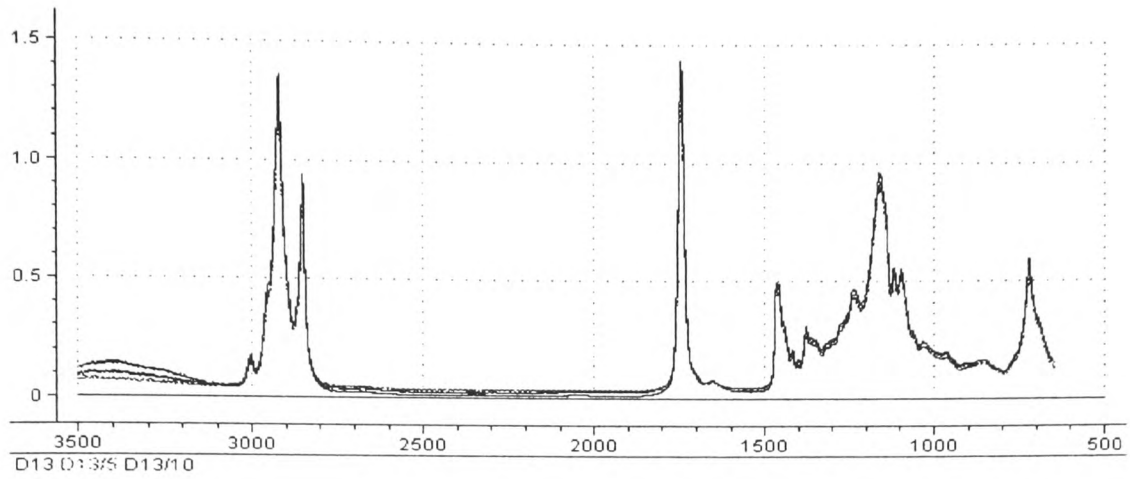


**Figure B13 Mid - infrared spectra of sample D13 and its adulterated mixtures**

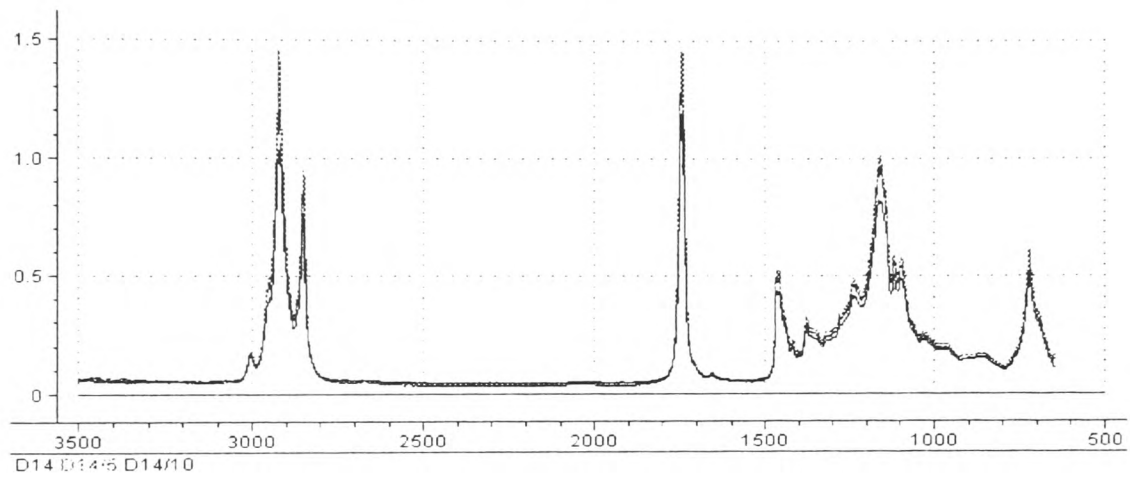


**Figure B14 Mid - infrared spectra of sample D14 and its adulterated mixtures**

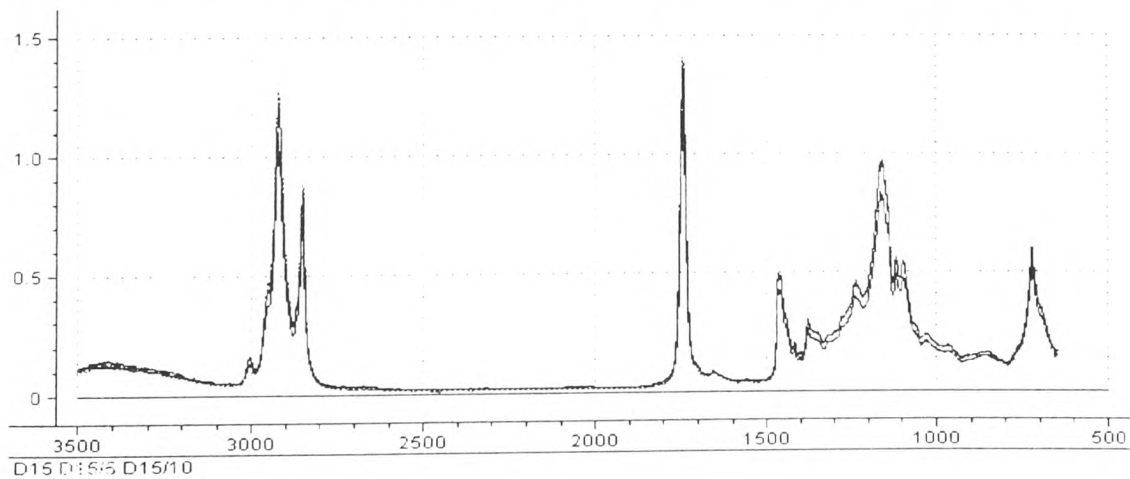


**Figure B15 Mid - infrared spectra of sample D15 and its adulterated mixtures**

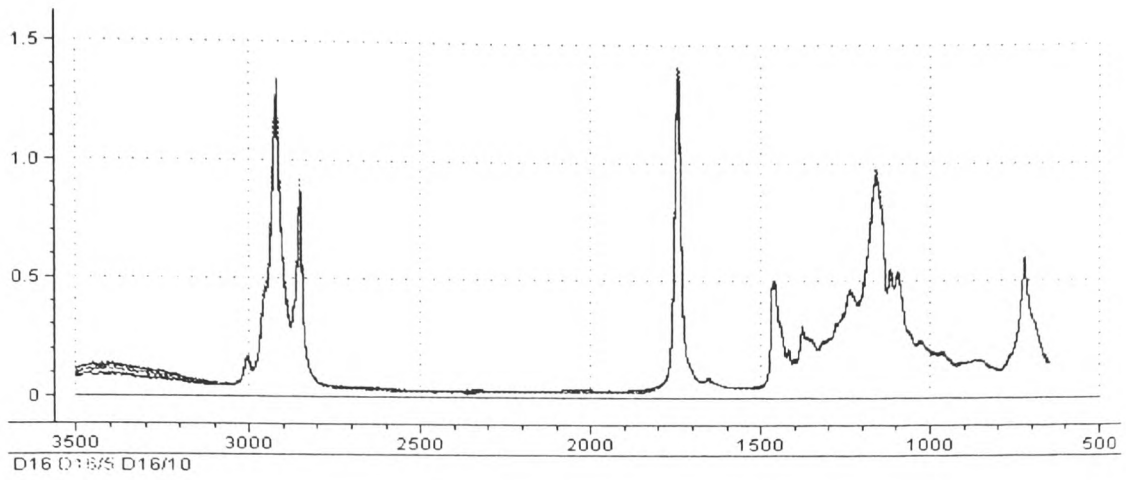


**Figure B16 Mid - infrared spectra of sample D16 and its adulterated mixtures**

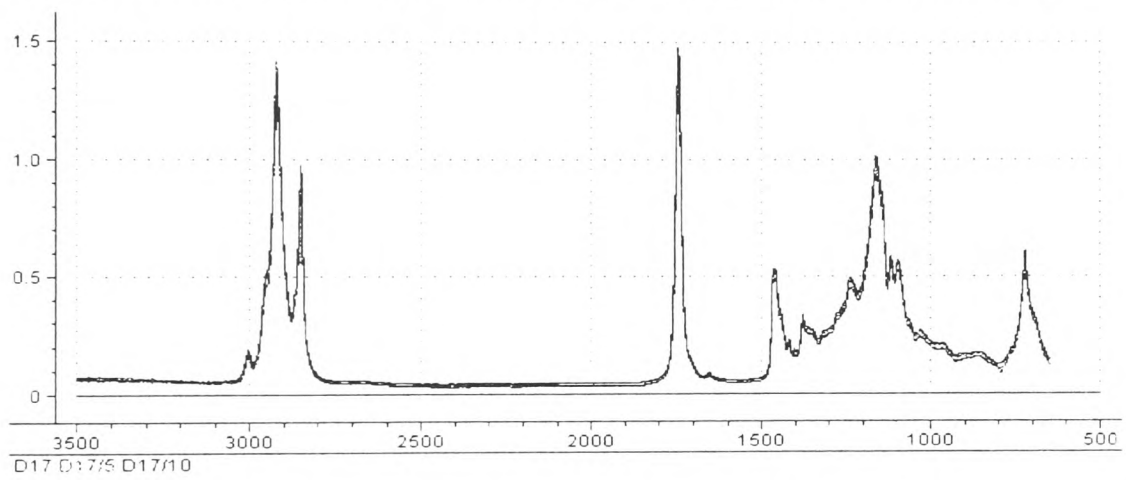


**Figure B17 Mid - infrared spectra of sample D17 and its adulterated mixtures**

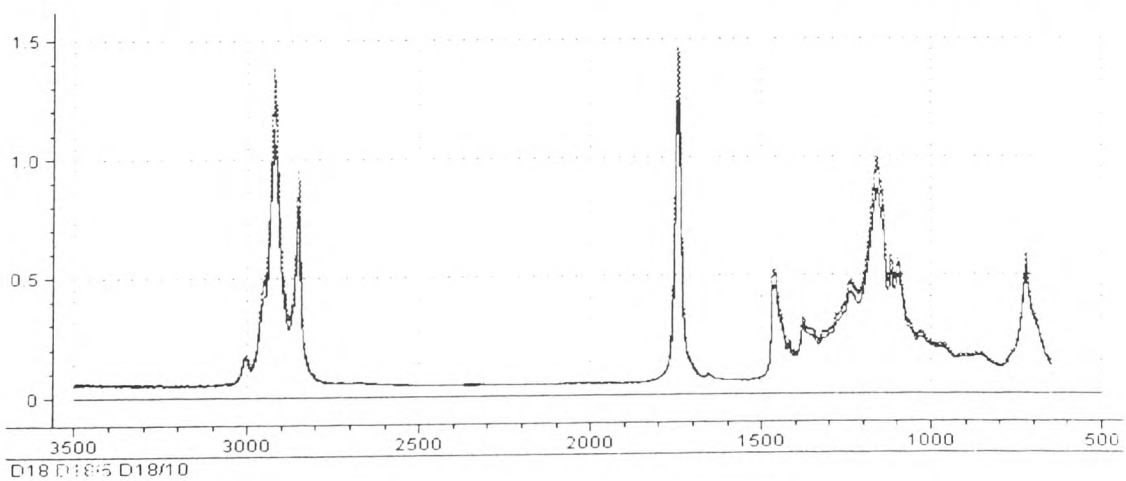


**Figure B18 Mid - infrared spectra of sample D18 and its adulterated mixtures**

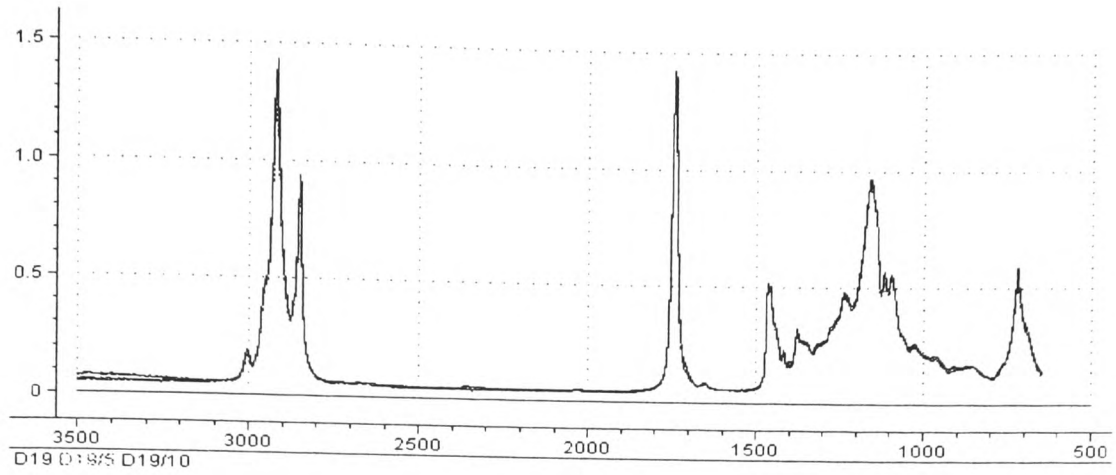


**Figure B19 Mid - infrared spectra of sample D19 and its adulterated mixtures**

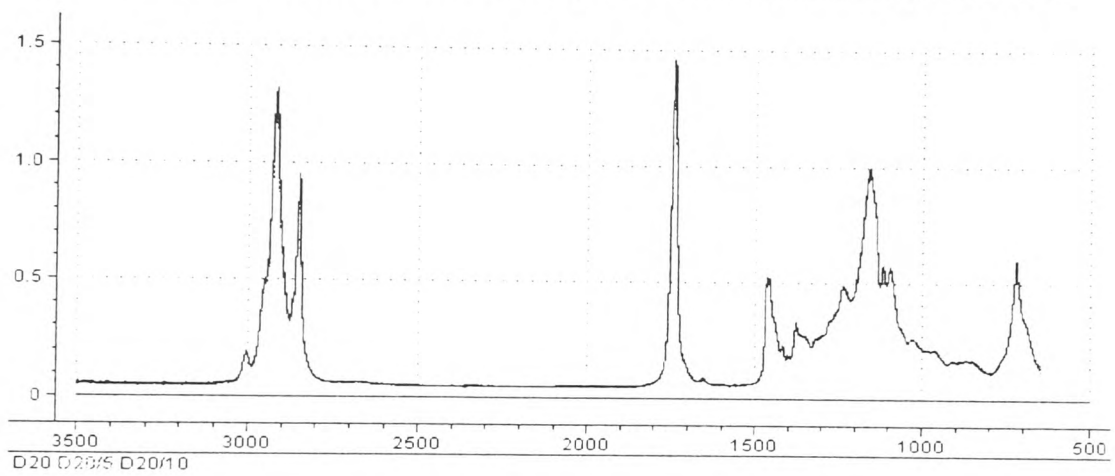


**Figure B20 Mid - infrared spectra of sample D20 and its adulterated mixtures**

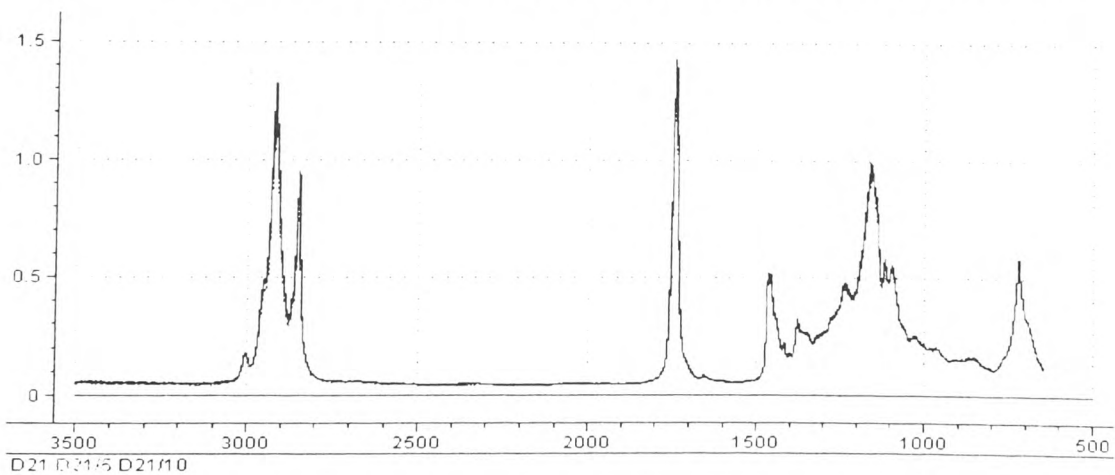


**Figure B21 Mid - infrared spectra of sample D21 and its adulterated mixtures**

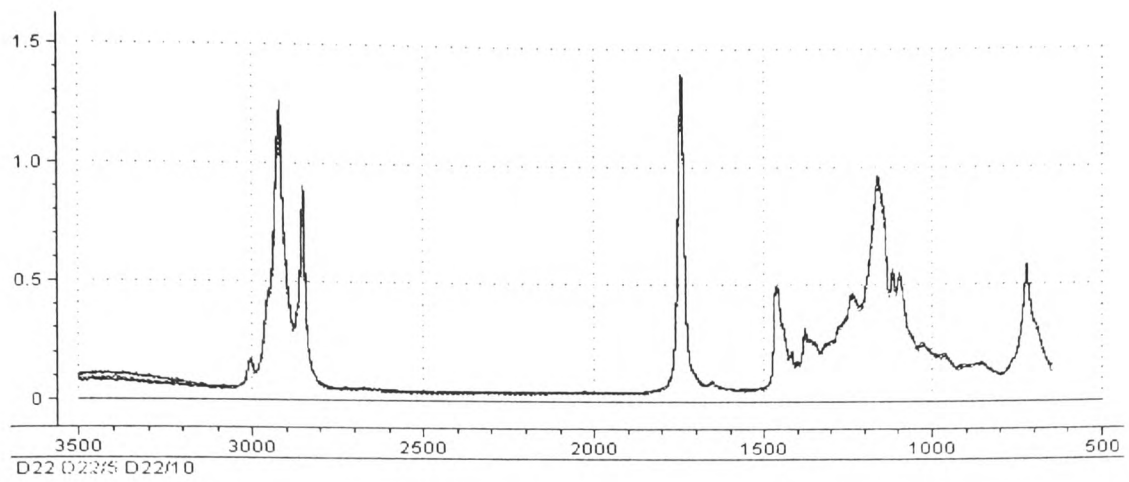


**Figure B22** Mid - infrared spectra of sample D22 and its adulterated mixtures

## APPENDIX C

Figure C1 Full $^{13}\text{C}$ NMR spectrum of sample D1.....	C1
Figure C2 Full $^{13}\text{C}$ NMR spectrum of sample D1 adulterated with 5 % w/w sunflower oil .. .....	C1
Figure C3 Full $^{13}\text{C}$ NMR spectrum of sample D1 adulterated with 10 % w/w sunflower oil .....	C1
Figure C4 Full $^{13}\text{C}$ NMR spectrum of sample D2.....	C2
Figure C5 Full $^{13}\text{C}$ NMR spectrum of sample D2 adulterated with 5 % w/w sunflower oil .. .....	C2
Figure C6 Full $^{13}\text{C}$ NMR spectrum of sample D2 adulterated with 10% w/w sunflower oil .....	C2
Figure C7 Full $^{13}\text{C}$ NMR spectrum of sample D3.....	C3
Figure C8 Full $^{13}\text{C}$ NMR spectrum of sample D3 adulterated with 5 % w/w sunflower oil .. .....	C3
Figure C9 Full $^{13}\text{C}$ NMR spectrum of sample D3 adulterated with 10% w/w sunflower oil .....	C3
Figure C10 Full $^{13}\text{C}$ NMR spectrum of sample D4.....	C4
Figure C11 Full $^{13}\text{C}$ NMR spectrum of sample D4 adulterated with 5 % w/w sunflower oil .....	C4

Figure C13 Full $^{13}\text{C}$ NMR spectrum of sample D5.....	C5
Figure C14 Full $^{13}\text{C}$ NMR spectrum of sample D5 adulterated with 5 % w/w sunflower oil .....	C5
Figure C15 Full $^{13}\text{C}$ NMR spectrum of sample D5 adulterated with 10 % w/w sunflower oil .....	C5
Figure C16 Full $^{13}\text{C}$ NMR spectrum of sample D6.....	C6
Figure C17 Full $^{13}\text{C}$ NMR spectrum of sample D6 adulterated with 5% w/w sunflower oil .....	C6
Figure C18 Full $^{13}\text{C}$ NMR spectrum of sample D6 adulterated with 10 % w/w sunflower oil .....	C6
Figure C19 Full $^{13}\text{C}$ NMR spectrum of sample D7.....	C7
Figure C20 Full $^{13}\text{C}$ NMR spectrum of sample D8.....	C7
Figure C21 Full $^{13}\text{C}$ NMR spectrum of sample D8 adulterated with 5% w/w sunflower oil .....	C7
Figure C22 Full $^{13}\text{C}$ NMR spectrum of sample D8 adulterated with 10% w/w sunflower oil .....	C8
Figure C23 Full $^{13}\text{C}$ NMR spectrum of sample D9.....	C8
Figure C24 Full $^{13}\text{C}$ NMR spectrum of sample D9 adulterated with 5% w/w sunflower oil .....	C8

Figure C25 Full $^{13}\text{C}$ NMR spectrum of sample D9 adulterated with 10% w/w sunflower oil .....	C9
Figure C26 Full $^{13}\text{C}$ NMR spectrum of sample D10.....	C9
Figure C27 Full $^{13}\text{C}$ NMR spectrum of sample D10 adulterated with 5% w/w sunflower oil .....	C9
Figure C28 Full $^{13}\text{C}$ NMR spectrum of sample D10 adulterated with 10% w/w sunflower oil .....	C10
Figure C29 Full $^{13}\text{C}$ NMR spectrum of sample D11.....	C10
Figure C30 Full $^{13}\text{C}$ NMR spectrum of sample D11 adulterated with 5% w/w sunflower oil .....	C10
Figure C31 Full $^{13}\text{C}$ NMR spectrum of sample D11 adulterated with 10% w/w sunflower oil .....	C11
Figure C32 Full $^{13}\text{C}$ spectrum NMR of sample D12.....	C11
Figure C33 Full $^{13}\text{C}$ spectrum NMR of sample D12 adulterated with 5 % w/w sunflower oil .....	C11
Figure C34 Full $^{13}\text{C}$ spectrum NMR of sample D12 adulterated with 10 % w/w sunflower oil .....	C12
Figure C35 Full $^{13}\text{C}$ spectrum NMR of sample D13.....	C12



Figure C36 Full $^{13}\text{C}$ spectrum NMR of sample D13 adulterated with 5 % w/w sunflower oil .....	C12
Figure C37 Full $^{13}\text{C}$ spectrum NMR of sample D13 adulterated with 10 % w/w sunflower oil .....	C13
Figure C38 Full $^{13}\text{C}$ spectrum NMR of sample D14.....	C13
Figure C39 Full $^{13}\text{C}$ spectrum NMR of sample D14 adulterated with 5 % w/w sunflower oil .....	C13
Figure C40 Full $^{13}\text{C}$ spectrum NMR of Sample D14 adulterated with 10 % w/w sunflower oil .....	C14
Figure C41 Full $^{13}\text{C}$ spectrum NMR of Sample D15 .....	C14
Figure C42 Full $^{13}\text{C}$ spectrum NMR of Sample D15 adulterated with 5 % w/w sunflower oil .....	C14
Figure C43 Full $^{13}\text{C}$ spectrum NMR of Sample D15 adulterated with 10 % w/w sunflower oil .....	C15
Figure C44 Full $^{13}\text{C}$ spectrum NMR of Sample D16 .....	C15
Figure C45 Full $^{13}\text{C}$ spectrum NMR of sample D16 adulterated with 5 % w/w sunflower oil .....	C15
Figure C46 Full $^{13}\text{C}$ spectrum NMR of sample D16 adulterated with 10% w/w sunflower oil .....	C16

Figure C47 Full $^{13}\text{C}$ spectrum NMR of sample D17 .....	C16
Figure C48 $^{13}\text{C}$ spectrum NMR of Sample D17 adulterated with 5% w/w sunflower oil	C16
Figure C49 Full $^{13}\text{C}$ spectrum NMR of Sample D17 adulterated with 10% w/w sunflower oil .....	C17
Figure C50 Full $^{13}\text{C}$ spectrum NMR of Sample D18 .....	C17
Figure C51 Full $^{13}\text{C}$ spectrum NMR of Sample D18 adulterated with 5% w/w sunflower oil .....	C17
Figure C52 Full $^{13}\text{C}$ spectrum NMR of Sample D18 adulterated with 10% w/w sunflower oil .....	C18
Figure C53 Full $^{13}\text{C}$ spectrum NMR of Sample D19 .....	C18
Figure C54 Full $^{13}\text{C}$ spectrum NMR of Sample D19 adulterated with 5% w/w sunflower oil .....	C18
Figure C55 Full $^{13}\text{C}$ spectrum NMR of Sample D19 adulterated with 10% w/w sunflower oil .....	C19
Figure C56 Full $^{13}\text{C}$ spectrum NMR of Sample D20 .....	C19
Figure C57 Full $^{13}\text{C}$ spectrum NMR of Sample D20 adulterated with 5% w/w sunflower oil .....	C19
Figure C58 Full $^{13}\text{C}$ spectrum NMR of Sample D20 adulterated with 10% w/w sunflower oil .....	C20

Figure C59 Full $^{13}\text{C}$ spectrum NMR of sample D21 .....	C20
Figure C60 Full $^{13}\text{C}$ spectrum NMR of Sample D21 adulterated with 5 % w/w sunflower oil .....	C20
Figure C61 Full $^{13}\text{C}$ spectrum NMR of Sample D21 adulterated with 10 % w/w sunflower oil .....	C21
Figure C62 Full $^{13}\text{C}$ spectrum NMR of Sample D22 .....	C21
Figure C63 Full $^{13}\text{C}$ spectrum NMR of Sample D22 adulterated with 5 % w/w sunflower oil .....	C21
Figure C64 Full $^{13}\text{C}$ spectrum NMR of Sample D22 adulterated with 10% w/w sunflower oil .....	C22

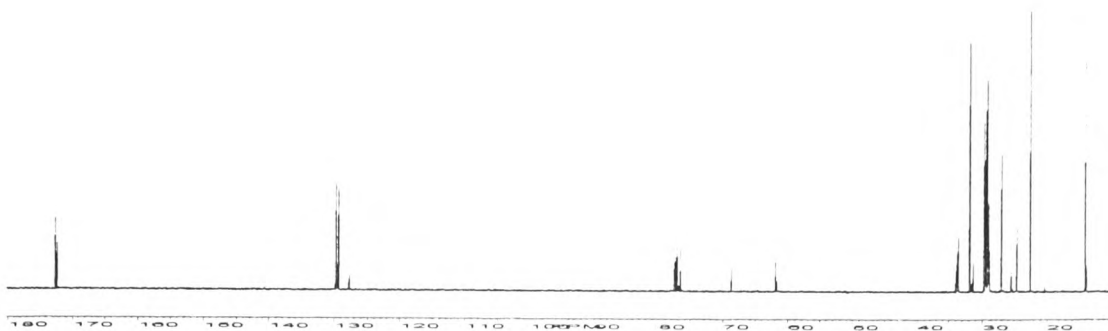


Figure C1 Full <sup>13</sup>C NMR spectrum of sample D1

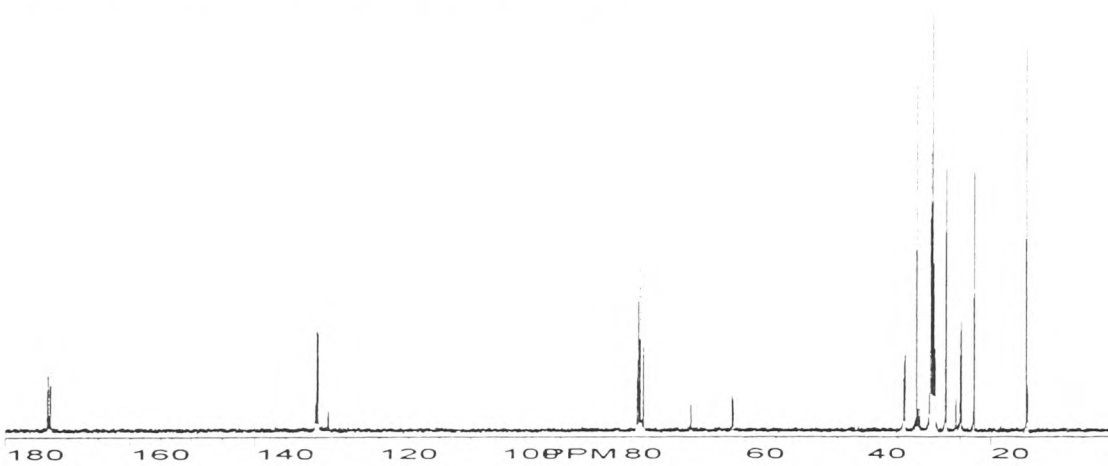


Figure C2 Full <sup>13</sup>C NMR spectrum of sample D1 adulterated with 5 % w/w sunflower oil

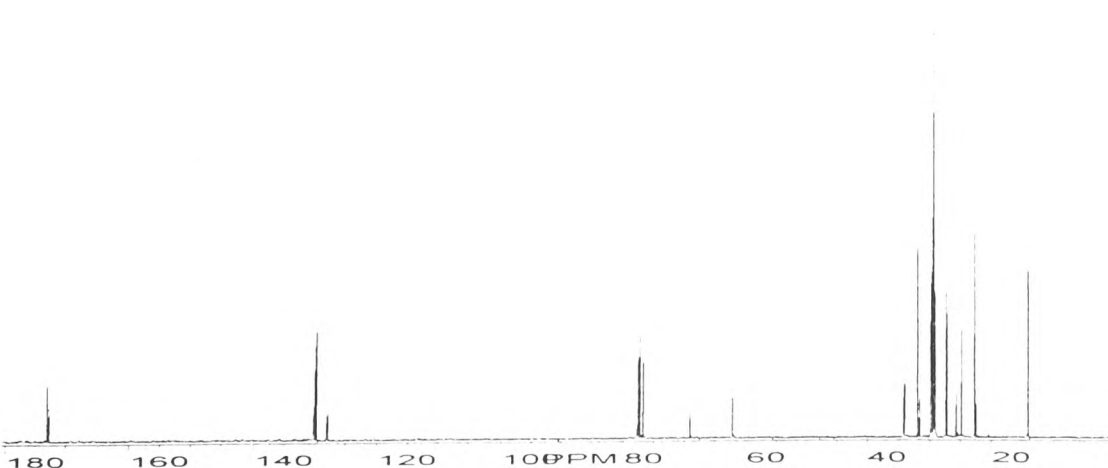


Figure C3 Full <sup>13</sup>C NMR spectrum of sample D1 adulterated with 10 % w/w sunflower oil

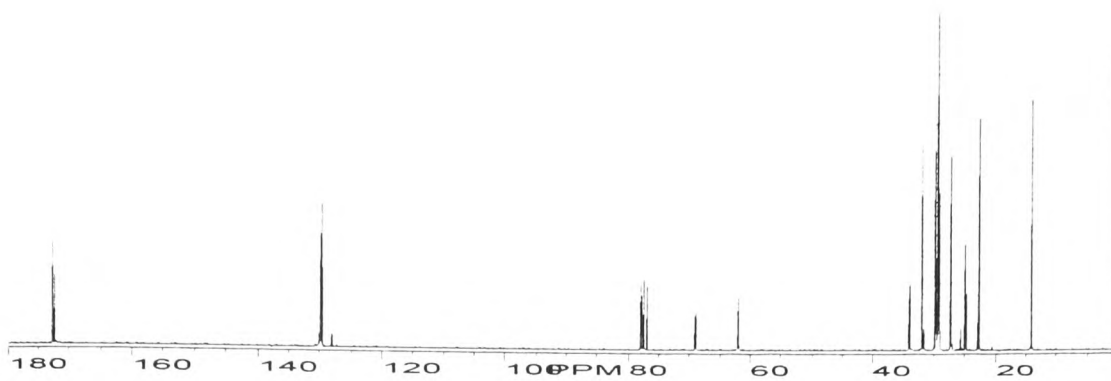


Figure C4 Full <sup>13</sup>C NMR spectrum of sample D2

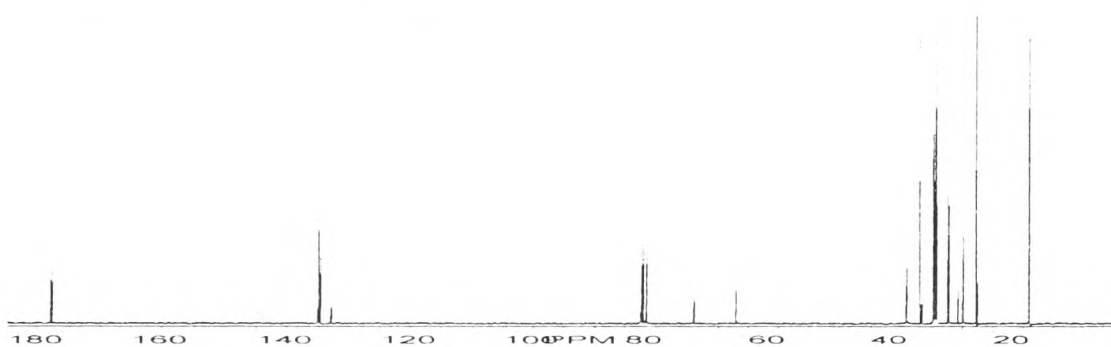


Figure C5 Full <sup>13</sup>C NMR spectrum of sample D2 adulterated with 5 % w/w sunflower oil

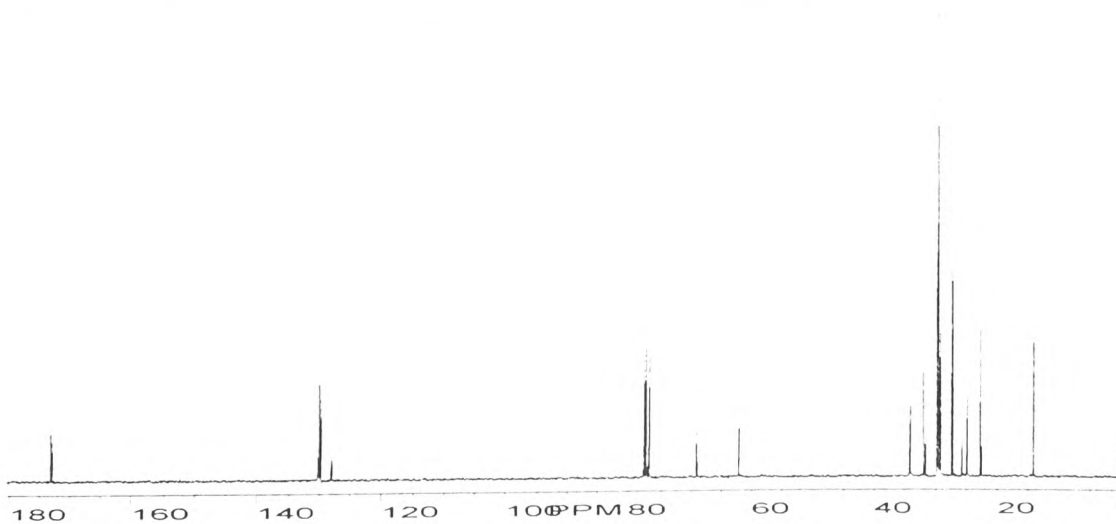


Figure C6 Full <sup>13</sup>C NMR spectrum of sample D2 adulterated with 10 % w/w sunflower oil

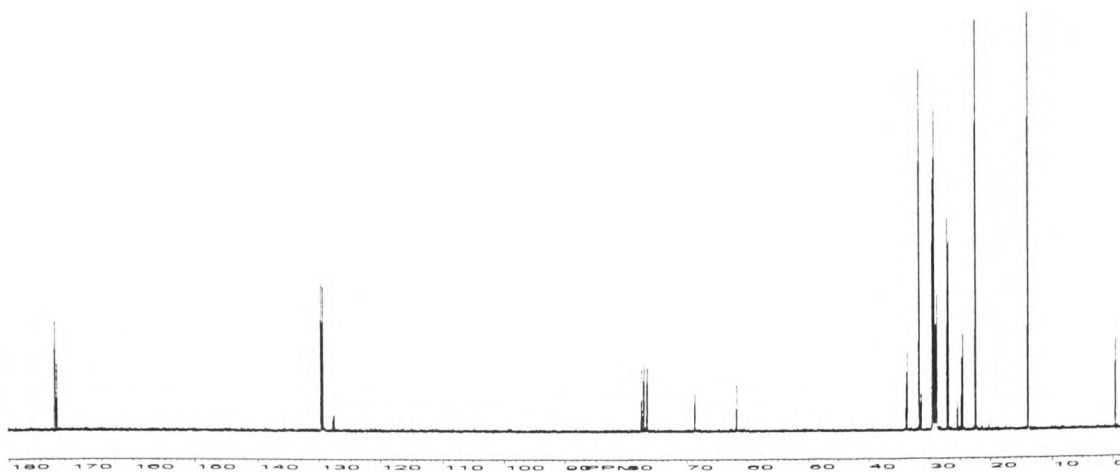


Figure C7 Full <sup>13</sup>C NMR spectrum of sample D3

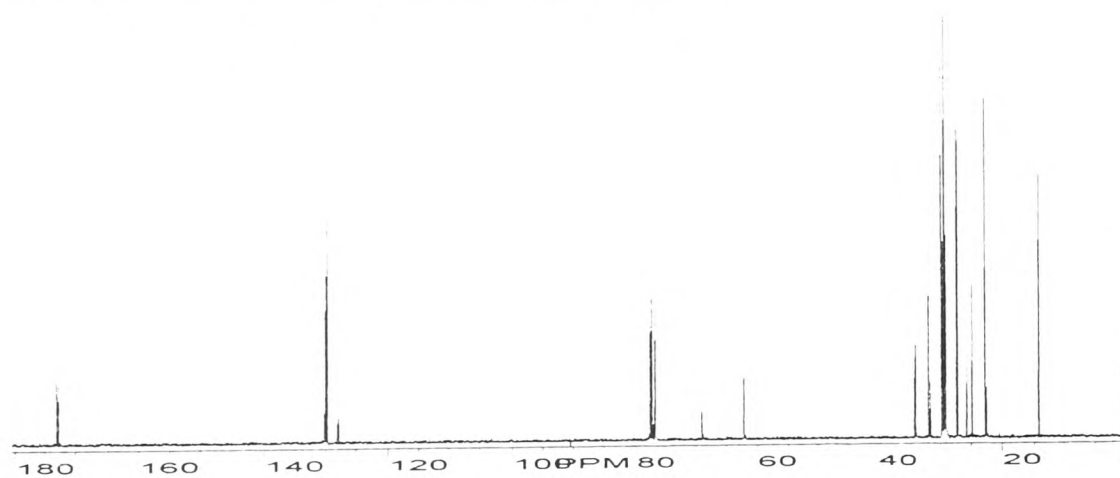


Figure C8 Full <sup>13</sup>C NMR spectrum of sample D3 adulterated with 5 % w/w sunflower oil

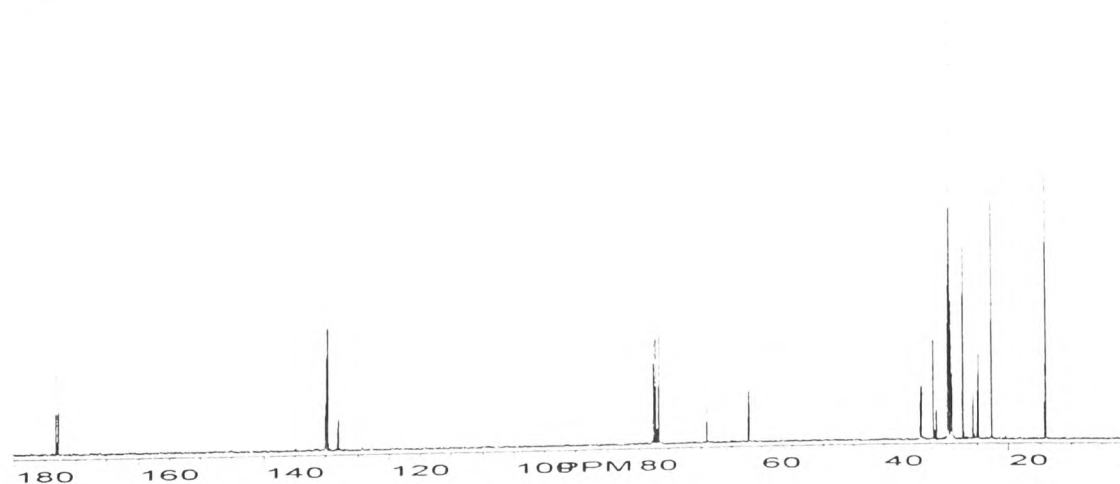


Figure C9 Full <sup>13</sup>C NMR spectrum of sample D3 adulterated with 10 % w/w sunflower oil

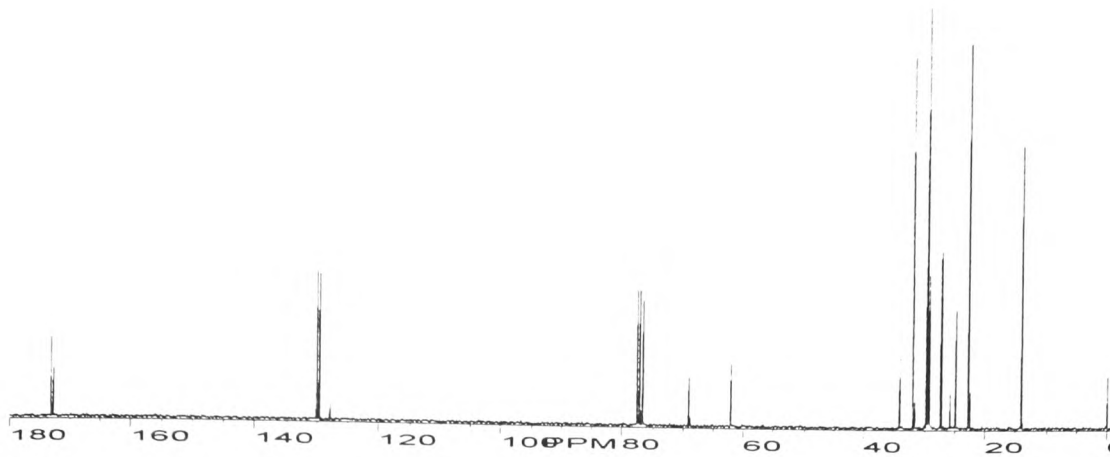


Figure C10 Full  $^{13}\text{C}$  NMR spectrum of sample D4

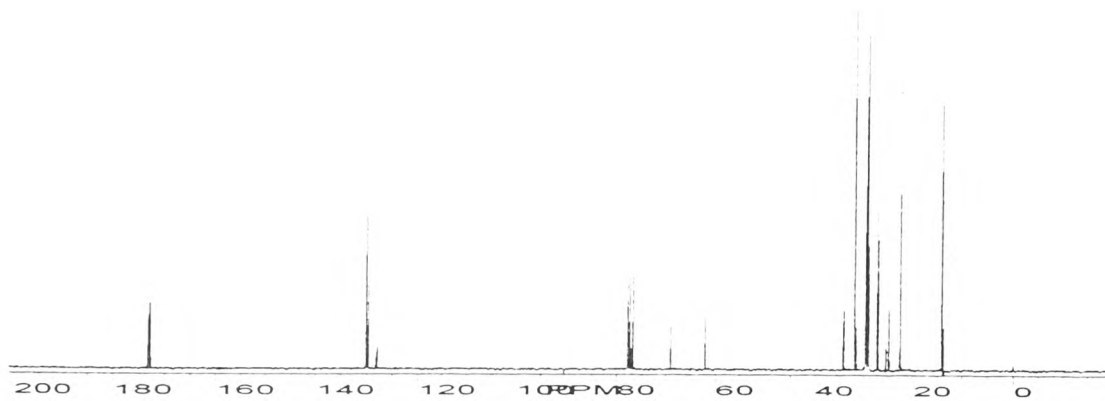


Figure C11 Full  $^{13}\text{C}$  NMR spectrum of sample D4 adulterated with 5 % w/w sunflower oil

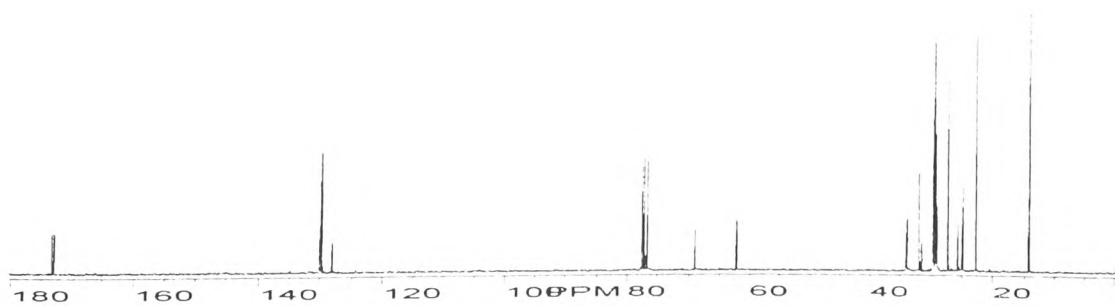


Figure C12 Full  $^{13}\text{C}$  NMR spectrum of sample D4 adulterated with 10 % w/w sunflower oil

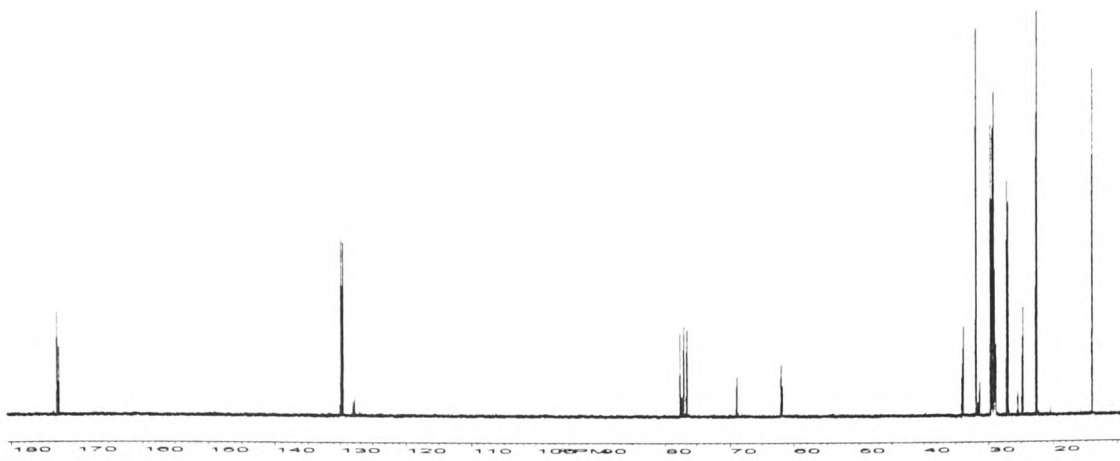


Figure C13 Full <sup>13</sup>C NMR spectrum of sample D5

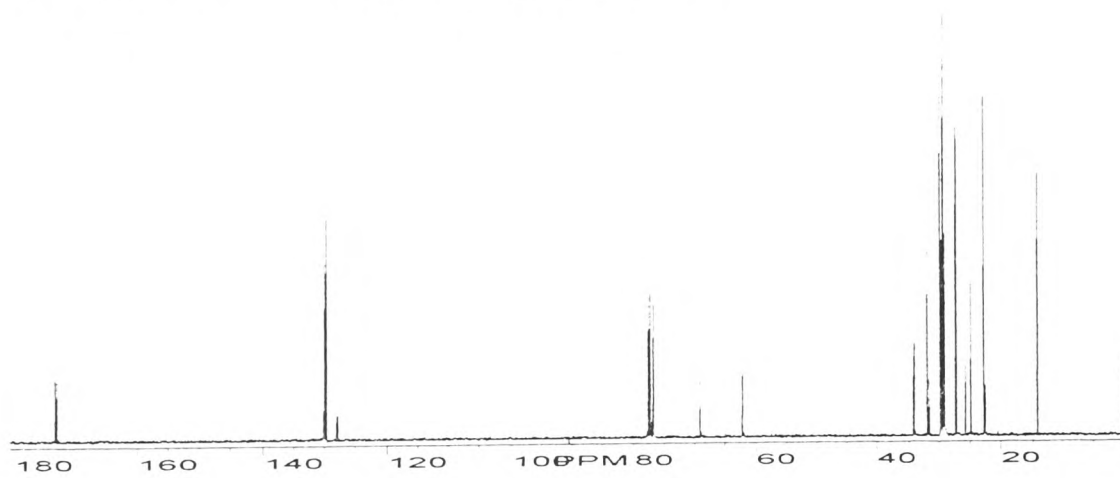


Figure C14 Full <sup>13</sup>C NMR spectrum of sample D5 adulterated with 5 % w/w sunflower oil

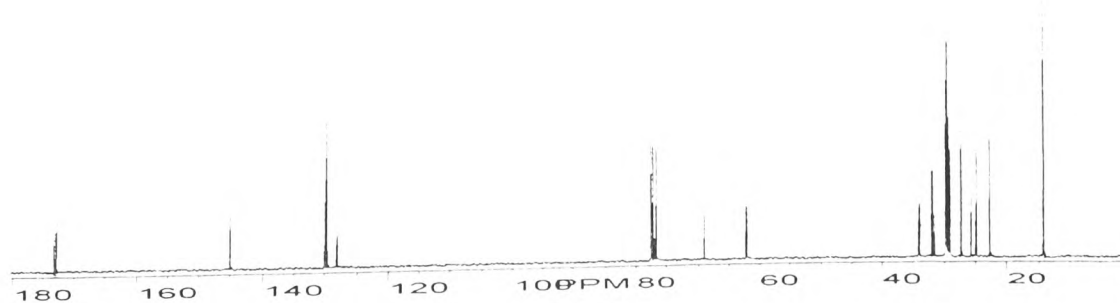


Figure C15 Full <sup>13</sup>C NMR spectrum of sample D5 adulterated with 10 % w/w sunflower oil



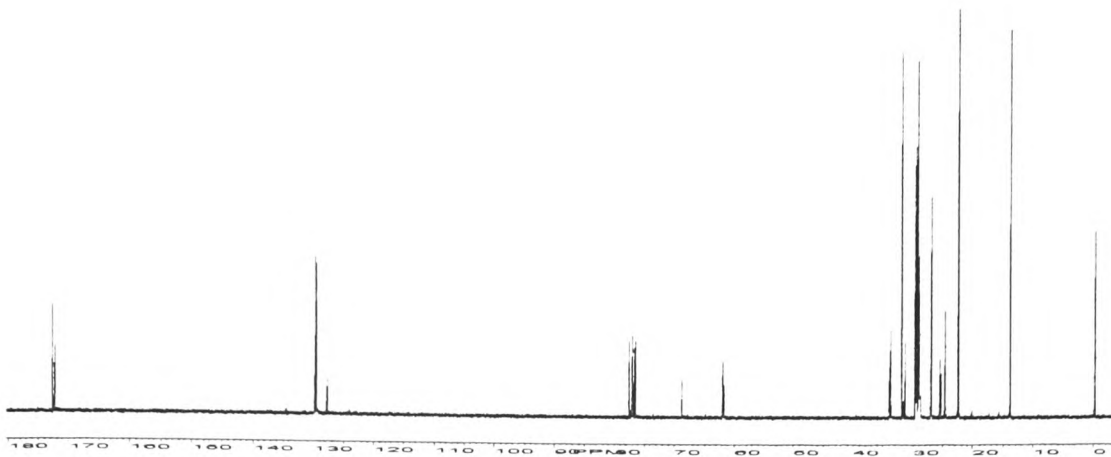


Figure C16 Full <sup>13</sup>C NMR spectrum of sample D6

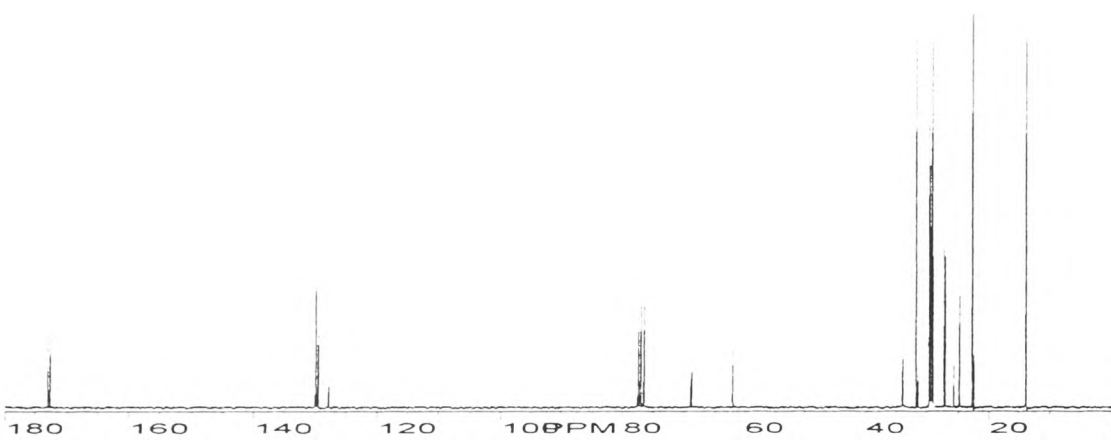


Figure C17 Full <sup>13</sup>C NMR spectrum of sample D6 adulterated with 5 % w/w sunflower oil

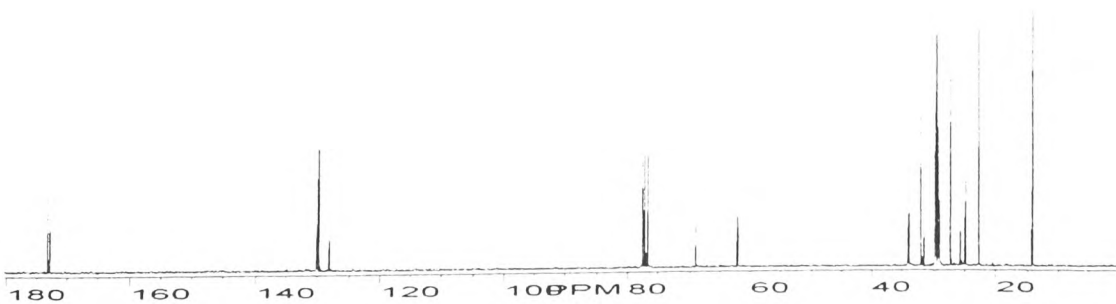


Figure C18 Full <sup>13</sup>C NMR spectrum of sample D6 adulterated with 10 % w/w sunflower oil

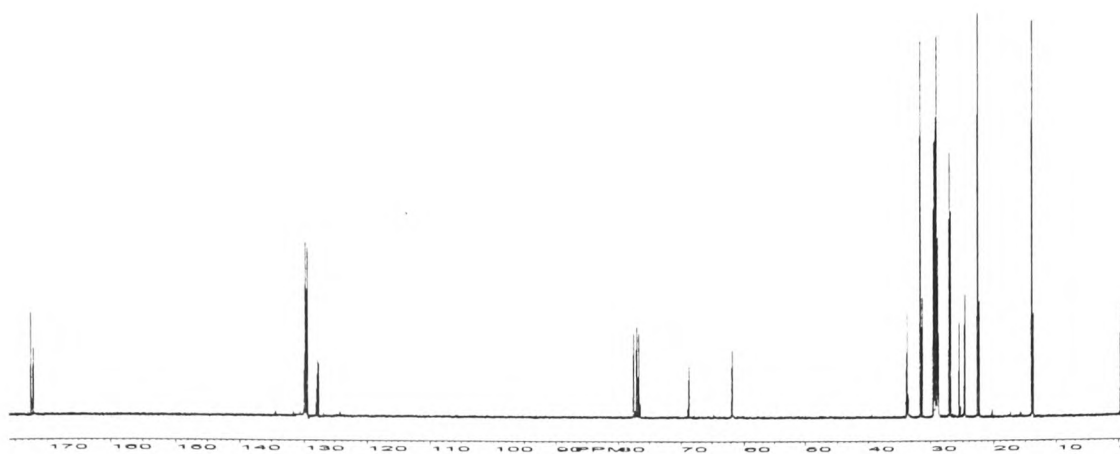


Figure C19 Full <sup>13</sup>C NMR spectrum of sample D7

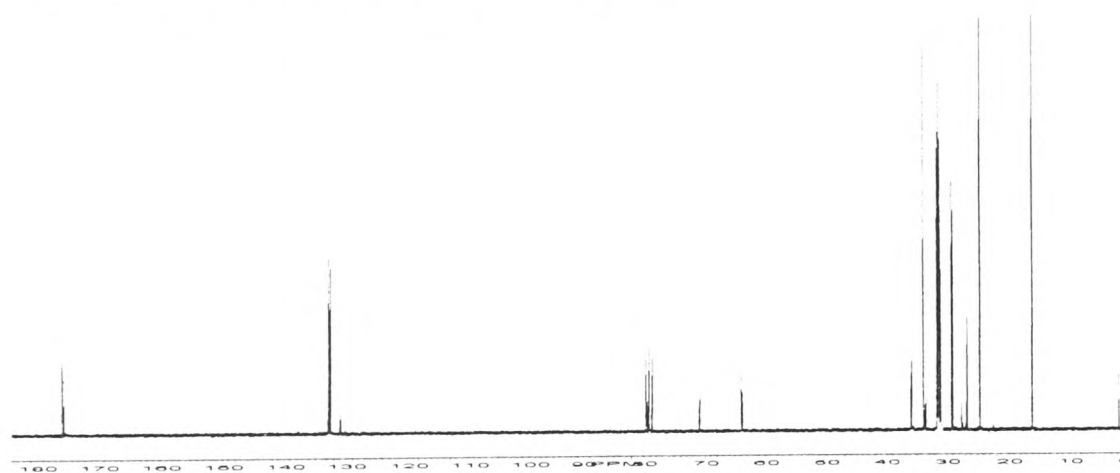


Figure C20 Full <sup>13</sup>C NMR spectrum of sample D8

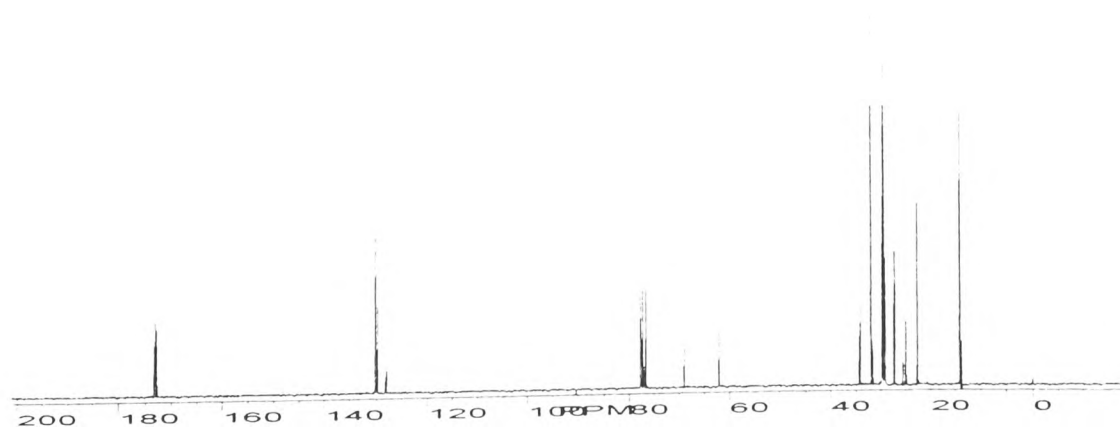


Figure C21 Full <sup>13</sup>C NMR spectrum of sample D8 adulterated with 5 % w/w sunflower oil

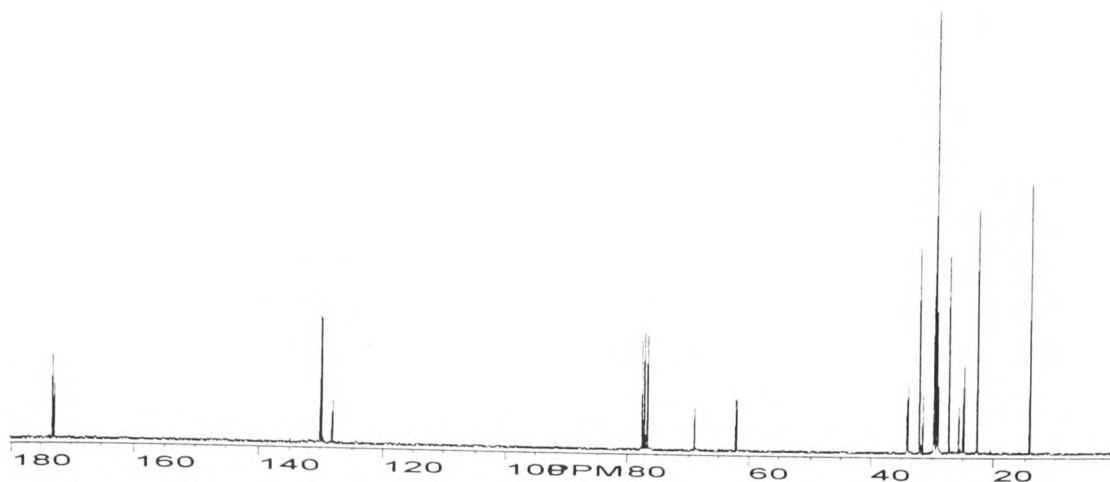


Figure C22 Full  $^{13}\text{C}$  NMR spectrum of sample D8 adulterated with 10 % w/w sunflower oil

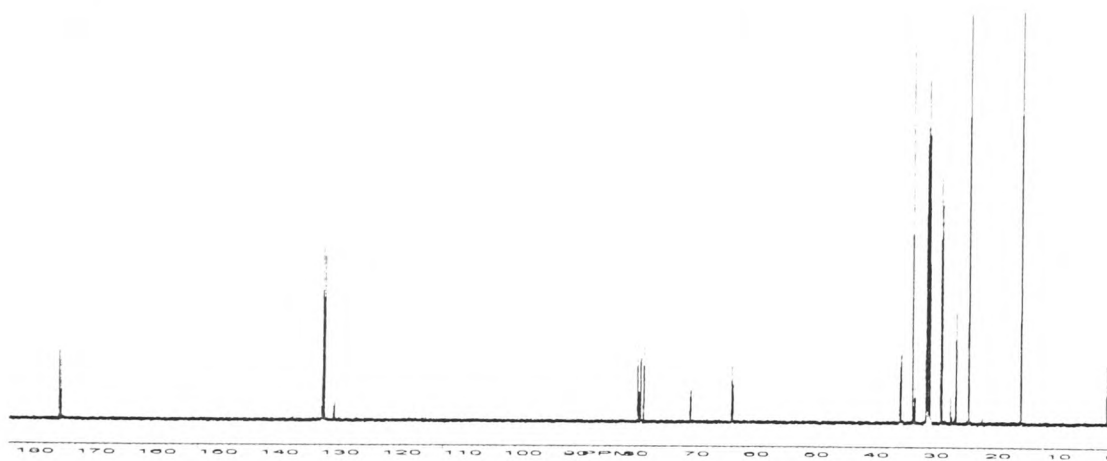


Figure C23 Full  $^{13}\text{C}$  NMR spectrum of sample D9

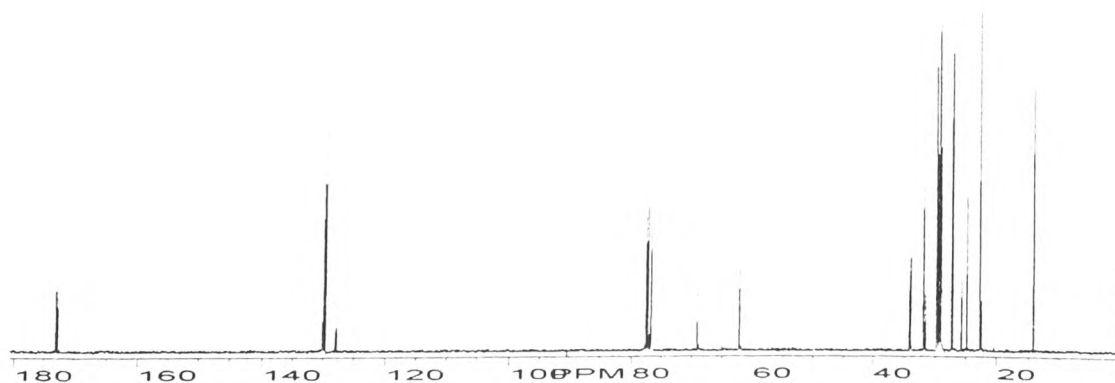


Figure C24 Full  $^{13}\text{C}$  NMR spectrum of sample D9 adulterated with 5 % w/w sunflower oil

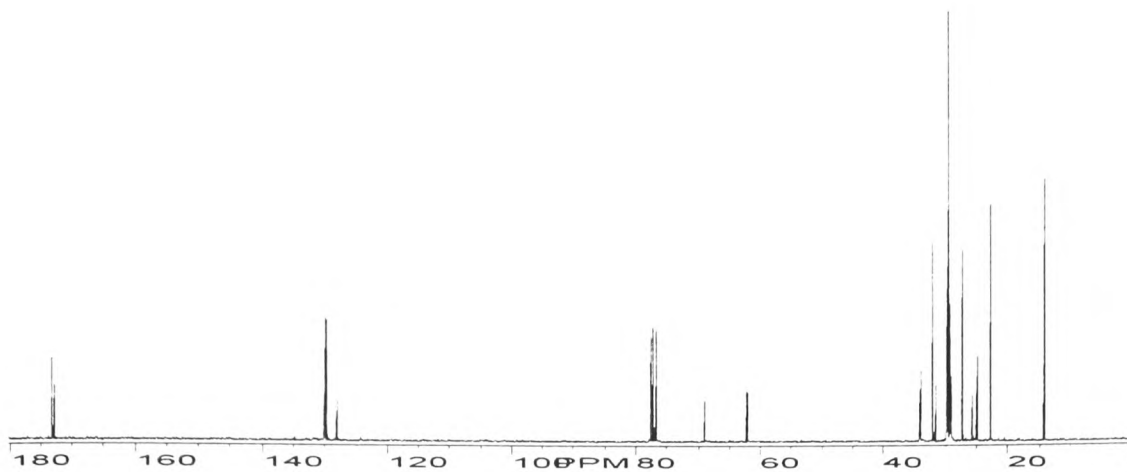


Figure C25 Full <sup>13</sup>C NMR spectrum of sample D9 adulterated with 10 % w/w sunflower oil

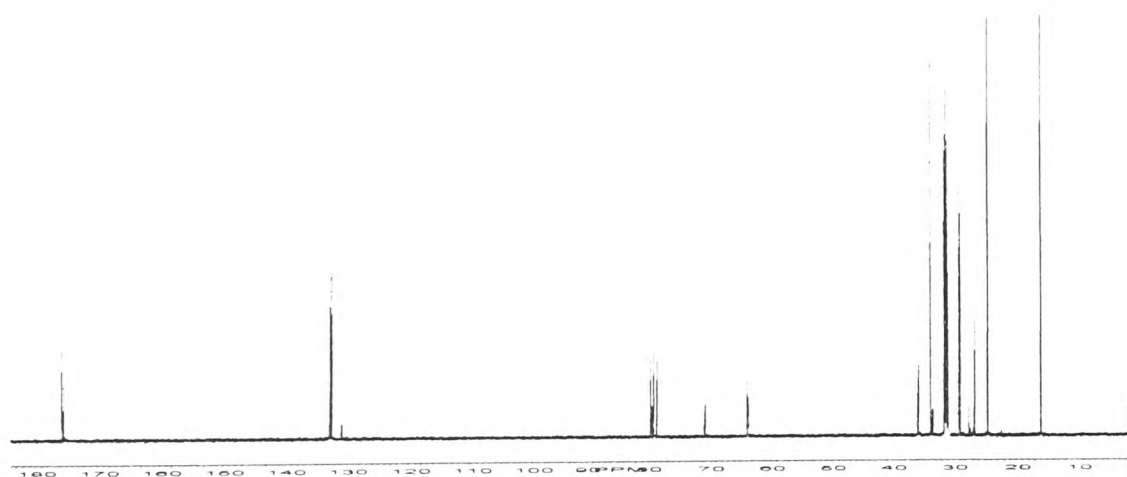


Figure C26 Full <sup>13</sup>C NMR spectrum of sample D10

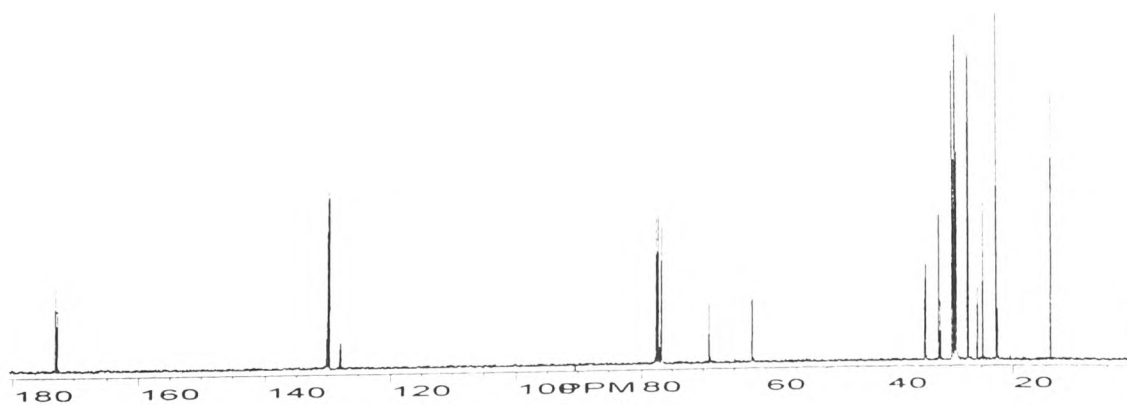
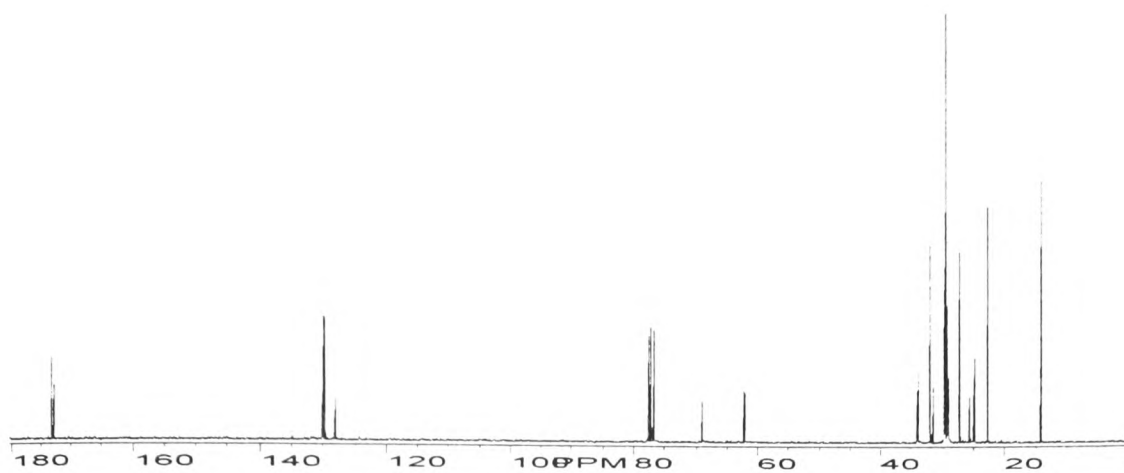
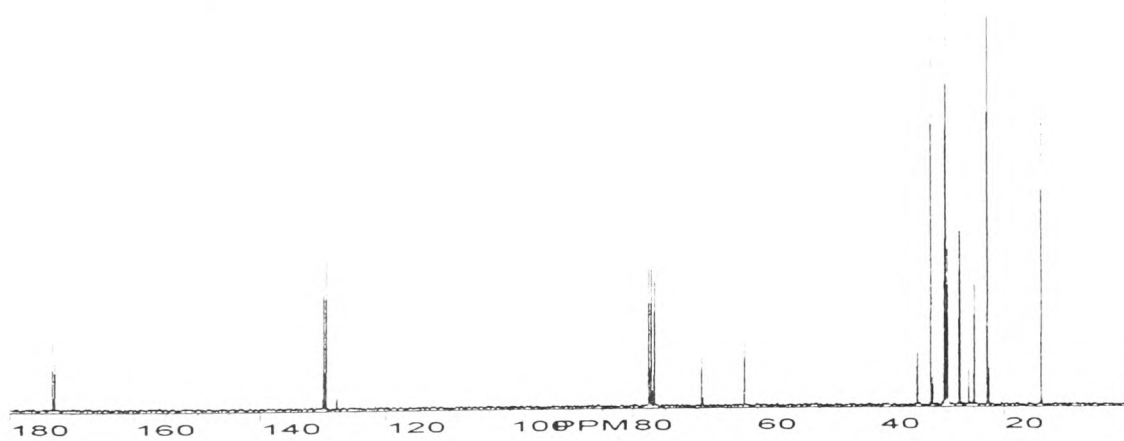


Figure C27 Full <sup>13</sup>C NMR spectrum of sample D10 adulterated with 5 % w/w sunflower oil



**Figure C28 Full <sup>13</sup>C NMR spectrum of sample D10 adulterated with 10 % w/w sunflower oil**



**Figure C29 Full <sup>13</sup>C NMR spectrum of sample D11**

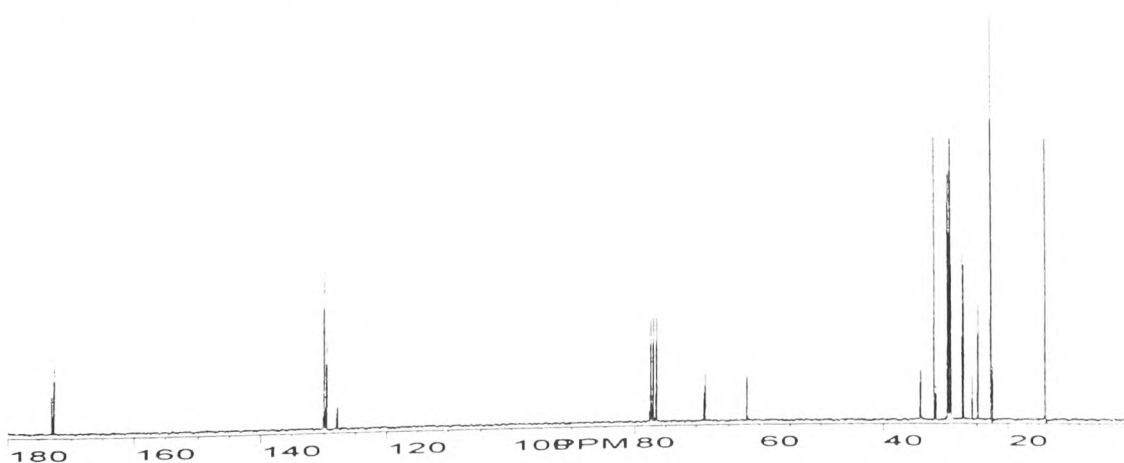


**Figure C30 Full <sup>13</sup>C NMR spectrum of sample D11 adulterated with 5 % w/w sunflower oil**

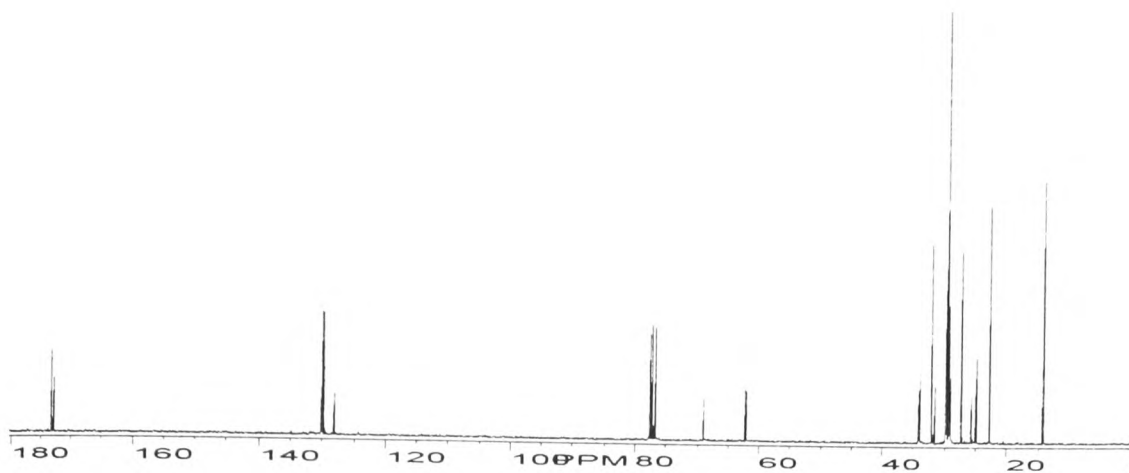


Figure C31 Full <sup>13</sup>C NMR spectrum of sample D11 adulterated with 10 % w/w sunflower oil

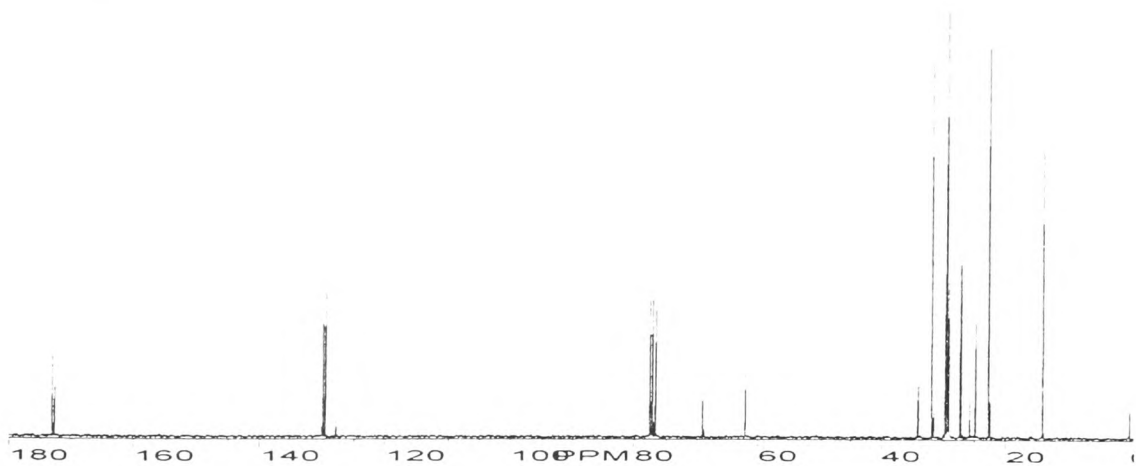


Figure C32 Full <sup>13</sup>C spectrum NMR of sample D12

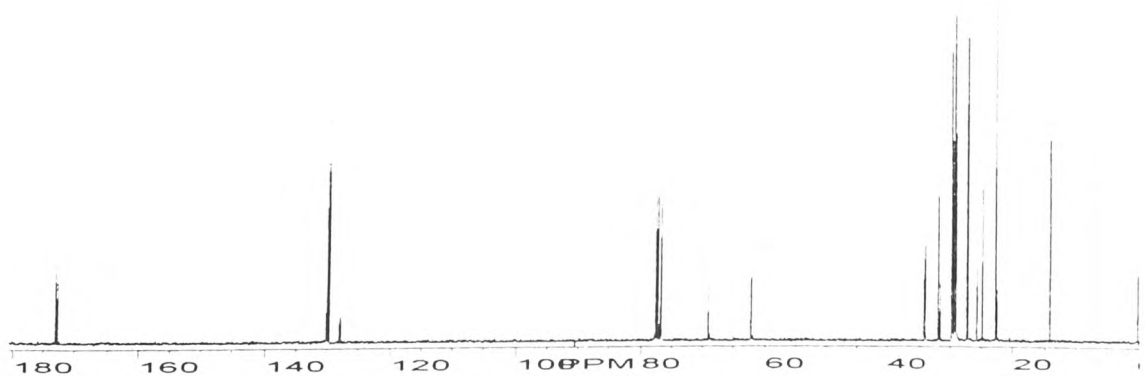


Figure C33 Full <sup>13</sup>C spectrum NMR of sample D12 adulterated with 5 % w/w sunflower oil

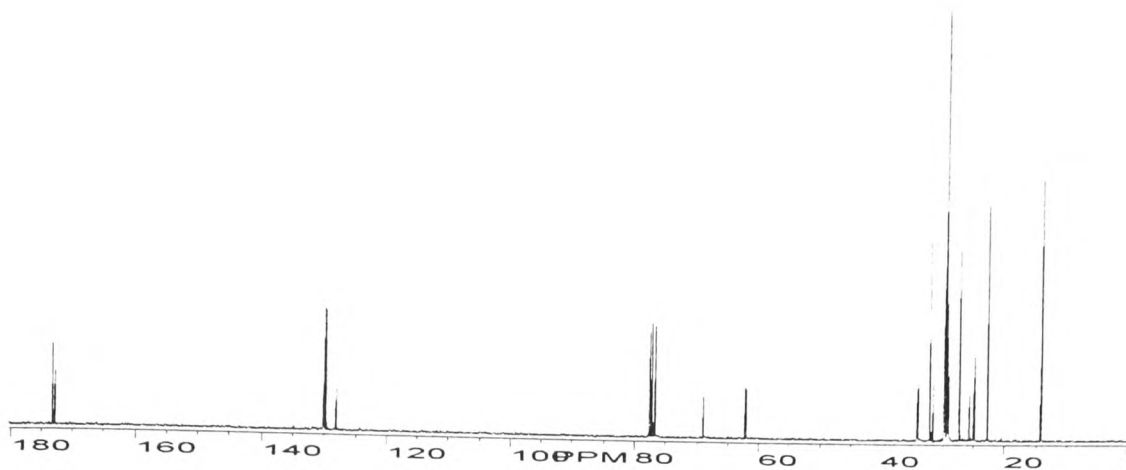


Figure C34 Full <sup>13</sup>C spectrum NMR of sample D12 adulterated with 10 % w/w sunflower oil

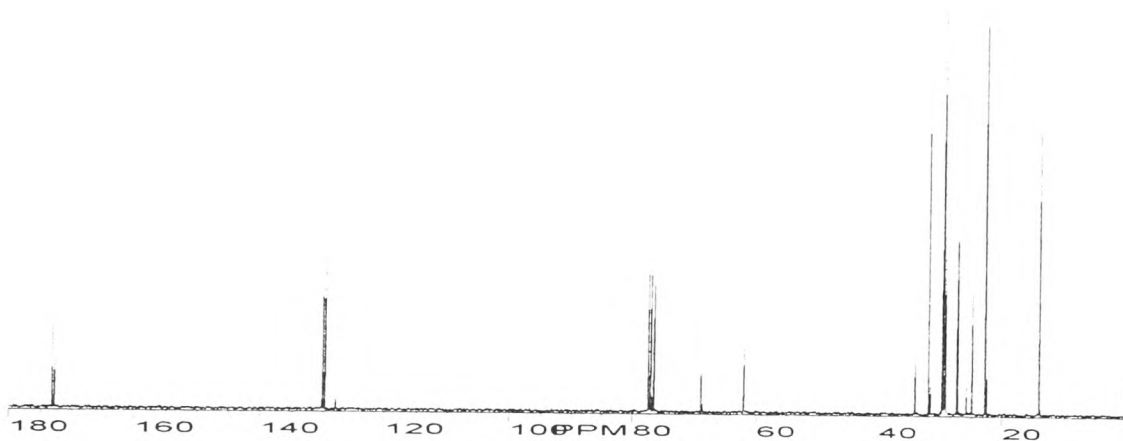


Figure C35 Full <sup>13</sup>C spectrum NMR of sample D13

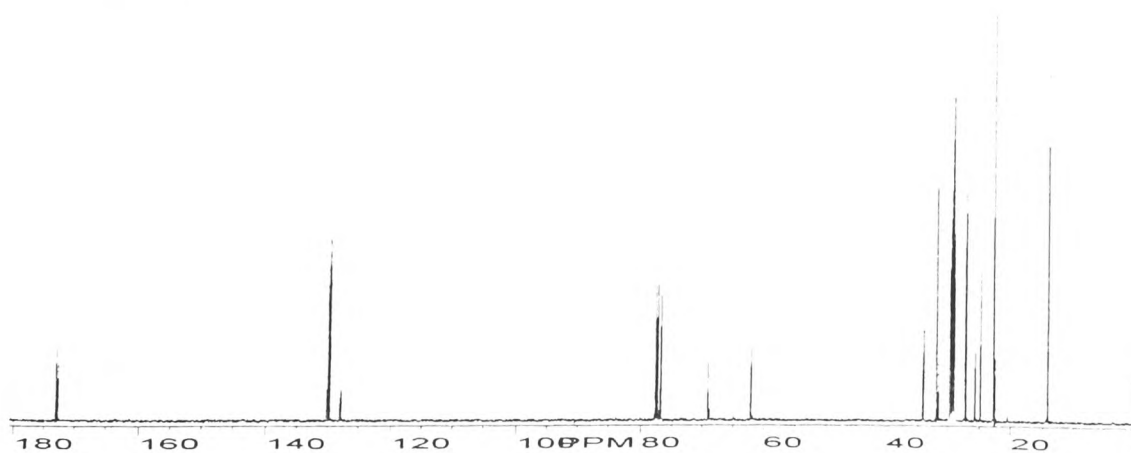


Figure C36 Full <sup>13</sup>C spectrum NMR of sample D13 adulterated with 5 % w/w sunflower oil

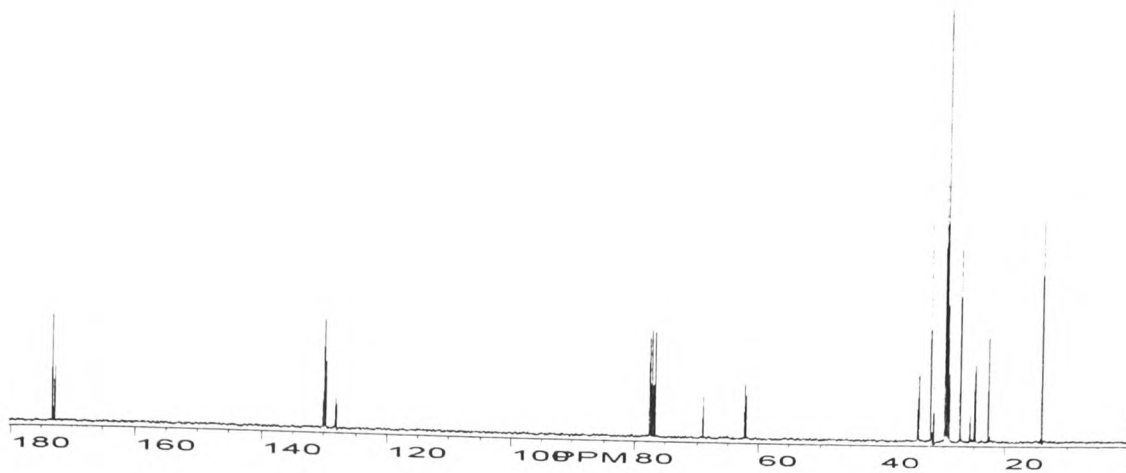


Figure C37 Full <sup>13</sup>C spectrum NMR of sample D13 adulterated with 10 % w/w sunflower oil

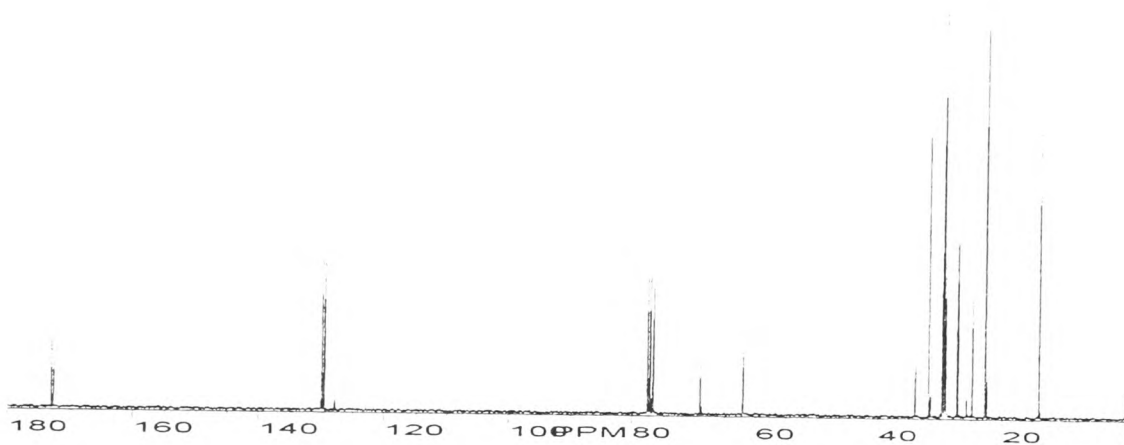


Figure C38 Full <sup>13</sup>C spectrum NMR of sample D14

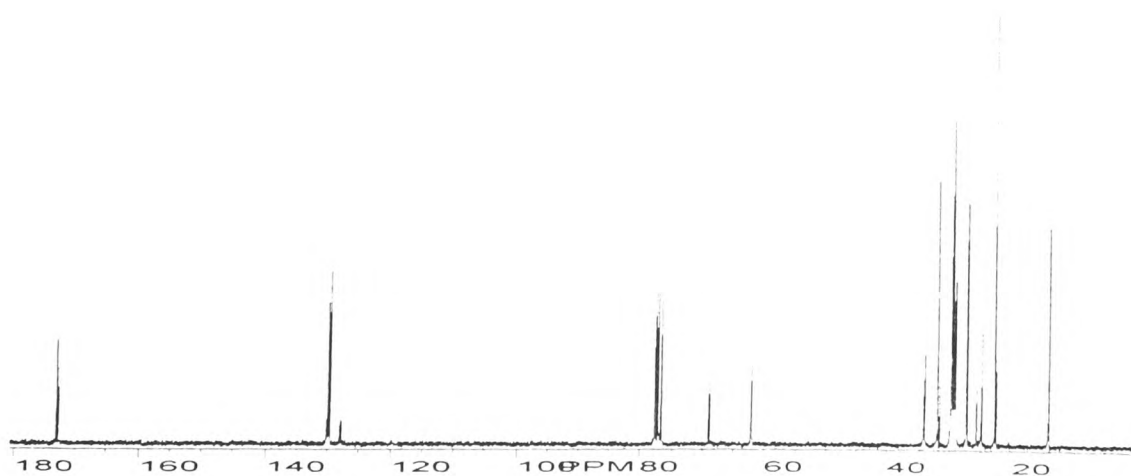


Figure C39 Full <sup>13</sup>C spectrum NMR of sample D14 adulterated with 5 % w/w sunflower oil



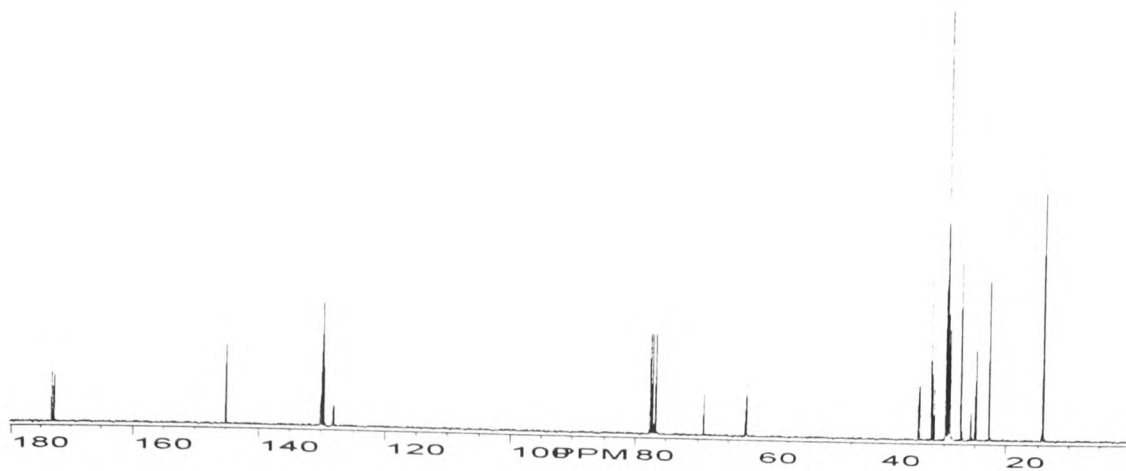


Figure C40 Full <sup>13</sup>C spectrum NMR of sample D14 adulterated with 10 % w/w sunflower oil

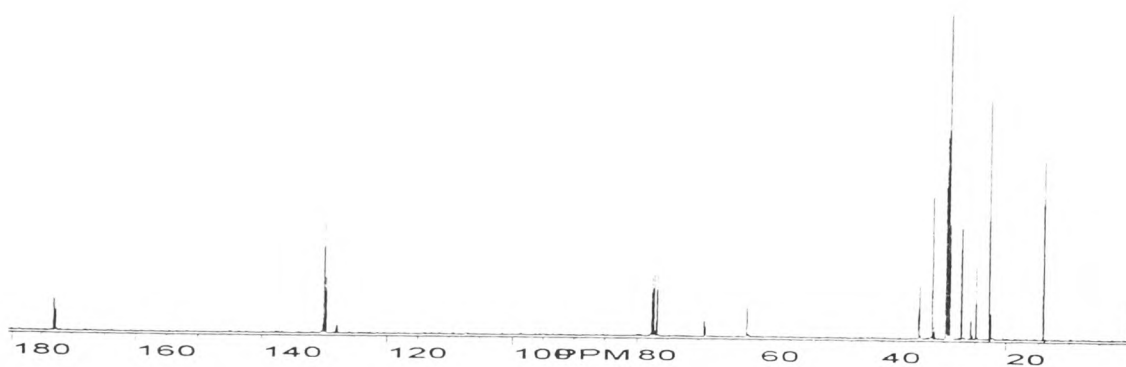


Figure C41 Full <sup>13</sup>C spectrum NMR of sample D15

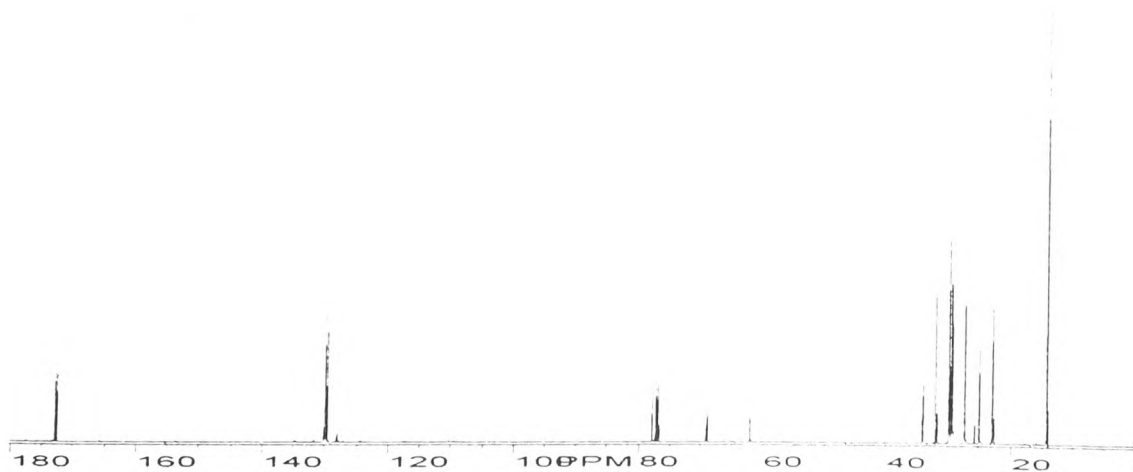


Figure C42 Full <sup>13</sup>C spectrum NMR of sample D15 adulterated with 5 % w/w sunflower oil

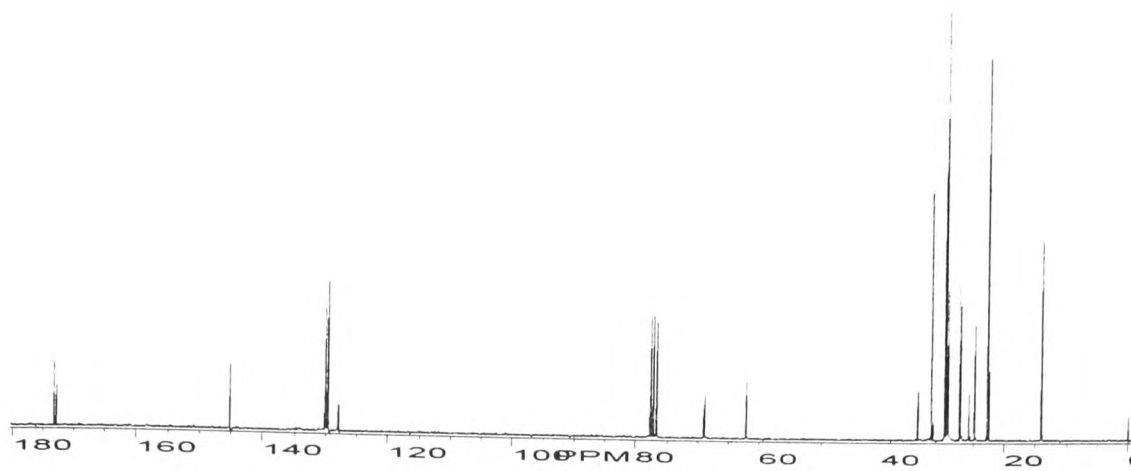


Figure C43 Full <sup>13</sup>C spectrum NMR of sample D15 adulterated with 10 % w/w sunflower oil

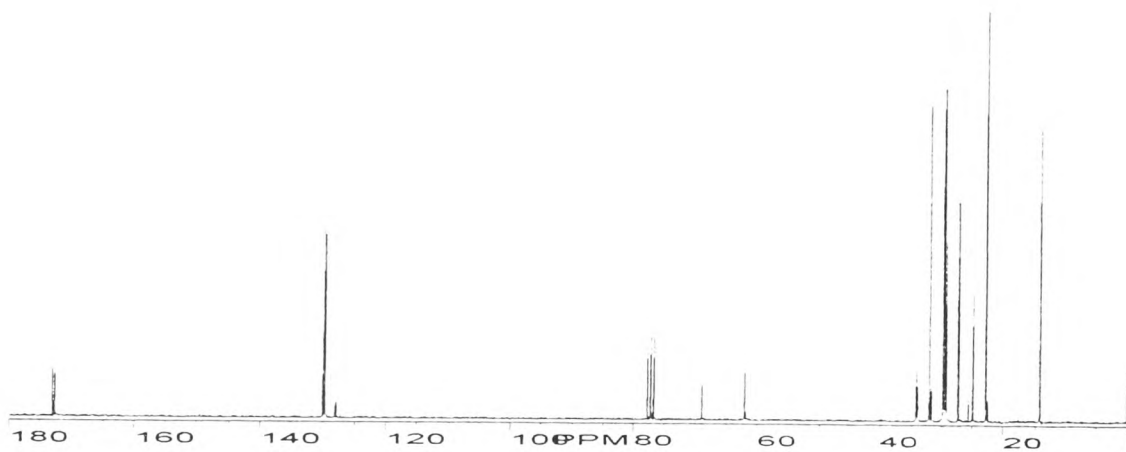


Figure C44 Full <sup>13</sup>C spectrum NMR of sample D16

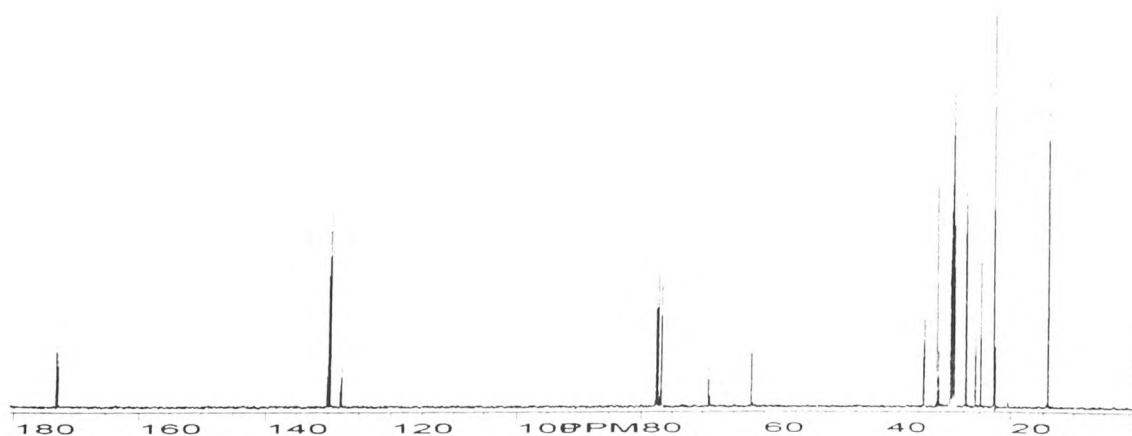


Figure C45 Full <sup>13</sup>C spectrum NMR of sample D16 adulterated with 5 % w/w sunflower oil

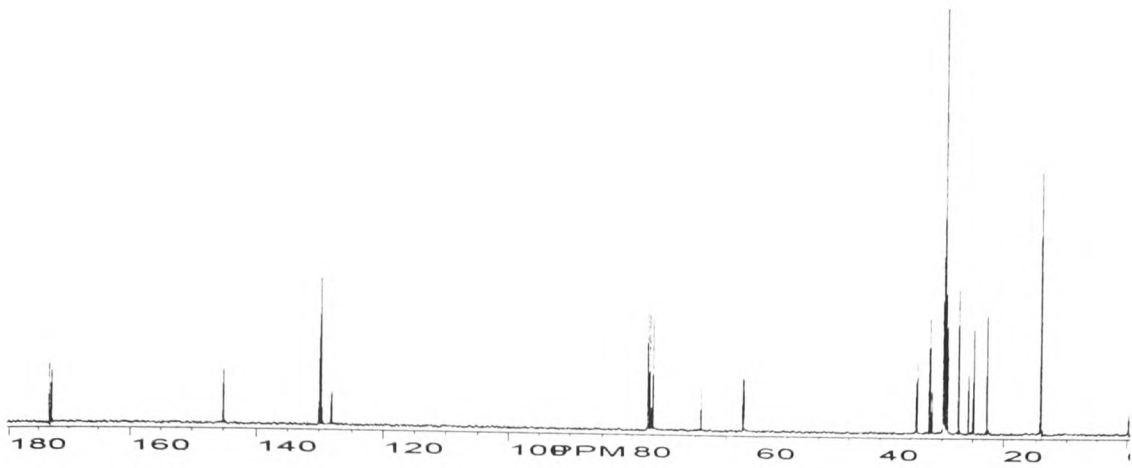


Figure C46 Full  $^{13}\text{C}$  spectrum NMR of sample D16 adulterated with 10% w/w sunflower oil

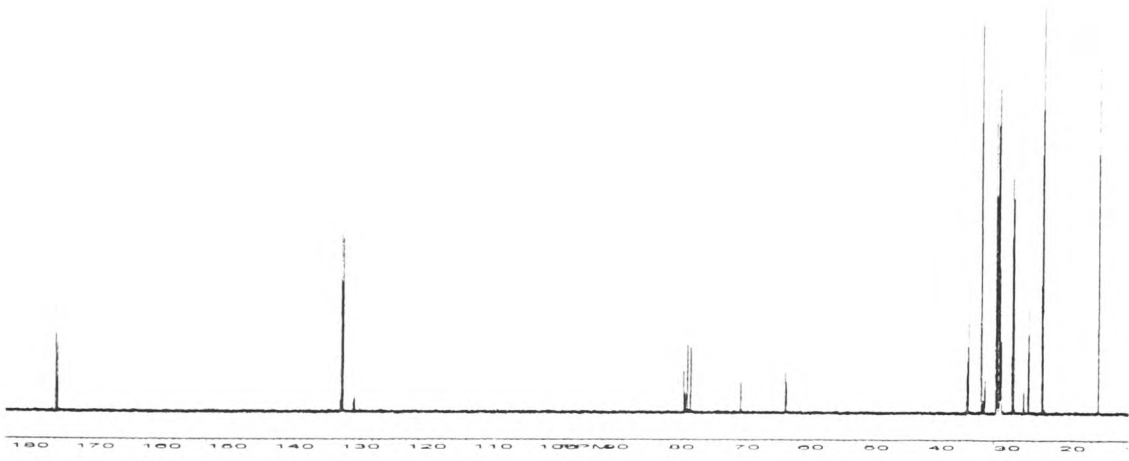


Figure C47 Full  $^{13}\text{C}$  spectrum NMR of sample D17

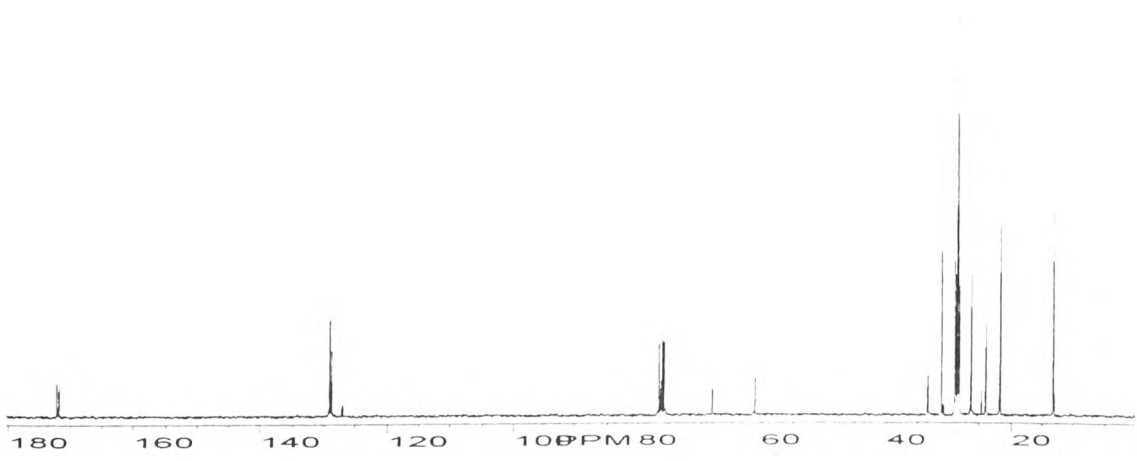


Figure C48  $^{13}\text{C}$  spectrum NMR of sample D17 adulterated with 5% w/w sunflower oil

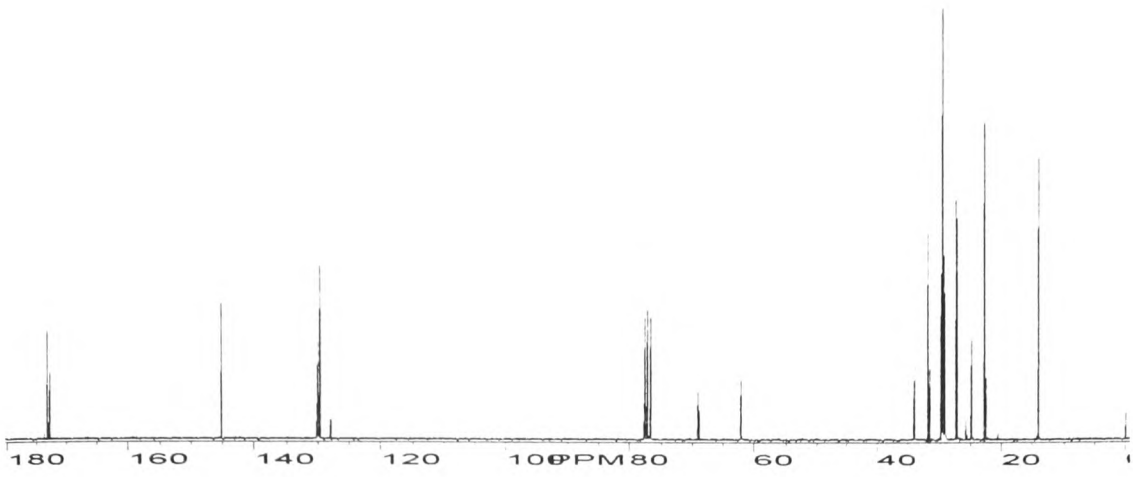


Figure C49 Full  $^{13}\text{C}$  spectrum NMR of sample D17 adulterated with 10% w/w sunflower oil

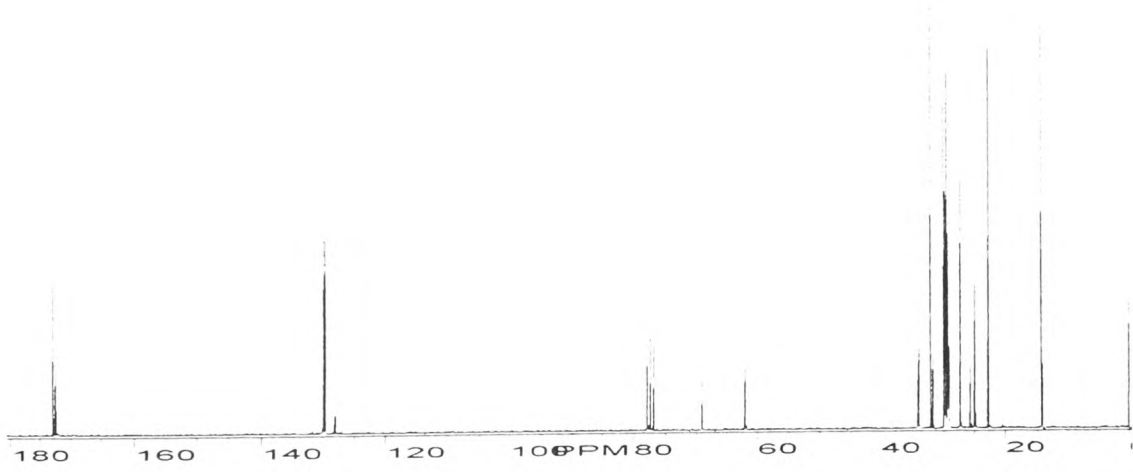


Figure C50 Full  $^{13}\text{C}$  spectrum NMR of sample D18

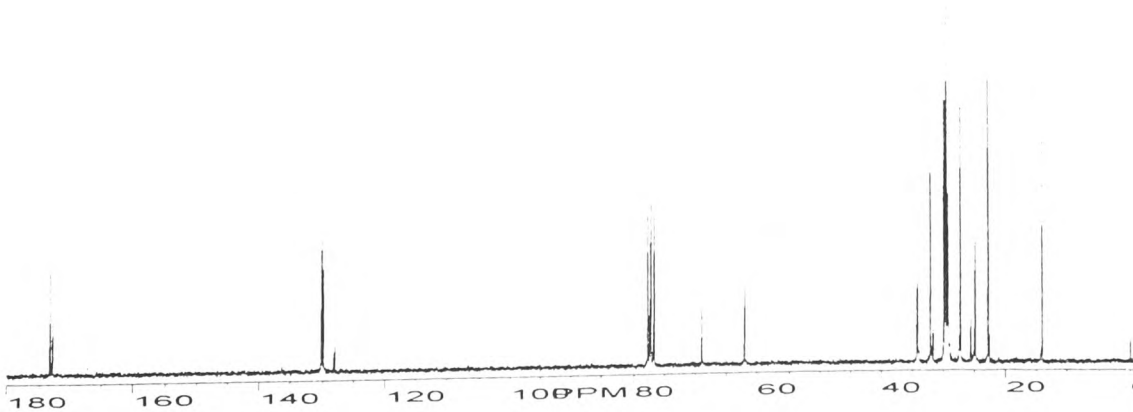


Figure C51 Full  $^{13}\text{C}$  spectrum NMR of sample D18 adulterated with 5% w/w sunflower oil

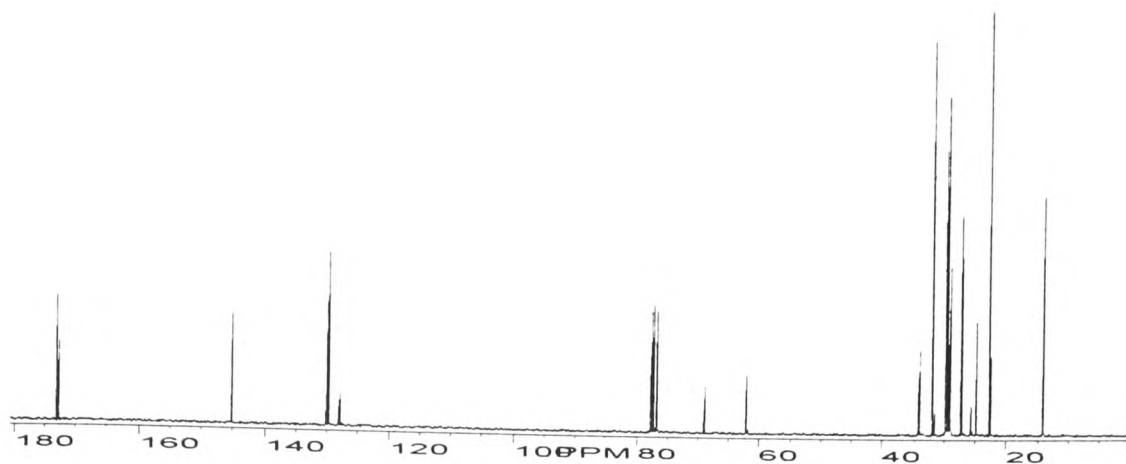


Figure C52 Full  $^{13}\text{C}$  spectrum NMR of sample D18 adulterated with 10% w/w sunflower oil

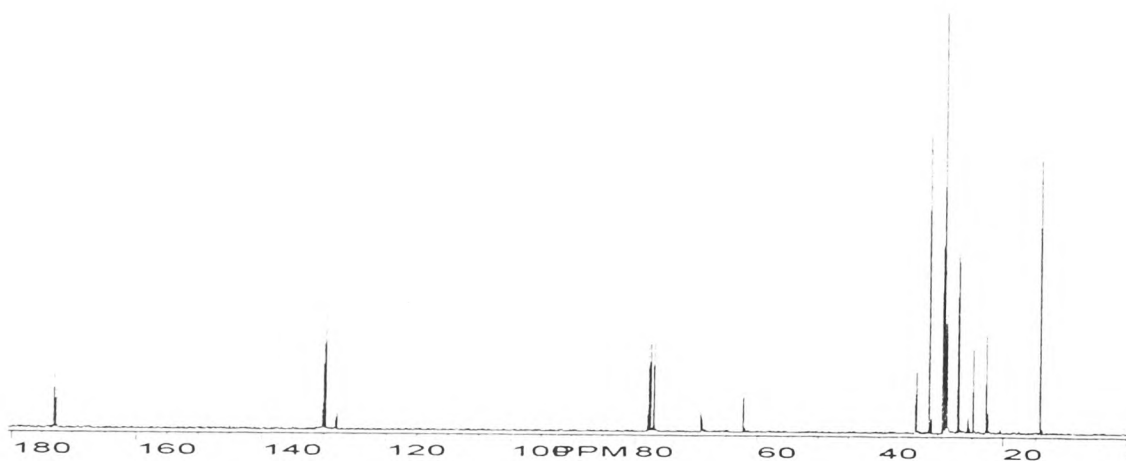


Figure C53 Full  $^{13}\text{C}$  spectrum NMR of sample D19

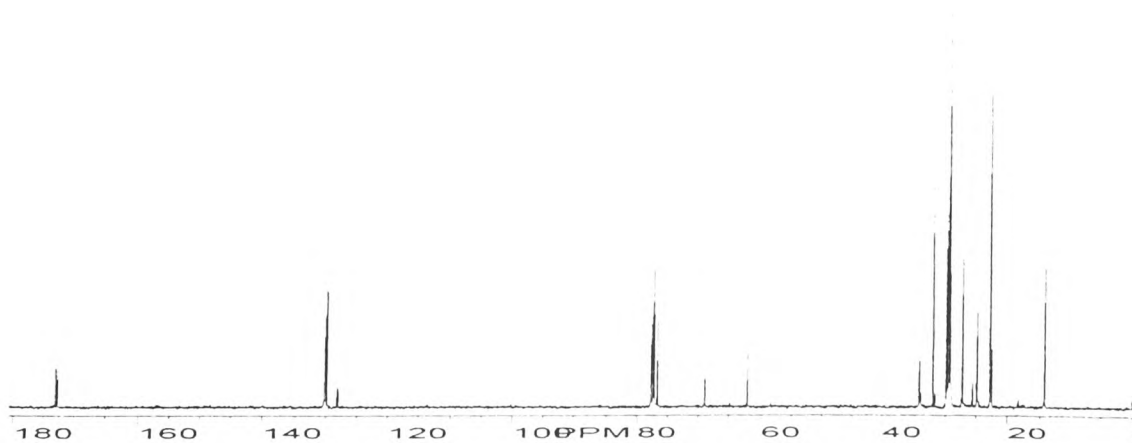


Figure C54 Full  $^{13}\text{C}$  spectrum NMR of sample D19 adulterated with 5% w/w sunflower oil

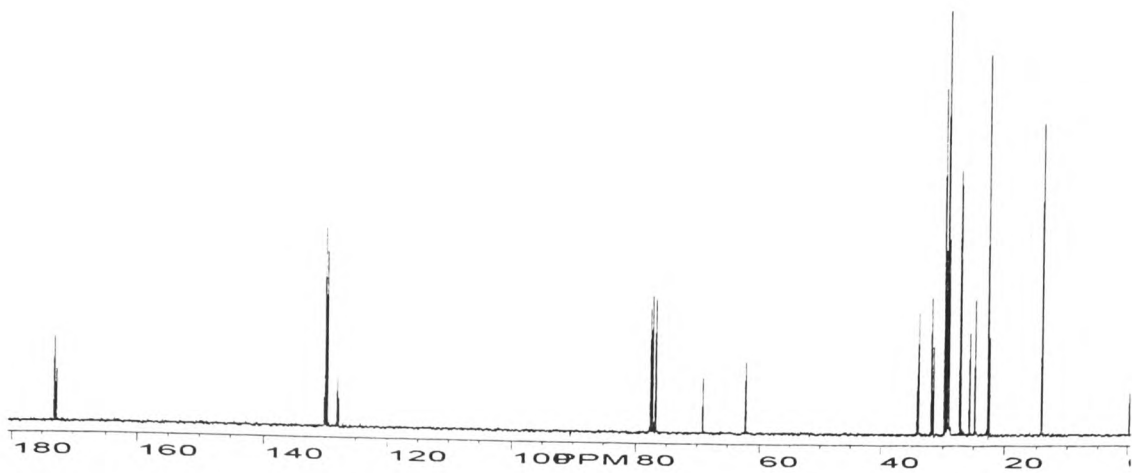


Figure C55 Full  $^{13}\text{C}$  spectrum NMR of sample D19 adulterated with 10% w/w sunflower oil

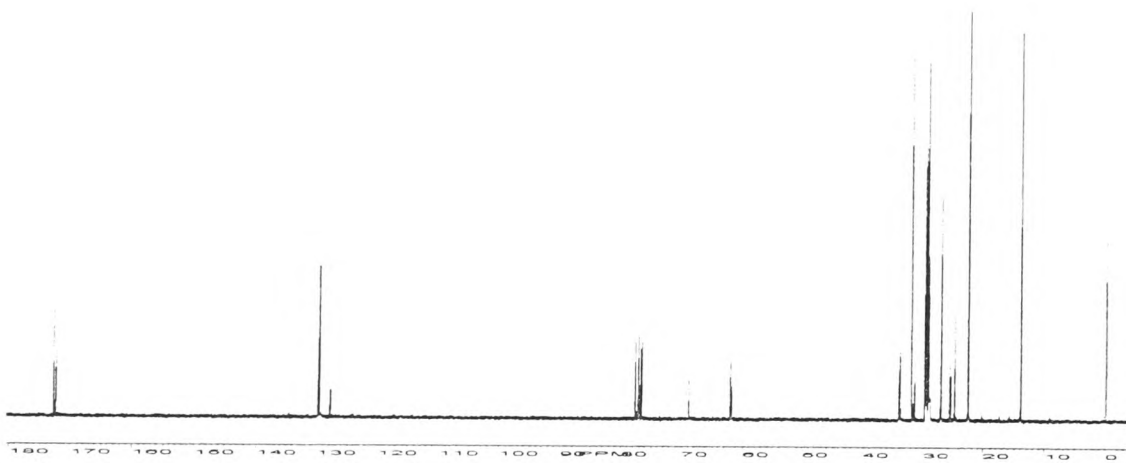


Figure C56 Full  $^{13}\text{C}$  spectrum NMR of sample D20

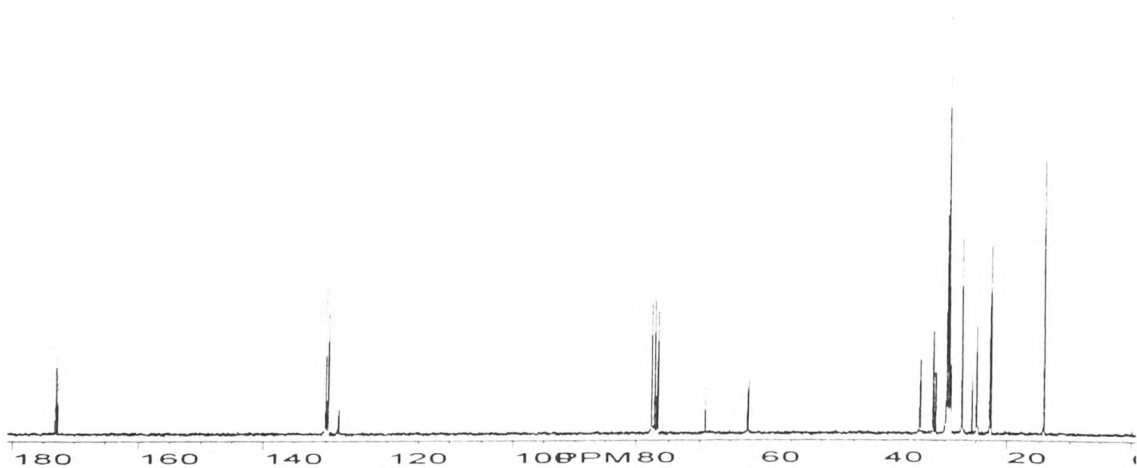


Figure C57 Full  $^{13}\text{C}$  spectrum NMR of sample D20 adulterated with 5% w/w sunflower oil

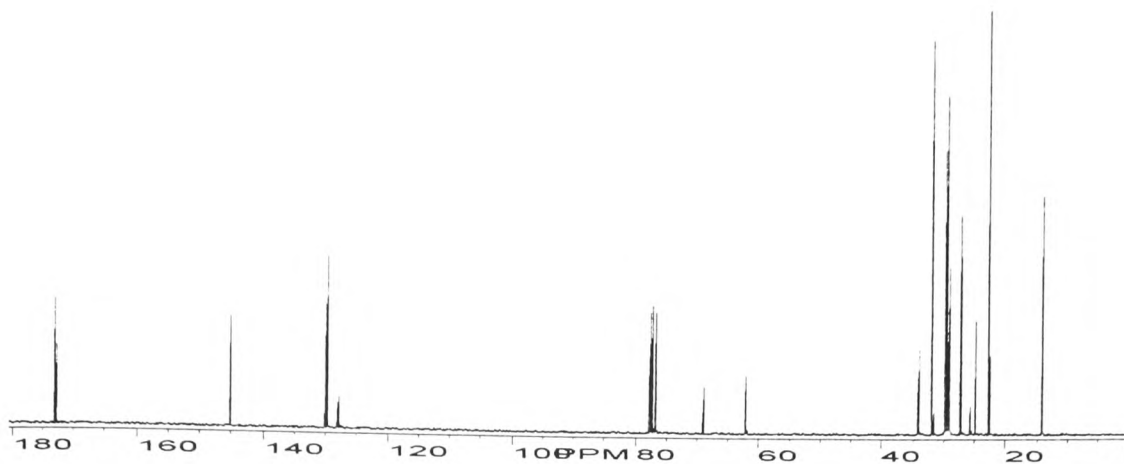


Figure C58 Full <sup>13</sup>C spectrum NMR of sample D20 adulterated with 10% w/w sunflower oil

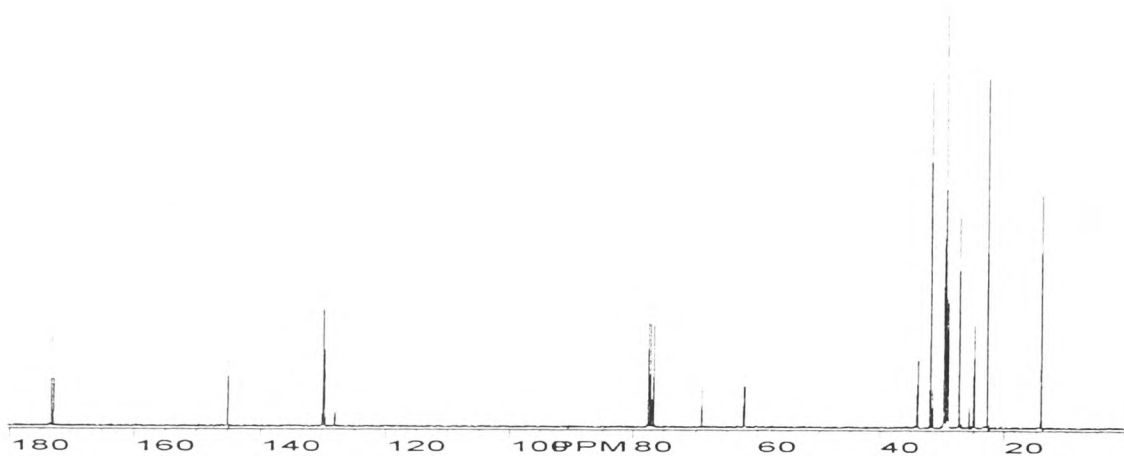


Figure C59 Full <sup>13</sup>C spectrum NMR of sample D21

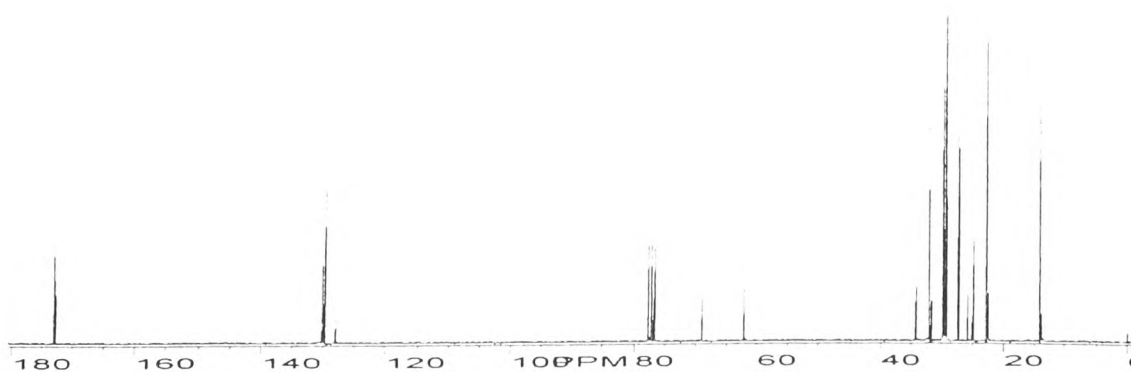


Figure C60 Full <sup>13</sup>C spectrum NMR of sample D21 adulterated with 5 % w/w sunflower oil

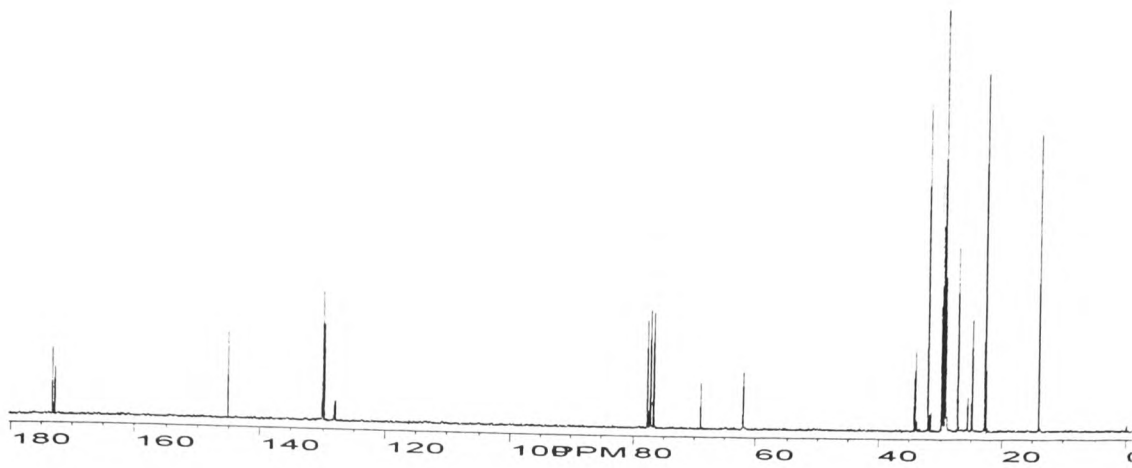


Figure C61 Full  $^{13}\text{C}$  spectrum NMR of sample D21 adulterated with 10 % w/w sunflower oil

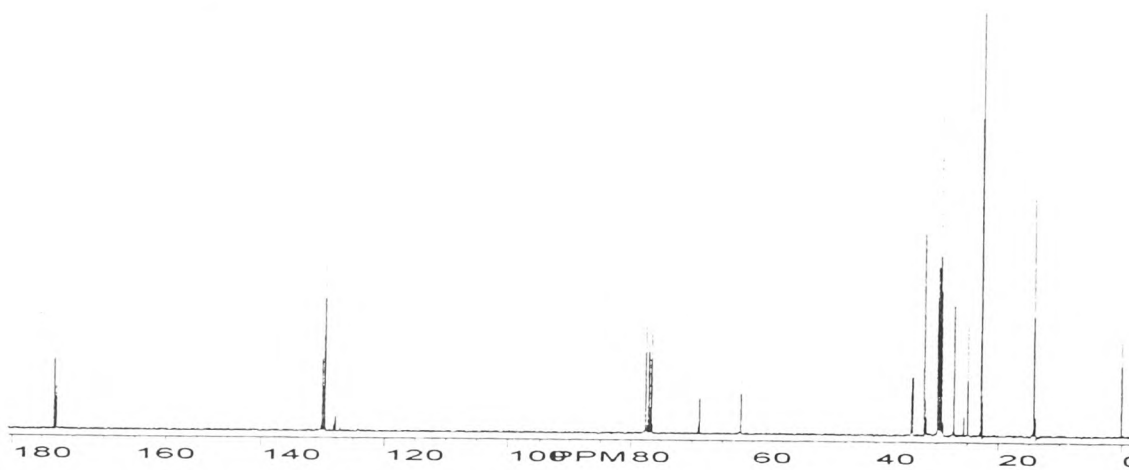


Figure C62 Full  $^{13}\text{C}$  spectrum NMR of sample D22

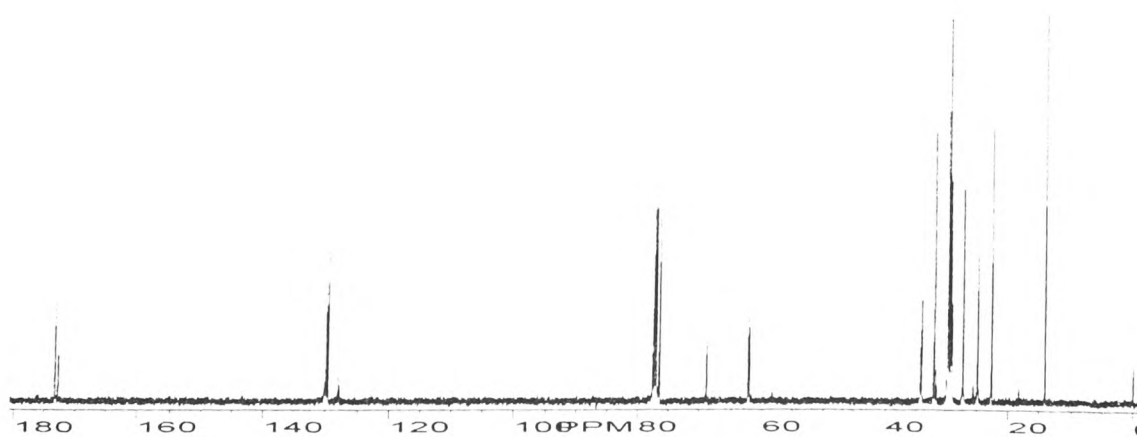
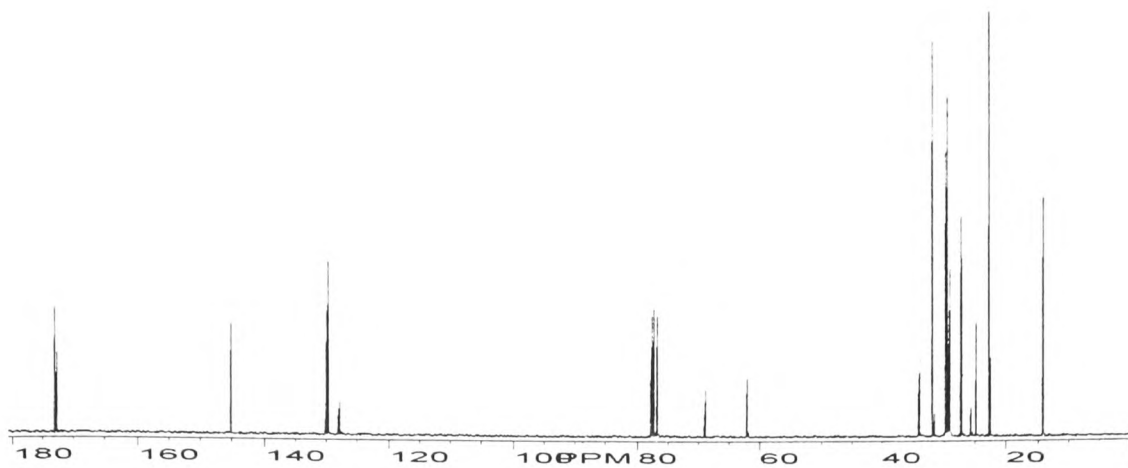


Figure C63 Full  $^{13}\text{C}$  spectrum NMR of sample D22 adulterated with 5 % w/w sunflower oil





**Figure C64 Full  $^{13}\text{C}$  spectrum NMR of sample D22 adulterated with 10% w/w sunflower oil**

## APPENDIX D

Figure D1 $^{13}\text{C}$ NMR alkene region of sample D1 .....	D1
Figure D2 $^{13}\text{C}$ NMR alkene region of sample D1 adulterated with 5 % w/w sunflower oil .....	D1
Figure D3 $^{13}\text{C}$ NMR alkene region of sample D1 adulterated with 10 % w/w sunflower oil .....	D1
Figure D4 $^{13}\text{C}$ NMR alkene region of sample D2 .....	D2
Figure D5 $^{13}\text{C}$ NMR alkene region of sample D2 adulterated with 5 % w/w sunflower oil .....	D2
Figure D6 $^{13}\text{C}$ NMR region of sample D2 adulterated with 10 % w/w sunflower oil .....	D2
Figure D7 $^{13}\text{C}$ NMR alkene region of sample D3 .....	D3
Figure D8 $^{13}\text{C}$ NMR alkene region of sample D3 adulterated with 5 % w/w sunflower oil .....	D3
Figure D9 $^{13}\text{C}$ NMR alkene region of sample D3 adulterated with 10 % w/w sunflower oil .....	D3
Figure 10 $^{13}\text{C}$ alkene region of sample D4 .....	D4
Figure 11 $^{13}\text{C}$ NMR alkene region of sample D4 adulterated with 5 % w/w sunflower oil .....	D4

Figure D12 <sup>13</sup> C NMR alkene region of sample D4 adulterated with 10 % w/w sunflower oil.....	D4
Figure D13 <sup>13</sup> C NMR alkene region of sample D5 .....	D5
Figure D14 <sup>13</sup> C NMR alkene region of sample D5 adulterated with 5 % w/w sunflower oil.....	D5
Figure D15 <sup>13</sup> C NMR alkene region of sample D5 adulterated with 10 % w/w sunflower oil.....	D5
Figure D16 <sup>13</sup> C NMR alkene region of sample D6 .....	D6
Figure D17 <sup>13</sup> C NMR alkene region of sample D6 adulterated with 5 % w/w sunflower oil.....	D6
Figure D18 <sup>13</sup> C NMR alkene region of sample D6 adulterated with 10 % w/w sunflower oil.....	D6
Figure D19 <sup>13</sup> C NMR alkene region of sample D7 .....	D7
Figure D20 <sup>13</sup> C NMR alkene region of sample D7 adulterated with 5 % w/w sunflower oil.....	D7
Figure D21 <sup>13</sup> C NMR alkene region of sample D7 adulterated with 10 % w/w sunflower oil.....	D7
Figure D22 <sup>13</sup> C NMR alkene region of sample D8 .....	D8

Figure D23 <sup>13</sup> C NMR alkene region of sample D8 adulterated with 5 % w/w sunflower oil.....	D8
Figure D24 <sup>13</sup> C NMR alkene region of sample D8 adulterated with 10 % w/w sunflower oil.....	D8
Figure D25 <sup>13</sup> C NMR alkene region of sample D9 .....	D9
Figure D26 <sup>13</sup> C NMR alkene region of sample D9 adulterated with 5 % w/w sunflower oil.....	D9
Figure D27 <sup>13</sup> C NMR alkene region of sample D9 adulterated with 10 % w/w sunflower oil.....	D9
Figure D28 <sup>13</sup> C NMR alkene region of sample D10.....	D10
Figure D29 <sup>13</sup> C NMR alkene region of sample D10 adulterated with 5 % w/w sunflower oil.....	D10
Figure D30 <sup>13</sup> C NMR alkene region of sample D10 adulterated with 10 % w/w sunflower oil.....	D10
Figure D31 <sup>13</sup> C NMR alkene region of sample D11.....	D11
Figure D32 <sup>13</sup> C NMR alkene region of sample D11 adulterated with 5 % w/w sunflower oil.....	D11
Figure D33 <sup>13</sup> C NMR alkene region of sample D11 adulterated with 10 % w/w sunflower oil .....	D11

Figure D34 $^{13}\text{C}$ NMR alkene region of sample D12.....	D12
Figure D35 $^{13}\text{C}$ NMR alkene region of sample D12 adulterated with 5 % w/w sunflower oil.....	D12
Figure D36 $^{13}\text{C}$ NMR alkene region of sample D12 adulterated with 10 % w/w sunflower oil.....	D12
Figure D37 $^{13}\text{C}$ NMR alkene region of sample D13.....	D13
Figure D38 $^{13}\text{C}$ NMR alkene region of sample D13 adulterated with 5 % w/w sunflower oil.....	D13
Figure D39 $^{13}\text{C}$ NMR alkene region of sample D13 adulterated with 10 % w/w sunflower oil.....	D13
Figure D40 $^{13}\text{C}$ NMR alkene region of sample D14.....	D14
Figure D41 $^{13}\text{C}$ NMR alkene region of sample D14 adulterated with 5 % w/w sunflower oil.....	D14
Figure D42 $^{13}\text{C}$ NMR alkene region of sample D14 adulterated with 10 % w/w sunflower oil.....	D14
Figure D43 $^{13}\text{C}$ NMR alkene region of sample D15.....	D15
Figure D44 $^{13}\text{C}$ NMR alkene region of sample D15 adulterated with 5 % w/w sunflower oil.....	D15

Figure D45 <sup>13</sup> C NMR alkene region of sample D15 adulterated with 10 % w/w sunflower oil .....	D15
Figure D46 <sup>13</sup> C NMR alkene region of sample D16.....	D16
Figure D47 <sup>13</sup> C NMR alkene region of sample D16 adulterated with 5 % w/w sunflower oil .....	D16
Figure D48 <sup>13</sup> C NMR alkene region of sample D16 adulterated with 10 % w/w sunflower oil .....	D16
Figure D49 <sup>13</sup> C NMR alkene region of sample D17.....	D17
Figure D50 <sup>13</sup> C NMR alkene region of sample D17 adulterated with 5 % w/w sunflower oil .....	D17
Figure D51 <sup>13</sup> C NMR alkene region of sample D17 adulterated with 10 % w/w sunflower oil .....	D17
Figure D52 <sup>13</sup> C NMR alkene region of sample D18.....	D18
Figure D53 <sup>13</sup> C NMR alkene region of sample D18 adulterated with 5 % w/w sunflower oil .....	D18
Figure D54 <sup>13</sup> C NMR alkene region of sample D18 adulterated with 10 % w/w sunflower oil .....	D18
Figure D55 <sup>13</sup> C NMR alkene region of sample D19.....	D19

Figure D56 <sup>13</sup> C NMR alkene region of sample D19 adulterated with 5 % w/w sunflower oil .....	D19
Figure D57 <sup>13</sup> C NMR alkene region of sample D19 adulterated with 10 % w/w sunflower oil .....	D19
Figure D58 <sup>13</sup> C NMR alkene region of sample D20.....	D20
Figure D59 <sup>13</sup> C NMR alkene region of sample D20 adulterated with 5 % w/w sunflower oil.....	D20
Figure D60 <sup>13</sup> C NMR alkene region of sample D20 adulterated with 10 % w/w sunflower oil .....	D20
Figure D61 <sup>13</sup> C NMR alkene region of sample D21.....	D21
Figure D62 <sup>13</sup> C NMR alkene region of sample D21 adulterated with 5 % w/w sunflower oil.....	D21
Figure D63 <sup>13</sup> C NMR alkene region of sample D21 adulterated with 10 % w/w sunflower oil.....	D21
Figure D64 <sup>13</sup> C NMR alkene region of sample D22.....	D22
Figure D65 <sup>13</sup> C NMR alkene region of sample D22 adulterated with 5 % w/w sunflower oil.....	D22
Figure D66 <sup>13</sup> C NMR alkene region of sample D22 adulterated with 10 % w/w sunflower oil .....	D22

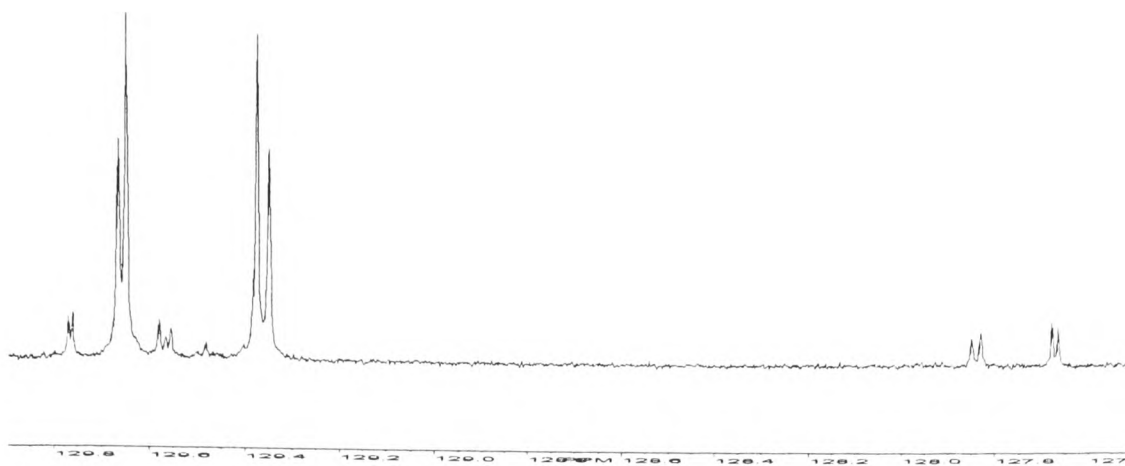


Figure D1  $^{13}\text{C}$  NMR alkene region of sample D1

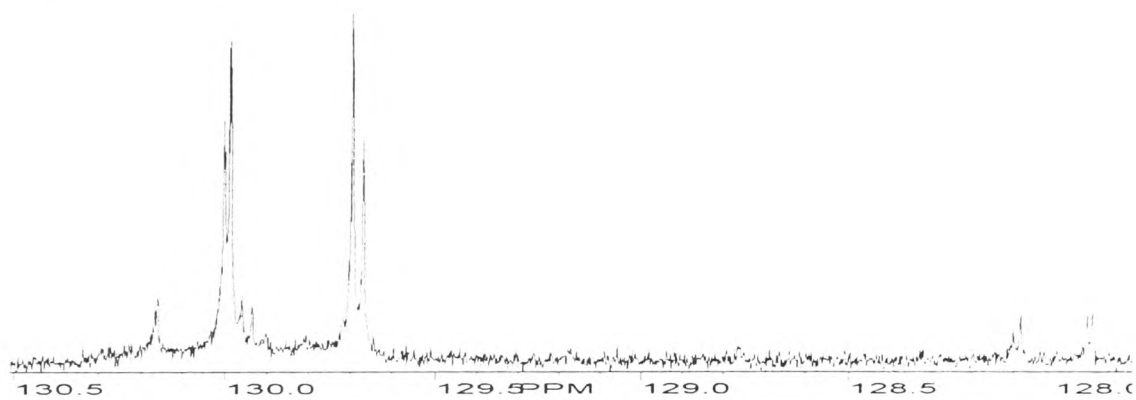


Figure D2  $^{13}\text{C}$  NMR alkene region of sample D1 adulterated with 5 % w/w sunflower oil

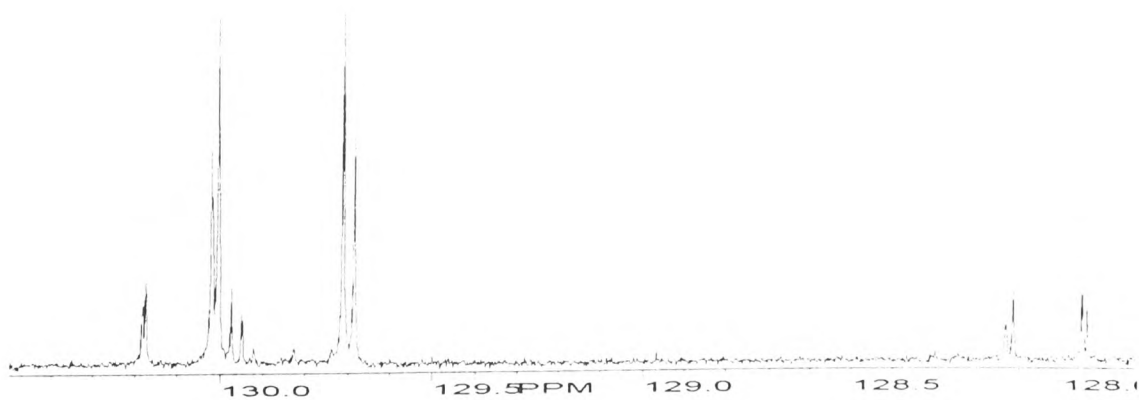


Figure D3  $^{13}\text{C}$  NMR alkene region of sample D1 adulterated with 10 % w/w sunflower oil



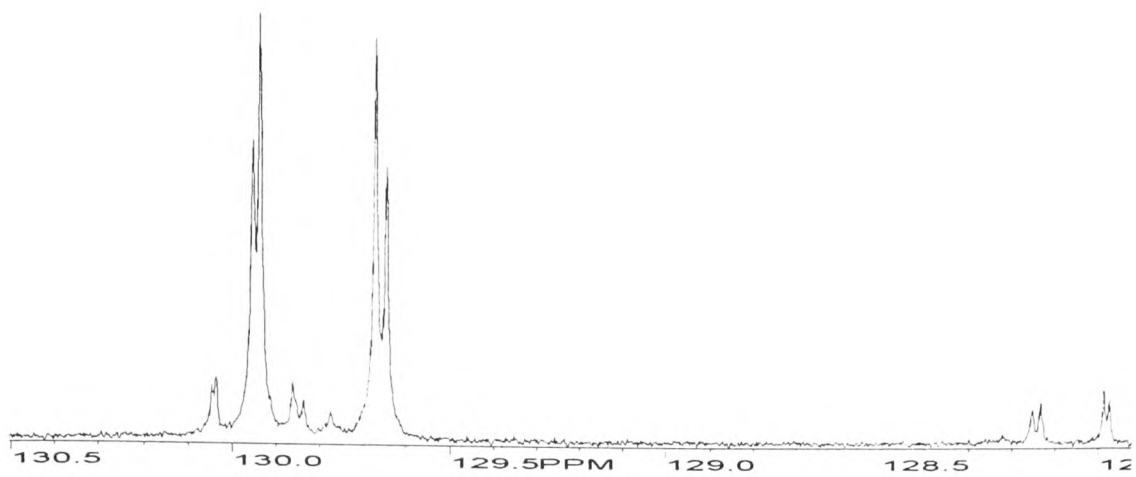


Figure D4  $^{13}\text{C}$  NMR alkene region of sample D2

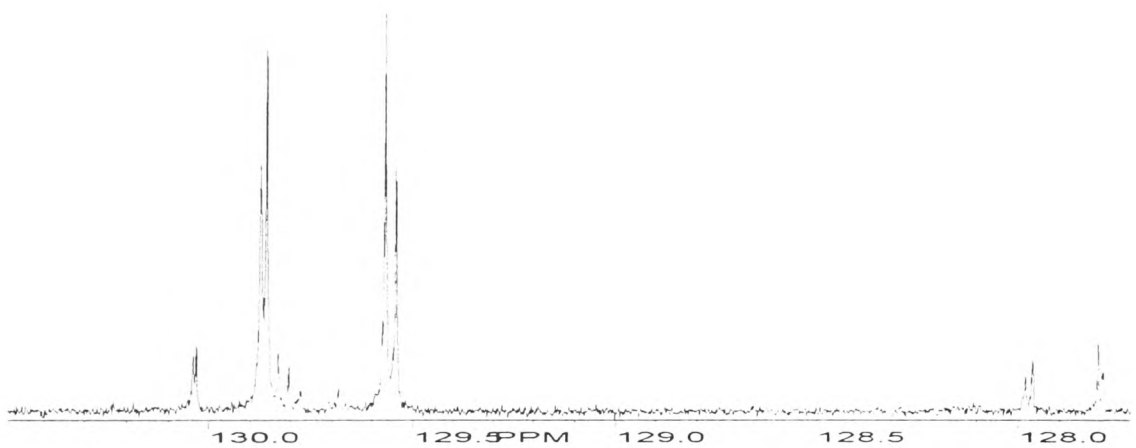


Figure D5  $^{13}\text{C}$  NMR alkene region of sample D2 adulterated with 5 % w/w sunflower oil

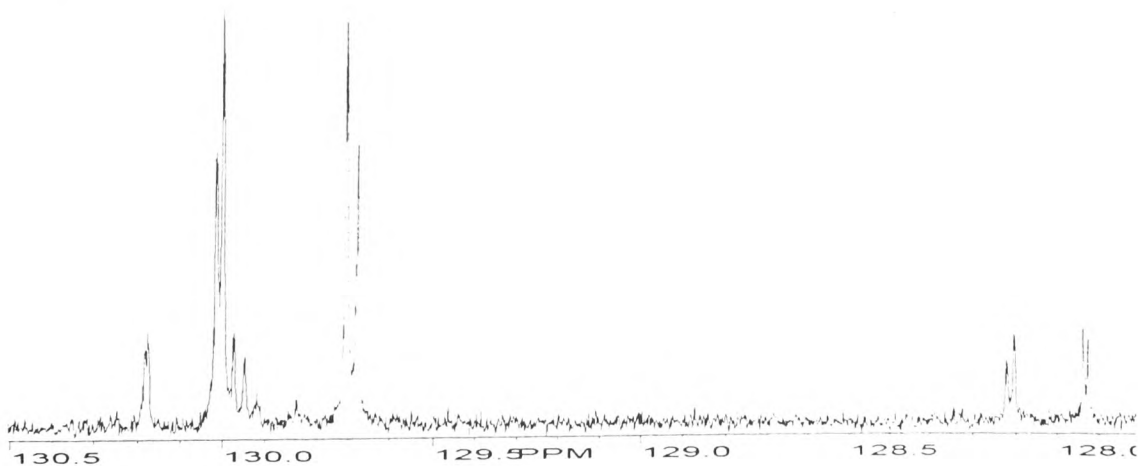


Figure D6  $^{13}\text{C}$  NMR region of sample D2 adulterated with 10 % w/w sunflower oil

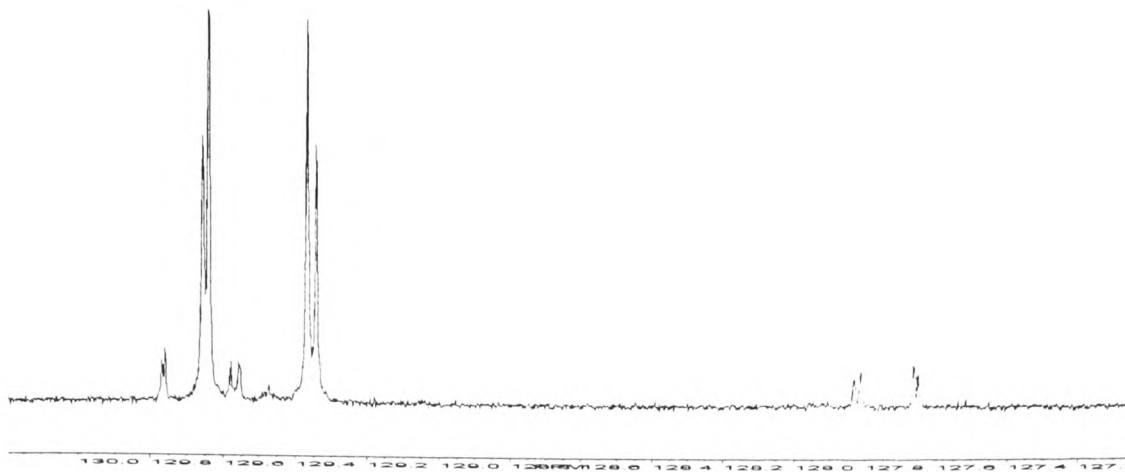


Figure D7  $^{13}\text{C}$  NMR alkene region of sample D3

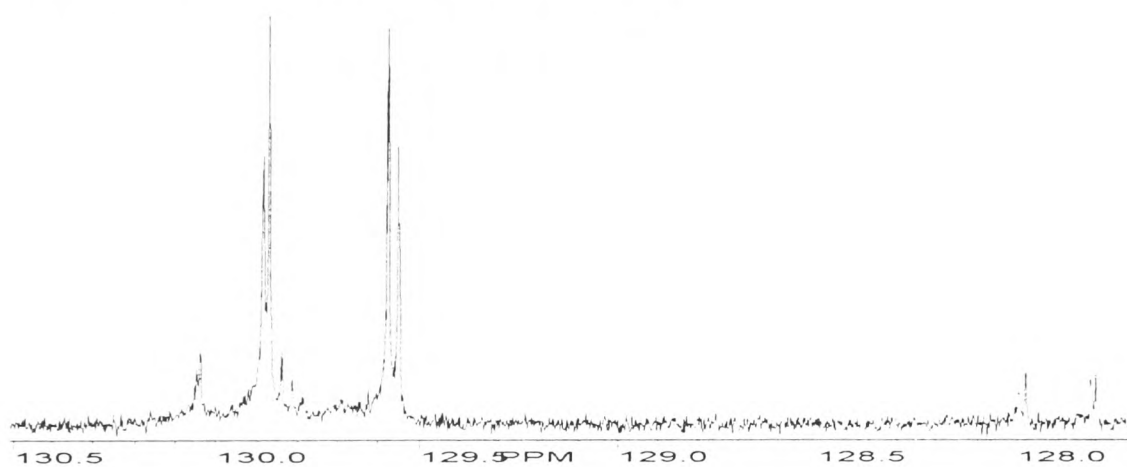


Figure D8  $^{13}\text{C}$  NMR alkene region of sample D3 adulterated with 5 % w/w sunflower oil

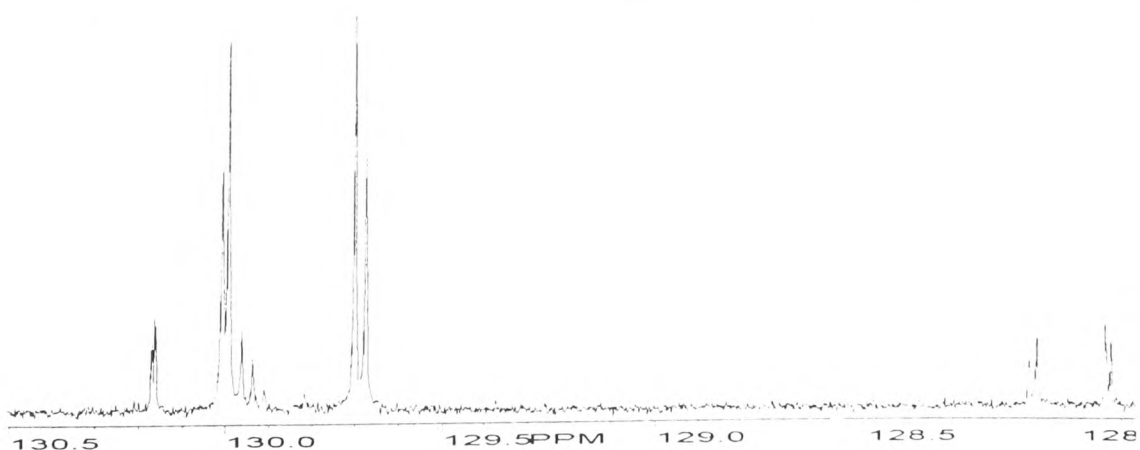


Figure D9  $^{13}\text{C}$  NMR alkene region of sample D3 adulterated with 10 % w/w sunflower oil

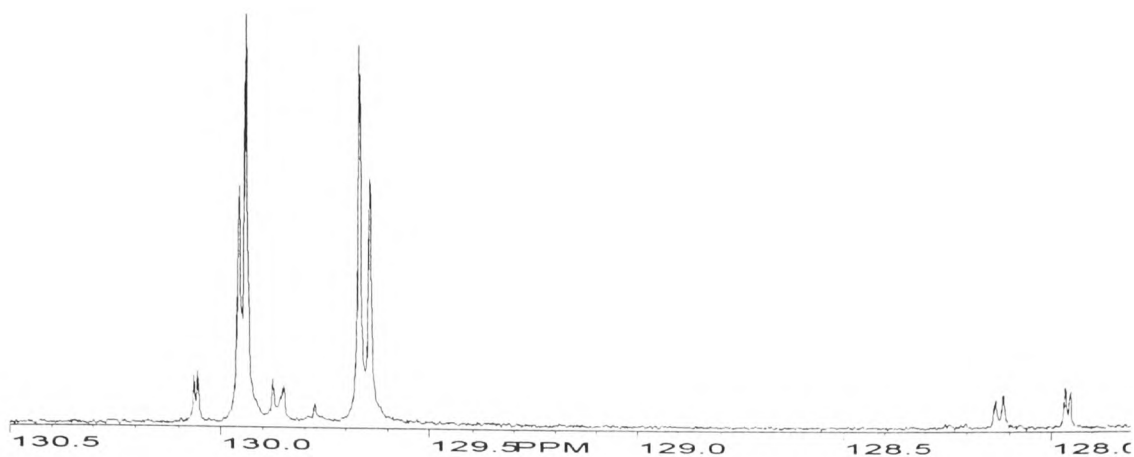


Figure D10  $^{13}\text{C}$  alkene region of sample D4

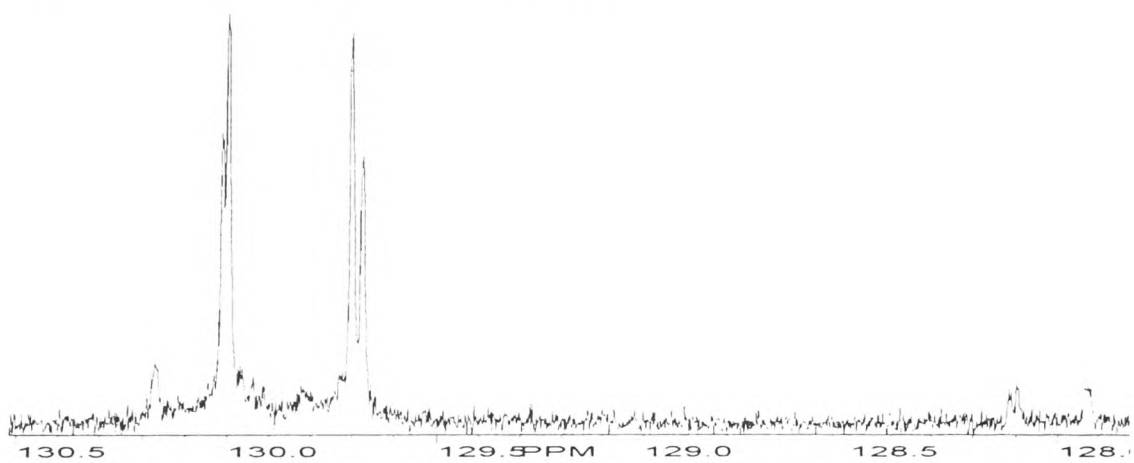


Figure D11  $^{13}\text{C}$  NMR alkene region of sample D4 adulterated with 5 % w/w sunflower oil

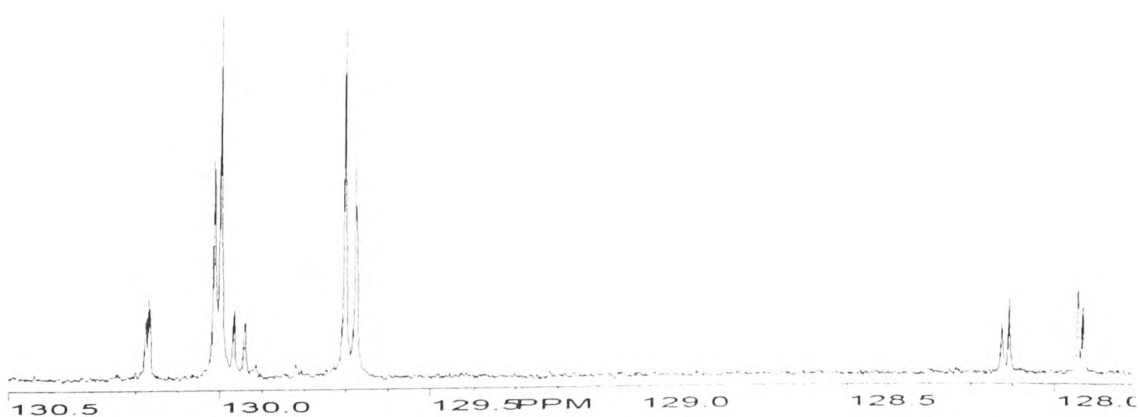


Figure D12  $^{13}\text{C}$  NMR alkene region of sample D4 adulterated with 10 % w/w sunflower oil

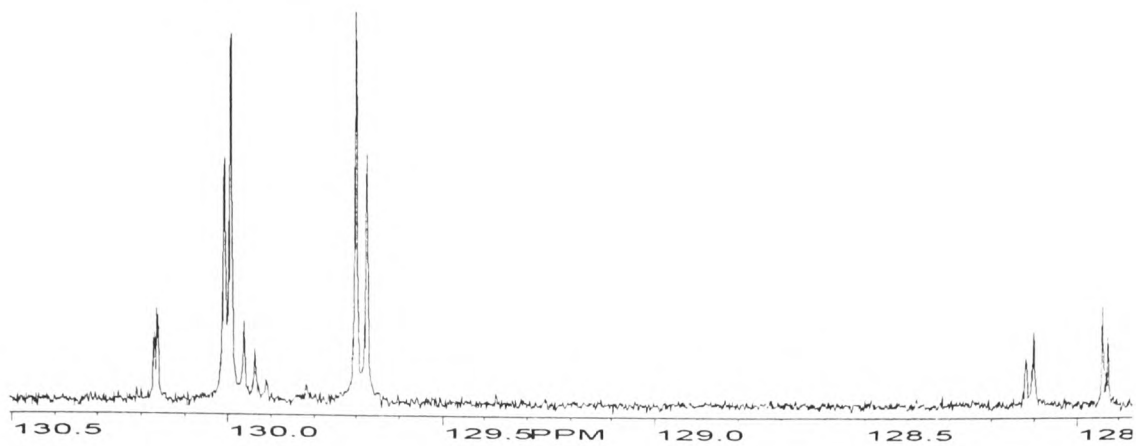


Figure D13  $^{13}\text{C}$  NMR alkene region of sample D5

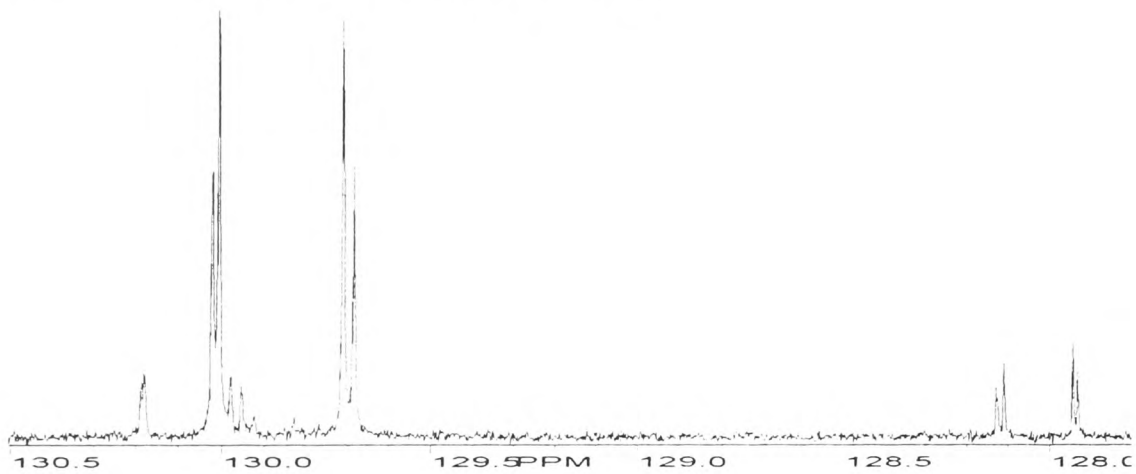


Figure D14  $^{13}\text{C}$  NMR alkene region of sample D5 adulterated with 5 % w/w sunflower oil

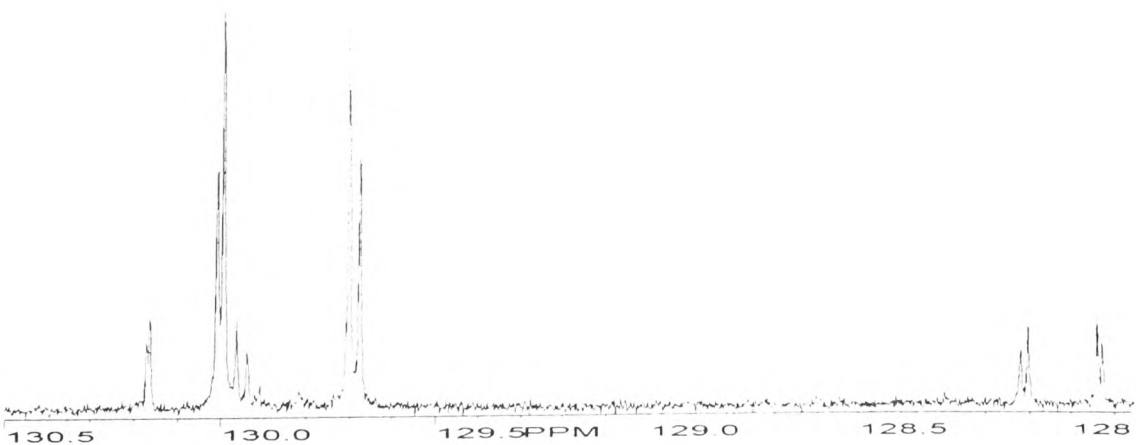


Figure D15  $^{13}\text{C}$  NMR alkene region of sample D5 adulterated with 10 % w/w sunflower oil

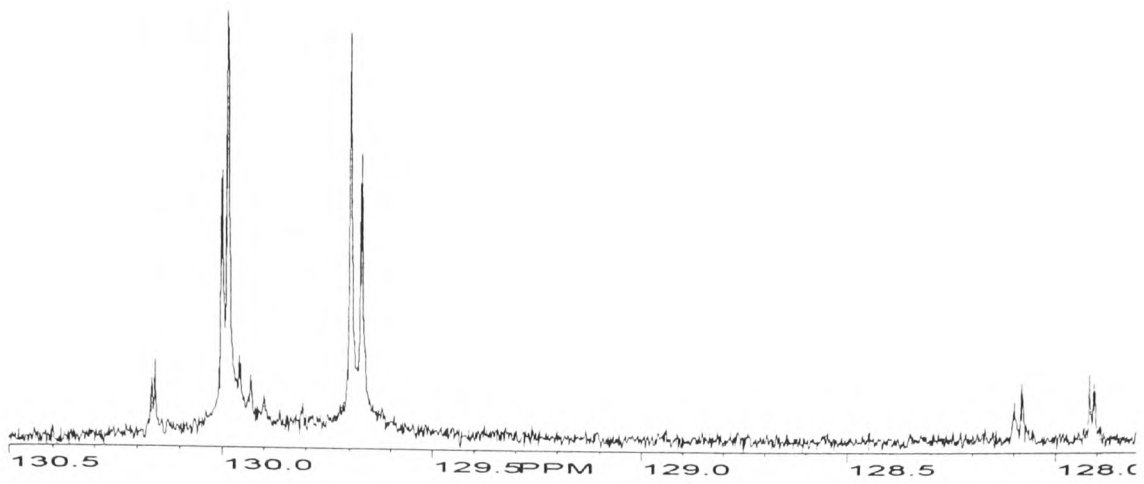


Figure D16 <sup>13</sup>C NMR alkene region of sample D6

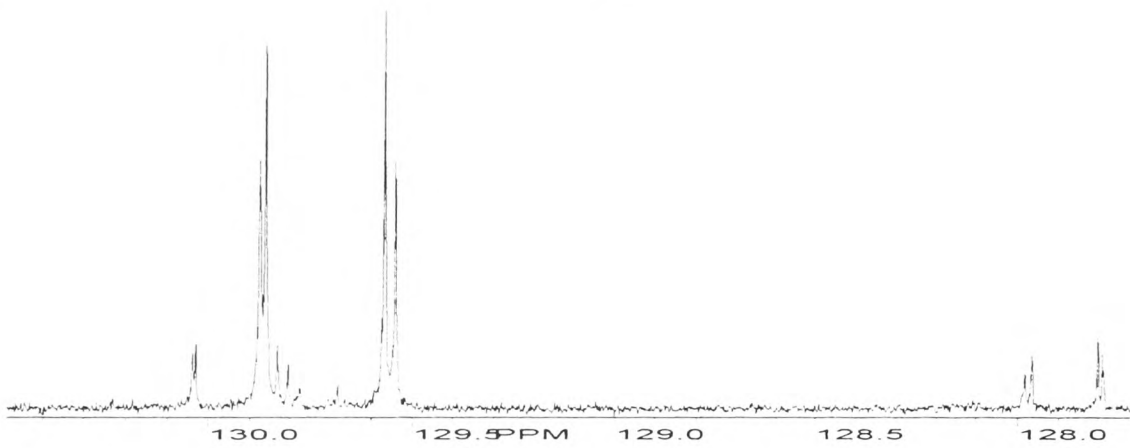


Figure D17 <sup>13</sup>C NMR alkene region of sample D6 adulterated with 5 % w/w sunflower oil

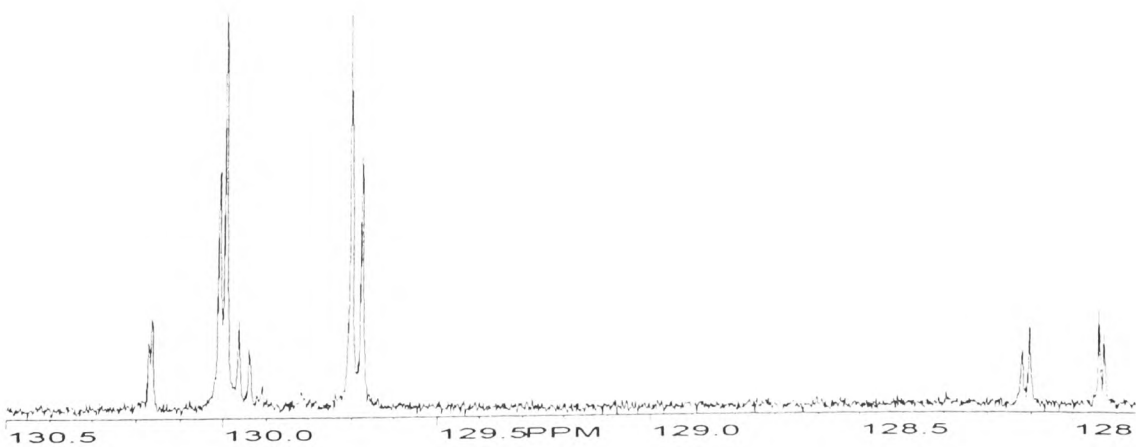


Figure D18 <sup>13</sup>C NMR alkene region of sample D6 adulterated with 10 % w/w sunflower oil

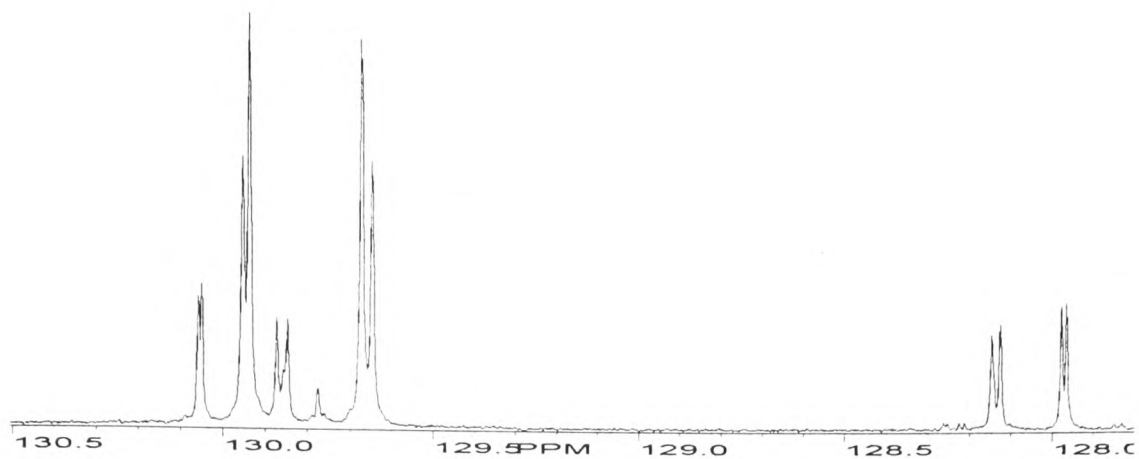


Figure D19  $^{13}\text{C}$  NMR alkene region of sample D7

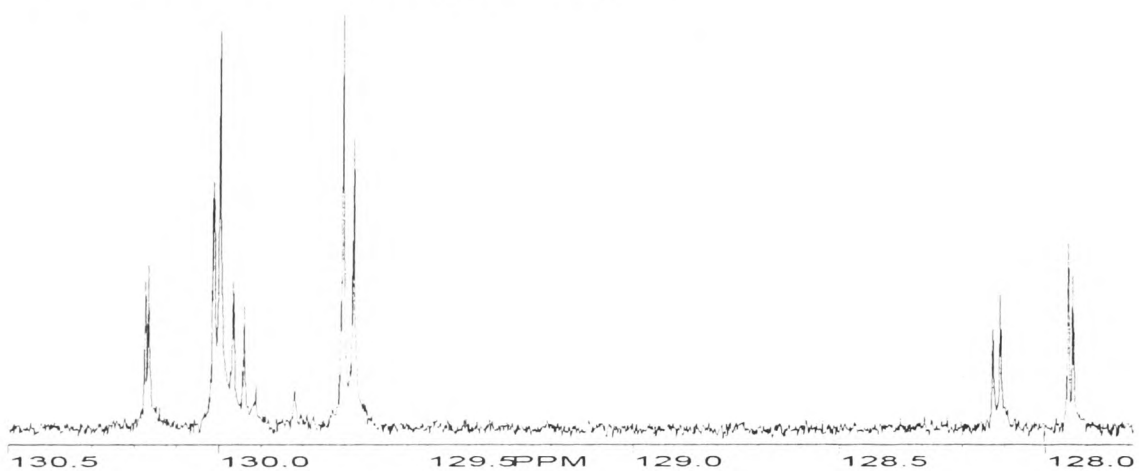


Figure D20  $^{13}\text{C}$  NMR alkene region of sample D7 adulterated with 5 % w/w sunflower oil

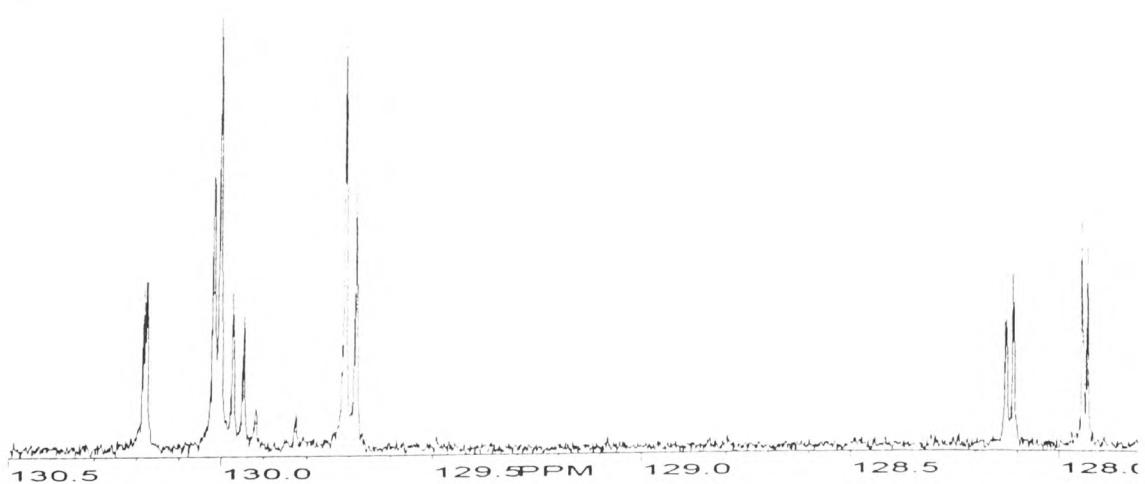


Figure D21  $^{13}\text{C}$  NMR alkene region of sample D7 adulterated with 10 % w/w sunflower oil

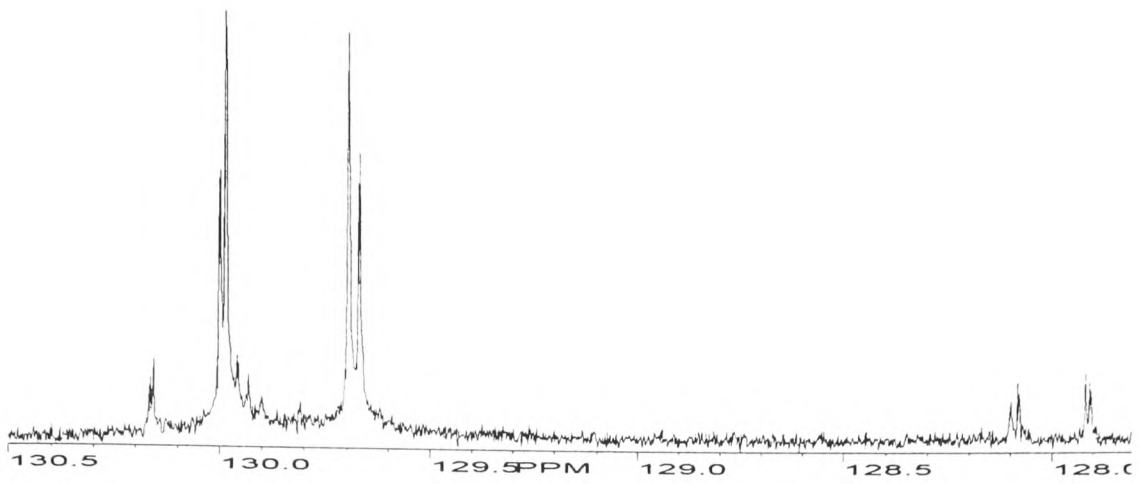


Figure D22  $^{13}\text{C}$  NMR alkene region of sample D8

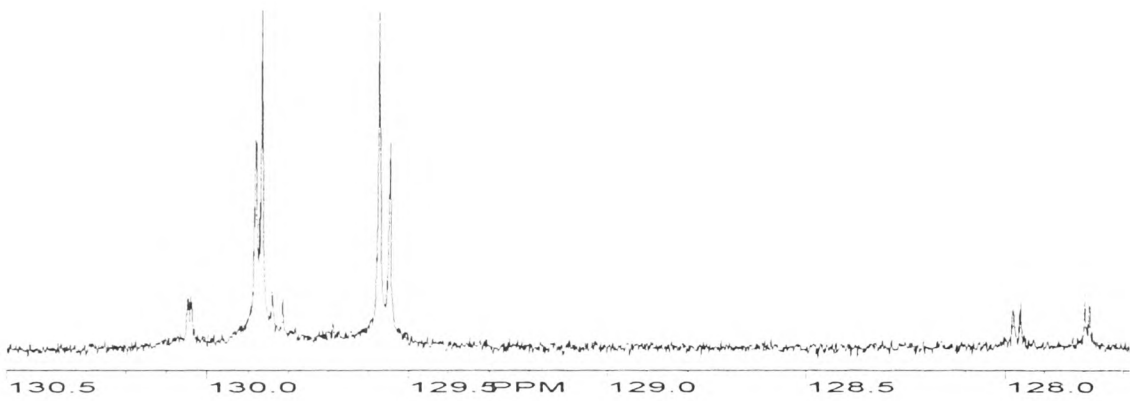


Figure D23  $^{13}\text{C}$  NMR alkene region of sample D8 adulterated with 5 % w/w sunflower oil

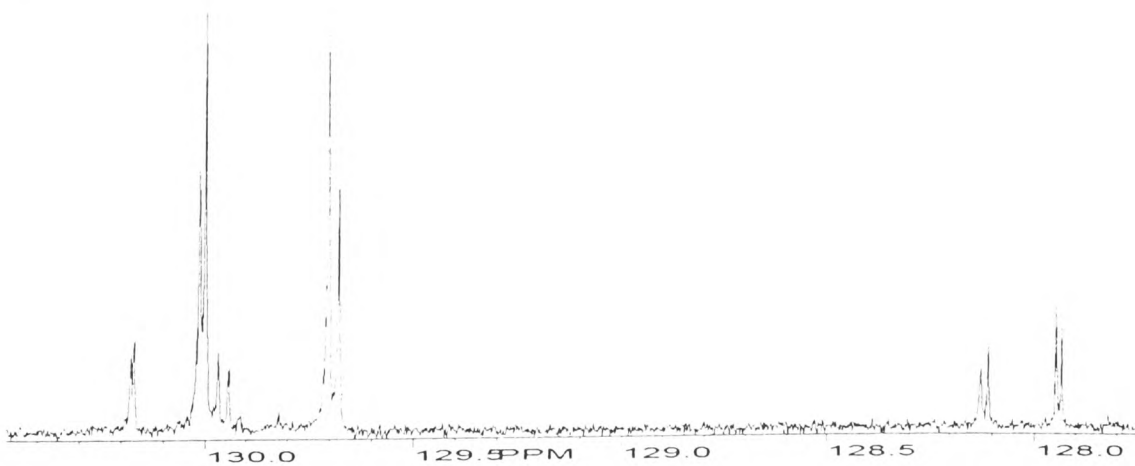


Figure D24  $^{13}\text{C}$  NMR alkene region of sample D8 adulterated with 10 % w/w sunflower oil

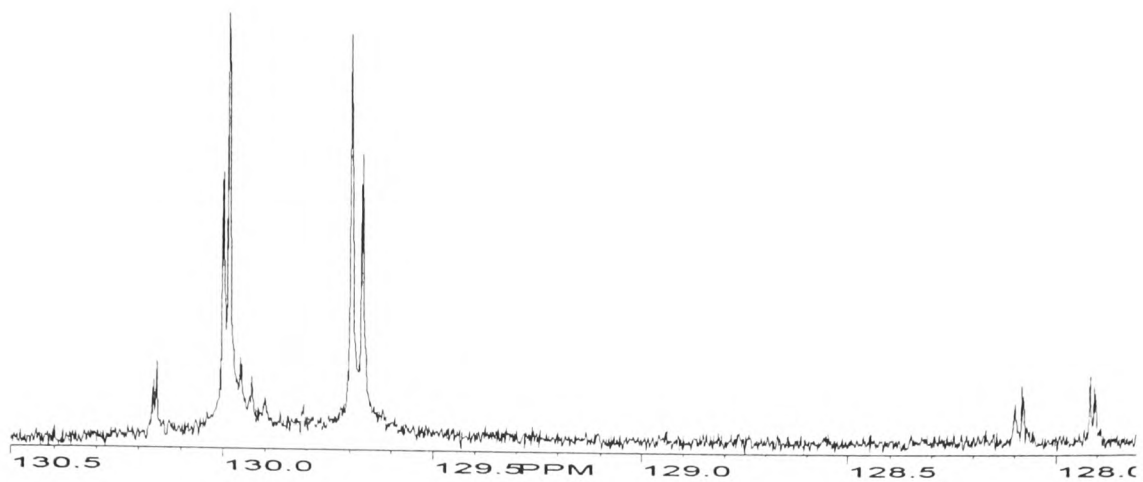


Figure D25  $^{13}\text{C}$  NMR alkene region of sample D9

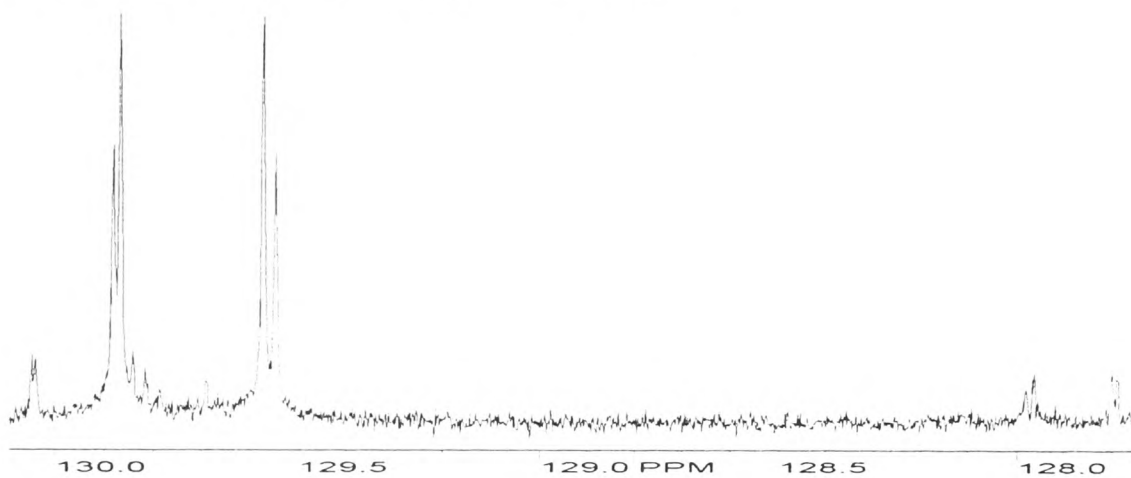


Figure D26  $^{13}\text{C}$  NMR alkene region of sample D9 adulterated with 5 % w/w sunflower oil

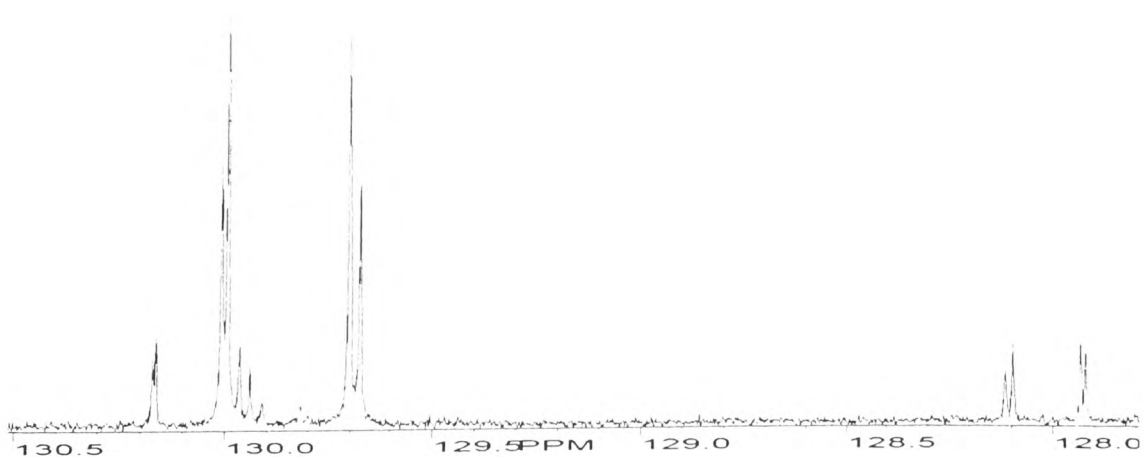


Figure D27  $^{13}\text{C}$  NMR alkene region of sample D9 adulterated with 10 % w/w sunflower oil



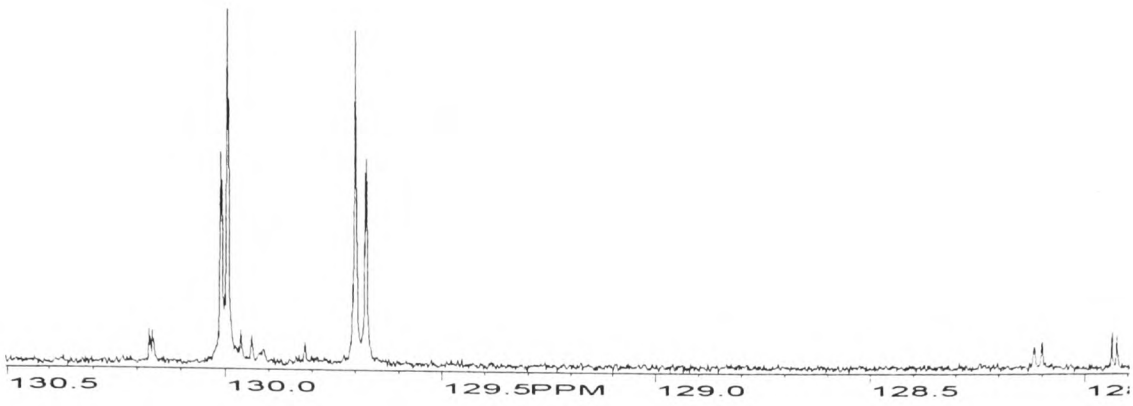


Figure D28  $^{13}\text{C}$  NMR alkene region of sample D10

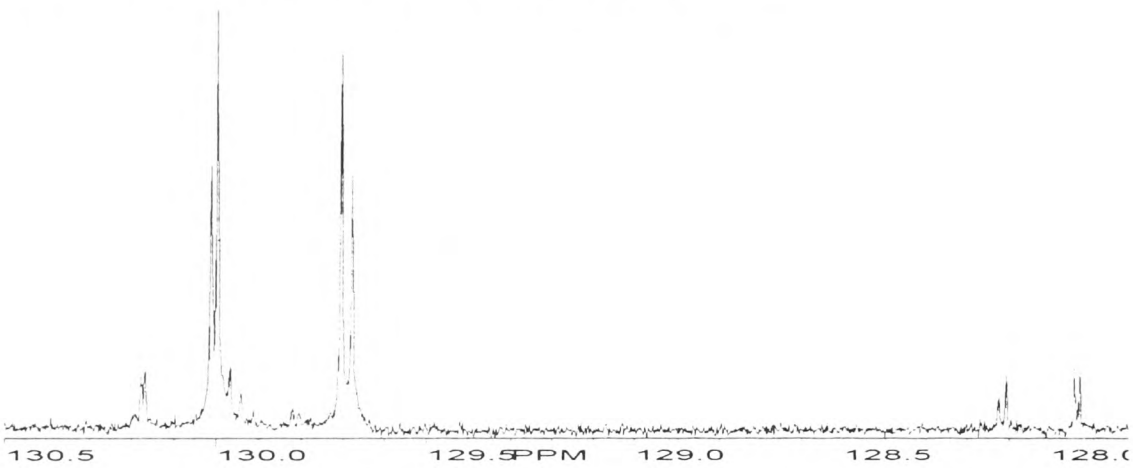


Figure D29  $^{13}\text{C}$  NMR alkene region of sample D10 adulterated with 5 % w/w sunflower oil

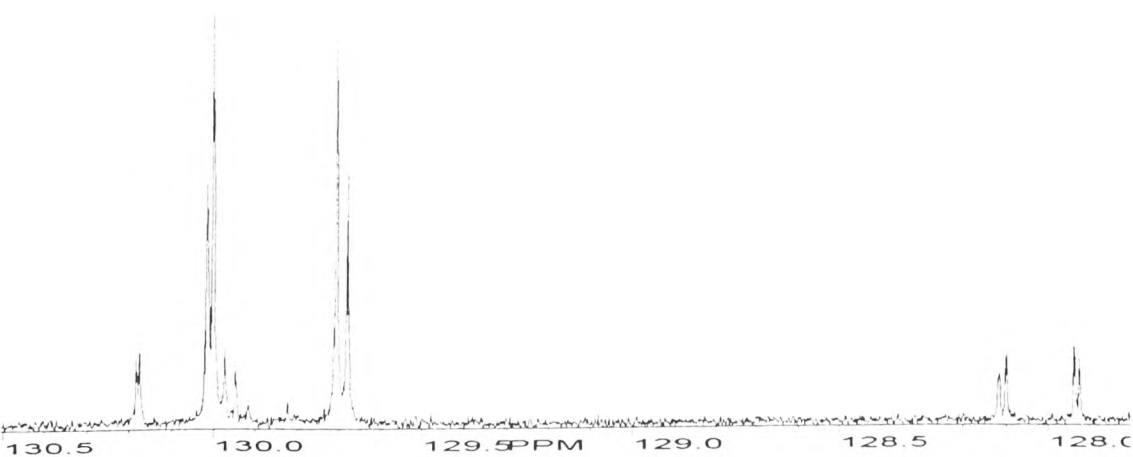


Figure D30  $^{13}\text{C}$  NMR alkene region of sample D10 adulterated with 10 % w/w sunflower oil

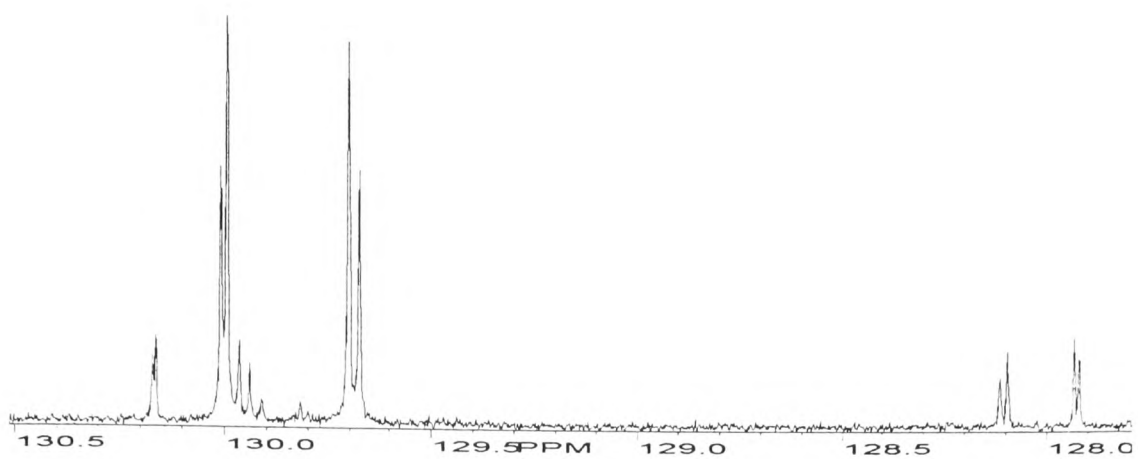


Figure D31  $^{13}\text{C}$  NMR alkene region of sample D11

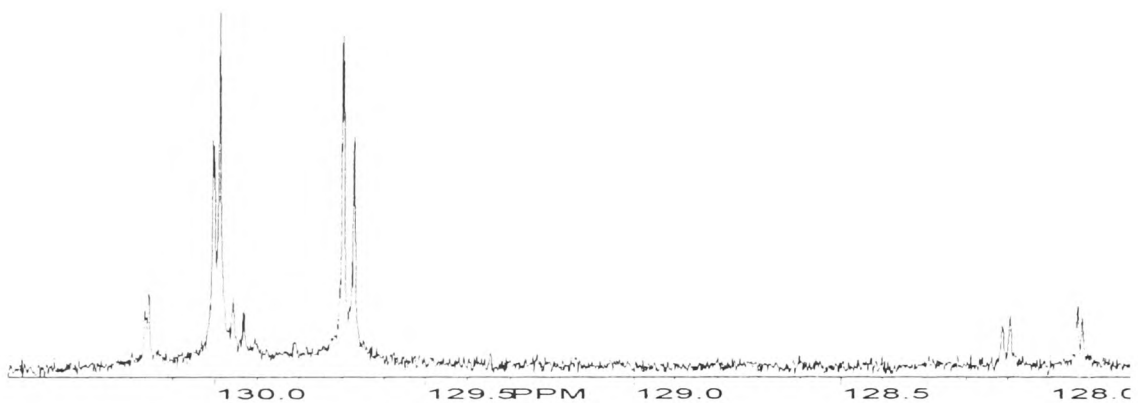


Figure D32  $^{13}\text{C}$  NMR alkene region of sample D11 adulterated with 5 % w/w sunflower oil

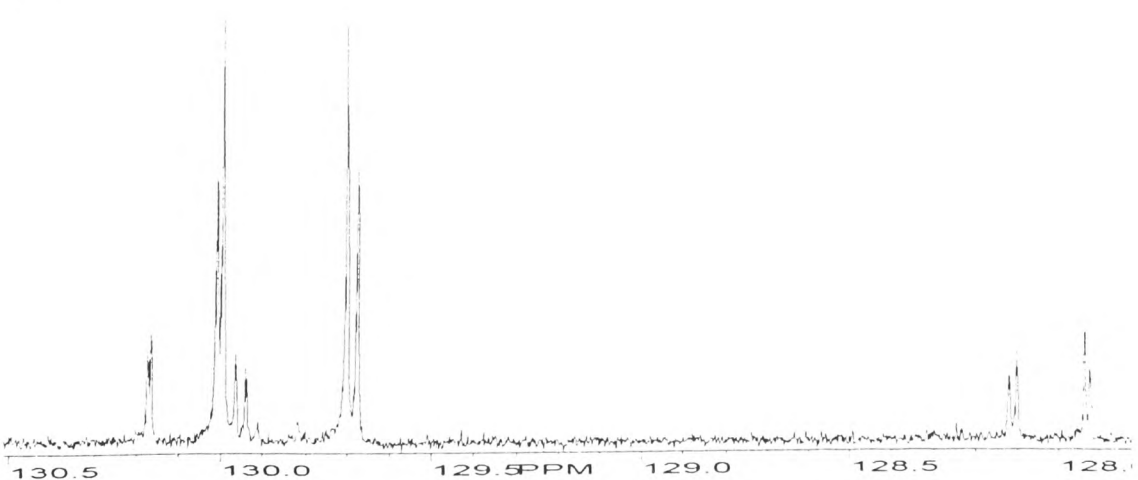


Figure D33  $^{13}\text{C}$  NMR alkene region of sample D11 adulterated with 10 % w/w sunflower oil

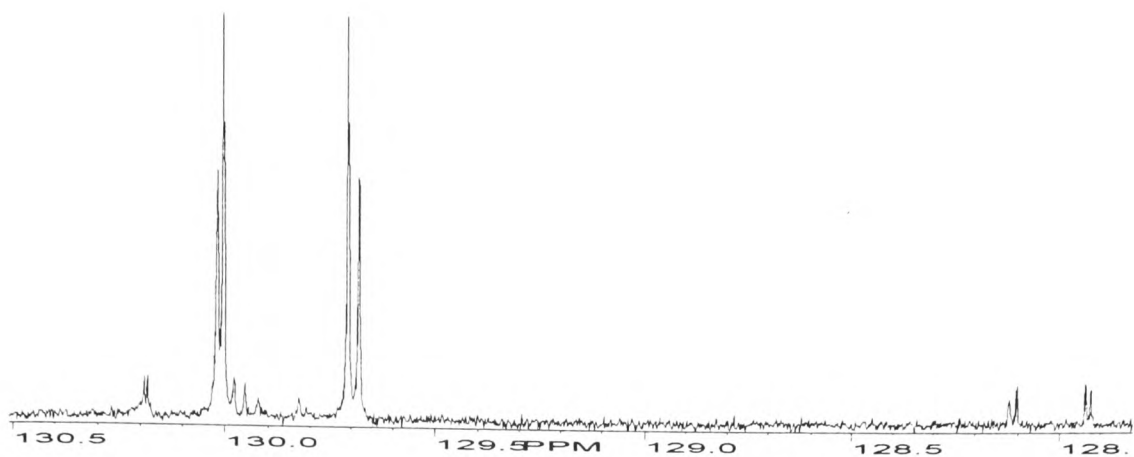


Figure D34  $^{13}\text{C}$  NMR alkene region of sample D12

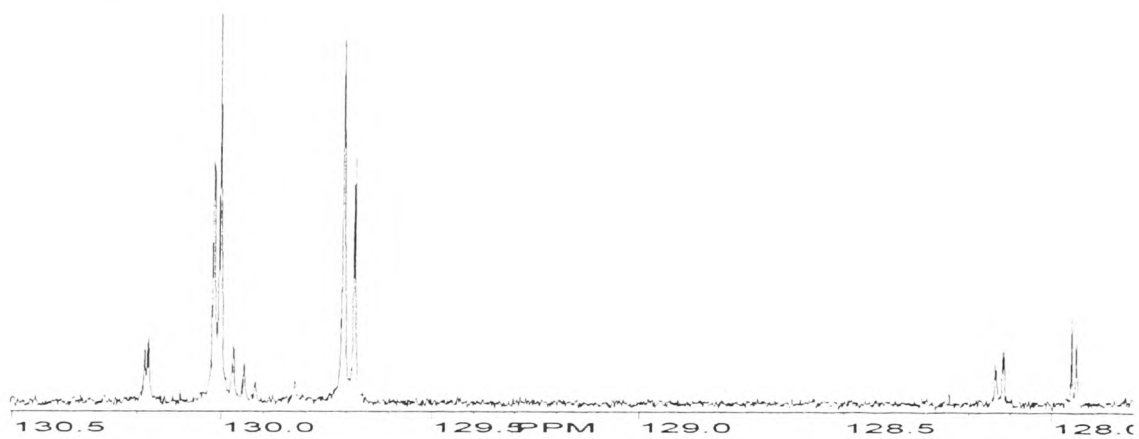


Figure D35  $^{13}\text{C}$  NMR alkene region of sample D12 adulterated with 5 % w/w sunflower oil

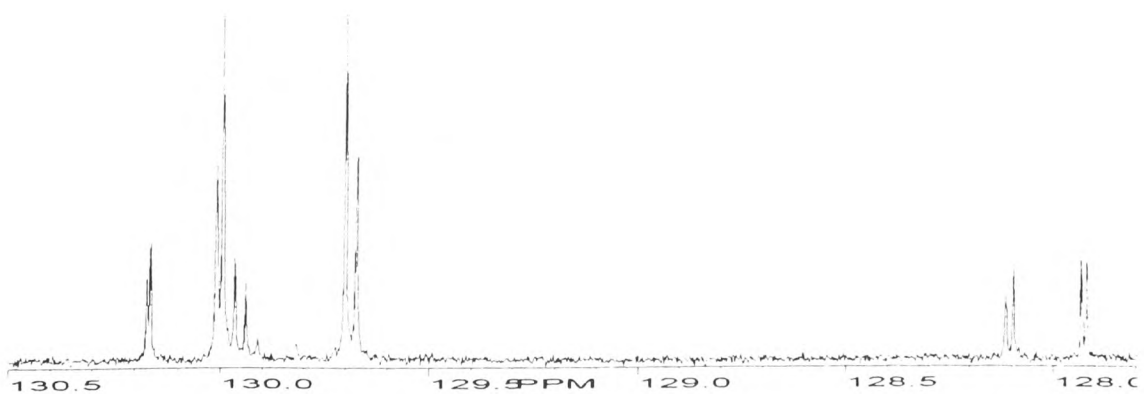


Figure D36  $^{13}\text{C}$  NMR alkene region of sample D12 adulterated with 10 % w/w sunflower oil

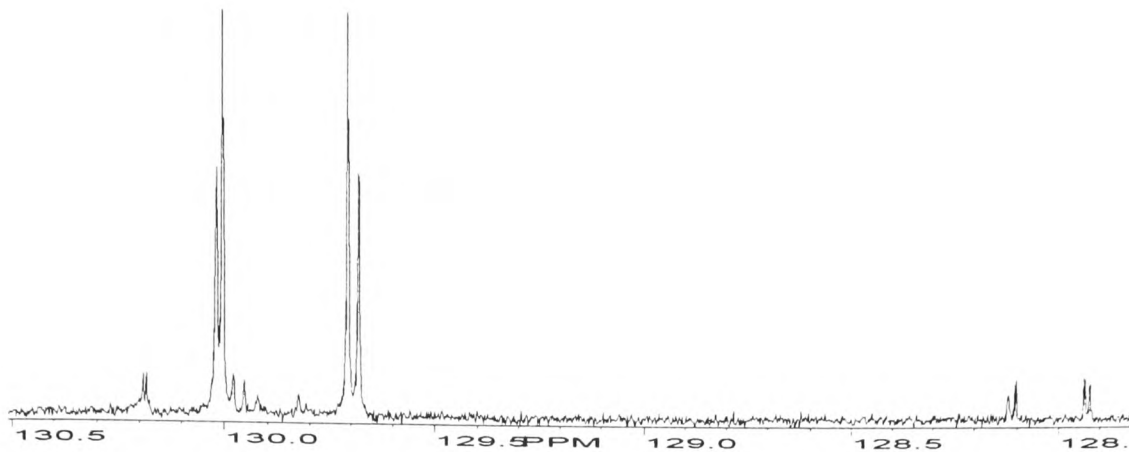


Figure D37  $^{13}\text{C}$  NMR alkene region of sample D13

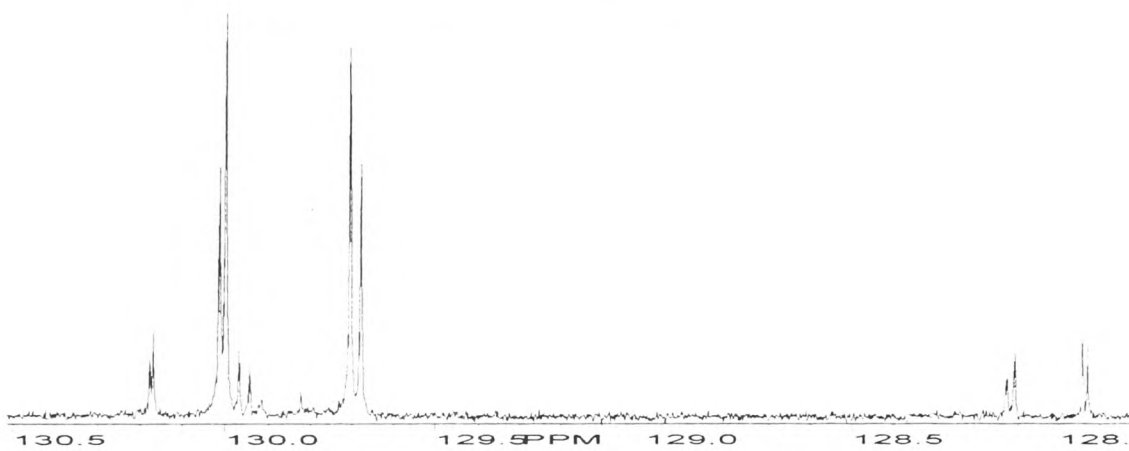


Figure D38  $^{13}\text{C}$  NMR alkene region of sample D13 adulterated with 5 % w/w sunflower oil

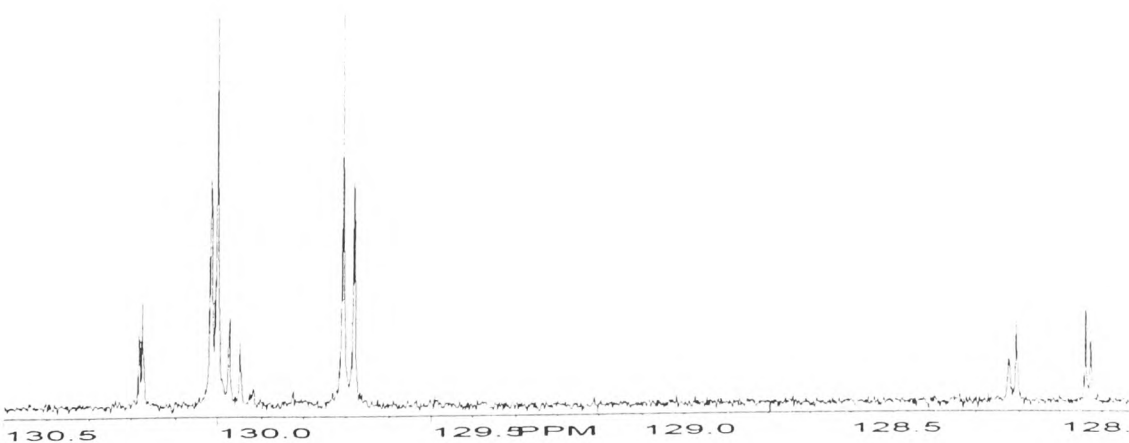
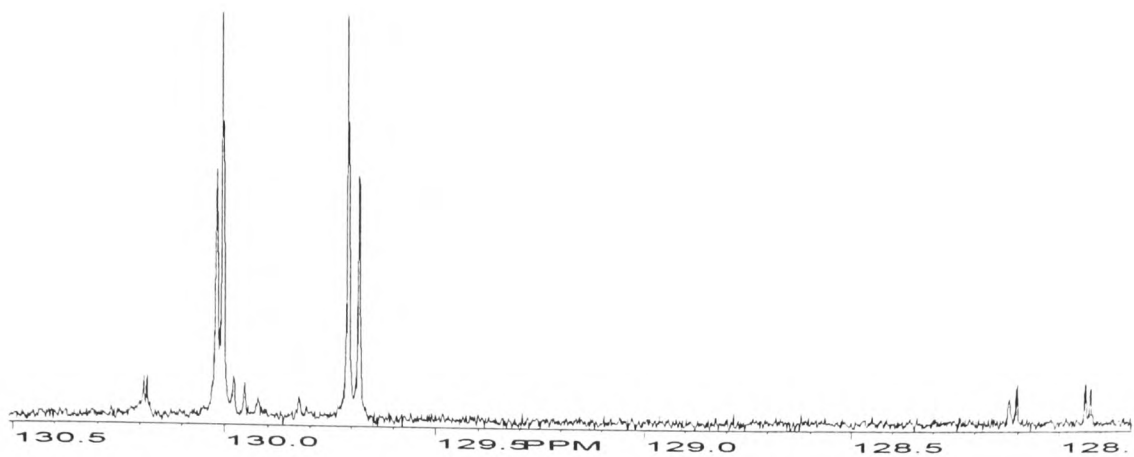
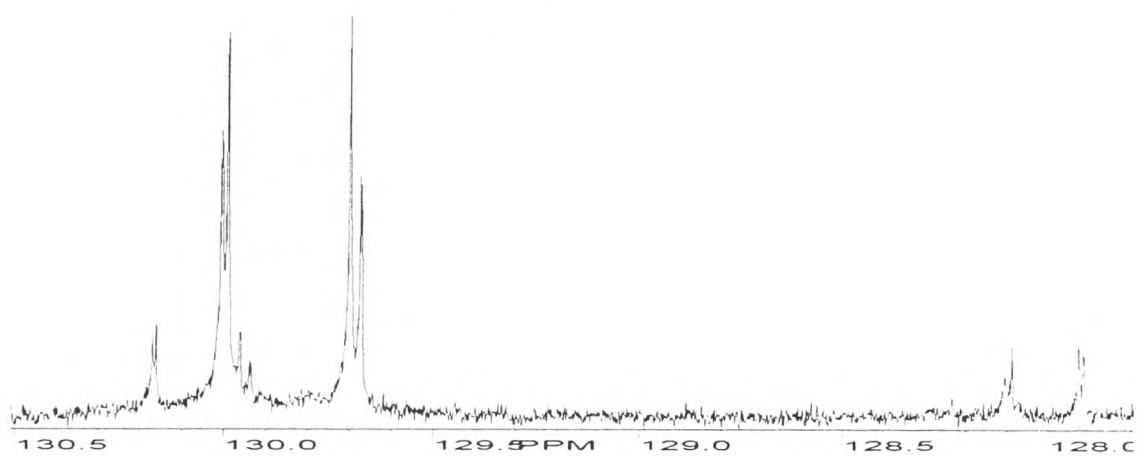


Figure D39  $^{13}\text{C}$  NMR alkene region of sample D13 adulterated with 10 % w/w sunflower oil



**Figure D40**  $^{13}\text{C}$  NMR alkene region of sample D14



**Figure D41**  $^{13}\text{C}$  NMR alkene region of sample D14 adulterated with 5 % w/w sunflower oil

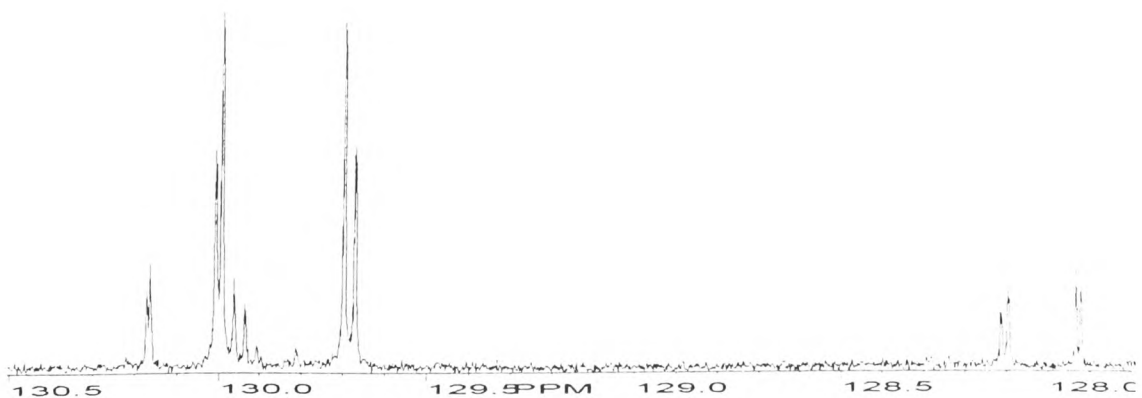


**Figure D42**  $^{13}\text{C}$  NMR alkene region of sample D14 adulterated with 10 % w/w sunflower oil

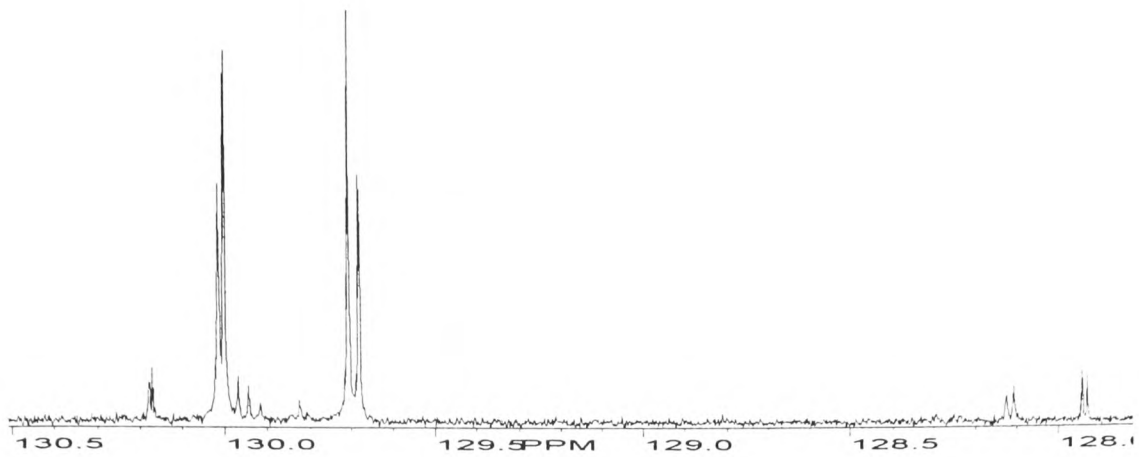


Figure D43  $^{13}\text{C}$  NMR alkene region of sample D15

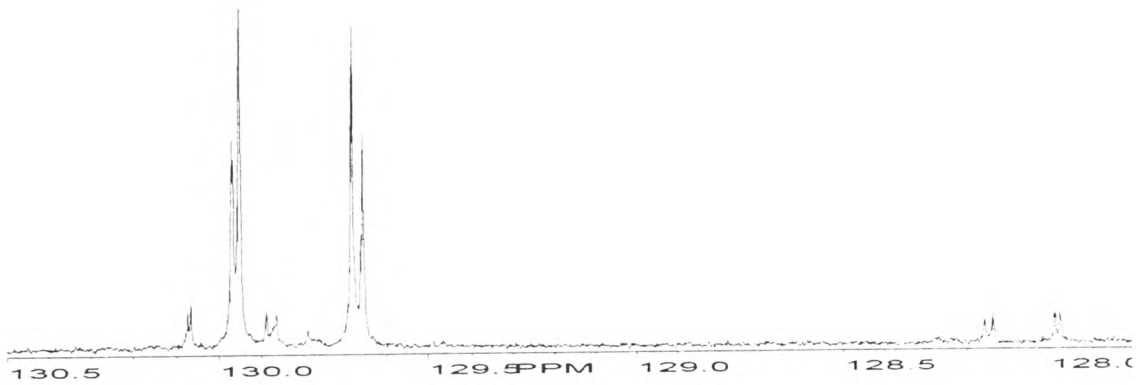


Figure D44  $^{13}\text{C}$  NMR alkene region of sample D15 adulterated with 5 % w/w sunflower oil

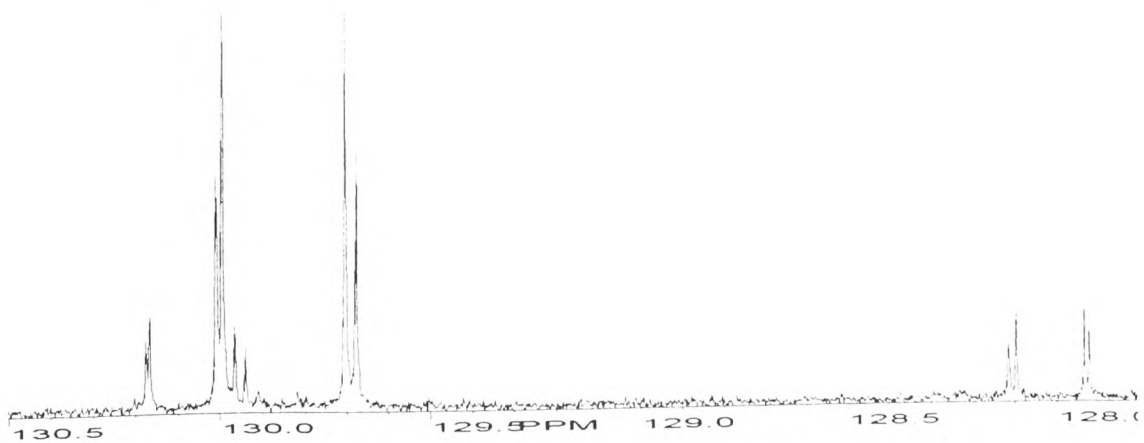


Figure D45  $^{13}\text{C}$  NMR alkene region of sample D15 adulterated with 10 % w/w sunflower oil

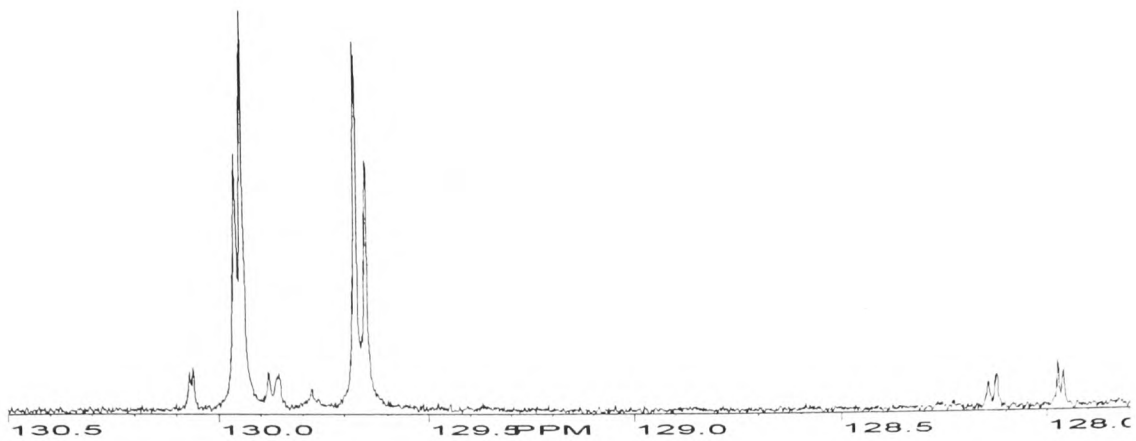


Figure D46  $^{13}\text{C}$  NMR alkene region of sample D16

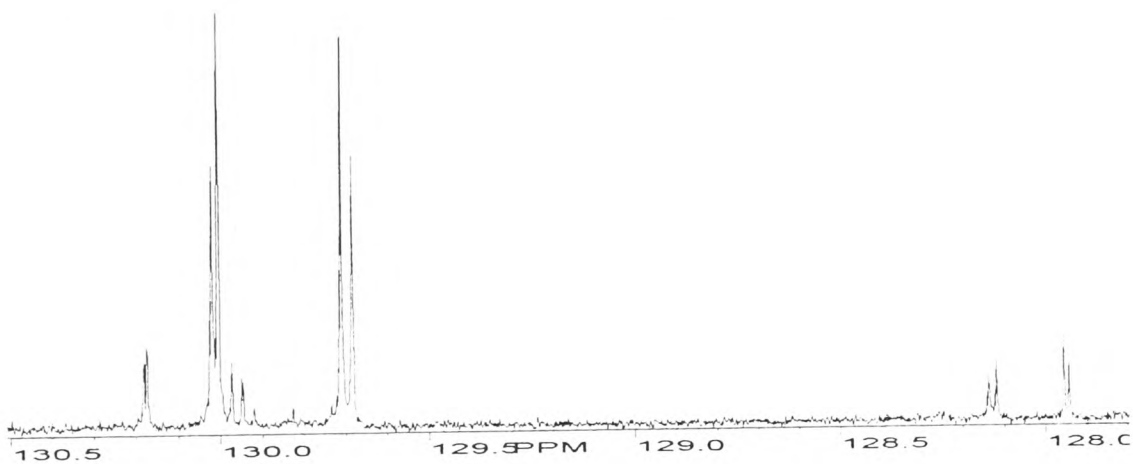


Figure D47  $^{13}\text{C}$  NMR alkene region of sample D16 adulterated with 5 % w/w sunflower oil

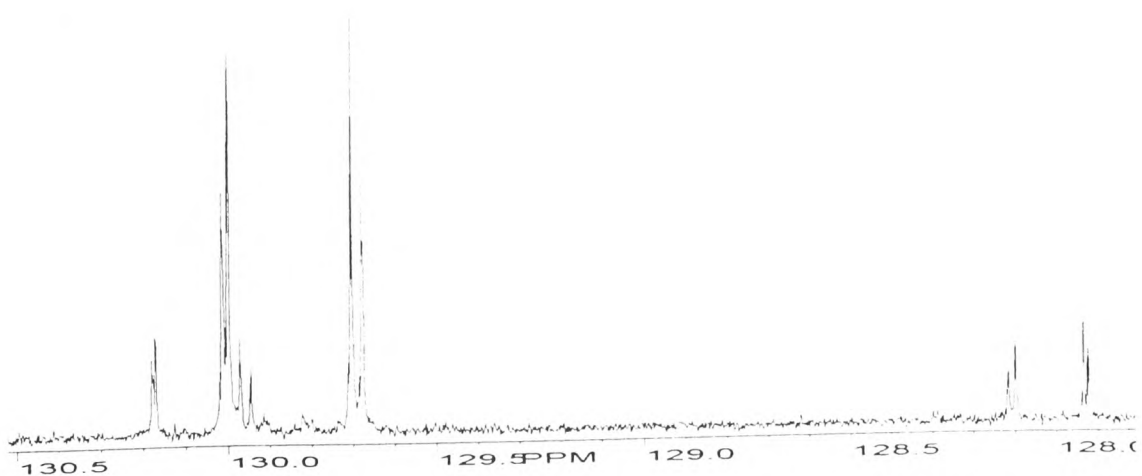


Figure D48  $^{13}\text{C}$  NMR alkene region of sample D16 adulterated with 10 % w/w sunflower oil

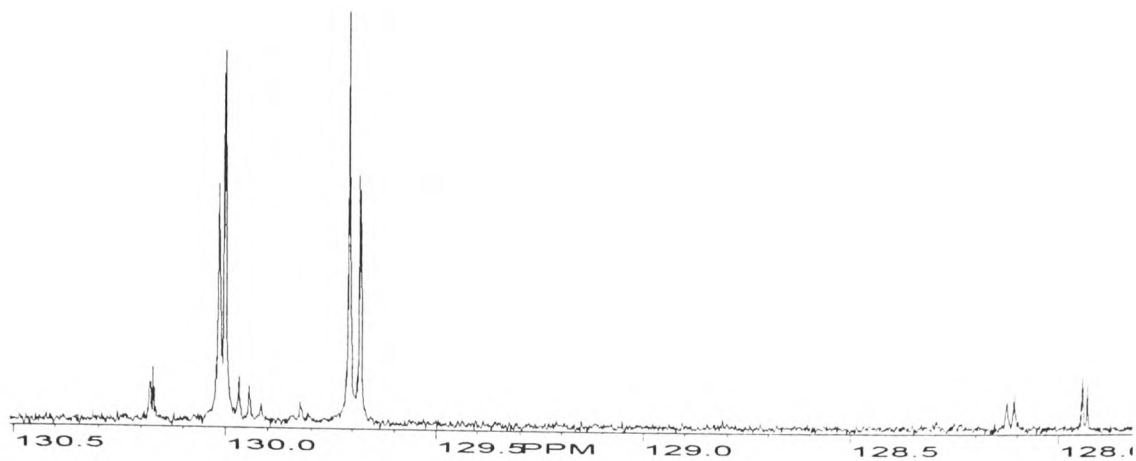


Figure D49  $^{13}\text{C}$  NMR alkene region of sample D17

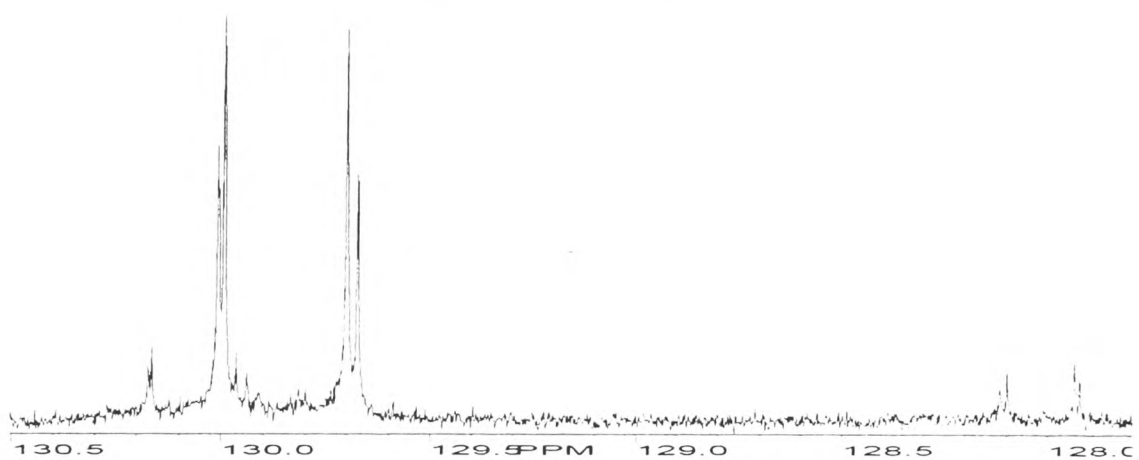


Figure D50  $^{13}\text{C}$  NMR alkene region of sample D17 adulterated with 5 % w/w sunflower oil

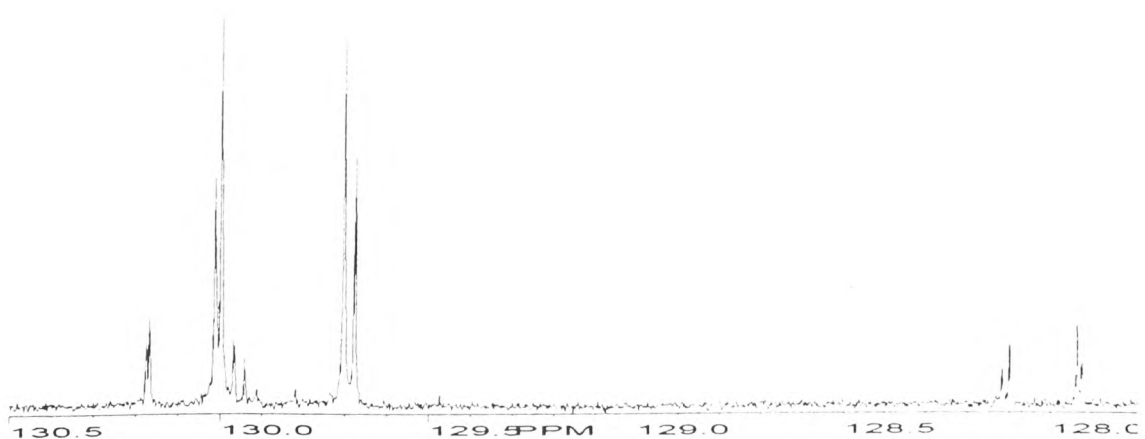
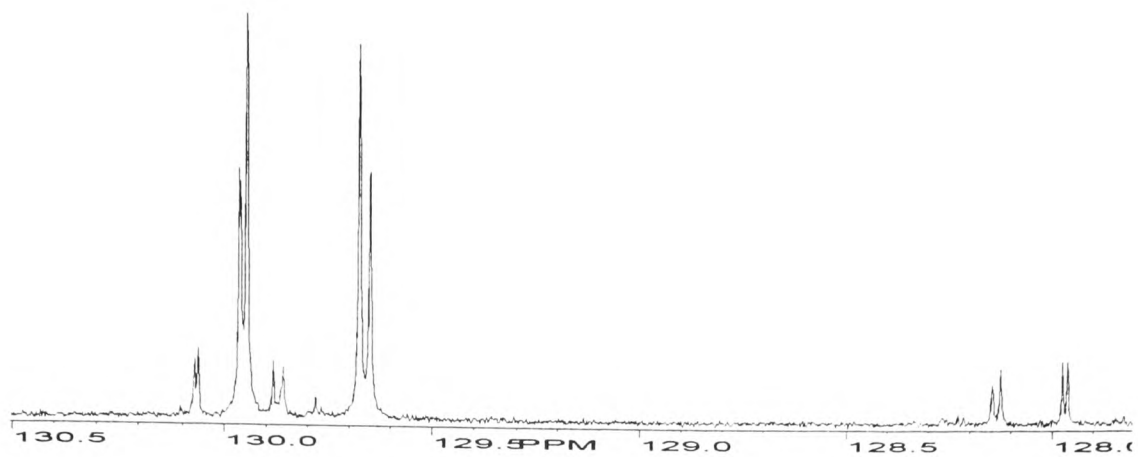
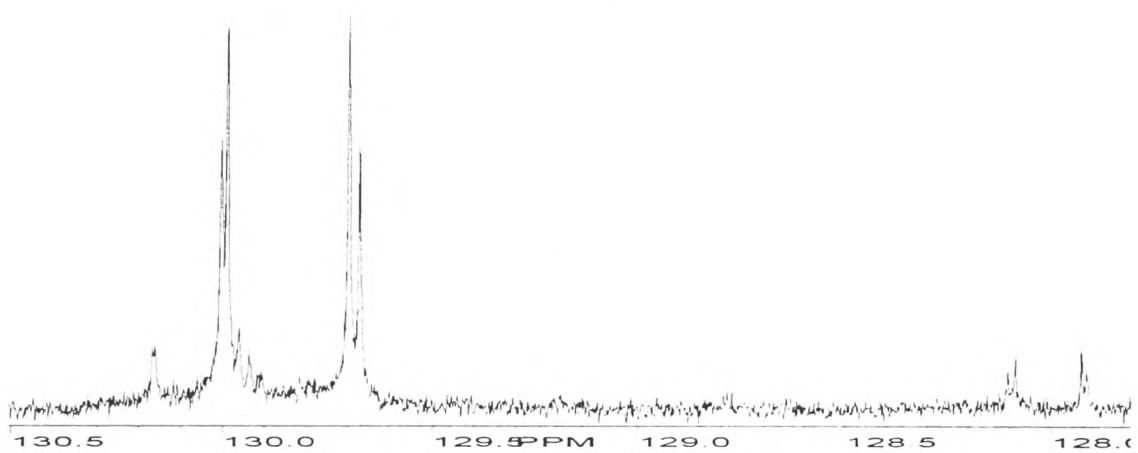


Figure D51  $^{13}\text{C}$  NMR alkene region of sample D17 adulterated with 10 % w/w sunflower oil





**Figure D52**  $^{13}\text{C}$  NMR alkene region of sample D18



**Figure D53**  $^{13}\text{C}$  NMR alkene region of sample D18 adulterated with 5 % w/w sunflower oil

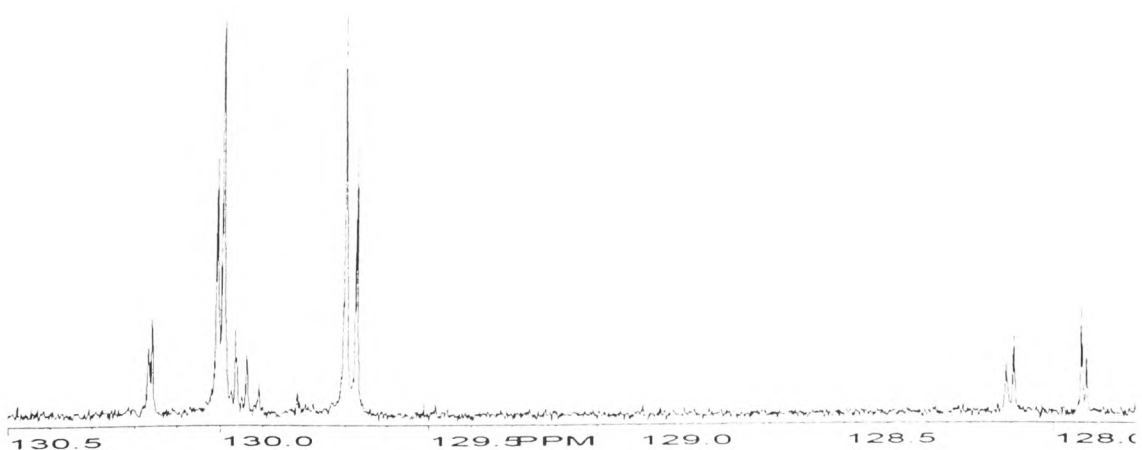


**Figure D54**  $^{13}\text{C}$  NMR alkene region of sample D18 adulterated with 10 % w/w sunflower oil

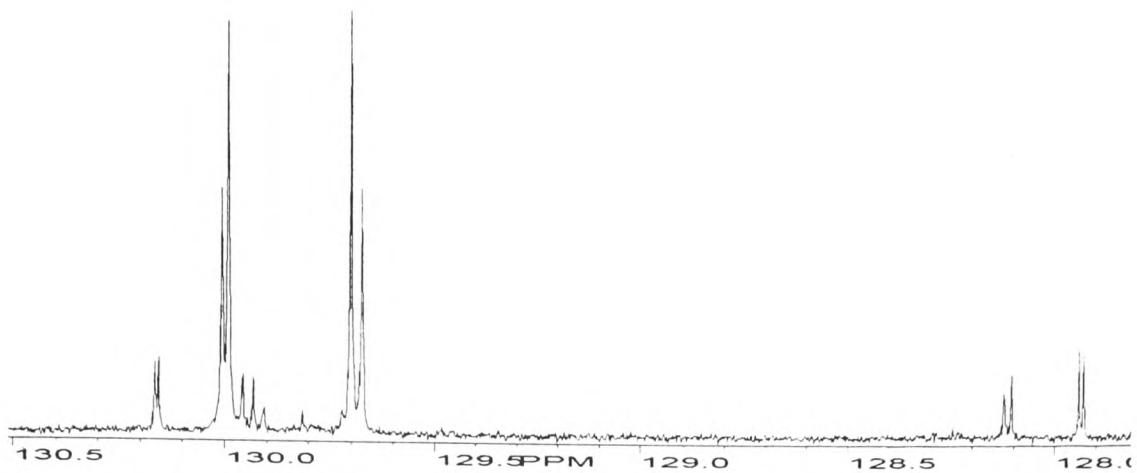


Figure D55  $^{13}\text{C}$  NMR alkene region of sample D19

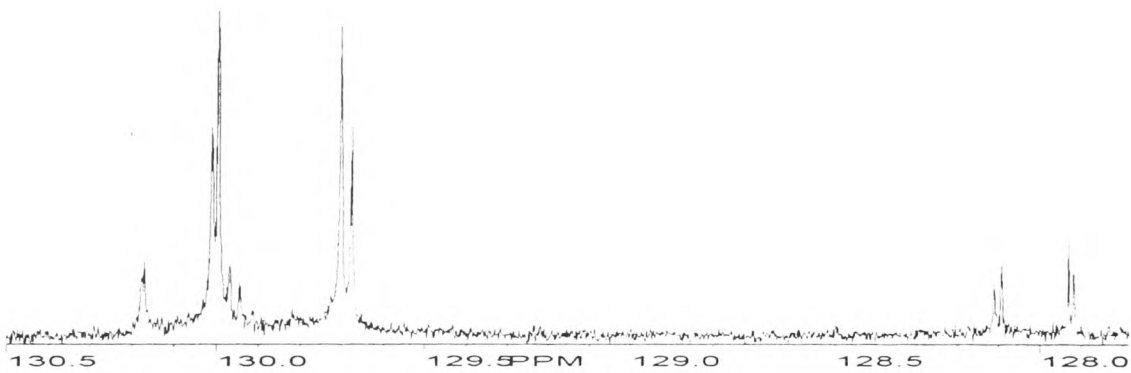


Figure D56  $^{13}\text{C}$  NMR alkene region of sample D19 adulterated with 5 % w/w sunflower oil

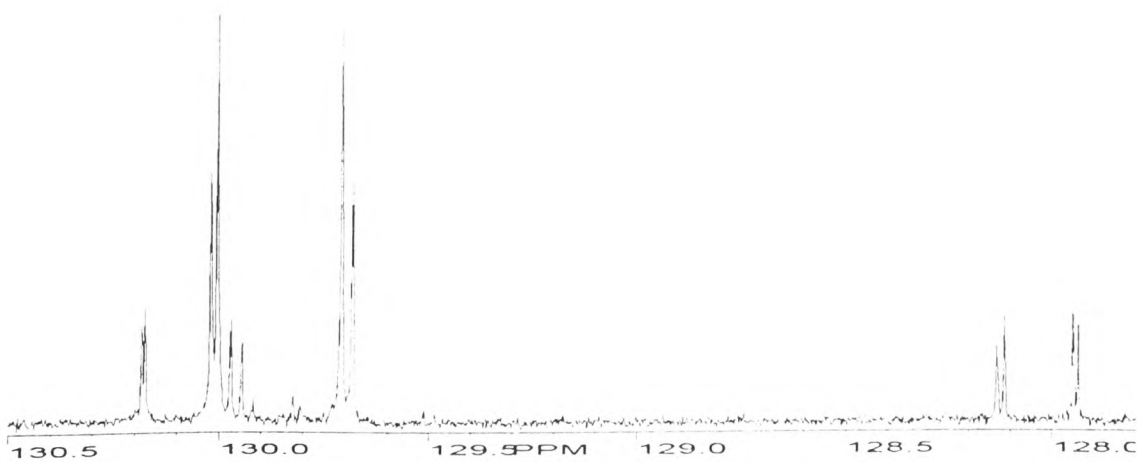
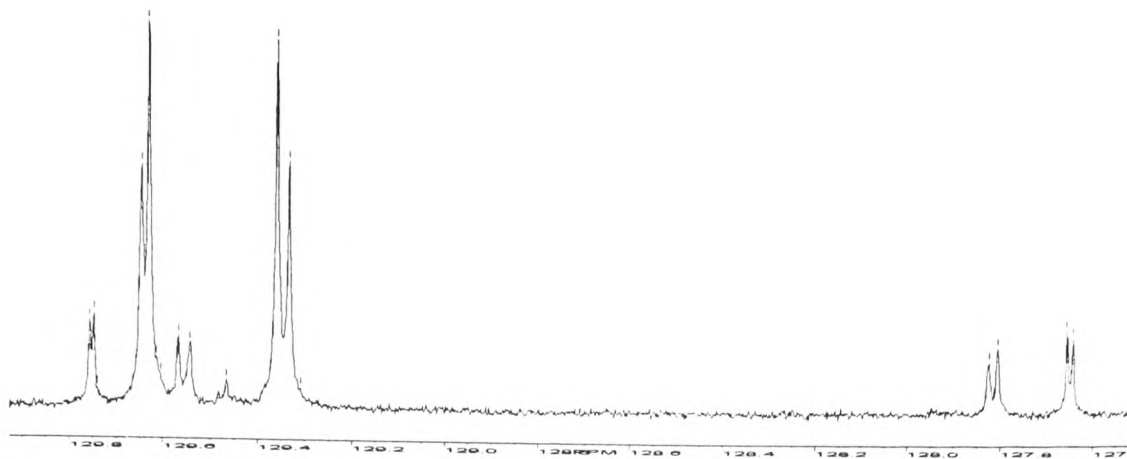
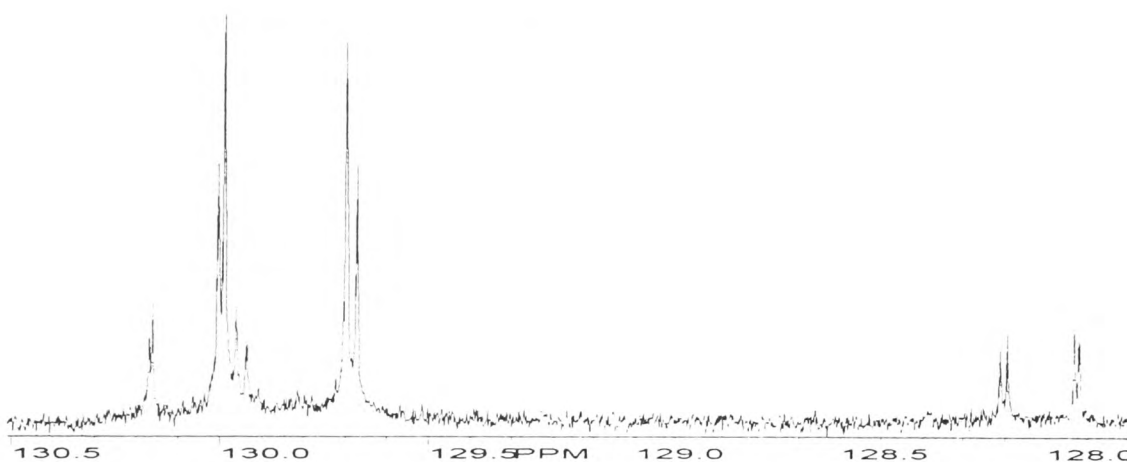


Figure D57  $^{13}\text{C}$  NMR alkene region of sample D19 adulterated with 10 % w/w sunflower oil



**Figure D58**  $^{13}\text{C}$  NMR alkene region of sample D20



**Figure D59**  $^{13}\text{C}$  NMR alkene region of sample D20 adulterated with 5 % w/w sunflower oil

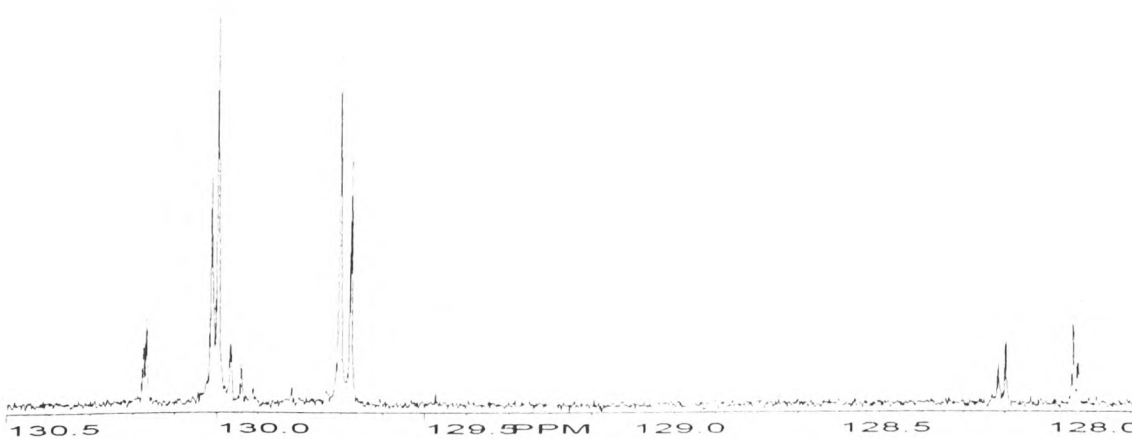


**Figure D60**  $^{13}\text{C}$  NMR alkene region of sample D20 adulterated with 10 % w/w sunflower oil

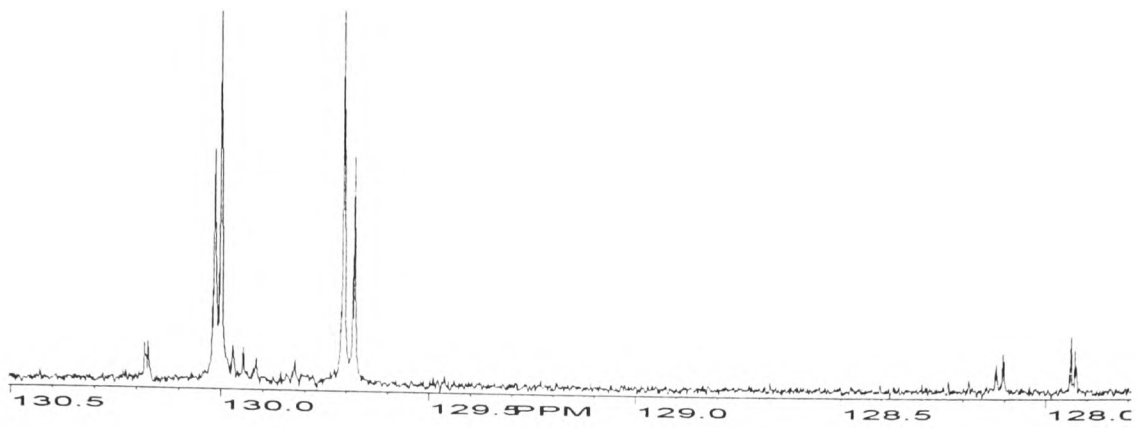


**Figure D61**  $^{13}\text{C}$  NMR alkene region of sample D21

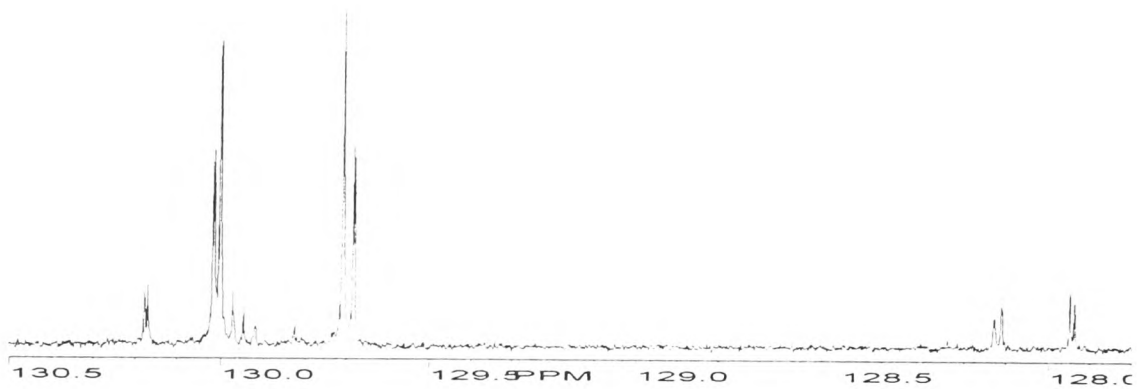


**Figure D62**  $^{13}\text{C}$  NMR alkene region of sample D21 adulterated with 5 % w/w sunflower oil

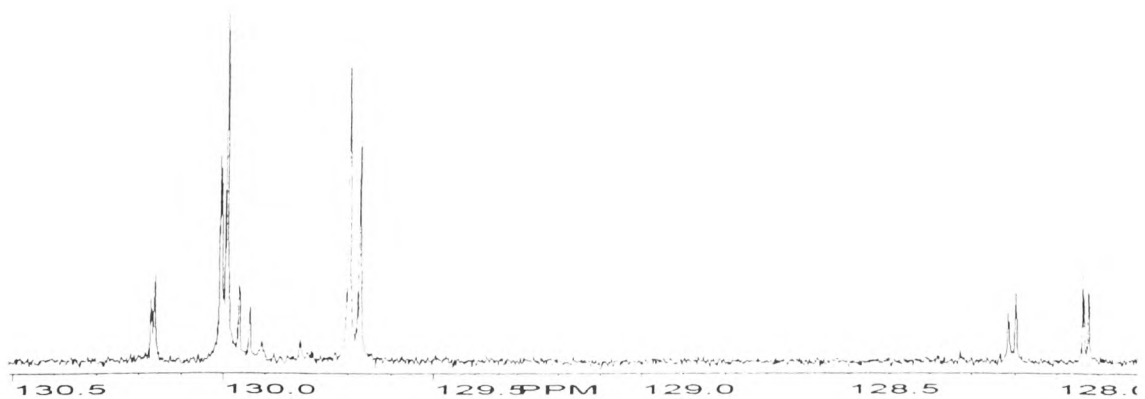


**Figure D63**  $^{13}\text{C}$  NMR alkene region of sample D21 adulterated with 10 % w/w sunflower oil

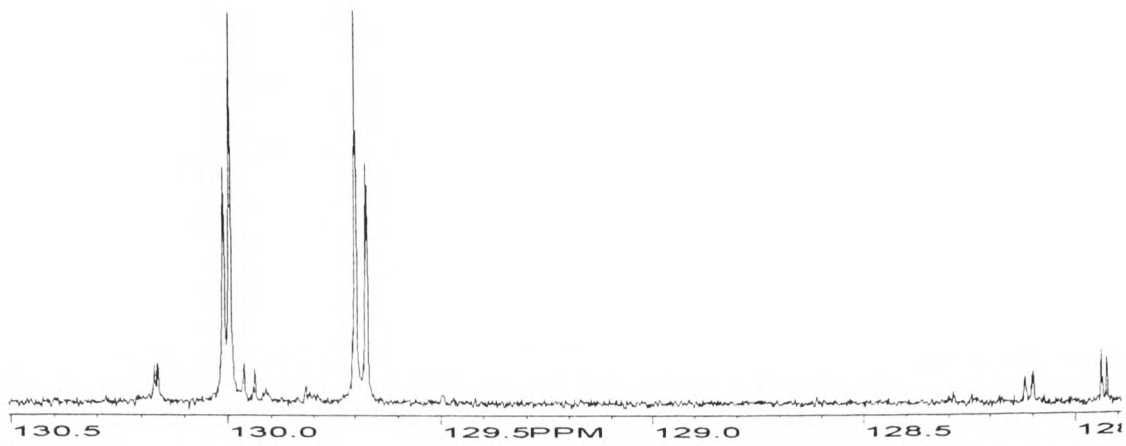


Figure D64  $^{13}\text{C}$  NMR alkene region of sample D22

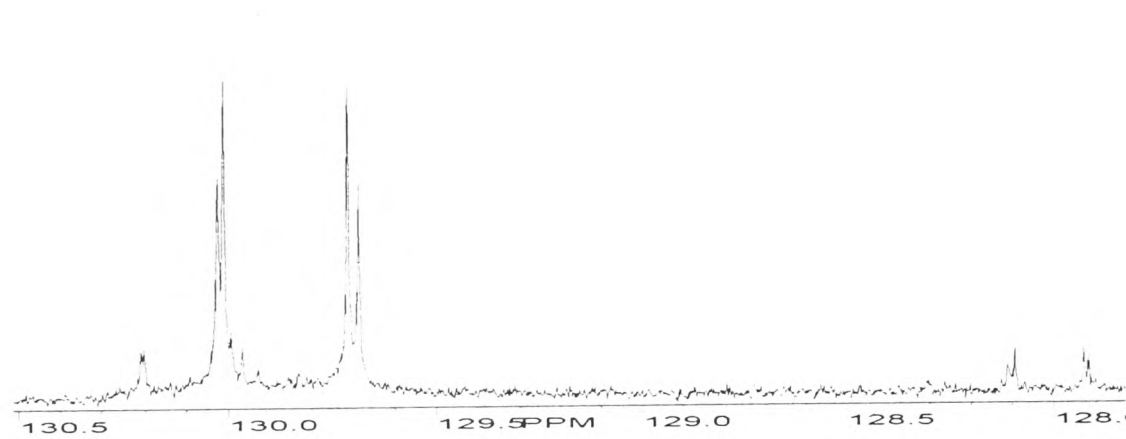


Figure D65  $^{13}\text{C}$  NMR alkene region of sample D22 adulterated with 5 % w/w sunflower oil

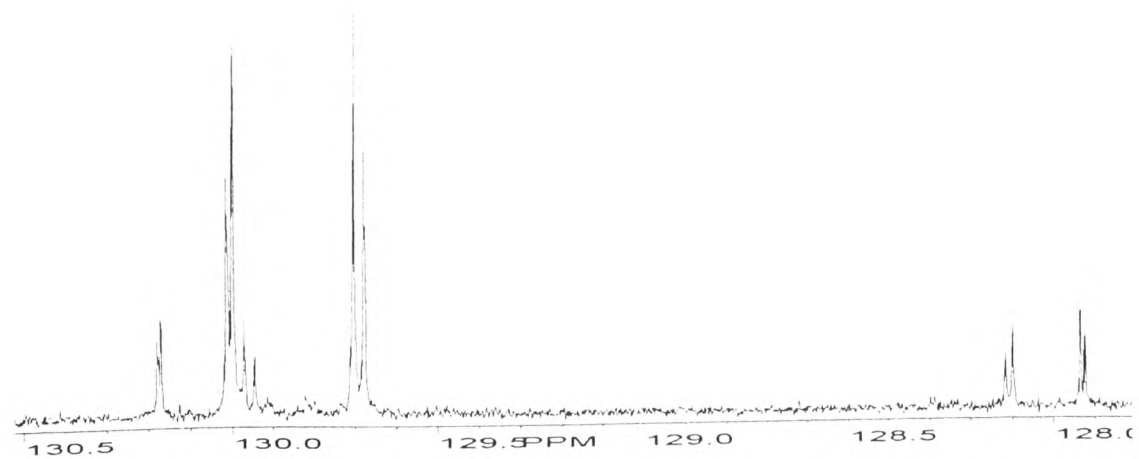


Figure D66  $^{13}\text{C}$  NMR alkene region of sample D22 adulterated with 10 % w/w sunflower oil

## APPENDIX E

Figure E1 $^1\text{H}$ NMR spectrum of sample D1.....	E1
Figure E2 $^1\text{H}$ NMR spectrum of sample D1 adulterated with 5 % w/w sunflower oil .....	E1
Figure E3 $^1\text{H}$ NMR spectrum of sample D1 adulterated with 10 % w/w sunflower oil ...	E1
Figure E4 $^1\text{H}$ NMR spectrum of sample D2.....	E2
Figure E5 $^1\text{H}$ NMR spectrum of sample D2 adulterated with 5 % w/w sunflower oil .....	E2
Figure E6 $^1\text{H}$ NMR spectrum of sample D2 adulterated with 10 % w/w sunflower oil ...	E2
Figure E7 $^1\text{H}$ NMR spectrum of sample D3.....	E3
Figure E8 $^1\text{H}$ NMR spectrum of sample D3 adulterated with 5 % w/w sunflower oil .....	E3
Figure E9 $^1\text{H}$ NMR spectrum of sample D3 adulterated with 10 % w/w sunflower oil ...	E3
Figure E10 $^1\text{H}$ NMR spectrum of sample D4.....	E4
Figure E11 $^1\text{H}$ NMR spectrum of sample D4 adulterated with 5 % w/w sunflower oil ...	E4
Figure E12 $^1\text{H}$ NMR spectrum of sample D4 adulterated with 10 % w/w sunflower oil .	E4
Figure E13 $^1\text{H}$ NMR spectrum of sample D5.....	E5
Figure E14 $^1\text{H}$ NMR spectrum of sample D5 adulterated with 5 % w/w sunflower oil ...	E5
Figure E15 $^1\text{H}$ NMR spectrum of sample D5 adulterated with 10 % w/w sunflower oil .	E5
Figure E16 $^1\text{H}$ NMR spectrum of sample D6.....	E6

Figure E17 $^1\text{H}$ NMR spectrum of sample D6 adulterated with 5 % w/w sunflower oil ...	E6
Figure E18 $^1\text{H}$ NMR spectrum of sample D6 adulterated with 10 % w/w sunflower oil .	E6
Figure E19 $^1\text{H}$ NMR spectrum of sample D7.....	E7
Figure E20 $^1\text{H}$ NMR spectrum of sample D7 adulterated with 5 % w/w sunflower oil ...	E7
Figure E21 $^1\text{H}$ NMR spectrum of sample D7 adulterated with 10 % w/w sunflower oil .	E7
Figure E22 $^1\text{H}$ NMR spectrum of sample D8.....	E8
Figure E23 $^1\text{H}$ NMR spectrum of sample D8 adulterated with 5 % w/w sunflower oil ...	E8
Figure E24 $^1\text{H}$ NMR spectrum of sample D8 adulterated with 10 % w/w sunflower oil .	E8
Figure E25 $^1\text{H}$ NMR spectrum of sample D9.....	E9
Figure E26 $^1\text{H}$ NMR spectrum of sample D9 adulterated with 5 % w/w sunflower oil ...	E9
Figure E27 $^1\text{H}$ NMR spectrum of sample D9 adulterated with 10 % w/w sunflower oil .	E9
Figure E28 $^1\text{H}$ NMR spectrum of sample D10.....	E10
Figure E29 $^1\text{H}$ NMR spectrum of sample D10 adulterated with 5 % w/w sunflower oil	E10
Figure E30 $^1\text{H}$ NMR spectrum of sample D10 adulterated with 10 % w/w sunflower oil ....	E10
.....	E10
Figure E31 $^1\text{H}$ NMR spectrum of sample D11.....	E11
Figure E32 $^1\text{H}$ NMR spectrum of sample D11 adulterated with 5 % w/w sunflower oil	E11

Figure E33 <sup>1</sup> H NMR spectrum of sample D11 adulterated with 10 % w/w sunflower oil ....	E11
Figure E34 <sup>1</sup> H NMR spectrum of sample D12.....	E12
Figure E35 <sup>1</sup> H NMR spectrum of sample D12 adulterated with 5 % w/w sunflower oil	E12
Figure E36 <sup>1</sup> H NMR spectrum of sample D12 adulterated with 10 % w/w sunflower oil ....	E12
Figure E37 <sup>1</sup> H NMR spectrum of sample D13.....	E13
Figure E38 <sup>1</sup> H NMR spectrum of sample D13 adulterated with 5 % w/w sunflower oil	E13
Figure E39 <sup>1</sup> H NMR spectrum of sample D13 adulterated with 10 % w/w sunflower oil ....	E13
Figure E40 <sup>1</sup> H NMR spectrum of sample D14.....	E14
Figure E41 <sup>1</sup> H NMR spectrum of sample D14 adulterated with 5 % w/w sunflower oil	E14
Figure E42 <sup>1</sup> H NMR spectrum of sample D14 adulterated with 10 % w/w sunflower oil ....	E14
Figure E43 <sup>1</sup> H NMR spectrum of sample D15.....	E15
Figure E44 <sup>1</sup> H NMR spectrum of sample D15 adulterated with 5 % w/w sunflower oil	E15
Figure E45 <sup>1</sup> H NMR spectrum of sample D15 adulterated with 10 % w/w sunflower oil ....	E15
Figure E46 <sup>1</sup> H NMR spectrum of sample D16.....	E16



Figure E47 <sup>1</sup> H NMR spectrum of sample D16 adulterated with 5 % w/w sunflower oil	E16
Figure E48 <sup>1</sup> H NMR spectrum of sample D16 adulterated with 10 % w/w sunflower oil ....	E16
Figure E49 <sup>1</sup> H NMR spectrum of sample D17.....	E17
Figure E50 <sup>1</sup> H NMR spectrum of sample D17 adulterated with 5 % w/w sunflower oil	E17
Figure E51 <sup>1</sup> H NMR spectrum of sample D17 adulterated with 10 % w/w sunflower oil ....	E17
Figure E54 <sup>1</sup> H NMR spectrum of sample D18.....	E18
Figure E55 <sup>1</sup> H NMR spectrum of sample D18 adulterated with 5 % w/w sunflower oil	E18
Figure E56 <sup>1</sup> H NMR spectrum of sample D18 adulterated with 10 % w/w sunflower oil ....	E18
Figure E57 <sup>1</sup> H NMR spectrum of sample D19.....	E19
Figure E58 <sup>1</sup> H NMR spectrum of sample D19 adulterated with 5 % w/w sunflower oil	E19
Figure E59 <sup>1</sup> H NMR spectrum of sample D19 adulterated with 10 % w/w sunflower oil ....	E19
Figure E60 <sup>1</sup> H NMR spectrum of sample D20.....	E20
Figure E61 <sup>1</sup> H NMR spectrum of sample D20 adulterated with 5 % w/w sunflower oil	E20
Figure E62 <sup>1</sup> H NMR spectrum of sample D20 adulterated with 10 % w/w sunflower oil ....	E20

Figure E63 $^1\text{H}$ NMR spectrum of sample D21 .....	E21
Figure E64 $^1\text{H}$ NMR spectrum of sample D21 adulterated with 5 % w/w sunflower oil	E21
Figure E65 $^1\text{H}$ NMR spectrum of sample D21 adulterated with 10 % w/w sunflower oil .... .....	E21
Figure E66 $^1\text{H}$ NMR spectrum of sample D22 .....	E22
Figure E67 $^1\text{H}$ NMR spectrum of sample D22 adulterated with 5 % w/w sunflower oil	E22
Figure E68 $^1\text{H}$ NMR spectrum of sample D22 adulterated with 10 % w/w sunflower oil .... .....	E22

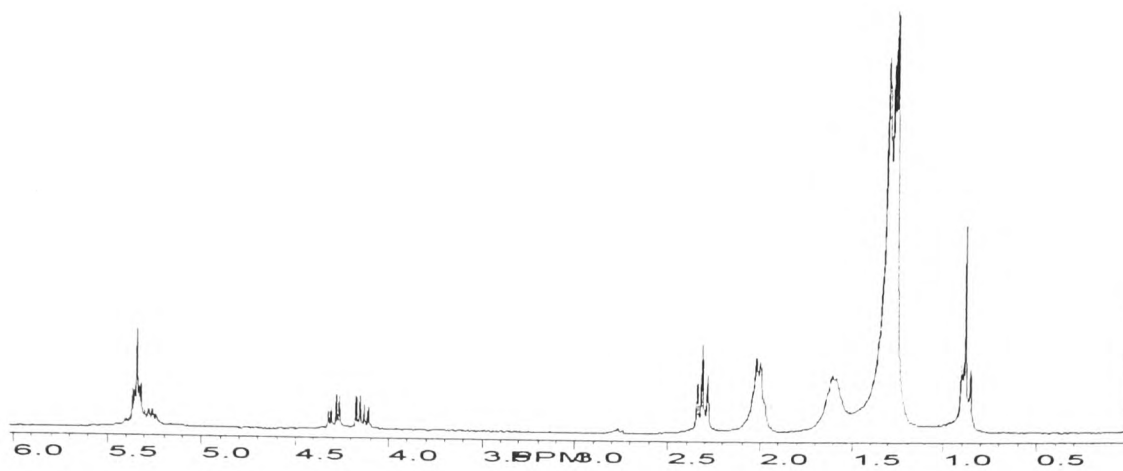


Figure E1  $^1\text{H}$  NMR spectrum of sample D1

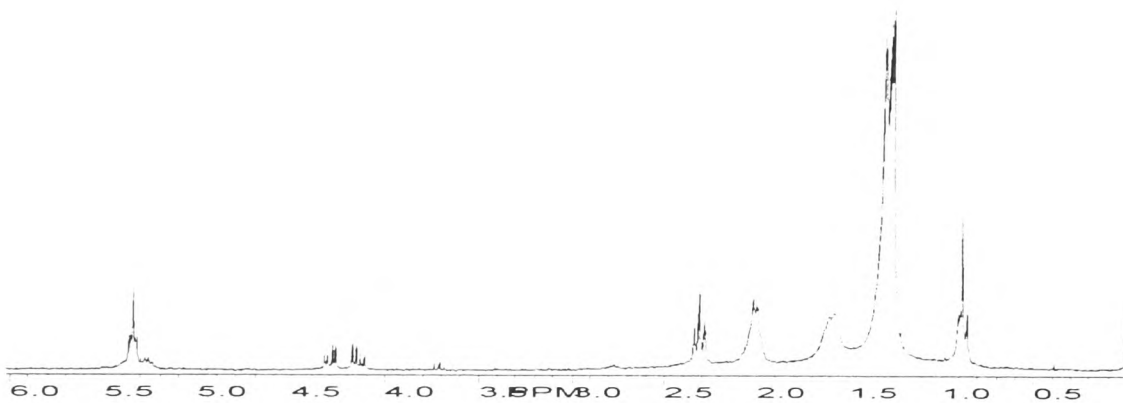


Figure E2  $^1\text{H}$  NMR spectrum of sample D1 adulterated with 5 % w/w sunflower oil

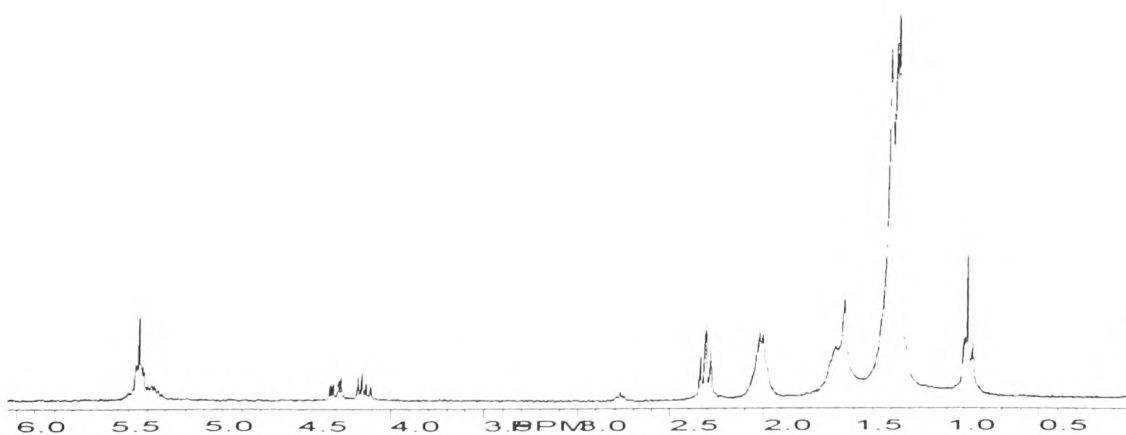


Figure E3  $^1\text{H}$  NMR spectrum of sample D1 adulterated with 10 % w/w sunflower oil

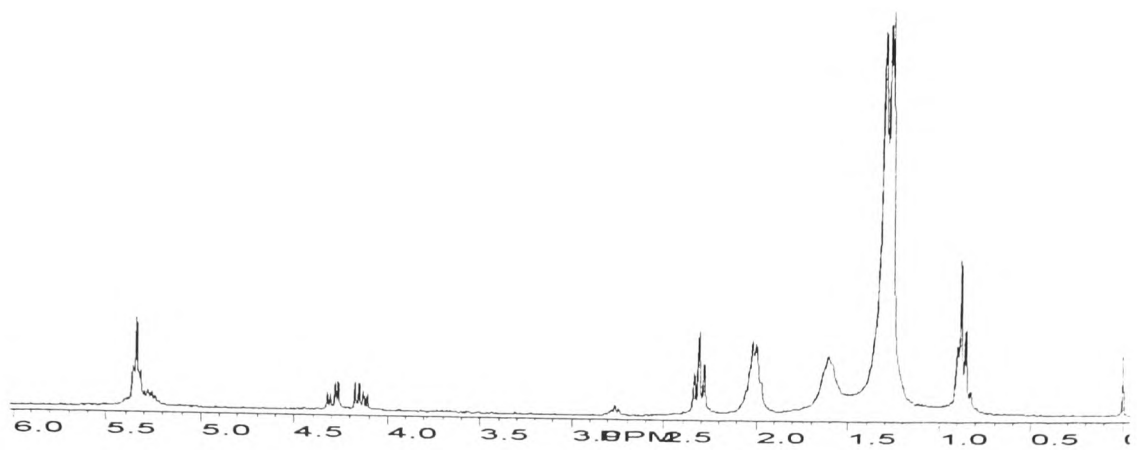


Figure E4 <sup>1</sup>H NMR spectrum of sample D2

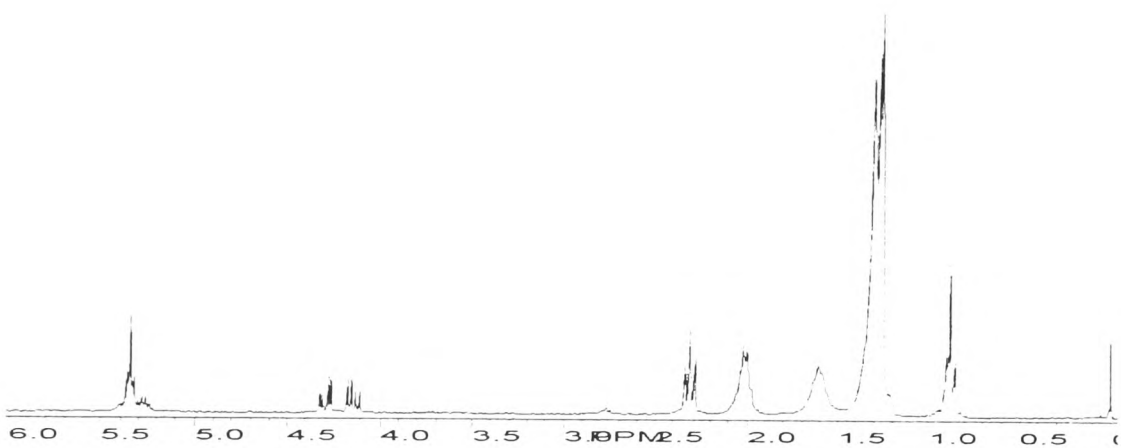


Figure E5 <sup>1</sup>H NMR spectrum of sample D2 adulterated with 5 % w/w sunflower oil

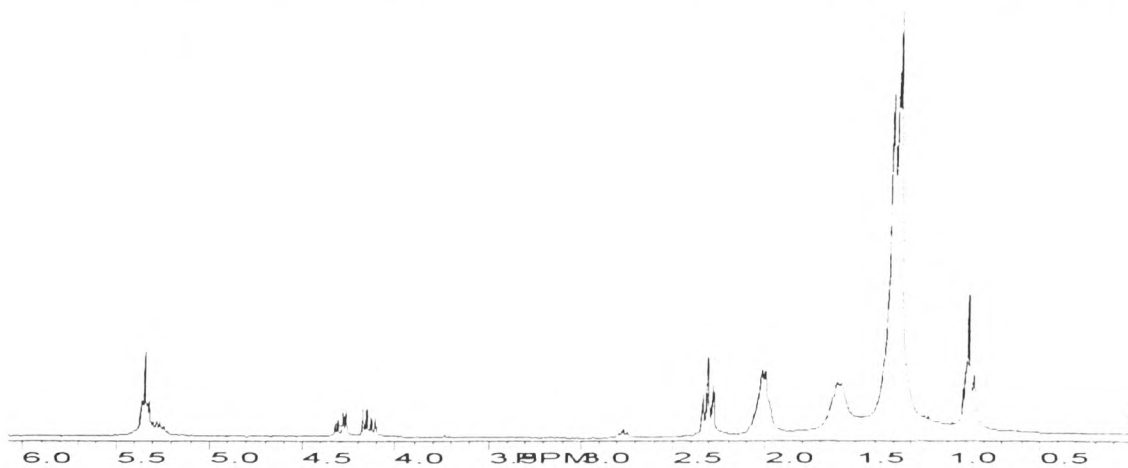


Figure E6 <sup>1</sup>H NMR spectrum of sample D2 adulterated with 10 % w/w sunflower oil

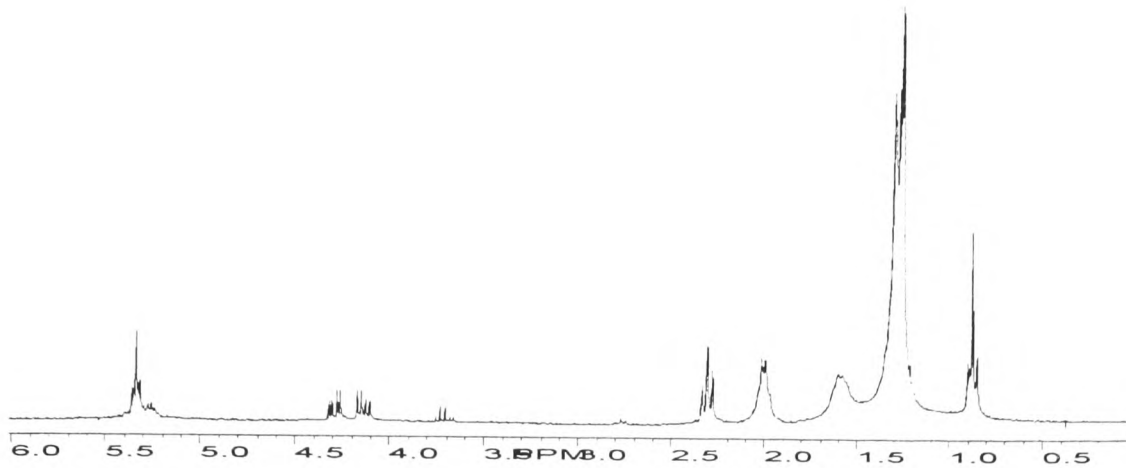


Figure E7 <sup>1</sup>H NMR spectrum of sample D3

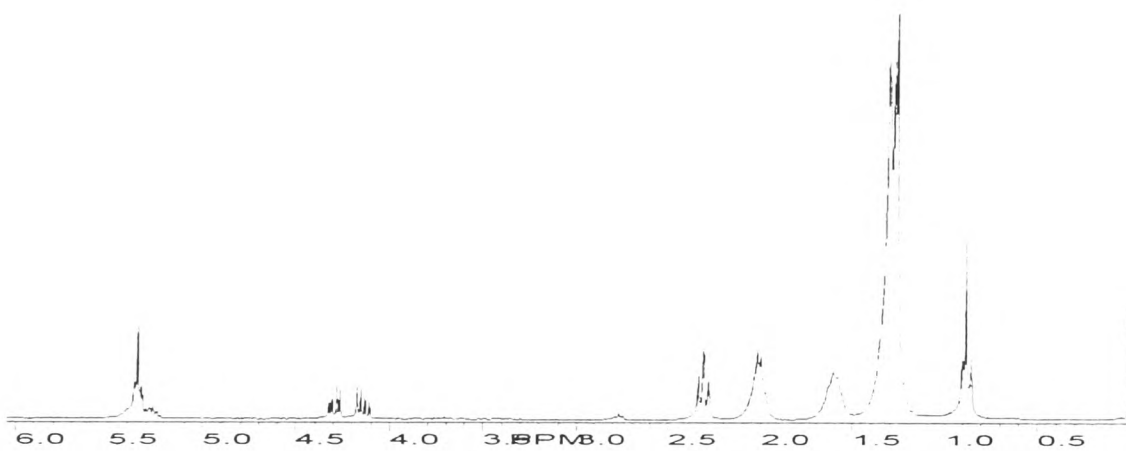


Figure E8 <sup>1</sup>H NMR spectrum of sample D3 adulterated with 5 % w/w sunflower oil

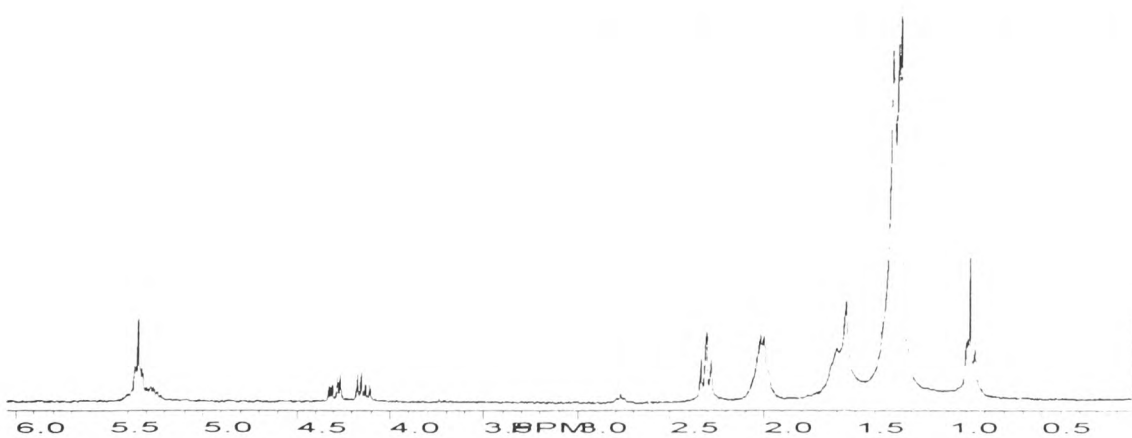


Figure E9 <sup>1</sup>H NMR spectrum of sample D3 adulterated with 10 % w/w sunflower oil

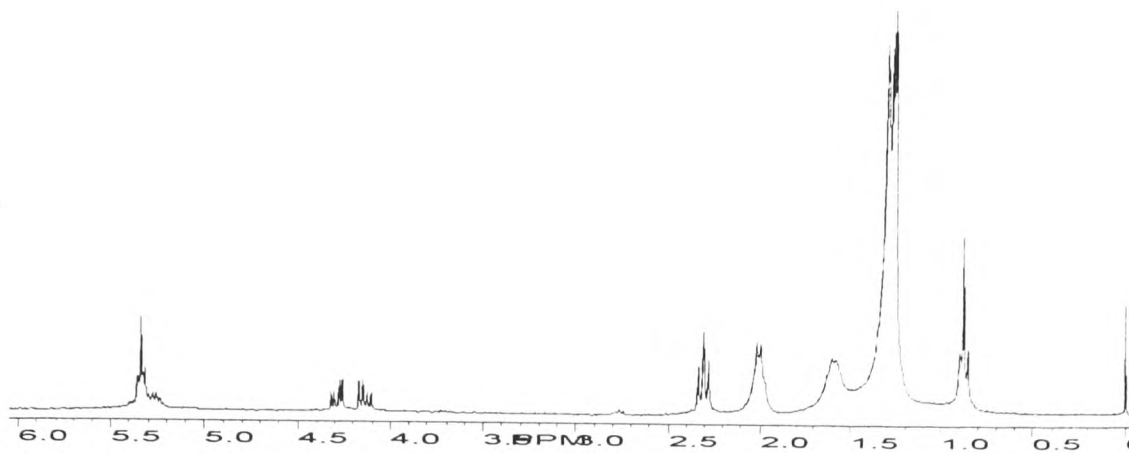


Figure E10 <sup>1</sup>H NMR spectrum of sample D4

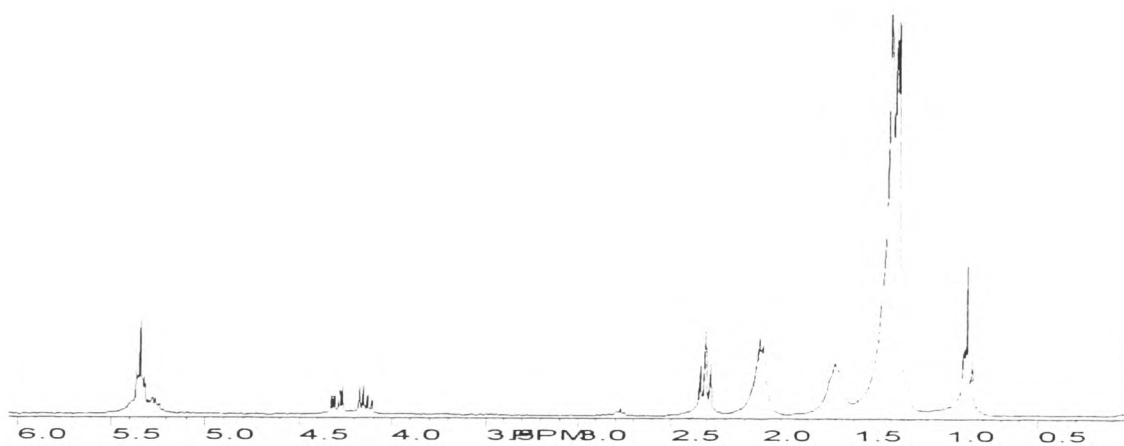


Figure E11 <sup>1</sup>H NMR spectrum of sample D4 adulterated with 5 % w/w sunflower oil

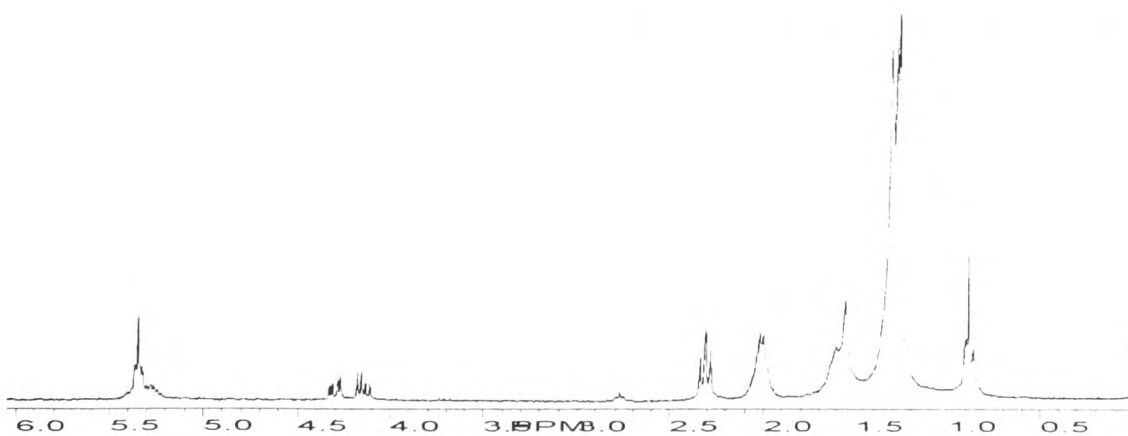


Figure E12 <sup>1</sup>H NMR spectrum of sample D4 adulterated with 10 % w/w sunflower oil

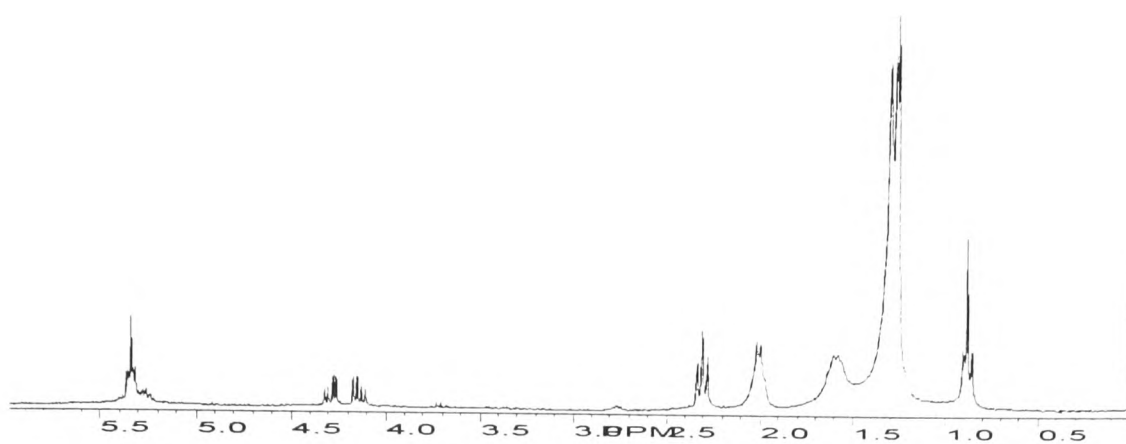


Figure E13 <sup>1</sup>H NMR spectrum of sample D5

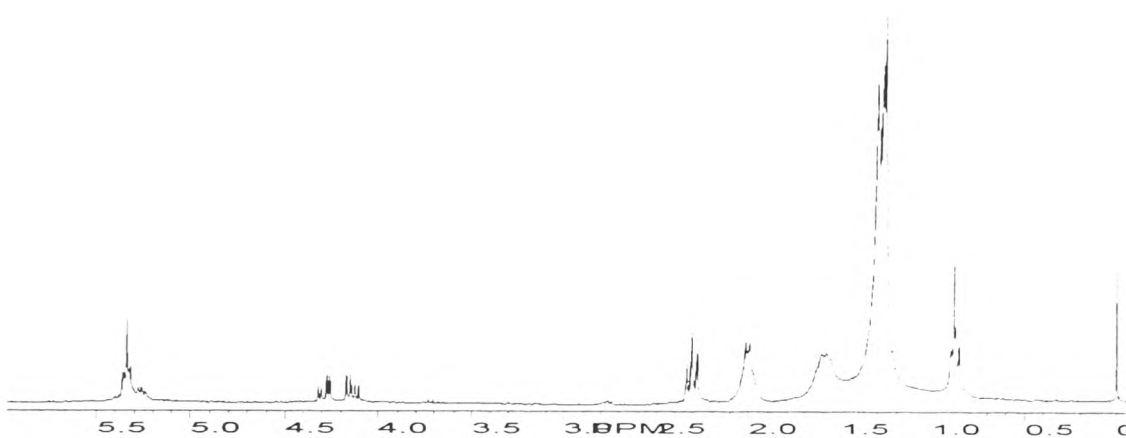


Figure E14 <sup>1</sup>H NMR spectrum of sample D5 adulterated with 5 % w/w sunflower oil

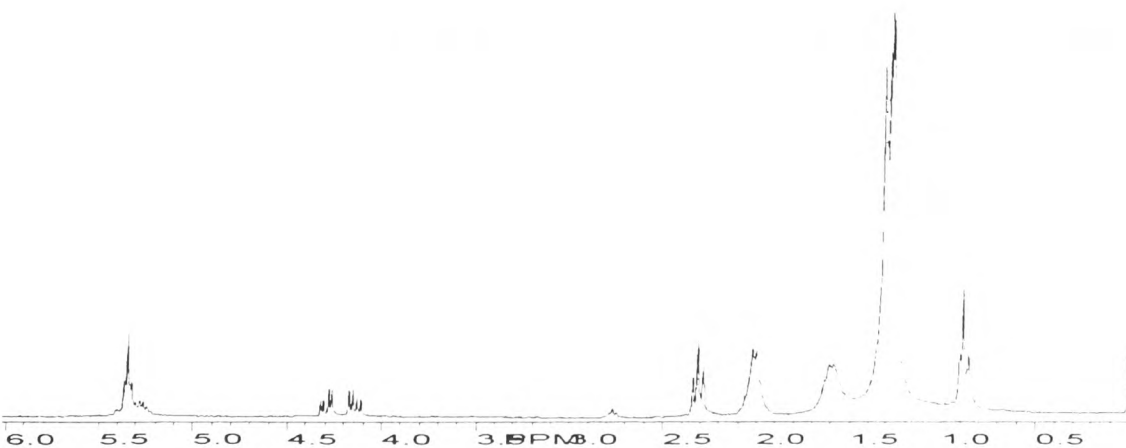


Figure E15 <sup>1</sup>H NMR spectrum of sample D5 adulterated with 10 % w/w sunflower oil

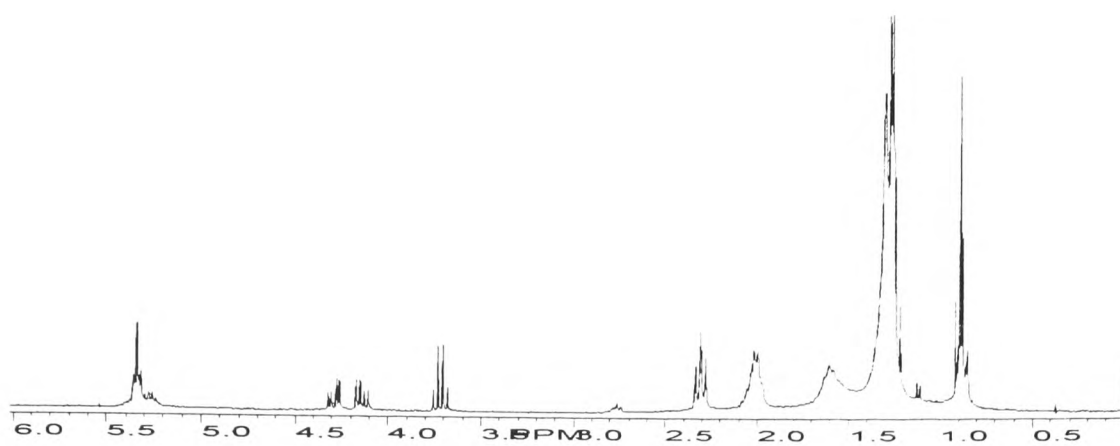


Figure E16 <sup>1</sup>H NMR spectrum of sample D6

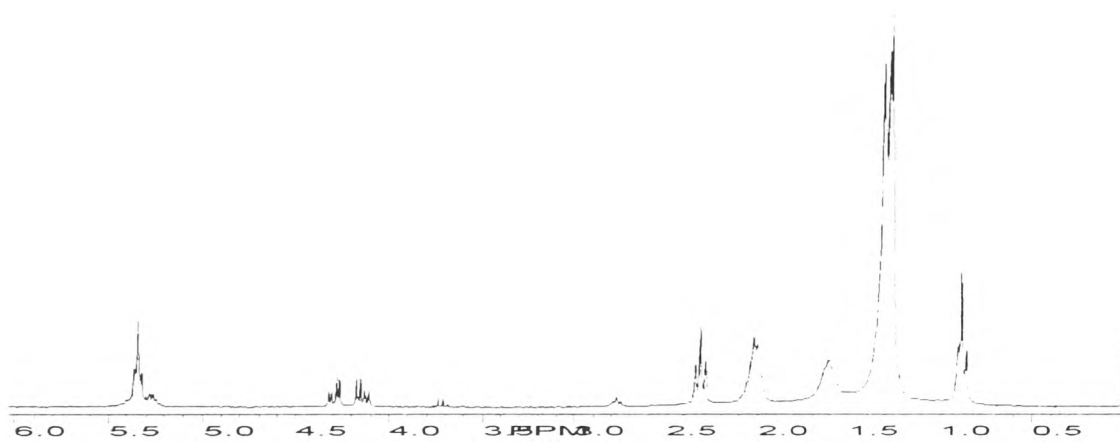


Figure E17 <sup>1</sup>H NMR spectrum of sample D6 adulterated with 5 % w/w sunflower oil

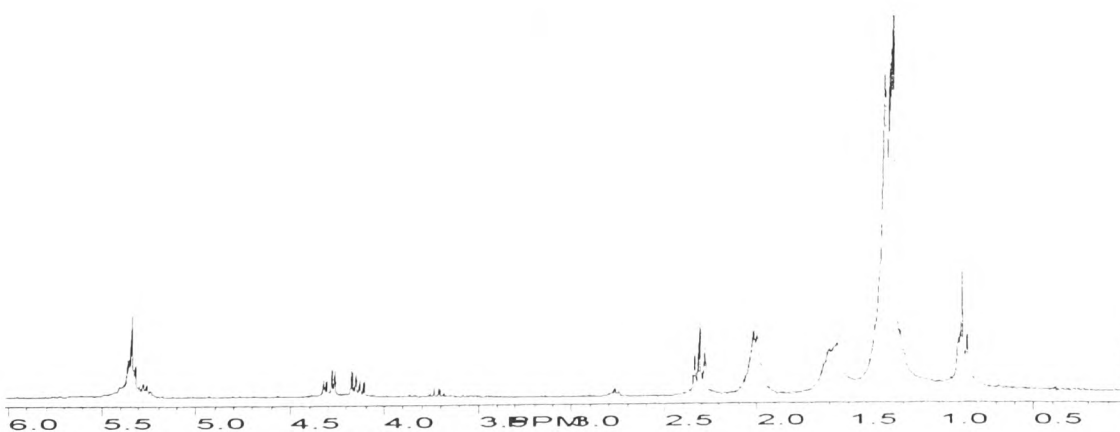
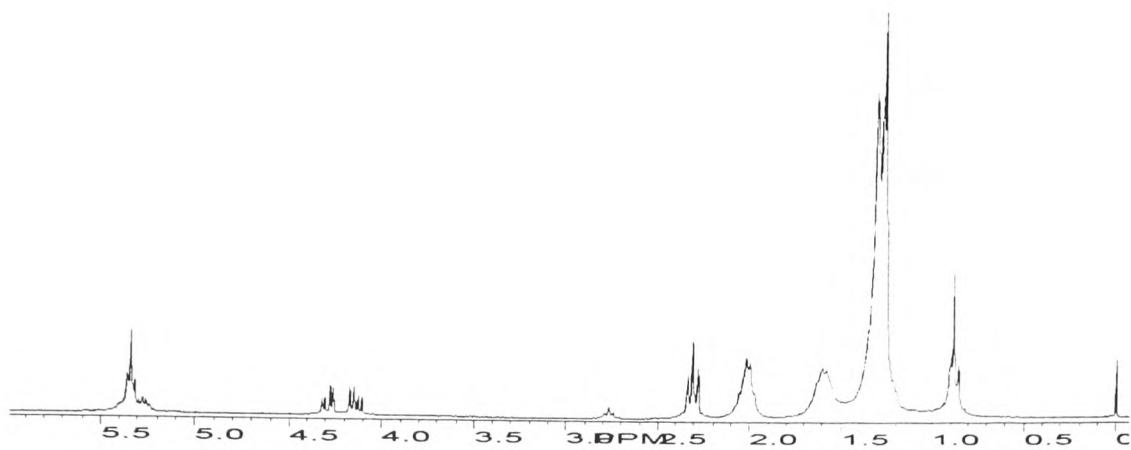
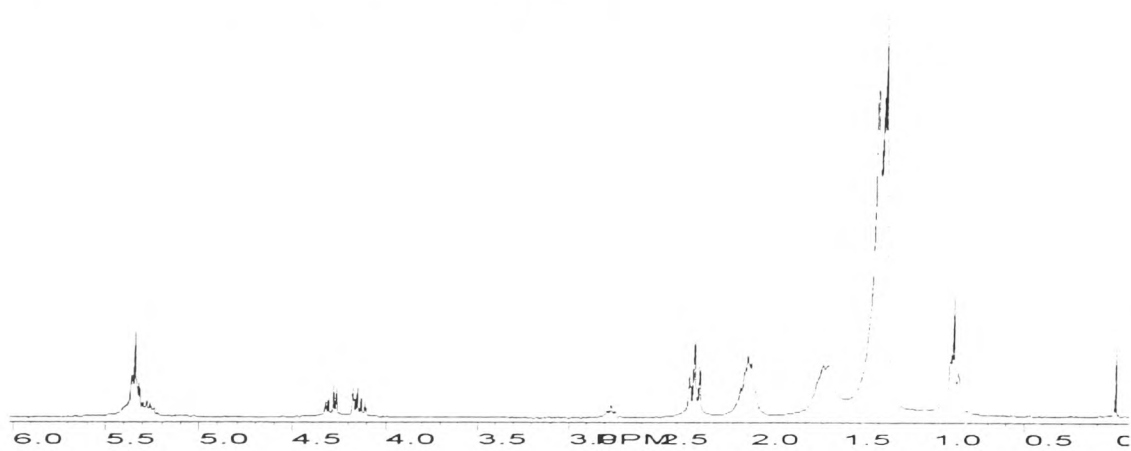


Figure E18 <sup>1</sup>H NMR spectrum of sample D6 adulterated with 10 % w/w sunflower oil





**Figure E19** <sup>1</sup>H NMR spectrum of sample D7



**Figure E20** <sup>1</sup>H NMR spectrum of sample D7 adulterated with 5 % w/w sunflower oil

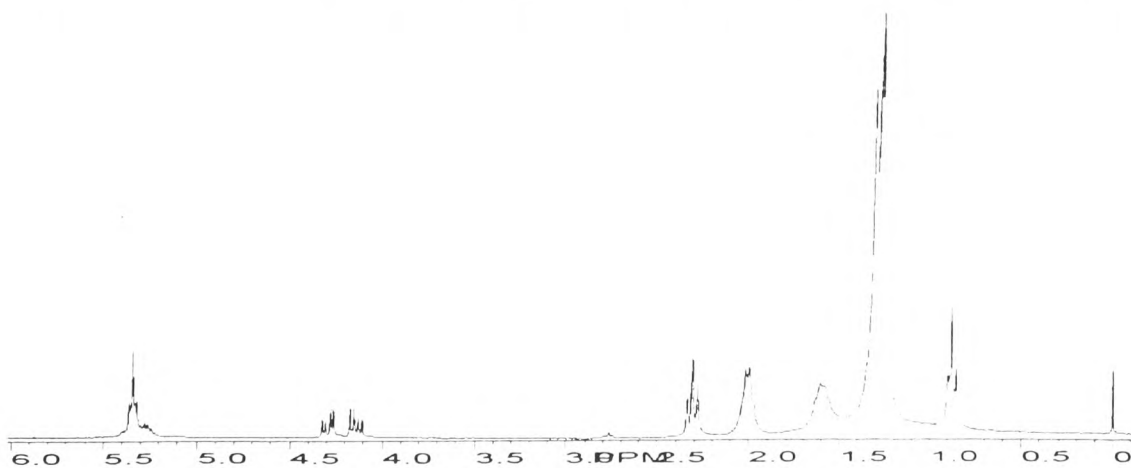


**Figure E21** <sup>1</sup>H NMR spectrum of sample D7 adulterated with 10 % w/w sunflower oil

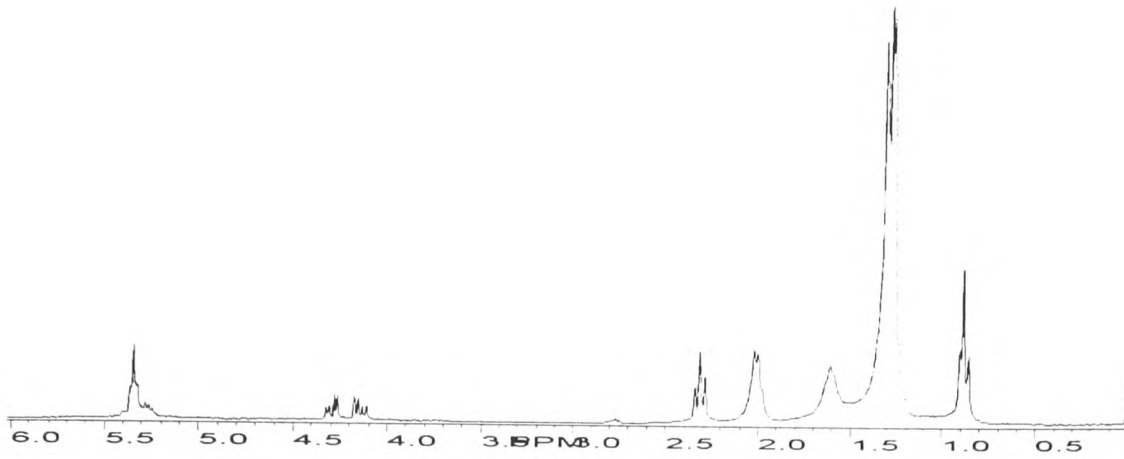


Figure E22 <sup>1</sup>H NMR spectrum of sample D8

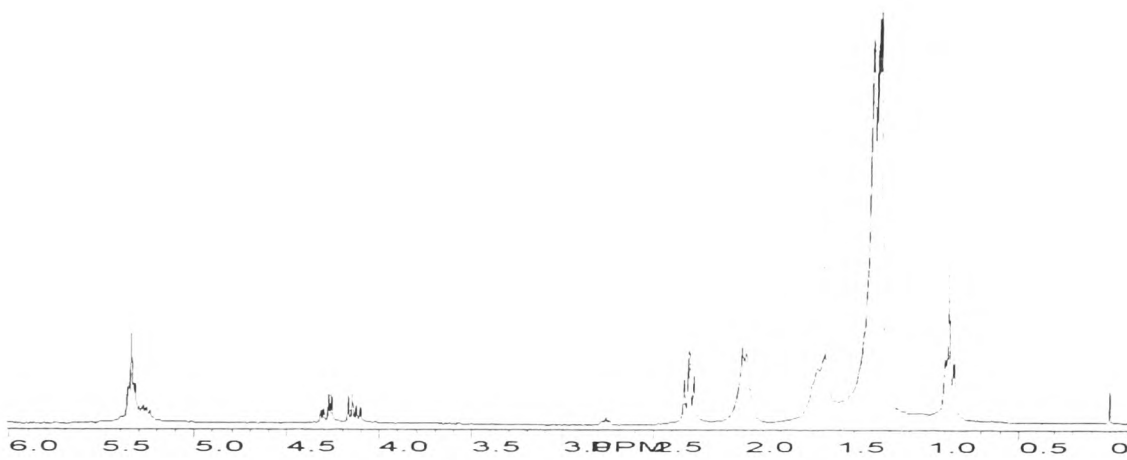


Figure E23 <sup>1</sup>H NMR spectrum of sample D8 adulterated with 5 % w/w sunflower oil

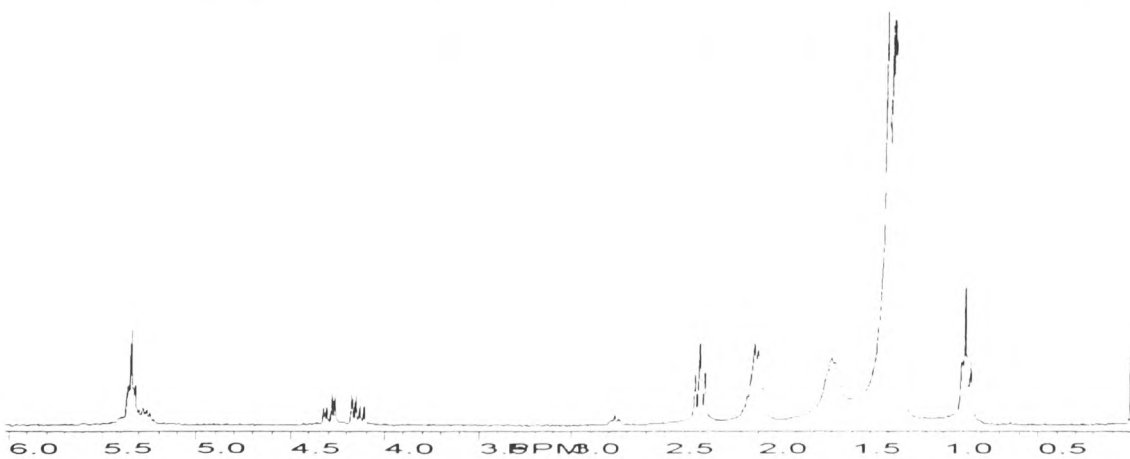


Figure E24 <sup>1</sup>H NMR spectrum of sample D8 adulterated with 10 % w/w sunflower oil

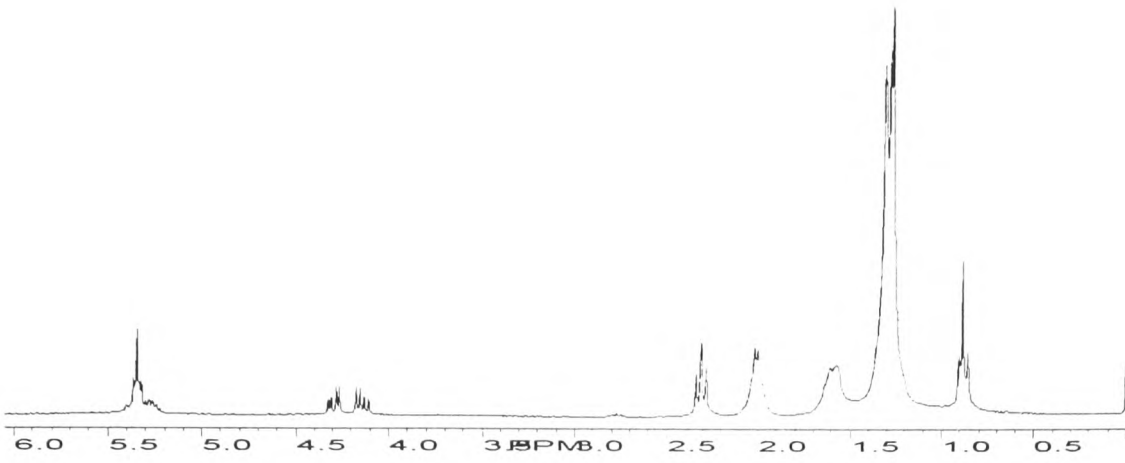


Figure E25 <sup>1</sup>H NMR spectrum of sample D9

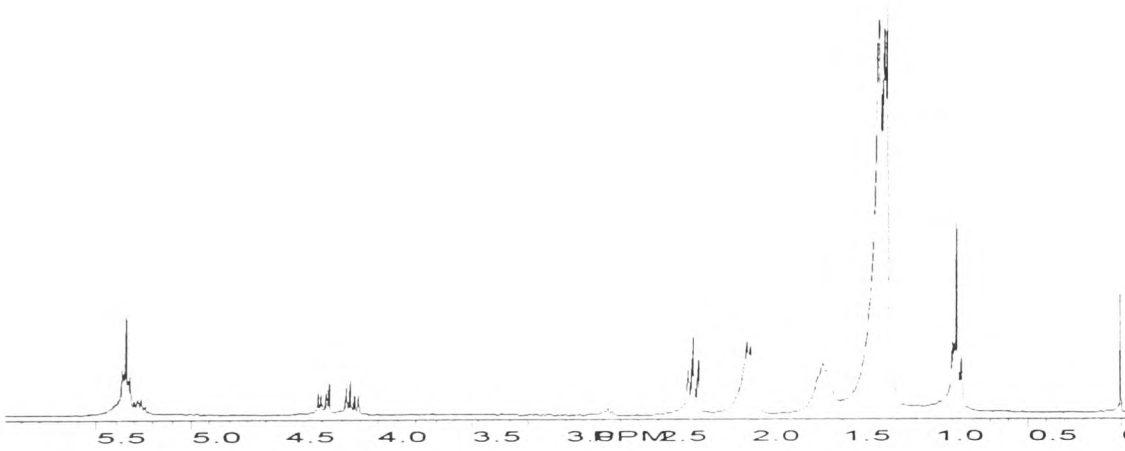


Figure E26 <sup>1</sup>H NMR spectrum of sample D9 adulterated with 5 % w/w sunflower oil

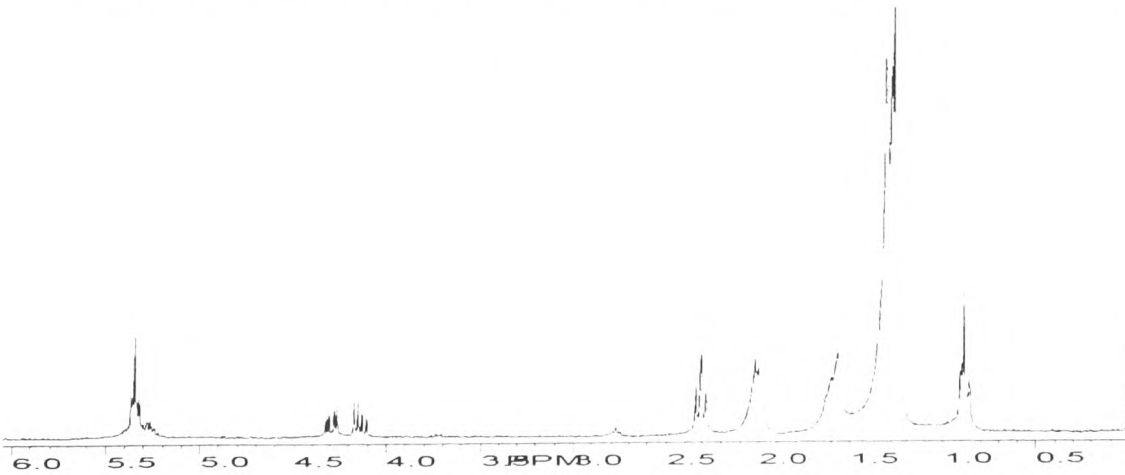


Figure E27 <sup>1</sup>H NMR spectrum of sample D9 adulterated with 10 % w/w sunflower oil

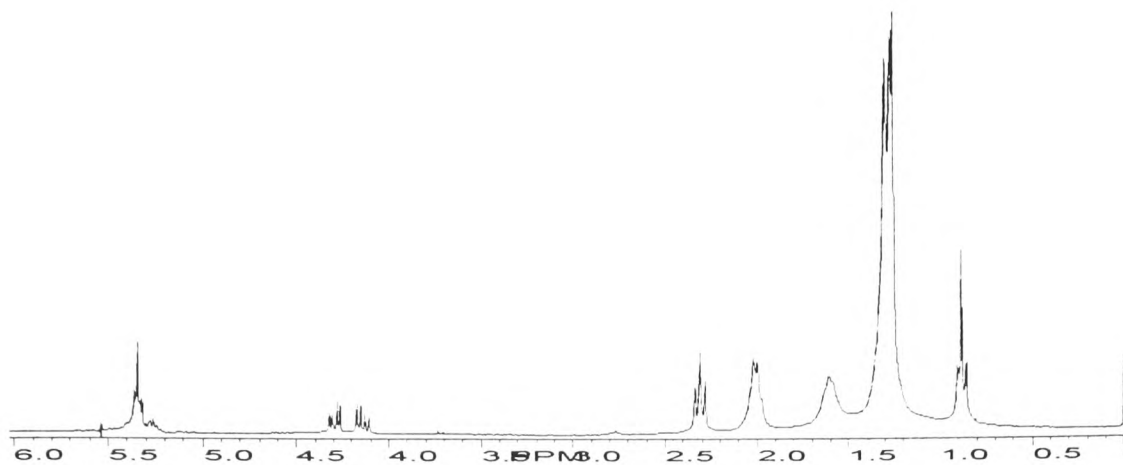


Figure E28  $^1\text{H}$  NMR spectrum of sample D10

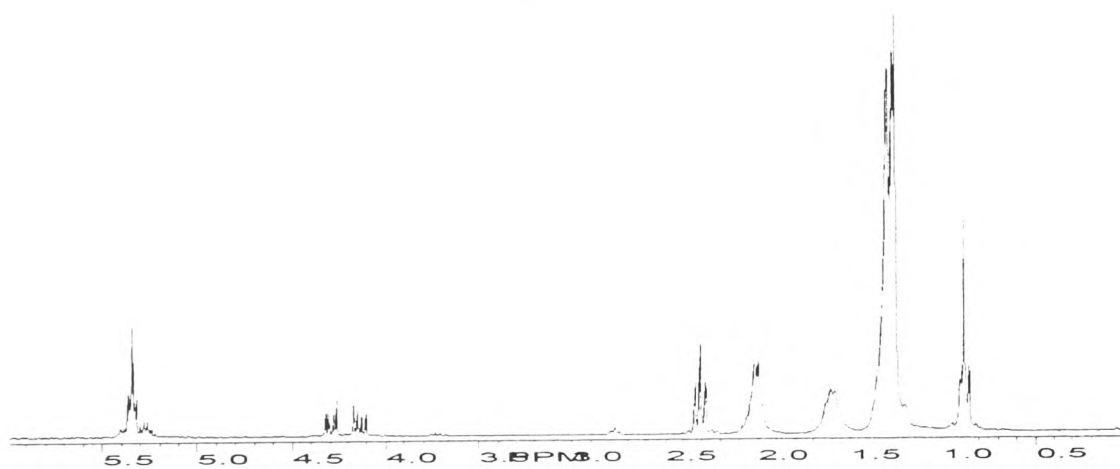


Figure E29  $^1\text{H}$  NMR spectrum of sample D10 adulterated with 5 % w/w sunflower oil

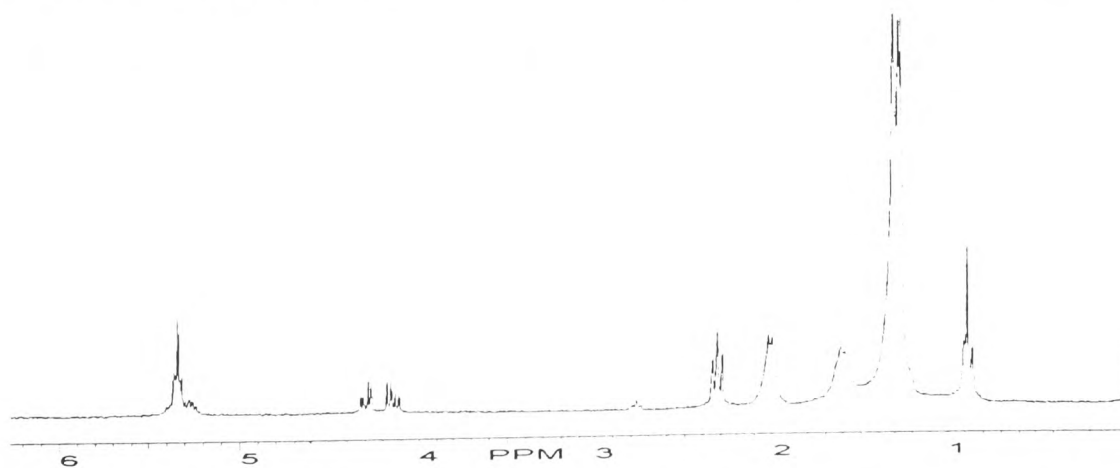


Figure E30  $^1\text{H}$  NMR spectrum of sample D10 adulterated with 10 % w/w sunflower oil

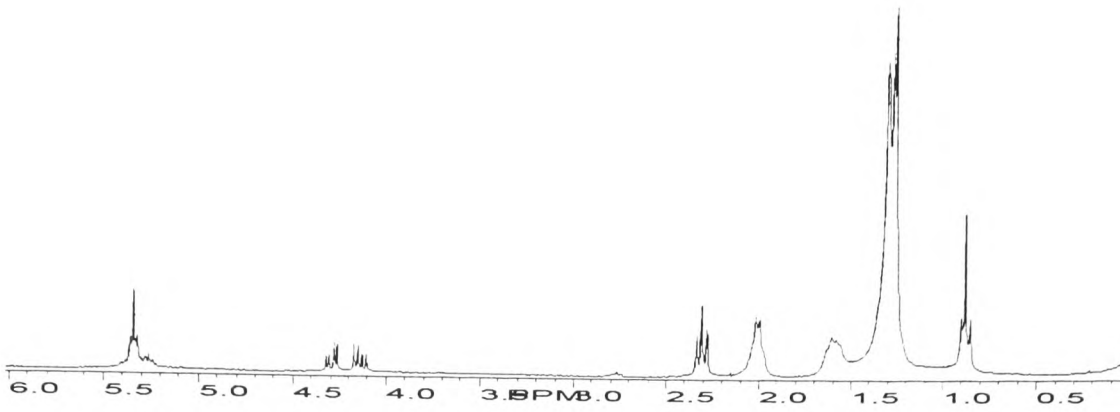


Figure E31 <sup>1</sup>H NMR spectrum of sample D11

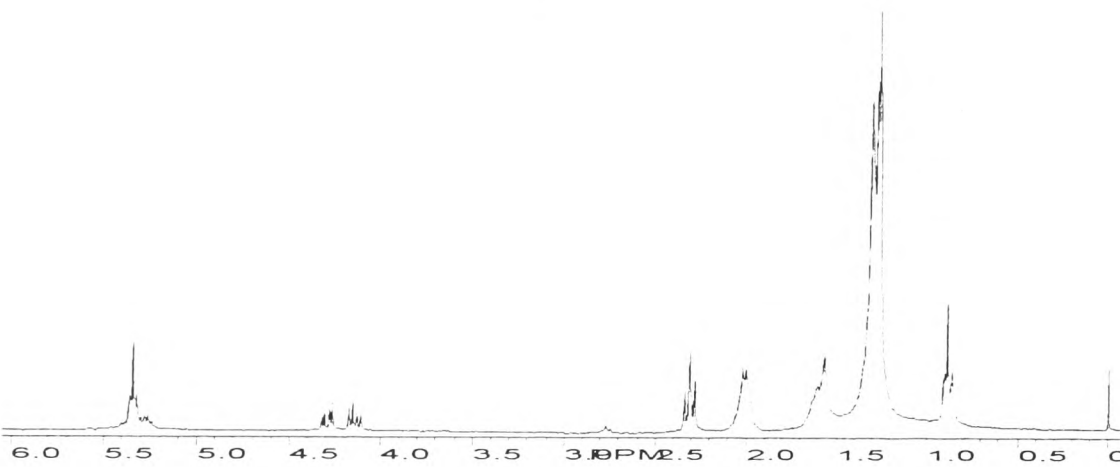


Figure E32 <sup>1</sup>H NMR spectrum of sample D11 adulterated with 5 % w/w sunflower oil

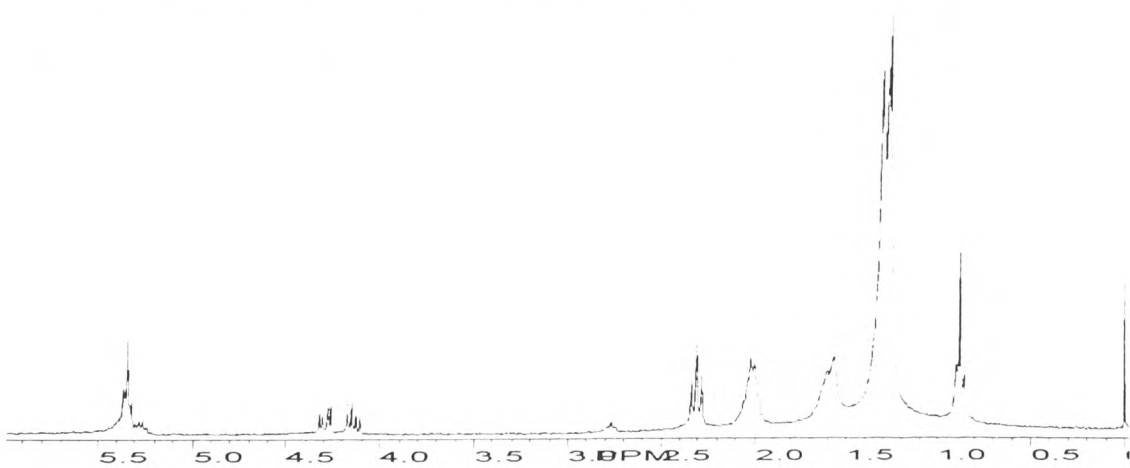


Figure E33 <sup>1</sup>H NMR spectrum of sample D11 adulterated with 10 % w/w sunflower oil

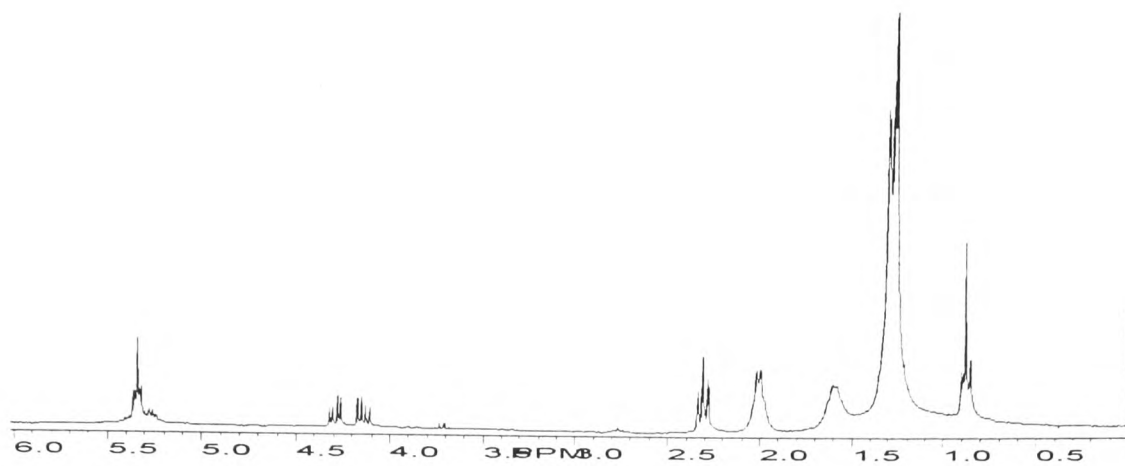


Figure E34 <sup>1</sup>H NMR spectrum of sample D12

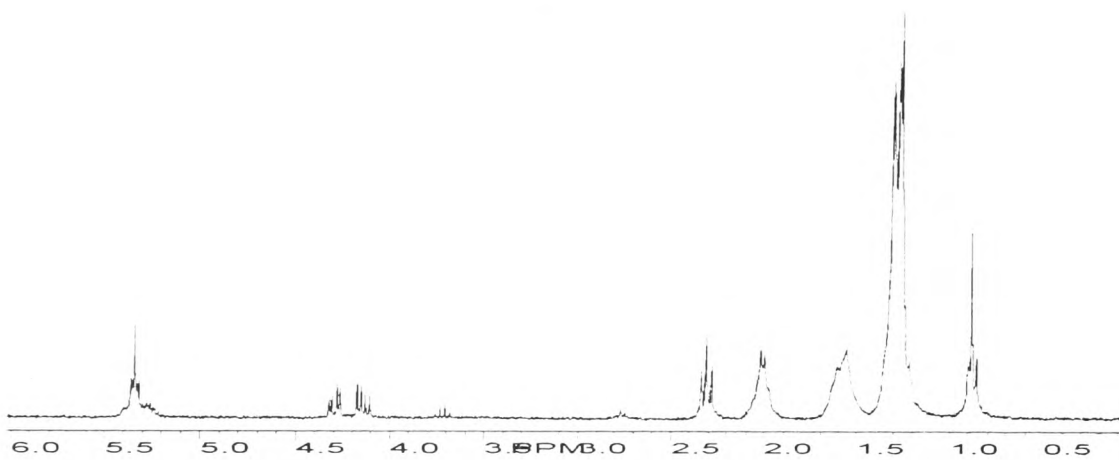


Figure E35 <sup>1</sup>H NMR spectrum of sample D12 adulterated with 5 % w/w sunflower oil

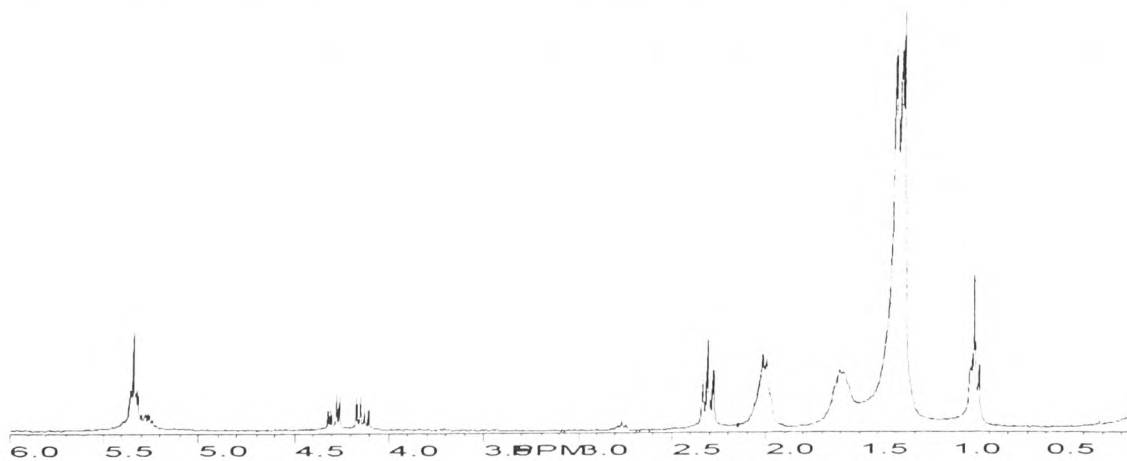


Figure E36 <sup>1</sup>H NMR spectrum of sample D12 adulterated with 10 % w/w sunflower oil

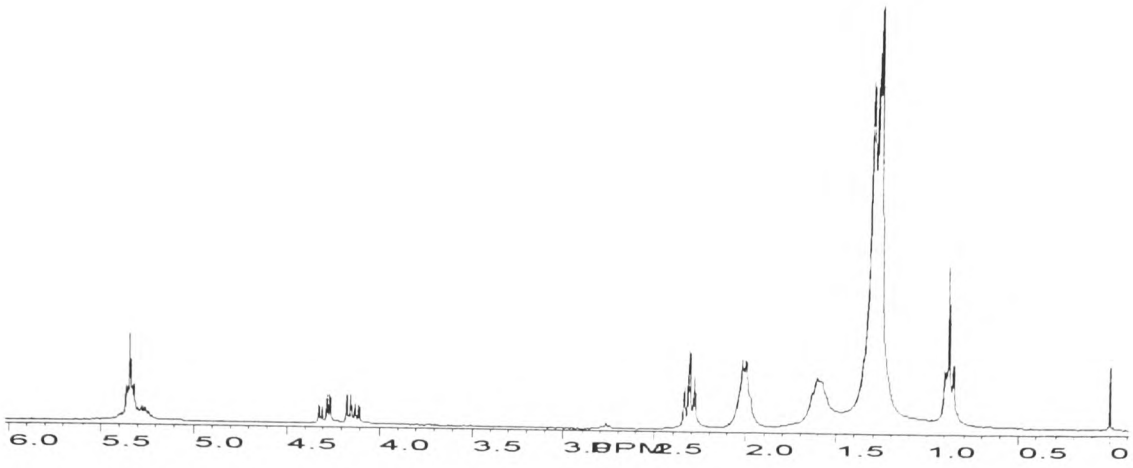


Figure E37 <sup>1</sup>H NMR spectrum of sample D13

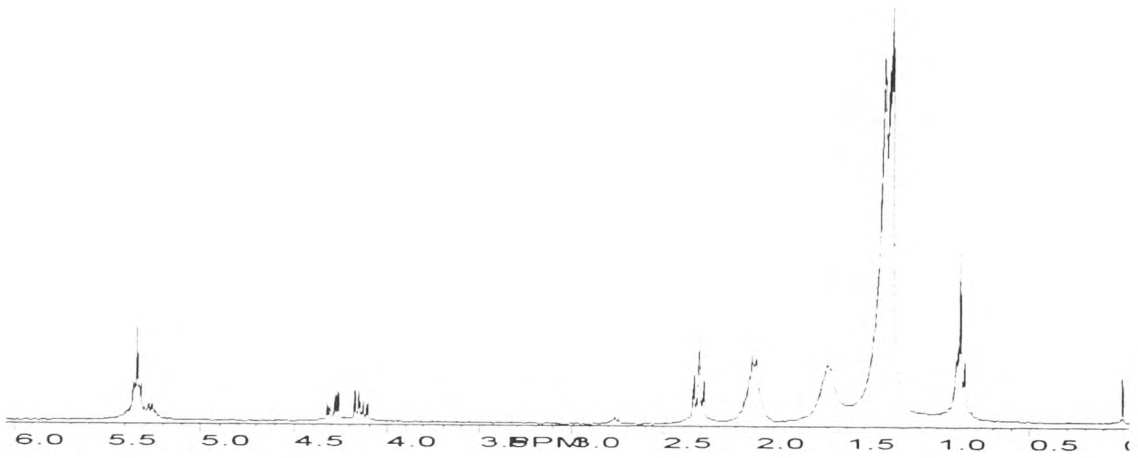


Figure E38 <sup>1</sup>H NMR spectrum of sample D13 adulterated with 5 % w/w sunflower oil

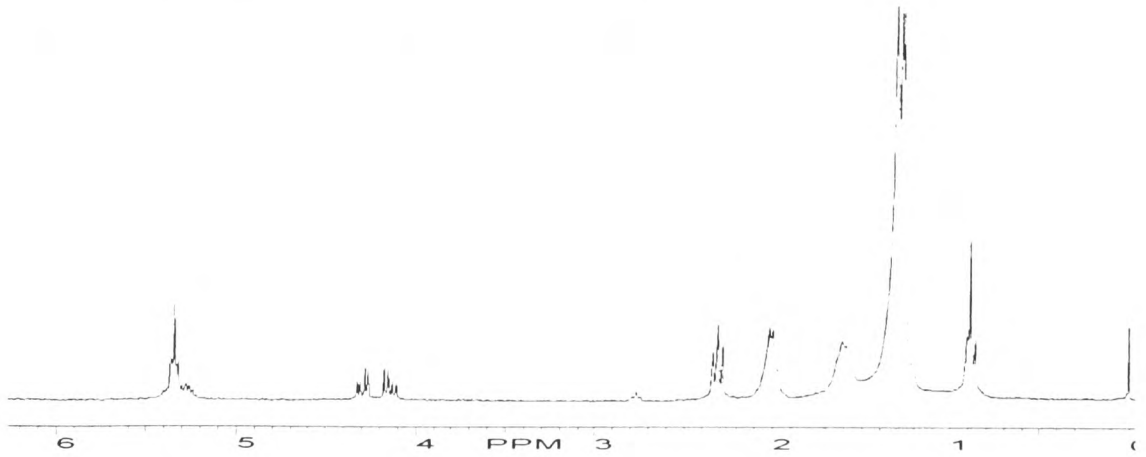


Figure E39 <sup>1</sup>H NMR spectrum of sample D13 adulterated with 10 % w/w sunflower oil

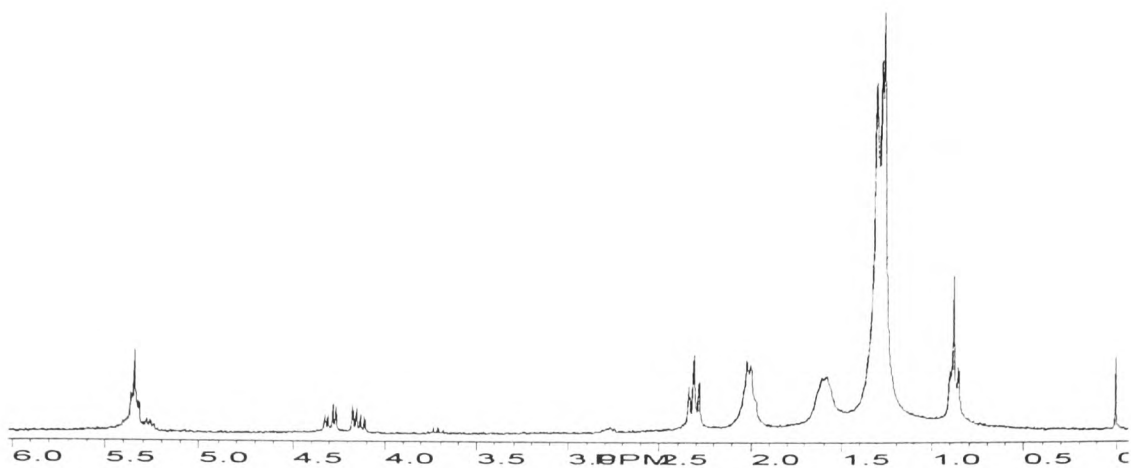


Figure E40 <sup>1</sup>H NMR spectrum of sample D14

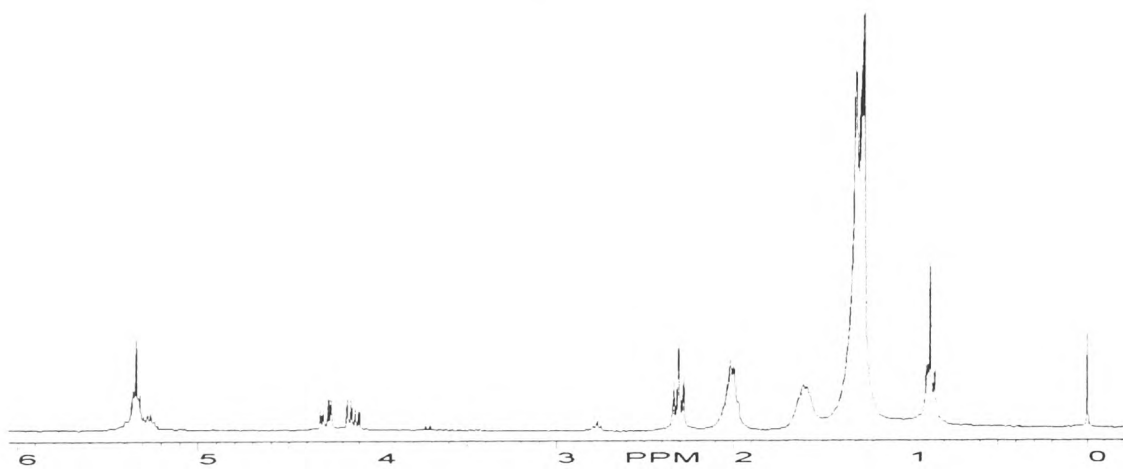


Figure E41 <sup>1</sup>H NMR spectrum of sample D14 adulterated with 5 % w/w sunflower oil

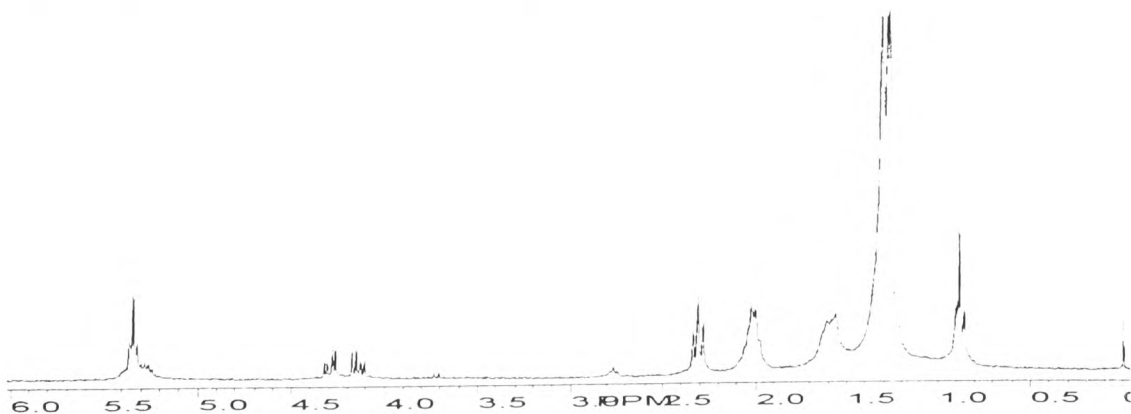


Figure E42 <sup>1</sup>H NMR spectrum of sample D14 adulterated with 10 % w/w sunflower oil



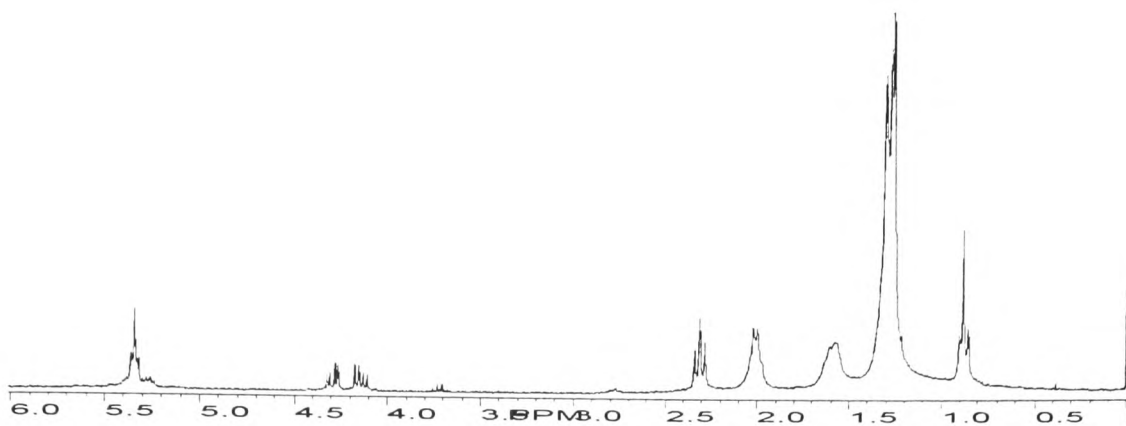


Figure E43 <sup>1</sup>H NMR spectrum of sample D15

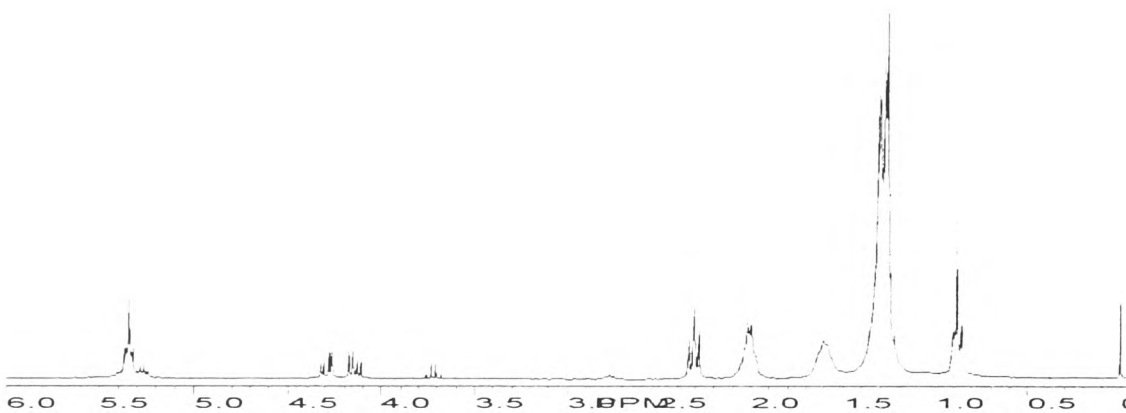


Figure E44 <sup>1</sup>H NMR spectrum of sample D15 adulterated with 5 % w/w sunflower oil

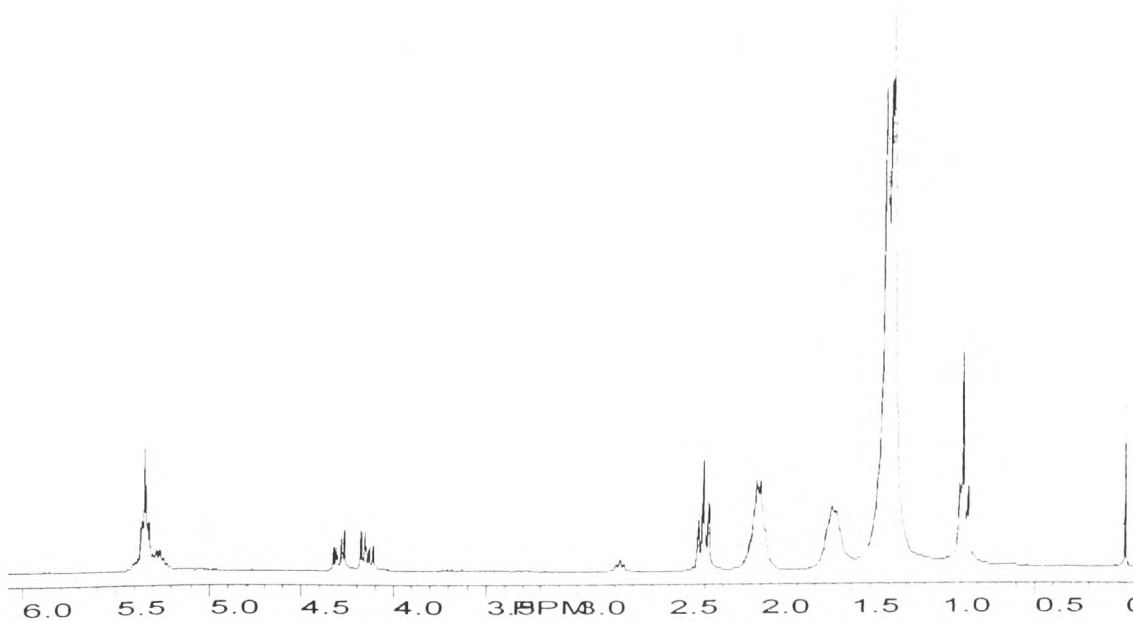
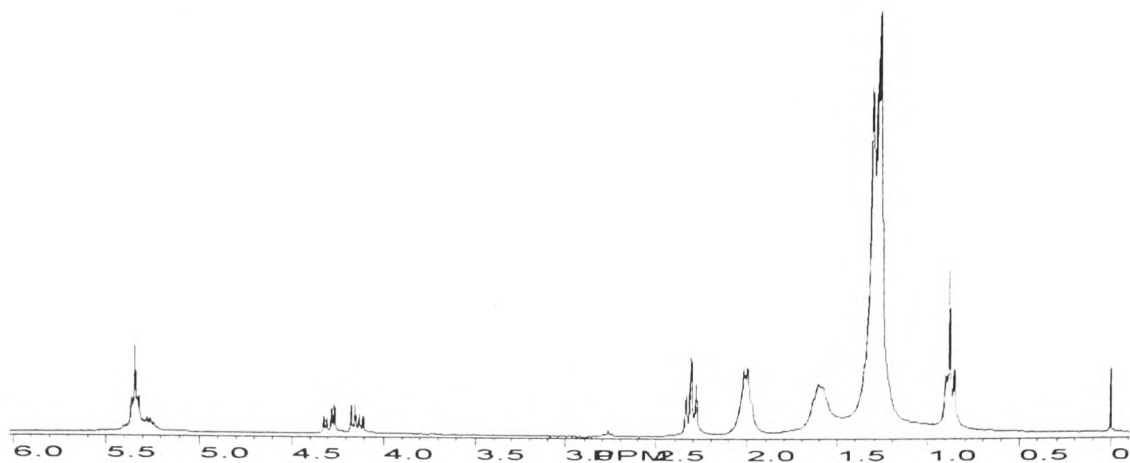
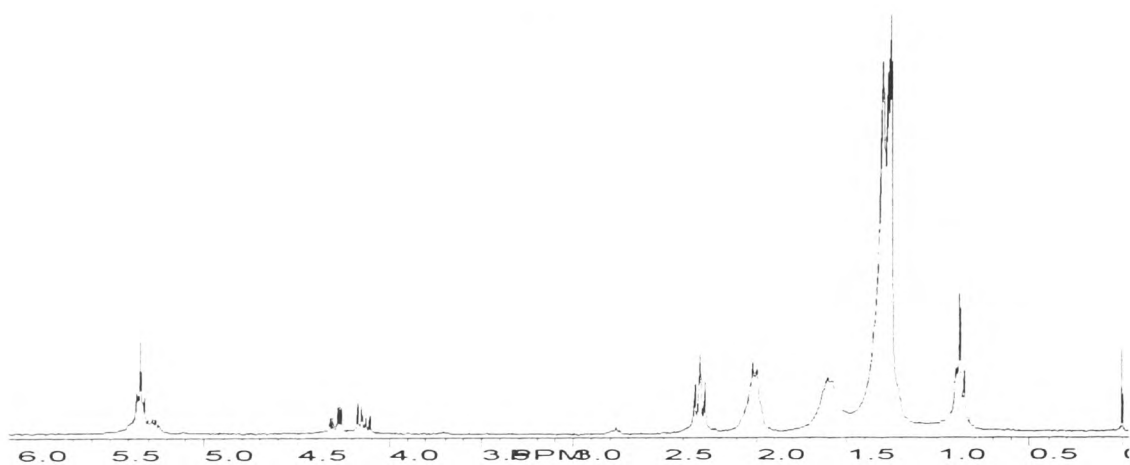


Figure E45 <sup>1</sup>H NMR spectrum of sample D15 adulterated with 10 % w/w sunflower oil



**Figure E46** <sup>1</sup>H NMR spectrum of sample D16



**Figure E47** <sup>1</sup>H NMR spectrum of sample D16 adulterated with 5 % w/w sunflower oil

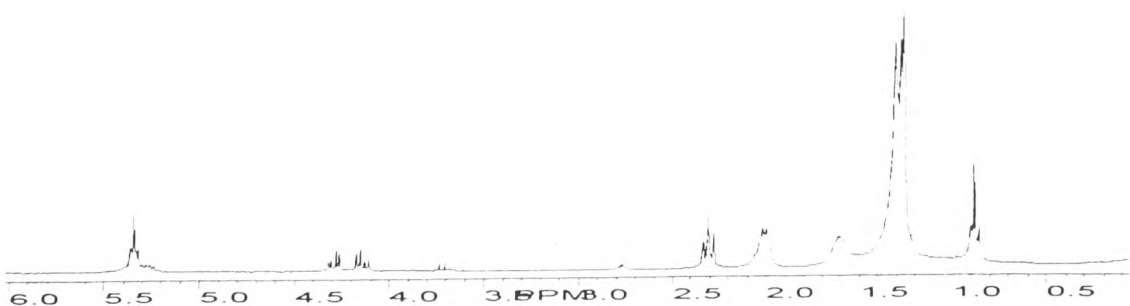


**Figure E48** <sup>1</sup>H NMR spectrum of sample D16 adulterated with 10 % w/w sunflower oil

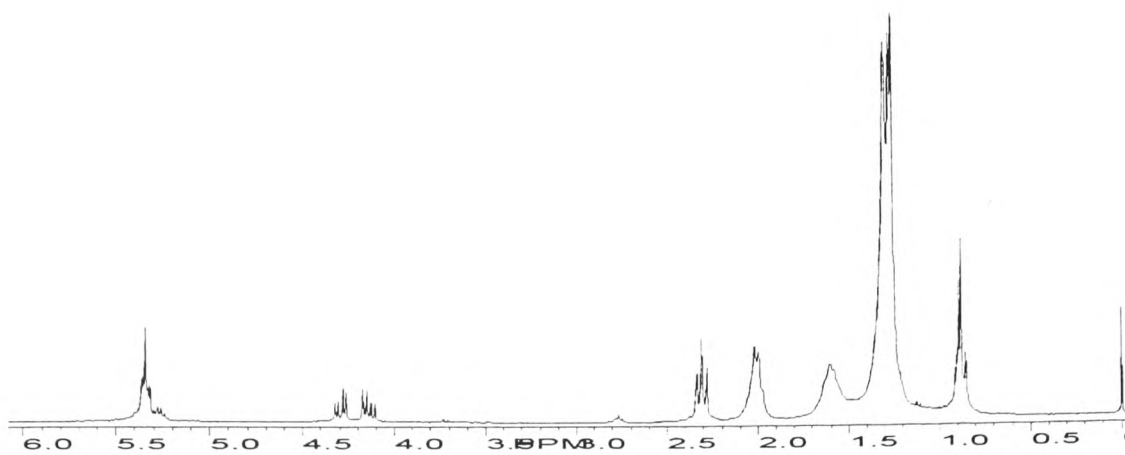


**Figure E49** <sup>1</sup>H NMR spectrum of sample D17

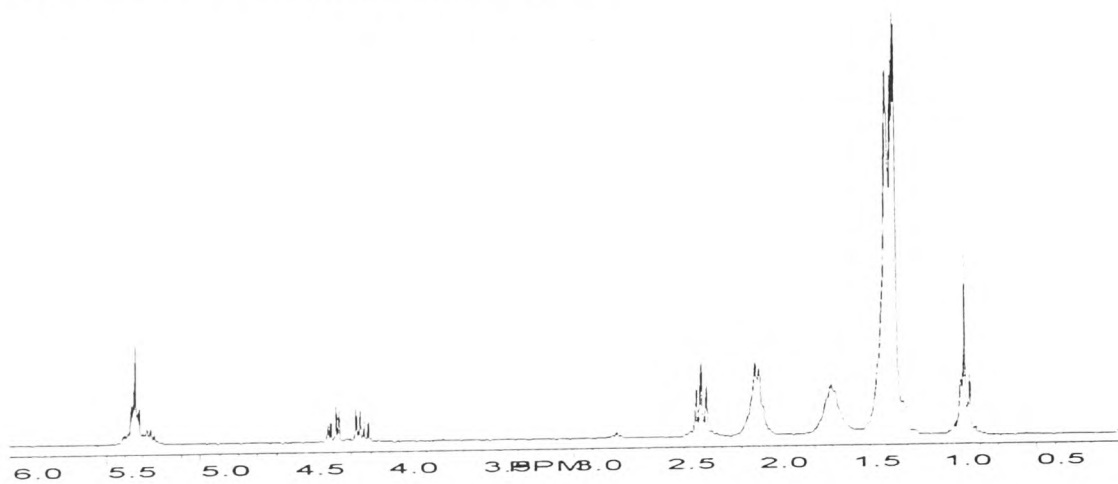


**Figure E50** <sup>1</sup>H NMR spectrum of sample D17 adulterated with 5 % w/w sunflower oil

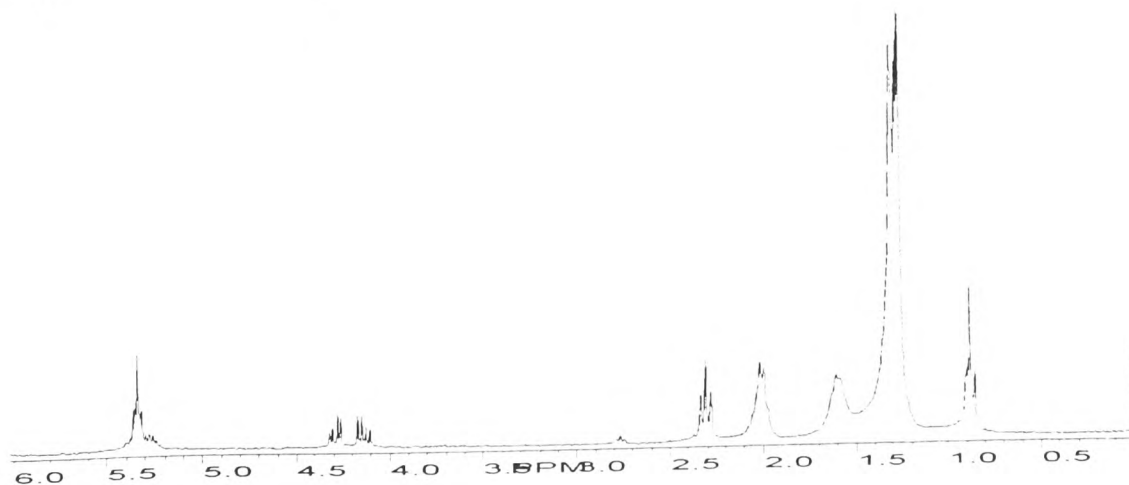


**Figure E51** <sup>1</sup>H NMR spectrum of sample D17 adulterated with 10 % w/w sunflower oil

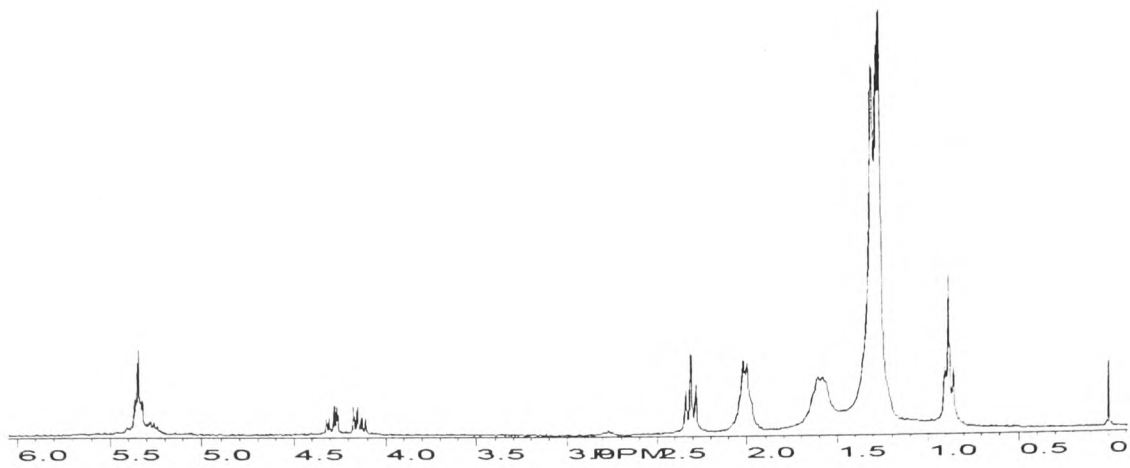


Figure E52  $^1\text{H}$  NMR spectrum of sample D18

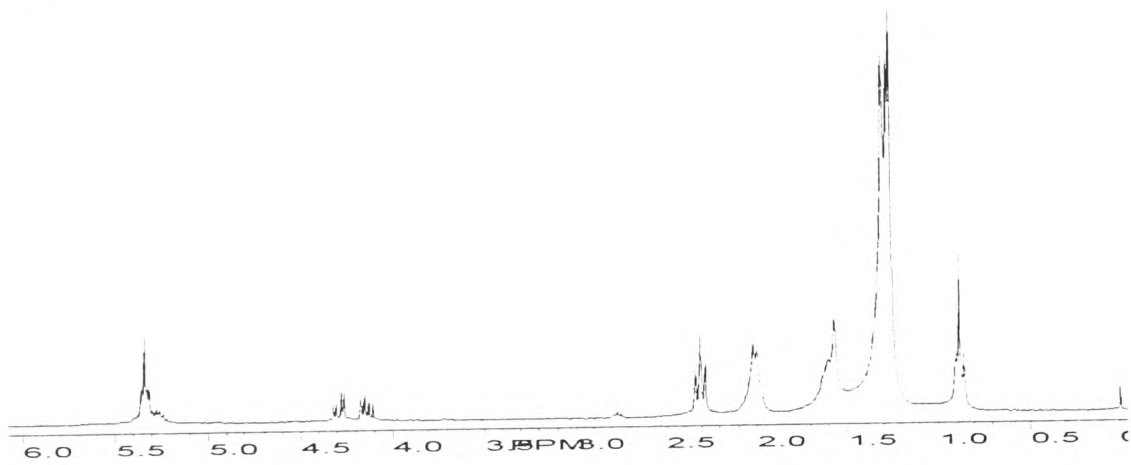


Figure E53  $^1\text{H}$  NMR spectrum of sample D18 adulterated with 5 % w/w sunflower oil

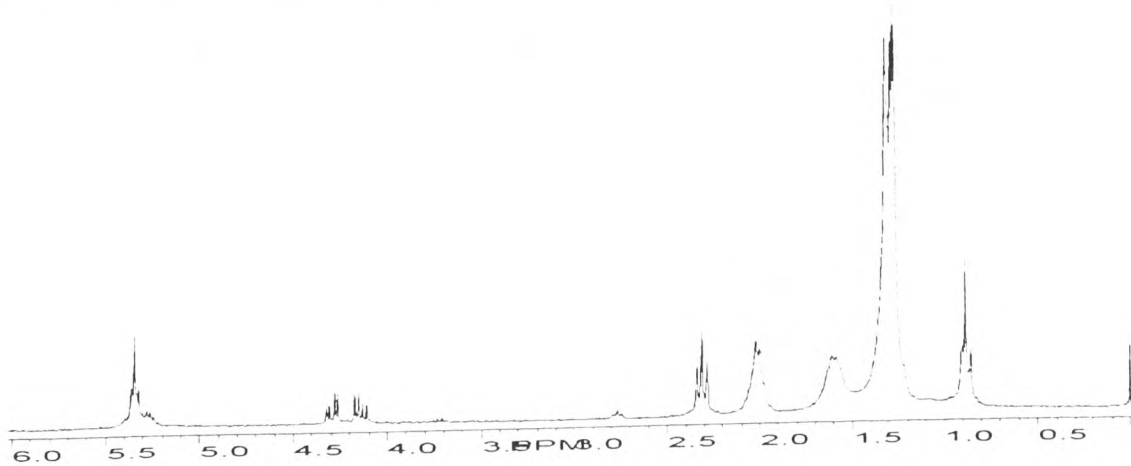


Figure E54  $^1\text{H}$  NMR spectrum of sample D18 adulterated with 10 % w/w sunflower oil

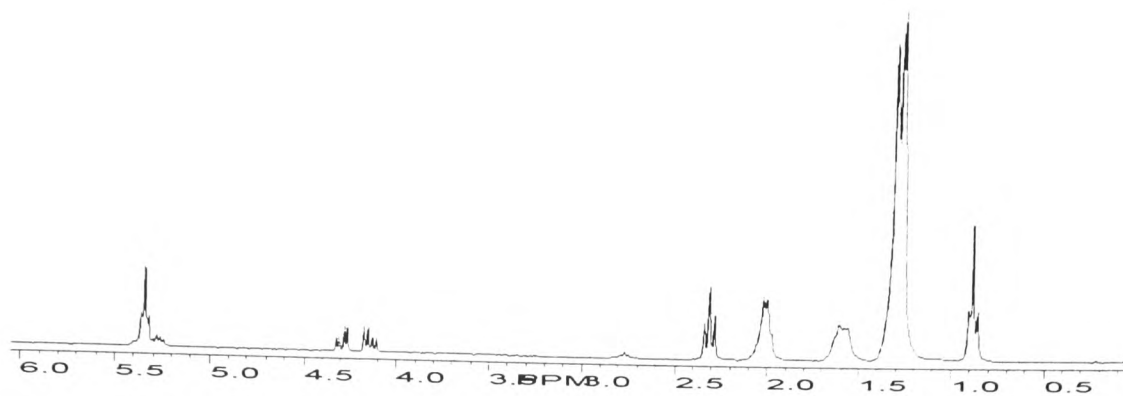


Figure E55 <sup>1</sup>H NMR spectrum of sample D19

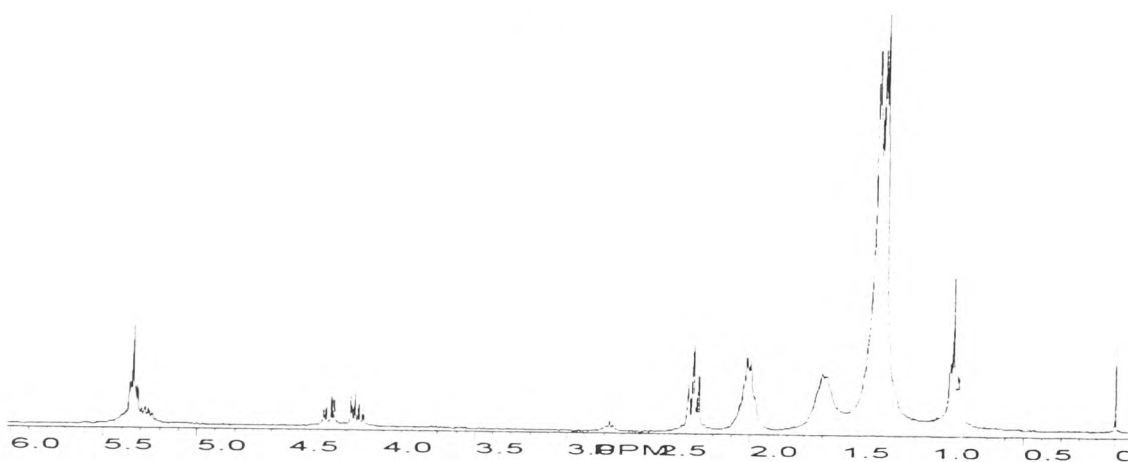


Figure E56 <sup>1</sup>H NMR spectrum of sample D19 adulterated with 5 % w/w sunflower oil

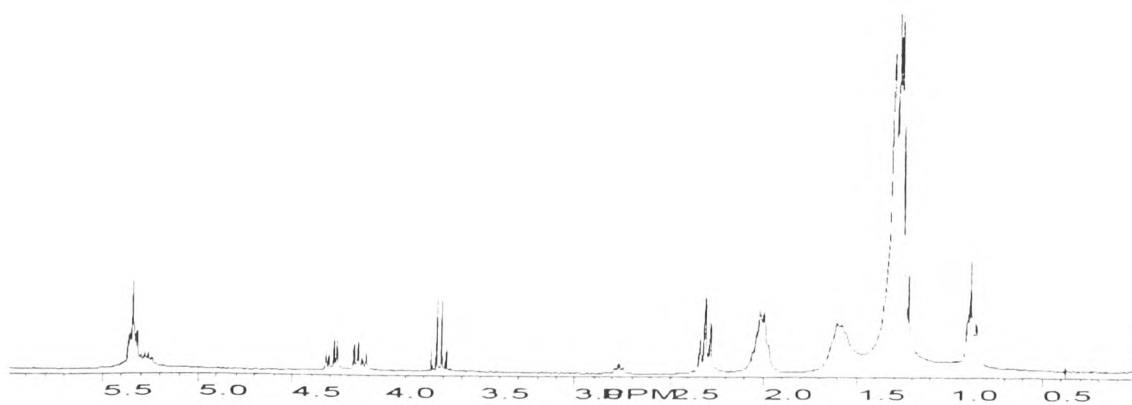


Figure E57 <sup>1</sup>H NMR spectrum of sample D19 adulterated with 10 % w/w sunflower oil

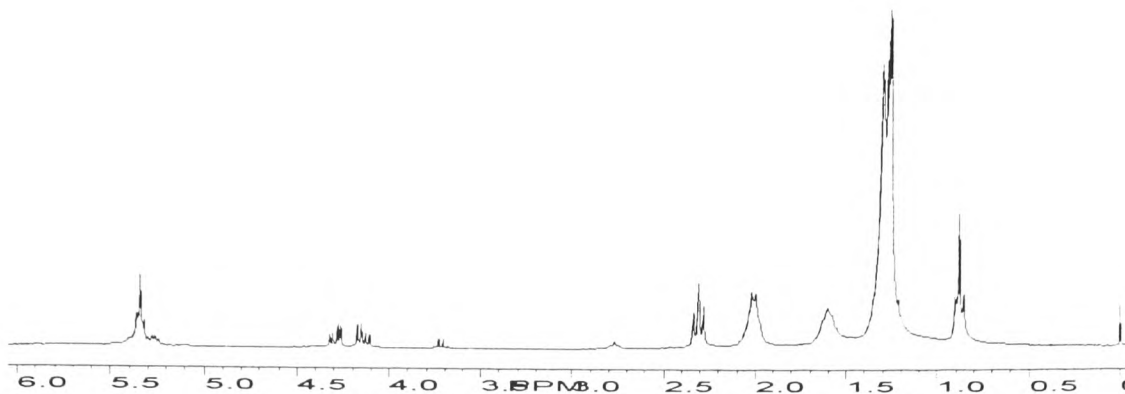


Figure E58 <sup>1</sup>H NMR spectrum of sample D20

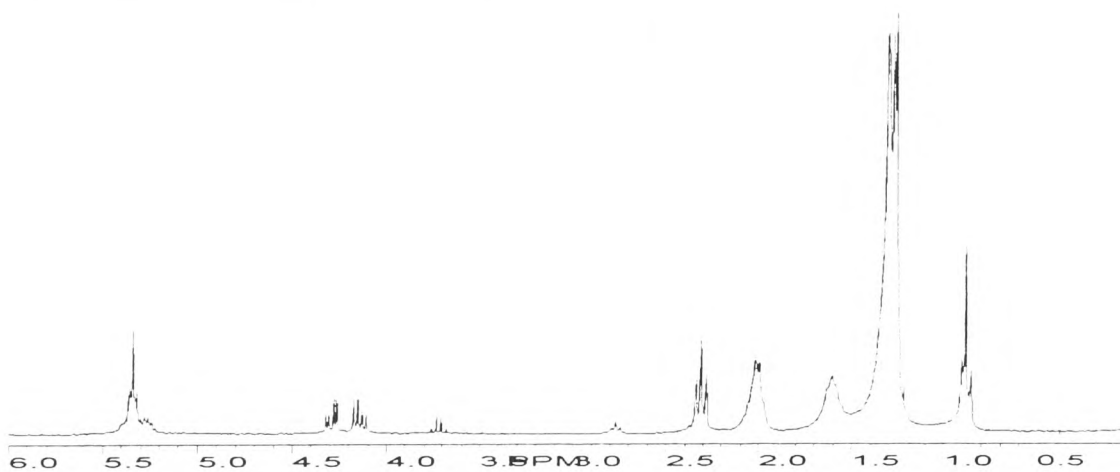


Figure E59 <sup>1</sup>H NMR spectrum of sample D20 adulterated with 5 % w/w sunflower oil

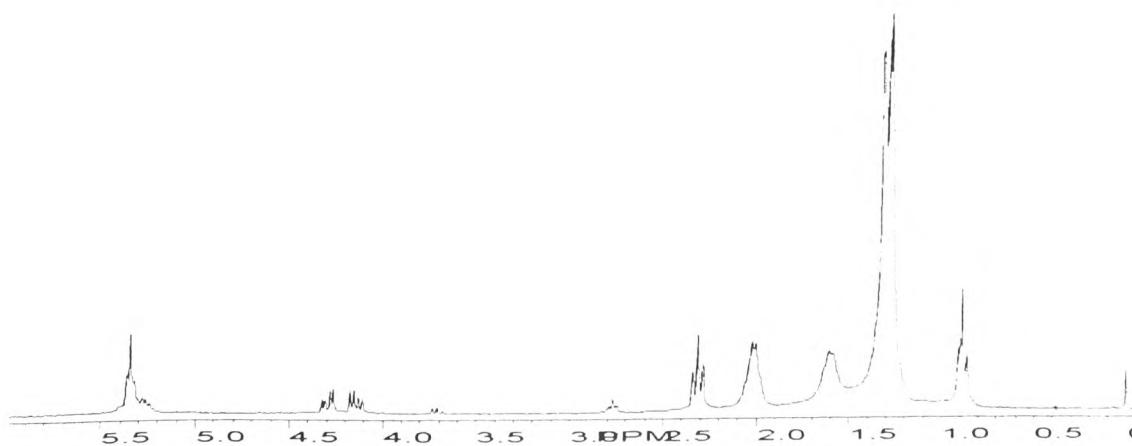
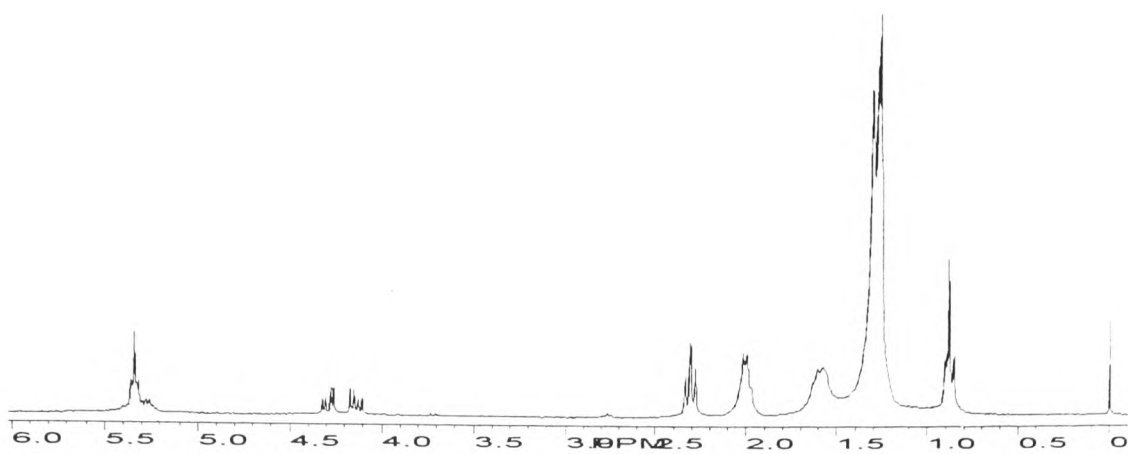
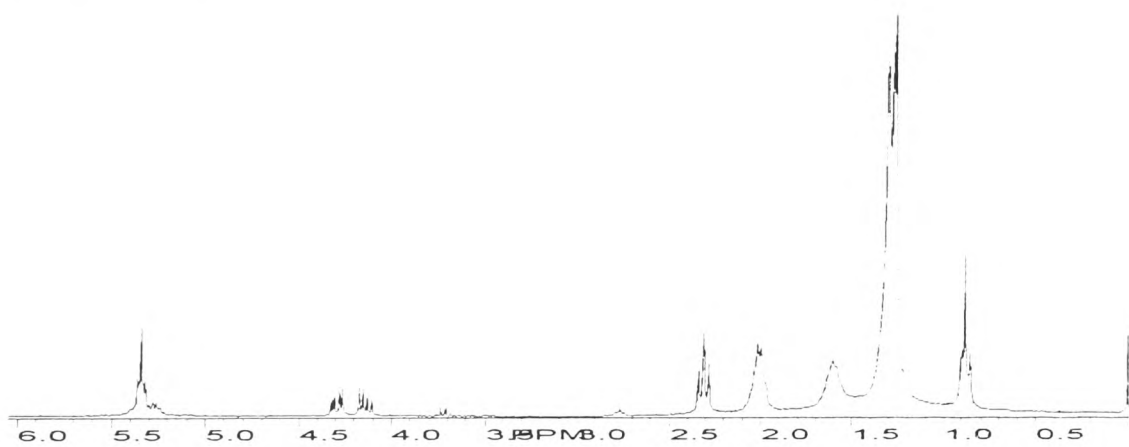


Figure E60 <sup>1</sup>H NMR spectrum of sample D20 adulterated with 10 % w/w sunflower oil



**Figure E61** <sup>1</sup>H NMR spectrum of sample D21



**Figure E62** <sup>1</sup>H NMR spectrum of sample D21 adulterated with 5 % w/w sunflower oil

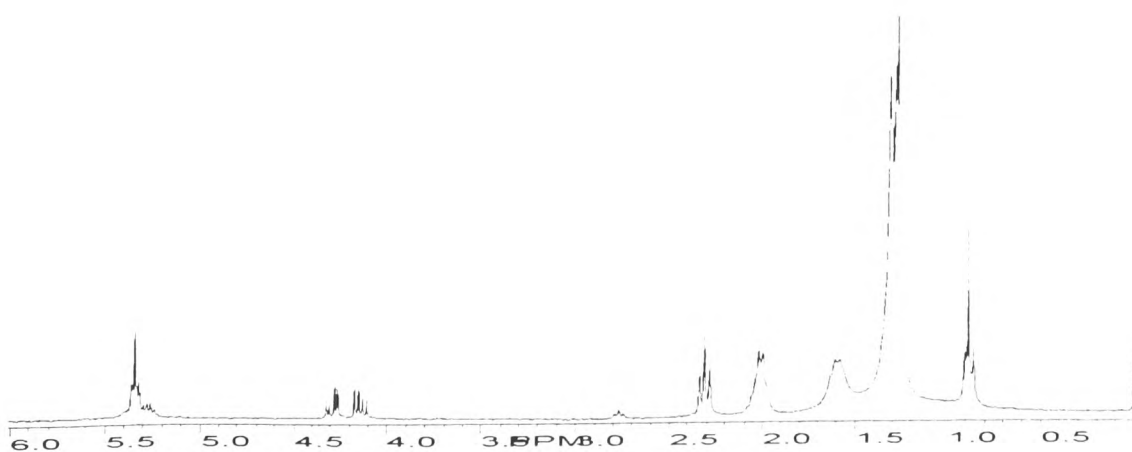


**Figure E63** <sup>1</sup>H NMR spectrum of sample D21 adulterated with 10 % w/w sunflower oil

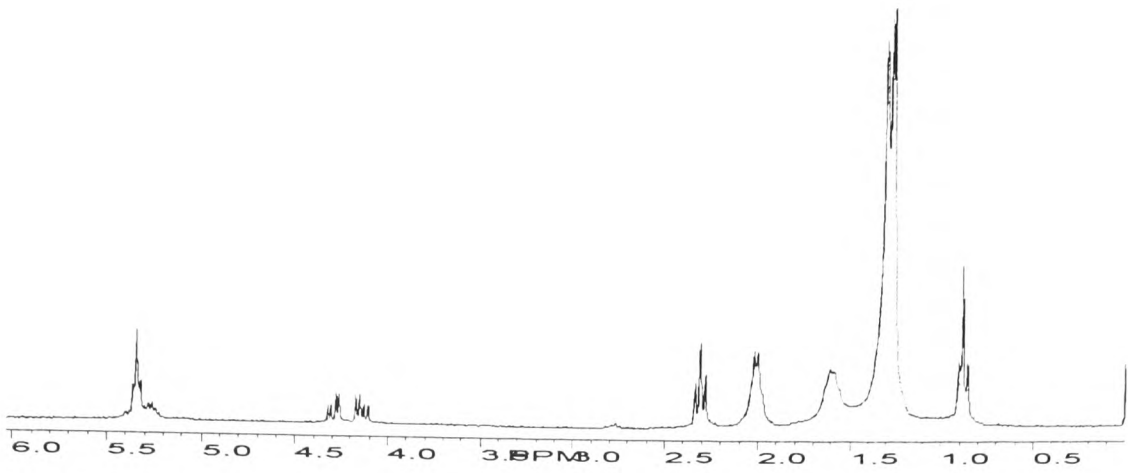


Figure E64 <sup>1</sup>H NMR spectrum of sample D22

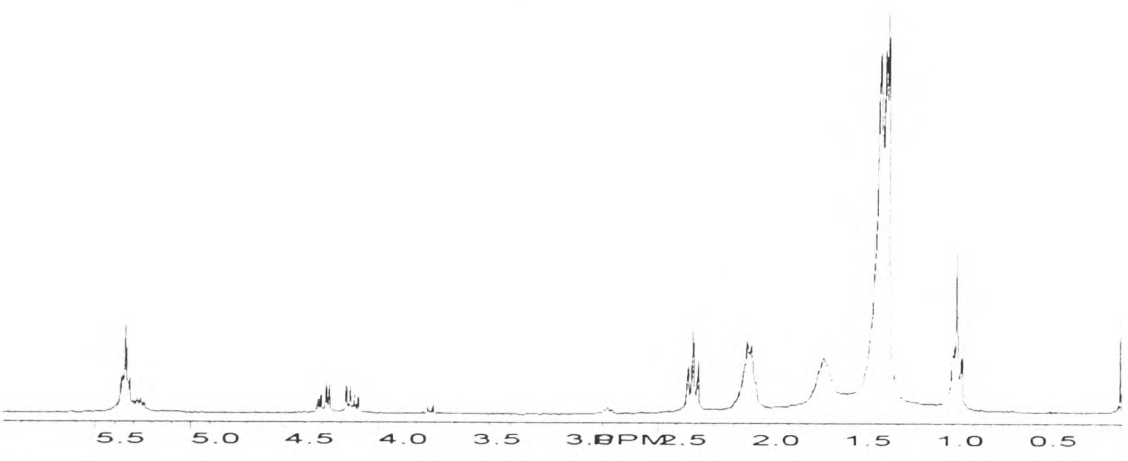


Figure E65 <sup>1</sup>H NMR spectrum of sample D22 adulterated with 5 % w/w sunflower oil

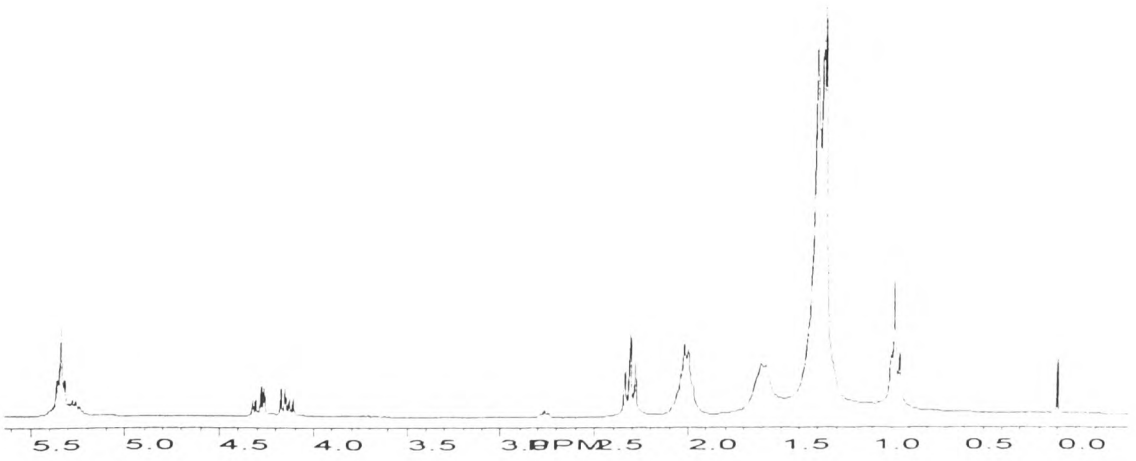


Figure E66 <sup>1</sup>H NMR spectrum of sample D22 adulterated with 10 % w/w sunflower oil



## APPENDIX F

Figure F1 Score plot of authentic Training set.....	F1
Figure F2 Score plot of Adult/2% Training set.....	F1
Figure F3 Score plot of Adult/5 % Training set.....	F1
Figure F4 Score plot of Adult/10 % Training set.....	F2
Figure F5 Score plot of Authfcv Training set.....	F2
Figure F6 Score plot of Authfcv/2 % Training set.....	F2
Figure F7 Score plot of Authfcv/5 % Training set.....	F3
Figure F8 Score plot of Authfcv/10 % Training set.....	F3
Figure F9 Score plot of Original Training set.....	F3
Figure F10 Score plot of Sun /2 % training set.....	F4
Figure F11 Score plot of Sun /5 % Training set.....	F4
Figure F12 Score plot of Sun /10 % Training set.....	F4
Figure F13 Score plot of Finorg Training set.....	F5
Figure F14 Score plot of Fin/2 % Training set.....	F5
Figure F15 Score plot of Fin/5 % Training set.....	F5
Figure F16 Score plot of Fin/10 % Training set.....	F6

Figure F17 Score plot of Finorg3 Training set.....	F6
Figure F18 Score plot of Fin3/2 % Training set.....	F6
Figure F19 Score plot of Fin3/5 % Training set.....	F7
Figure F20 Score plot of Fin3/10 % Training set.....	F7
Figure F21 Score plot of Fin8/2 % Training set.....	F7
Figure F22 Score plot of Finorg8 Training set.....	F8
Figure F23 Score plot of Fin8/5 % Training set.....	F8
Figure F24 Score plot of Fin8/10 % Training set.....	F8
Figure F25 Score plot of Pelop Training set.....	F9
Figure F26 Score plot of Rorgpel2 Training set.....	F9
Figure F27 Score plot of Rorgpel5 Training set.....	F9
Figure F28 Score plot of Rorgpel10 Training set.....	F10
Figure F29 Score plot of Pelfin Training set.....	F10
Figure F30 Score plot of Pel/2 % Training set.....	F10
Figure F31 Score plot of Pel/5 % Training set.....	F11
Figure F32 Score plot of Pel/10 % Training set.....	F11
Figure F33 Score plot of Crete Training set.....	F11

Figure F34 Score plot of Crete/2 % Training set .....	F12
Figure F35 Score plot of Crete/5 % Training set .....	F12
Figure F36 Score plot of Crete/10 % Training set .....	F12
Figure F37 Score plot of org1 Training set (containing authentic samples) using reduced FIR data 3050 - 2752 .....	F13
Figure F38 score plot of org1 Training set (containing authentic samples adulterated with 10 % w/w sunflower) using reduced IR data 3050 - 2752 .....	F13
Figure F39 Score plot of ore Training set (containing authentic samples) using reduced IR data 3100 - 2500, 1800 - 1000 .....	F13
Figure F40 Score plot of selo Training set (containing authentic samples from selective IR region) .....	F14
Figure F41 Score plot of sel2 Training set (containing authentic samples adulterated with 2 % w/w sunflower) on selective data region .....	F14
Figure F42 Score plot of sel5 Training set (containing authentic samples adulterated with 5 % w/w sunflower) on selective data region .....	F14
Figure F43 Score plot of sel10 Training set (containing authentic samples adulterated with 10 % w/w sunflower) on selective data region .....	F15
Figure F44 Score plot of Carkorg Training set .....	<b>F1Error! Bookmark not defined.</b>
Figure F45 Score plot of Carb5 Training set.....	F15

Figure F46 Score plot of Carb10 Training set.....	F16
Figure F47 Score plot of Caralkborg Training set.....	F16
Figure F48 Score plot of Calkalk5 Training set .....	F16
Figure F49 Score plot of Calkalk10 Training set .....	F17
Figure F50 Score plot of Crevar Training set.....	F17
Figure F51 Score plot of Pelvar Training set .....	F17
Figure F52 Score plot of Protorg Training set.....	F18
Figure F53 Score plot of Prot5 Training set .....	F18
Figure F54 Score plot of Prot10 Training set .....	F18
Figure F55 Score plot of Procre Training set.....	F19
Figure F56 Score plot of Propel Training set .....	F19

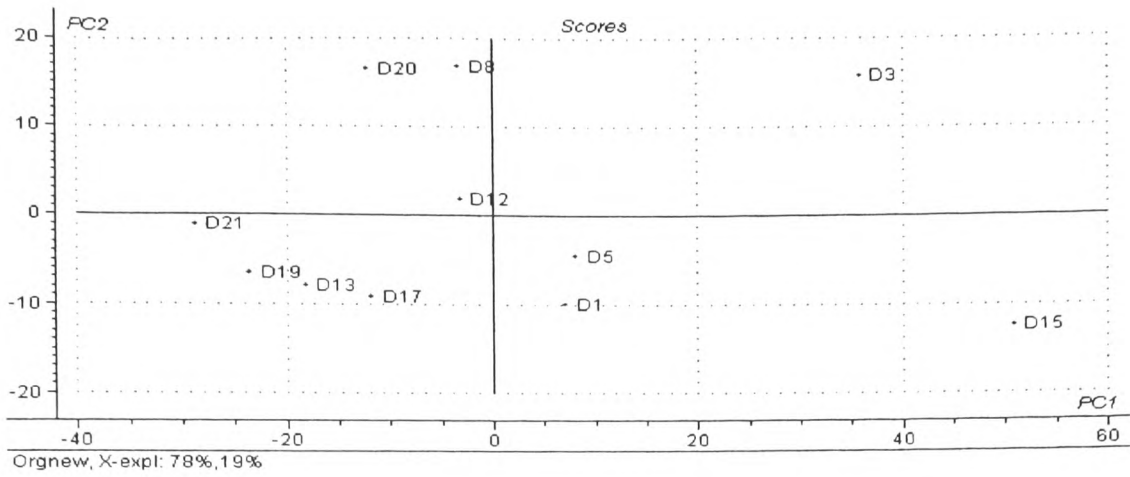


Figure F1 Score plot of Authentic Training set

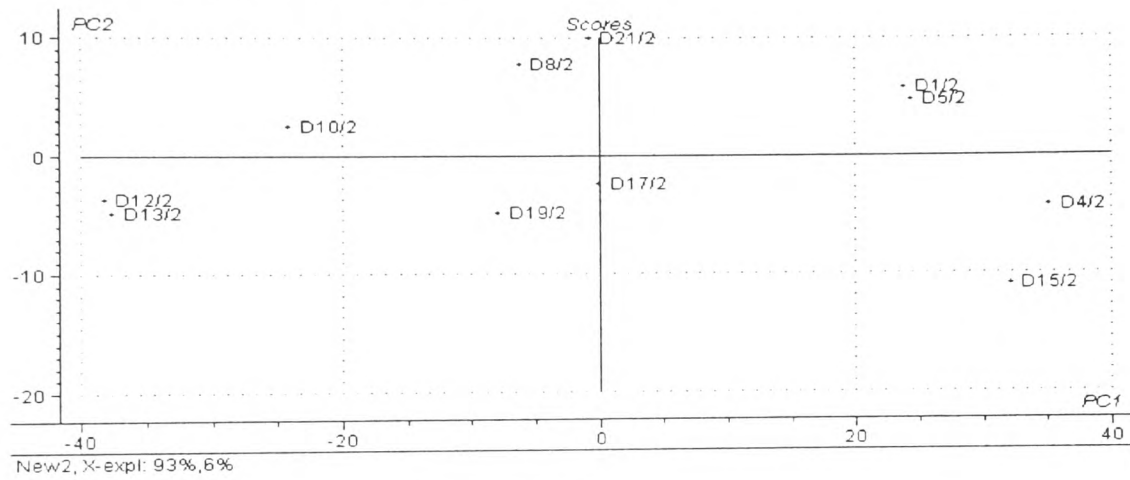


Figure F2 Score plot of Adult/2 % Training set

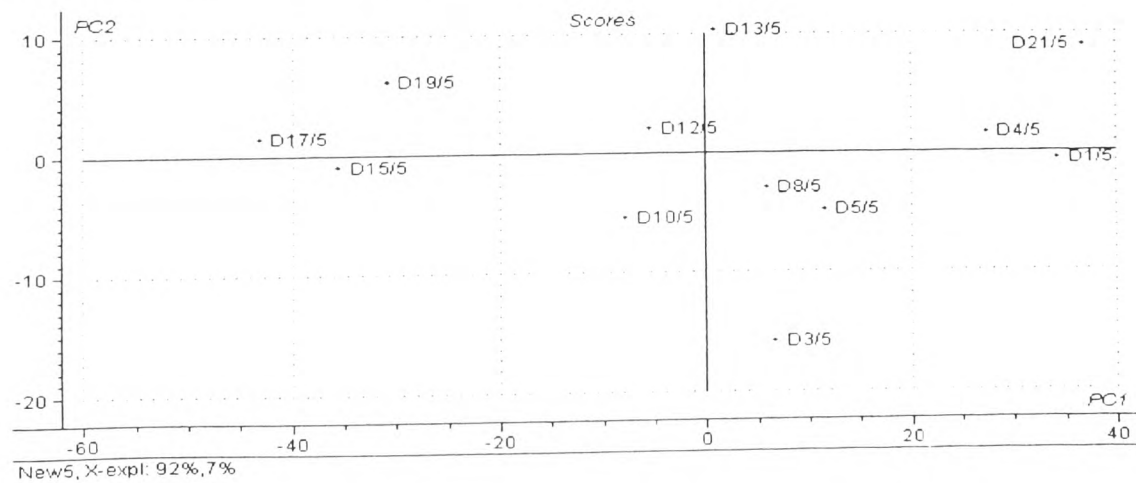


Figure F3 Score plot of Adult/5 % Training set

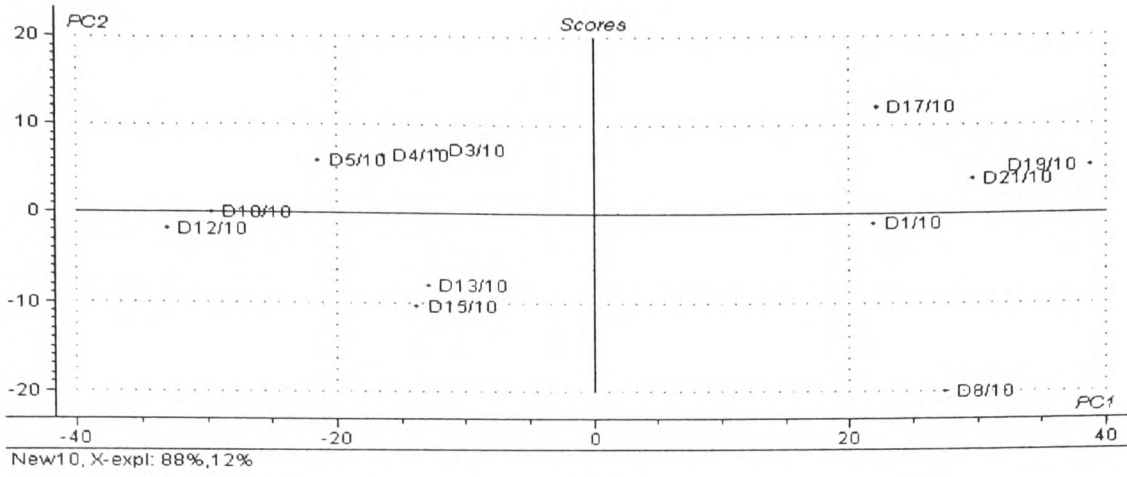


Figure F4 Score plot of Adult/10 % Training set

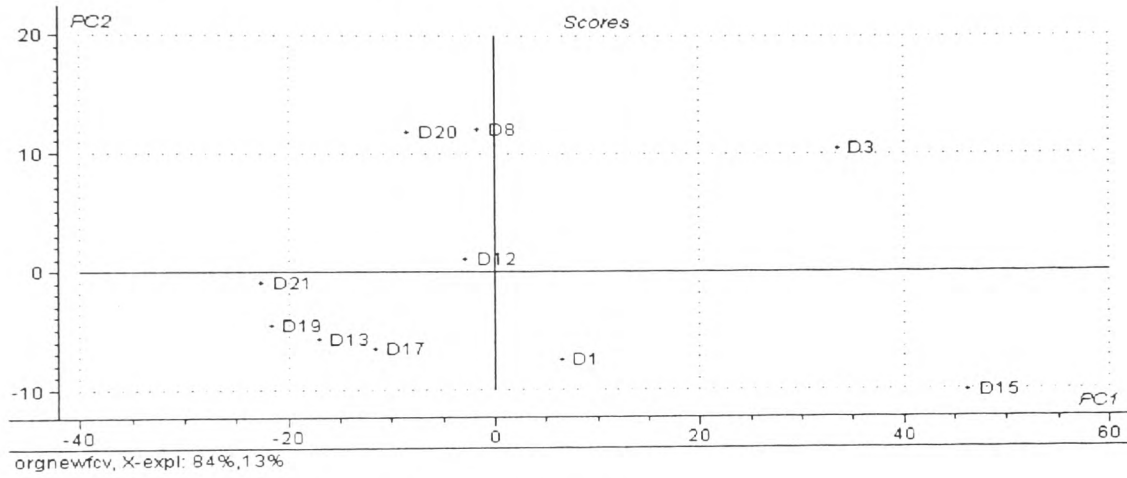


Figure F5 Score plot of Authfcv Training set

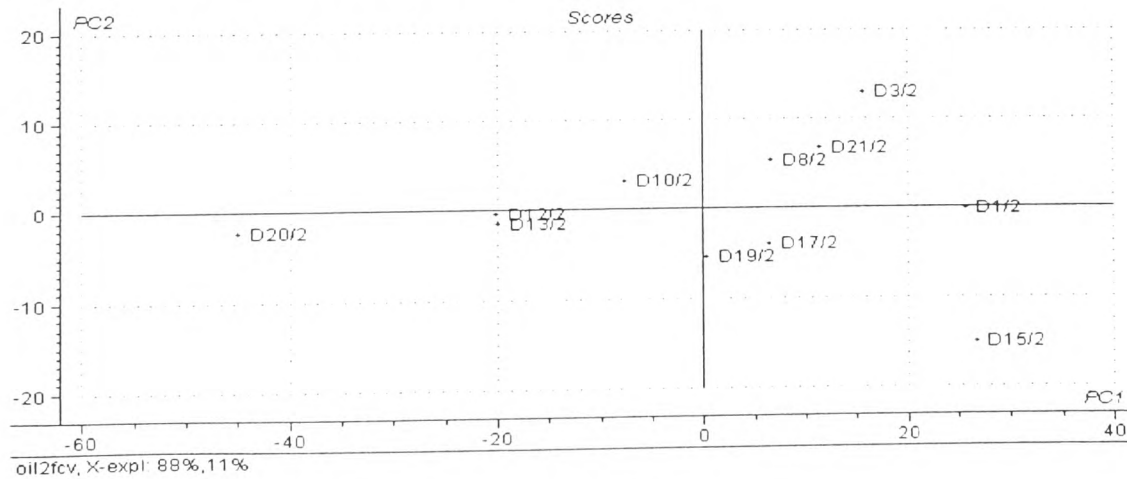


Figure F6 Score plot of Authfcv/2 % Training set

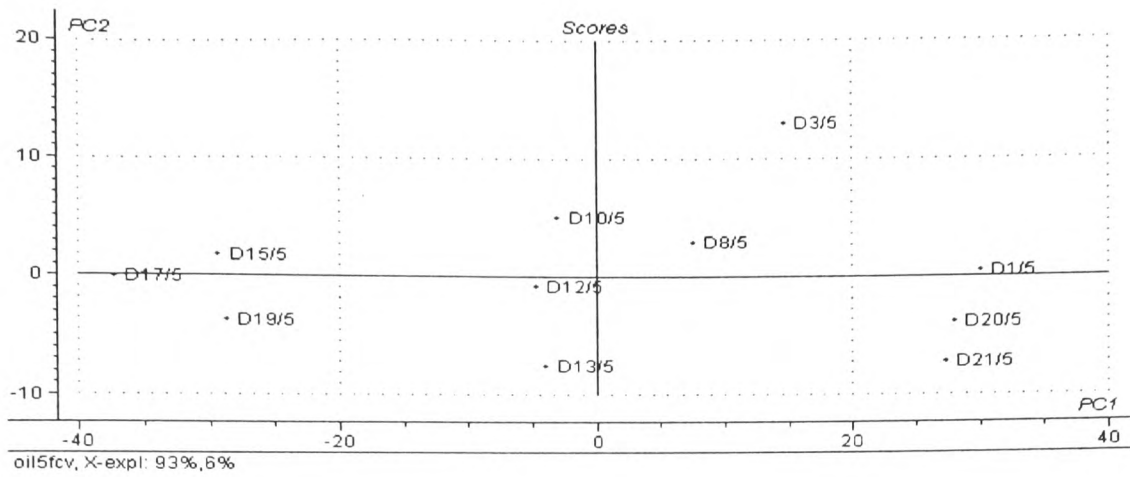


Figure F7 Score plot of Authfcv/5 % Training set

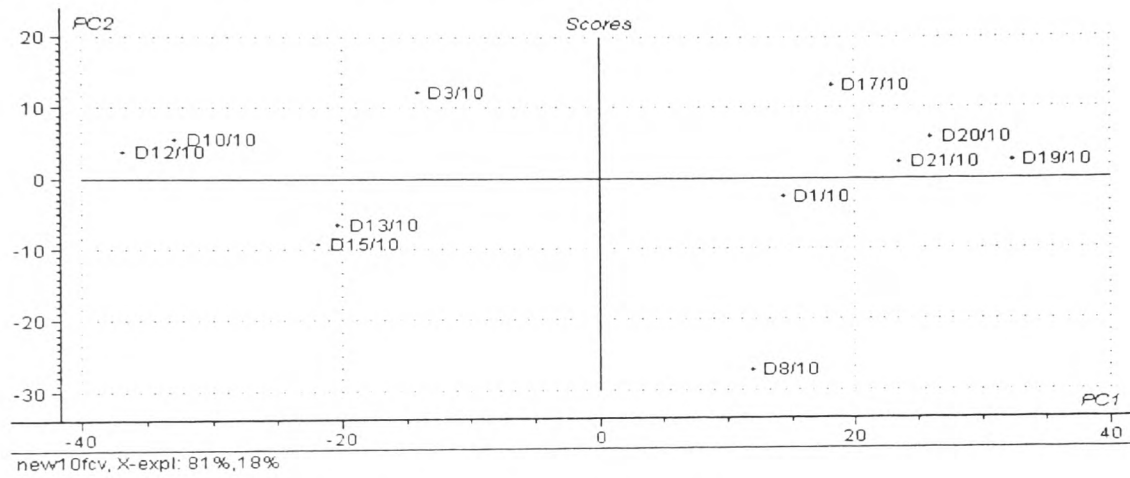


Figure F8 Score plot of Authfcv/10 % Training set

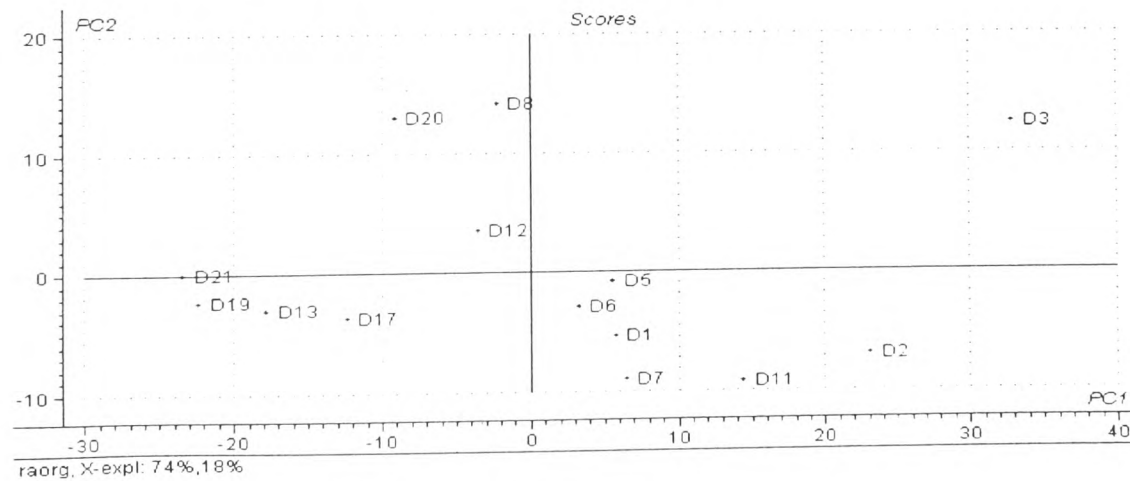


Figure F9 Score plot of Original Training set

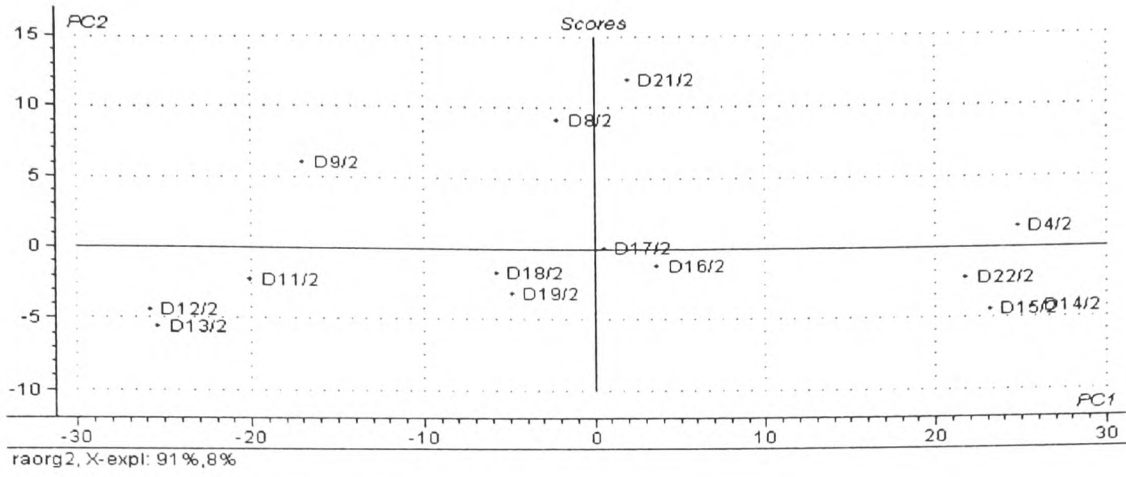


Figure F10 Score plot of Sun /2 % Training set

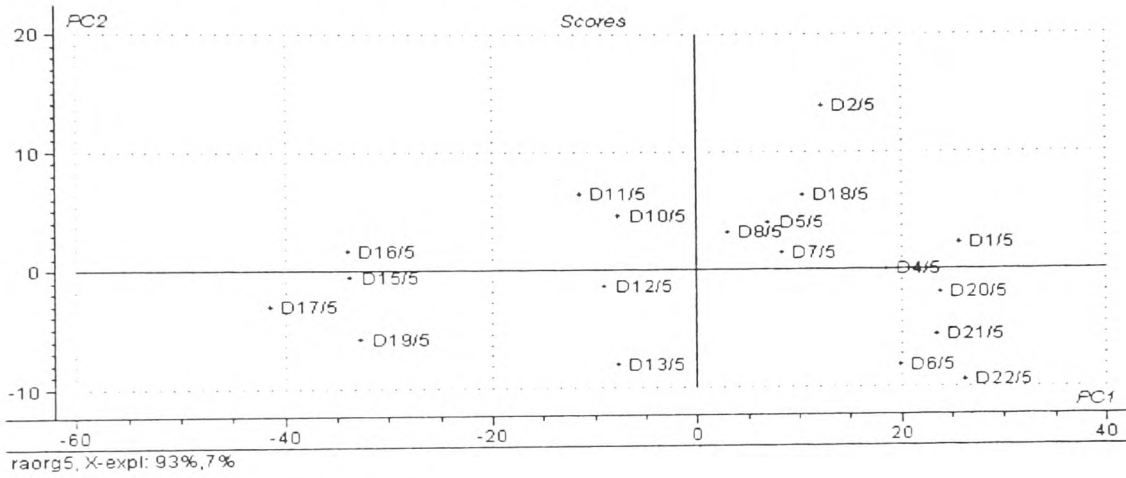


Figure F11 Score plot of Sun /5 % Training set

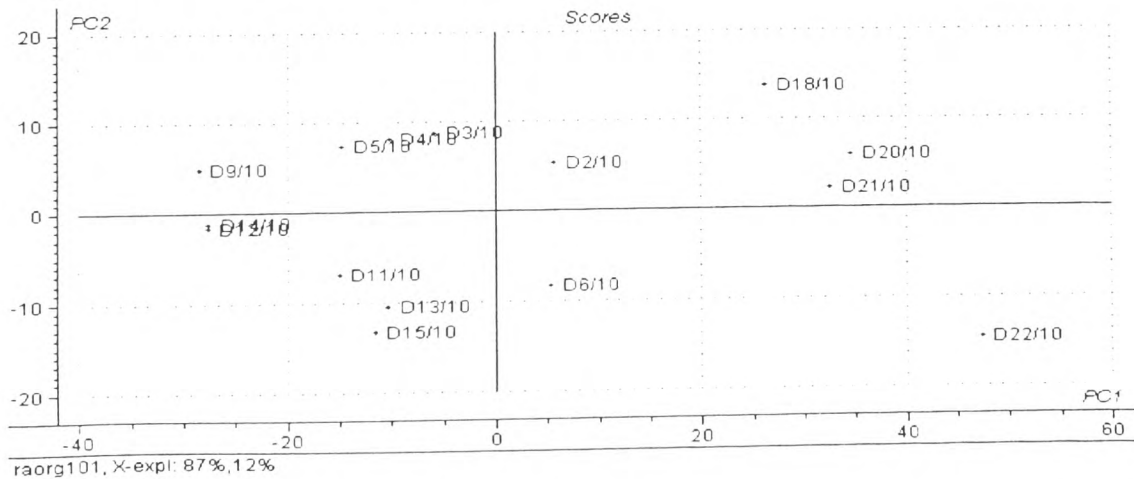


Figure F12 Score plot of Sun /10 % Training set



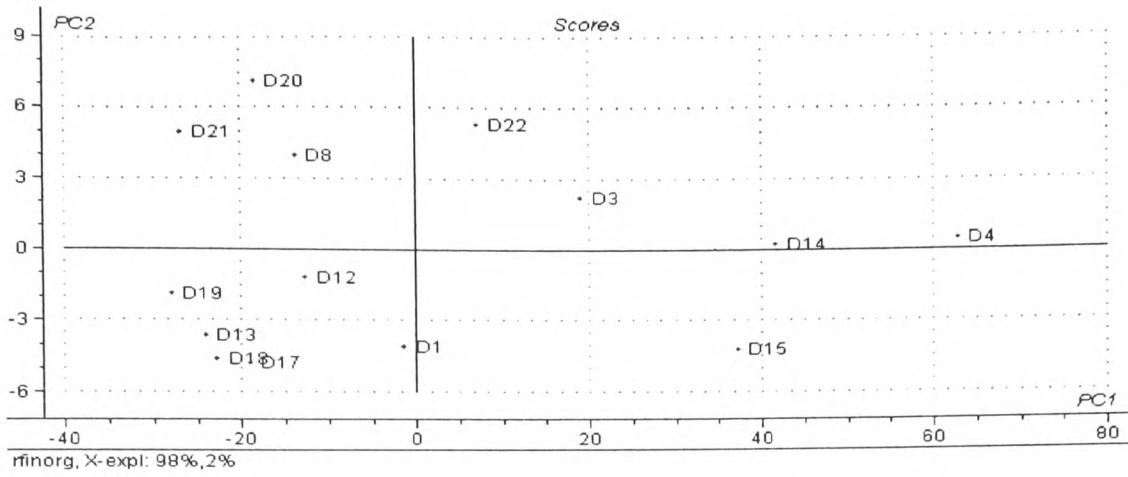


Figure F13 Score plot of Finorg Training set

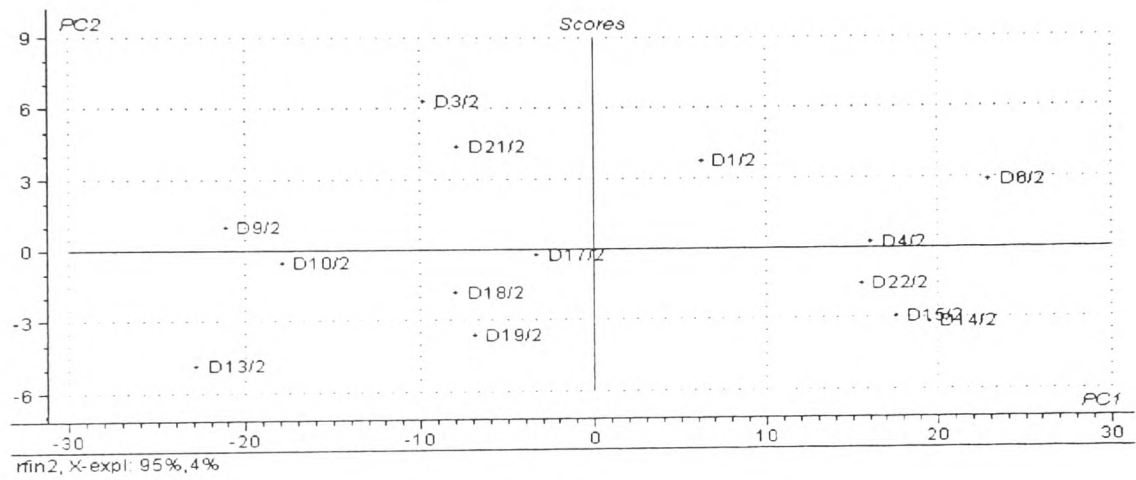


Figure F14 Score plot of Fin/2 % Training set

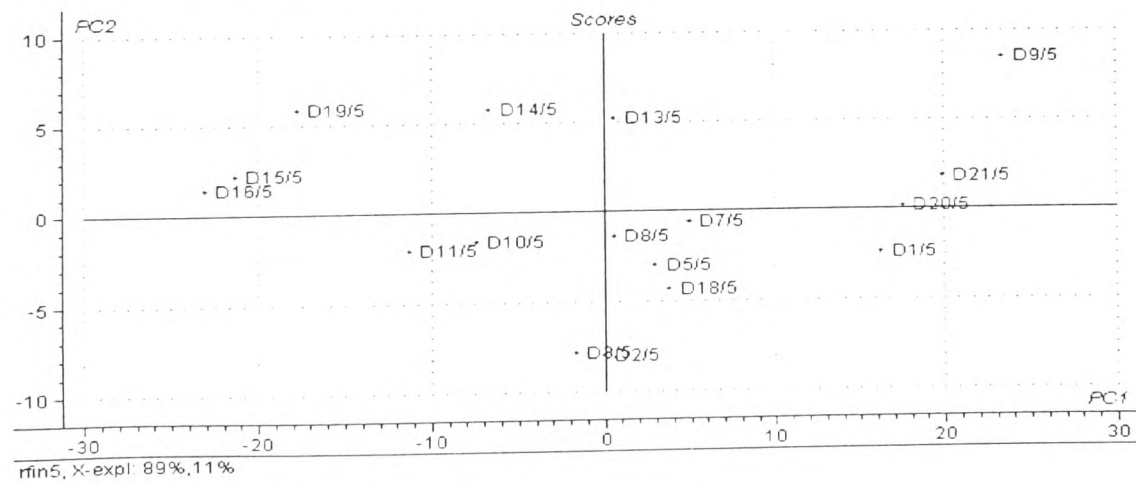


Figure F15 Score plot of Fin/5 % Training set

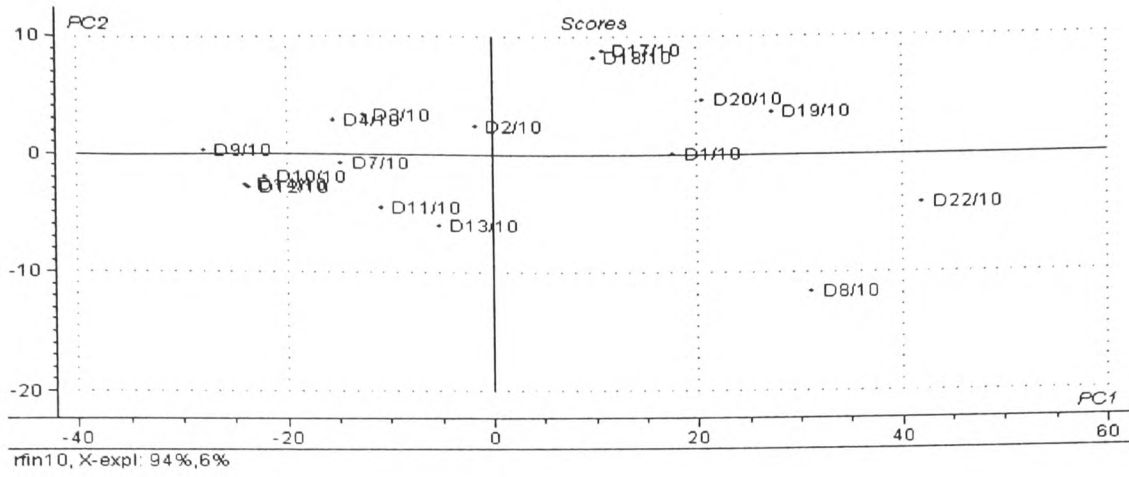


Figure F16 Score plot of Fin/10 % Training set

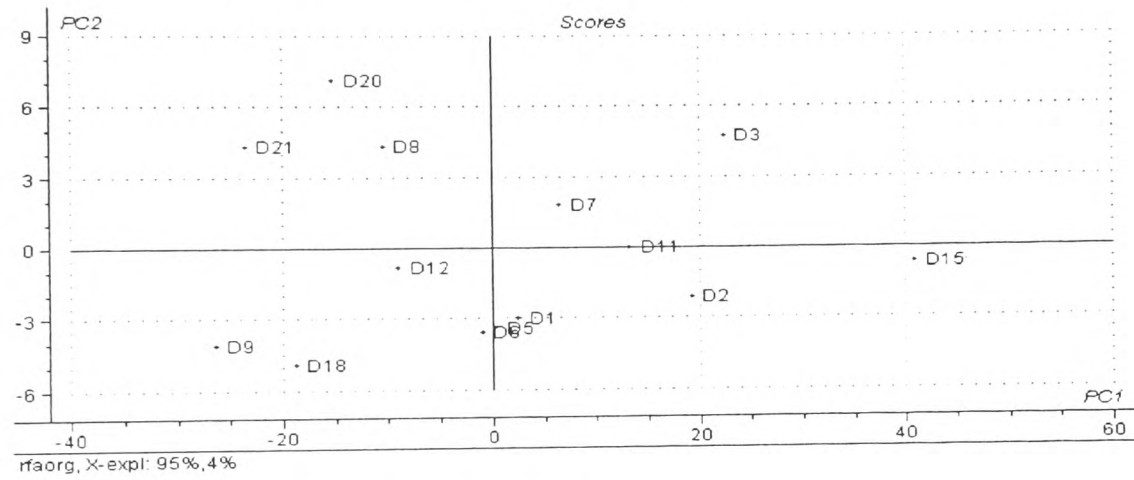


Figure F17 Score plot of Finorg3 Training set

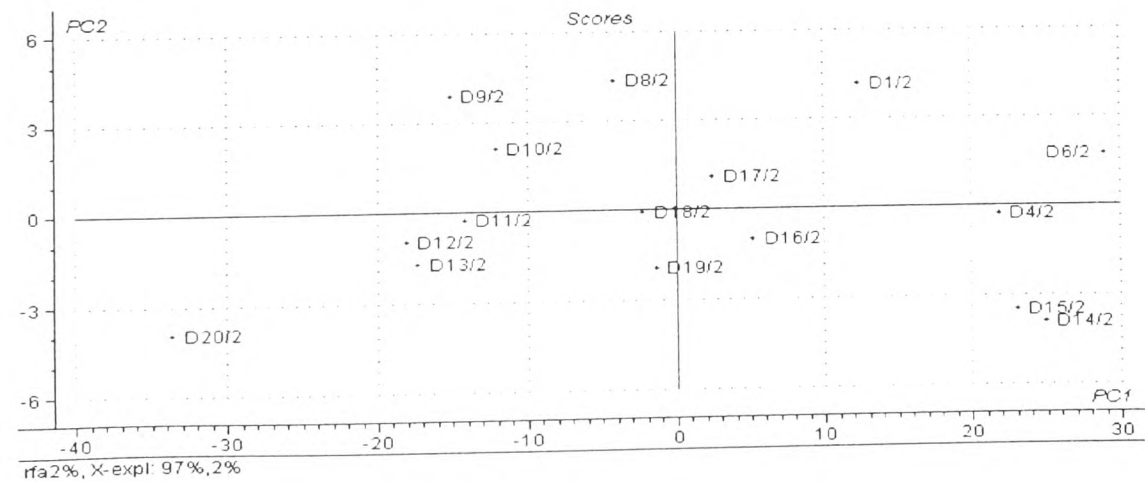


Figure F18 Score plot of Fin3/2 % Training set

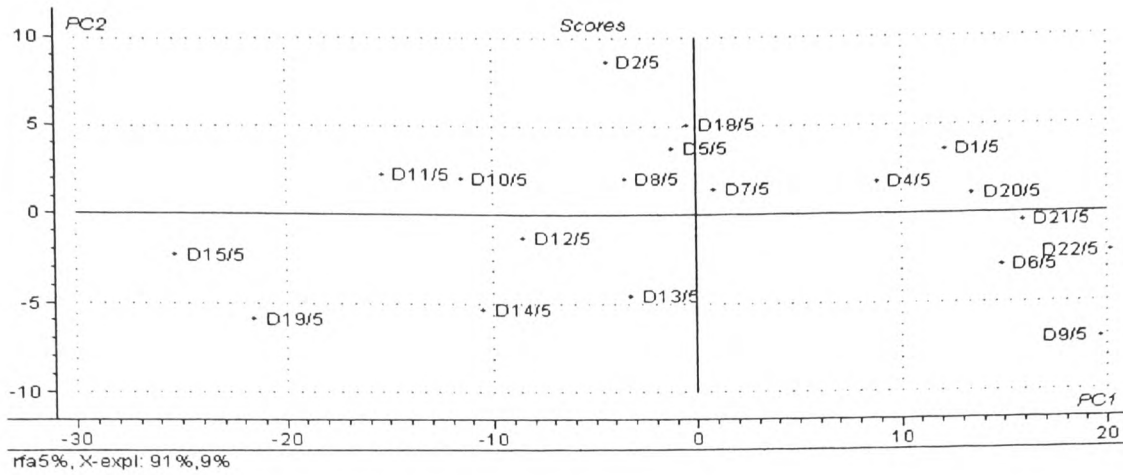


Figure F19 Score plot of Fin3/5 % Training set

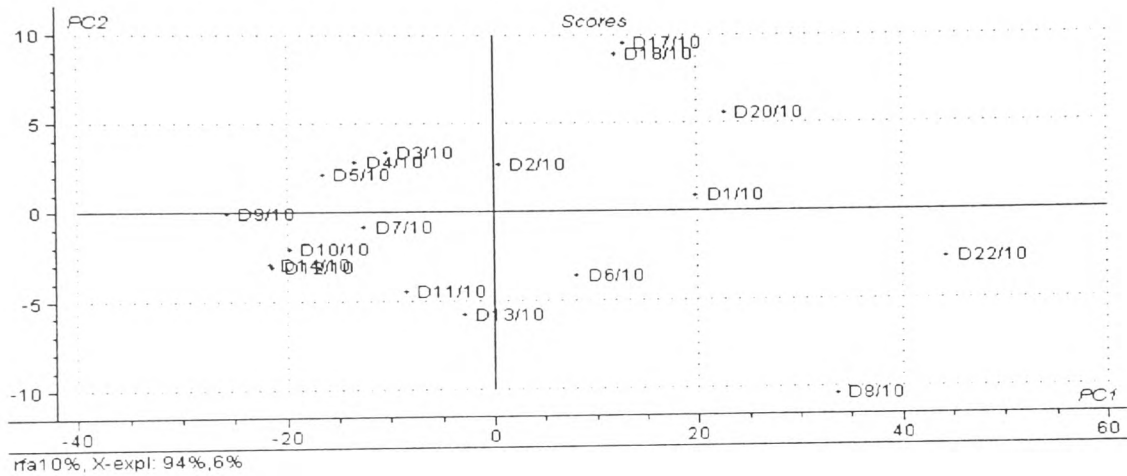


Figure F20 Score plot of Fin3/10 % Training set

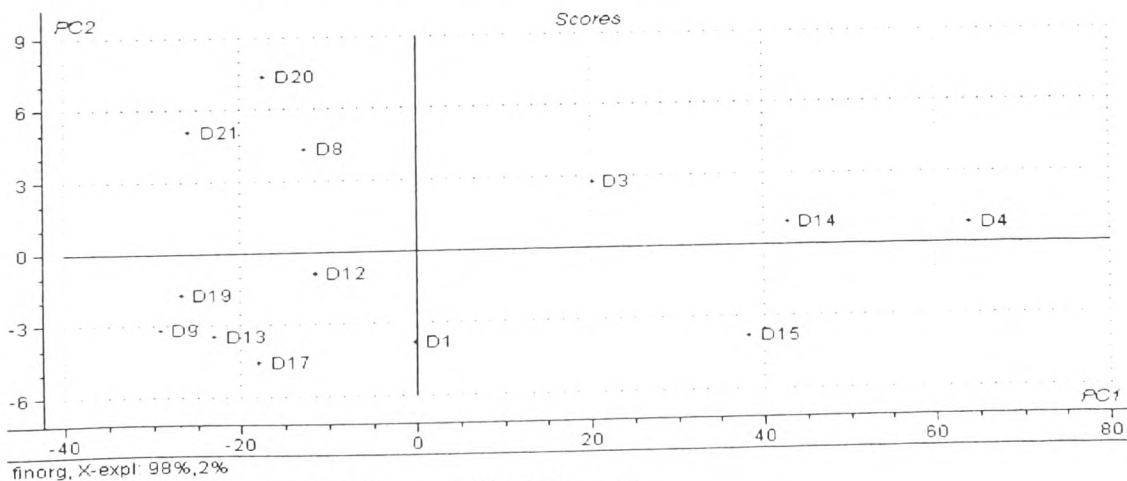


Figure F21 Score plot of Finorg8 Training set

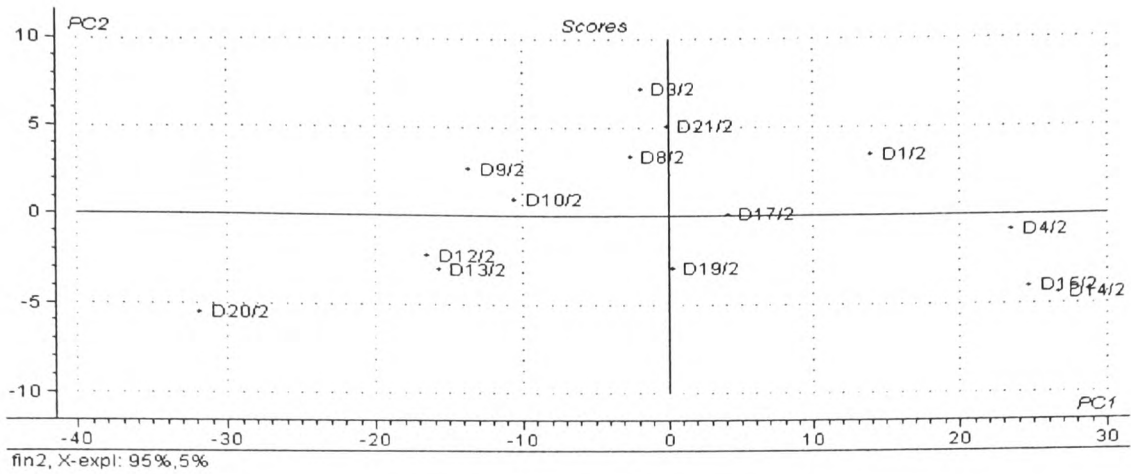


Figure F22 Score plot of Fin8/2 % Training set

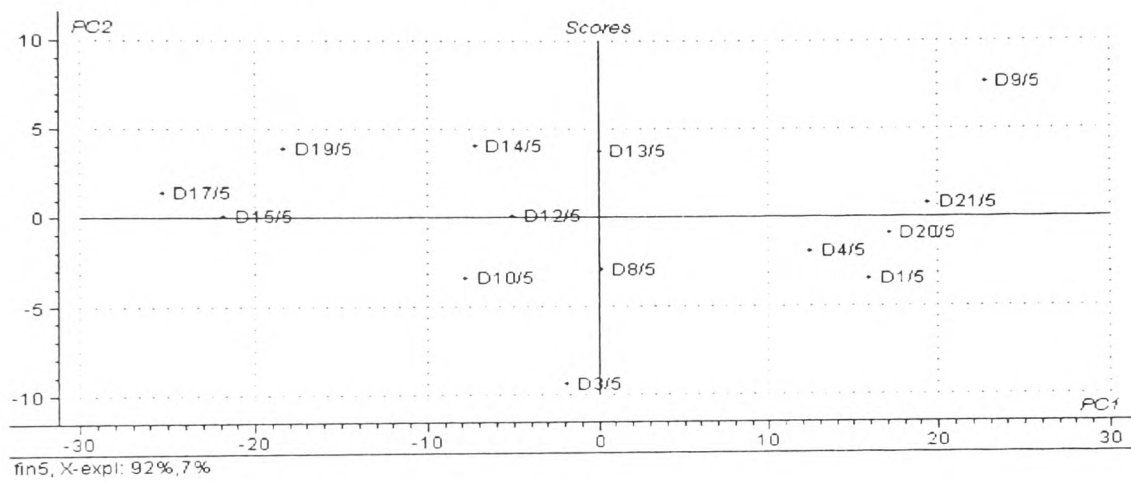


Figure F23 Score plot of Fin8/5 % Training set

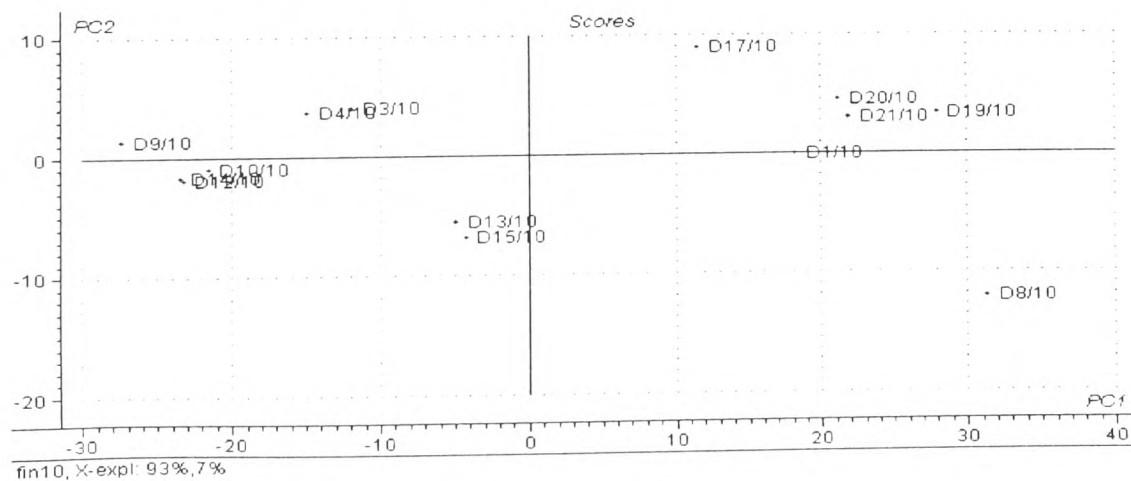


Figure F24 Score plot of Fin8/10 % Training set

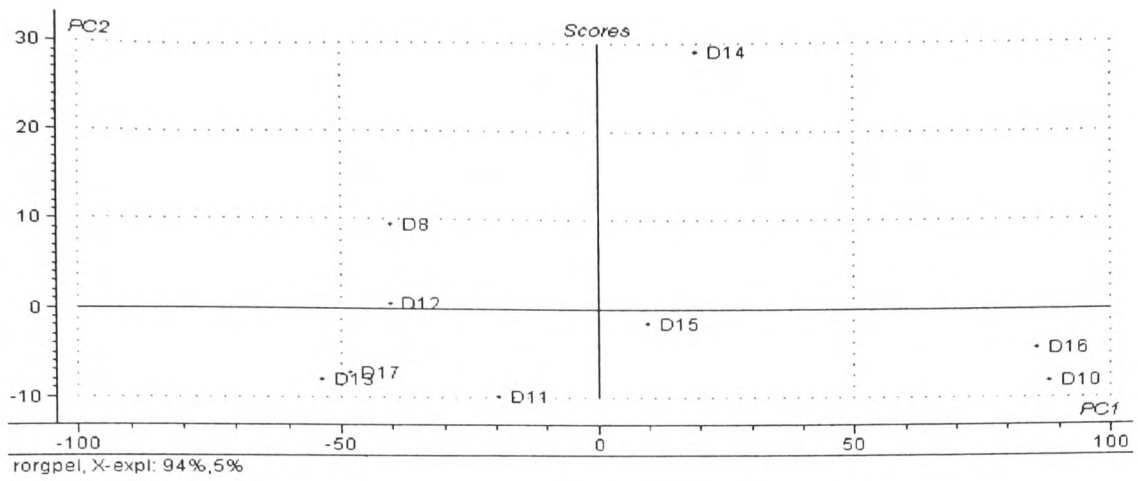


Figure F25 Score plot of Pelop Training set

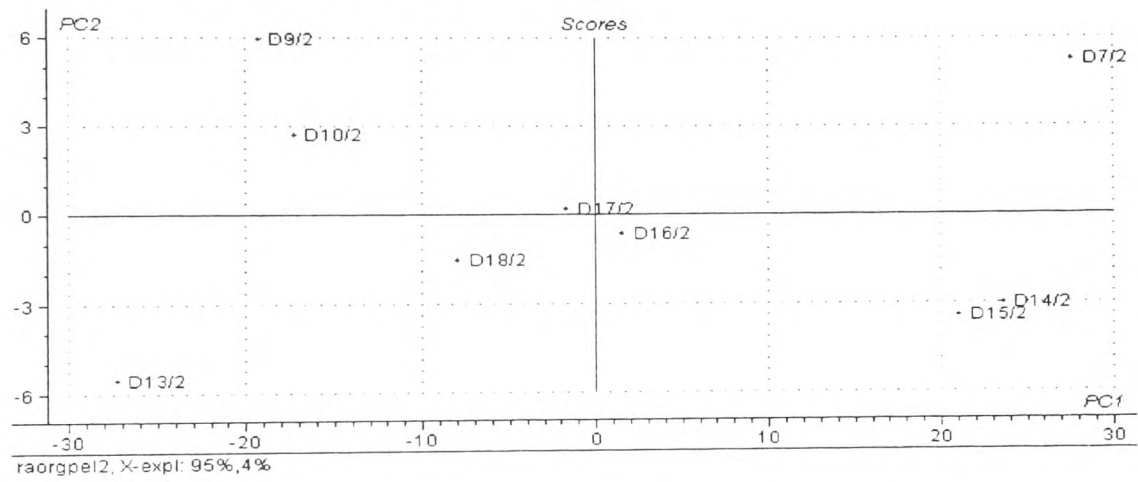


Figure F26 Score plot of Rorgpel2 Training set

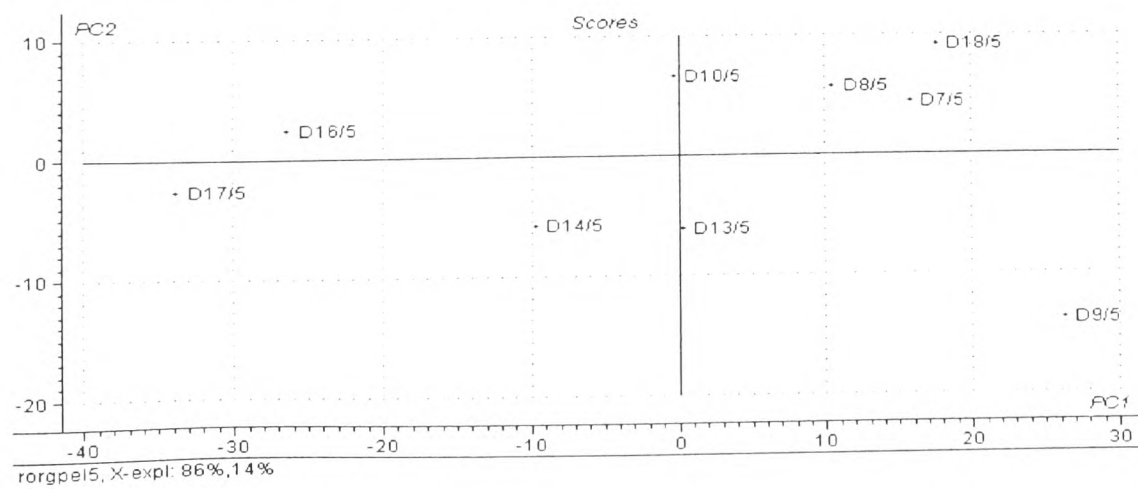


Figure F27 Score plot of Rorgpel5 Training set

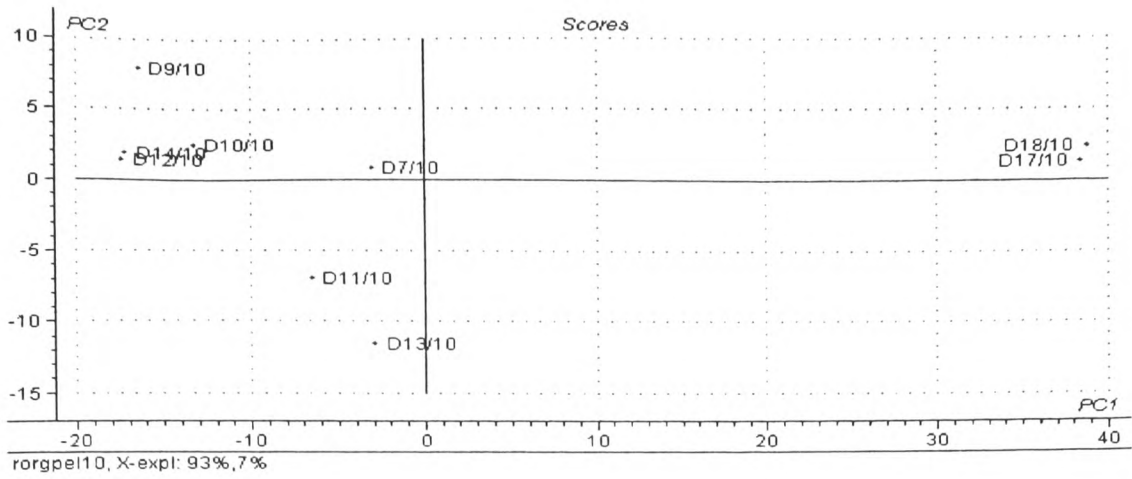


Figure F28 Score plot of Rorgpel10 Training set

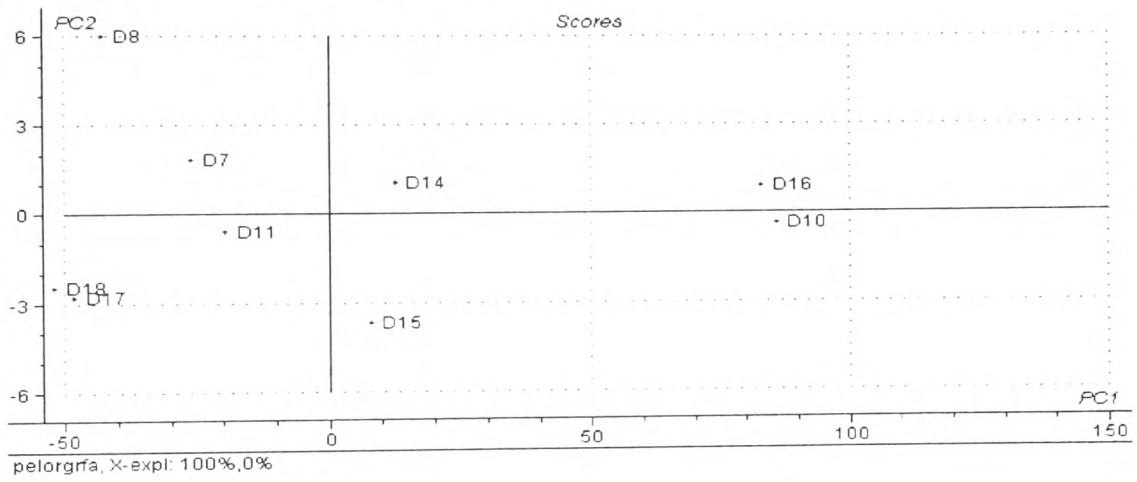


Figure F29 Score plot of Pelfin Training set

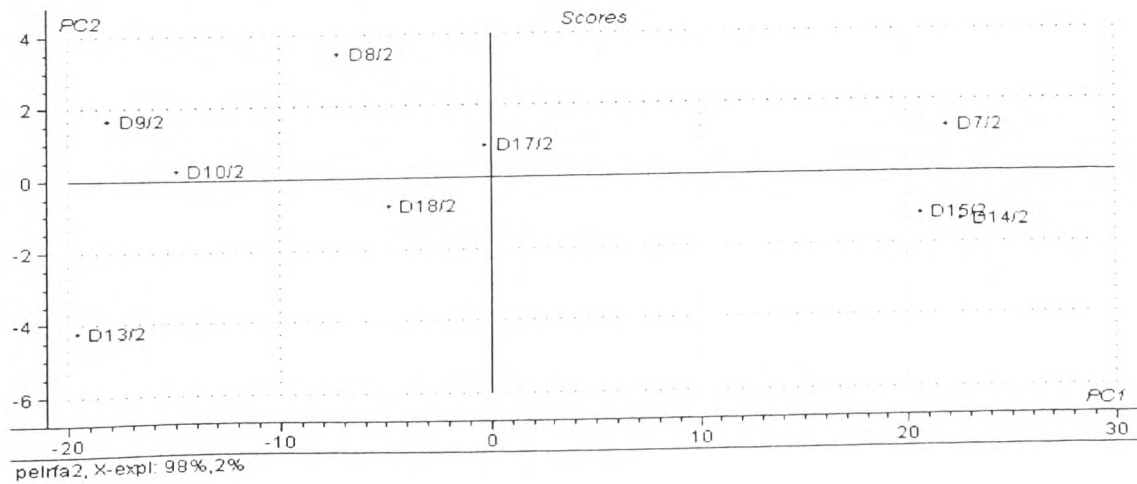


Figure F30 Score plot of Pel/2 % Training set

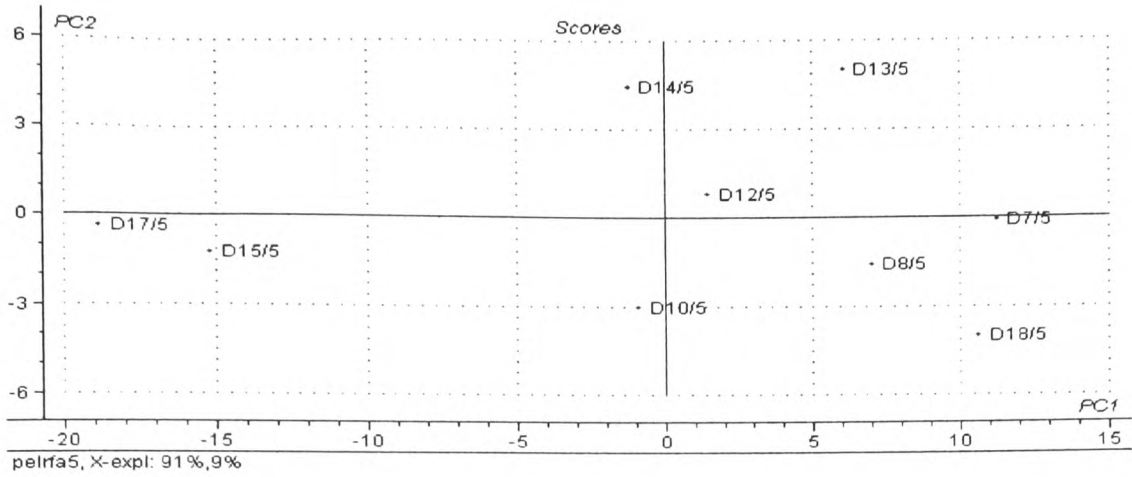


Figure F31 Score plot of Pel/5 % Training set

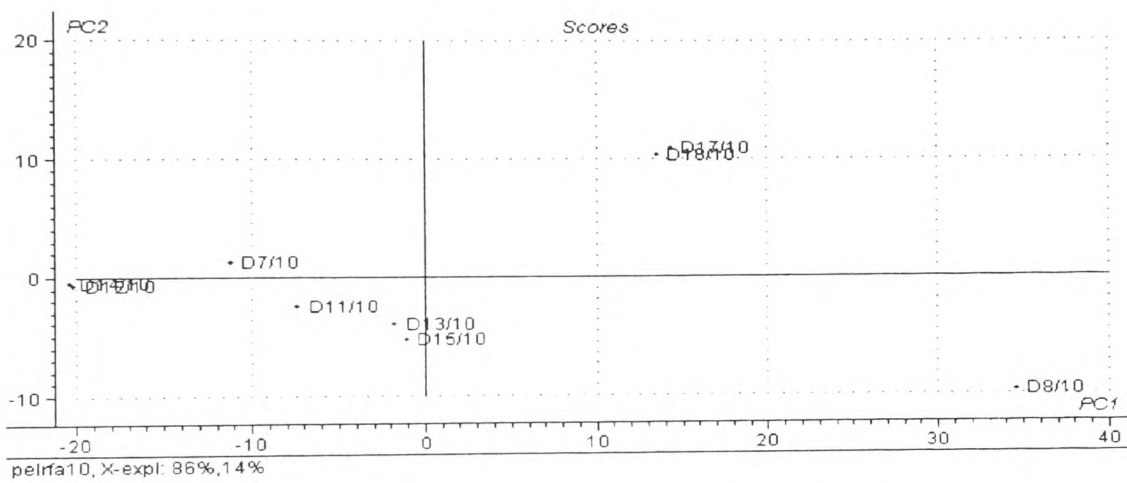


Figure F32 Score plot of Pel/10 % Training set

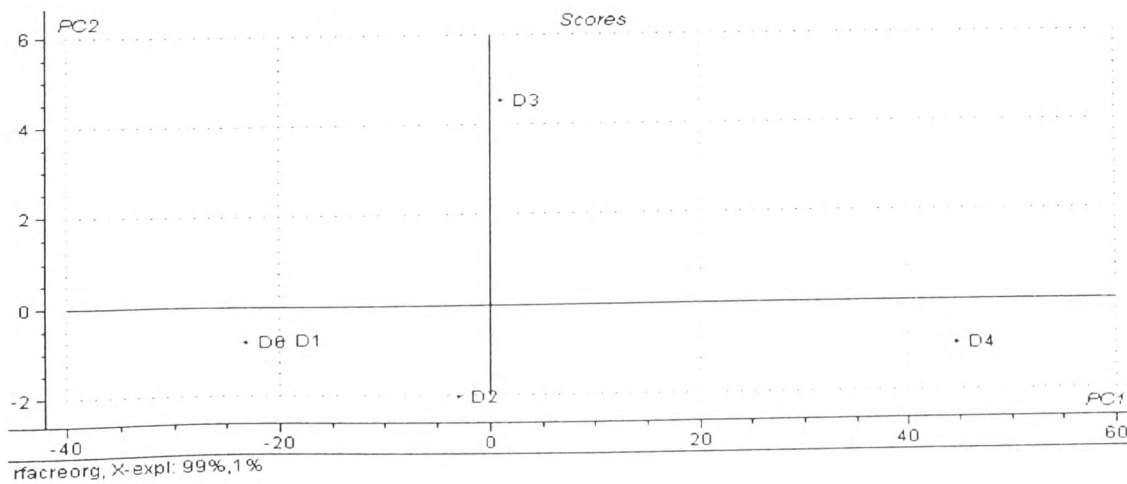


Figure F33 Score plot of Crete Training set

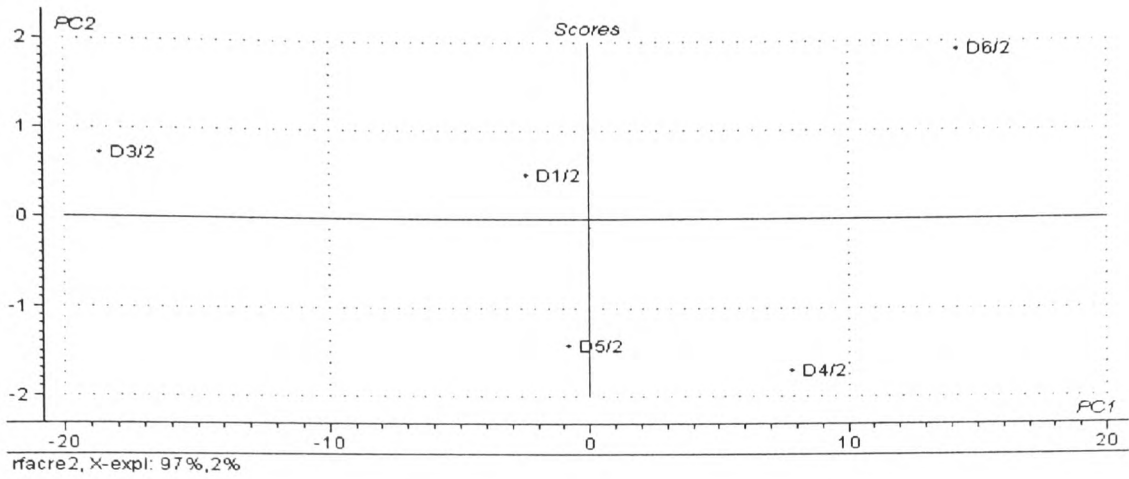


Figure F34 Score plot of Crete/2 % Training set

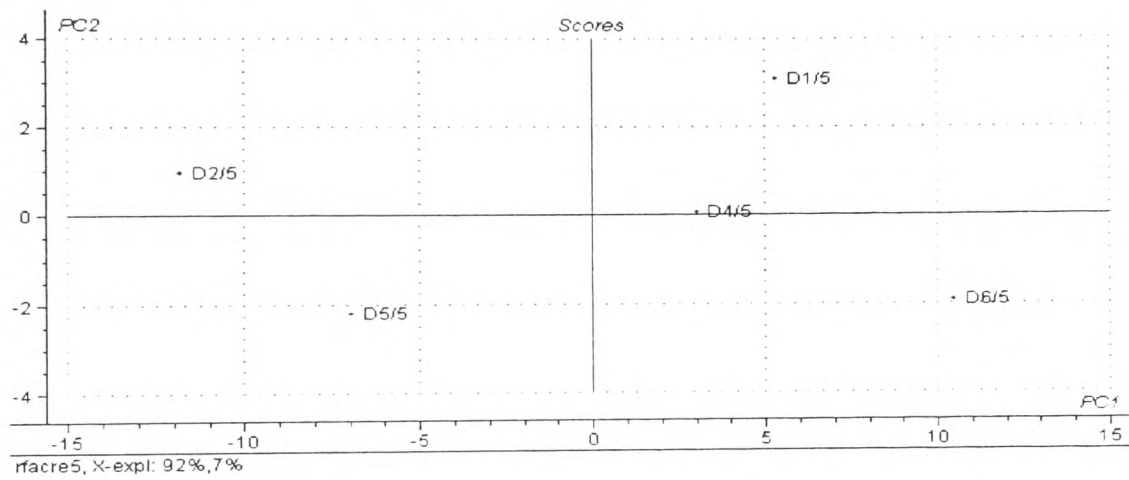


Figure F35 Score plot of Crete/5 % Training set

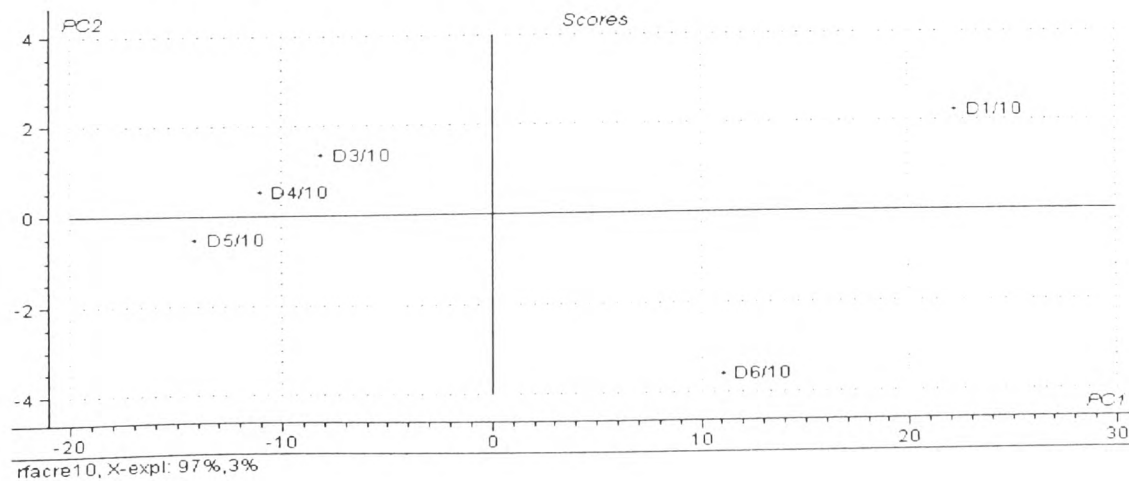
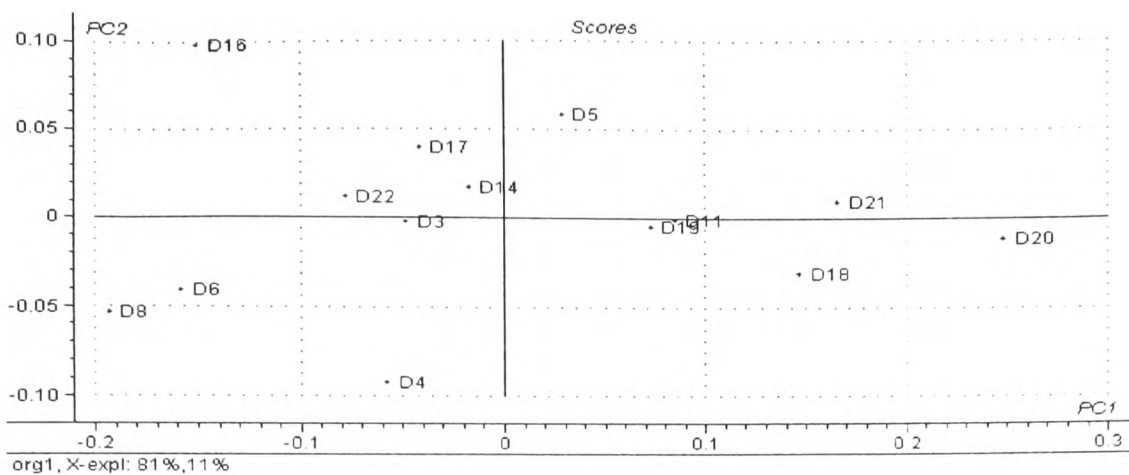
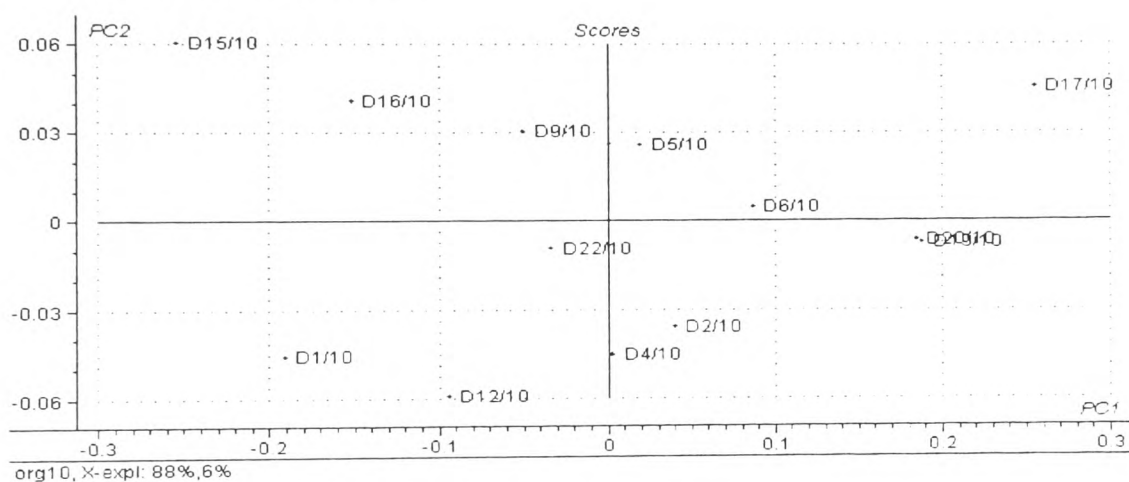


Figure F36 Score plot of Crete/10 % Training set





**Figure F37** Score plot of org1 Training set (containing authentic samples) using reduced IR data 3050 - 2752



**Figure F38** Score plot of org1 Training set (containing authentic samples adulterated with 10 % w/w sunflower) using reduced IR data 3050 - 2752  $\text{cm}^{-1}$

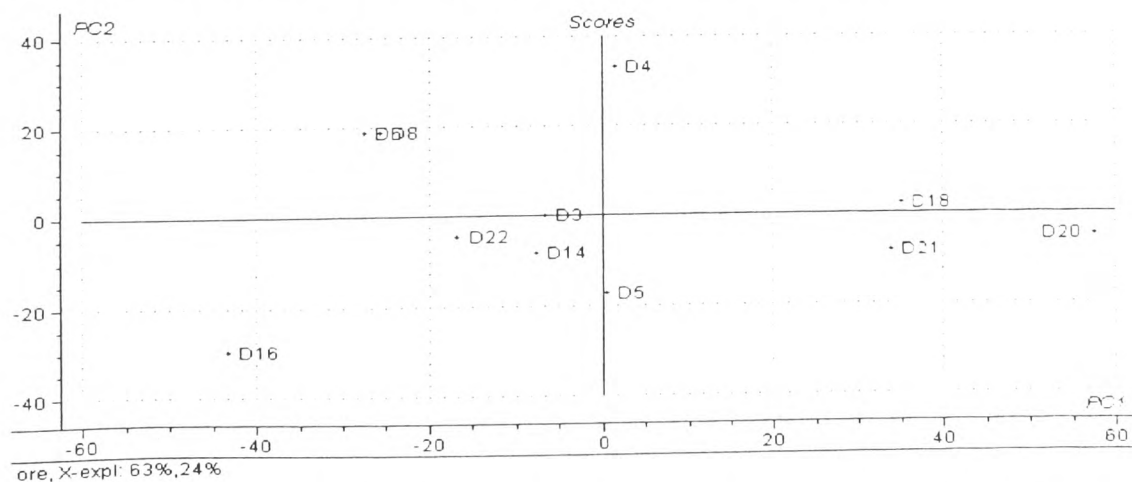


**Figure F39** Score plot of ore Training set (containing authentic samples) using reduced IR data 3100 - 2500  $\text{cm}^{-1}$ , 1800 - 1000  $\text{cm}^{-1}$

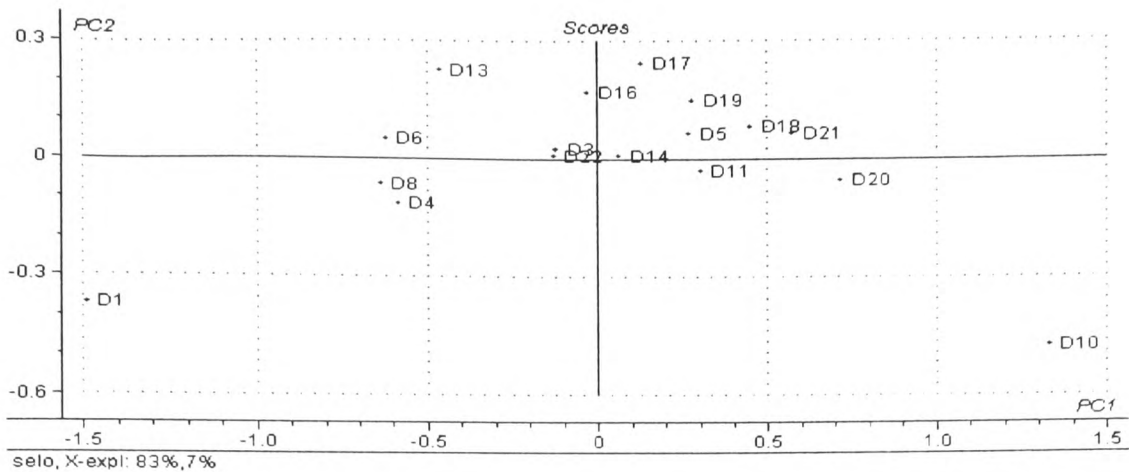


**Figure F40** Score plot of sel0 Training set (containing authentic samples from selective IR region)

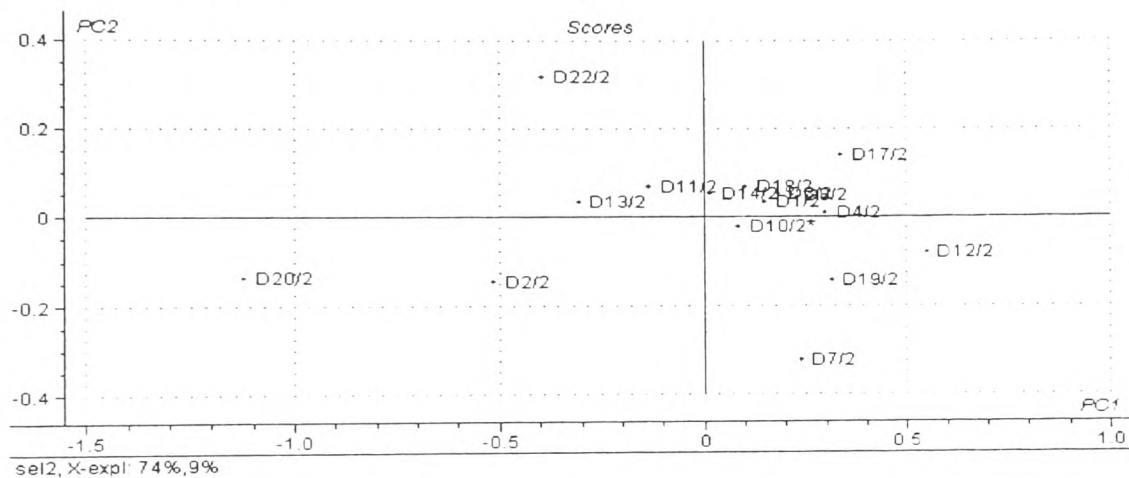


**Figure F41** Score plot of sel2 Training set (containing authentic samples adulterated with 2 % w/w sunflower) on selective data region

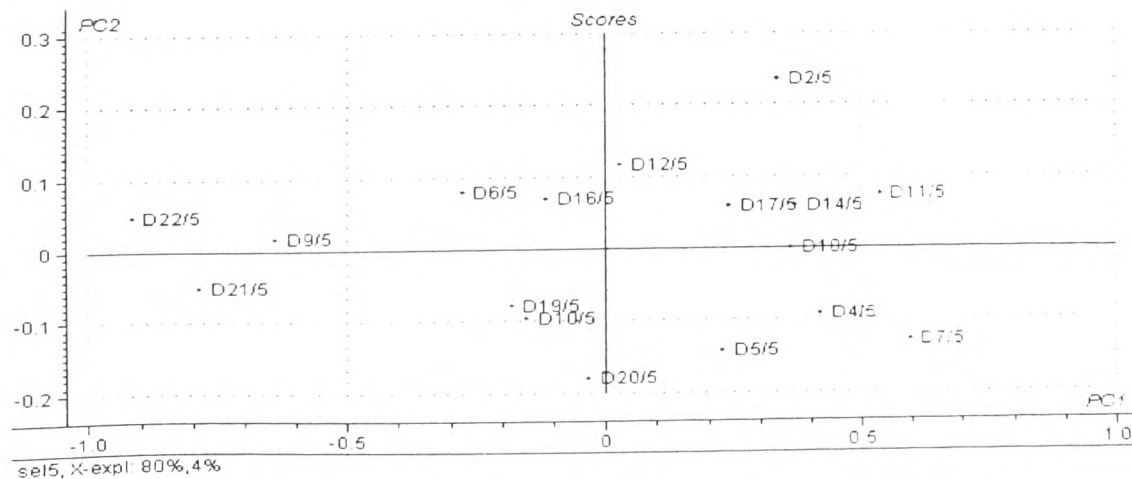


**Figure F42** Score plot of sel5 Training set (containing authentic samples adulterated with 5 % w/w sunflower) on selective IR data region

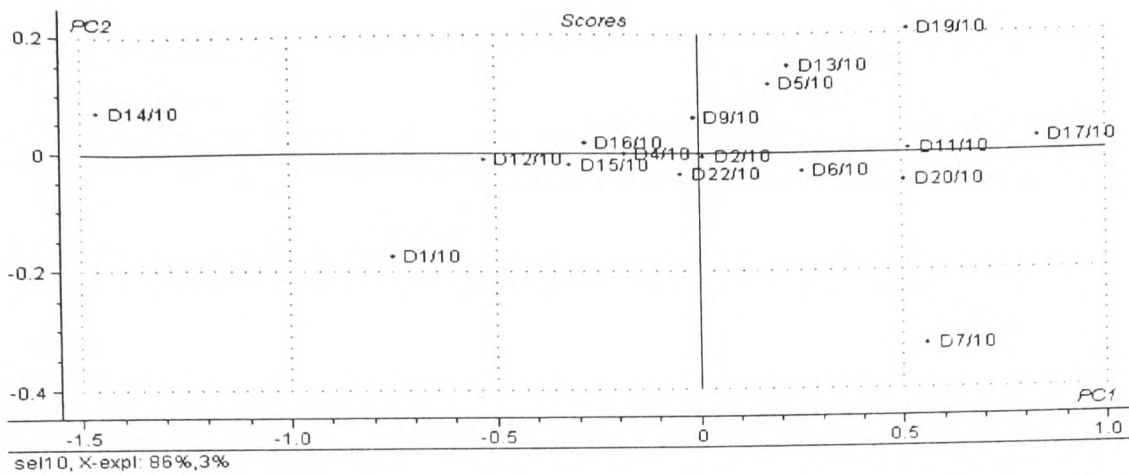


**Figure F43 Score plot of sel10 Training set (containing authentic samples adulterated with 10 % w/w sunflower) on selective data region**

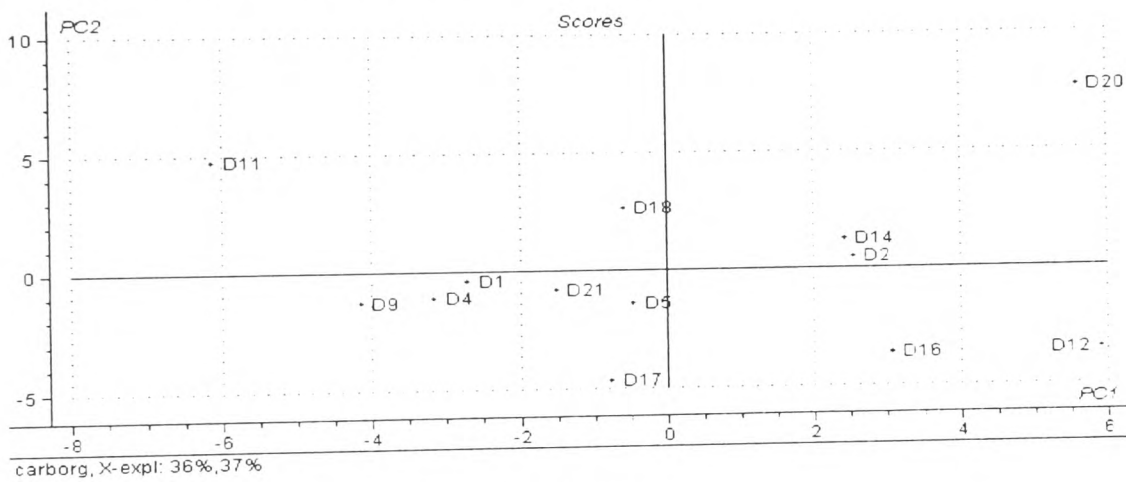


**Figure F44 Score plot of Carborg Training set**

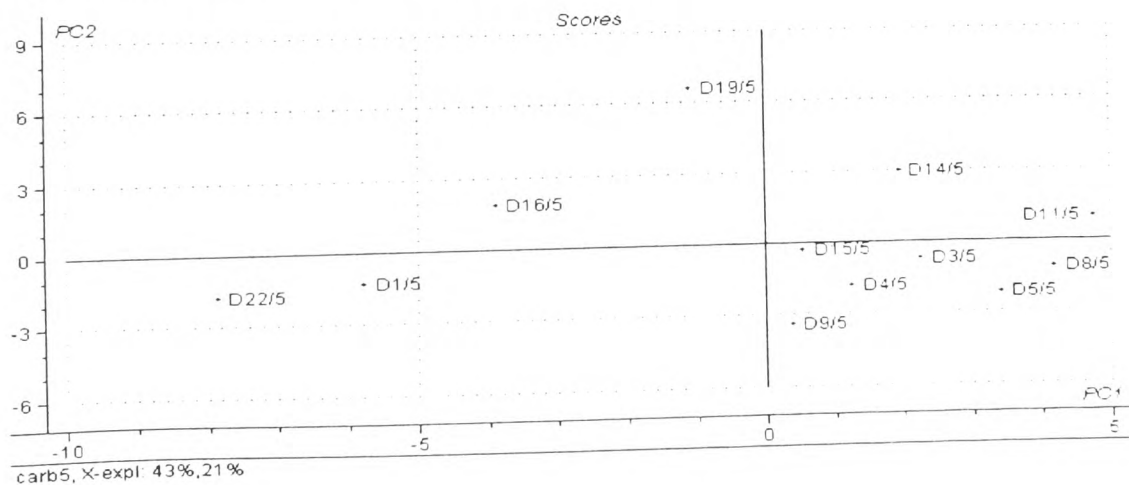


**Figure F45 Score plot of Carb5 Training set**

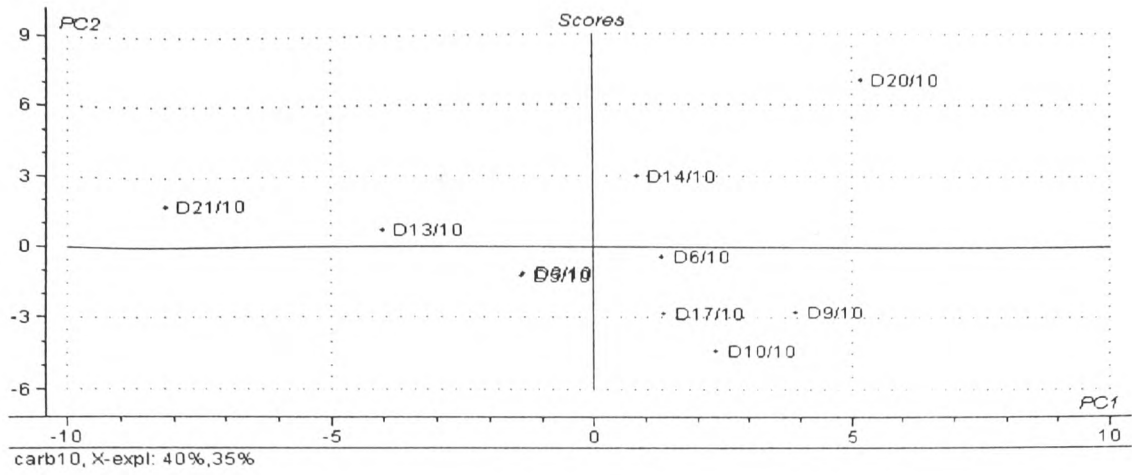


Figure F46 Score plot of Carb10 Training set

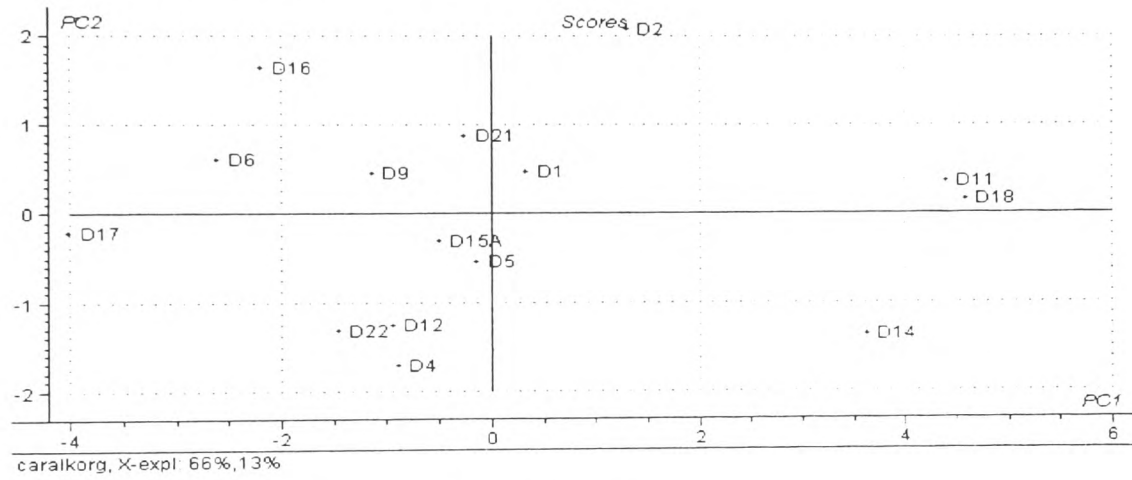


Figure F47 Score plot of Caralkborg Training set

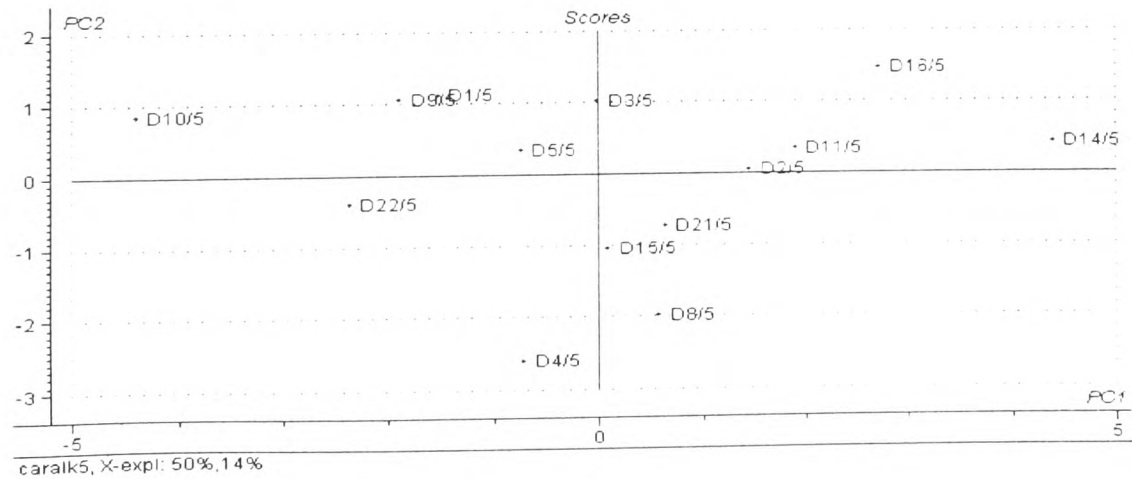


Figure F48 Score plot of Calkalk5 Training set

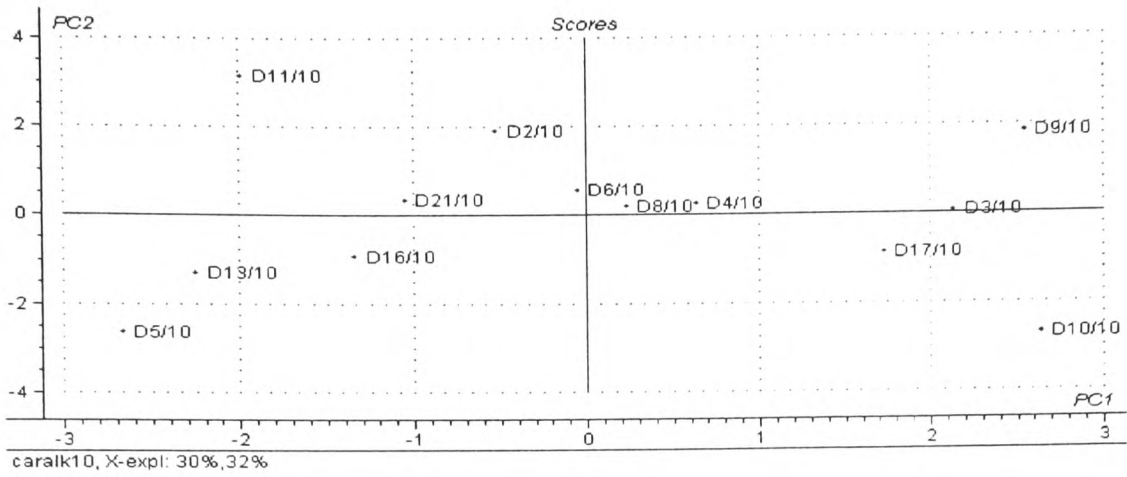


Figure F49 Score plot of Calkalk10 Training set

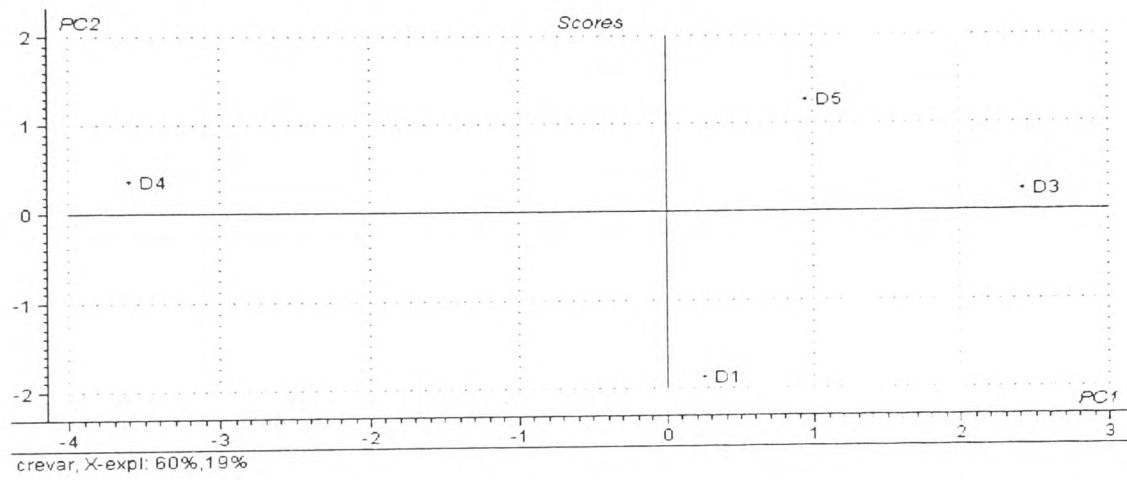


Figure F50 Score plot of Crevar Training set

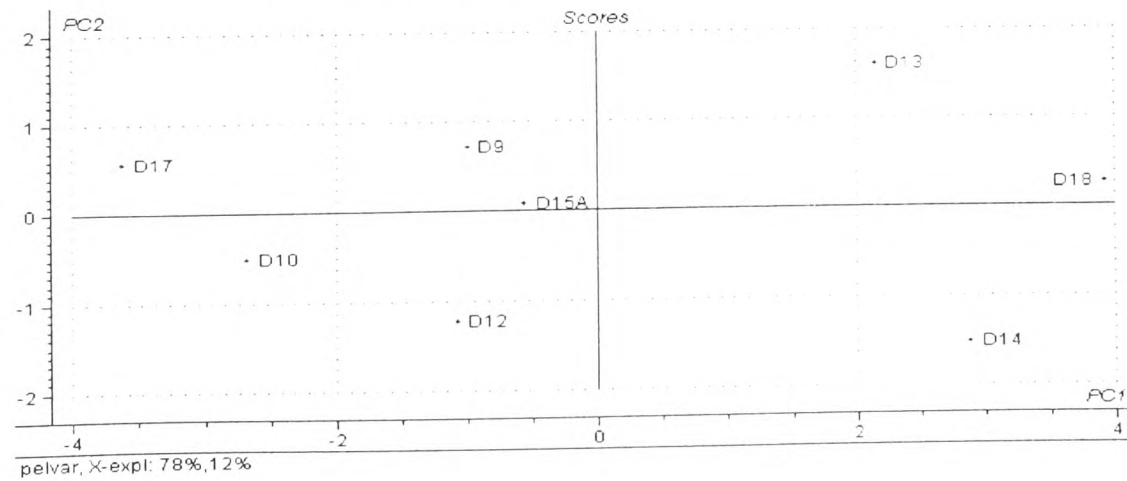


Figure F51 Score plot of Pelvar Training set

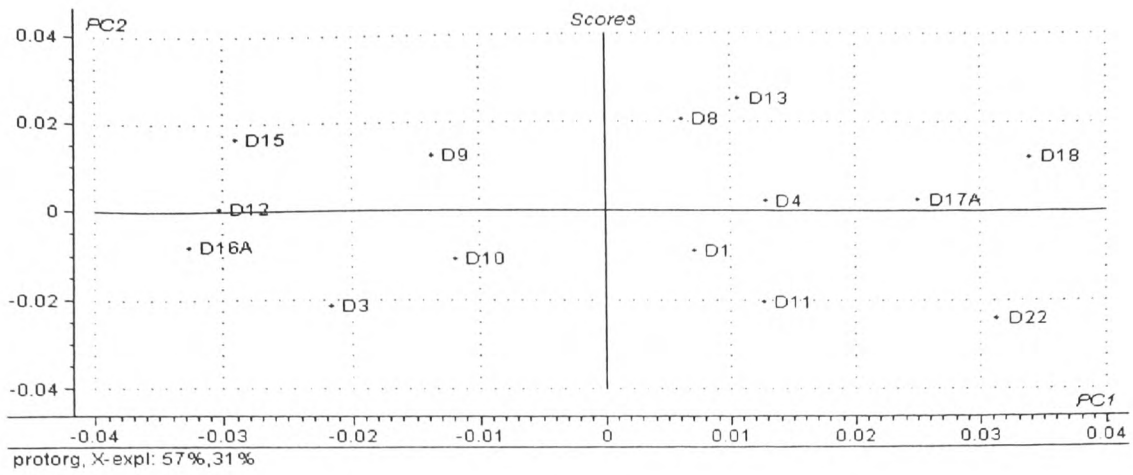


Figure F52 Score plot of Protorg Training set

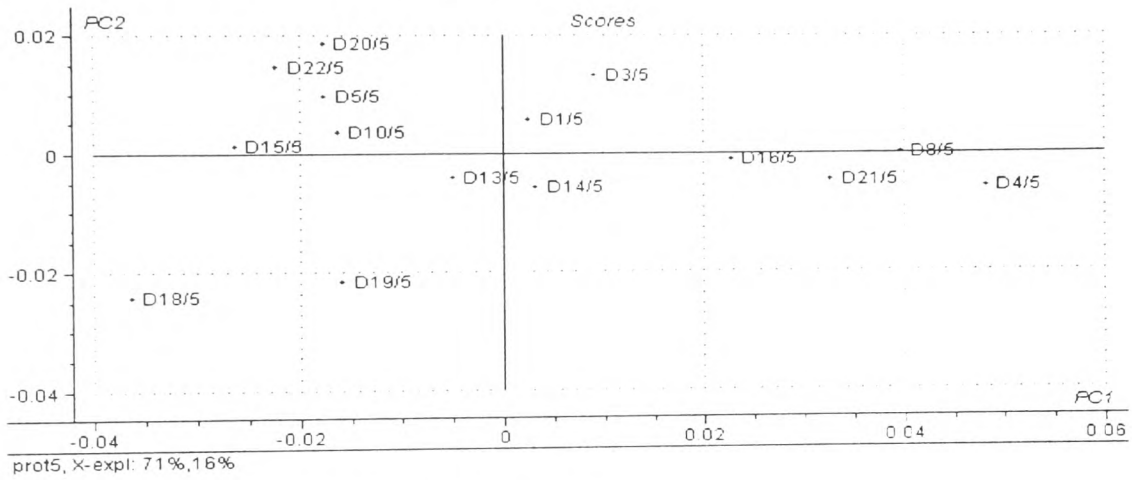


Figure F53 Score plot of Prot5 Training set

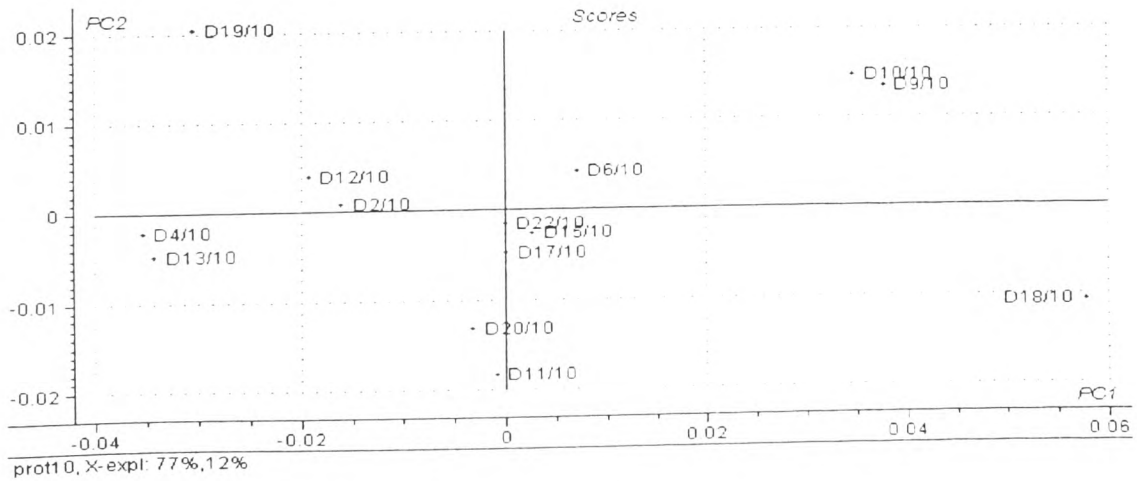
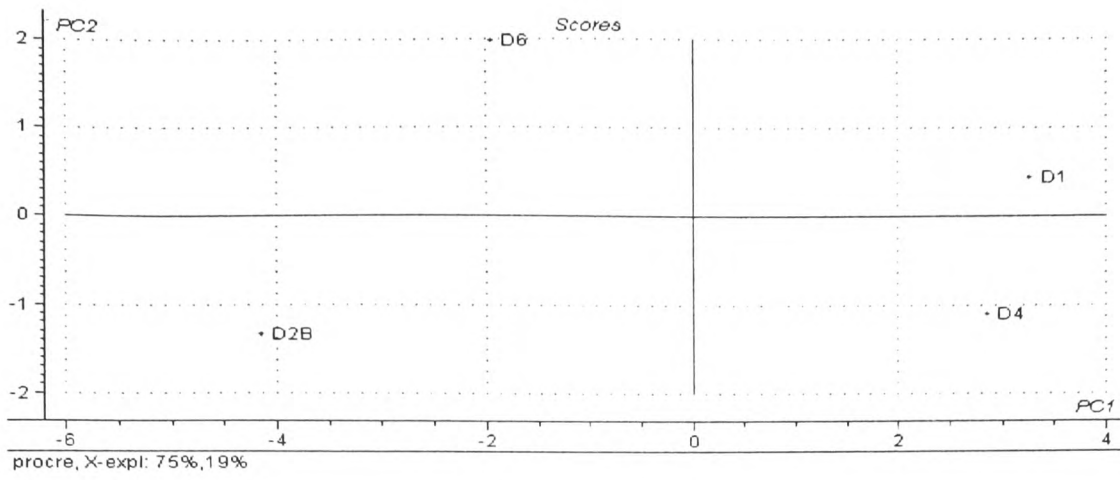
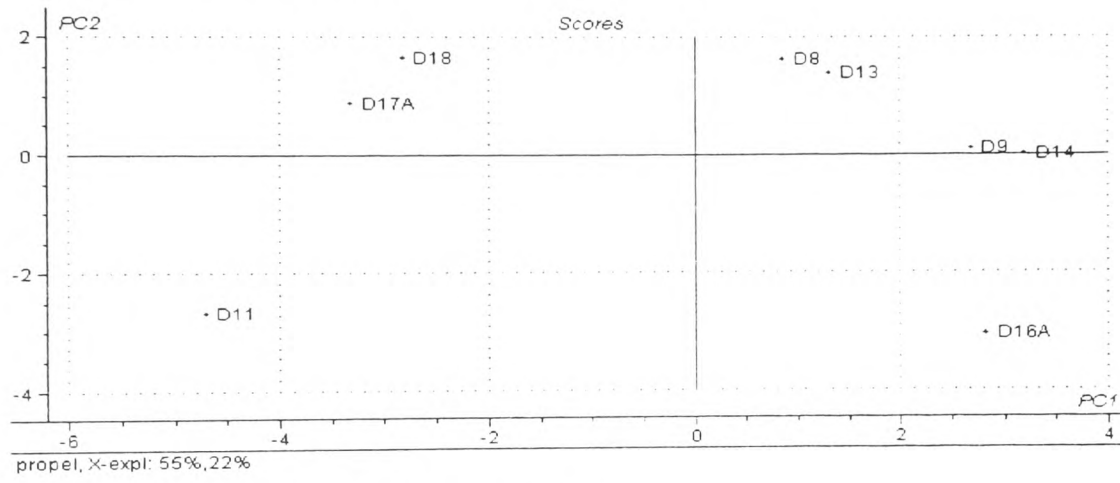


Figure F54 Score plot of Prot10 Training set



**Figure F55** Score plot of Procre Training set



**Figure F56** Score plot of Propel Training set